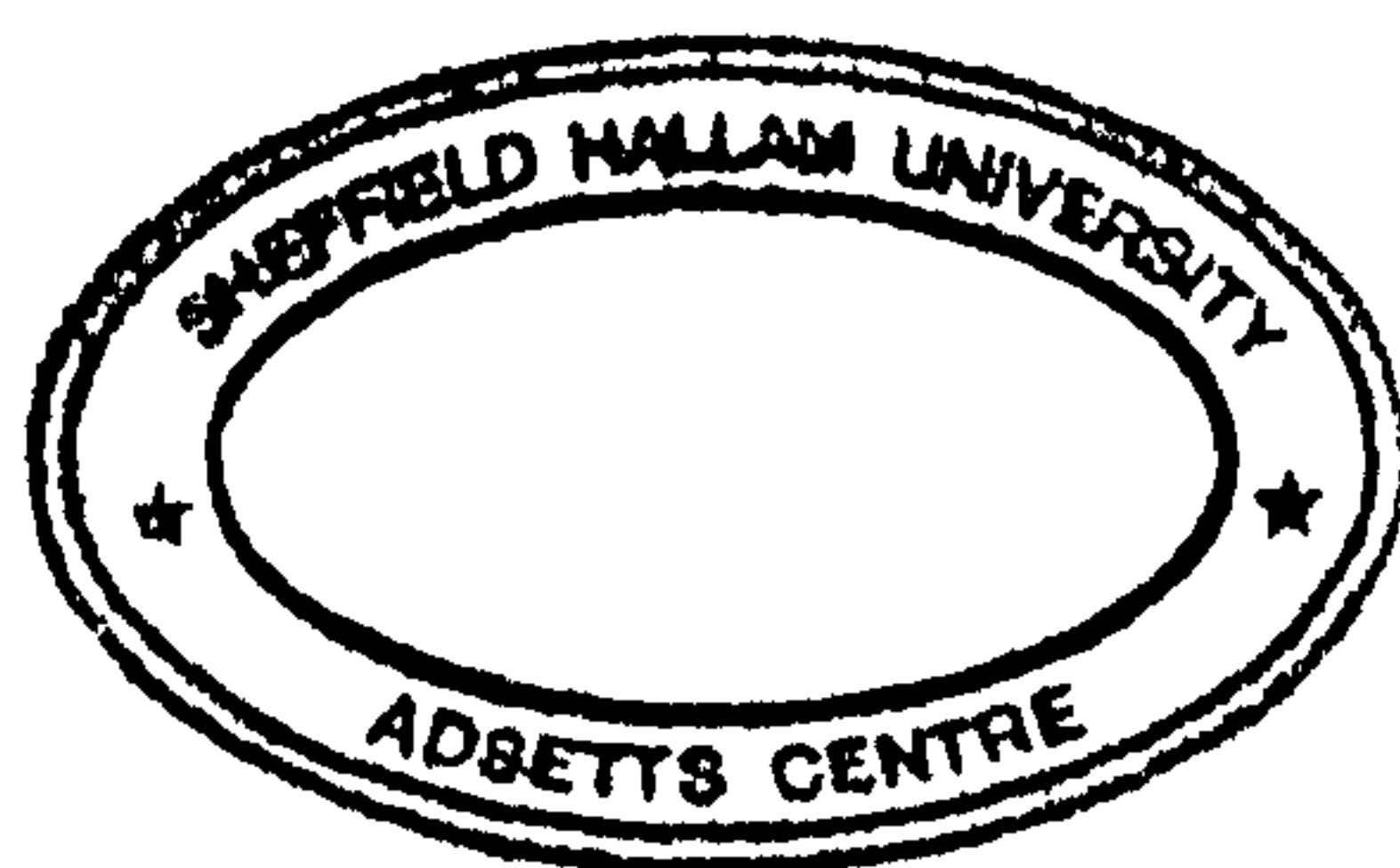


# ROAD TRAFFIC NOISE BARRIER DESIGN: MEASUREMENTS AND MODELS CONCERNING MULTIPLE-WALLS AND AUGMENTED EARTH MOUNDS

Inan Ekici



A thesis submitted in partial fulfilment of the  
requirements of Sheffield Hallam University for a  
degree of Doctor of Philosophy

January 2004

## **Abstract:**

This research programme is concerned with the design of road traffic noise barriers, in particular, the use of multiple-walls on the ground and on top of earth mound type barriers.

As part of this research, a comprehensive up-to-date review of the research carried out on noise barriers was undertaken. A number of areas requiring further research were identified. The discussion of these resulted in the proposal of a simplified noise barrier selection method which would be of use particularly to non-acousticians. This method indicated that acoustic information available for the design of earth mounds was limited, although this barrier type is commonly used in practice and is known to have a number of non-acoustic benefits. Initial investigations showed that the performance of an earth mound could be enhanced by the use of multiple-walls on its top.

A detailed investigation was undertaken into the acoustic performance of multiple-walls both on the ground and on top of earth mounds. Both physical and numerical modelling techniques were used for this purpose. The physical scale modelling experiments were carried out both under uniform field conditions and in two different semi-anechoic chambers in the presence of a continuous noise source, using a model scale of 1:10. The numerical modelling was applied using indirect boundary element method formulation. The commercial software named SYSNOISE was employed for the computations. It was found that numerical modelling results and the semi-anechoic chamber experiments generally agreed very well. The level of accuracy of the uniform field experiments depended on the choice of source and receiver locations as well as the size of the model geometry.

This investigation resulted in acoustic advice on the use of multiple walls both on their own and on top of earth mounds. Under favourable conditions, the multiple-wall configurations were shown to provide substantial attenuations of up to 26dB. The physical parameters involved in their design and their noise attenuation mechanisms were identified. In addition to long-wave scattering and diffraction effects, it was identified that surface wave generation mechanisms and interference effects played a role in attenuating noise. The acoustic advice for the design of earth mounds was extended to the applications of single, double and multiple-walls on their top.

This work also showed that uniform field conditions in conjunction with a continuous noise source could be used for physical modelling. It was found that for small-sized geometries good agreements were observed between physical modelling (both types) and numerical simulations. There were lesser agreements between the sets of data for larger geometries.

The multiple-wall configurations investigated as part of this research programme could be used as noise mitigating measures in central reservations of dual carriageways. However, further research would be required into their acoustic performance and engineering design. The results obtained from this investigation have led to the identification of a number of research areas which could be undertaken in the future.



# TABLE OF CONTENTS

<b>1</b>	<b>GENERAL INTRODUCTION.....</b>	<b>1</b>
<b>1.1</b>	<b>EFFECTS OF NOISE</b>	<b>1</b>
1.1.1	Interference with Speech Communication	1
1.1.2	Sleep Disturbance Effects	1
1.1.3	Psycho-Physiological Effects	2
1.1.4	Mental Health Effects	2
1.1.5	Performance Effects	2
1.1.6	Residential Effects and Annoyance	2
1.1.7	Economic Costs	3
<b>1.2</b>	<b>EUROPEAN NOISE POLICY</b>	<b>3</b>
<b>1.3</b>	<b>ROAD TRAFFIC NOISE CONTROL IN THE U.K.</b>	<b>5</b>
<b>1.4</b>	<b>CONCLUDING REMARKS</b>	<b>8</b>
<b>1.5</b>	<b>THE WAY FORWARD</b>	<b>9</b>
<b>1.6</b>	<b>REFERENCES</b>	<b>12</b>
<b>2</b>	<b>SOUND PROPAGATION IN OUTDOOR ENVIRONMENTS.....</b>	<b>14</b>
<b>2.1</b>	<b>BACKGROUND</b>	<b>14</b>
2.1.1	Geometric Spreading, $A_s$	14
2.1.2	Atmospheric Absorption, $A_a$	15
2.1.3	Ground Effect, $A_g$	15
2.1.4	Atmospheric Effects, $A_{atm}$	18
2.1.5	Barrier Attenuation, $A_b$	19
<b>2.2</b>	<b>INFLUENCE OF ATMOSPHERIC AND GROUND EFFECTS ON BARRIER PERFORMANCE</b>	<b>21</b>
2.2.1	Ground Conditions	21
2.2.2	Atmospheric Conditions	22
<b>2.3</b>	<b>NUMERICAL METHODS</b>	<b>23</b>

<b>2.4</b>	<b>THEORETICAL CONCEPTS OF BARRIER ATTENUATION IN HOMOGENOUS ATMOSPHERE</b>	<b>24</b>
2.4.1	Geometrical Diffraction Methods	25
2.4.2	Numerical wave - based methods: Boundary Element Methods	28
<b>2.5</b>	<b>CONCLUSIONS</b>	<b>30</b>
<b>2.6</b>	<b>REFERENCES</b>	<b>32</b>
<b>3</b>	<b>REVIEW OF ROAD TRAFFIC NOISE CONTROL BY MEANS OF BARRIERS .....</b>	<b>36</b>
<b>3.1</b>	<b>INTRODUCTION</b>	<b>36</b>
<b>3.2</b>	<b>RESEARCH INTO BARRIER PERFORMANCE</b>	<b>37</b>
3.2.1	Analytical Methods	37
3.2.2	Physical Scale Modelling	39
3.2.3	Full Scale Testing	41
<b>3.3</b>	<b>FACTORS AFFECTING THE ACOUSTIC DESIGN OF ENVIRONMENTAL BARRIERS</b>	<b>42</b>
3.3.1	Barrier profile	42
3.3.2	Height	42
3.3.3	Length	42
3.3.4	Source - to - barrier distance	43
3.3.5	Barrier - to - receiver distance	43
3.3.6	Source and receiver heights	43
3.3.7	Frequency content of the traffic noise	43
3.3.8	Transmission loss through the barrier	43
<b>3.4</b>	<b>NOISE BARRIER TYPES</b>	<b>44</b>
3.4.1	Vertical alignment of road	44
3.4.2	Thin Vertical Reflective Barriers	44
3.4.3	Earth Mounds	45
3.4.4	Multiple- Edged Barriers	46
3.4.5	Random-Edged Barriers	48
3.4.6	Absorptive Barriers	48
3.4.7	Enclosure Type Barriers	50
3.4.8	Bio-Barriers and Vegetation	51

3.4.9	Sloped barriers	51
3.4.10	Interference - Based Barriers	52
3.4.11	Low-height Parallel Walls	53
3.4.12	Picket Barriers	53
3.4.13	Reactive Barriers	55
3.4.14	Helium- Filled Barriers	55
3.4.15	Dispersive Barriers	56
<b>3.5</b>	<b>DISCUSSION</b>	<b>56</b>
<b>3.6</b>	<b>CRITICAL APPRAISAL</b>	<b>57</b>
3.6.1	Barrier Design	57
3.6.2	Methods for Investigating Barrier Performance	58
3.6.3	Way Forward	58
<b>3.7</b>	<b>CONCLUSIONS AND RECOMMENDATIONS FOR FUTURE WORK</b>	<b>59</b>
<b>4</b>	<b>A SIMPLIFIED METHOD OF SELECTING BARRIERS .....</b>	<b>72</b>
<b>4.1</b>	<b>INTRODUCTION</b>	<b>72</b>
<b>4.2</b>	<b>DESIGN PHILOSOPHY</b>	<b>72</b>
4.2.1	The Design Process	72
4.2.2	Design Analogy	74
<b>4.3</b>	<b>EXISTING DESIGN GUIDELINES</b>	<b>75</b>
<b>4.4</b>	<b>PROPOSED DESIGN GUIDELINES</b>	<b>76</b>
4.4.1	Multiple Reflections	77
4.4.2	New Barriers	80
4.4.3	Existing Barriers	82
<b>4.5</b>	<b>DISCUSSION</b>	<b>85</b>
<b>4.6</b>	<b>CONCLUSIONS</b>	<b>86</b>
<b>4.7</b>	<b>REFERENCES</b>	<b>87</b>
<b>5</b>	<b>EXPLORATORY WORK TO DEFINE RESEARCH AREA AND METHODOLOGY .....</b>	<b>89</b>
<b>5.1</b>	<b>INTRODUCTION</b>	<b>89</b>



<b>5.2</b>	<b>PREVIOUS WORK ON MULTIPLE - SIDED BARRIERS</b>	<b>90</b>
<b>5.3</b>	<b>FACTORS FAVOURING THE APPLICATION OF EARTH MOUNDS</b>	<b>93</b>
5.3.1	Acoustics	93
5.3.2	Aesthetics	94
5.3.3	Cost	94
5.3.4	Acceptability	94
5.3.5	Environmental friendliness	95
<b>5.4</b>	<b>ACOUSTICAL GUIDANCE ON EARTH MOUNDS</b>	<b>95</b>
5.4.1	Applications in Europe	95
5.4.2	Earth mounds in U.K.	95
<b>5.5</b>	<b>OUTDOOR NOISE MEASUREMENTS ON THE PERFORMANCE OF AN EARTH MOUND</b>	<b>97</b>
5.5.1	Measurements	97
5.5.2	Results	99
5.5.3	Prediction of Noise Levels	100
5.5.4	Prediction of Insertion Loss	102
5.5.5	Concluding Remarks	102
<b>5.6</b>	<b>PHYSICAL SCALE MODELLING OF EARTH MOUNDS WITH SMALL HEIGHT BARRIERS</b>	<b>103</b>
5.6.1	Introduction	103
5.6.2	Experimental Method	103
5.6.3	Results	104
5.6.4	Discussion	108
<b>5.7</b>	<b>TECHNIQUES AVAILABLE FOR THE INVESTIGATION OF BARRIERS</b>	<b>109</b>
5.7.1	Noise Measurements	109
5.7.2	Physical Modelling	110
5.7.3	Numerical Modelling	111
<b>5.8</b>	<b>CONCLUSIONS</b>	<b>111</b>
<b>5.9</b>	<b>REFERENCES</b>	<b>113</b>

<b>6</b>	<b>THEORETICAL APPRAISAL OF THE ACOUSTICS OF RIB STRUCTURES .....</b>	<b>115</b>
<b>6.1</b>	<b>INTRODUCTION</b>	<b>115</b>
<b>6.2</b>	<b>BACKGROUND</b>	<b>116</b>
6.2.1	A series of edges on the ground	116
6.2.2	Noise barrier with a reactive cylindrical top	117
6.2.3	Noise barrier with a reactive horizontal cap	118
6.2.4	Use of quarter-wave resonators in building ventilation openings	118
6.2.5	Seat dip effect in auditoria	119
6.2.6	Diffusors	119
6.2.7	Propagation over ground having small-sized irregularities	120
<b>6.3</b>	<b>PRESSURE RELEASE SURFACES</b>	<b>121</b>
6.3.1	Boundary Conditions	121
6.3.2	Quarter-wave Resonators	122
<b>6.4</b>	<b>DIFFRACTION GRATINGS</b>	<b>125</b>
<b>6.5</b>	<b>SURFACE WAVES</b>	<b>128</b>
<b>6.6</b>	<b>CONCLUSIONS</b>	<b>130</b>
<b>6.7</b>	<b>REFERENCES</b>	<b>132</b>
<b>7</b>	<b>AN INVESTIGATION INTO THE EXPERIMENTAL SET-UP .....</b>	<b>135</b>
<b>7.1</b>	<b>PHYSICAL SCALE MODELLING UNDER UNIFORM FIELD CONDITIONS</b>	<b>135</b>
7.1.1	Background	135
7.1.2	Testing Room	136
7.1.3	Background Noise	136
7.1.4	Scale Factor	137
7.1.5	Modelling Materials	137
7.1.6	Noise Source and Receiver	138
<b>7.2</b>	<b>REVERBERATION TIME MEASUREMENTS</b>	<b>139</b>
7.2.1	Background	139
7.2.2	Aim of the Experiment	140
7.2.3	The Level Recorder Experiments	140

7.2.4	The NC10 Experiments	146
7.2.5	Comparative results for two methods	155
<b>7.3</b>	<b>SOURCE DIRECTIVITY</b>	<b>156</b>
7.3.1	Aim of the Experiment	156
7.3.2	Experimental Apparatus, Set-up and Procedure	157
7.3.3	Results	157
<b>7.4</b>	<b>ESTIMATION OF REVERBERANT FIELD</b>	<b>162</b>
7.4.1	Background	162
7.4.2	Experimentation	163
7.4.3	Results	164
<b>7.5</b>	<b>COMPARISON TO PREVIOUSLY PUBLISHED WORK</b>	<b>169</b>
7.5.1	De Jong et al.'s Model	169
7.5.2	Hutchins et al.'s Model	171
<b>7.6</b>	<b>IMPEDANCE TUBE MEASUREMENTS</b>	<b>176</b>
7.6.1	Aim of the Experiment	176
7.6.2	Experimental Apparatus Set-Up and Procedure	176
7.6.3	Results	177
<b>7.7</b>	<b>FLOW RESISTIVITY OF THE ABSORBING MATERIAL</b>	<b>181</b>
<b>7.8</b>	<b>GENERAL DISCUSSION</b>	<b>182</b>
7.8.1	Reverberant Field within Testing Space	182
7.8.2	Absorptive Properties of Model Materials	185
<b>7.9</b>	<b>CONCLUSIONS</b>	<b>186</b>
<b>7.10</b>	<b>REFERENCES</b>	<b>188</b>
<b>8</b>	<b>PHYSICAL SCALE MODELLING: UNIFORM FIELD TESTS .....</b>	<b>189</b>
<b>8.1</b>	<b>EXPERIMENTAL METHOD</b>	<b>189</b>
<b>8.2</b>	<b>RESULTS</b>	<b>192</b>
8.2.1	Multiple Edges on the Ground	192
8.2.2	Multiple Edges on a Low Rectangular Barrier	203
8.2.3	Multiple Edges on a Flat-Topped Mound	207



<b>8.3</b>	<b>DISCUSSION</b>	<b>210</b>
<b>8.4</b>	<b>CONCLUSIONS</b>	<b>218</b>
<b>9</b>	<b>PHYSICAL SCALE MODELLING: SEMI-ANECHOIC CHAMBER EXPERIMENTS .....</b>	<b>221</b>
<b>9.1</b>	<b>EXPERIMENTAL METHOD</b>	<b>221</b>
<b>9.2</b>	<b>MULTIPLE EDGES ON THE GROUND</b>	<b>225</b>
9.2.1	Progressive Increase in the Number of Edges	225
9.2.2	Doubling of the Number of Wells	227
9.2.3	Effect of Additional Edges at Different Receivers	230
<b>9.3</b>	<b>ADDITIONAL EXPERIMENTS ON RECEIVER HEIGHT</b>	<b>234</b>
<b>9.4</b>	<b>COMPARISON OF DIFFERENT WELL DEPTHS</b>	<b>238</b>
<b>9.5</b>	<b>MULTIPLE EDGES ON A LOW RECTANGULAR BARRIER</b>	<b>243</b>
<b>9.6</b>	<b>MULTIPLE EDGES ON A FLAT-TOPPED MOUND</b>	<b>249</b>
<b>9.7</b>	<b>DISCUSSIONS</b>	<b>252</b>
<b>9.8</b>	<b>CONCLUSIONS</b>	<b>258</b>
<b>10</b>	<b>NUMERICAL MODELLING USING BOUNDARY ELEMENT METHODS 260</b>	
<b>10.1</b>	<b>BACKGROUND</b>	<b>260</b>
<b>10.2</b>	<b>DETAILS OF THE NUMERICAL MODEL</b>	<b>263</b>
10.2.1	Process of Modelling	263
10.2.2	Junctions	270
10.2.3	Irregular Frequencies	273
<b>10.3</b>	<b>MODELLING OF A TEST GEOMETRY FROM LITERATURE</b>	<b>276</b>
<b>10.4</b>	<b>NUMERICAL MODELLING OF SELECTED GEOMETRIES INVESTIGATED BY PHYSICAL MODELLING</b>	<b>279</b>
10.4.1	The rib structure	279
10.4.2	The edges on the ground	280
10.4.3	The edges on rectangle	283

10.4.4	The edges on earth mound	285
<b>10.5</b>	<b>MODIFICATIONS TO AN EXISTING EARTH MOUND</b>	<b>287</b>
10.5.1	Description of the Geometry	287
10.5.2	Numerical Modelling Results	290
<b>10.6</b>	<b>EQUAL HEIGHT REACTIVE MOUND</b>	<b>295</b>
<b>10.7</b>	<b>DISCUSSION</b>	<b>298</b>
<b>10.8</b>	<b>CONCLUSIONS</b>	<b>300</b>
<b>10.9</b>	<b>REFERENCES</b>	<b>302</b>
<b>11</b>	<b>COMPARISON OF MODELLING RESULTS.....</b>	<b>304</b>
<b>11.1</b>	<b>VALIDATION OF THE RESULTS FROM THE SCALE MODELLING</b>	<b>304</b>
11.1.1	Edges on the Ground	305
11.1.2	Edges on Rectangle	310
11.1.3	Edges on Earth Mound	312
11.1.4	Effects of Rib-structure at Different Receiver Heights	313
<b>11.2</b>	<b>DISCUSSIONS</b>	<b>318</b>
11.2.1	Edges on the ground	318
11.2.2	Edges on rectangle	319
11.2.3	Earth Mound	319
11.2.4	Rib-structure	320
<b>11.3</b>	<b>CONCLUSIONS</b>	<b>320</b>
<b>12</b>	<b>GENERAL DISCUSSION.....</b>	<b>322</b>
<b>12.1</b>	<b>BACKGROUND</b>	<b>322</b>
<b>12.2</b>	<b>IDENTIFYING RESEARCH NEEDS</b>	<b>325</b>
<b>12.3</b>	<b>A SIMPLIFIED METHOD FOR BARRIER SELECTION</b>	<b>326</b>
<b>12.4</b>	<b>EXPLORATORY WORK</b>	<b>327</b>
<b>12.5</b>	<b>MAIN MODELLING WORK</b>	<b>329</b>
<b>12.6</b>	<b>EXTENDING GUIDANCE ON EXISTING EARTH MOUNDS</b>	<b>337</b>

<b>13</b>	<b>CONCLUSIONS AND FUTURE WORK.....</b>	<b>342</b>
<b>13.1</b>	<b>MODELLING</b>	<b>342</b>
<b>13.2</b>	<b>AN ALTERNATIVE BARRIER TYPE</b>	<b>342</b>
13.2.1	Physical Parameters	343
13.2.2	Attenuation Mechanisms	343
<b>13.3</b>	<b>SPECIFIC FINDINGS</b>	<b>343</b>
<b>13.4</b>	<b>RESEARCH FINDINGS</b>	<b>345</b>
<b>13.5</b>	<b>FUTURE WORK</b>	<b>346</b>
<b>13.6</b>	<b>REFERENCES</b>	<b>348</b>



# TABLE OF FIGURES

Figure 2.1 : Sound propagation over a flat boundary .....	16
Figure 2.2 : Path length difference $\delta$ .....	24
Figure 2.3 : Sound path diagrams without and with a barrier .....	25
Figure 2.4 : Two-dimensional model showing source ( $r_o$ ), receiver ( $r$ ), barrier ( $y$ ) and ground ( $y_9$ ) configuration and the reference coordinate system. ....	28
Figure 3.1 : Roads in Cuttings .....	44
Figure 3.2 : Elevated Roads.....	44
Figure 3.3 : Thin vertical barriers (a) single, (b) multiple, and (c) median barrier configurations	45
Figure 3.4 : Various earth mound / wedge configurations .....	46
Figure 3.5 : Multiple edged barrier configurations showing (a) thick barrier, (b) T – capped barrier, (c) brackets attached to main barrier, (d) arrow profile, (e) Y – profile, (f) Y – profile with additional edges, (g) branched profile, (h) U – profile, (i) fir tree section, (j) double barriers .....	47
Figure 3.6 : Random edged barrier (Longitudinal view showing part of length) .....	48
Figure 3.7 : Barriers with absorptive treatment, (a) cylindrically capped, (b) mushroom capped, and (c) horizontally louvred barriers.....	49
Figure 3.8 : Enclosure type barriers (a) tunnel, (b) louvered cover, (c) cantilevered barrier, (d), partially inclined barrier, (e) open box section.....	51
Figure 3.9 : Sloped noise barrier.....	52
Figure 3.10 : Interference based noise barriers (source to the left).....	52
Figure 3.11 : Phase reversal barriers (a) slow – waveguide, (b) basic dipolar type, (c) halfguide dipolar type, and (d) quadrupolar type .....	53
Figure 3.12 : Longitudinal and cross-sectional views of various picket barriers, (a) picket fence, (b) flat topped picket, (c) saw toothed picket, (d) splitter type picket. ....	54
Figure 3.13 : Plan view of a vertically louvred barrier (part of whole length).....	54
Figure 3.14 : Barriers with reactive surfaces (a) series of parallel ribs on the ground, (b) waterwheel, (c) constant depth reactive T-capped barrier, and (d) variable depth reactive T-capped barrier.....	55
Figure 3.15 : Plan view, showing part of whole length, of (a)zigzag, (b)wave and (c) castellated profiled barriers.....	56
Figure 4.1 : The main issues involved in environmental barrier design.....	74

Figure 4.2 : The six factors perceived as the individual pieces of a jigsaw puzzle.....	74
Figure 4.3 : The completed jigsaw puzzle.....	75
Figure 4.4 : Effective solution for an environmental barrier. ....	75
Figure 4.5 : Multiple reflection mechanisms.....	78
Figure 4.6 : Selection process for new barriers .....	82
Figure 4.7 : Improvements to existing wall type barriers .....	83
Figure 5.1 : Earth mounds investigated by Hutchins et al. ....	91
Figure 5.2 : Geometries investigated by Hothersall et al. ....	91
Figure 5.3 : Geometries investigated by Hothersall et al. ....	92
Figure 5.4 : The sketch showing the cross-section through the site and the receiver locations. .....	98
Figure 5.5 : A-weighted sound pressure levels ( $L_{A10}$ ) compared for receivers 1 and 3. ....	100
Figure 5.6 : Details of the source / receiver locations and the dimensions of the basic geometry. .....	104
Figure 5.7 : Relative performance in dB of various edge conditions combined with different absorption characteristics over plain earth mound.....	105
Figure 5.8 : Comparison of the effects of different absorption characteristics over the performance for given edge conditions. ....	106
Figure 5.9 : Comparison of the effects of different edge conditions over the performance for given absorption characteristics. ....	107
Figure 6.1 : A typical diffraction grating.....	126
Figure 6.2 : Path length difference for a plane wave .....	127
Figure 7.1 : Plan of testing room and the general location of models .....	136
Figure 7.2 : The background noise levels within the uniform testing space .....	137
Figure 7.3 : Experimental set-up for level recorder tests .....	141
Figure 7.4 : Plan view of the testing room showing the source-receiver configuration for the starting pistol tests.....	141
Figure 7.5 : Plan view of the testing room showing the source-receiver configuration for the speaker tests. ....	141
Figure 7.6 : Plan view of the testing room showing the source-receiver configurations for the double-speaker tests .....	142
Figure 7.7 : Sample decay curve .....	143

Figure 7.8 : Starting pistol sound pressure levels obtained for different tests throughout the testing range.....	143
Figure 7.9 : Reverberation times obtained for the starting pistol tests .....	144
Figure 7.10 : Reverberation times obtained for the single wedge speaker tests.....	145
Figure 7.11 : Reverberation times obtained for the double wedge speaker tests .....	145
Figure 7.12 : Experimental set-up showing NC10 tests.....	146
Figure 7.13 : Digital Noise Analyser NC10 used for reverberation time measurements .....	146
Figure 7.14 : The NC10 Analyser, microphone and calibrator.....	147
Figure 7.15 : Source-receiver configuration for the reverberation time tests undertaken by NC10 using a wedge speaker as the source.....	147
Figure 7.16 : Source-receiver configuration for the reverberation time tests undertaken by NC10 using a starting pistol as the source. ....	147
Figure 7.17 : Average reverberation times for the NC10 tests using the wedge speaker as the source.....	150
Figure 7.18 : Correlation of the T30 test results using the wedge speaker. ....	150
Figure 7.19 : Correlation of the T20 test results using the wedge speaker. ....	151
Figure 7.20 : Correlation of the early decay times (EDT) using the wedge speaker. ....	151
Figure 7.21 : Average reverberation times for the pistol tests. ....	152
Figure 7.22 : Correlation of the T30 test results using the starting pistol. ....	152
Figure 7.23 : Correlation of the T20 test results using the starting pistol. ....	153
Figure 7.24 : Correlation of the early decay times (EDT) using the starting pistol. ....	153
Figure 7.25 : Decay curves for selected frequency bands for the starting pistol. ....	154
Figure 7.26 : Decay curves for selected frequency bands for the wedge speaker.....	154
Figure 7.27 : Average reverberation times between 800 Hz and 4 kHz for various tests. ....	155
Figure 7.28 : Average reverberation times between 500 Hz and 16 kHz for starting pistol / pen-recorder and the NC10 tests. ....	156
Figure 7.29 : Polar plot of sound pressure levels for 2, 2.5, 3.15 and 4 kHz.....	158
Figure 7.30 : Polar plot of sound pressure levels for 5, 6.3, 8 and 10 kHz.....	159
Figure 7.31 : Polar plot of sound pressure levels for 12.5, 16 and 20 kHz.....	160
Figure 7.32 : Directivity indices for each 1 / 3 octave band frequency between 2 - 20 kHz ....	161
Figure 7.33 : Directivity factors for each 1 / 3 octave band frequency between 2 - 20 kHz. ...	161
Figure 7.34 : Variation of the sound pressure levels .....	165



Figure 7.35 : Measured and predicted sound pressure levels for 1.9668 kHz ( $Q = 2$ ,  $R_c = 100$ ; assumed  $L_w = 55$  dB)..... 166

Figure 7.36 : Measured and predicted sound pressure levels for 3.2081 kHz ( $Q = 3.5$ ,  $R_c = 100$ ; assumed  $L_w = 56$  dB)..... 167

Figure 7.37 : Measured and predicted sound pressure levels for 22.067 kHz ( $Q = 8.5$ ,  $R_c = 7619$ ; assumed  $L_w = 49$  dB) ..... 168

Figure 7.38 : De Jong et al.'s geometry. .... 169

Figure 7.39 : The testing geometry obtained by scaling the reference geometry by 1.7..... 170

Figure 7.40 : Comparison of the measured insertion losses with those of De Jong et al. .... 170

Figure 7.41 : Hutchins et al. geometry. .... 171

Figure 7.42 : Comparison of the measured insertion losses with those of Hutchins et al. .... 172

Figure 7.43 : Measured and predicted sound pressure levels at a specific receiver location in the presence of barrier. .... 174

Figure 7.44 : The directivity effect of the source..... 175

Figure 7.45 : Experimental set-up and apparatus for the impedance tube measurements..... 177

Figure 7.46 : Absorption coefficients obtained for glass fibre quilt. .... 178

Figure 7.47 : Absorption coefficients obtained for the medium density fibre (m.d.f.)..... 179

Figure 7.48 : Summary of absorption coefficients obtained for the three cases..... 180

Figure 8.1 : A 3D sketch showing the testing room ..... 189

Figure 8.2 : The plan view of the testing room..... 190

Figure 8.3 : General test arrangement..... 191

Figure 8.4 : Experimental set-up for investigating effect of up to 8 edges..... 193

Figure 8.5 : Progressive reduction of sound pressure levels with increased number of edges. .... 194

Figure 8.6 : Sound pressure levels in the presence of a single edge and 8 - edges..... 194

Figure 8.7 : Insertion loss values for a single edge and for 8 - edges. .... 195

Figure 8.8 : The two configurations investigated showing the source and the receiver locations. The dB values included give the relative improvements over a single edge situated 0.5 m from the source..... 196

Figure 8.9 : Relative performance of 8 edges over a single edge (receiver distance = 0.5 m). .... 197

Figure 8.10 : Relative performance of 8 edges over a single edge (receiver distance = 1 m) 197

Figure 8.11 : Relative performance of 14 edges over a single edge (receiver distance = 0.5 m)	198
Figure 8.12 : Relative performance of 14 edges over a single edge (receiver distance = 1 m).	198
Figure 8.13 : The height of the wells is 0.008 m. The spacing between the edges is 0.017 m. Total width of the reactive surface is approximately 0.22 m.	200
Figure 8.14 : The height of the wells is 0.017 m. The spacing between the edges is 0.008 m. Total width of the reactive surface is approximately 0.10 m.	200
Figure 8.15 : The height of the wells is 0.025 m. The spacing between the edges is 0.025 m. Total width of the reactive surface is approximately 0.325 m.	200
Figure 8.16 : Relative improvement of 14-edges over a single edge (edge height 0.008 m, edge spacing 0.017 m, receiver 0.50 m from first edge)	201
Figure 8.17 : Relative improvement of 14-edges over a single edge (edge height 0.008 m, edge spacing 0.017 m , receiver 1 m from first edge)	201
Figure 8.18 : Relative improvement of 14-edges over a single edge (edge height 0.017 m, edge spacing 0.008 m, receiver 0.5 m from first edge)	202
Figure 8.19 : Relative improvement of 14-edges over a single edge (edge height 0.017 m, edge spacing 0.008 m, receiver 1 m from first edge)	202
Figure 8.20 : Detail showing the cross - section through the rectangular platform on which the edges were placed.	203
Figure 8.21 : The basic shape showing the position of the source and the first edge on the rectangular platform.	203
Figure 8.22 : Comparison of the insertion loss values for the rectangular barrier alone and the reactive rectangular barriers with various well depths	204
Figure 8.23 : Effect of multiple edges of various heights placed on the rectangular barrier....	205
Figure 8.24 : Effect of single barriers of various heights placed on the rectangular barrier. ...	206
Figure 8.25 : Cross-sectional view showing test arrangement.	207
Figure 8.26 : Plan view of flat-topped earth mound configuration	207
Figure 8.27 : The frequency spectrum of gains for various reactive configurations.	209
Figure 8.28 : Difference between the sound pressure levels in the presence of a single edge SPL (1) and 8-edges SPL (8).	211
Figure 9.1 : General experimental set-up in Sheffield chamber	222
Figure 9.2 : The background noise levels at the semi-anechoic chambers.	222
Figure 9.3 : Experimental set-up for investigating effect of up to 8 edges	225

Figure 9.4 : Progressive reduction of sound pressure levels with increased number of edges 226

Figure 9.5 : Insertion loss values for a single edge and for 8 – edges. .... 226

Figure 9.6 : The configurations for investigating effect of doubling of wells. .... 227

Figure 9.7 : Relative performance of 8 edges over a single edge. .... 228

Figure 9.8 : Relative performance of 8 edges over a single edge ..... 229

Figure 9.9 : Relative performance of 14 edges over a single edge (receiver distance = 0.5 m)  
..... 229

Figure 9.10 : Relative performance of 14 edges over a single edge (receiver distance = 1 m).  
..... 230

Figure 9.11 : Variation in SPL with increased number of edges, Receiver (0.5, 0)..... 231

Figure 9.12 : Variation in SPL with increased number of edges, Receiver (1, 0)..... 231

Figure 9.13 : Variation in SPL with increased number of edges, Receiver (0.5, 0.04)..... 232

Figure 9.14 : Variation in SPL with increased number of edges, Receiver (1, 0.04)..... 232

Figure 9.15 : Variation in SPL with increased number of edges, Receiver (0.5, 0.15)..... 233

Figure 9.16 : Variation in SPL with increased number of edges, Receiver (1, 0.15)..... 233

Figure 9.17 : Experimental set-up for investigating different receiver heights..... 234

Figure 9.18 : Receiver height = 0m..... 235

Figure 9.19 : Receiver height = 0.05m..... 235

Figure 9.20 : Receiver height = 0.1m..... 236

Figure 9.21 : Receiver height 0.15m..... 236

Figure 9.22 : Receiver height = 0.2m..... 237

Figure 9.23 : Receiver height = 0.25m..... 237

Figure 9.24 : Receiver height = 0.30m..... 238

Figure 9.25 : The height of the wells is 0.008 m (well spacing is 0.017 m). .... 238

Figure 9.26 : The height of the wells is 0.017 m (well spacing is 0.008 m). .... 239

Figure 9.27 : The height of the wells is 0.025 m (well spacing is 0.025 m). .... 239

Figure 9.28 : Insertion Loss of 14-edges (edge height 0.008 m, edge spacing 0.017 m) ..... 240

Figure 9.29 : Relative improvement of 14-edges over a single edge (edge height 0.008 m, edge  
spacing 0.017 m)..... 240

Figure 9.30 : Insertion Loss of 14-edges (edge height 0.017m, edge spacing 0.008m) ..... 241

Figure 9.31 : Relative improvement of 14-edges over a single edge (edge height 0.017 m, edge  
spacing 0.008 m)..... 241



Figure 9.32 : Insertion Loss of 14-edges (edge height 0.025m, edge spacing 0.025m) ..... 242

Figure 9.33 : Relative improvement of 14-edges over a single edge (edge height 0.025m, edge spacing 0.025m)..... 242

Figure 9.34 : Detail showing the cross - section through the rectangular platform on which the edges were placed. .... 243

Figure 9.35 : The basic shape showing the position of the source and the first edge on the rectangular platform. .... 243

Figure 9.36 : Experimental set-up for the reactive rectangles ..... 244

Figure 9.37 : Improvement in performance over plain rectangles by different edge heights (Rec. ht = 0.5, 0). .... 245

Figure 9.38 : Improvement in performance over plain rectangles by different edge heights (Rec. ht = 0.5, 0.04). .... 245

Figure 9.39 : Insertion loss of plain rectangle and combined edges plus rectangle (Rec. ht = 0.5, 0) ..... 246

Figure 9.40 : Insertion loss of plain rectangle and combined edges plus rectangle (Rec. ht = 0.5, 0.04) ..... 246

Figure 9.41 : Effect of multiple edges of various heights placed on the rectangular barrier.... 247

Figure 9.42 : Effect of single barriers of various heights placed on the rectangular barrier. ... 248

Figure 9.43 : Reference case showing dimensions of basic geometry and the source / receiver locations. .... 249

Figure 9.44 : The frequency spectrum of gains for various reactive configurations. .... 251

Figure 10.1 : Two - dimensional barrier problem. .... 261

Figure 10.2 : Block diagram showing the numerical modelling process..... 263

Figure 10.3 : The geometry pre-processed as field points in SYSNOISE ..... 265

Figure 10.4 : The model with the symmetry plane..... 266

Figure 10.5 : Element normal vectors ..... 267

Figure 10.6 : All free edges forming the model ..... 268

Figure 10.7 : Free edges on symmetry plane ..... 268

Figure 10.8 : Free edges on which zero jump of pressure is applied ..... 269

Figure 10.9 : Node duplication at junctions..... 270

Figure 10.10 : The geometry for investigating the influence of junctions ..... 271

Figure 10.11 : Element nodes as modelled originally ..... 271

Figure 10.12 : Node duplication at junctions..... 271

Figure 10.13 : The effects of junctions on sound pressure field at receiver (5,0)..... 272

Figure 10.14 : The effects of junctions on sound pressure field at receiver (5, 04)..... 273

Figure 10.15 : Model with and without the singular impedance elements. .... 273

Figure 10.16 : The source and receivers for investigating irregular frequencies..... 274

Figure 10.17 : Differences in sound pressure levels at receiver 4 due to singular impedance elements. .... 274

Figure 10.18 : Differences in sound pressure levels at 1400 and 1300 Hz throughout receivers 1 - 9. .... 275

Figure 10.19 : Details of Lai geometry ..... 276

Figure 10.20 : Insertion loss values for Receiver 1..... 276

Figure 10.21 : Insertion loss values for Receiver 2..... 277

Figure 10.22 : Path length difference at Receiver 1 ..... 277

Figure 10.23 : Path length difference at Receiver 2 ..... 278

Figure 10.24 : Experimental set-up investigating various receiver heights ..... 279

Figure 10.25 : The effect of 21 edges over a single edge ..... 280

Figure 10.26 : The height of the wells is 0.08 m. The spacing between the edges is 0.17 m. . 281

Figure 10.27 : The height of the wells is 0.17 m. The spacing between the edges is 0.08 m. . 281

Figure 10.28 : The height of the wells is 0.25 m. The spacing between the edges is 0.25 m. . 281

Figure 10.29 : Effect of 14 x 0.08m edges relative to a single edge (on the ground)..... 282

Figure 10.30 : Effect of 14 x 0.17m edges relative to a single edge (on the ground)..... 282

Figure 10.31 : Effect of 14 x 0.25m edges relative to a single edge (on the ground)..... 283

Figure 10.32 : Experimental set-up for the reactive rectangles ..... 284

Figure 10.33 : Effect of reactive configurations over a plain rectangle (receiver 5, 0)..... 284

Figure 10.34 : Effect of reactive configurations over a plain rectangle (receiver 5, 0.4) ..... 285

Figure 10.35 : The earth mound with edges ..... 285

Figure 10.36 : The effect of multiple edges on top of a plain earth mound ..... 286

Figure 10.37 : The basic earth mound geometry and receivers locations..... 287

Figure 10.38 : The details of the modifications made on top of the basic shape..... 289

Figure 10.39 :Insertion loss spectra for receivers 20m from the centreline..... 291

Figure 10.40 : Insertion loss values for receivers 50m from the centreline ..... 291

Figure 10.41 : Insertion loss values for receivers 100m from the centreline ..... 292



Figure 10.42 : Spectra at receiver 4 comparing profiles with the same edge heights to the reference case. .... 294

Figure 10.43 : Spectra of the reactive configurations compared with the reference case at receiver 4. .... 295

Figure 10.44 : Reactive mound (well depth = 0.17 m) with an overall height of 3 m compared with the reference case and model 13 (receiver 4). .... 296

Figure 10.45 : Reactive mound (well depth = 0.25 m) with an overall height of 3 m compared with the reference case and model 10 (receiver 4). .... 297

Figure 11.1 : The height of the wells is 0.08 m. The spacing between the edges is 0.17 m. ... 306

Figure 11.2 : The height of the wells is 0.17 m. The spacing between the edges is 0.08 m. ... 306

Figure 11.3 : The height of the wells is 0.25 m. The spacing between the edges is 0.25 m. ... 306

Figure 11.4 : Effects of 0.08m wells on the ground ..... 307

Figure 11.5 : Effects of 0.17m wells on the ground ..... 308

Figure 11.6 : Effects of 0.25m wells on the ground ..... 309

Figure 11.7 : Experimental set-up for the reactive rectangles ..... 310

Figure 11.8 : Effect of reactive configurations over a plain rectangle..... 311

Figure 11.9 : The earth mound with edges ..... 312

Figure 11.10 : Measured and modelled results at the single receiver location for the reactive mound geometry. .... 312

Figure 11.11 : Experimental set-up investigating various receiver heights ..... 313

Figure 11.12 : Receiver height = 0..... 314

Figure 11.13 : Receiver height = 0.5m..... 314

Figure 11.14 : Receiver height = 1m..... 315

Figure 11.15 : Receiver height = 1.5m..... 315

Figure 11.16 : Receiver height = 2m..... 316

Figure 11.17 : Receiver height = 2.5m..... 316

Figure 11.18 : Receiver height = 3m..... 317

Figure 12.1 : Improvements to existing earth mound type barriers. .... 339

Figure 12.2 : Change in insertion loss of an existing earth mound due to various modifications. .... 340

# **1 GENERAL INTRODUCTION**

## **1.1 EFFECTS OF NOISE**

Noise can have a variety of effects depending on type, duration and timing of the noise source as well as the susceptibility of the recipient. Continued exposure to loud noise may cause hearing loss which can be of temporary or permanent nature. However, according to World Health Organisation guidelines<sup>1</sup> and the background research to these guidelines<sup>2</sup>, noise harms more than our ears. Some of the adverse effects of noise on humans and human life have been identified in these documents as interference with speech communication, sleep disturbance effects, psycho-physiological effects, mental health effects, performance effects, residential effects and annoyance as well as economic costs. These are briefly discussed below.

### **1.1.1 Interference with Speech Communication**

Interference of noise with speech communication can result in problems with concentration, fatigue, uncertainty and lack of self-confidence, irritation, misunderstandings, decreased working capacity, problems in human relations, and a number of reactions to stress.

### **1.1.2 Sleep Disturbance Effects**

Social survey data indicate that sleep disturbance is considered to be a major environmental noise effect. Exposure to noise can induce disturbances of sleep in terms of difficulty to fall asleep, alterations of sleep pattern or depth, and awakenings. These are known as primary effects. Other primary physiological effects that can be induced by noise during sleep are reactions such as increased blood pressure, increased heart rate, increased finger pulse amplitude, vasoconstriction, and change in respiration and cardiac arrhythmia. Exposure to night-time noise can also induce secondary effects or after-effects, that is, effects that can be measured in the morning or the day after the noise exposure. These secondary effects include reduced perceived sleep quality, increased fatigue, decreased mood or well-being and decreased performance.

### **1.1.3 Psycho-Physiological Effects**

A large body of research exists relating noise effects to stress response, cardiovascular effects, psycho-endocrine and immunological effects as well as physical health such as bodily fatigue. However most of these studies have not been able to provide information on the temporal relationship between noise exposure and start of a disease.

### **1.1.4 Mental Health Effects**

Exposure to high levels of occupational noise has been associated with development of neurosis and irritability and exposure to high levels of environmental noise with mental health.

Mental health in noise research covers a variety of symptoms, ranging from anxiety, emotional stress, nervous complaints, nausea, headaches, instability, argumentativeness, sexual impotency, changes in general mood and anxiety, and social conflicts, to more general psychiatric categories like neurosis, psychosis and hysteria.

Noise is not believed to be a direct cause of mental illness but might accelerate and intensify the development of latent mental disorders. The relationship among noise annoyance, noise sensitivity and mental morbidity is complex and not yet well understood. The consumption of tranquilizers and sleeping pills has been proposed as an indication of latent disease or mental disturbance in noise-exposed communities.

### **1.1.5 Performance Effects**

The effects of noise on human performance are very complex. Acute noise exposure appears to disrupt tasks that demand attention to multiple cues, tasks in which high levels of working memory capacity are required, and tasks where continuous and detailed attention to frequent signals is required. There are well documented aftereffects, particularly of uncontrollable noise, on human performance that demands sustained effort. Chronic noise exposure affects reading acquisition in children.

### **1.1.6 Residential Effects and Annoyance**

The annoyance-inducing capacity of a noise depends mainly upon its intensity and spectral characteristics, and variations of these with time. However, annoyance reactions are sensitive to many non-acoustic factors of a social, psychological, or



economic nature and there are considerable differences in individual reactions to the same noise. Furthermore, community annoyance varies with activity (speech communication, relaxation, listening to radio and TV, etc.). Annoyance is affected by the equivalent sound level, the highest sound level of a noise event, the number of such events, and the time of the day. It should be noted that a large proportion of low frequency components in the noise may increase annoyance considerably.

### **1.1.7 Economic Costs**

In order to fully assess the costs of noise in monetary terms, the following would all need to be considered: the societal costs for noise-induced illnesses, disabilities, loss of psychological well-being, healthcare costs, as well as the losses in productivity. In addition to these primary costs, secondary costs involved are related to a further deterioration of life quality, for instance in the form of discomfort and annoyance caused by noise exposure. In the short term, increased noise pollution would usually result in lowered market values of real estate, population segregation, and general deterioration of residential areas.

## **1.2 EUROPEAN NOISE POLICY**

It has been discussed above that, environmental noise, caused by traffic, industrial and recreational activities is one of the main local environmental problems and the source of an increasing number of complaints from the public. Generally however action to reduce environmental noise has had a lower priority than that taken to address other environmental problems such as air and water pollution.

Regarding research on environmental noise, Europe has been lagging behind North America and Japan. The European Commission Green Paper on "Future Noise Policy"<sup>3</sup>, published in 1996, stresses the fact that in Europe the data available on noise exposure is generally poor in comparison to that collected to measure other environmental problems and often difficult to compare due to the different measurement and assessment methods. According to the statistics in the Green Paper, it has been estimated that around 20 % of the European Union's population or close to 80 million people suffer from noise levels that scientists and health experts consider to be unacceptable which is a level more than 65 dB(A), where most people become annoyed, where sleep is disturbed and where adverse health effects are to be feared. An additional 170 million citizens are living in so-called 'grey areas', which are areas subject to levels between 55 and 65 dB(A), where the noise levels are such to cause serious annoyance during the daytime.

According to the statistics in the Green Paper the economical costs of noise to society especially transport noise is estimated in the range between 0.2 % and 2 % of GDP. Using the lower figure of 0.2% of GDP represents an annual cost to society of over 12 billion ECU.

With regard to nuisance due to excessive noise levels, road traffic noise is the main culprit as it accounts for the 90 % of the cases experienced by the 80 million people exposed to levels more than 65 dB(A). Thanks to the legislation and technological progress significant reductions of noise from individual sources have been achieved since 1970. However, data covering the past 15 years does not show significant improvements in exposure to environmental noise especially road traffic noise. The growth and spread of traffic in space and time and the development of leisure activities and tourism have partly offset the technological improvements. In the case of motor vehicles other factors such as the dominance of tyre noise above quite low speeds (50 km/h) and the absence of regular noise inspection and maintenance procedures are also important.

The measurements of noise exposure levels and the exposure of populations remain far from comprehensive and the data are infrequently updated often using simplistic models. The European Commission believes that improvements in noise data, harmonisation of methods of assessment of noise exposure to enable the comparability, monitoring and mutual exchange of information, and the provision of information to the public are the main priorities for short and medium term action. In order to establish a framework for the actions above the Commission recently passed a legislation in the form of a directive<sup>4</sup>. The new directive establishes the noise indicators to be used for the assessment of noise throughout the member countries. According to the directive, the local authorities in all major cities of Europe are responsible for producing strategic noise maps and preparing action plans based on these for tackling noise.

The Commission hopes, the results could help overcome the shortcomings mentioned above and can assist national and local authorities and the European Community to take more informed decisions about the noise measures for which they are responsible.

In order to achieve the objectives set out in the Green Paper, the Commission has formed various Working Groups to cover topics such as harmonisation of noise indices, calculation and assessment methods, noise maps, provision of information on the effects of noise and on the effectiveness of noise abatement measures, and emission control of railway vehicles. The working group 5 (WG 5) on abatement measures is set up to provide guidelines to be used by local authorities for designing noise abatement



plans and the execution of those plans. Among the objectives of the WG 5 is making an inventory of the various noise mitigation methods such as land use planning, speed limits, car free areas, noise barriers, building blocks used as noise barriers, porous road surfaces, tunnels, prohibition of certain activities during parts of the day, permits, noise monitoring and road pricing.

These guidelines, whenever made available, can only be implemented subject to the policies of local / national governments in a specific country. The following section discusses how legislation and government policy in the U.K. starting from 1970s to the present day affected practice of road traffic noise control.

### **1.3 ROAD TRAFFIC NOISE CONTROL IN THE U.K.**

There are several methods available worldwide for controlling road traffic noise in practice. These are environmental barriers, low noise road surfaces, alteration of horizontal or vertical alignment of the roads (realignment, natural screening by use of cuttings), noise insulation of properties, traffic management (traffic control devices, prohibition of certain vehicle types, modified speed limits, exclusive lane designations), and the acquisition of property to serve as a buffer zone to prevent future development. The relevant legislation currently in place and the policy of the national / local authorities will dictate which of these approaches will be implemented. The U.K. is no different and the road traffic noise control practice has been heavily and - up to recent times - adversely influenced by legislation and policies.

The Land Compensation Act 1973<sup>5</sup> is the earliest example of these. This legislation was introduced to provide compensation to owners whose property has been devalued as a result of public works including all road schemes. The Noise Insulation Regulations were introduced in 1975<sup>6</sup> enabling part of this compensation for house holders to be the provision of noise insulation where the exposure to noise would be increased to 68 dBA,  $L_{10,18hr}$  due to a new or altered road. In order to qualify for a grant the necessary calculations had to be carried out in accordance with the official road traffic noise prediction method, namely Calculation of Road Traffic Noise (CRTN) published in 1975<sup>7</sup>. The CRTN was revised in 1988<sup>8</sup>, following the amendment of The Noise Insulation Regulations<sup>9</sup>. This revision retained the basic approach provided 13 years earlier, only extending the method to cover a wider range of applications.

It has always been recognised that control of noise at source is more desirable than providing noise insulation at the affected properties. As traffic volumes and noise levels increase, the numbers of properties adversely affected grow and it becomes an increasingly viable option to provide screening for roads. The CRTN can also be used

for environmental appraisal of road schemes, highway design and land use planning and therefore includes guidance on purpose built noise barriers. CRTN was - and still is - far from meeting these demands, even in its revised form. The guidance it includes on prediction of barrier performance was very simplistic and did not make allowances for possible developments in barrier design.

In 1990 The Government summarised its policy on the environment in the White Paper "This Common Inheritance"<sup>10</sup>. The White Paper noted the significance of selection of lines and levels for roads in such a way to minimise noise and the role of noise barriers and earth mounds as a means of protecting people from noise. It also anticipated that quieter surfaces would be used to reduce noise at source.

Even though it was government's policy to provide screening rather than insulation, initial cost considerations seemed to take precedent over value. Overlooking the wider environmental issues meant the people continue to be exposed to traffic noise in their gardens, parks or even in their homes if they preferred to keep their double-glazed windows open. The CRTN, the Land Compensation Act 1973 and high permissible noise levels compared with other European countries are shown to be among the main reasons inhibiting the UK use of high performance barriers<sup>11</sup>.

The Department of Transport issued guidance on the use of barriers in the form of The Design Manual for Roads and Bridges (DMRB) Volume 10, Section 5<sup>12,13</sup>. These documents provided advice on how the impact of the barrier itself on its surroundings can be minimised by the appropriate choice of form and materials used, at the same time taking advantage of developments in the techniques of noise attenuation. It is recognised that a new road can have a profound effect on the quality of life for residents in the vicinity. This could be in the form of noise, dust, fumes caused by traffic, restriction of access to local facilities and the obstruction of the views of the surroundings. Barriers can therefore be incorporated into the overall scheme to mitigate the immediate effects of traffic, but they may create an oppressive sense of enclosure unless they are sensitively designed. The aim should be to make them as unobtrusive in the landscape as possible, or to provide visual quality whenever full integration is not feasible. Even though the overall design philosophy is presented in detail, information on the acoustic design of different barrier profiles is inadequate.

DMRB Volume 11, Section 2, Part 3 (1993)<sup>14</sup> recognises that some measures mitigate more than one effect. The bunds are given as an example for reducing visual intrusion and the noise levels, and planting is recognised to reduce the effects for people and also benefit wildlife. DMRB Volume 11, Section 3, Part 7 (1993)<sup>15</sup> lists possible mitigation measures generally applicable to noise and vibration. Provision of



environmental barriers both earth mounding and acoustic fencing is among the options provided.

The Planning Policy Guidance No. 24 on Planning and Noise<sup>16</sup> provided guidance to the local authorities on the use of their planning powers to minimise the adverse impacts of noise. Among the possible mitigation measures was the provision of purpose built barriers and sound insulation. It also states that special consideration should be given to designated areas and the countryside.

The Integrated Transport White Paper<sup>17</sup>, published in 2001, also stresses the sensitivity of transport noise issues and the environment. The transport plan is expected to cost £180 billion over the next 10 years. As far as the roads are concerned, the expenditure is proposed to result in 70 local bypasses, 50 of which are in rural areas, 130 other local road schemes, 567 km of trunk road and motorway widening and 30 strategic route bypasses.

As stated in the Integrated Transport White Paper, there will be a strong presumption against schemes that would significantly affect environmentally sensitive sites, or important species, habitats or landscapes. All road schemes will include high standards of environmental mitigation to ensure that, so far as reasonably possible, noise and the impact on biodiversity, the landscape and heritage are minimised. Among the outcomes expected to be achieved are reductions in traffic noise benefiting 3 million people within 600 m of trunk roads. This is to be achieved by the application of lower noise surfaces on 60% of the trunk road network, the construction of new bypasses, better public transport, reduced congestion and improved traffic management in towns and cities.

Contrary to the ideas put forward in the Integrated Transport White Paper the bypasses running through the rural areas, rather than helping with the noise problem, are going to be critical since they will introduce noise levels previously non - existent in these sensitive environments. The improvement in the road network is naturally expected to help the growth and spread of traffic in space and time. This is the very reason, according to the findings of the European Commission's Green Paper, which rendered improvements in noise levels useless. The recommended use of low noise surfaces is encouraging, even though it is not made clear what the expected overall effect will be both in the short term, and in the longer term as such surfaces are worn away in time.

Following the Integrated Transport White Paper the news that The Highway Agency abandoned whisper concrete and porous asphalt in favour of the thin asphalt surfacings came as a shock to the industry. Both of these surfaces were developed a decade earlier and were thought to be unrivalled in the industry. These surfaces are going through a dynamic research and development phase and there are still questions

surrounding their short and long term acoustic performance and non - acoustic characteristics.

The above summary indicates the transformation in the U.K. traffic noise control policy and practice. Over the years the preference shifted from noise insulation of properties in 1970s towards the use of environmental barriers in 1990s and finally to the application of low noise surfaces in 2000s.

## **1.4 CONCLUDING REMARKS**

The European Commission recognised environmental noise as a major problem only as recent as five years ago. Accordingly road transport noise is the dominant source. However action to reduce these have not been given priority.

The U.K. has not been any less indifferent to the environmental noise problem. The shift in policy and practice over the years is a positive sign of the recognition of the reality of noise. It is good common sense and environmentally more acceptable to address the problem at the source rather than at the receiver. The sound insulation of the properties is simply to avoid the problem. Low noise surfaces, if they could be effective on their own, would be the best way to control noise at source. However, low noise surfaces are unable to offer a full solution to the problem presently and are likely to be used in conjunction with environmental noise barriers. When built as close to the traffic source as possible, the screening becomes a method of control at the source containing the noise within the corridor around the road. In addition, there are continuing reservations about the cost, durability, maintenance requirements and the long-term acoustic performance of alternative road surfaces. The indecisiveness of the Highway Agency as to which surface to adopt indicates these surfaces are passing through a dynamic research and development stage. The maximum allowable noise levels in the U.K., highest of all European countries, is also making the noise problem appear smaller than it actually is. Possible lowering of these levels is bound to demand more effective solutions possibly incorporating barriers and low noise surfaces. The growth and spread of traffic in space and time, when added on top of all these, is expected to make the semi-urban and rural areas more susceptible to noise impacts.

Currently screening provides the well-proven, widely used option for securing considerable reductions in roadside noise levels with no long-term decrease in performance. Barriers also have the added advantage over alternative road surfaces of reducing dust, dirt, litter, fumes and headlight glare from the highways and improving the visual quality of the surroundings if well conceived. The expertise needed in the design, construction and maintenance of special road surfaces is not essential in the

case of noise barriers, provided basic guidelines are provided for the designers by experts. When the developing countries reach the awareness of the developed nations in accepting the adverse impacts of noise on the built environment, barriers are the likely candidates to offer off-the-shelf solutions for their needs which will also be economically, aesthetically, acoustically and environmentally effective.

The role of environmental noise barriers in road traffic noise control is not thought to diminish in any case in the foreseeable future. At present there is a need for research into their acoustic performance. The real concern however is how to provide environmentally sensitive noise reducing systems with even better acoustical performance than ever.

## **1.5 THE WAY FORWARD**

One of the objectives of this research project is to devise environmentally sensitive noise reducing systems to counter the noise impacts due to the growth and spread of traffic in space and time.

The general structure of this thesis comprises three main parts. Part I is where general topic of research is identified. This includes Chapters 2, 3 and 4. Part II is on the specific research area and the methodology. This part consists of Chapters 5 and 6. The findings of the main investigation are discussed in Part III. This part consists of Chapters 7 to 11, inclusive. The following is a description of the work undertaken in various chapters.

Chapter 2 provides background information on the issues related to propagation of sound in outdoor environments. The likely influence of atmospheric and ground effects on the performance of a noise barrier is highlighted. The main theoretical approaches for the investigation of noise barriers in homogeneous atmospheric conditions are presented. The discussions of these issues help define the scope and limitations of the current work.

Chapter 3 reviews the theoretical and practical work done in the field of environmental noise barriers. Different barrier profiles available and their acoustic design parameters are discussed in detail. This review results in recommendations for further research in the field. It is shown that there is a lack of simple but substantial guidance on environmental barrier design as well as environmentally sensitive noise reducing systems.

In Chapter 4, a simplified method for the design of environmental barriers is proposed based on the findings and recommendations of the previous chapter. The wall type



barriers and earth mounds are given equal emphasis as part of this method provided certain practical limitations permit their applications. However the limited available information on the acoustical characteristics of earth mounds indicated the need for further research into these.

It would be essential to explain why a specific barrier type, mainly ignored by the scientific community, should deserve more attention. Chapter 5 undertakes a detailed study of the benefits of earth mounds in addition to the acoustic ones. Some real life applications are presented as examples of earth mounds being the clear favourites in certain sensitive surroundings. This is supported by on-site investigations of the performance of an earth mound. The theoretical and practical work done on earth mounds or similar shapes is reviewed, which also serves as a basis for ideas for developing an alternative barrier shape. The likely improvements and their possible benefits are discussed as part of these ideas. Physical scale modelling under uniform field conditions identified single and multiple small height barriers on top of earth mounds as the likely candidates which could improve the performance. This chapter describes the research methodology to be used in the forthcoming chapters for carrying out the main experimental investigation into alternative earth mound profiles.

The multiple edges or rib structures identified in the previous chapter are investigated in greater detail in Chapter 6. This chapter is a theoretical appraisal into their acoustic performance. The aim of the chapter is to identify some of the mechanisms and physical parameters involved in the attenuation of noise. These are explained by the approaches used in the study of resonators and gratings. This chapter is central to shaping the main experimental work, in terms of both the edge configurations investigated and the discussion of the findings of the modelling work.

Chapter 7 details the findings of the investigation into the experimental set-up which is directed towards assessing the suitability of the physical scale modelling technique to be applied in forthcoming chapters. Reverberation time measurements are undertaken to find out the suitability of the test room for uniform field modelling work and to quantify the effects of the reverberant field. Directivity tests are carried out to help determine the source characteristics. The findings of these tests are used to draw conclusions on the likely effects of the reflections from the room boundaries. Two geometries are selected from the literature as test cases to quantify the likely effects of the reverberant field. Impedance tube measurements are performed to establish the properties of the model materials to be used as part of this work. The findings of previous research using airflow resistivity are provided in support of some of the absorption characteristics identified by impedance tube experiments.

**Chapter 8 investigates a number of models consisting of rib structures both on the ground and on other earth mound type barriers under uniform field conditions.**

**Chapter 9 provides discussions of the results of experiments repeated in semi-anechoic chambers. This chapter undertakes additional experiments to explain some of the noise attenuation mechanisms and the parameters involved better.**

**Chapter 10 provides the details of the numerical model to be used in the next chapter for validating experimental work. The numerical modelling using boundary element methods is used to model a number of models investigated by physical modelling. These are extended to investigation of alternative earth mound profiles consisting of various edge conditions using more realistic receiver positions.**

**Chapter 11 undertakes a comparative discussion of experimental findings from uniform field experiments and semi-anechoic chambers. The findings of the numerical modelling using boundary element methods are used to validate results.**

**In Chapter 12, a general discussion of the main findings of this work is presented. The advice provided in Chapter 4 on the selection of noise barriers is extended further to include earth mounds. This advice incorporates some of the findings resulting from this research programme.**

**Concluding statements arising from this research programme and the future work required to further develop some of its findings are given in Chapter 13.**

## **1.6 REFERENCES**

- 
- <sup>1</sup> Guidelines for Community Noise, edited by Brigitta Berglund, Thomas Lindvall  
Dietrich Schwela, Kee-Tai Goh, on behalf of World Health Organisation, ISBN: 9971-  
88-770-3, 2000
- <sup>2</sup> Community Noise, Birgitta Berglund and Thomas Lindvall, Centre for Sensory  
Research, Stockholm, ISSN 1400-2817, ISBN 91-887-8402-9, 1995
- <sup>3</sup> Commission of the European Communities, Green Paper on "Future Noise Policy",  
COM(96) 540, Brussels, November 1996
- <sup>4</sup> Commission of the European Communities, Directive 2002/49/EC of The European  
Parliament and of The Council relating to the "Assessment and Management of  
Environmental Noise", Brussels, 25 June 2002
- <sup>5</sup> Land Compensation Act, 1973, HMSO, London
- <sup>6</sup> Department of the Environment, 1975, Statutory Instruments, 1975 No 1763, Building  
and Buildings, The Noise Insulation Regulations, HMSO, London
- <sup>7</sup> Department of Transport, Welsh Office, 1975, HMSO, London
- <sup>8</sup> Department of Transport, Welsh Office, 1988, HMSO, London
- <sup>9</sup> Department of the Environment, 1988, Statutory Instruments, 1988 No 2000, Building  
and Buildings, The Noise Insulation (Amendment) Regulations, HMSO, London
- <sup>10</sup> This Common Inheritance : Britain's Environmental Strategy, Cm 1200, 1990,  
HMSO, London
- <sup>11</sup> High Performance Acoustic Barriers In The U.K., Highways and Transportation,  
43(05), May 1996, 7-12
- <sup>12</sup> Highways Agency, Design Manual for Roads and Bridges, Volume 10 :  
Environmental Design and Management, Section 5 : Environmental Barriers, Part 1 :  
HA 65/94 Design Guide For Environmental Barriers, 1994
- <sup>13</sup> Highways Agency, Design Manual for Roads and Bridges, Volume 10 :  
Environmental Design and Management, Section 5 : Environmental Barriers, Part 2 :  
HA 66/95 Environmental Barriers : Technical Requirements, 1995

---

<sup>14</sup> Highways Agency, Design Manual for Roads and Bridges, Volume 11 :  
Environmental Assessment, Section 2 : General Principles of Environmental  
Assessment, Part 3 : Mitigation, June 1993

<sup>15</sup> Highways Agency, Design Manual for Roads and Bridges, Volume 11 :  
Environmental Assessment, Section 3 : Environmental Assessment Techniques, Part 7  
: Traffic Noise and Vibration, (Amended) August 1994

<sup>16</sup> Department of The Environment, Welsh Office, Planning Policy Guidance 24,  
Planning and Noise, July 1994

<sup>17</sup> Department of the Environment, Transport and the Regions, Integrated Transport  
White Paper "Transport 2010 : The 10 Year Plan", London, July 2000



## 2 SOUND PROPAGATION IN OUTDOOR ENVIRONMENTS

In the previous chapter environmental noise barriers have been identified as the focus of this research project. This chapter provides background information on the issues related to propagation of sound in outdoor environments. The likely influence of atmospheric and ground effects on the performance of a noise barrier is highlighted. The main theoretical approaches used in the investigation of noise barriers in homogeneous atmospheric conditions are presented.

### 2.1 BACKGROUND

The total noise attenuation in an outdoor environment,  $A_T$ , could be defined as the sound pressure level difference between a source and a receiver. This attenuation is affected by a number of factors. This section provides a review of the research which has been carried out by others to investigate these factors <sup>1, 2, 3, 4, 5</sup>. The total attenuation can be expressed as follows.

$$A_T = A_s + A_a + A_g + A_{atm} + A_b$$

where;

$A_s$  is the attenuation due to geometric spreading

$A_a$  is the attenuation due to atmospheric absorption

$A_g$  is the attenuation due to presence of ground in homogeneous atmosphere

$A_{atm}$  is the attenuation due to atmospheric effects (refraction and turbulence)

$A_b$  is attenuation due to presence of barrier

These factors are briefly investigated below.

#### 2.1.1 Geometric Spreading, $A_s$

A general expression for the spreading loss  $A_s$ , in decibels, between any two positions at distances  $r_1$ ,  $r_2$  from an acoustic source can be given in the form<sup>5</sup>.



$$A_s = 20g \log \left( \frac{r_2}{r_1} \right)$$

where  $r_2$ ,  $r_1$  are the distances between the acoustic centre of the source and the farthest (i.e. receiver) and closest (i.e. source) positions respectively.

$g = 0$  for **plane** wave propagation such as within a uniform pipe (i.e. no spreading loss)

$g = \frac{1}{2}$  for **cylindrical** propagation from a line source (3 dB per doubling of distance)

$g = 1$  for **spherical** wave propagation from a point source (6 dB per doubling of distance)

### 2.1.2 Atmospheric Absorption, $A_a$

A sound wave travelling through air free of any particles is attenuated due to atmospheric absorption caused by<sup>5</sup>.

- (1) classical (heat conduction and shear viscosity) losses
- (2) molecular relaxation losses associated with an exchange between molecular translational and molecular rotational or vibration energy

These loss components vary with **temperature** and **atmospheric pressure** and for molecular vibrational relaxation, with **humidity** content.

$$A_a = ar$$

where  $a$  is the attenuation coefficient in decibels per meter and  $r$  is the distance travelled in meters

Some atmospheric attenuation also occurs in fog, in dust in the air, and from absorption due to electromagnetic radiation of moist air molecules at frequencies less than 10 Hz.

### 2.1.3 Ground Effect, $A_g$

The sound pressure  $p$ , due to propagation between a source  $S$  and a receiver  $R$  in a still, uniform atmosphere over a path near the ground surface can be described as shown in the equation below<sup>1, 6</sup>.

$$p(S,R) = \left( \frac{e^{-ikr_1}}{r_1} \right) + R_p \left( \frac{e^{-ikr_2}}{r_2} \right) + (1 - R_p) \cdot F(w) \left( \frac{e^{-ikr_1}}{r_2} \right)$$

In order to describe the physical meaning of various terms in this equation, the following basic geometry can be considered.

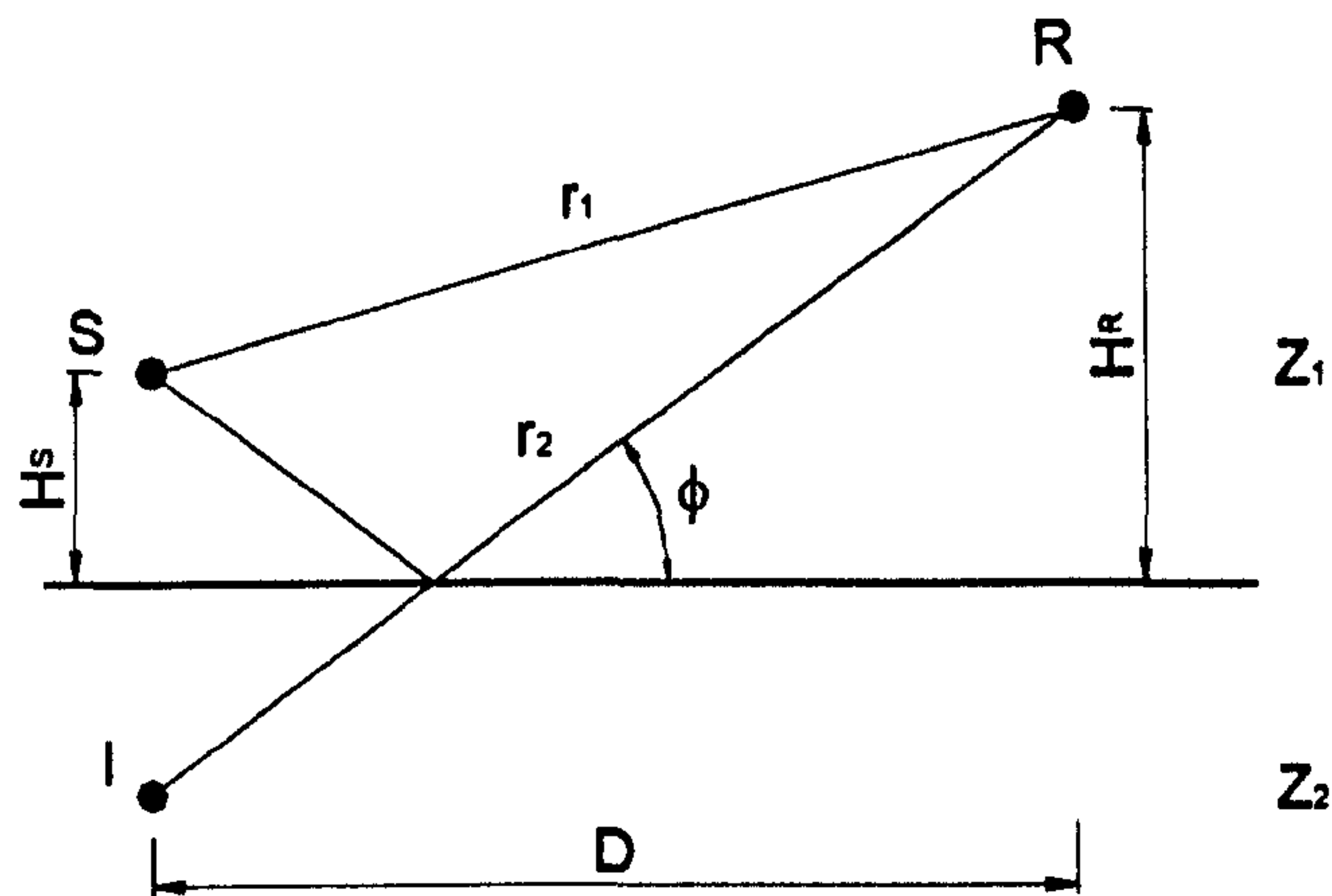


Figure 2.1 : Sound propagation over a flat boundary

The first term on the right hand side of the equation is the contribution from **direct wave**, represented by path  $r_1$ . The second term is the contribution from the **ground reflected wave**, represented by path  $r_2$ . The third term defines the behaviour of **ground and surface waves**. It arises mathematically from the need to match the boundary conditions of a spherical wave front, which due to its curvature, meets a plane boundary at different points and has varying incidence angles along the surface.

The term  $R_p$  is the **plane-wave reflection coefficient** for a plane sound wave incident obliquely on a plane **locally reacting surface** and is given by

$$R_p = \frac{\sin \phi - Z_1 / Z_2}{\sin \phi + Z_1 / Z_2}$$

where,

$\phi$  is the incidence angle

$Z_1 = \rho c$  is the characteristic impedance of air (where  $\rho$  is the air density and  $c$  is the velocity of sound in air)

$Z_2$  is the acoustic impedance of the surface

and

$F(w)$  is the **boundary loss factor** expressed as a function of  $w$ , which is a numerical distance.

The ground wave embodied in the boundary loss factor  $F(w)$  is augmented by a surface wave which can exist provided certain conditions are met.

In order to include the change of phase as well as amplitude on reflection, complex notation is used for both  $R_p$  and  $Z_2$ .

The characteristics of a particular locally reacting surface may be represented by complex impedance,

$$Z_2 = r + jx$$

where  $r$  is called the specific acoustic resistance and  $x$  the specific acoustic reactance of the medium for the particular wave being considered.

Phase angle  $\psi = \tan^{-1}(x/r)$

The hypothetical cases considered below are aimed at explaining the physical meaning of various terms involved<sup>4</sup>.

#### **1) PLANE - WAVE PROPAGATION – SOURCE AND RECEIVER BOTH ON A HARD GROUND.**

Assume a plane wave propagation for source and receiver both situated on a perfectly hard surface, where the phase change on reflection would be zero. This signifies that  $R_p = 1$ . The implication is that  $Z_2$  would have to be infinite, which in practice is impossible. Since  $Z_2$  is very large but finite, the ratio of  $Z_1/Z_2$  cannot be zero. Under these circumstances and at a grazing angle of  $\phi = 0$ ,  $R_p = -1$ , which represents a phase change of 180° on reflection. This implies a cancellation of direct and ground reflected rays even though the path length difference between these are the same. Therefore plane waves propagating at grazing incidence over a plane surface with finite acoustic impedance signifies a shadow zone. The depth of this shadow depends on the value of the ground impedance  $Z_2$ .

#### **2) EFFECT OF PATH LENGTH DIFFERENCES – SOURCE AND RECEIVER BOTH ABOVE A HARD GROUND.**

When both source and receiver are above the ground the total phase change is a function of phase change due to path length difference between direct and ground reflected propagation paths and phase change on reflection.

If we consider propagation above a hard, smooth surface (reflection coefficient,  $R_p = 1$  and hence no phase change on reflection), the effect of the path length difference alone can be

investigated. Dips in excess attenuation spectra are the result of cancellation between direct and reflected rays for path-length differences of an *odd number of half-wavelengths*.

### 3) **GROUND WAVES – SOURCE AND RECEIVER BOTH ON A HARD GROUND.**

When both source and receiver are on the ground ( $h_s = h_r = 0$  and  $\phi = 0$ ) and the boundary is resistive (phase angle  $\chi = 0$ ), the direct and reflected waves cancel completely to form a shadow zone as described above. This shadow zone is penetrated by the ground wave which is represented by the third term.

### 4) **SURFACE WAVES – SOURCE AND RECEIVER BOTH ON A GRASS COVERED GROUND.**

This could be explained by comparing propagation over hard and soft surfaces. The phase angle  $\chi$  for grassy surface is known to vary between approximately  $45^\circ$  and  $60^\circ$  over the audible range of frequencies. The amplitude of the function  $F(w)$  for this range of  $\chi$  differs from that for  $\chi = 0$  (i.e. for a hard ground) by the presence of a substantial increase in the vicinity of  $\omega = 1$ . This increase in the function  $F(w)$  is attributed to mainly the contribution of a *surface wave* in the air.

This wave is coupled to the ground surface owing to the latter's stiffness reactance but propagates in the air, with an amplitude that decreases exponentially with height above the boundary. Therefore, propagation of sound energy between a point source and receiver which are both placed on a grassy surface ( $h_s = h_r = 0$  and  $\phi = 0$ ) is by a *ground wave* augmented by a *surface wave*.

## 2.1.4 Atmospheric Effects, $A_{atm}$

The atmospheric effects considered in this section are refraction by non-homogeneous atmosphere and scattering or diffraction effects due to turbulence<sup>5</sup>.

### 2.1.4.1 Refraction

The speed of sound relative to the ground is a function of temperature and wind velocity. Under most weather conditions temperature and the wind velocity vary with height above the ground. These cause the sound waves to propagate along curved paths.

A temperature lapse is a common daytime condition during most of the year and causes ray paths to curve upward. This occurs during the day when solar radiation heats the



earth's surface, resulting in warmer air near the ground. It is most noticeable on sunny days but can also exist under overcast skies. After sunset, there is often radiation cooling of the ground. This produces cooler air near the surface and forms a temperature inversion. Under conditions of a **temperature inversion**, the temperature increases with increasing height and ray paths curve downward.

When there is wind, its speed decreases with decreasing height. Because of drag on the moving air at the ground the layer of air next to ground tends to be stationary. Therefore, the speed of sound relative to the ground increases with height during **downwind** propagation, and ray paths curve downward. For propagation **upwind** the sound speed decreases with height, and ray paths curve upward. There is no refraction in the vertical direction produced by wind when the sound propagates directly crosswind.

The temperature and wind gradients can result in measured noise levels being very different from those obtained by predictions using conventional methods. These effects are particularly important beyond propagation distances greater than few hundred meters. The effect of the downward refracting rays is to modify ground attenuation by increasing the grazing angle. These also tend to reduce the shadow zone behind a barrier.

#### **2.1.4.2 Turbulence**

The atmosphere is an unsteady medium with random variations in temperature, wind velocity, pressure, and density. The most influential of these are the **temperature** and **wind velocity** variations. During the daytime fluctuations in temperature of 5°C that last several seconds are common and 10°C fluctuations not uncommon. The wind velocity fluctuates in a similar manner and has a standard deviation about its mean value that is commonly one-third of the average value. When sound waves propagate through the atmosphere, these random fluctuations over a short time period scatter the sound energy resulting in random fluctuations in amplitude and phase.

An important effect of atmospheric turbulence is the degradation of the ground attenuation and the reduction of the deep shadows produced behind barriers or during propagation in upward refraction conditions.

#### **2.1.5 Barrier Attenuation, $A_b$**

The attenuation due to the presence of a solid barrier can occur due to diffraction, reflection or scattering effects. These can be in the form of purpose built environmental

noise barriers, buildings, naturally occurring hills, cuttings, embankments or small and large undulations in ground levels.

Under homogeneous atmospheric conditions, when a large solid body intercepts the sound field, the ray theory of sound predicts a shadow region behind the body with sharply defined boundaries. In practice this shadow zone is penetrated by diffraction and scattering due to the presence of the obstacle<sup>2</sup>.

The insertion loss of barriers is generally observed to be higher when the intervening ground is hard rather than soft. The reason may be related to the presence of ground and surface waves. As recalled from earlier,

$$R_p = \frac{\sin \phi - Z_1 / Z_2}{\sin \phi + Z_1 / Z_2}$$

When a barrier intercepts the line-of-sight between a source and a receiver, it has an effect of raising the propagation height and increasing the grazing angle. As the height of the barrier increases, the incidence angle  $\phi$  tends to 90 degrees and the term  $\sin \phi$  approaches 1.

In the cases where the ratio  $Z_1/Z_2 \ll \sin \phi$ , then  $R_p \approx 1$ . This could occur when  $Z_2$  approaches to infinity. (i.e. perfectly hard ground). From the equation describing the general propagation over a ground surface, it can be seen that the third term becomes zero, i.e. no ground or surface waves.

Conversely, if  $Z_1/Z_2 \gg \sin \phi$ , then  $R_p \approx -1$ . This is expected to occur when  $Z_2$  is zero (i.e. perfectly soft ground). Under these circumstances, if the direct and ground reflected paths are equal in length ( $r_1 = r_2$ ), the first two terms would cancel each other and the sound field would be dominated by the third term i.e. by ground and surface waves. The direct and ground reflected paths would practically be equal on both sides of the barrier if the source and receiver heights are small.

The cases in presence of a barrier can be combined as follows with the findings of previously identified cases in presence of ground only.

Ground type	Without barrier	With barrier	Insertion Loss Performance
Perfectly hard ground	Direct and ground reflected waves	Direct and ground reflected waves	Substantial up to 100m Effective up to 300m
Perfectly soft ground	Ground and surface wave	Ground and surface waves	Considerable up to 100m Negligible at 300m

**Table 2-1 : Hypothetical cases showing the dominant components of sound propagation**

Over soft ground, the dominance of ground and surface waves both with and without a barrier appears to limit the potential reductions by a barrier. Over hard ground, barrier diffraction losses are able to provide attenuation of direct and ground reflected paths which pass over the top edge of the barrier. This makes barriers more effective over greater distances. Over several hundred metres, irrespective of the ground type, the performance of any barrier type is negligible due to atmospheric effects discussed earlier. The effects of ground and atmosphere on the performance of a barrier are discussed below.

## **2.2 INFLUENCE OF ATMOSPHERIC AND GROUND EFFECTS ON BARRIER PERFORMANCE**

The acoustic performance of noise barriers can be determined, to some extent, by geometrical considerations and noise barrier properties<sup>7, 8</sup>. These parameters also form a significant part of the design guidance provided by official documents<sup>9, 10</sup>. However atmospheric and ground effects heavily influence on-site performance of noise barriers.

### **2.2.1 Ground Conditions**

The ground surface plays an important role in determining the performance of a barrier. Its type decides the absorption characteristics and its shape governs whether sound will propagate coherently or if it will be scattered.

Comparing the effect of a depressed road with a certain depth and that of a barrier with the same height, Jonasson<sup>11</sup> showed that the road in a cutting is likely to be most efficient at large distances while the opposite should be the case at short distances. Further work by Jonasson<sup>12</sup> indicated that an acoustic barrier is most effective at places where the ground attenuation is low before the insertion of a barrier, for example in the cases where the receiver is situated well above the ground or where the ground is acoustically hard.



The performance of barriers in the presence of various ground surfaces has been studied by scale modelling<sup>13</sup>. In the presence of hard ground (asphalt), the insertion loss maxima corresponded to frequencies which are odd multiples of one-half wavelength of the path length differences between the direct and the ground reflected waves. The attenuation due to the ground surface alone was small and therefore the increase in insertion loss around a particular frequency could be attributed to destructive interference and hence to the geometry of the source-receiver-barrier configuration. In the presence of a soft ground (grass surface), attenuation due to the ground surface alone existed which, in this particular case, was centred around 500 Hz. This was the result of cancellation between direct and reflected waves caused primarily by phase changes on reflection. Following the insertion of a barrier, this beneficial ground effect disappeared. At higher frequencies, destructive interference still existed, this time, corresponding to even multiples of one-half wavelength of the path length differences between the direct and the ground reflected waves. However at lower frequencies, the ground effect was shifted due to the presence of the barrier.

In addition to complex impedance value of the ground surface and interference effects due to path length differences, rough boundaries also contribute to the ground effect. Surface roughness of small dimensions was shown to have significant influence on near-grazing sound propagation at low frequencies, especially for acoustically hard surface materials<sup>14</sup>.<sup>15</sup>. The presence of a noise barrier may interfere with the ground effect by shifting the frequency at which the maximum ground effect takes place or by raising the effective propagation height. The frequency at which these changes take place should be carefully considered.

### **2.2.2 Atmospheric Conditions**

The propagation of sound is influenced by sound velocity gradients which may be caused by a temperature gradient or a wind speed gradient<sup>16</sup>. The main atmospheric effects which influence the performance of a noise barrier are refraction and scattering due to atmospheric turbulence<sup>17</sup>.

Atmospheric turbulence was shown to be the main reason why the sound pressure levels measured behind barriers are higher than those predicted by theory, causing the noise barriers to be less effective than expected<sup>18</sup>. Atmospheric turbulence acts in a way to scatter the sound energy from its original path, degrading the coherence of the sound field. This tends to limit reduction in sound levels, typically to a maximum of 25-30 dB(A), depending on frequency<sup>19</sup>. Insertion loss is similarly limited to about 15-25 dB<sup>5</sup>.



Refraction occurs due to variations in temperature and wind velocity with height above the ground. This causes the sound rays to travel in curved paths either upwards or downwards. The assumption that sound travels in straight paths as in still uniform atmosphere is invalid, especially at propagation distances greater than a few hundred metres. In the cases where propagation causes the rays to bend downwards, the effectiveness of a noise barrier would be reduced since the rays from the source could reach the receiver by curving over the barrier top<sup>5</sup>. This occurs under temperature inversions and downwind propagation conditions.

## 2.3 NUMERICAL METHODS

This section reviews some of the main numerical techniques applicable to sound propagation in non-homogeneous conditions. These are the fast-field programs (FFP), parabolic equation (PE) method, substitute - sources method (SSM) and scattering cross-section method.

**Fast-field programs (FFP)** permit the prediction of sound pressure in a refracting atmosphere at an arbitrary receiver on or above a flat continuous ground from a point source somewhere above the ground. The basis of the FFP method is to work numerically from exact integral representations of the sound field within the layered atmosphere in terms of coefficients that may be determined from the ground impedance<sup>5</sup>. The method gets its name from the discrete Fourier transform used to evaluate these integrals.<sup>20</sup>

**Parabolic equation (PE)** model assumes that wave motion for a particular problem is always directed away from the source or that there is very little backscattering. This assumption reduces the boundary value problem to an initial boundary value problem that results in differential equation which is easier to compute.<sup>20</sup>

One limitation of PE method is that its accuracy is limited to low angles from the horizontal. Therefore the applications are restricted to cases where all parts of the medium, ground or barrier which may influence the sound field have to be situated at low angles compared with the source-to-receiver distance<sup>26</sup>. The main advantage of the PE over most methods is that it is able to take into account the variations in the ground and atmosphere along the propagation direction<sup>21</sup>.

In the **substitute - sources method (SSM)**, the sound field due to an original source is represented by a distribution of sources on a plane surface. The surface is called a substitute surface and the sources are called substitute sources. The propagation is

calculated in steps from one surface to the next. In the case of turbulent atmosphere each step takes into account the energy losses of the coherent field into a residual, random field<sup>22</sup>. Turbulence can also be included in the PE and FFP methods discussed above<sup>23,24</sup>.

Another method of predicting the influence of turbulence is the **scattering cross-section method**. This uses a single-scattering approximation and predicts a much weaker influence of turbulence than the SSM<sup>25</sup>. This enables the wave incident on an inhomogeneity to be approximated by the wave calculated for a non-turbulent atmosphere<sup>26</sup>.

Recent developments include hybrid models which can account for the barrier and ground interaction as well as the meteorological effects<sup>27,28,29</sup>.

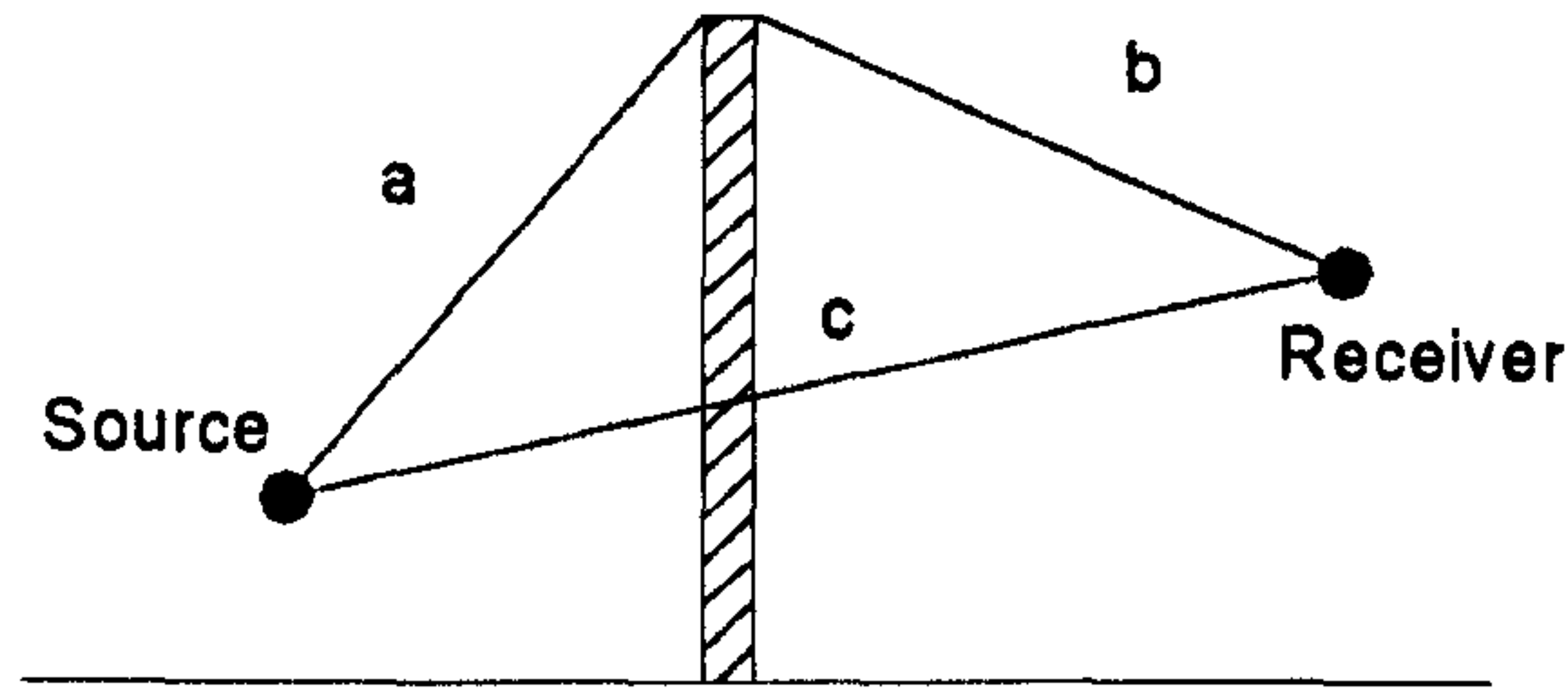
The following section is an account of the two of the main models used in the modelling of noise barriers under homogeneous atmospheric conditions and in the presence of a ground surface.

## **2.4 THEORETICAL CONCEPTS OF BARRIER ATTENUATION IN HOMOGENOUS ATMOSPHERE**

In order to identify the benefits or the shortfalls in relative performance of different noise barrier profiles, comparisons are generally made in isolation from the effects of atmospheric phenomena. This section presents theoretical approaches which can be used to determine the performance of a noise barrier in homogeneous atmospheric conditions but in presence of a ground surface.

The acoustical performance of a vertical thin barrier is generally determined by the ratio of path length difference,  $\delta$ , to the acoustic wavelength,  $\lambda$ . The path difference  $\delta$  can be defined as the difference between the direct sound path from source to receiver when there is no barrier (path c) and the top diffracted path when a barrier is installed in between (path a & b). Figure 2.2 shows the path length difference schematically.

$$\delta = a + b - c \quad (1)$$



**Figure 2.2 : Path length difference  $\delta$**

The path length difference,  $\delta$ , and wavelength of sound in air,  $\lambda$ , are combined as follows to give the Fresnel number,  $N$ .

$$N = \frac{2\delta}{\lambda} \quad (2)$$

This is a non-dimensional variable which has commonly been used in simple models to express the performance of a barrier. The two important descriptors of barrier performance are attenuation and insertion loss. Attenuation is the sound level difference at the receiver position, when both the barrier and the ground are present, relative to propagation in free space.

$$\text{Attenuation} = -20 \log \left| \frac{\Phi_{\text{Total}}}{\Phi_{\text{Free-field}}} \right| \quad (3)$$

where  $\Phi_{\text{Total}}$  is the sound pressure due to geometrical spreading in the presence of ground and barrier and  $\Phi_{\text{Free-field}}$  is the sound pressure at the same receiver due to the same source in free - field. Insertion loss is the change in sound level with and without the barrier but with the ground present in both cases.

$$\text{Insertion Loss} = -20 \log \left| \frac{\Phi_{\text{Total}}}{\Phi_{\text{Ground}}} \right| \quad (4)$$

where  $\Phi_{\text{Total}}$  is the total sound pressure due to geometrical spreading in the presence of ground and barrier and  $\Phi_{\text{Ground}}$  is the sound pressure at the same receiver due to the same source in the presence of ground. Previous work has shown that the Attenuation and Insertion Loss calculated by 2D models are applicable to equivalent 3D cases.

The following is an account of two of the main theoretical approaches employed in determining the insertion loss of a barrier in homogeneous atmosphere. These are the geometrical diffraction methods and the numerical wave based methods.

### 2.4.1 Geometrical Diffraction Methods

In order to determine insertion loss of a barrier due to a source, S, the sound field at a receiver, R, has to be determined both without and with the barrier, in the presence of ground in both cases. The possible sound paths are as shown in Figure 2.3.

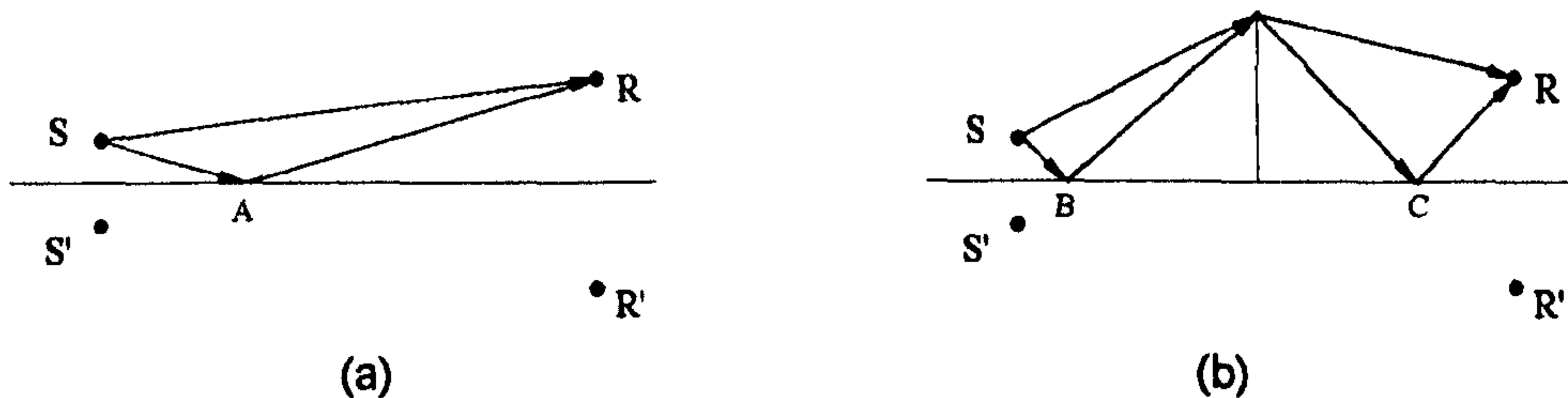


Figure 2.3 : Sound path diagrams without and with a barrier

Insertion loss can be calculated as shown in equation (4). The sound pressure at a receiver R, in the presence of ground surface alone,  $\Phi_{Ground}$ , can be calculated as follows.

$$\Phi_{Ground} = \frac{e^{ikd_{SR}}}{d_{SR}} + \frac{e^{ikd_{S'R}}}{d_{S'R}} \{R_A + (1 - R_A)F(w_A)\} \quad (5)$$

Where

$R_A$  is the pressure reflection coefficient about the point of specular reflection A

$F(w_A)$  is the boundary loss factor

$k$  is the wave number ( $= 2\pi / \lambda$ )

$d_{SR}$  and  $d_{S'R}$  correspond to the length of relevant sound paths as shown in Figure 2.3 (a).

Plane-wave pressure reflection coefficient about the reflection point A, can be defined as follows.

$$R_A = \frac{Z_s \sin \phi - 1}{Z_s \sin \phi + 1} \quad (6)$$

Where;

$\phi$  is the grazing angle

$Z_s$  is the surface impedance



The two of the more commonly known models for determining ground impedance are those of Delany & Bazley<sup>30</sup> and Attenborough<sup>31</sup>. The use of complex notation for both  $Z$ , and  $R_A$  enables the inclusion of the changes of phase as well as amplitude on reflection.

The boundary loss factor  $F(w)$  defines the ground waves, and surface waves if present, as a function of the numerical distance,  $w$ . Numerical expressions for these terms can be found in most studies concerned with ground effects<sup>1, 2, 3</sup>. The numerical distance,  $w$ , is a function of propagation distance, frequency, grazing angle and surface impedance.

The importance of the term  $F(w)$  can be explained by considering a configuration where both the source and the receiver are resting on a hard surface. This condition implies the direct and ground reflected waves would cancel each other forming a shadow zone. However the presence of the ground waves, signified by the boundary loss factor, ensures this is not the case. The differences in the magnitude of this term, observed around  $w=1$ , for different phase angles, are attributed to the presence of surface waves. The influence of ground and surface waves become more prominent at longer propagation distances and at low frequencies<sup>4</sup>.

In the presence of a barrier, the total sound pressure  $\Phi_{Total}$  at a receiver R behind a barrier, could be expressed as the sum of pressures from the real source S, Image source in the ground S', and the contributions of these pressures at the image of the receiver R'<sup>32</sup>. Possible sound paths are shown in Figure 2.3 (b).

$$\Phi_{Total} = \Phi_{SR} + \Phi_{S'R} + \Phi_{SR'} + \Phi_{S'R'} \quad (7)$$

The above calculation is applicable to problems where the diffracted paths round the ends of a barrier do not contribute to the total. In finite length barrier problems additional end diffracted ray paths similarly need to be accounted for. It has been noted that there are ten possible paths for the 3D geometry, however only eight of these are applicable for any source-receiver configuration<sup>33</sup>.

The first component of the field above,  $\Phi_{SR}$ , consists of the top diffracted field,  $\Psi_{SR}$ . The remaining three components of the total field,  $\Phi_{S'R}$ ,  $\Phi_{SR'}$ , and  $\Phi_{S'R'}$ , are modified by the presence of ground surfaces. These can be expressed in Equation 8, 9, 10 and 11 as follows<sup>32</sup>.

$$\Phi_{SR} = \Psi_{SR} \quad (8)$$

$$\Phi_{S'R} = \Psi_{S'R} \{R_B + (1 - R_B) F(w_B)\} \quad (9)$$

$$\Phi_{SR'} = \Psi_{SR'} \{R_C + (1 - R_C) F(w_C)\} \quad (10)$$

$$\Phi_{S'R'} = \Psi_{S'R'} \{R_B + (1 - R_B) F(w_B)\} \cdot \{R_C + (1 - R_C) F(w_C)\} \quad (11)$$

The sound pressure contribution from the image source to the real receiver depends on the properties of the ground surface on the source side, and the pressure from the real source to the image receiver depends on the ground properties on the receiver side. The pressure from image source to image receiver is modified by the ground on both sides.

The diffracted pressures, defined by the change in propagation path due to the presence of a solid thin barrier, can be given by  $\Psi_{SR}$ ,  $\Psi_{S'R}$ ,  $\Psi_{SR'}$ , and  $\Psi_{S'R'}$  for each path. These can be determined from an appropriate diffraction model. A detailed assessment of different models has been undertaken by Isei et al.<sup>34</sup> in which they compared five diffraction theories with each other and with results of outdoor measurements. An approximate expression for  $\Psi_{SR}$  can be given as follows<sup>32</sup>

$$\Psi_{SR} = \pm i \sqrt{\frac{2}{\pi l (l + l_{SR})}} \cdot \exp\left(ikl_{SR} + i\frac{\pi}{4}\right) \cdot E(\xi_{SR}) \quad (12)$$

where  $l$  is the minimum distance in the diffracted path from source to receiver

$l_{SR}$  is the distance from S to R

$k$  is the wave number

$E(\xi_{SR})$  represents the complex Fresnel integral

$$\text{where } \xi_{SR} = \pm \sqrt{k(l + l_{SR})} \quad (13)$$

$$\text{and } E(x) = \int_x^\infty \exp(i\mu^2) d\mu \quad (14)$$

Diffracted pressures  $\Psi_{S'R}$ ,  $\Psi_{SR'}$ , and  $\Psi_{S'R'}$  can be similarly determined from equations 12, 13 and 14.

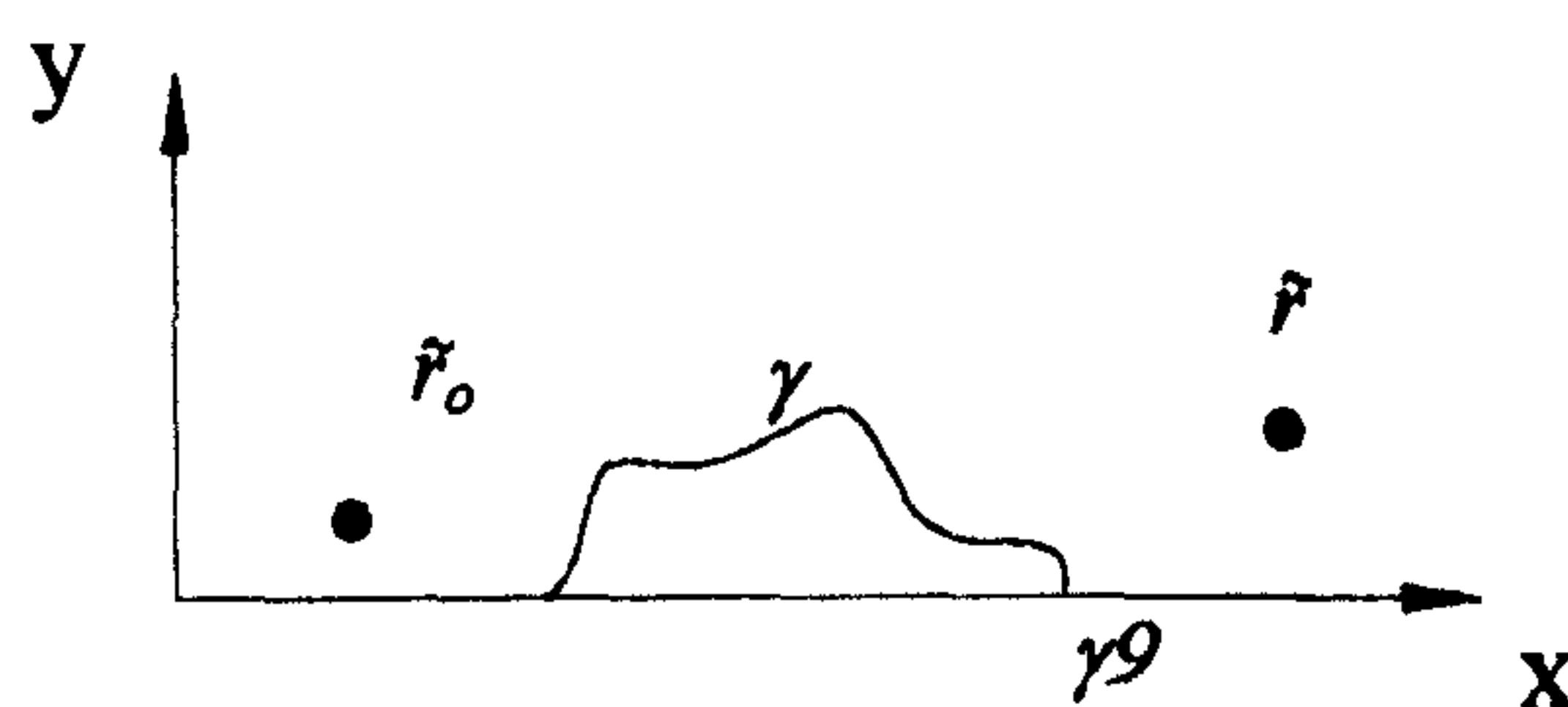
In the cases where there may be variations in the grazing angles,  $\phi$ , or the ground impedances,  $Z_s$ , between the source and receiver sides of the barrier,  $R_B$  and  $R_C$  can be used to represent the plane-wave pressure reflection coefficients about the points of

specular reflection B and C respectively, as shown in Figure 2.3 (b) and  $F(w_B)$  and  $F(w_C)$  are the corresponding boundary loss factors.

The accuracy of geometrical diffraction methods depend mainly on the choice of appropriate diffraction and ground models and on the number of sound paths included in the model.

## 2.4.2 Numerical wave - based methods: Boundary Element Methods

Boundary element methods (BEM) have been used as an efficient tool for calculating the sound field for complex barrier geometries. The main theoretical principles will be examined using the notation defined in Figure 2.4. The description included below is restricted to applications of BEM to 2D models.



**Figure 2.4 : Two-dimensional model showing source ( $\tilde{r}_0$ ), receiver ( $\tilde{r}$ ), barrier ( $\gamma$ ) and ground ( $\gamma_0$ ) configuration and the reference coordinate system.**

The sound pressure  $\phi(\tilde{r})$  at a receiver can be described in terms of the Helmholtz equation and appropriate boundary conditions (i) on the ground, (ii) on the barrier and (iii) at infinity. The boundary value problem can be expressed as follows<sup>35, 36</sup>

$$(\Delta + k^2)\phi(\tilde{r}) = f(\tilde{r}) \quad (15)$$

Where,

$k$  is the wave number, defined earlier

$f(\tilde{r}) = \delta(\tilde{r} - \tilde{r}_0)$  where  $\delta$  denotes the Dirac delta function

$\tilde{r} = (x, y)$  is the receiver position

$\tilde{r}_0 = (x_0, y_0)$  is the source position

Assuming locally reacting boundary conditions on ground and barrier, the normal derivative of the sound pressure can be written as a function of the sound pressure at receiver,  $\tilde{r}$ , as follows:

$$\frac{\partial(\tilde{r})}{\partial n} = ik\beta(\tilde{r}) \cdot \phi(\tilde{r}), \text{ } n \text{ indicating the normal out of the propagating medium}$$

At infinity, the Sommerfeld radiation condition on the diffracted part of the field  $\phi_d$  ensures there are only outgoing waves at infinity:

$$\lim_{r \rightarrow \infty} r^\varepsilon \left( \frac{\partial \phi_d}{\partial r} - ik\phi_d \right) = 0, \text{ where } r = |\tilde{r}| \text{ and } \varepsilon = \frac{1}{2} \text{ in two-dimensions}$$

By applying Green's second theorem to the boundary value problem described above, it has been shown that the following boundary integral equation is obtained.<sup>35, 37</sup>

$$\varepsilon(\tilde{r}) \cdot p(\tilde{r}, \tilde{r}_o) = G_{\beta_c}(\tilde{r}_o, \tilde{r}) + \int_{\gamma} \left( \frac{\partial G_{\beta_c}(\tilde{r}_s, \tilde{r})}{\partial_n(\tilde{r}_s)} - ik\beta(\tilde{r}_s) G_{\beta_c}(\tilde{r}_s, \tilde{r}) \right) p(\tilde{r}_s, \tilde{r}_o) ds(\tilde{r}_s) \quad (16)$$

$p(\tilde{r}, \tilde{r}_o)$  is the acoustic pressure at the receiver  $\tilde{r}$  due to the source  $\tilde{r}_o$  in the presence of the barrier.

$\gamma$  denotes the barrier surface

$\beta(\tilde{r}_s)$  is the normalised surface admittance at the point  $\tilde{r}_s = (x_s, y_s)$  located on  $\gamma$

$ds(\tilde{r}_s)$  is the arc-length of an element of  $\gamma$  at  $r_s$

$\frac{\partial}{\partial_n(\tilde{r}_s)}$  is the partial derivative in the direction of the normal to  $\gamma$  at  $r_s$ , directed out of the propagating medium

$k$  is the wave number

$\varepsilon(\tilde{r}) = 1$  when  $\tilde{r}$  is in propagating medium, except on  $\gamma$

$\varepsilon(\tilde{r}) = \frac{1}{2}$  if  $\tilde{r}$  is on  $\gamma$ , provided it is not a corner point

$\varepsilon(\tilde{r}) = \varsigma / 2\pi$  if  $\tilde{r}$  is a corner point, where  $\varsigma$  is the angle in the medium subtended by the two tangents to the boundary at  $\tilde{r}$ <sup>37</sup>

$G_{\beta_c}(\tilde{r}, \tilde{r}_o)$  is the acoustic pressure at the receiver  $\tilde{r}$  due to the source  $\tilde{r}_o$  in the absence of the barrier, with only the flat ground.



In the case of perfectly reflecting ground ( $\beta_c = 0$ ) of homogeneous admittance, the acoustic pressure at  $r$  due to a source at  $r_o$  can be written as follows

$$G_{\beta_c}(\tilde{r}, \tilde{r}_o) = -\frac{i}{4} \left( H_o^{(1)}(k|r_o - r|) + H_o^{(1)}(k|r'_o - r|) \right) \quad (17)$$

$r'_o = (x_o, -y_o)$  is the image of the source in the ground

$H_o^{(1)}$  is the Hankel function of the first kind of order zero

Therefore the barrier insertion loss can be calculated as follows:

$$Insertion\ Loss = 20 \log \left( \frac{p(\tilde{r}, \tilde{r}_o)}{G_{\beta_c}(\tilde{r}, \tilde{r}_o)} \right) \quad (18)$$

Geometrical diffraction methods and boundary element methods are both able to model the interaction of ground with the barrier. The advantage of boundary element methods over geometrical diffraction methods is that it can handle complex geometries. However, neither of these models includes the influence of atmosphere. Therefore the expressions used for insertion loss could be considered as a 'theoretical value' providing useful indications on 'relative' performance.

## 2.5 CONCLUSIONS

This chapter examined various factors affecting sound propagation outdoors. These have been identified as geometric spreading, atmospheric absorption, turbulence, refraction, ground effects, and barrier attenuation.

Published work on the likely influence of atmospheric and ground effects on the performance of a noise barrier has been reviewed. The main numerical methods used in the study of atmospheric effects on outdoor noise propagation were described. It is well documented that barrier attenuation measured outdoors is often much lower than predicted by theory or scale modelling. This is commonly attributed to atmospheric conditions. Although theoretical understanding of the atmospheric phenomena has improved over the years, there still is not a comprehensive approach which can account for all the effects, in the form of a simple and practical model.

The theoretical concepts in the investigation of the performance of barriers in the presence of a ground surface but under homogeneous atmospheric conditions can be broadly

classified into two categories. These are geometrical diffraction methods and boundary element methods. They were both shown to be able to model the interaction of ground with the barrier. The advantage of boundary element methods over geometrical diffraction methods is that it can handle complex geometries. However, neither of these models includes the influence of atmosphere.

When assessing the relative performance of different barrier shapes it would be reasonable to minimise atmospheric and ground effects such that the acoustic benefits of various shapes can be determined free from external factors. Therefore for the purposes of this work homogenous atmospheric conditions will be assumed. The boundary on which noise barriers are to be located will be assumed to be flat, smooth and reflective to minimise absorption and scattering effects due to ground surface.

The following Chapter will review the up - to - date research carried out on noise barriers. This is expected to result in recommendations for further research needs in the field which will inform the rest of this research programme.

- 
- <sup>1</sup> EMBLETON, T.F.W., PIERCY, J.E., and OLSON, N., Outdoor Sound Propagation Over Ground of Finite Impedance, J.Acoust.Soc.Am., Vol. 59, No. 2, 267-277, 1976
  - <sup>2</sup> EMBLETON, T.F.W., PIERCY, J.E., and DAIGLE, G.A., Effective Flow Resistivity of Ground Surfaces Determined by Acoustical Measurements, J.Acoust.Soc.Am., Vol. 74, No. 4, 1239-1244, 1980
  - <sup>3</sup> ATTENBOROUGH, K., Predicted Ground Effect for Highway Noise, Journal of Sound and Vibration, 81(3), 413-424, 1982
  - <sup>4</sup> PIERCY, J.E., EMBLETON, T.F.W., and SUTHERLAND, L.C., Review of Noise Propagation in the Atmosphere, J.Acoust.Soc.Am., Vol. 61, No. 6, 1403-1418, June 1977
  - <sup>5</sup> SUTHERLAND, L. C., and DAIGLE, G. A., Atmospheric Sound Propagation, Chapter 28, Handbook of Acoustics, M. J. Crocker (Editor), 305-329, 1998
  - <sup>6</sup> DURNIN, J., and BERTONI, H., Acoustic propagation over ground having inhomogeneous surface impedance, J.Acoust.Soc.Am., Volume 70, No. 3, 852-859, 1981
  - <sup>7</sup> JACKSON, G.M., A Review of Highway Noise Barriers, The Journal of the Institution of Highway Engineers, 13-16, November 1979
  - <sup>8</sup> WATTS, G., Factors Affecting the Performance of Traffic Noise Barriers, Proceedings of Inter-Noise 2000, Nice – France, August 27-30, Volume 1, 515-520, 2000
  - <sup>9</sup> The Highways Agency, Design Manual for Roads and Bridges, Volume 10, Section 5, Part 2, HA 66/95 - Environmental Barriers: Technical Requirements HMSO, 1995
  - <sup>10</sup> Highway Traffic Noise Analysis and Abatement Policy and Guidance, U.S. Department of Transportation, Federal Highway Administration Office of Environmental and Planning, Noise and Air Quality Branch, Washington, D.C., June 1995
  - <sup>11</sup> JONASSON, H.G. Diffraction By Wedges of Finite Acoustic Impedance With Applications to Depressed Roads, J.Sound Vib., 25(4), 1972, 577-585
  - <sup>12</sup> JONASSON, H.G. Sound Reduction By Barriers On The Ground, Journal of Sound and Vibration, 22(1), 113-126, 1972
  - <sup>13</sup> HUTCHINS, D.A., JONES, H.W., and RUSSELL, L.T., Model Studies of Barrier Performance in The Presence of Ground Surfaces. Part I - Thin, Perfectly Reflecting Barriers, J.Acoust.Soc.Am., 75(6), June 1984, 1807-1816

- 
- <sup>14</sup> BOULANGER, P., ATTENBOROUGH, K., TAHERZADEH, S., WATERS-FULLER, T., KAI, M.L., Ground Effect Over Hard Rough Surfaces, *J. Acoust. Soc. Am.*, 104(3), Pt. 1, 1474-1482, September 1998
- <sup>15</sup> ATTENBOROUGH, K., Understanding and Controlling Acoustic Effects of Outdoor Surfaces, IMechE Seminar Publication 2000-3, Noise and Vibration, Advances in Research and Development, S682/003/99, 29-38, 2000
- <sup>16</sup> RASMUSSEN, K. B., Outdoor Sound Propagation Under The Influence of Wind and Temperature Gradients, *Journal of Sound and Vibration*, 104(2), 321-335, 1986
- <sup>17</sup> HALLBERG, B., LARSSON, C., and ISRAELSSON, S., Some Aspects on Sound Propagation Outdoors, *Acustica*, Vol. 66, 109-112, 1988
- <sup>18</sup> DAIGLE, G.A., Diffraction of Sound By A Noise Barrier In The Presence of Atmospheric Turbulence, *J.Acoust.Soc.Am.*, 71(4), 847-854, April 1982
- <sup>19</sup> SCHOLLES, W.E., SALVIDGE, A.C., and SARGENT, J.W., Field Performance of A Noise Barrier, *Journal of Sound and Vibration*, 16(4), 627-642, 1971
- <sup>20</sup> ATTENBOROUGH, K., et al., Benchmark Cases for Outdoor Propagation Models, *J.Acoust.Soc.Am.*, 97(1), 173-191, January 1995
- <sup>21</sup> SALOMONS, E.M., Diffraction by a screen in downwind sound propagation: A parabolic-equation approach, *J.Acoust.Soc.Am.*, 95(6), 3109-3117, June 1994.
- <sup>22</sup> FORSSEN, J., An Extended substitute-sources method for a turbulent atmosphere: Calculations for upward refraction, *Acta Acustica United with Acustica*, Vol. 89, 225-233, 2003
- <sup>23</sup> RASPET, R., and WU, W., Calculation of Average Turbulence Effects on Sound Propagation Based on The Fast-Field Program Formulation, *J.Acoust.Soc.Am.*, Vol. 97, 145-153, 1995
- <sup>24</sup> GILBERT, K.E., RASPET, R., and DI, X., Calculation of Turbulence Effects in an Upward Refracting Atmosphere, *J.Acoust.Soc.Am.*, Vol. 87, 2428-2437, 1990
- <sup>25</sup> FORSSEN, J., Calculation of noise barrier performance using substitute-sources method for a three-dimensional turbulent atmosphere, *Acta Acustica United with Acustica*, Vol. 88, 181-189, 2002



- 
- <sup>26</sup> FORSSEN, J., Calculation of Sound Reduction by a Screen in A Turbulent Atmosphere Using the Parabolic Equation Method, *Acta Acustica United with Acustica*, Vol. 84, 599-606, 1998
- <sup>27</sup> TAHERZADEH, S., ATTENBOROUGH, K. and LI K.M., A Hybrid BIE/FFP Scheme for Predicting Barrier Efficiency Outdoors, *J.Acoust.Soc.Am.*, 110 (2), 918-925, 2001
- <sup>28</sup> PREMAT, E. and GABILLET, Y., A New Boundary Element Method with Inhomogeneous Green's Function for Predicting Noise Barriers Efficiency with Meteorological Effects, *Inter-Noise 98*, Auckland, 1998
- <sup>29</sup> PREMAT, E. and GABILLET, Y., A New Boundary-Element Method for Predicting Outdoor Sound Propagation and Application to the Case of a Sound Barrier in the Presence of Downward Refraction, *J.Acoust.Soc.Am.*, 108(6), 2775-2783, 2000
- <sup>30</sup> DELANY, M.E., and BAZLEY, E.N., Acoustical Properties of Fibrous Absorbent Materials, *Applied Acoustics*, Vol. 3, 105-116, 1970
- <sup>31</sup> ATTENBOROUGH, K., Acoustical Impedance Models For Outdoor Ground Surfaces, *Journal of Sound and Vibration*, 99(4), 521-544, 1985
- <sup>32</sup> ISEI, T., Absorptive Noise Barrier on Finite Impedance Ground, *J.Acoust.Soc.Jpn.(E)*, Vol. 1, No. 1, 3-10, 1980
- <sup>33</sup> MURADALI, A., and FYFE, K.R., A Study of 2D and 3D Barrier Insertion Loss using Improved Diffraction-based Methods, *Applied Acoustics*, Vol. 53, No 1-3, 49-75, 1998
- <sup>34</sup> ISEI, T., EMBLETON, T.F.W., and PIERCY, J.E., Noise Reduction by Barriers on Finite Impedance Ground, *J.Acoust.Soc.Am.*, 67(1), 46-58, January 1980
- <sup>35</sup> SEZNEC, R., Diffraction of Sound Around Barriers : Use of The Boundary Elements Technique, *Journal of Sound and Vibration*, 73(2), 195-209, 1980
- <sup>36</sup> CHANDLER-WILDE, S.N., and HOTHERSALL, D.C., Sound Propagation Above An Inhomogeneous Impedance Plane, *Journal of Sound and Vibration*, 98(4), 475-491, 1985
- <sup>37</sup> HOTHERSALL, D.C., CHANDLER-WILDE, S.N., HAJMIRZAE, N.M., Efficiency of single noise barriers. *J.Sound and Vibration*, Vol 146, 303-322, 1991

### **3 REVIEW OF ROAD TRAFFIC NOISE CONTROL BY MEANS OF BARRIERS**

#### **3.1 INTRODUCTION**

The control of road traffic noise attracted a number of solutions depending on the nature of the problem and the political decisions in the specific countries. In the U.K., the Land Compensation Act 1973 encouraged sound insulation of properties and paying for the land subjected to noise levels set by the legislation. By offering double glazing noise was kept out of the homes. This only avoided the problem rather than solving it and it did not take into consideration the need for the people to open their windows or use their gardens, in which case this particular noise control would be rendered useless<sup>1</sup>.

Traffic management is another means of traffic noise control. The three main parameters affecting traffic noise are traffic volume, speed and composition. Traffic management attempts to control these parameters by various measures. These include traffic control devices, prohibition of certain vehicle types during certain times from sensitive areas, modification of speed limits or horizontal / vertical realignment of the traffic relative to the noise sensitive areas. These measures do have their practical limitations and some may also require a strict enforcing (control / policing) mechanism until they take effect.

Two of the more commonly preferred and implemented noise mitigation measures are the use of barriers and alternative road surfaces. In the U.K. porous road surfaces were developed to allow water to drain rapidly through the surface material and consequently help to prevent water forming on the surface during heavy rainfall. These surfaces reduce spray from passing vehicles and give better skid resistance. However, it's been realised that in addition to the reduction in the so called "splash noise", the tyre/road generated noise was also absorbed to some extent due to the porous nature of the road surface under dry conditions<sup>2</sup>. This technique of noise control "at the source" has been developed over the years and implemented into practice<sup>3,4</sup>. Durability<sup>5</sup>, maintenance<sup>6,7</sup>, reduction of acoustic effectiveness in time<sup>8</sup> and cost<sup>9</sup> (both application and maintenance) are still a concern. However promising progress has been made and reductions in traffic noise in

real life situations are encouraging. The use of this method is also emphasised in the European Commission's Green Paper<sup>10</sup>.

The most commonly preferred traffic noise control method has been the use of noise barriers. Although it is a method of noise control by intercepting the transmission path, due to the ease of implementation and its effectiveness, it attracted wide interest among the scientific community. This method has the advantage over noise insulation that it protects people more effectively, whether they are inside or outside their homes. Barriers take immediate effect and do not require a transition period required by certain traffic management measures. Although noise control at source is always more effective, low noise surfaces are still in the process of being developed and require technical expertise - not necessarily possessed by developing countries - to be implemented. Problems inhibiting their implementation may be overcome over the years but low noise surfaces may still be required to be used in conjunction with noise barriers for a more effective traffic noise control<sup>11</sup>. Therefore there are potential benefits in investigating the noise barriers further.

This chapter reviews the research carried out on environmental noise barriers using analytical and physical modelling as well as on-site measurements. The main parameters affecting the performance of barriers, other than atmospheric and ground effects, are highlighted. Different noise barrier types available in the literature are critically reviewed and their noise attenuation mechanisms are identified. The discussion of this work leads to recommendations on further research needs in the general field of environmental noise control by means of barriers.

## **3.2 RESEARCH INTO BARRIER PERFORMANCE**

Research into the performance of noise barriers is usually undertaken using either full scale testing or modelling techniques. There are two types of modelling techniques for investigating barrier performance. These are physical scale modelling and numerical modelling. The former provides a simple tool for laboratory testing while the latter is a convenient method for investigation. The ultimate test for the performance of a noise barrier is on-site measurements where the real performance of a barrier can be assessed under realistic ground and atmospheric conditions. The following is a review of the research on barrier performance.



### 3.2.1 Analytical Methods

Diffraction of sound over, around and through a barrier has a fundamental effect on its performance. Rigorous mathematical solutions of this problem have been developed over the years. Sommerfeld<sup>12</sup> presented the exact solution for the diffraction of a plane wave by a semi-infinite plane screen and Macdonald<sup>13</sup> for the diffraction of a cylindrical wave. However, for the purposes of noise barrier design, simplified and approximate methods are generally preferred. Early studies investigated diffraction over a barrier edge where the ground effects were not explicitly considered and the atmospheric effects were ignored. Redfearn<sup>14</sup> and Fehr<sup>15</sup> provided charts for predicting screen attenuation. Maekawa<sup>16,17</sup> proposed a design chart based on experimental data for calculating the shielding effect of a screen. This chart relates Fresnel number,  $N$ , to attenuation relative to free-space. Ground effect is taken into account empirically by applying a 2dB correction. A number of engineering formulae have since been developed to represent this chart<sup>18, 19, 20</sup>. Kurze and Anderson<sup>21</sup> investigated the difference between the results for a point source and for a straight-line source. The excess attenuation was found to be consistent with experimental results of Maekawa<sup>17</sup> and Rathe<sup>22</sup>. Fujiwara et al. proposed simplified methods for estimating the excess attenuation by a thick<sup>23</sup> and an absorptive barrier<sup>24</sup>. Various diffraction techniques have been employed to investigate diffraction over a wedge<sup>25, 26, 27</sup>, three-sided barrier<sup>28</sup>, many-sided barrier or a pillar<sup>29</sup> and polygonal shapes<sup>30</sup>.

The combined barrier and ground effects are modelled by taking into account the ground reflected ray paths as discussed earlier. Isei et al.<sup>31</sup> compared five different diffraction theories which differed in their approach to the theory of diffraction and the model they used for ground impedance. Additional analytical methods for calculating the insertion loss of finite length barriers on the ground have been explored further<sup>32, 33, 34, 35, 36, 37</sup>.

Muradali and Fyfe<sup>38</sup> compared improved diffraction based methods to the numerical wave-based boundary element methods (BEM) and showed they were in good agreement. Another comparison of a ray based model and numerical methods based on Fourier BEM was undertaken by Salomons et al.<sup>39</sup> which investigated traffic noise situations with multiple diffractions and reflections. The benchmark paper on boundary element modelling of noise barriers is the work of Seznec<sup>40</sup>. It was shown that this model can be applied to any system with arbitrary shape and boundary conditions but in practice computation times would be a limiting factor. The BEM is suitable for external problems and only the boundary of a model needs to be discretised, as opposed to the whole body discretisation as in finite element methods (FEM). This method has been used for the systematic



comparison of the effects of varying barrier shapes, orientation and absorption properties and also to undertake a study of relative performances of different barrier profiles<sup>41, 42</sup>.

Geometrical diffraction methods have their limitations in that they are specific to certain types of barriers and they cannot cope with diffraction around novel shaped barriers. Numerical wave-based methods, particularly boundary element methods, on the other hand, have the flexibility of being able to model any complicated barrier shape. All of these studies excluded the effects of atmosphere on barrier performance. Under non-homogenous atmospheric conditions, the ray paths are bent by the vertical sound speed gradient and become curves. Under strong downward refracting situations, it is possible that a path can curve over the barrier to reach a receiver that does not have a direct line of sight to the source.

Attenborough et al.<sup>43</sup> have presented a comparison of a range of ray and wave based models for outdoor sound propagation over flat ground. This extensive investigation included the effects of both the ground and the atmosphere in the absence of screening from barriers and showed that sophisticated wave based methods agree with the analytical solutions. Interaction of barriers with the atmosphere has been the subject of investigations using a number of numerical models such as parabolic equations (PE)<sup>44, 45</sup>, substitute-sources method<sup>46, 47</sup> and scattering cross-section models<sup>48</sup>. Salomons developed a semi-analytical ray model for downwind propagation of sound in the absence of a barrier<sup>49</sup>. This method does not suffer from the problem of large computation times at high frequencies, which is a disadvantage of the wave-based methods. Muradali and Fyfe<sup>50</sup> proposed an improved diffraction-based sound barrier performance model combined with a heuristic atmospheric model. Comparisons with parabolic equation method showed good agreement.

Ray and wave based analytical methods have been successfully used to model the interaction of barriers with the atmosphere and ground. Although theoretical understanding of the atmospheric phenomena has improved over the years, there is not, as yet, a comprehensive approach which can account for all the effects, in the form of a simple and practical model. Ray based models are restricted to simple barrier shapes and their accuracy depends on the level of detail they consider. Numerical wave based methods are able to model complex barrier geometries in a still, homogeneous atmosphere, but have difficulties dealing with complex barrier geometries in a non-homogeneous atmosphere.

### 3.2.2 Physical Scale Modelling

Acoustic modelling has been used extensively in the design of auditoria and concert halls<sup>51</sup>. It is also applicable to the modelling of complex urban environments which would be difficult to investigate analytically. The principle of physical scale modelling, for many classes of acoustic phenomena, is relatively simple. It involves the scaling of physical dimensions, wavelengths and acoustic properties appropriately by a chosen scale factor. As the scale factor becomes smaller, the model frequencies need to be further into the ultrasonic range. It becomes more difficult to produce and to detect these frequencies. The investigation of various atmospheric effects, such as wind and turbulence, by this technique is complex and requires tests to be carried out in wind tunnels. The following is an account of some of the main considerations when applying this technique to the modelling of noise barriers.

#### 3.2.2.1 Testing Medium

The testing room should ideally be a purpose built anechoic or semi-anechoic chamber. These provide a testing space free of reverberant field, practically eliminating the reflections<sup>52</sup>. An anechoic chamber could be in a two-dimensional form, for the investigation of an infinitely long barrier with a uniform longitudinal profile<sup>53</sup>. Impulsive sound sources of short enough duration in conjunction with fast sampling times<sup>16, 54</sup> could be used to avoid reflections from room boundaries. Short enough sampling times would ensure only the direct component of the sound is taken into account.

Investigation of the effects of wind on barriers can be performed in wind tunnels<sup>55, 56</sup>. These are closed-circuit structures where constant air flow simulates the outdoor conditions.

Air absorption can be modelled by air drying or gas substitution<sup>51</sup>. At higher testing frequencies it may have to be computationally corrected for, since simulation becomes impossible. Alternatively, comparative measurements taken at the same receiver position, with and without the barrier in between, could cancel air absorption effects.<sup>57</sup>

#### 3.2.2.2 Scale Factor

Various scale factors can be employed depending on the nature of the environmental problem to be examined. Some examples are 1:5<sup>58</sup>, 1:10, 1:16<sup>54, 59</sup>, 1:20<sup>60, 61</sup>, 1:40<sup>35</sup>, 1:50<sup>62, 63</sup>, 1:80<sup>57, 64</sup>, 1:100<sup>32</sup>. This clearly shows that the practical choices made are based on individual circumstances<sup>65</sup>.

### **3.2.2.3 Modelling Materials**

In order to model the acoustic properties of real surfaces, a wide range of materials have been used. Aluminium<sup>57, 61</sup> has been used to simulate reflective surfaces, such as asphalt, due to its high impedance. Plywood<sup>68, 58</sup> has been employed as barrier model material. Various other materials such as carpet<sup>58</sup>, pressboard<sup>36</sup>, acryl, wool<sup>35</sup>, polystyrol<sup>66</sup>, fibreglass<sup>47</sup> have all been used in conjunction with specific scale factors and according to the nature of the surfaces to be simulated.

### **3.2.2.4 Noise Source**

The source can be modelled as a point source or a line source or a combination of two for realistic traffic flow simulations. Point source can be a spark source<sup>32, 67</sup>, ultrasonic whistle<sup>57, 64</sup>, air jet<sup>51, 61, 62</sup> or a small sized tweeter<sup>16, 35, 38, 51, 60, 68</sup>. A line source can be simulated by a series of point sources closely positioned in a line or in the form of a mechanical sound source, with a series of balls loosely attached in a metal channel<sup>68</sup>.

### **3.2.2.5 Other Factors**

Other factors of importance are transmission loss through the model material, length of the model and weak points in the model where sound leakage can occur. The model material has to provide sufficient transmission loss such that the top diffracted noise is at least 10 dB more than that passing through the model. The model has to be long enough so that the side-diffracted noise does not interfere with the top diffracted waves.

The simplicity of physical scale modelling makes it possible to investigate real life problems, such as different traffic flow combinations and barriers having varying longitudinal profiles. It is also useful in providing a practical appreciation of the problem at hand. However the requirements for specialist equipment and purpose built testing rooms may limit the applications of this technique.

## **3.2.3 Full Scale Testing**

Field performance of noise barriers has been investigated with localised sound sources<sup>69</sup> and real traffic noise<sup>70, 71</sup>. The determination of the insertion loss of a barrier or the effect of a device on top of a barrier usually takes the shape of 'before' and 'after' measurements. Potential difficulties with on-site insertion loss measurements have been demonstrated<sup>72</sup>. In order to obtain meaningful comparisons, all external factors have to be monitored and



their effects need to be taken into account. In the case of short term measurements variations in traffic and atmosphere need to be considered. In long term measurements variations in ground conditions may also have to be monitored. Although the field tests are expensive and require careful monitoring of many variables, they are the ultimate test for determining the true performance of a noise barrier.

### **3.3 FACTORS AFFECTING THE ACOUSTIC DESIGN OF ENVIRONMENTAL BARRIERS**

The main factors which affect the acoustic design of environmental barriers are discussed below. Some of these have also been reported recently by Watts<sup>73</sup>.

#### **3.3.1 Barrier profile**

As it will be discussed later in this chapter, by modifying the shape of a barrier slightly, especially in the regions where the noise is passing over the top, considerable gains can be achieved, even in excess of that due to path length difference.

#### **3.3.2 Height**

Typically, minimum height is determined by the relative positions of the source and the receiver so that the line-of-sight from the source to the receiver is intercepted. In that case, the acoustic shielding provided by the barrier is 5 dB(A) and it increases up to about 15 dB(A), as the path length difference between the direct rays and the top diffracted rays increases. This corresponds to approximately 1.5 dB(A) additional noise level reduction for each meter of increase in height after the barrier breaks the line-of-sight.

The theoretical maximum of 20 dB(A), which corresponds to a 99% reduction in acoustic energy of the noise levels, is almost impossible to achieve in practice. The target level of 15 dB(A) reduction would be very difficult to achieve. This would imply a 97% reduction in the acoustic energy.

#### **3.3.3 Length**

A barrier should stretch in both directions enough to protect the receiver from the end diffracted rays. As a rule of thumb, the minimum length of a barrier is taken as 20 times the distance between the source and the receiver to be protected<sup>74</sup>. A different approach is that the barrier should extend 4 times as far in each direction as the distance from the



receiver to the barrier<sup>75</sup>. Both of the above methods are, in essence, trying to achieve a high angle of view. A barrier covering an angle of  $160^\circ$  subtended from the receiver to the road will ensure that the end diffracted rays are not significant.

### **3.3.4 Source - to - barrier distance**

For maximising its efficiency, the barrier should be installed as close to the noise source as possible. Obviously in the case of traffic noise, this parameter is not for the designer to determine in most cases, but is decided by the specific site conditions.

### **3.3.5 Barrier - to - receiver distance**

Horizontal separation between the residential homes and the erected barrier depends on the specific geometric configuration. The performance of the barriers decreases as the distance increases, and usually net effect is negligible beyond 300 m, if the ground surface behind the barrier is absorbing.

### **3.3.6 Source and receiver heights**

In the UK's official traffic noise calculation method<sup>76</sup> the traffic noise height is taken as 0.5 m above the ground surface. The receiver height again depends on the number of storeys in the residential homes. For example, the height of the bedroom window of a two-storey residential home can be taken as 3.5 m. If the receiver is so high that it remains in the illuminated zone (i.e. the line of sight is not intercepted by the barrier), then the noise levels will not only be reduced but could even be increased due to diffracted sound towards that zone.

### **3.3.7 Frequency content of the traffic noise**

Maximum intensity of A-weighted traffic noise is somewhere between the mid frequencies of 500 Hz and 1500 Hz, taken as 1000 Hz in the CRTN for convenience.

### **3.3.8 Transmission loss through the barrier**

Due to the noise finding its way through the barrier, and not being forced to go over the top edge, the performance of an acoustic screen can be diminished greatly. This can happen either when the superficial mass ( $\text{kg/m}^2$ ) of the barrier material is insufficient or when the barrier is not airtight. The latter case is more likely to happen due to the gaps at the joints,

especially in the panel type of construction. Adequate superficial mass is easy to ensure because all we require from the transmission loss is to be a minimum of 10 dB, in which case, due to the logarithmic nature of the addition of noise levels, transmitted noise will not have an effect on the top diffracted noise level.

## 3.4 NOISE BARRIER TYPES

The literature on different barrier systems world-wide has been reviewed<sup>77</sup> where cost effective designs and materials for barrier construction were presented. This section will undertake an up to date review of the available barrier profiles with an emphasis on the physical principles on which they perform and their possible applications.

### 3.4.1 Vertical alignment of road

Vertical alignment of a road can be used as a means of screening traffic noise. Roads in cuttings, either with natural absorptive slopes or artificially retained reflective sides, are common examples in practice (Figure 3.1). Roads elevated above the surrounding ground on embankments or on other structures such as viaducts can create shadow zones for receivers situated close to the roads (Figure 3.2).



Figure 3.1 : Roads in Cuttings



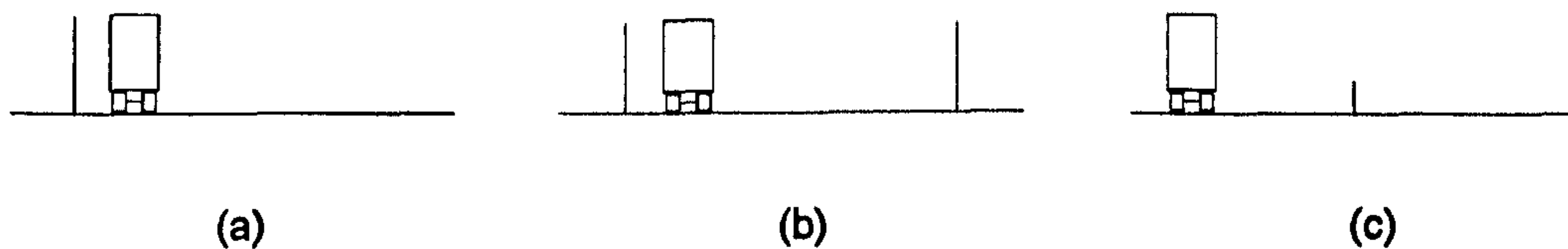
Figure 3.2 : Elevated Roads

### 3.4.2 Thin Vertical Reflective Barriers

The acoustic effectiveness of different barrier types is generally assessed by comparison with thin vertical walls. Early studies investigated the performance of semi-Infinite screens as discussed in previous sections. The side diffracted waves were shown to be influential in the interference patterns behind a rectangular constant height barrier for barrier lengths

which were up to 4 to 5 times their height<sup>66</sup>. In the case of a single receiver point situated on a flat ground, the optimised noise barrier shape was found to result in a Gaussian-like shape<sup>78</sup>. The use of a median barrier in central reservation of a dual carriageway was shown to produce an improvement of 1 to 2 dB in insertion loss depending on surrounding ground type<sup>79</sup>.

Transparent barriers are essentially thin vertical walls which are preferred mainly for visual and aesthetic reasons. They provide optical transparency without compromising the acoustics<sup>80, 81</sup>. However, these may need frequent maintenance and suffer from vandalism.



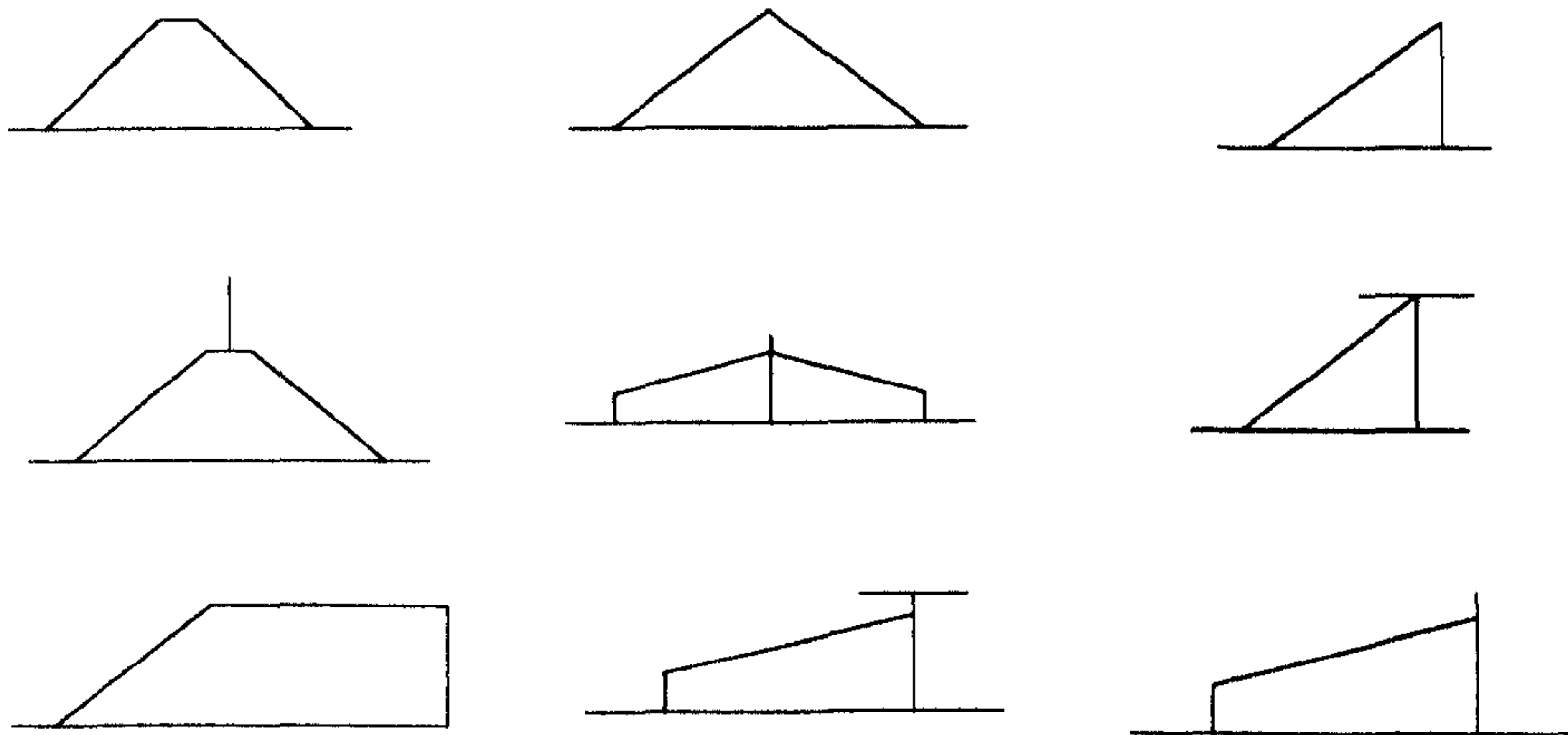
**Figure 3.3 : Thin vertical barriers (a) single, (b) multiple, and (c) median barrier configurations**

Figure 3.3 shows some applications for thin vertical barriers. Various practical concerns have led to the development of alternative barrier types which are discussed below.

### **3.4.3 Earth Mounds**

Earth mounds reduce noise in a number of ways such as increased effective barrier height, scattering and double diffraction losses on the barrier top, and absorption effects on grass-covered slopes.

Hajek's finding was that provided an earth berm is covered by grass, the insertion loss performance is comparable to that of a thin vertical wall of equal height<sup>82</sup>. It was found that inserting a relatively low thin wall or placing absorptive material on top of an earth mound were both acoustically beneficial. Numerical modelling by boundary element methods demonstrated that decreasing the slope angle of the wedge shaped barrier was beneficial in improving the performance<sup>Error! Bookmark not defined.</sup>. It was found that an absorbing flat-topped mound gave 3 dB improvement over an absorbing wedge of equivalent overall height. A thin vertical barrier provided a 1 dB improvement over the flat - topped grass - covered mound. In practice, it may be difficult to detect this difference due to atmospheric and ground effects. The variations on a mound or a wedge profile have been investigated by Hutchins et al.<sup>64</sup> as shown in Figure 3.4.



**Figure 3.4 : Various earth mound / wedge configurations**

The insertion loss of an earth mound is increased for cases where source and receiver are close to it<sup>83</sup>. The main reason was found to be enhanced high frequency performance. Mounting a thin-wall on top of an absorptive - topped earth berm initially reduces the beneficial effect of the absorptive top. The performance is recovered as the height of the thin-wall increases. This finding, which was also observed by others<sup>84</sup>, contradicts the findings of Hajek<sup>82</sup>.

Earth mounds are aesthetically pleasing, environmentally acceptable and have considerable perceived acoustic effectiveness compared to conventional barriers<sup>85</sup>. A noise barrier may be erected on top of an earth mound to reduce the horizontal land take. There is inconclusive evidence that this could in some cases diminish the acoustic performance of earth mounds<sup>84</sup>. However, further research is required to quantify the effects of a small height barrier on top of an earth mound.

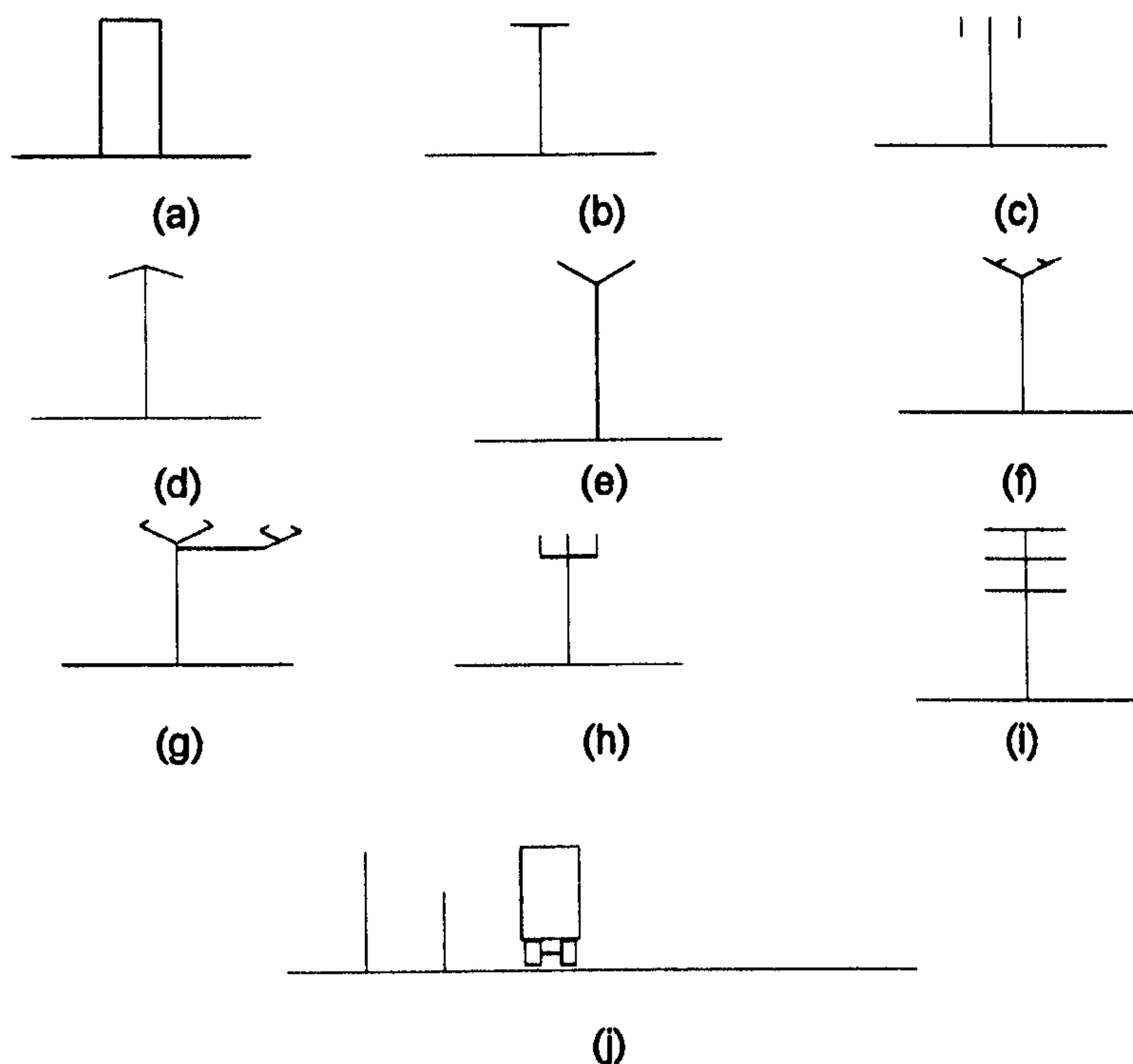
### **3.4.4 Multiple- Edged Barriers**

Double barrier configurations, in which the line of sight from the source to the rear barrier grazes the upper edge of the first barrier, were shown to be extremely efficient in attenuating road traffic noise, in comparison with a vertical screen of the same effective height<sup>86</sup>. This clearly demonstrated that the simple path length difference approach is insufficient for predicting the performance of multiple-edged barriers accurately. The beneficial effects of additional diffracting edges can be seen in the case of U-sections<sup>87</sup>, which involves extra panels connected to the main screen by brackets<sup>87, 88</sup>, fir tree profiles<sup>89</sup>, T-profile barriers and their associated Y-profile and arrow-profiled barriers<sup>64</sup>



and branched barriers<sup>90</sup>. All of these profiles introduce some form of additional diffracting edge and also change the effective height of the barriers by doing so.

By using numerical methods, Alfredson and Du<sup>89</sup> compared the performance of barriers with extra diffracting edges, to that of a thin barrier, and concluded that gains of the order of 5 dB(A) were possible without an increase in barrier height. Full scale tests of multiple edge barriers by Watts et al showed that an average improvement in the insertion loss of 2.5 dB(A) can be achieved without the use of relatively costly absorptive materials<sup>88</sup>. More recent work by Watts with a similar profile tested at three sites, revealed that under favourable conditions, improvements above 3 dB(A) are possible in the barrier screening performance<sup>70</sup>. The performance of various shapes of branched barriers investigated along highways was found to be 3 to 4 dB better than a thin vertical barrier of similar height<sup>90</sup>.



**Figure 3.5 : Multiple edged barrier configurations showing (a) thick barrier, (b) T – capped barrier, (c) brackets attached to main barrier, (d) arrow profile, (e) Y – profile, (f) Y – profile with additional edges, (g) branched profile, (h) U – profile, (i) fir tree section, (j) double barriers**

A number of barrier profiles designed to benefit from double or multiple diffraction are shown in Figure 3.5. Barrier profiles with extra diffracting edges are, so far, the most promising designs as far as cost effectiveness and acoustical performance is concerned.

### 3.4.5 Random-Edged Barriers

Random edged barriers (Figure 3.6) have been investigated in an attempt to interrupt the deterministic phase variations which occur in the case of straight edged barriers<sup>91, 92, 93</sup>.



**Figure 3.6 : Random edged barrier (Longitudinal view showing part of length)**

The wave front from a stationary point source meets the barrier top at different locations. The barrier edge itself could be considered as an infinite number of point sources along its length. The phase and strength of each source varies monotonically along the edge away from the point of closest approach, and this variation depends on the distance from the real point source. Coherent addition of the sound pressure from the effective sources results in destructive and constructive interference patterns depending on the location of the receiver and the frequency. Introduction of random edges is aimed at preventing the constructive interference patterns. Different edges would represent different point sources at various heights above ground. These would no longer be in phase and the secondary source effects would be reduced by de-correlation. The distinct ground effects observed in the case of a single constant-height barrier would not occur in the case of random-edge barriers.

The jagged-edge barrier was found to be better above about 5 kHz. The improvement was shown to increase as the distance from the barrier to the receiver decreased. In the frequency range in which the jagged barrier has the higher insertion loss, the improvement was 3-7 dB however the performance diminished at lower frequencies. Insertion loss was greatest when the edge was as jagged or rapidly fluctuating as possible. The experimental findings indicate that the improvement was modest, varying from 2.5 dB to 5 dB. It was noted that it was possible to choose a random-edge fluctuation that resulted in a worse performance than that of a straight-edge barrier of same average height.

### 3.4.6 Absorptive Barriers

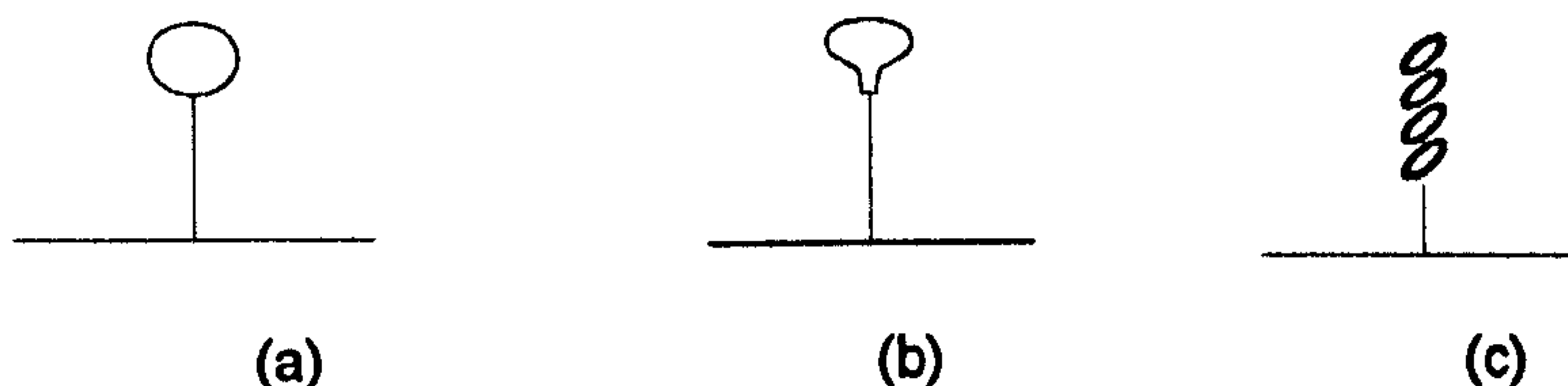
Absorptive barriers could be investigated under two categories. Firstly where the absorptive treatment is applied around the free edges of a barrier to reduce the energy of diffracted sound paths, and secondly where it is applied on the vertical face of a barrier to prevent reverberant build-up of traffic noise due to multiple reflections. Some examples of absorptive treatments for diffraction and reflection problems are given below.

### 3.4.6.1 Treatment around Diffracting Edges

Research showed that for the full improvement in attenuation to be realised, absorbent treatment was only needed within one wavelength of the edge of a rigid screen<sup>94, 95</sup>. Test results on a 4.2m high barrier indicated that, with an effective height of 0.46 m of absorptive material at the top of a barrier, an equivalent noise reduction to that of an additional barrier height of up to 1.1 m could be achieved<sup>96</sup>.

The noise shielding efficiency of different shapes of absorbing obstacles on top of a barrier edge was investigated by modelling and on-site testing. It was concluded that these devices were able to provide improvements of up to 3 dB and are appropriate where an increase in barrier height may not be possible<sup>97, 98, 99, 100, 101</sup>.

It's been shown in the case of T-profile barriers that adding absorptive material on top of the horizontal cap causes certain acoustical gains. The numerical modelling technique presented by Hothersall et al.<sup>102</sup> indicated that the improvement in performance depended on the surface area and the absorptive properties of the treatment being applied. The scale model testing of T – profiled barriers<sup>54</sup> showed improvements of the order of 2 dB in performance due to the use of absorptive materials on the horizontal cap. However, real life testing of T-profile barriers<sup>103</sup> did not reveal a statistically significant difference between the noise reduction produced by the absorptive and reflective configurations. Further full-scale investigations concluded that the addition of absorptive material had a small but statistically significant effect of 0.6 dB on the insertion loss performance of a 1 m wide T-shaped profile at normal incidence<sup>88</sup>. Figure 3.7 shows some practical applications where absorptive materials could be used around the free edges of a barrier.



**Figure 3.7 : Barriers with absorptive treatment, (a) cylindrically capped, (b) mushroom capped, and (c) horizontally louvred barriers**

The beneficial effects of using absorbing materials have also been investigated as part of numerous other multiple-edged and picket type barriers. The benefits of using absorptive materials is generally noted, however there is no agreement on the magnitude of these effects. The long term performance of absorbing materials in outdoor applications is a concern.

### **3.4.6.2 Treatment on Barrier Surface**

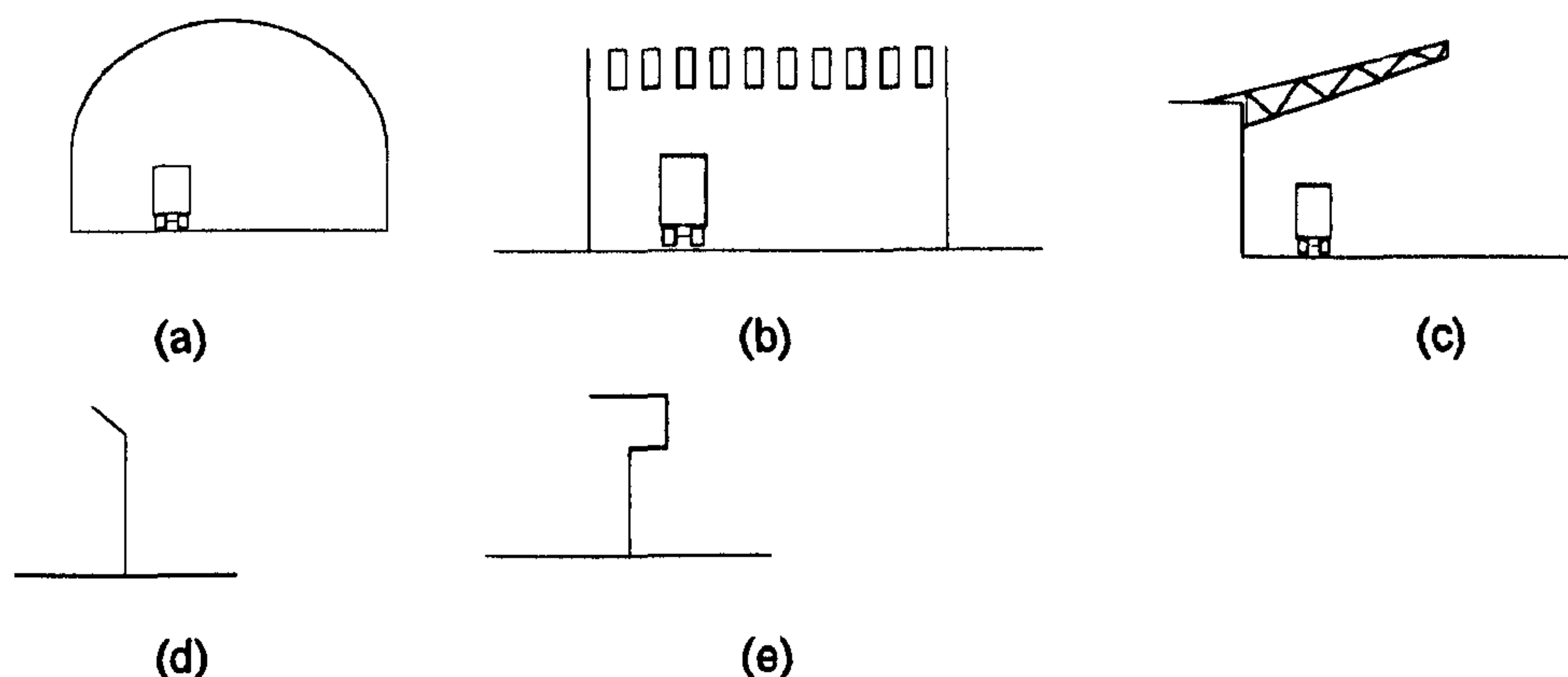
Barriers with absorptive faces have been considered to combat reverberant build-up of traffic noise. This may occur when the traffic is enclosed by reflecting surfaces, for instance, due to the presence of another barrier on the opposite side of the road or high-sided reflective vehicles running close to the barrier. The case of reflections from high-sided vehicles was investigated by 2D analytical modelling<sup>104</sup>. For the configurations considered it was found that multiple reflections significantly degraded performance particularly when the vehicle was higher than the barrier. Use of an absorbing surface on the source side of the barrier was found to restore the attenuation to the levels when no multiple reflections existed. A progressive improvement was observed with an increase in area of the absorber.

The use of absorptive treatment to combat reverberant build-up of traffic noise in parallel barrier configurations was investigated in full scale tests. This investigation indicated that the sound absorptive barriers were effective in counteracting the degradation in single barrier performance resulting from unwanted reflected paths<sup>105</sup>. More recent work however indicated that the measured effects of applying absorptive materials to the roadside barriers were generally less than 1 dB on the  $L_{Aeq}$  and  $L_{A10}$  scales and most recorded changes were not statistically significant<sup>106</sup>.

### **3.4.7 Enclosure Type Barriers**

Tunnels are examples of full enclosure barriers. The internal surfaces of a tunnel may need to be lined with absorptive materials to avoid reverberant build-up of noise. The cost of construction and provision of sufficient ventilation are major non-acoustic considerations in tunnels. There are also partial enclosure solutions such as partially inclined barriers<sup>107</sup>, cantilevered barriers, galleried barriers and louvered covers<sup>81</sup>. These solutions do not have the problems of reverberant build-up or decreased air quality associated with the tunnels. Enclosure and partial enclosure type barriers are illustrated in Figure 3.8.





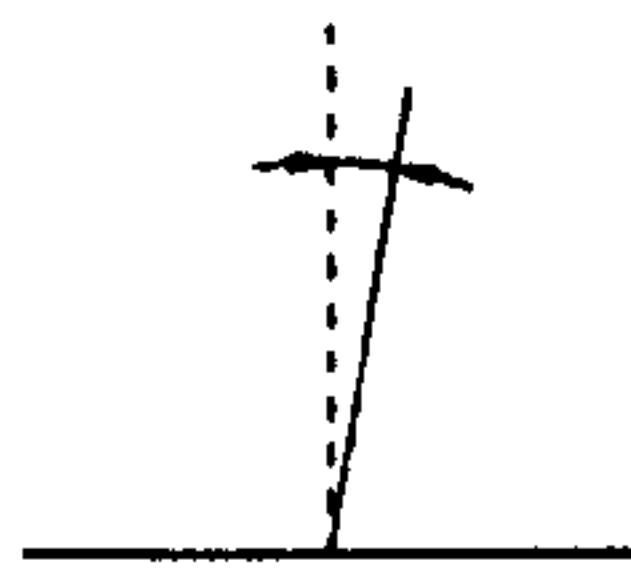
**Figure 3.8 : Enclosure type barriers (a) tunnel, (b) louvered cover, (c) cantilevered barrier, (d), partially inclined barrier, (e) open box section**

### **3.4.8 Bio-Barriers and Vegetation**

The use of vegetation in noise control has been studied as an environmentally and aesthetically alternative to wall type barriers. Wide belts of tall dense trees appear to offer substantial reductions in noise levels of the order of 5-8 dB. However a combination of trees with a solid form of barrier is recommended for effectiveness<sup>108</sup>. It has been shown from field measurements that a dense belt of vegetation 30 m thick, could provide a noise reduction of 6 dB(A)L<sub>10</sub> greater than the same depth of grassland. The effectiveness of the vegetation is greatest close to the road<sup>109</sup>. Bio-barriers, which make use of vegetation combined with an earth mound have also been used due to their smaller space requirement and natural appearance<sup>81, 110</sup>. These may require extensive maintenance.

### **3.4.9 Sloped barriers**

Sloped barriers have been used to overcome multiple reflection problems. The mechanisms for control of the reverberant build-up of traffic noise are similar to those discussed earlier for barriers with absorbing vertical faces. Due to the initial cost of application of the sound absorbing treatments and the requirement for periodic maintenance, the possibility of tilting the barriers backwards, as illustrated in Figure 3.9, was explored as an alternative means of eliminating undesirable reflection paths.



**Figure 3.9 : Sloped noise barrier**

Results show that the performance improved, compared to vertical barriers. The insertion loss increased to a maximum when the angle of the tilt reached 10 degrees and then dropped to lower values as the angle of tilt was increased further<sup>111</sup>. Other research showed that, relatively small angles of tilt can restore almost all of the single barrier insertion loss, counteracting the degradation due to multiple reflections.

The conclusion was that a barrier tilt of 3 degrees for wide roadways are enough but greater angles of 10-15 degrees are required for narrow roadways<sup>112</sup>. Full scale tests supported the observations above<sup>105</sup>. The reverberant build-up depends on the height of the barriers, the separation distance between barriers and the vertical and horizontal location of the source with respect to the barriers.

### **3.4.10 Interference - Based Barriers**

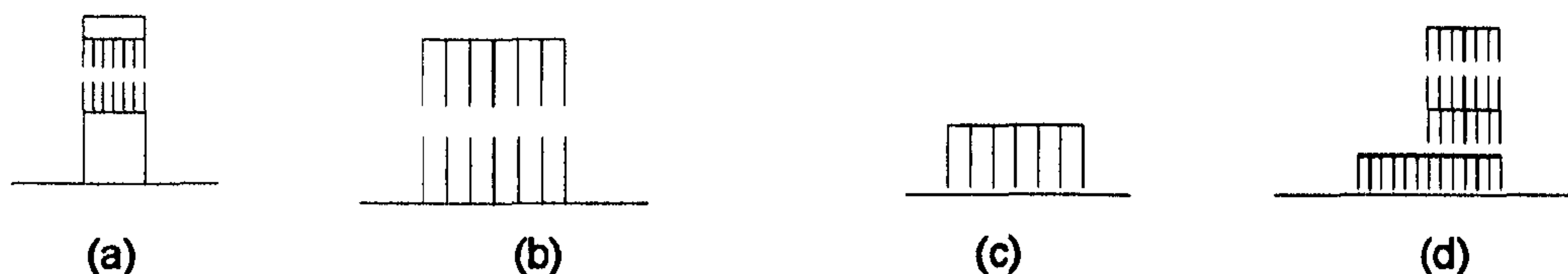
The concept of interference-based barriers was reported by Mizuno et al., where they described a three-sided barrier consisting of hollow passages at an angle to the ground<sup>113, 114</sup> (as seen in Figure 3.10 (a)).



**Figure 3.10 : Interference based noise barriers (source to the left)**

Two adjacent hollow passages have different lengths and the difference between any two adjacent hollow passages is constant. Sound waves are effectively refracted or deflected when passing through this structural phase lag circuit. Top diffracted sound waves interfere with the refracted sound destructively in some areas resulting in noise reduction. The device was developed further and tested at full scale (Figure 3.10 (b)). The maximum reduction in noise levels due to the device was reported to be 6 dB<sup>116</sup>. Further full scale tests concluded that when the additional height of the barrier is taken into account the device provides an estimated gain in average screening performance of 1.9 dB of which 0.7 dB is considered to be due to an interference effect<sup>116</sup>. The primary reason for the noise reduction was considered to be diffraction due to the presence of the back panel.

Barriers containing perforations or openings were reported to have enhanced low frequency performance. Some examples are wave guides<sup>117</sup> and phase reversal barriers<sup>118</sup>, shown in Figure 3.11.



**Figure 3.11 : Phase reversal barriers (a) slow – waveguide, (b) basic dipolar type, (c) halfguide dipolar type, and (d) quadrupolar type**

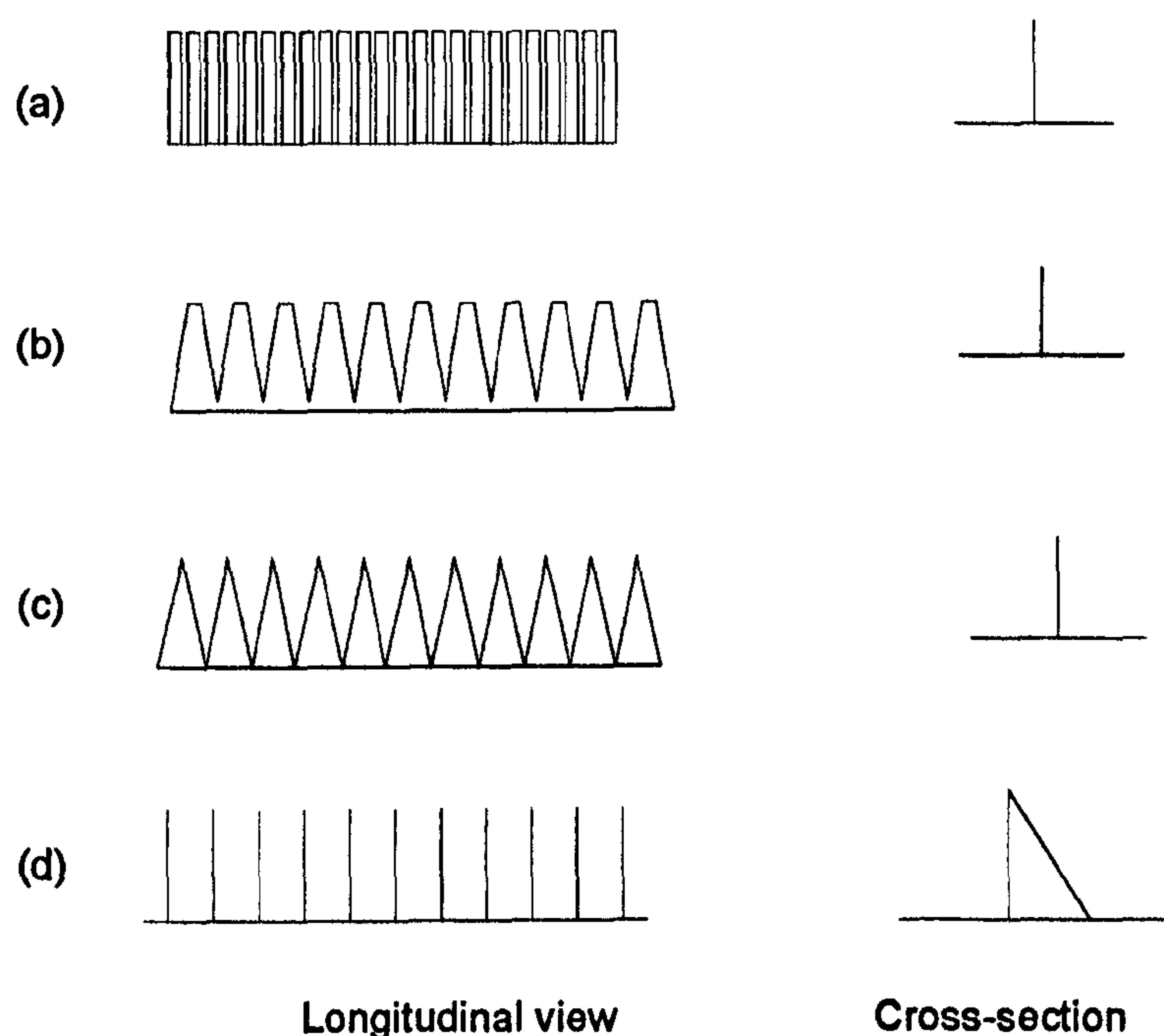
These consist of an open network of rigid stripes which delay the transmitted sound. The sound passing along the rigid stripes propagates more slowly than in free air which results in refraction. The noise reduction is achieved by the destructive interference of the waves going through the openings with the waves diffracted over the top. When compared with a solid barrier, these provided up to 5 dB improvement in performance at low frequencies<sup>118</sup>. Measurements showed that at higher frequencies, degradation of performance was possible and it was suggested that these devices would be better suited to unique and dominant pure tones at low frequencies<sup>117</sup>.

### 3.4.11 Low-height Parallel Walls

Van der Heijden and Martens<sup>119</sup> investigated the possibility of reducing traffic noise by means of a series of parallel low-height walls in the ground. The authors used the term '*rib structure*' or '*parallel ribs*' to describe these low-height parallel walls. Based on a number of theoretical considerations, this rib structure was described to operate by surface wave exclusion. Further discussion of surface waves will be undertaken in the forthcoming chapters. It was reported that attenuations of up to 20 dB at low frequencies was offset by increased noise levels of up to 12 dB at high frequencies. The average insertion loss was found to be around 4 dB(A).

### 3.4.12 Picket Barriers

'Thnadners'<sup>120</sup>, picket barriers<sup>121</sup>, and vertically louvred noise barriers<sup>122</sup> have been investigated as both optically and acoustically open alternatives to barrier design. These are shown in Figure 3.12 and Figure 3.13.



**Figure 3.12 : Longitudinal and cross-sectional views of various picket barriers, (a) picket fence, (b) flat topped picket, (c) saw toothed picket, (d) splitter type picket.**



**Figure 3.13 : Plan view of a vertically louvred barrier (part of whole length)**

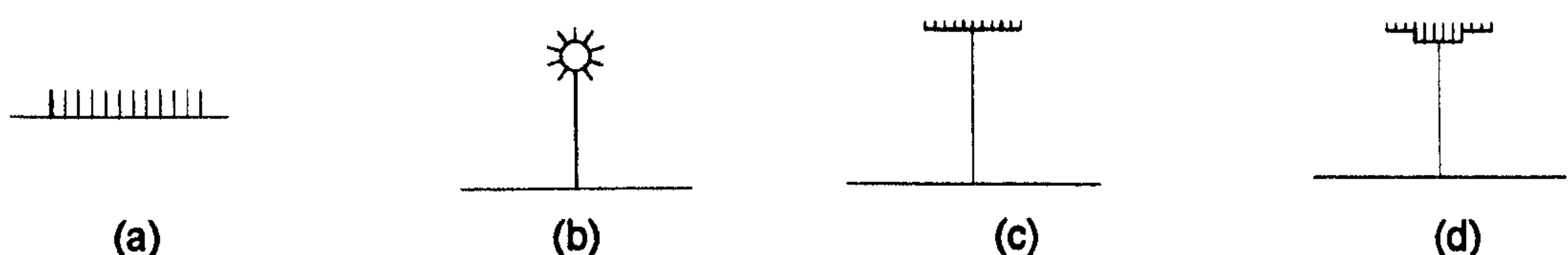
Thnadners<sup>120</sup> create deeper shadow zones by varying amplitude or phase gradients. It was pointed out that if a shadow zone is deepened in one region, sound has to be louder in another and it was suggested this bright region could be designed to be in a relatively harmless direction. Improvements of 1 to 4 dB were reported compared to a reflective barrier with a flat top picket of 25% open area. As the proportion of the open area is increased, as in saw tooth pickets (50%) and splitter panels (85%), the performance was reported to diminish. The main attribute of this profile is its open design which reduces dead weights and, more importantly, wind loading on barrier foundations. These are important considerations when designing noise barriers on top of bridges and similar structures. Wassilieff<sup>121</sup> investigated the performance of picket fences with regular perforations using diffraction theory. The improvement was found to be due to destructive interference of low frequency sound between the sound transmitted through the gaps and that passing over the barrier top. It was found the high frequency performance could be



increased by the use of sound absorbing materials in the gaps. Performance of vertically louvred noise barriers, with varying louver angles, was investigated by models and measurements<sup>122</sup>. Compared with a solid 3m high barrier, a louvred noise barrier with a louver angle of 9°, gave a noise increase of 9.5 dB(A) behind the barrier. Fully absorptive louvers on both the source and receiver side reduced this increase to 3 dB(A). Widening the louver angles reduced the acoustic performance. It was concluded that careful consideration of the compromise in acoustic performance is essential for achieving the best visual transparency.

### 3.4.13 Reactive Barriers

Two recent applications of barriers with reactive surfaces are Waterwheel<sup>123</sup> and T-profile with a reactive surface<sup>53</sup>. A T-shaped barrier with a soft upper surface was shown to produce an improvement of 8.3 dB for all frequencies in the mean insertion loss compared to a plane rigid screen of the same overall height. Measurements in experimental models show smaller gains since in practice the soft surface can not be expected to be equally effective over the whole range of frequencies. The barrier with a "waterwheel" on top of a thin vertical barrier provided 10 dB average improvement in the frequency range it was intended for. These designs consist of a series of tubes, open on one side and rigid at the other, as illustrated in Figure 3.14.



**Figure 3.14 : Barriers with reactive surfaces (a) series of parallel ribs on the ground, (b) waterwheel, (c) constant depth reactive T-capped barrier, and (d) variable depth reactive T-capped barrier.**

The depth of the tubes can be tuned to the quarter wavelength of the resonant frequency to be reduced. These designs appear to have a large potential for noise reduction, however further research is required to establish their acoustic and non-acoustic performance in outdoor environments.

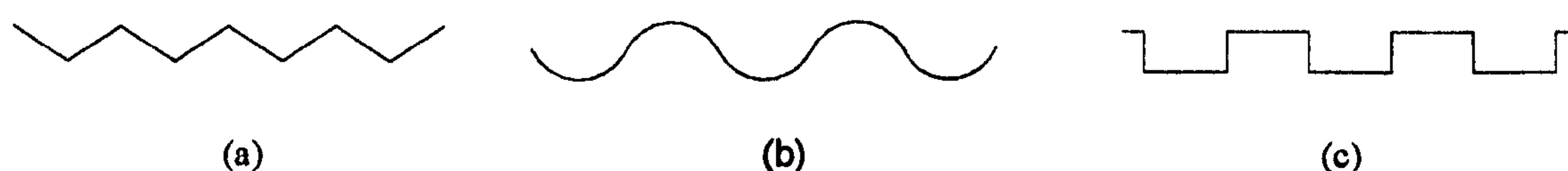
### 3.4.14 Helium- Filled Barriers

Helium filled barrier was investigated as light-weight noise barriers for temporary applications, such as at construction sites or ballistic ranges<sup>124</sup>. This barrier is filled with helium gas which is lighter than air. The waves being transmitted through the barrier are refracted away from it since the sound waves are travelling from a denser medium (air)

into a less dense medium (helium). It was found that this barrier is capable of performing as efficiently as any similar sized barrier over the entire audible frequency spectrum.

### 3.4.15 Dispersive Barriers

Dispersive barriers could present an alternative solution to the problem of performance degradation due to reverberant build-up of traffic noise in parallel barrier configurations or multiple reflections from high-sided vehicles. As shown in Figure 3.15, these barriers have contoured surfaces (zigzag, wavy, castellated) in an attempt to scatter the sound waves which impinge onto the barrier surface in order to prevent unwanted reflections.



**Figure 3.15 : Plan view, showing part of whole length, of (a)zigzag, (b)wave and (c) castellated profiled barriers.**

Gatwick Airport's 11 m high "wave wall" is an example of a noise barrier with a contoured surface<sup>125</sup>. These types of barriers take up more space on the ground compared to thin vertical walls; however they possess aesthetic and structural benefits. The pockets of free space could potentially be used for vegetation to create environmentally friendly and visually interesting designs. Panel elements making up the symmetrical and interlocking structure are inherently self-supporting and this could minimise the foundation requirements.

## 3.5 DISCUSSION

Investigation of barrier performance is generally undertaken by a combination of modelling and full scale testing. Full scale on-site testing gives the true performance of a barrier. However, the need to monitor many variables in an outdoor environment and the time required to undertake representative testing can make this method very expensive. Therefore, before undertaking any on-site testing, modelling techniques are generally employed, which provide well - controlled test environments. In this way, barrier profiles likely to perform better than others can be identified. For instance, if modelling has not yielded substantial differences between the performances of two barrier types, there may not be any need for on-site testing since these small differences will probably be masked by external factors such as atmospheric effects.

Modelling can be carried out using physical scale models. This is a useful technique for appreciating the practicalities of a problem. The fundamentals of the technique are relatively simple for most classes of acoustic phenomena. However, it may not always be an accessible tool due to the requirements for specialist equipment and testing rooms. Analytical modelling, on the other hand, offers a convenient method for investigating different profiles easily. Underlying assumptions and simplifications in an analytical model may make it less accurate than physical scale modelling. Data preparation and computation times can be an issue depending on the complexity of the model being considered.

There has been extensive research on a variety of noise barrier profiles using the above investigation techniques. Early studies have looked at diffraction over a barrier top which is an important factor in determining performance. However multiple diffractions, multiple reflections, scattering, interference, absorption and refraction have all been shown to play a significant role. Therefore simple geometrical diffraction methods may not adequately describe the relative barrier performance. Numerical wave-based methods, such as boundary element methods, have emerged as efficient tools for assessing complex barrier geometries and ground in a homogeneous atmosphere. The absolute performance of barriers is very much dependent on atmospheric effects and these have been investigated using numerical methods such as parabolic equations and substitute-sources.

## **3.6 CRITICAL APPRAISAL**

A detailed review of the literature on noise barriers identified a number of areas which required further attention. This section will look into these to determine the course of work in the forthcoming chapters.

### **3.6.1 Barrier Design**

The main document providing guidance on the design of environmental barriers in the U.K. does not incorporate many of the practical aspects of barrier design discussed earlier. The guidance on different barrier profiles is not encouraging for the designer. Details on acoustic performance are scarce and novel barrier profiles which are promising in real life applications are mentioned in passing. The shortcomings of this method will be highlighted further in the forthcoming chapters. The most visible gap in the field is the requirement for a simple method for the selection of noise barriers.



The parameters involved in the design of environmental barriers show that there are a limited number of ways to increase the performance of a barrier. The source and receiver configurations, and the frequency content of the traffic noise are beyond the control of a designer. The transmission loss through a barrier or the overall length of a barrier are simply the minimum design requirements. Barrier height is an obvious choice in enhancing the performance of a barrier, but due to structural and aesthetic reasons, the height can not be increased at will so as to increase the path length travelled by the sound. Therefore the edge conditions are particularly important and realistically have the potential to have an impact on the performance of a barrier. Any attempt to enhance the performance of a barrier should therefore focus on developing a new profile with an alternative edge condition.

### **3.6.2 Methods for Investigating Barrier Performance**

The three main methods for investigating barrier performance were identified as numerical and physical modeling as well as on-site measurements. The methodology to be adopted for this work will be determined in Chapter 5, after discussing the findings of investigations using some of these techniques.

### **3.6.3 Way Forward**

The up-to-date research reviewed in this chapter, using mathematical and physical modelling techniques as well as on-site measurements, showed that barriers with multiple diffracting edges are likely to be the most efficient designs. Recent work revealed that barriers with reactive surfaces are equally promising if not superior. However, attention in both cases was given to the applications involving the wall type barriers. Categorical refusal to try to incorporate these modifications in environmentally sensitive designs, such as earth barriers, is a question which awaits an answer. The wall type barriers have established themselves as effective noise control devices in congested urban environments. However environmentally sensitive areas with a rural or semi-urban surroundings demand differing solutions. Factors affecting the decision for implementing a solution are not solely acoustics. Traditionally, noise solutions for such surroundings have been the earth barriers. Apart from combining them with conventional barriers, there have not been any attempts to enhance their performance further without increasing their overall height or diminishing their aesthetic appeal. Also such solutions would have implications for a shorter earth barrier requirement for a similar performance. Considering that the amount of material required for their construction and the horizontal land-take can be the



two factors which restrict their use, this could make the earth barriers clear favourites in noise control solutions in certain sensitive environments.

### **3.7 CONCLUSIONS AND RECOMMENDATIONS FOR FUTURE WORK**

A comprehensive review of the up-to-date work carried out on environmental barriers has been undertaken which covered both theory and practice. This has helped identify the aspects of problems needing further attention and informed the discussion of various research methods described in the forthcoming chapters in order to identify the most suitable one to be used for this research project for addressing these problems. This review of previous research revealed a number of areas which need further attention. These are related to the performance as well as the design of barriers.

- **The mechanisms of reverberant build-up of traffic noise** need to be studied further. Degradation of barrier performance due to multiple reflections in parallel barrier situations is generally agreed on, in qualitative terms. There is some disagreement as to the magnitude of this performance loss, especially on-site. The case of reflections from high-sided reflective vehicles running close to a barrier, which potentially could have even bigger adverse impacts, need to be validated with on-site measurements under real traffic situations.
- **Dispersive barriers** and their applicability to multiple reflection problems deserve further attention. Sloped and absorbing barriers have been considered as possible solutions. In practice, the long-term performance of absorptive treatment is a real concern. The use of sloping barriers may not be an adequate solution in situations where there are high rise buildings near the road. Therefore, dispersive barriers could be considered as alternatives. These could be designed to have the added benefit of visual interest.
- **Reactive barriers** have been shown to provide substantial improvement over conventional barriers. Their applicability on their own (by the roadside, or on central reservations) or possibly on short height structures (small bunds, garages etc) needs to be investigated. Their performance when used in conjunction with absorbing surfaces (i.e. on top of earth mounds with substantial grass-covered slopes), or scattering bodies (i.e. with vegetation) is not known.
- **Open barriers**, both due to visual and structural considerations, have some advantages. Initial findings indicated their reduced acoustic effectiveness

compared with a conventional barrier. More work is required to determine the acoustic compromise which may be expected in situations where conventional noise barriers would not be applicable.

- The use of **multiple diffracting edges and absorbing obstacles** on top of conventional barriers has been reported to have beneficial effects on barrier performance. These are reported to give improvements of up to 4 dB. Further measurements need to be undertaken to confirm the range of validity of these observations.
- **Earth mounds combined with conventional noise barriers** are commonly used in practice. However, there are conflicting findings that the presence of a noise barrier on top a mound may interfere with the beneficial ground effect. This needs to be quantified to determine the optimum barrier height that will maximise both ground absorption and additional barrier diffraction.
- **Single number indicators** used for defining barrier performance do not accurately represent the response of the public to traffic noise problems. Lack of sufficient information on subjective response to frequency content of noise prevents the ground effects from being taken into account adequately and prohibits the use of **interference based barriers**. Barriers could be designed to use destructive interference for reducing noise at selected frequencies.
- Generally the role of consultation with the public at the early design stage is acknowledged as being vital for the success of any noise barrier solution. However, the subjective response of the public to the **perceived effectiveness** of different noise barriers based on non-acoustic factors is not well established.
- Clearly the true performance of any barrier depends heavily on the influence of the **ground, the atmosphere** and reflective surfaces in built-up areas. Further work on the on-site performance of barriers is required to validate their performance under carefully monitored outdoor conditions over a wide range of distances.
- There is a need for accurate and efficient **numerical models** to assess the barrier-ground-atmosphere interaction. Reliable and accessible computer-based tools could help more effective barrier solutions to be developed and, in the long term, could reduce the need for on-site measurements.
- Whilst a barrier may not be suitable in some cases it may offer the most favourable solution in a specific situation. **Advice** is needed on all the acoustic and non-acoustic aspects of alternative barrier types. This would help practitioners make an

informed decision based on the knowledge of the advantages and limitations of a barrier.

A great deal of theoretical work has been done on the modelling and performance prediction of barriers, especially on those designed for the urban context. The information on the actual on-site performance of barriers is not as detailed, or rather, accessible, even though the noise barriers are now widely used traffic noise reducing tools across the developed countries of the world. The most obvious gap in the knowledge appears to be the missing link between the theory and practice, to incorporate the latest findings of research into real life. There is a need for simple and practical guidelines to offer substantial advice to inexperienced designer. There is also a need for alternative noise barrier solutions which address the wider environmental issues more effectively. These are addressed in the next chapter.

- 
- <sup>1</sup> High Performance Acoustic Barriers In The UK, Highways and Transportation, 43(5), 7-12, May 1996,
- <sup>2</sup> NELSON, P.M., UNDERWOOD, M.C.P., Lorry Tyre Noise, Vehicle Noise and Vibration Conference, IMechE, Paper C139/84, London, 21-30, 1984
- <sup>3</sup> SANDBERG, U., A Road Surface for Reduction of Tire Noise Emission, The International Conference on Noise Control Engineering, Inter-Noise 79, Warszawa-Poland, September 11-13, 517-520, 1979
- <sup>4</sup> MEIARASHI, S., ISHIDA, M., FUJIWARA, T., HASEBE, M., NAKATSUJI, T., Noise Reduction Characteristics of Porous Elastic Road Surfaces, Applied Acoustics, Vol 47, No. 3, 239-250, 1996
- <sup>5</sup> CAMOMILLA, G., MALGARINI, M., GERVASIO, S., Sound Absorption and Winter Performance of Porous Asphalt Pavement, Transportation Research Record 1265, Porous Asphalt Pavements: An International Perspective, 1-8, 1990
- <sup>6</sup> PHILLIPS, S., NELSON, P., ABBOTT, P., Reducing Noise From Motorways: The Acoustic Performance of Porous Asphalt on The M4 at Cardiff, Technical Contribution, Acoustics Bulletin, 13-20, September / October 1995
- <sup>7</sup> NELSON, P.M. and ROSS, N.F., Noise From Vehicles Running on Open Textured Road Surfaces, Transport and Road Research Laboratory, TRRL Supplementary Report 696, Department of the Environment, Department of Transport, 1981
- <sup>8</sup> SANDBERG, U., Action Plan Against Exterior Tyre/Road Noise, Inter-Noise 93, Leuven-Belgium, August 24-26, 635-640, 1993
- <sup>9</sup> WOODSIDE, A.R., WOODWARD, W.D.H., ANDERSON, G., Reducing Road Traffic Noise by Altering the Surface Texture, Pro. 2nd European Symposium, Performance and Durability of Bituminous Materials, Leeds, 617-630, April 1997,
- <sup>10</sup> European Commission Green Paper, Future Noise Policy, COM(96) 540, Brussels, November 1996
- <sup>11</sup> WATTS, G.R., CHANDLER-WILDE, S.N., MORGAN, P.A., The combined effects of porous asphalt surfacing and barriers on traffic noise, Applied Acoustics, 58, 351-377, 1999



- 
- <sup>12</sup> SOMMERFELD, A., Mathematische Theorie der Diffraction, Math. Ann. 47, 317-374, 1896
- <sup>13</sup> MACDONALD, H.M., A Class of Diffraction Problems, Proc. London Math. Soc., 14, 410-427, 1915
- <sup>14</sup> REDFERN, S.W., Some Acoustical Source-Observer Problems, Philo. Mag. J. Sci., Ser 7, Vol. 30, No. 200, 223-236, 1940
- <sup>15</sup> FEHR, R.O., The Reduction of Industrial Machine Noise, Proceedings of Second Annual Noise Abatement Symposium, 93-103, October 1951
- <sup>16</sup> MAEKAWA, Z., Noise Reduction by Screens, Memoirs of The Faculty of Engineering, Kobe University, No. 11, 29-53, 1965
- <sup>17</sup> MAEKAWA, Z., Noise Reduction by Screens, Applied Acoustics, 1, 157-173, 1968
- <sup>18</sup> DELANY, M. E., A practical scheme for predicting noise levels (L10) arising from road traffic, National Physics Laboratory, Department of Trade and Industry, Acoustics Report Ac57, July 1972
- <sup>19</sup> TATGE, R.B., Barrier-wall attenuation with a finite-sized source, J.Acoust.Soc.Am., 53, 1317-1319, 1973
- <sup>20</sup> YAMAMOTO, K. and TAKAGI, K., Expression of Maekawa's Chart for Computation, Applied Acoustics, 37, 75-82, 1992
- <sup>21</sup> KURZE, U.J. and ANDERSON, G.S. Sound Attenuation By Barriers, Applied Acoustics, Vol. 4, 35-53, 1971
- <sup>22</sup> RATHE, E.J., Note on Two Common Problems of Sound Attenuation, J.Sound Vib., 10(3), 472-479, 1969
- <sup>23</sup> FUJIWARA, K., ANDO, Y., MAEKAWA, Z., Noise Control By Barriers - Part 1: Noise Reduction By A Thick Barrier, Applied Acoustics, Vol. 10, 147-159, 1977
- <sup>24</sup> FUJIWARA, K., ANDO, Y., MAEKAWA, Z., Noise Control By Barriers - Part 2: Noise Reduction By An Absorptive Barrier, Applied Acoustics, Vol. 10, 167-179, 1977
- <sup>25</sup> MEDWIN, H., Shadowing by finite noise barriers, J.Acoust.Soc.Am., 69(4), 1060-1064, April 1981
- <sup>26</sup> HADDEN, W.J. and PIERCE, A.D., Sound diffraction around screens and wedges for arbitrary point source locations. J.Acoust.Soc.Am., 69(5), 1266-1276, 1981

- 
- <sup>27</sup> MAEKAWA, Z. and OSAKI, S., A Simple Chart for the Estimation of the Attenuation by a Wedge Diffraction, *Applied Acoustics*, Vol. 18, 1985, 355-368
- <sup>28</sup> PIERCE, A.D., Diffraction of sound around corners and over wide barriers, *J.Acoust.Soc.Am*, Vol. 55, No. 5, 941-955, May 1974
- <sup>29</sup> KAWAI, T., Sound diffraction by many-sided barrier or pillar, *J. of Sound & Vib.*, 79(2), 229-242, 1981
- <sup>30</sup> YUZAWA, M., SONE, T., Noise Reduction By Various Shapes of Barrier, *Applied Acoustics*, Vol. 14, 1981, 65-73
- <sup>31</sup> ISEI, T., EMBLETON, T.F.W., and PIERCY, J.E., Noise Reduction by Barriers on Finite Impedance Ground, *J.Acoust.Soc.Am.*, 67(1), 46-58, January 1980
- <sup>32</sup> KOERS, P., Diffraction by An Absorbing Barrier or By an Impedance Transition, *Inter-Noise 83*, 1983, 311-314
- <sup>33</sup> L'ESPERANCE, A., NICOLAS, J., DAIGLE, G.A., Insertion loss of absorbent barriers on ground, *J. Acoust. Soc. Am.*, 86(3), September 1989, 1060-1064
- <sup>34</sup> L'ESPERANCE, A., The insertion loss of finite length barriers on the ground, *J.Acoust.Soc.Am.*, 86(1), July 1989, 179-183
- <sup>35</sup> LEANG, L.K., YAMASHITA, Y., MATSUI, M., Simplified calculation method for noise reduction by barriers on the ground, *J.Acoust.Soc.Jpn (E)*, Vol. 11, No. 4, 199-206, 1990
- <sup>36</sup> LAM, Y.M. and ROBERTS, S.C., A simple method for accurate prediction of finite barrier insertion loss, *J.Acoust.Soc.Am.*, 93(3), March 1993, 1445-1452
- <sup>37</sup> LAM, Y.W., Using Maekawa's Chart to Calculate Finite Length Barrier Insertion Loss, *Applied Acoustics*, Vol. 42, 29-40, 1994
- <sup>38</sup> MURADALI, A., and FYFE, K.R., A Study of 2D and 3D Barrier Insertion Loss using Improved Diffraction-based Methods, *Applied Acoustics*, Vol. 53, No 1-3, 49-75, 1998
- <sup>39</sup> SALOMONS, E., GEERLINGS, A.C., and DUHAMEL, D., Comparison of a Ray Model and a Fourier - Boundary Element Method for Traffic Noise Situations with Multiple Diffractions and Reflections, *Acustica - Journal of European Acoustics Association*, Vol. 83, No 1, 35-47, 1997
- <sup>40</sup> SEZNEC, R., Diffraction of Sound Around Barriers : Use of The Boundary Elements Technique, *Journal of Sound and Vibration*, 73(2), 195-209, 1980

- 
- <sup>41</sup> FYFE, K.R., and HARRISON, C.C., Modelling of Road Noise Optimal Barrier Design, Canada Mortgage and Housing Corporation, CMCH CR File 6585-F039, March 1995
- <sup>42</sup> CISKOWSKI, R.D., and BREBBIA, C.A., (Editors), Boundary Element Methods in Acoustics, Computational Mechanics Publications and Elsevier Applied Science (co-publishers), ISBN 1-85312-104-5 Computational Mechanics Publications, Southampton, 1991
- <sup>43</sup> ATTENBOROUGH, K., et al., Benchmark Cases for Outdoor Propagation Models, J.Acoust.Soc.Am., 97(1), 173-191, January 1995
- <sup>44</sup> SALOMONS, E.M., Diffraction by a Screen in Downward Sound Propagation: A Parabolic-equation Approach, J.Acoust.Soc.Am., Vol. 95, No. 6, 3109-3117, 1994
- <sup>45</sup> FORSSEN, J., Calculation of Sound Reduction by a Screen in a Turbulent Atmosphere Using the Parabolic Equation Method, Acustica - Acta Acustica, Vol. 84, 599-606, 1998
- <sup>46</sup> FORSSEN, J., Calculation of noise barrier performance in a turbulent atmosphere by using substitute sources above the barrier. Acustica - Acta Acustica, Vol. 86, 269-275, 2000
- <sup>47</sup> FORSSEN, J., Calculation of noise barrier performance using the substitute-sources method for a three-dimensional turbulent atmosphere, Acustica - Acta Acustica, Vol. 88, 181-189, 2002
- <sup>48</sup> FORSSEN, J. and OGREN, M., Barrier noise reduction in the presence of atmospheric turbulence: Measurements and numerical modelling, Applied Acoustics, Vol. 63, 173-187, 2001
- <sup>49</sup> SALOMONS, E.M., Downwind propagation of sound in an atmosphere with a realistic sound-speed profile: A semi-analytical ray model, J.Acoust.Soc.Am., Vol. 95, No. 5, 2425-2436, 1994
- <sup>50</sup> MURADALI, A. and FYFE, K.R. Accurate Barrier Modelling in the Presence of Atmospheric Effects, Applied Acoustics, 56, 1999, 157-182
- <sup>51</sup> LYON, R.H., and CANN, R.J., Acoustical Modelling in Urban Environments, Inter-noise 74, Washington, D.C., September 30 - October 2, 1974, 457-460
- <sup>52</sup> ANDERSON, J.S., BRATOS-ANDERSON, M., Noise Its Measurement, Analysis, Rating and Control, ISBN 0 291 39794 8, Published by Avebury Technical, 1993, 246-252



- 
- <sup>53</sup> FUJIWARA, K., HOTHERSALL, D.C., KIM, C., Noise Barriers with Reactive Surfaces, *Applied Acoustics*, Vol. 53, No. 4, 1998, 255-272
- <sup>54</sup> MAY, D.N. and OSMAN, M.M., Highway Noise Barriers: New Shapes, *Journal of Sound and Vibration*, 71(1), 1980, 73-101
- <sup>55</sup> DE JONG, R. and STUSNICK, E., Scale Model Studies of the Effects of Wind on Acoustic Barrier Performance, *Noise Control Engineering*, Volume 6, Number 3, May-June 1976, 101-109
- <sup>56</sup> VAN RENTERGHEM, T., BOTTELDOOREN, D., CORNELIS, W.M., and GABRIELS, D., Reducing Screen-Induced Refraction of Noise Barriers in Wind by Vegetative Screens, *Acustica - Acta Acustica*, Vol. 88, 231-238, 2002
- <sup>57</sup> HUTCHINS, D.A., JONES, H.W., and RUSSELL, L.T., Model Studies of Barrier Performance in The Presence of Ground Surfaces. Part I - Thin, Perfectly Reflecting Barriers, *J.Acoust.Soc.Am.*, 75(6), June 1984, 1807-1816
- <sup>58</sup> HAYEK, S.I., Noise Reduction by Absorbent Double Parallel Barriers Over Hard Ground, *Inter-noise 85*, Munich, 18-20 September, 1985, 495-498
- <sup>59</sup> NOVAK, J., Scale Model Measurements of Insertion Loss of Road Traffic Noise Barriers, *Proceedings of the 31st International Acoustical Conference, High Tatras 97*, European Acoustics Association (EAA) Symposium, 1997, 112-113
- <sup>60</sup> PIRINCHIEVA, R., Model Study of the Sound Propagation Behind Barriers of Finite Length, *J.Acoust.Soc.Am.* 87(5), May 1990, 2109-2113
- <sup>61</sup> TAKAGI, K., HOTTA, R., and YAMAMOTO, K., A Simple Method for The Calculation of Noise Attenuation by A Finite Length Barrier, *Applied Acoustics*, 43, 1994, 353-365
- <sup>62</sup> YAMASHITA, M., and YAMAMOTO, K., Scale Model Experiments for the Prediction of Road Traffic Noise and the Design of Noise Control Facilities, *Applied Acoustics*, 31, 1990, 185-196
- <sup>63</sup> HOTKA, M., Propagation of Road Traffic Noise Over Non-Flat Ground, *Proceedings of the 31st International Acoustical Conference, High Tatras 97*, European Acoustics Association (EAA) Symposium, 1997, 104-105
- <sup>64</sup> HUTCHINS, D.A., JONES, H.W., and RUSSELL, L.T., Model Studies of Barrier Performance in The Presence of Ground Surfaces. Part II - Different Shapes, *J.Acoust.Soc.Am.*, 75(6), June 1984, 1817-1826



- 
- <sup>65</sup> COHN, L.F., and HARRIS, R.A., Special Noise Barrier Applications, Phase III, Final Report, WA - RD 378.3, prepared for Washington State Department of Transportation, U.S. Department of Transportation and Federal Highway Administration, January 1996, p. 5
- <sup>66</sup> PIRINCHIEVA, R.K., The Influence of Barrier Size on Its Sound Diffraction, Journal of Sound and Vibration, 148(2), 1991, 183-192
- <sup>67</sup> HAJEK, J.J. and BLANEY, C.T., Evaluation of T – Profile Highway Noise Barriers, Transportation Research Record 983, Issues in Transportation Noise Mitigation: Highway and Railway Studies, 1984, 8-17
- <sup>68</sup> KOYASHU, M. and YAMASHITA, M., Scale Model Experiments on Noise Reduction By Acoustic Barrier of A Straight Line Source, Applied Acoustics, Vol. 6, 233-242, 1973
- <sup>69</sup> SCHOLLES, W.E., SALVIDGE, A.C., and SARGENT, J.W., Field Performance of A Noise Barrier, Journal of Sound and Vibration, 16(4), 627-642, 1971
- <sup>70</sup> WATTS, G.R. Acoustic Performance of a Multiple Edge Noise Barrier Profile at Motorway Sites, Applied Acoustics, Vol 47, 1996, 47-66
- <sup>71</sup> YAMAMOTO, K., TAYA, K., YAMASHITA, M., and KATSUNORI, T., Reduction of Road Traffic Noise by Absorptive Cylinder Adapted at The Top of A Barrier, Inter-noise 89, Newport Beach, CA, USA, December 4-6, 349-352, 1989
- <sup>72</sup> ANFOSSO-LEDEE, F., STEIMER, V. and DEMIZIEUX, P., In-situ Methods for Characterisation of Road Noise Barriers Efficiency, Proceedings of Inter-Noise 2000, Nice – France , August 27-30, Volume 1, 499-504, 2000
- <sup>73</sup> WATTS, G., Factors Affecting the Performance of Traffic Noise Barriers, Proceedings of Inter-Noise 2000, August 27-30, Volume 1, 515-520, 2000
- <sup>74</sup> The Highways Agency, Design Manual for Roads and Bridges, Volume 10, Section 5, Part 2, HA 66/95 - Environmental Barriers: Technical Requirements HMSO, 1995
- <sup>75</sup> Highway Traffic Noise Analysis and Abatement Policy and Guidance, U.S. Department of Transportation, Federal Highway Administration Office of Environmental and Planning, Noise and Air Quality Branch, Washington, D.C., June 1995
- <sup>76</sup> Calculation of Road Traffic Noise, Department of Transport, Welsh Office, HMSO, London, 1988

- 
- <sup>77</sup> WATTS, G. Acoustic Performance of Traffic Noise Barriers. A State-of-The-Art Review, Euro symposium 1992, The Mitigation of Traffic Noise in Urban Areas, 219-246, 1992
- <sup>78</sup> WATTS, G.R., Noise Barrier Optimisation, Acoustic Barriers – The Engineered Solution to Road and Rail Noise Pollution, Seminar organised by the environmental engineering group of the Institution of Mechanical Engineers, 1-6, 1990
- <sup>79</sup> MARTIN S.J., and HOTHERSALL D.C., Performance of Median Noise Barriers, Proceedings of Inter-Noise 2000, Nice – France , August 27-30, 489-492, 2000
- <sup>80</sup> ROCCHI, S.E. and PEDERSEN, S., Feasibility of Transparent Noise Barriers, Transportation Research Record 1255, Washington DC, 87-93, 1990
- <sup>81</sup> KOTZEN, B. and ENGLISH, C., Environmental Noise Barriers: A guide to their acoustic and visual design, E & FN SPON, 1999
- <sup>82</sup> HAJEK, J.J., Are Earth Berms Acoustically Better Than Thin-Wall Barriers?, Transportation Research Record, No. 896, Washington, D.C., 60-67, 1982
- <sup>83</sup> DAIGLE, G.A. (convenor of working party), Report by the International Institute of Noise Control Engineering Working Party on the Effectiveness of Noise Walls, Noise/News International, 13-35, 1998
- <sup>84</sup> BOUGDAH, H., and EKICI, I., An Experimental Investigation Into Acoustic Performance of Earth Mounds Combined with Short Noise Barriers, Proceedings of Inter-Noise 2000, Nice – France, 27-30 August 2000, Volume 3, 1455-1458, 2000
- <sup>85</sup> COHN, L.F., Highway Noise Barriers, National Cooperative Highway Research Program, Synthesis of Highway Practice 87, Transportation Research Board, Washington DC, 1981
- <sup>86</sup> CROMBIE, D.H., PELOW, A.T., CHANDLER-WILDE, S.N. and HOTHERSALL, D.C. Multiple Road Traffic Noise Barriers, Proc. I.O.A., Volume 13, Part 1, 1991, 27-34
- <sup>87</sup> HOTHERSALL, D.C. Modelling The Performance of Noise Barriers, Euro symposium 1992, The Mitigation of Traffic Noise in Urban Areas, 247-258, 1992
- <sup>88</sup> WATTS, G.R., CROMBIE, D.H. and HOTHERSALL, D.C. Acoustic Performance of New Designs of Traffic Noise Barriers: Full Scale Tests, Journal of Sound and Vibration, 177(3), 1994, 289-305
- <sup>89</sup> ALFREDSON, R.J., DU, X., Special Shapes And Treatment For Noise Barriers, Inter-Noise 95, Newport Beach, CA, USA, July 10-12 1995, 381-384

- 
- <sup>90</sup> SHIMA, H., WATANABE, T., YOKOI, T., MIZUNO, K., MATSUMOTO, K., YAMAMOTO, M., MIYAMA, T., Branched Noise Barriers, Inter-Noise 98, Christchurch, New Zealand, November 16-18 1998, 403-406
- <sup>91</sup> HO, S.S.T., BUSH-VISHNIAC, I.J., and BLACKSTOCK, D.T., Noise Reduction by A Barrier Having Random Edge Profile, J.Acoust.Soc.Am., 100(5), pt 1, 1997, 2669-2676
- <sup>92</sup> MENOUNOU, P. and BUSCH-VISHNIAC, I.J., Jagged Edge Noise Barriers, Building Acoustics, Vol. 7, No. 4, 2000, 179-200
- <sup>93</sup> SHAO, W, LEE, H.P. and LIM, S.P., Performance of noise barriers with random edge profiles, Applied Acoustics, Vol. 62, 2001, 1157-1170
- <sup>94</sup> BUTLER, G.F. A note on Improving The attenuation Given By A Noise Barrier, Journal of Sound and Vibration, 32(3), 1974, 367-369
- <sup>95</sup> RAWLINS, A.D. Diffraction of Sound by a Rigid Screen With A Soft or Perfectly Absorbing Edge, Journal of Sound and Vibration, 45(1), 1976, 53-67
- <sup>96</sup> GHARABEGIAN, A. Improving Sound wall Performance Using Route Silent, Inter-Noise 95, Newport Beach, CA, USA, 1995 July 10-12, 385-388
- <sup>97</sup> FUJIWARA, K. and FURUTA, N. Sound Shielding Efficiency of a Barrier With a Cylinder at The Edge, Noise Control Engineering Journal, July-August 1991, Volume 37, Number 1, 1991, 5-11
- <sup>98</sup> YAMAMATO, K., YAMASHITA, M., YOSHIDA, SHONO, Y., Application of Noise Abatement Devices At The Top of Highway Noise Barrier, Inter-Noise 95, Leuven-Belgium, August 24-26, 1993, 1719-1722
- <sup>99</sup> FUJIWARA, K., OHKUBO, T., OMOTO, A. A., Note On The Noise Shielding Efficiency Of A Barrier With Absorbing Obstacle At The Edge , 393-396, Inter-Noise 95, Newport Beach, CA, USA ,1995 July 10-12
- <sup>100</sup> YAMAMOTO, K., SHONO, Y., OCHIAI, H., HIRAO, Y, Measurements of Noise Reduction By Absorptive Devices Mounted At The Top of Highway Noise Barriers, Inter-Noise 95, Newport Beach, CA, USA, 1995, July 10-12, 389-392
- <sup>101</sup> MATSUMOTO, T., YAMAMOTO, K., and ISHIKITA, H., Efficiency of Highway Noise Barrier With Horizontal Louver – A Study by Full Scale Model Experiment, Proceedings of Inter-Noise 2000, Nice – France , August 27-30, 511-514, 2000

- 
- <sup>102</sup> HOTHERSALL, D.C. ,CROMBIE, D.H. and CHANDLER-WILDE, S.N. (1991) The performance of T-Profile and Associated Noise Barriers, *Applied Acoustics*, 32, 269-287, 1991
- <sup>103</sup> MAY, D.N., OSMAN, M.M. The performance of sound absorptive, reflective and T-profile noise barriers in Toronto, *J.Sound Vibration*, 71 (1980), 65-71
- <sup>104</sup> HOTHERSALL, D.C. and TOMLINSON, S.A. High-Sided Vehicles and Road Traffic Noise Barriers, *Acoustics Bulletin*, July / August 1996
- <sup>105</sup> WATTS, G.R. Acoustic Performance of Parallel Traffic Noise Barriers, *Applied Acoustics*, Vol 47, No 2, 95-119, 1996
- <sup>106</sup> WATTS, G.R. and GODFREY, N.S., Effects on roadside noise levels of sound absorptive materials in noise barriers, *Applied Acoustics* 58, 1999, 385-402
- <sup>107</sup> JIN, B.J., KIM, H.S., KANG, H.J., and KIM, J.S. Sound Diffraction by a partially inclined noise barrier, *Applied Acoustics*, 62, 2001, 1107-1121
- <sup>108</sup> COOK, D.I., Role of Plant Materials In Traffic Noise Control, *Transportation Research Record 789, Environmental Issues in Transportation: Analysis, Noise and Air Quality*, Washington DC, 35-40, 1981
- <sup>109</sup> HUDDART, L., The Use of Vegetation for Traffic Noise Screening, *TRRL, Research Report 238*, 1990
- <sup>110</sup> Building the Sound Barrier, *Surveyor*, 183(5393), 20 June 1996, 22-23
- <sup>111</sup> MENGE, C.W. (1978), Sloped Barriers For Highway Noise Control, *Inter-Noise 78*, 509-512
- <sup>112</sup> SLUTSKY, S. and BERTONI, H.L., Analysis and Programs for Assessment of Absorptive and Tilted Parallel Barriers, *Transportation Research record 1176*, 1988, 13-22
- <sup>113</sup> MIZUNO, K., SEKIGUCHI, H., IIDA, K., Research on a Noise Control Device, 1st Report, *Bulletin of Japanese Society of Mechanical Engineers*, Vol. 27, No 229, July 1984, Paper No 229-25, 1499-1505
- <sup>114</sup> MIZUNO, K., SEKIGUCHI, H., IIDA, K., Research on a Noise Control Device, 2nd Report, *Bulletin of Japanese Society of Mechanical Engineers*, Vol. 28, No 245, November 1985, Paper No 245-33, 2737-2743



- 
- <sup>115</sup> IIDA, K., KONDOH, Y. and OKADO, Y. Research on a Device for Reducing Noise, Transportation Research Record 983 ,Washington DC, 1984, 51-54
- <sup>116</sup> WATTS, G.R. and MORGAN, P.A. Acoustic Performance of an Interference-Type Noise-Barrier Profile, Applied Acoustics, 1996, Vol. 49, No 1, 1-16
- <sup>117</sup> NICHOLAS, J. and DAIGLE, G.A., Experimental study of a slow-wave guide barrier on finite impedance ground, J.Acoust.Soc.Am., Vol. 80, 1986, 869-876
- <sup>118</sup> AMRAM, M., CHVROJKA, V.J. and DROIN, L., Phase reversal barriers for better noise control at low frequencies: laboratory versus field measurements, Noise Control Engineering Journal, 28(1), 1987, 16-23
- <sup>119</sup> VAN DER HAIJDEN, L. A. M. and MARTENS, M. J. M., Traffic Noise Reduction by Means of Surface Wave Exclusion Above Parallel Grooves In the Roadside, Applied Acoustics, Vol. 15, 1982, 329-339
- <sup>120</sup> WIRT, L.S., The Control of Diffracted Sound by Means of Thnadners (Shaped Noise Barriers), Acustica, Vol. 42, No. 2, 1979, 73-88
- <sup>121</sup> WASSILIEFF, C., Improving the noise reduction of picket barriers, J.Acoust.Soc.Am., 84(2), August 1988, 645-650
- <sup>122</sup> WATTS, G.R., HOTHERSALL, D.C., and HOROSHENKOV, K.V., Measured and predicted acoustic performance of vertically louvred noise barriers, Applied Acoustics, Vol. 62, 2001, 1287-1311
- <sup>123</sup> OKUBO, T. and FUJIWARA, K., Efficiency of a noise barrier on the ground with an acoustically soft cylindrical edge, J.Sound.Vib., 216 (5), 1998, 771-790
- <sup>124</sup> AILMAN, C.M., A Light-Weight Helium-Filled Noise Barrier, Inter-noise 78, 8-10 May 1978, San Francisco, USA, 513-516
- <sup>125</sup> The New Civil Engineer, Supplement: 21st Century Airports, November 1997, p. 54.

## **4 A SIMPLIFIED METHOD OF SELECTING BARRIERS**

### **4.1 INTRODUCTION**

The previous chapter presented a comprehensive review of research carried out on environmental noise barriers within the last four decades. This work identified a large number of nominally independent research areas which needed further attention. It is difficult at this stage to prioritise these in any particular order. Additional work is required to explore which course the current research project should take. Therefore the available information has to be organised in a constructive and methodical manner to be able to achieve this.

This chapter intends to develop further the concepts discussed in the previous one with a view to putting forward a simplified approach to selecting the type of noise barrier for controlling road traffic noise. This approach would be of benefit particularly to those non-acousticians who are part of the decision making process.

The acoustic advice given below is based on the collective experience of the performance of barriers on site and observations of what is likely to be achievable in practice, as discussed in Chapter 3. However, the proposed design guidelines do not explicitly take into account atmospheric and ground effects highlighted in Chapter 2. The method aims to condense the large amount of research on noise barriers into a simple and accessible format. It also serves the purpose of identifying further research needs.

### **4.2 DESIGN PHILOSOPHY**

This section will discuss the process by which environmental noise barriers are designed and the role of the various agencies involved in the process. This would help identify the shortcomings, if any, that the current design method suffers from.

### **4.2.1 The Design Process**

The design and construction of environmental barriers requires the involvement of specialists from many disciplines. In addition to acousticians, architects, planners, landscape architects, civil engineers, highway engineers, structural engineers and geotechnical engineers, the community must also be involved for an effective and widely accepted solution<sup>1</sup>. Since noise barriers are intended, primarily, for the comfort and convenience of the people, two more factors should be added to the list of issues that inform the design process. These are the concerns of the local residents and those of the wider public representing various interest groups<sup>2</sup>.

The specialists involved and the considerations of importance that have been mentioned are inter-related. Acousticians have to ensure that the noise screening provided by the chosen option is satisfactory, both for the authorities involved and for the public. Architects, landscape architects and planners have to ensure that the solution fits the context of local environment. There are reported examples of options presented to the public to enable them to make the choice for themselves<sup>2</sup>. Civil and structural engineer, geotechnical engineer, highway engineer have to ensure the design and construction side of the matter including costs, safety implications, drainage and stability of the selected option. Probably this is the step which involves the least public involvement. Environmental specialists will deal with the impact of the project onto the character of the local environment, and onto to wildlife and ecology. Wider public will be represented in the form of various interest groups. These could be wildlife and ecology conservation groups or national heritage conservation groups, who will input into the environmental and aesthetic dimension of the project. Local residents will be concerned with the direct impact of the project on the quality of their life. Reduction of excessive noise levels will probably be the most important priority as far as the local residents are concerned. In doing so, however, visual pollution and restriction of the daylight falling onto their property should be at levels that could be compromised. Due to the subjective nature of noise, if local residents are somehow dissatisfied about various non-acoustic factors, the project will fail acoustically too, no matter how effective it is.

A barrier can be considered as a two dimensional structure which separates the space-time into two distinctive worlds. These two worlds can be named the "static side" and the "dynamic side" of a barrier, both in terms of movement and noise. The aesthetic requirements will obviously be different for either side. The static side will be free from excessive noise levels, and probably even from the sight of chaotically flowing traffic. This space may be used as a park or a footpath, required for peaceful and quiet activities. The dynamic side will be where the traffic is flowing continuously and the



noise levels are high. The motorists will have different aesthetic expectations on the dynamic side so that the barrier does not interfere with their driving concentration by providing a claustrophobic or rather monotonous sight.

### 4.2.2 Design Analogy

The main issues involved in environmental barrier design have been summarised above. These six main issues were identified as acoustics, aesthetics, engineering, environment and also the concerns of the local people and the wider public as seen in Figure 4.1.

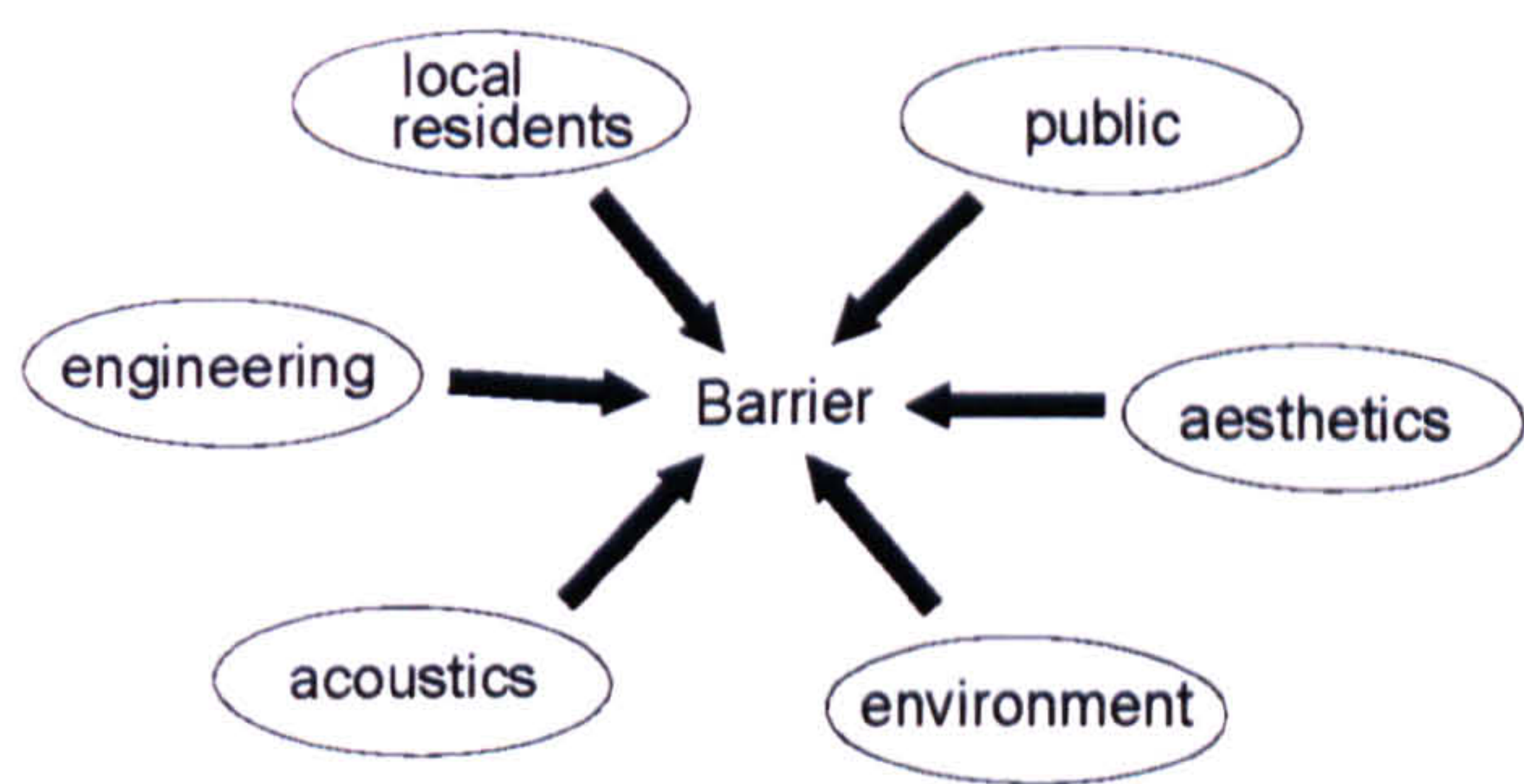


Figure 4.1 : The main issues involved in environmental barrier design.

We could relate all in an analogy. Environmental barrier design could be perceived as a jigsaw puzzle in which a number of "pieces" make up "the complete picture". The most effective solution to a specific noise problem would be the jigsaw puzzle in its completed form. The issues of importance would correspond to the individual pieces making up the jigsaw as seen in Figure 4.2.

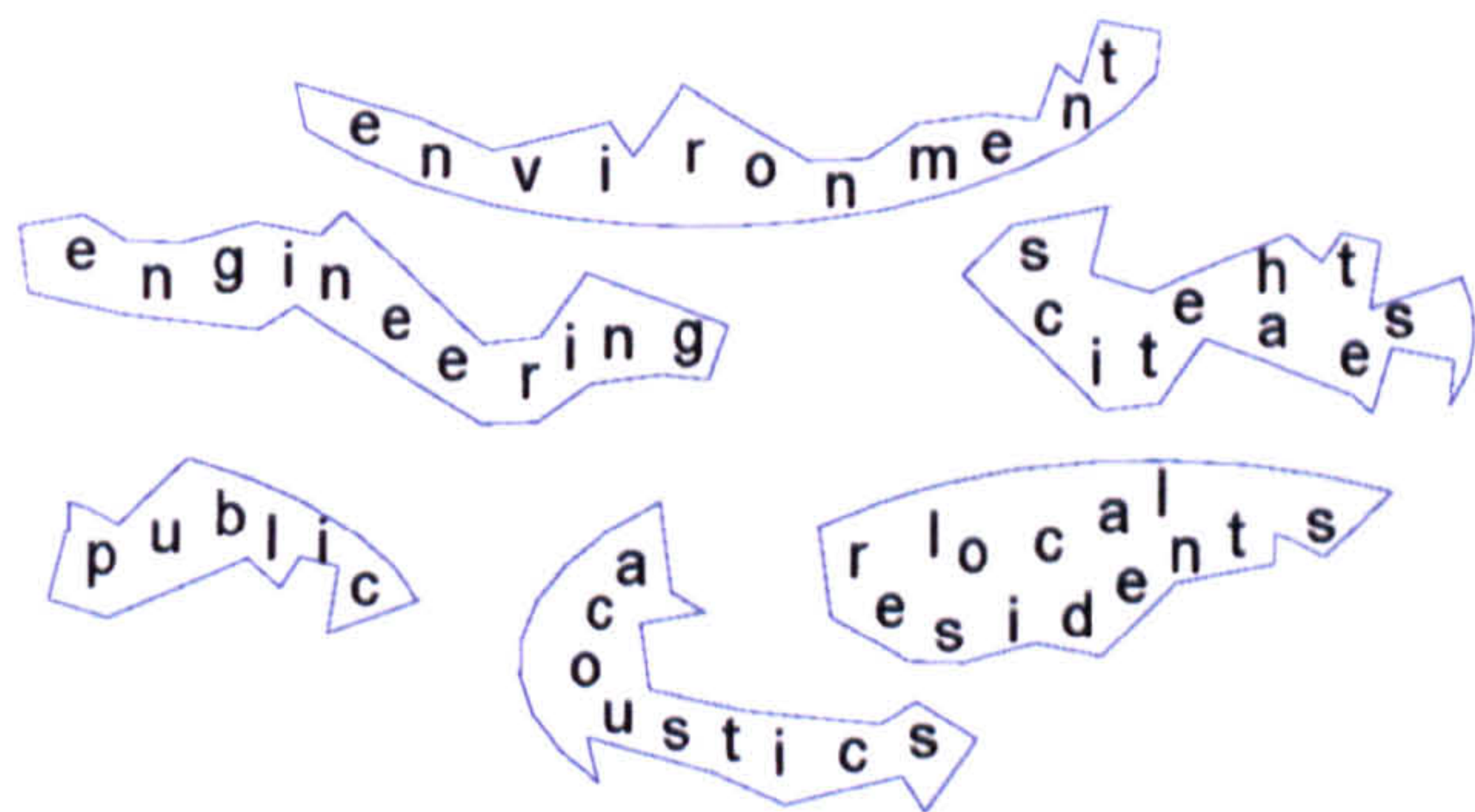
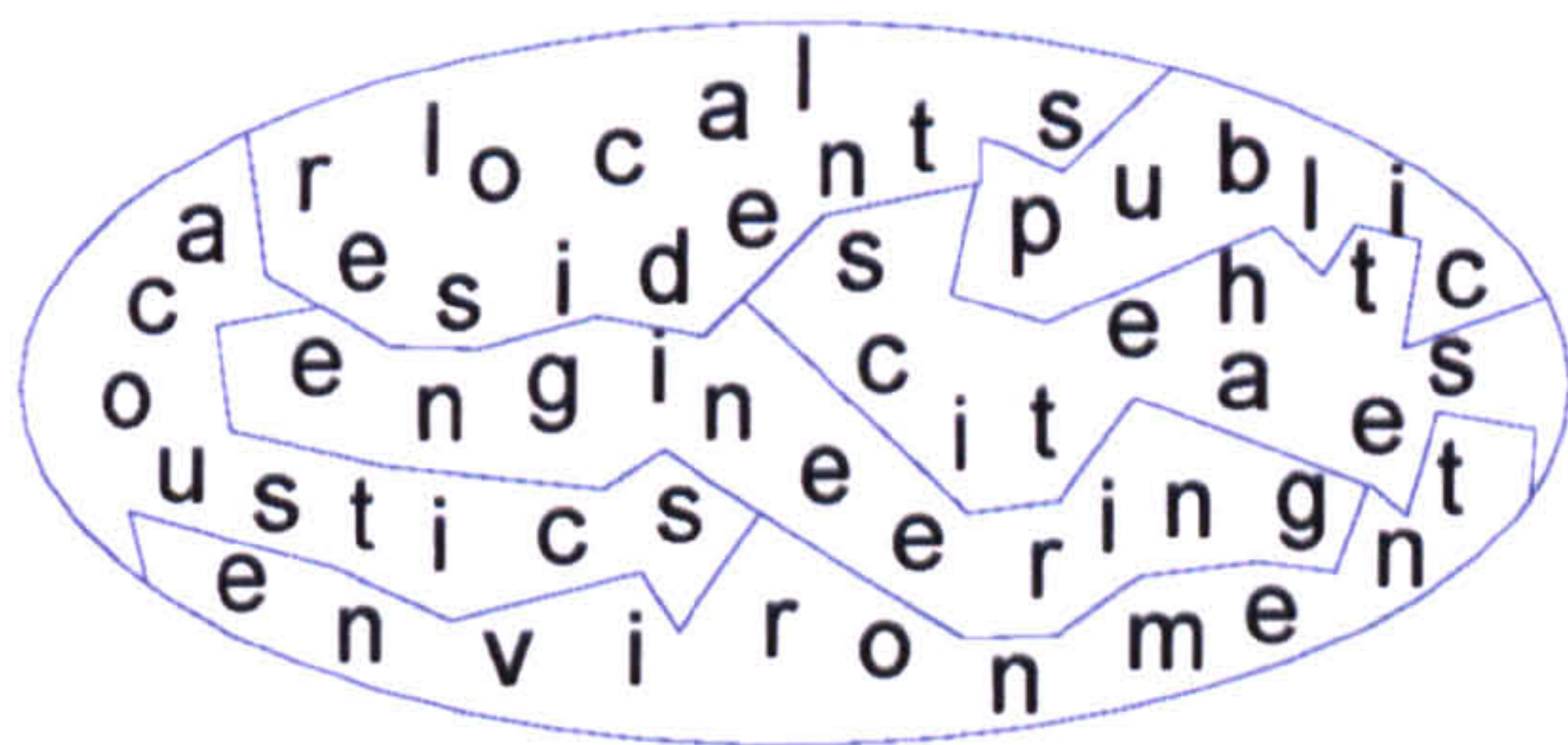


Figure 4.2 : The six factors perceived as the individual pieces of a jigsaw puzzle.

Nevertheless, like in every jigsaw, we have to start by placing one of the pieces first. Then we attach the rest one by one, until the picture grows into a whole. Therefore all

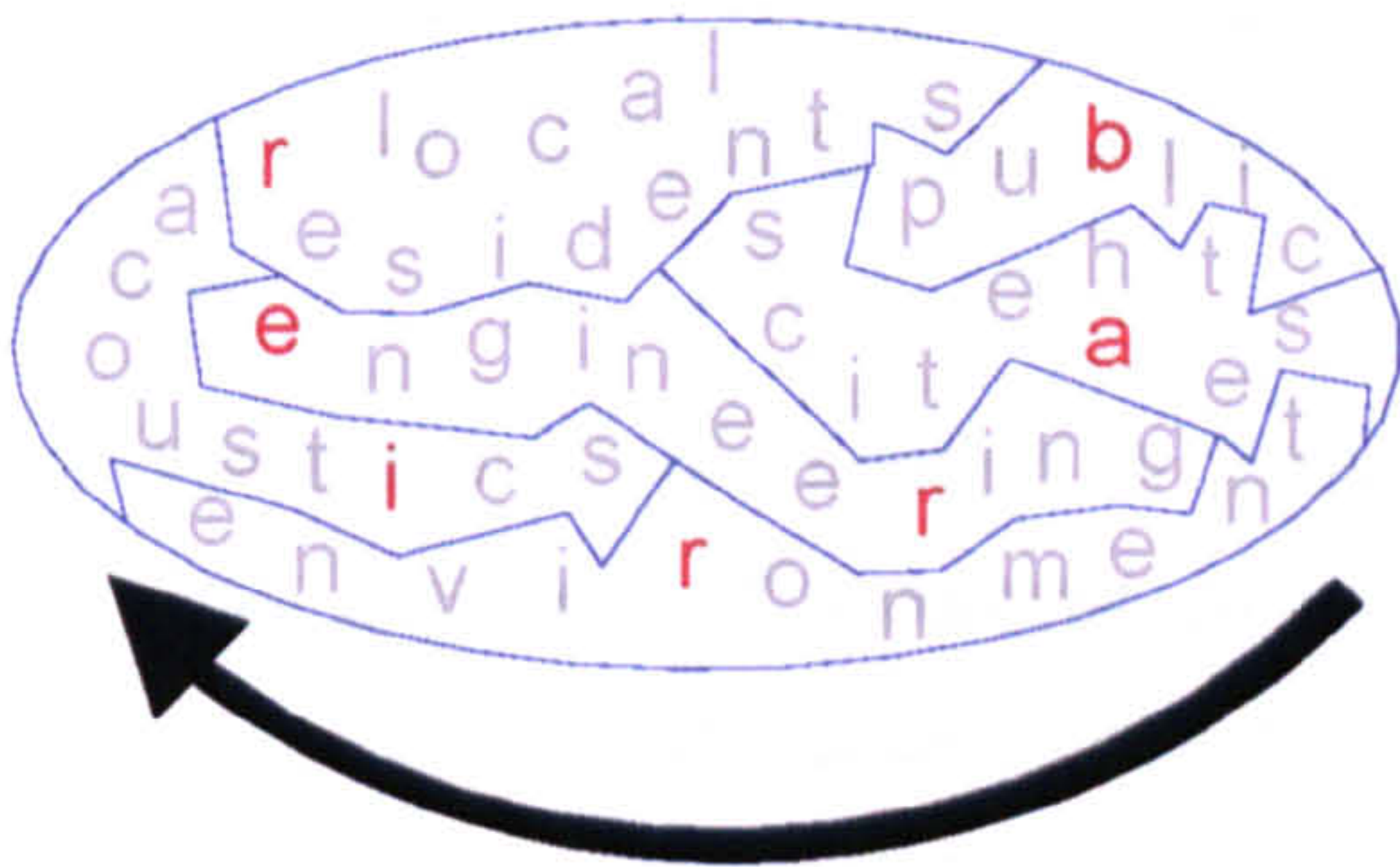


we know at the beginning is that we need to join the six individual pieces in an appropriate manner to solve the puzzle (Figure 4.3). The question is where do we start from? Which piece comes first?



**Figure 4.3 :** The completed jigsaw puzzle.

It is impossible to isolate one aspect of barrier design as the most important one from the others. All are needed for an effective solution. However, due to their distinguishing features, some pieces will have preference over the others in being the first choice. Distinguishing feature of this puzzle is the "acoustics" piece because the completed puzzle will reveal the "solution of a noise problem" in the form of a barrier (Figure 4.4).



**Figure 4.4 :** Effective solution for an environmental barrier.

Even though acoustics issues take precedence in the flow chart diagrams proposed in the forthcoming sections, non-acoustical factors can not be segregated from decision making process.



### **4.3 EXISTING DESIGN GUIDELINES**

With such an abundant number of design parameters related to barriers and with a great variety of profiles available, a potential designer would need specific guidance on a number of occasions concerning acoustical performance of barriers.

The main document for the design of environmental barriers in the U.K. is Section 5 in Volume 10 of the Design Manual for Roads & Bridges. Part 1 is mainly concerned with the impact of the barrier on the environment<sup>3</sup> while Part 2 deals with the technical requirements including the acoustic performance and engineering details<sup>4</sup>.

These two documents cover a wide range of information about different aspects of barrier design, however alternative barrier profiles are only mentioned in passing. The information is not presented as guidance to help the designer choose the right option, but merely to quote certain examples of performance. In certain cases, the designer is simply advised to seek further help elsewhere (i.e. dispersive barriers and multiple diffracting edges). In some cases, the guidance can be contradictory as in the case of earth mounds. A short acoustic screen erected on top of an earth mound is promoted due to its beneficial effects, however the designer is also warned that this could diminish the noise absorbent effect of the vegetated slopes.

Although these documents provide the designers with an overview, acoustical guidance is not presented in an easily accessible manner. This may, sometimes, force inexperienced designers to seek solutions to detailed acoustical problems which may be beyond their capabilities.

It is clearly stated that the guide is not intended to "prescribe a standard range of barriers from which to make a selection"<sup>3</sup>. However, more substantial information on different types of barriers and their acoustical performance would give the designer the flexibility to deal with other factors more effectively.

Established barrier options could be listed, together with their acoustical performance, and non-acoustical limitations, so that the few effective barrier options can be identified. The next step would be to refine this option with input from the local residents and the wider public so that the impact of the design on the environment is minimised. In order to ensure the effectiveness of the solution, full construction details associated with each recommended option need to be included.

## **4.4 PROPOSED DESIGN GUIDELINES**

The design method presented here attempts to augment the advice provided in the existing guidelines. Information is presented in an easy-to-follow flow chart diagram. The designer progresses to the next step by the aid of simple questions, which mainly require yes/no answers. The method consists of two stages. The first one is where the main type of barrier is decided upon and the second one provides the essential refinements, if any, to be made to the design. With minor modifications, the method can also be used for checking or improving the acoustical efficiency of an existing design.

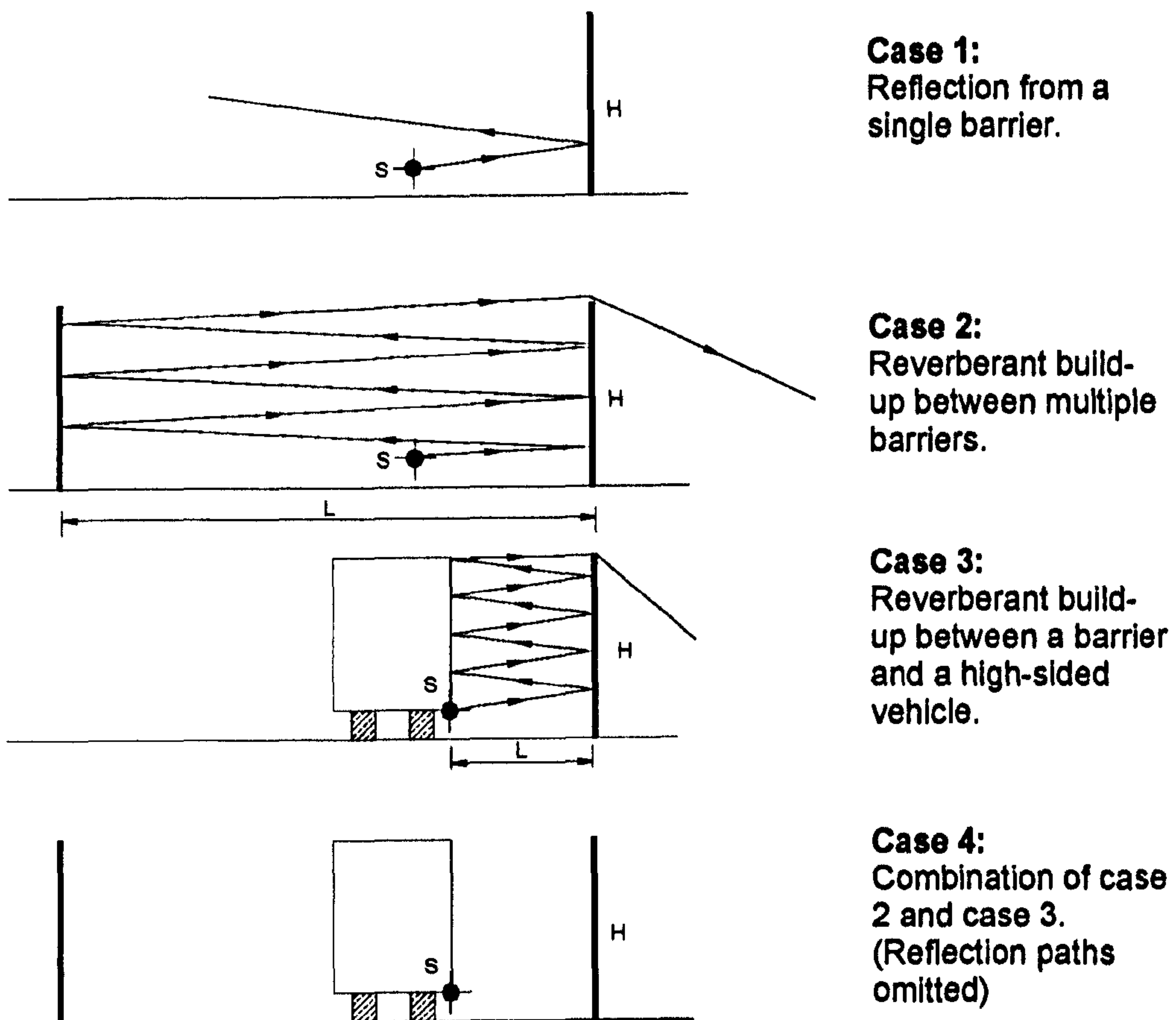
### **4.4.1 Multiple Reflections**

When designing new barriers or improving the performance of existing ones, main consideration is to ensure multiple reflections do not degrade the barrier performance. Therefore before presenting a simplified method for the design of noise barriers, the adverse effects of multiple reflections and the options that are available for counteracting this problem will be discussed.

The mechanism of multiple reflections acts in a way to raise the effective source height by causing a reverberant build up of sound energy between the faces of two vertical barriers. In order to maximise the efficiency of a barrier of given height and also because of the increasing use of noise barriers in urban situations where site restrictions can occur, noise barriers are often situated very close to the edge of the road. In these conditions too, multiple reflections between a high sided vehicle and a barrier can cause a degradation of performance<sup>5</sup>. Similarly nearby buildings can present unwanted reflection paths.

Four main "reflection mechanisms" investigated by other workers are summarised in the sketches in Figure 4.5. The first one is where a single reflective vertical barrier is already available and the effect of the reflections on a receiver on the opposite side of the road is investigated. In the second case, the effect of a second reflective vertical barrier on the performance of the former one is investigated. Then the second reflective barrier is replaced by a high-sided vehicle, which effectively represents a reflective surface of similar height much closer to the existing barrier. The last one is a combination of two reflective vertical barriers with high-sided vehicles running between them.





**Figure 4.5 : Multiple reflection mechanisms**

It has been pointed out that, the effective noise insertion loss of many practical barrier schemes being typically of the order of 5-10 dB(A) for receivers 30-60 metres away from the barriers, degradation of 3 dB(A) or more, would significantly counteract the benefits of this abatement measure<sup>6</sup>.

The possibility of sound reflections from a single barrier causing an increase in noise levels at exposed facades on the opposite side of the motorway was examined by on-site measurements, however the workers' finding was that in practical situations this increase in  $L_{10}$  is unlikely to exceed 1.0 dB(A). They also did not find any evidence that multiple reflections occurring between parallel barriers caused an increase in noise levels at the chosen measurement positions<sup>7</sup>.

It was concluded by Watts that the screening performance of a single 2 m high barrier on the nearside is reduced by 4 dB(A) when a reflective barrier of similar height is erected at the edge of the farside carriageway<sup>8</sup>. Both tilted barriers (10 degrees of

inclination) and the absorptive barriers were effective in restoring the performance of these barriers.

Where a barrier had been erected on one side of the carriageway the maximum change (between a reflective and absorptive barrier facing the reflections) in level  $L_{A10}$  measured opposite the barrier at a distance of 25 m from the road edge was negligibly small<sup>9</sup>.

Parallel barriers placed on either side of a dual-carriageway (situated in a shallow cutting) gave a maximum effect of around 2 dB between a reflective and absorptive barrier<sup>9</sup>.

Numerical modelling used in order to investigate the effects of a high-sided vehicle running close to a reflective barrier indicated degradation in performance of around 4-5 dB. Use of absorbing surface on the source side of the barrier restored the performance<sup>5</sup>.

One particular example investigated by using a computer model, gave predicted degradation from 3 dB(A) to 9 dB(A) depending on the percentage truck composition of the traffic<sup>10</sup>. The "truck compositions" investigated in this model do not necessarily correspond to the "high-sided vehicle compositions" and are intended to represent different traffic scenarios. However this investigation potentially resembles the case 4.

Degradation in barrier performance due to multiple reflections led to two possible solutions for this problem. These are the application of *sound absorptive materials* onto the barrier surfaces or *tilting the barrier* backwards from its vertical position.

In order to avoid the effects that can be caused due to multiple reflections when screens are installed on either side of a road, the following recommendations are provided by certain official standards across Europe<sup>11</sup>.

$H > L / 5$ , Absorbent material should be used in the screens.

$L / 5 > H > L / 10$ , The decision to use absorbent material depends on the environment and on the possibility of sloping the screens. The efficiency of the two solutions should be studied.

$L / 10 > H > L / 20$ , Sloping screens are to be preferred to the use of absorbent materials, because generally they are more effective.

$H < L / 20$ , The use of absorbent material or sloping screens hardly affects the final result.

where, H is the height of the screens and L is the distance between the two screens located opposite one another.

This is an interesting example of the type of practical guidance that can be included in a prediction method. Even though the provisions above are for two barriers facing each other, they could be extended to apply to high-sided vehicles. High-sided vehicles would be considered as vertical screens situated very close to the existing barrier. This assumption would imply the traffic consists of high-sided vehicles alone which is not the case in reality. Further work on the percentage composition of high-sided vehicles - and not necessarily trucks or heavy vehicles- in relation to the overall traffic composition would reveal the critical case where reflections from these surfaces start causing a problem. When making recommendations in overcoming the problem of multiple reflections, these guidelines will be followed wherever applicable.

#### **4.4.2 New Barriers**

For the purpose of the proposed guidelines, environmental barriers are classified broadly into three main categories. These are the wall type barriers, the earth mounds and the bio-barriers or mounds with reinforced slopes.

Earth barriers have the advantage of being aesthetically pleasing and environmentally friendly. Due to their natural appearance they blend into the local environment and the public perception of these barriers is high<sup>12</sup>. Depending on the availability of sufficient space and local fill material, their construction can be cost-effective. Therefore earth barriers are given priority over wall type barriers even though a flat-topped grass-covered earth mound has been shown to perform less well than a thin vertical wall of an equal height<sup>13</sup>. With so many factors favouring the applications of earth mounds, less effective acoustic performance can be remedied by making them higher. An increased height in the case of earth barriers have less visual impact and is not subjected to structural limitations such as wind loading.

According to the flow chart in Figure 4.6, the first question to be answered is whether the right-of-way situation provides readily available land for the construction of earth mounds. Where the available space for achieving the required design height is sufficient, the availability of local fill material needs to be considered. Where a road construction contract produces surplus material, the earth mounds can be constructed for a negligible cost<sup>4</sup>, otherwise the cost of transporting fill material from another site should be considered. This adds to the construction cost of an earth mound.

If the availability of space is limited, naturally resting soil would not be self-supporting and reinforced slopes would be essential to achieve the vertical height required, within a limited horizontal stretch. In this case, bio-barriers and mounds with steeper reinforced slopes are always available as options. They may appear man-made due to their unnatural slope angles and hence aesthetics will be a consideration. The need for



maintenance and irrigation to ensure the presence of dense plantation at all times are other factors which increase the unwillingness of the designer to put these options into practice. However successful designs do exist and examples of bio-barriers in real life applications can be seen throughout Europe<sup>2</sup>.

Where space is not available, the opportunity of buying the land should be explored. This would have additional cost implications. The next point would be the consideration of whether the land to be purchased is enough or limited for the purpose of constructing an earth mound. If the space is neither available nor can it be acquired, then erection of wall type barriers may be inevitable.

If a wall type barrier is the preferred option, the second stage of the design procedure would provide the necessary or possible refinements to the design. In this case, degradation due to multiple reflections should be a prime consideration. The options available for the prevention of multiple reflections have been discussed earlier. The distance between the reflective surfaces (L) in relation to the barrier height (H) determines which option should be used. The decision shifts from absorbing barriers towards tilted barriers, as this distance increases. When the reflecting surface is situated up to 5 times the barrier height, the use of absorbent materials is recommended. As the separating distance increases up to 10 times the barrier height or more, sloping the barrier becomes a more feasible option <sup>14</sup>. Tilt angles of 10 - 15 degrees are required for narrow roadways but 3 degrees are enough for wide roadways<sup>15</sup>.

Should it be desirable, the height of a wall type barrier can be reduced by considering the options explained in the flow chart. These options will be explored in greater depth in the next section.

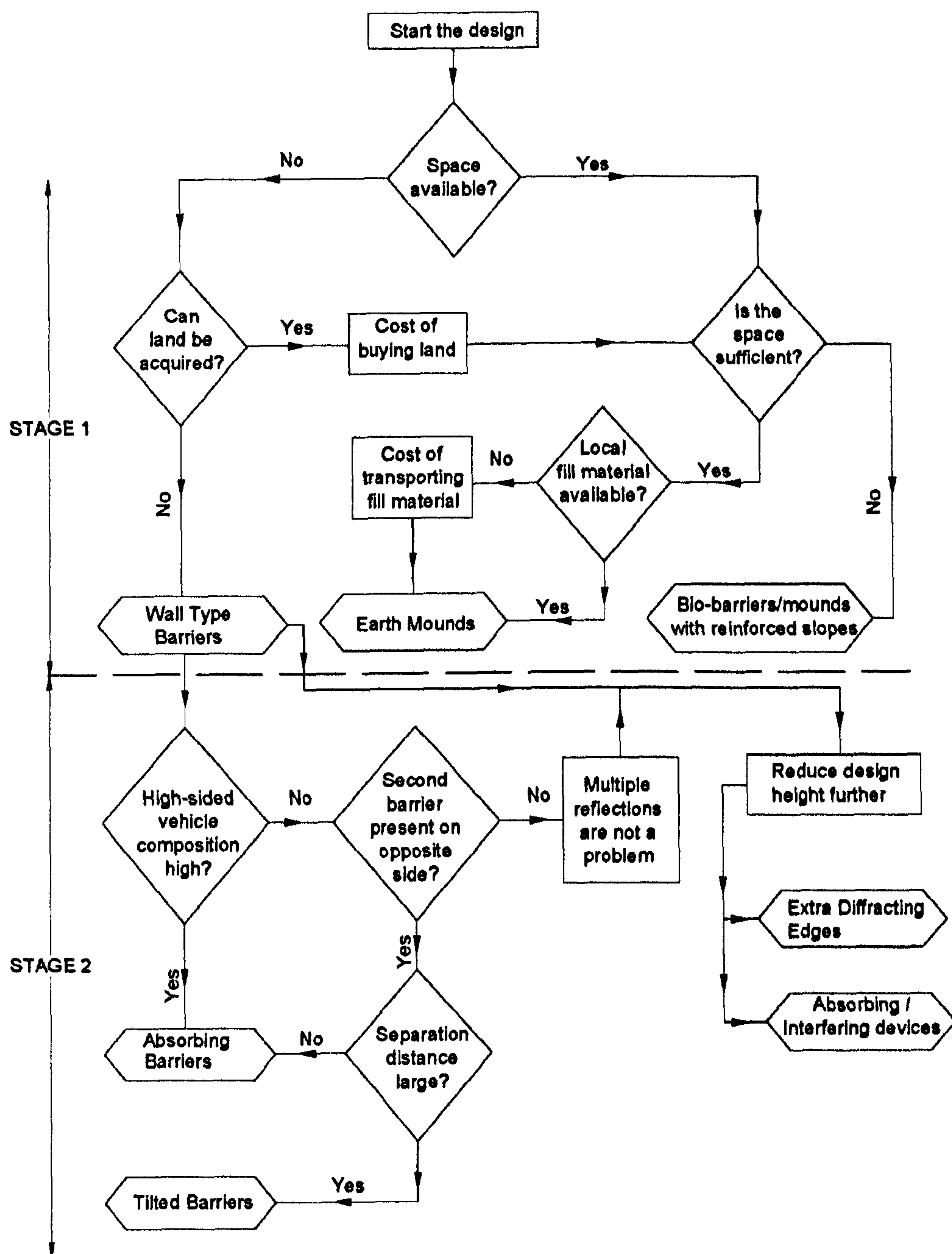


Figure 4.6 : Selection process for new barriers

### 4.4.3 Existing Barriers

In urban and semi-urban environments, wall type barriers are commonly used instead of earth mounds due to physical constraints. With time, these barriers can have their

screening effect reduced as a consequence of ever increasing traffic volumes or as a result of multiple reflections from a second barrier opposite an existing one.

Before even considering how the acoustic performance of an existing wall type barrier can be improved, it is vital to ensure there is no degradation in the design performance of a screen due to multiple reflections. As mentioned before, these may occur when there are highly reflecting surfaces present close to the noise source.

The distinction made earlier between high-sided vehicles and a second reflective barrier in terms of their proximity to the existing barrier is avoided here. According to Figure 4.6, the presence of either the high-sided vehicles or a second barrier on the opposite side is treated as a potential problem. Under these conditions application of absorbing materials is recommended as a solution. For this to be effective, the average absorption coefficient of the absorbing materials in practice should be at least 0.8<sup>4</sup>. It is not feasible to tilt an already constructed vertical barrier at a later stage. Therefore this eliminates the solution of a potential problem where two vertical barriers with a large separation distance might exist in practice. Application of absorbing treatment is not expected to be effective in these cases. This is a setback in the method, justified by practical constraints.

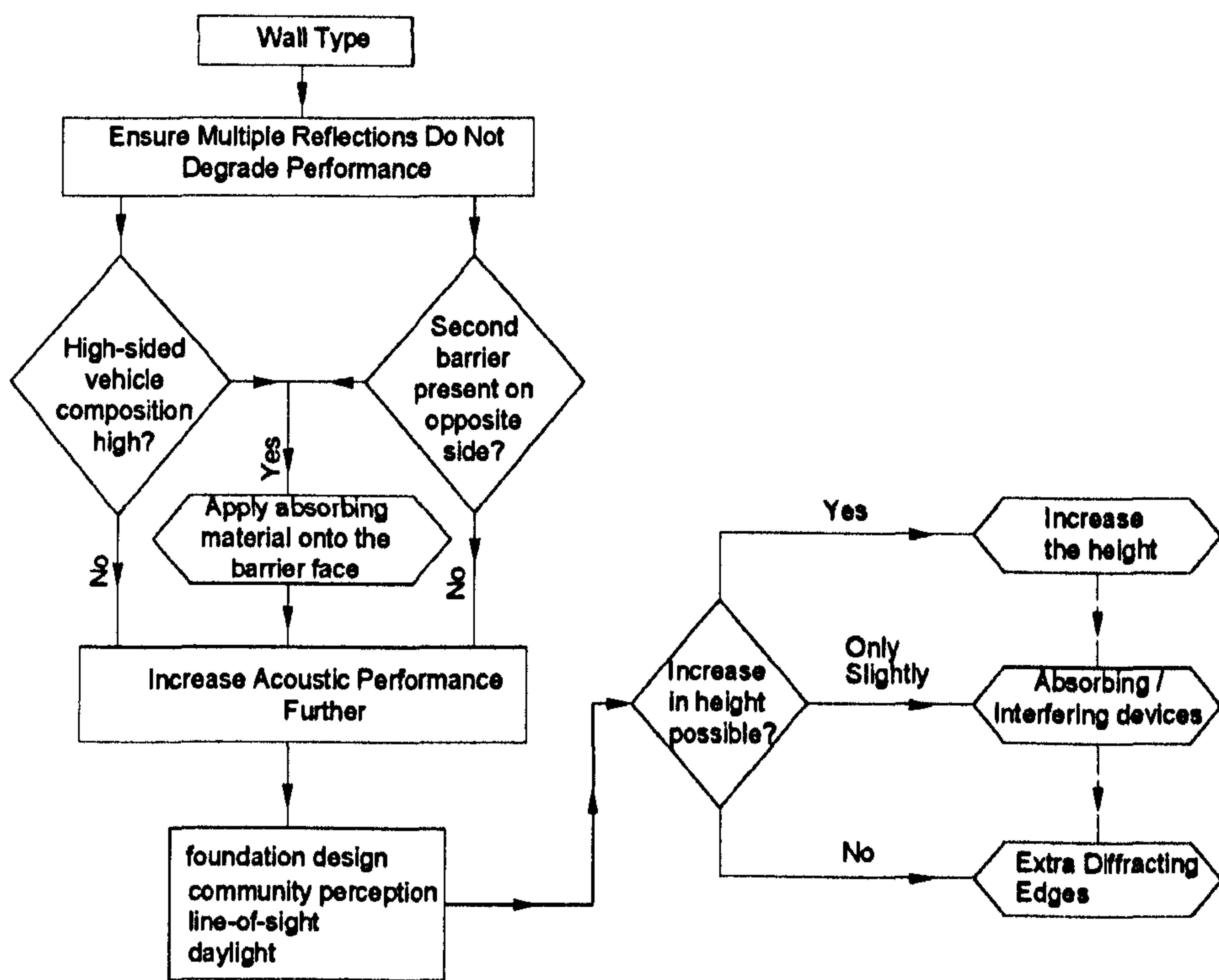


Figure 4.7 : Improvements to existing wall type barriers



Once “multiple reflections” have been considered, the designer can concentrate on increasing the acoustical efficiency of the barrier to offset any increase in noise levels due to large traffic volumes.

Modifications that can be made to an existing wall type barrier are classified into three different categories. The decision depends on how much height increase is possible. If no increase in height is allowed the only option is attaching extra diffracting edges. If a slight increase is allowed, then interfering/absorbing devices can also be used. If there is no such restriction, then increase in height is also a consideration as well as the other options mentioned above. Although it may not be desirable to increase the height of a barrier due to non-acoustic considerations, there may well be cases requiring or allowing this option. After the line-of-sight has been intercepted, every additional metre of barrier height is expected to provide 1.5 dB(A) improvement in the insertion loss. The factors influencing the decision whether or not the height could be increased are non-acoustic considerations which will be discussed below.

Increasing the barrier height could bring with it complaints from the local community that the daylight falling onto their gardens and windows is reduced, or the line-of-sight from their property has been restricted. Even if this option is justified with the consensus of the public, extra load on the foundations due to the wind should be considered. This problem can be solved by strengthening the foundations, which will incur extra costs. Alternatively, the extra height could be constructed in the form of transparent panels to avoid obstructing the line-of-sight further, or reducing the amount of daylight falling onto the property. In addition to the high cost of the transparent panels and the frequent need for maintenance, extra wind loading would still be a problem.

Attaching sound absorbing or interfering devices onto the top of an existing barrier has been reported to have considerable acoustical effects. In Japan absorbing devices, namely absorbing cylinders<sup>16</sup> or absorbing mushrooms<sup>17</sup>, have been used, and the reported acoustical gains are 2-3 dB(A). In the UK, barriers with interfering devices attached on top have been tested on site<sup>18</sup>. Although the full-scale performance was around 2 dB(A), it was found that most of this was due to diffraction and not to interference. These devices cause only a small increase in the height of a barrier.

Extra diffracting edges have been proven to be both acoustically and structurally sound solutions. Addition of a horizontal cap<sup>19</sup> or vertical shallow panels attached on either side of the barrier top<sup>20</sup> can increase the acoustical efficiency, partly due to increase in the path difference and mainly due to extra diffraction. The main non-acoustical advantage of these solutions is that the height of the barrier is not increased. In the case of T-profile barriers the snow loading and the lifting effect of the wind on the

horizontal cap are structural considerations which will need attention during the design. In this respect the vertical shallow panels appear like a more cost-effective solution compared to the horizontal cap, especially when their slightly higher acoustical performance is taken into account.

## **4.5 DISCUSSION**

Before proposing a solution to the acoustic design of noise barriers, the design philosophy has been examined closer in order to demonstrate the complexity of the process.

The main source of advice for the design of environmental barriers is the Manual for the Design of Roads and Bridges. The information contained in this document is often difficult to interpret particularly when the designer is inexperienced. The need for a simple approach to select the appropriate design option has been argued for in this chapter. The method being put forward covers both new barriers as well as existing ones.

The abundance of different barrier shapes have been pointed out in Chapter 3. Only the most promising profiles have been included in this design method where on-site performance checks indicated positive gains. Considerable acoustic gains have also been reported concerning the reactive barriers <sup>21,22</sup>, as mentioned earlier. As the acoustic performance of these designs are confirmed with measurements and as the engineering problems inhibiting their use are overcome, there can be no excuse for avoiding their applications.

The design process for new barriers can be undertaken in two stages. Initially, the most favourable type of barrier is selected on the basis of availability of space for erection and the cost implications. The second stage is where the type of acoustic treatment to be applied to the barrier is selected on the basis of some simple logical tests, where no specialist knowledge of acoustics is required.

Considering the average insertion loss of barriers in practice was observed to lie between 5 and 12 dB(A)<sup>23</sup>, the targeted insertion loss values should be at least 10 dB(A). This reduction will be subjectively perceived as halving the noise levels.

Similarly a design procedure, for improving the performance of existing wall type barriers, based on simple yes/no tests and little knowledge of acoustics is being proposed. The main advantage of both methods is the shortening of the design process and the reduction in the costs of afterthought mitigating measures.

The reported benefits of the modifications discussed in the preceding section vary. However, almost all are said to have made only modest contributions to an existing barrier, up to about 3 dB(A) in real life applications. An existing barrier may already possess high degree of screening performance and it may prove difficult to enhance this performance greatly. Realistically, 3 dB(A) should be the targeted additional increase in the acoustic performance, which is subjectively the smallest noticeable change in noise levels.

When a modification is being made to an existing design there is always the danger of not putting it into the context of the already existing. It is always desirable to get the design right from the first time. In the cases however, where improvements are necessary and unavoidable, even if the acoustical benefits of a modification sound tempting, extreme care should be shown so that the extra additions do not seem like "an after thought".

## **4.6 CONCLUSIONS**

The discussion of the design process has highlighted further the need for simplified noise barrier design guidelines as previously identified. An alternative design method consisting of a series of flow chart diagrams is presented to aid the inexperienced designer in making decisions on the most favourable design options without the need to consider detailed acoustical performance. The method can be used for both new and existing barriers. It is hoped the proposed method will shorten the design process which in turn would produce more effective design solutions at lower costs.

The method does not address the atmospheric and ground effects and therefore the acoustic benefits or deficiencies of one barrier over another are indicative.

The earth mounds and the wall type barriers have been given equal emphasis as part of the method as being the two main barrier types. Since, the wall type barriers have attracted large amount of interest, the findings of this research have been incorporated into the method. However this was not the case for earth mounds as reflected in the proposed flowcharts for new and existing barriers. The limited available information on acoustical characteristics of earth mounds has indicated the need for further research.

The next chapter is an investigation into the acoustical and non-acoustical merits of earth mounds. Together with published work reviewed in earlier chapters, it helps identify the research methodology to be used for the main investigation into the performance of environmental barriers.



## **4.7 REFERENCES**

- 
- <sup>1</sup> Highway Traffic Noise Analysis And Abatement Policy And Guidance, U.S. Department Of Transportation, Federal Highway Administration Office of Environment And Planning, Noise and Air Quality Branch, Washington, D.C., June 1995
- <sup>2</sup> Environmental Noise Barriers - A Guide to Their Acoustic and Visual Design, Bentz Kotzen and Colin English, E & FN Spon, 1999
- <sup>3</sup> Volume 10 Environmental Design, Section 5, Environmental Barriers, Part 1 HA 65/94 Design Guide For Environmental Barriers, 1994
- <sup>4</sup> Volume 10 Environmental Design, Section 5, Environmental Barriers, Part 2 HA 66/95 Environmental Barriers – Technical Requirements, 1995
- <sup>5</sup> HOTHERSALL, D.C. and TOMLINSON, S.A. High-Sided Vehicles and Road Traffic Noise Barriers, Acoustics Bulletin, July / August 1996
- <sup>6</sup> LEE, V.M., MICHALOVE, R.A., SLUTSKY, S. (1988) Tilted Parallel Barrier Program :Application and Verification, Transportation Research Record 1176, 23-33
- <sup>7</sup> NELSON, P.M., ABBOTT, P.G., SALVIDGE, A.C. (1976), Acoustic Performance of the M6 Noise Barriers, TRRL Lab Report 731
- <sup>8</sup> WATTS, G.R. Acoustic Performance of Parallel Traffic Noise Barriers, Applied Acoustics, Vol 47, No 2, 95-119, 1996
- <sup>9</sup> WATTS, G.R. and GODFREY, N.S., Effects on roadside noise levels of sound absorptive materials in noise barriers, Applied Acoustics, Vol. 58, 385-402, 1999
- <sup>10</sup> BOWLBY, W. and COHN, L.F. (1986), A Model for Insertion Loss Degradation for Parallel Highway Noise Barriers, J.Acoust.Soc.Am., Vol 80, No 3, 855-868
- <sup>11</sup> OECD, Organisation For Economic Co-operation and Development, Roadside Noise Abatement, 1995, Chapter VI- Noise Barriers, 105-142
- <sup>12</sup> COHN, L.F., Highway Noise Barriers, National co-operative highway research program, Synthesis of highway practice 87, Transportation Research Board, Washington D.C., December 1981
- <sup>13</sup> HOTHERSALL, D.C., CHANDLER-WILDE, S.N. and HAJMIRZAE, M.N., Efficiency of Single Noise Barriers, Journal of Sound and Vibration, 146(2), 303-322, 1991
- <sup>14</sup> Roadside Noise Abatement, Chapter VI - Noise Barriers, 105-142, I.R.R.D. Publication, O.E.C.D (publisher), Source number: 9510TR190E, 1995

- 
- <sup>15</sup> SLUTSKY, S. and BERTONI, H.L. Analysis and Programs for Assessment of Absorptive and Tilted Parallel Barriers, Transportation Research Record 1176, 13-22, 1988
- <sup>16</sup> YAMAMOTO, K., TAYA, K., YAMASHITA, M., and TANAKA, K., Reduction of Road Traffic Noise By Absorptive Cylinder Adapted At The Top Of A Barrier, Inter-Noise 89, Newport Beach, CA, USA, December 4-6, 349-352, 1989
- <sup>17</sup> YAMAMOTO, K., SHONO, Y., OCHIAI, H., HIRAO, Y., Measurements Of Noise Reduction By Absorptive Devices Mounted At The Top Of Highway Noise Barriers, Inter-Noise 95, Newport Beach, CA, USA, July 10-12, 389-392, 1995
- <sup>18</sup> WATTS, G.R., and MORGAN, P.A., Acoustic Performance of an Interference-Type Noise Barrier Profile, Applied Acoustics, Vol. 49, No 1, 1-16, 1996
- <sup>19</sup> WATTS, G.R., CROMBIE, D.H. and HOTHERSALL, D.C., Acoustic Performance of New Designs of Traffic Noise Barriers: Full Scale Tests, Journal of Sound and Vibration, 177 (3), 289-305, 1994
- <sup>20</sup> WATTS, G.R., Acoustic Performance of Multiple Edge Noise Barrier Profile at Motorway Sites, Applied Acoustics, Vol. 47, 47-66, 1996
- <sup>21</sup> FUJIWARA, K., HOTHERSALL, D.C., and KIM, C., Noise Barriers With Reactive Surfaces, Applied Acoustics, Vol. 53, No. 4, 255-272, 1998
- <sup>22</sup> OKUBO, T., FUJIWARA, K., Efficiency of A Noise Barrier on the Ground With an Acoustically Soft Cylindrical Edge, J.Sound Vib., 216(5), 771-790, 1998
- <sup>23</sup> DAIGLE, G.A. Report by the International Institute of Noise Control Engineering Working Party on the Effectiveness of Noise Walls, Noise/News International, 13-35, March 1998

## **5 EXPLORATORY WORK TO DEFINE RESEARCH AREA AND METHODOLOGY**

### **5.1 INTRODUCTION**

This chapter, together with the next one, will describe the research methodology to be adopted for this research. It will also identify the specific areas of research together with the techniques to be used to carry out the experimental investigation.

The proposed guidelines in Chapter 4 addressed acoustic and environmental issues in a simple and practical manner. Special emphasis was placed on the environmental and aesthetic issues by giving priority to the earth mounds wherever the practical constraints permit their applications.

It was demonstrated in previous chapters that the wall type barriers have been investigated in exhaustive detail. The lack of interest in earth mounds was found to be due to acoustical as well as non-acoustical limitations. These types of barriers require space and fill material for their construction. In addition the slopes of a mound prevent the highest part of the barrier to be situated close to the road, where the maximum acoustic benefits could be obtained. These barriers also perform slightly less well than an equivalent height thin vertical wall with centrelines situated at the same place. It is considered that developing a novel earth mound with enhanced acoustical performance would be necessary to promote their applications in real life.

This chapter outlines the previous work carried out on earth mound type barriers. The reasons for selecting earth mounds for further studies are described in detail by examining the acoustical and non-acoustical factors favouring their applications. The idea of combining earth mounds with conventional barriers is extended to the possibility of incorporating multiple short height barriers.

This chapter explores the methodology by which the performance of an alternative shape could be investigated. The details of exploratory research into performance of earth mounds are presented. These consist of on-site measurements and physical scale modelling work. In the light of this research, the details of the investigative methods are described.



## **5.2 PREVIOUS WORK ON MULTIPLE - SIDED BARRIERS**

The previous work on earth mounds was reviewed in Chapter 3. This is a more detailed account of this research. It aims to identify the physical mechanisms and design elements which could be explored further to improve the performance.

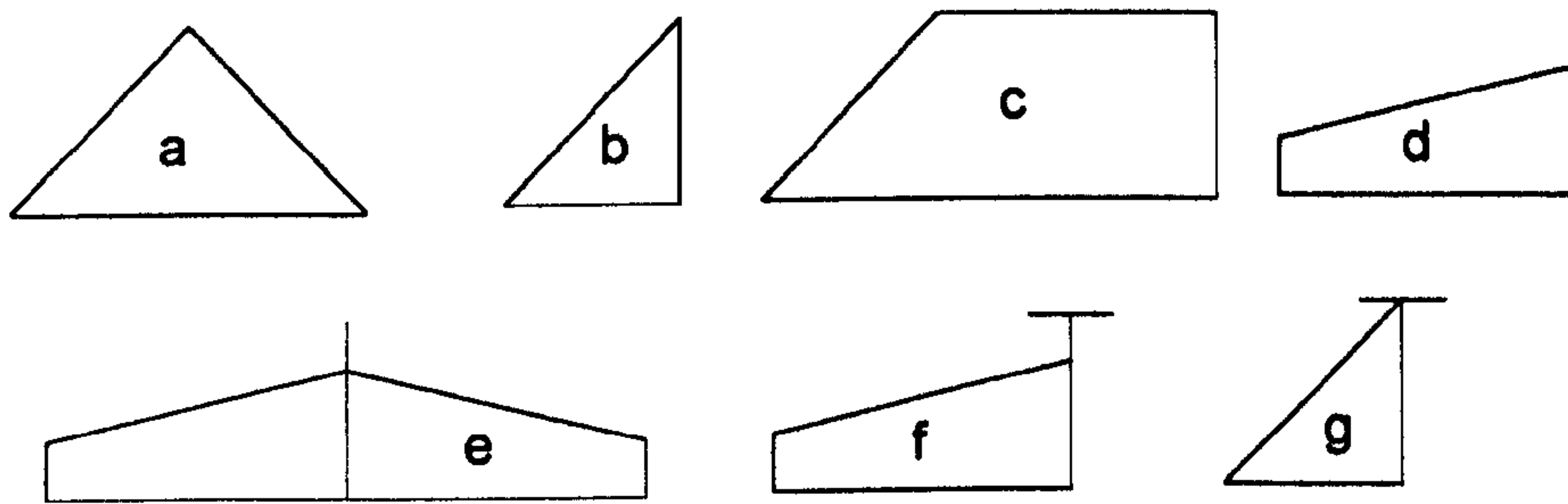
The wedges, flat-topped earth mounds and building blocks are some examples of many sided barriers which have been studied extensively by numerical methods and to some extent by on-site experiments and physical modelling.

Various forms of single/double diffraction techniques were employed to investigate diffraction over a wedge<sup>1</sup>, three-sided barrier<sup>2</sup> and many sided barrier or a pillar<sup>3</sup>. De Jong et al.<sup>4</sup> tested a model for the calculation of effects of ground and a screen/wedge barrier on the sound propagation with outdoor measurements. Their investigation of the combined effect of ground and an earth barrier gave slight discrepancy when compared with the measured data. The calculated results were slightly shifted towards the higher end of the frequency spectrum compared with the measured spectrum of transmission loss. According to the authors, one possible explanation of the shift in the calculated results could be the approximation of the barrier cross section by a wedge, where in reality it was a flat topped mound. They suggested the use of double edge diffraction theories for an improvement in the results.

Rasmussen<sup>5</sup> described various models on outdoor sound propagation over wedge barriers and three sided barriers. Theoretical results were compared with measured data for sound propagation over grass-covered earth berms, both from a loudspeaker source and a real road traffic noise. The measured and calculated results were shown to agree well, except for a frequency shift in the case where road traffic noise was the source. This was attributed to the wind speeds.

There have also been studies of more practical nature. A method for estimating the attenuation by a thick barrier, related the total attenuation to the combined effect of thickness and an equal height thin barrier<sup>6</sup>. A simple chart for the estimation of the attenuation by a wedge diffraction has been proposed<sup>7</sup>, relating the wedge attenuation to that combined with the effect of a thin screen and the effect of the wedge angle.

Hutchins et. al investigated the frequency dependence of barrier insertion loss for various barrier designs with physical scale modelling<sup>8</sup>. Their work shows the interference effects of different ground surfaces on the barrier performance. The various profiles associated with earth mounds are shown below. These were all covered with absorbing material. The profile "d" was also investigated with a reflective top.

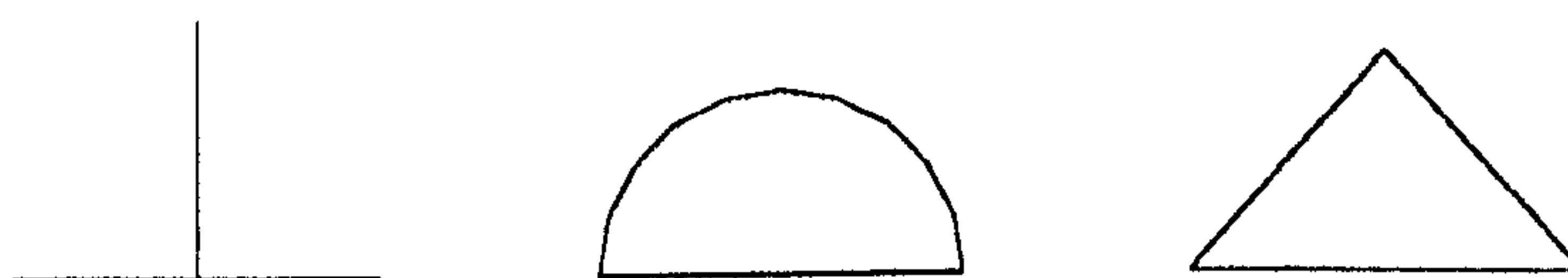


**Figure 5.1 : Earth mounds investigated by Hutchins et al.**

In the presence of a grass covered ground surface, a and b performed similar to a thin vertical barrier. A large change was observed when the overall width of profile c was 12 m. The low frequency performance of this profile was 15 dB but decreased steadily at higher frequencies. Profiles d, e, f, g all gave improved insertion loss performance at selected frequencies, due to destructive interference<sup>8</sup>.

Compared with an equivalent height thin vertical wall in the presence of an asphalt ground, the profiles a and b resulted in similar forms of insertion loss curves with some additional attenuation. Profiles d and e gave great improvement over thin vertical barrier at 500 Hz. Profiles d and e provided 10 dB and 20 dB additional insertion loss respectively over that produced by a thin vertical barrier. The reflective version of d gave improvements at 1 kHz and profiles f and g provided improvements at 550 Hz<sup>8</sup>.

Numerical modelling by boundary element methods demonstrated a 3 dB/octave increase in the insertion loss values of various profiles above 500 Hz as the sides of the profiles became more vertical<sup>9</sup>.



**Figure 5.2 : Geometries investigated by Hothersall et al.**

Similar trends were observed when the wedge angle of a wedge shaped barrier was decreased. As the sides of the profile became more vertical with the decreased wedge angles, the insertion loss improved, particularly at the low frequency. The difference between an absorbing and a reflective wedge shaped barrier with a wedge angle of 127 degrees was also investigated. 3 dB/octave increase in insertion loss in the case of reflective wedge increased to a 4.5 dB/octave increase when the sides were absorbing. Similar investigation of with a wedge angle of 53 degrees yielded only a small difference between the reflective and the absorptive cases<sup>9</sup>.

Insertion loss provided by a wedge, flat topped mound and a thin vertical barrier gave consistent trends beyond horizontal distances of 20 m behind the barrier. The absorbing flat-topped mound gave a 3 dB improvement over an absorbing wedge of equivalent overall height. The thin vertical barrier gave, in turn, 1 dB improvement over the flat topped barrier<sup>9</sup>.



**Figure 5.3 : Geometries investigated by Hothersall et al.**

Road traffic noise propagation over earth mounds was investigated by Hothersall et al.<sup>10</sup> by site measurements. The predicted insertion loss values were found to be small. This was attributed to the introduction of the barrier which removed the beneficial ground attenuation of the grass-covered ground.

Chew investigated the possibility of using grass embankments for screening road traffic noise. The reductions were reported to be in excess of 6 dB(A) when the slope angles were greater than 10 degrees. However, for high-rise buildings, the benefits were found to be non-existent for residents living in 10th storey and above<sup>11</sup>.

The observations on earth type barriers, most of which are explained above, were summarised by the working party on the effectiveness of noise walls<sup>12</sup>.

It was emphasised that the insertion loss for a hard-surface wedge was lower than for a vertical barrier and no consensus existed on the magnitude of this effect. Increasing the wedge angle in the case of wedge shaped barriers reduced the performance progressively. The introduction of absorbing materials at the sides of a shallow-sided barrier improved the high frequency performance. In the cases where the wedge angle exceeds 45 degrees, the performance of a wedge shaped barrier was noted to be less than that of an equal height barrier. A flat-topped grass covered berm performed similar to a vertical wall. For source and receiver geometries close to an earth berm, insertion loss was increased, mainly due to enhanced high frequency performance. Mounting a thin-wall on top of an absorptive-topped earth mound was found to initially reduce the beneficial effect of the absorptive top. As the height of the thin-wall was increased, the performance recovered.



## **5.3 FACTORS FAVOURING THE APPLICATION OF EARTH MOUNDS**

In urban areas, the unavailability of space and the magnitude of the noise problem make the application of wall type barriers more favourable. Increased awareness on the impact of noise on the environment is focusing the attention to semi-urban and rural areas where noise was not perceived to be such a great threat. The spread and growth of traffic noise in space and time is threatening these environmentally sensitive areas which have a lower tolerance threshold for noise to begin with. Noise control solutions to be implemented in these areas will not only have to address the noise pollution, but also the environmental fragility of the surroundings themselves.

The following is an account of acoustic and non-acoustic factors which could favour the applications of earth mounds in certain situations.

### **5.3.1 Acoustics**

An equal height wall type barrier will perform better than an earth mound due to the fact that the highest "part" of the wall can be constructed closer to the highway<sup>13</sup>. However earth type barriers can be made higher without much visual impact and are not subjected to stringent structural constraints like those of the wall type barriers. Increase in height implies an increase in wind loading in the case of wall type barriers and foundation design has to be reviewed.

Typical insertion loss values have been reported to be 15-16 dB (A) for a 3-4 m high earth berm with shrubbery, for some representative installations.<sup>14</sup>

When a flat-topped earth mound is compared against a thin wall with their centrelines running exactly the same distance from a source, the difference is only 1 dB as seen before<sup>9</sup>. It is likely that when tested outdoors, a difference of this magnitude may not necessarily be quantified, given the variations in traffic, atmospheric and ground conditions.

A conventional barrier is not effective against low frequency noise, however due to its dimensions, an earth mound has the potential to intercept much larger wavelengths.

The transmission loss through a wall type barrier is a major consideration, due to the choice of materials and the type of construction. Not only the material has to be dense enough, but also all the gaps have to be sealed. A minimum surface density of 20 kg / m<sup>2</sup> is recommended <sup>14</sup>. Earth mounds would not possess these limitations due to the very nature of their construction.

Therefore acoustically there is not much against the earth mounds, when compared against wall type barriers, to outweigh their applications.

### **5.3.2 Aesthetics**

The aesthetic design of environmental noise barriers requires careful planning. The choice of colours, textures, materials all need to be considered. In the case of earth mounds these may not be an issue. Because of their sloping sides they may not create the claustrophobic feeling that the motorists might perceive in the case of vertical walls. This would mean there is neither the need nor the expectation to vary the design of the longitudinal profile. Due to their natural appearance they may not appear to be a noise barrier at all. Planting the top of the barrier with vegetation and the slopes of it with grass could make it very appealing.

### **5.3.3 Cost**

The costs incurred during the design, construction and maintenance of a barrier are very important considerations. The cost of a scheme could in most instances single-handedly determine if a noise barrier can be built.

In the cases where a new road is being built there may be enough excess material to construct the earth barrier at a negligible cost. In those circumstances, getting rid of that material by transporting it somewhere where it can be disposed of would normally add to the cost of the project. In some cases, earth mounds could even be the dumping ground for demolition and power station waste. These do not have any adverse environmental impact and would need to be recycled or otherwise disposed of.

Earth barriers usually have unlimited life span and are less costly to maintain. They would not be exposed to acts of vandalism, such as graffiti or stone throwing. The earth barriers may not require additional safety barriers which are considered essential in the case of wall type barriers against vehicle collision. Unlike in the case of walls, there would not be provisions made for snow or wind loading, snow clearance from the roads, shock, fire or corrosion resistance of the barrier materials or dynamic loading from by-passing vehicles. All these factors could reduce the money and time spent on designing the barrier<sup>14</sup>.

### **5.3.4 Acceptability**

Due to the subjective nature of the noise, unless a noise mitigation measure is taken by the common consensus and approval of the public, it will not be appreciated even though acoustically and aesthetically it is effective. It is well known that earth type

barriers have high acceptability among the public and because of this reason they will be widely preferred and deemed acoustically effective<sup>15</sup>.

In U.S., prediction models even allow an extra 3 dB(A) attenuation, due to its perceived effectiveness, when a barrier is specified as a berm.<sup>15</sup>

### **5.3.5 Environmental friendliness**

An earth type barrier can be made to fit into the local environment and to reflect its character by embracing local wild life, either plants or animals, and hence making it even more popular with local communities.

They typically allow more sunshine and better air circulation than walls.<sup>14</sup>

## **5.4 ACOUSTICAL GUIDANCE ON EARTH MOUNDS**

### **5.4.1 Applications In Europe**

In Austria one-third of the total of 500 km of barriers consist of earth berms, earth with a wall on top or earth with steep slopes. Earth berms are mainly used when new roadway sections are constructed.<sup>14</sup>

Attempts have been made to apply a special variation of building a wall on top of an earth berm. 1 m high, earth-filled, wooden troughs have been fixed to earthberm crowns without any foundation, saving the cost of a traditional foundation and purchase of additional property.<sup>14</sup>

Steep earth berms have been used where available space was too small for an earth berm with natural slopes. However, these have higher construction and maintenance costs, and a shabbier appearance in winter months. They are difficult and costly to maintain.<sup>14</sup>

In Denmark, if desired height of the barrier has been more than 4-5 m, then earth berms have most often been easier to fit into the landscape than noise barriers. The earth berms have primarily been used in natural surroundings and in less densely populated areas, as the earth berms require relatively large amount of space.<sup>14</sup>

### **5.4.2 Earth mounds In U.K.**

A recent example on the use of earth mounds has been constructed as part of the Channel Tunnel Rail Link which opened in September 2003<sup>16</sup>. The proposed noise mitigation works were undertaken in the form of noise bunds where appropriate,



utilising the surplus soil in a carefully designed new landscape form. The new landform was functional both in terms of noise control and the subsequent use thereafter. The use of surplus soil in this way generated enormous cost savings and environmental benefits to the project by removing the need for taxable offsite waste disposal at remote locations, thus keeping heavy lorries off the public highway.

Another proposed major road widening project, which is expected to start in 2005, is the £165 million A3 Hindhead widening scheme<sup>17</sup>. This project will involve a twin bore tunnel passing through Devil's Punch Bowl in Surrey, which is a Site of Special Scientific Interest (SSSI) and Special Protection Area (SPA). Therefore environmental concerns dictated all aspects of the design. As part of the noise mitigation works and to hide the traffic from the view, earth mounds with heights of up to 5m have been proposed<sup>18</sup>.

"Environmental Barriers", Part 1<sup>19</sup> encourages the use of earth mounds both for rural and semi-urban contexts. Where the acoustic performance of an earth type barrier needs to be improved, combination with a "conventional" type barrier is recommended throughout the document. Some examples are quoted from the Part 1:

- 2.17 - "...similarly, short barriers at the top of cuttings can improve their acoustic efficiency."
- 4.3 - "...earth mounds can be combined with barriers if the skyline is softened with planting."
- 4.13 - "...a short fence type of barrier can be used on top of a mound to increase the degree of screening"

Part 2<sup>20</sup> continues to promote the beneficial effects of using a short height barrier as a diffracting edge in conjunction with an earth mound, however with the addition of a probable worry that the ground absorption may be diminished.

- 4.12 "...it might therefore be beneficial to provide a short acoustic screen on top of an earth mound to obtain maximum benefit, but the noise absorbent effect of the vegetated slope may be diminished."

The above paragraph is about the only mention given to an application which has the potential to be very useful in practice. This leaves the designer in a dilemma whether to use a short height barrier or not. Therefore a question that needs to be addressed is the minimum possible barrier height that would provide significant acoustical benefit, while keeping the visual impact to the surrounding environment minimal.

The following two sections aim to obtain an indication of the on-site performance of an earth mound type barrier and to explore the possibility, by physical scale modelling, of using small height barriers on top of earth mounds to increase their performance.

## **5.5 OUTDOOR NOISE MEASUREMENTS ON THE PERFORMANCE OF AN EARTH MOUND**

This section will present the results of a road traffic noise survey which are intended to demonstrate the noise attenuation on site due to the presence of an earth mound. Results will be compared to those predicted by the official traffic noise calculation method, called *Calculation of Road Traffic Noise (CRTN)*<sup>21</sup>.

### **5.5.1 Measurements**

The measurements were taken between 16:45 - 18:00 hours on a Saturday on Mosborough by-pass known as the A57. The road under consideration is a dual carriageway and the speed of the traffic is subjected to a 60 miles / hour limit.

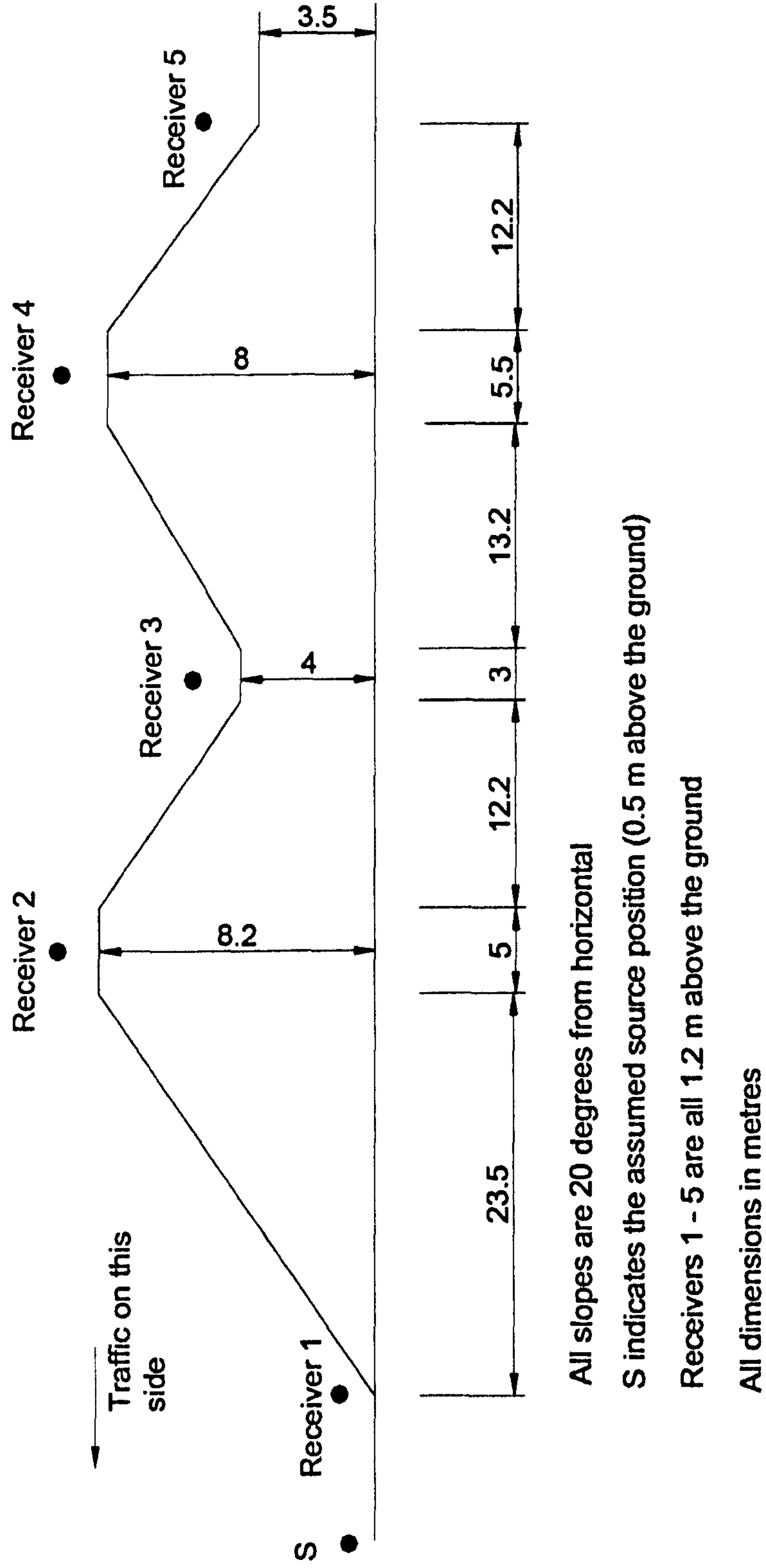


Figure 5.4 : The sketch showing the cross-section through the site and the receiver locations.



The section of the road where the measurements were carried out was a straight segment, with an estimated gradient of approximately 10 %. The lay-by which was chosen as a convenient location for easy access to the selected site, was roughly in the middle of the road segment, with no other traffic sources affecting the results. The only potential source of unwanted traffic is envisaged to come from the roundabout at one end of the by-pass, which is 2 miles away from the site.

The section where the measurements were taken is shown in Figure 5.4. The barrier under investigation is an earth mound. Rather than being a purpose built noise reducing device, it is the outcome of the roadworks undertaken during the construction of the by-pass. There is a public footpath running immediately behind the earth mound. The earth mound was continuous along the road segment and was running parallel to the road. All the slopes shown are 20 degrees and are covered with grass. The receiver heights are all 1.2 m. The relative distances and relative heights of the receiver positions 1 - 5 can be seen in the sketch of the section provided.

The traffic conditions could be considered free flowing traffic. The total number of vehicles accounted was 1750 vehicles over the hour of measurement period, traffic being constant with approximately 300 vehicles running every 10 minutes in both directions. The amount of heavy vehicles was negligible. 10 - 15 heavy vehicles were counted, most of which were double-decker buses and a few light trucks, accounting for less than 1% of the total number of vehicles. Wind speed did not exceed 2 m/s.

Two sound level meters were used for the purposes of this investigation after they were calibrated on site. The first sound level meter was used to monitor the traffic noise levels at the reference point. It was positioned 5 m away from the nearside edge of the carriageway, placed 1.2 m above the ground level. The second receiver was used for sampling the noise levels for 15 minute durations at receiver locations 2, 3, 4, and 5. The receiver heights were all 1.2 m above the ground that they were resting. The relative locations of the receivers are as seen in Figure 5.4. To enable direct comparison, the sound level meter at receiver 1 was reset every time the second sound level meter was moved to a different receiver location. Measurements were taken in 1/3 octave band frequencies between 8 Hz and 16 kHz and various noise indices were determined.

### **5.5.2 Results**

The frequency spectrum behind the barrier shows some typical features. The frequencies less than 63 Hz are only reduced by 7 - 8 dB. The reductions continue increasing up to the 500 Hz, which corresponds to a distinctive trough of around 32 dB reduction. Immediately afterwards, there is a distinctive peak at 1000 Hz which is



following the shape of the previous curve corresponding to the before-the-barrier curve. After the 1000 Hz, the curve again dips down roughly following the other curve as above. The reductions between 250 Hz and 8 kHz are between 20 - 30 dB.

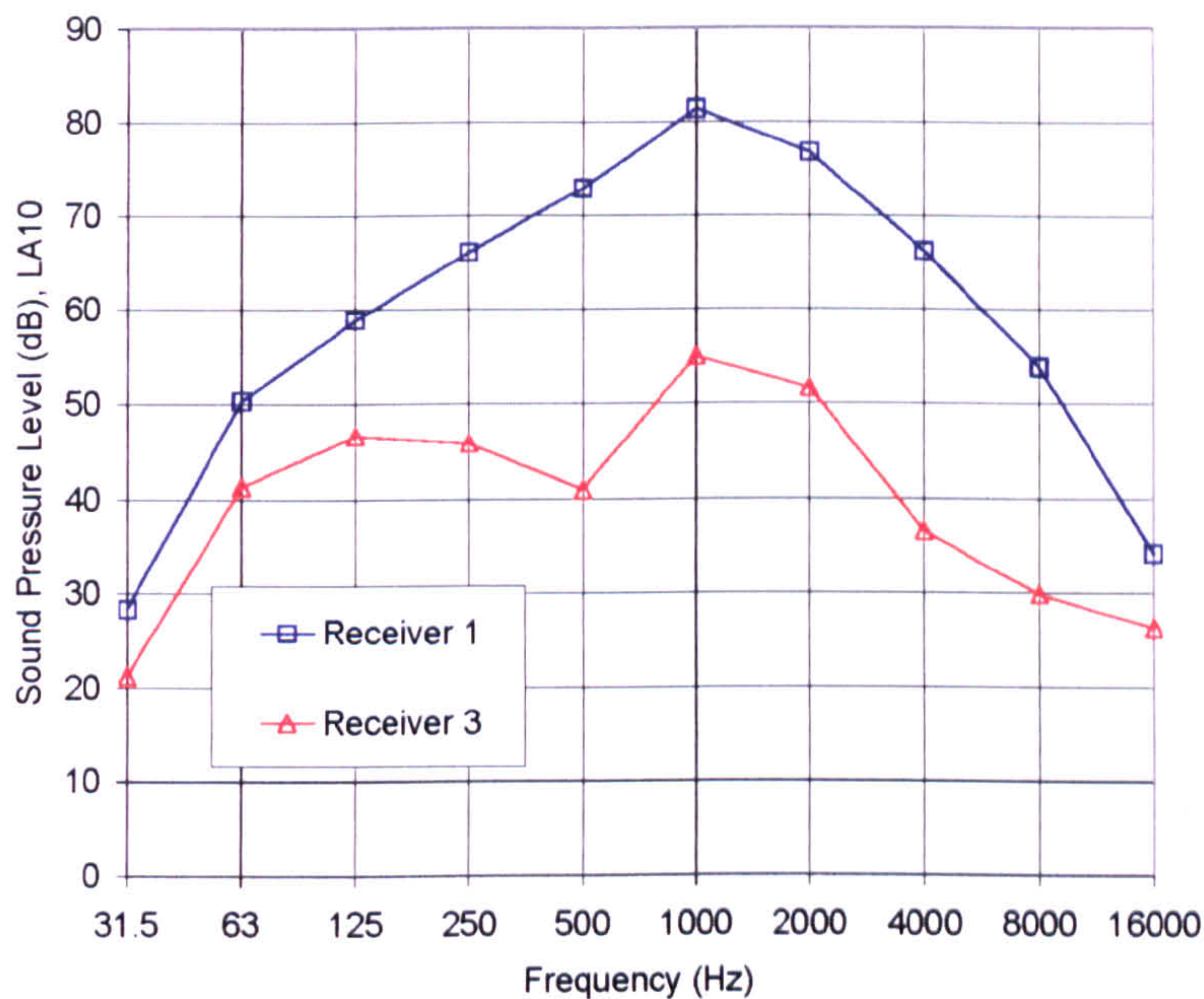


Figure 5.5 : A-weighted sound pressure levels (LA10)compared for receivers 1 and 3.

Figure 5.5 provides useful information on the frequency characteristics of a typical traffic noise spectrum which has a parabolic shape with a peak at around 1000Hz. However the frequency spectrum behind the screen has a very prominent trough at around 500 Hz which somehow distorts the parabolic shape of the spectrum. Reductions at frequencies above 250 Hz are the most noticeable, and the low frequencies below 250 are not reduced as effectively.

The effects of barrier screening and geometrical spreading can be seen together in the results presented above. In the next section, it will be attempted to separate the two components and to predict the effect of screening alone.

### 5.5.3 Prediction of Noise Levels

The prediction method used is the UK’s official ‘Calculation of Road Traffic Noise (CRTN)’ method. All the graphs, charts and equations referred to are from the named traffic noise calculation method.

According to the CRTN, the source height is 0.5 m and it is situated 3.5 m inside of the nearside carriageway edge. The basic noise level at a reference distance of 10 m away from the nearside carriageway edge is obtained from the traffic flow, the speed of the traffic, the composition of the traffic, the gradient of the road and the road surface. The basic noise level is then subjected to further corrections such as the effects of distance



from the line source, the nature of the ground surface, and screening from any intervening obstacles. The method of calculating the effects of propagation and screening can generally be broken down into separate parts.

- (i) Calculate the correction for distance disregarding the presence of ground or intervening obstacles.
- (ii) Decide whether the road segment is obstructed or unobstructed.
- (iii) For unobstructed road segment calculate the effect of absorbing ground where necessary.
- (iv) For obstructed road segment apply a screening correction.

The noise levels at receiver positions 1 - 5 have been predicted following the guidelines provided by the CRTN. The summary of results can be seen in Table 5.1 below. All the noise levels listed in the table are LA<sub>10</sub> dB(A). The square brackets refer to the noise levels predicted by an alternative interpretation of the examples given in CRTN for practical guidance.

LA <sub>10</sub> dB(A)	Receiver Location				
	1	2	3	4	5
Measured	83.3	77.3	57.1	59.4	51.3
Predicted	81.1	71.5	57.6	59.5	55.1 [51.9]

**Table 5.1 : Measured and predicted levels for receivers 1 - 5.**

The predicted values of 55.1 dB(A) and 51.9 dB(A), obtained for receiver 5 are the result of two different approaches (Examples provided in Annex 11 and Annex 12 of the CRTN). The double - screening correction (Annex 11) gave an overprediction of 3.8 dB(A) and the approach of “screening by flat - topped buildings” (Annex 12 ) gave an overprediction of 0.6 dB(A). Although the CRTN is open to interpretation, double - barrier correction is thought to be a more realistic approach, giving a discrepancy of 3.8 dB(A).

The predicted noise levels at receivers 3 and 4 have shown reasonable agreement with measured levels. Therefore, it could be argued there should not be any shortcoming of the screening correction within the method, which is the only correction applied together with the distance correction. The receiver 1 gave 2.2 dB(A) underprediction. This shows there is a potential overprediction of the screening correction which counterbalances the underprediction incurred earlier. When we look at the predicted level at Receiver 5, this argument can be supported more. The double - screening correction applied for this location gave an overprediction of 3.8 dB(A) which is consistent with the trend. The alternative method of calculation, the result of which is presented in square brackets in Table 5.1, gives a much smaller overprediction of 0.6



dB(A), which is considered acceptable. The former method (Annex 11) is the "double screening effect" and the latter one (Annex 12) is an "equivalent single barrier" approach which gives a much larger path difference, hence resulting in larger correction which brings the normally overpredicted results much closer to the measured levels.

### **5.5.4 Prediction of Insertion Loss**

The noise level at receiver 3 was predicted to be 57.6 dB(A). The measured value was very close to predictions which meant the CRTN could be used further to predict the insertion loss performance of the first earth mound. Starting from the basic noise level, which is the noise level at a reference distance of 10 m away from the nearside carriageway edge, the noise level at receiver 3 can be predicted pretending the earth mound does not exist at all. The corrections which need to be applied are the distance and ground correction. Distance correction is as before (i.e. 5.8 dB(A)) and the ground correction can be predicted from Chart 8 ( $d = 50$  m and  $H = 2$  m) as 5 dB(A). When these two are subtracted from the basic noise level, the resulting noise level is found as 68.3 dB(A). Difference between "with the barrier" (measured) and "without the barrier" (predicted) noise levels gives the insertion loss. Therefore the insertion loss is predicted as 10.7 dB(A).

### **5.5.5 Concluding Remarks**

The agreement between the measurements and the predictions is good where only screening correction is applied.

The site is unique in that it contains double-earth mounds. It is not clear from the CRTN how to predict the noise levels behind the second mound (receiver 5). Following the guidance given in the method, two different approaches were employed, giving different results.

Considering the CRTN is a simple and practical method, all predictions gave reasonable agreement with the measurements, probably with the exception of receiver 2. Since the sampling durations were unrepresentative, a more involved traffic survey is expected to provide a better agreement.

A typical A-weighted traffic noise spectrum was obtained showing that highest levels are concentrated around 1 kHz. The linear traffic noise is governed by low frequency noise.

Insertion loss provided by a receiver behind the earth mound situated in the deep shadow zone was calculated to be 10.7 dB(A).

## **5.6 PHYSICAL SCALE MODELLING OF EARTH MOUNDS WITH SMALL HEIGHT BARRIERS**

### **5.6.1 Introduction**

A possible gain in acoustic performance with the use of a small height barrier on top of an earth mound would mean the same performance can be achieved with a lower height barrier. The implications would be lesser requirement for fill material and lesser horizontal land take. It should be recalled that these are the two main physical limitations inhibiting the use of earth type barriers.

It is obvious that higher the barrier on top, better the acoustic performance due to an increase in path length. However, the main asset of the earth mounds is their natural appearance and therefore the height of any barrier on top has to be small enough so that it blends into the background and the visual impact is minimised. If the required performance cannot be achieved by a single edge, the double or multiple configurations could be considered.

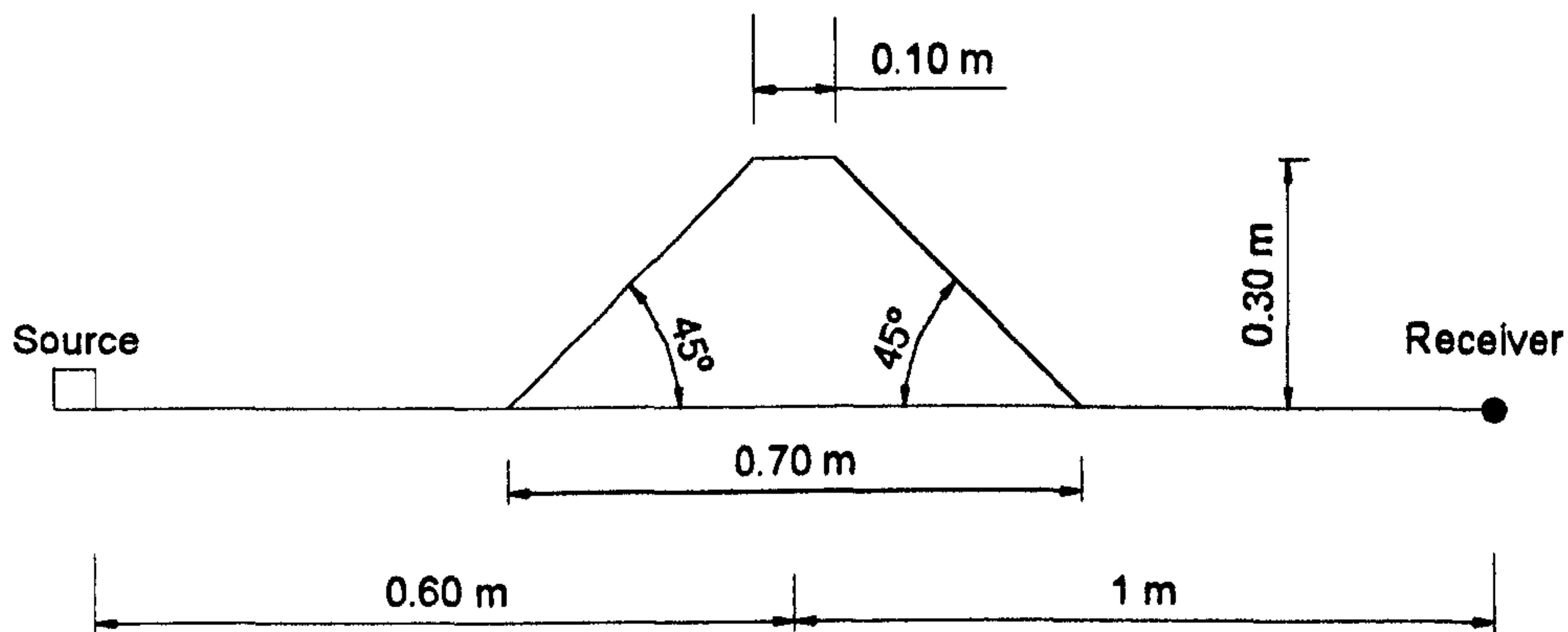
This section will investigate the relative effects of small height barriers, or edges, on top of earth mounds using physical scale modelling.

### **5.6.2 Experimental Method**

For the purpose of this investigation a scale of 1:10 was used. Using this scale factor, frequencies ranging from 100 Hz and 2000 Hz were modelled at 1/3 octave intervals giving a modelled range between 1 kHz and 20 kHz.

An earth mound of trapezoid shape was modelled to which combination of different heights of screens and absorbing materials were added to create 15 configurations. The physical dimensions of the mound were 24 m long, 7 m wide (base) and 3 m high with 45 degree slopes giving a width of 1 m at the top. Details can be seen in Figure 5.6.

The model was constructed from 4 mm thick medium density fibreboard and the absorbing material used was glass fibre quilt of 8 mm thickness. The absorbing characteristics of these materials are detailed in Chapter 7.



**Figure 5.6 : Details of the source / receiver locations and the dimensions of the basic geometry.**



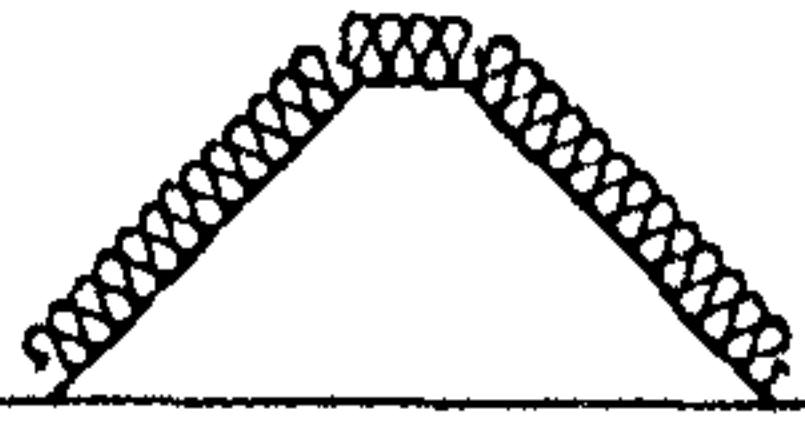
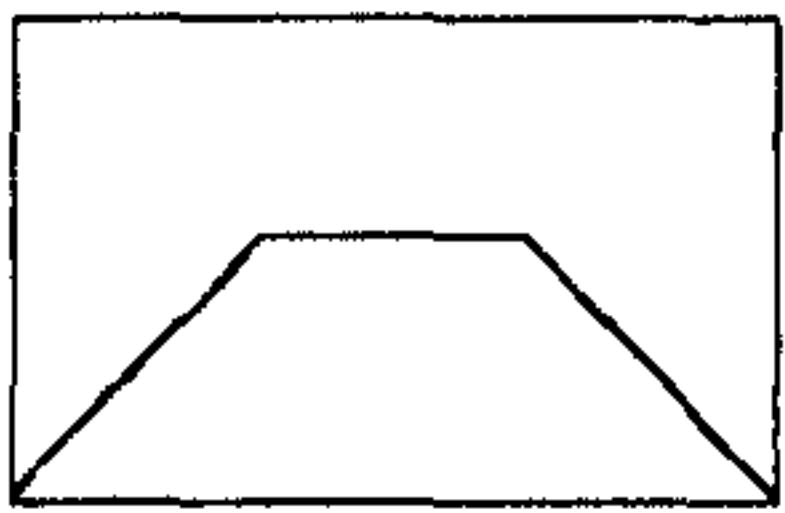
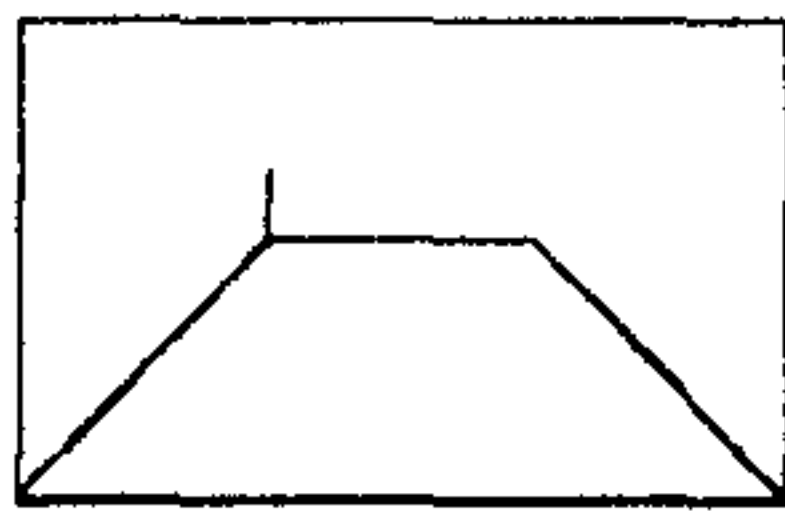
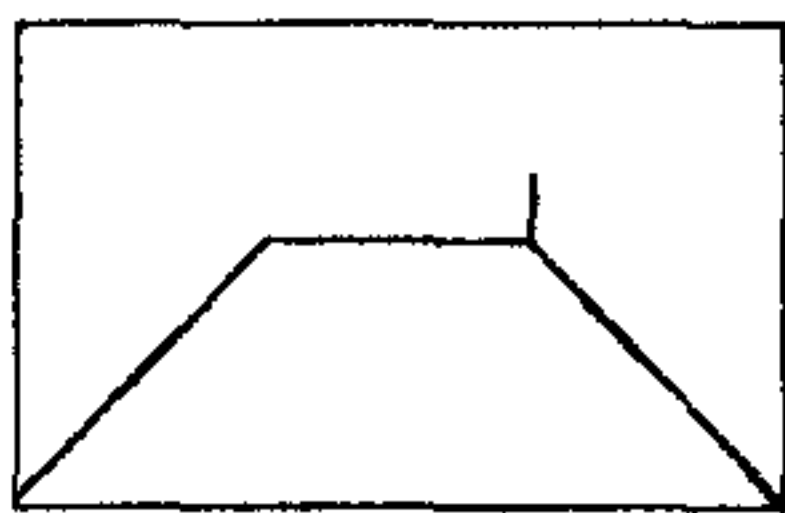
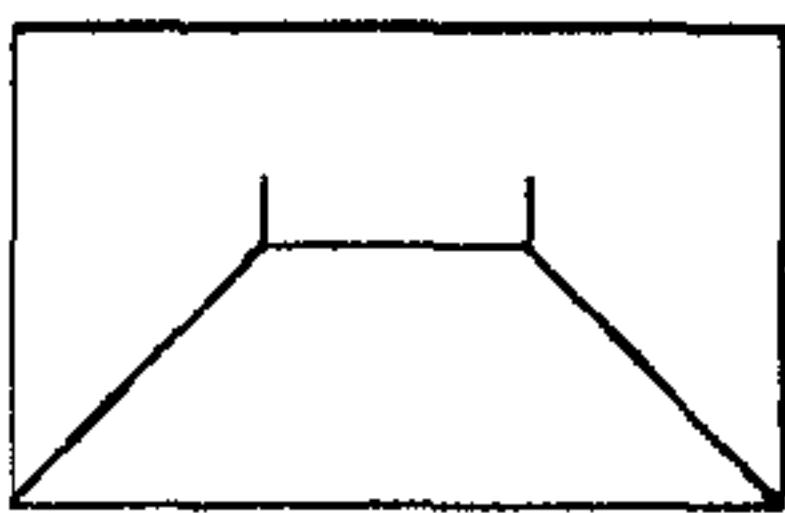
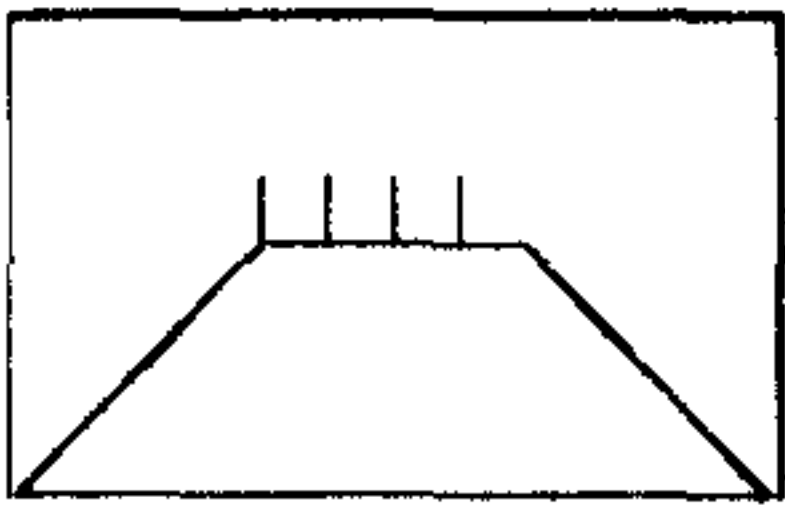
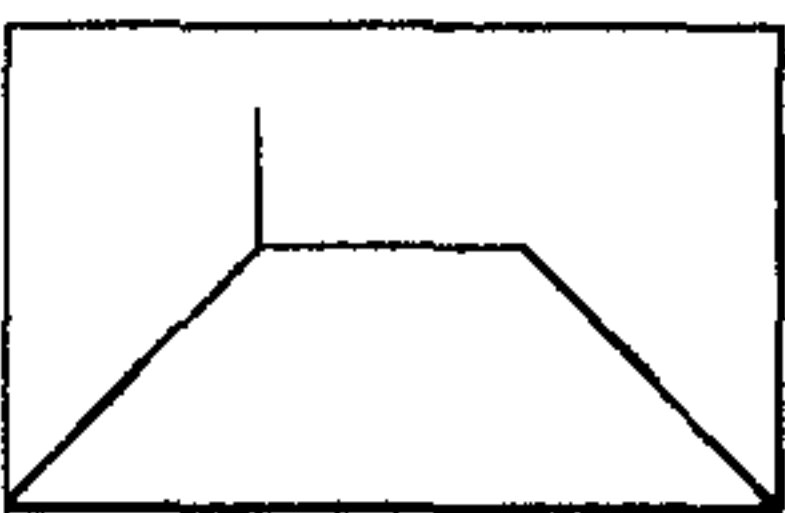
The set-up was placed on top of a bench in the centre of the room with the source-receiver axis being parallel to the room length. The source was located on the bench, 0.6 m away from the centreline of the model. The receiver was 1 m from the centreline of the model, positioned on the opposite side of the model and resting on the bench.

The reference noise levels were measured 0.05 m from the source. This distance was thought to be close enough to the source to give a good representation of the output noise levels, and to characterise the source accurately. The source was connected to a random noise generator and an amplifier where a constant and continuous output of noise was produced. The sound level meter was run through a frequency sweep both at the reference point on the source side and at the receiver position. The tests were repeated 4 times for each configuration and their average was taken. The difference between the average values of the two levels for each frequency band gave the relative acoustical performance of each modification at the receiver position under investigation.

### **5.6.3 Results**

The 15 configurations investigated are shown in Figure 5.7. Each edge condition combined with one of the three slope absorption characteristics represents a different profile where applicable. The summary of results shows the relative performance of the profiles over the reference case. The reference case was chosen as the plain mound with no edges (Profile A). The single number ratings in dB are determined from the difference in the sound pressure levels between the reference point and the receiver position, averaged linearly for the whole testing frequency range.



Edge height	Details of the edge conditions on the horizontal top.	Plain Mound	Partial Absorption	Full Absorption
				
No edge		PROFILE A 0	PROFILE B +3.3	PROFILE C +3.8
0.025 m		PROFILE D +0.3	PROFILE E +3.2	PROFILE F +3.3
		PROFILE G -2.1	PROFILE H +1.9	PROFILE I +3.6
		PROFILE J -0.6	N / A	PROFILE K +4.8
		PROFILE L -0.7	N / A	PROFILE M* +3.3
0.05 m		PROFILE N -0.5	PROFILE O +0.9	N / A

**Figure 5.7 : Relative performance in dB of various edge conditions combined with different absorption characteristics over plain earth mound.**

*\* The profile M does not have absorptive material on horizontal top section due to presence of multiple edges.*



The relative differences between each profile and the reference case throughout the whole frequency range under investigation are also shown in Figure 5.8 and Figure 5.9.

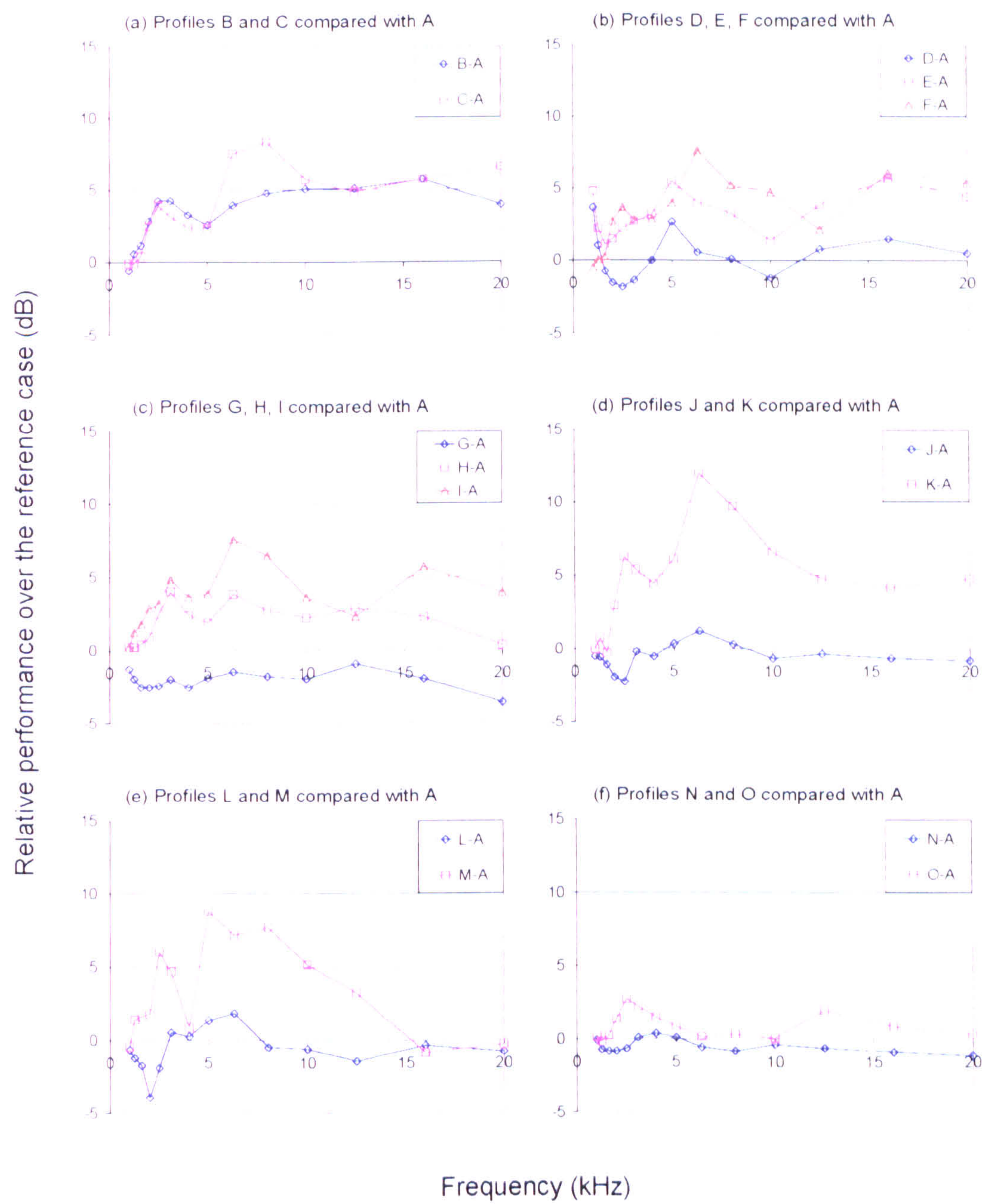


Figure 5.8 : Comparison of the effects of different absorption characteristics over the performance for given edge conditions.



The relative differences between each profile and the reference case throughout the whole frequency range under investigation are also shown in Figure 5.8 and Figure 5.9.

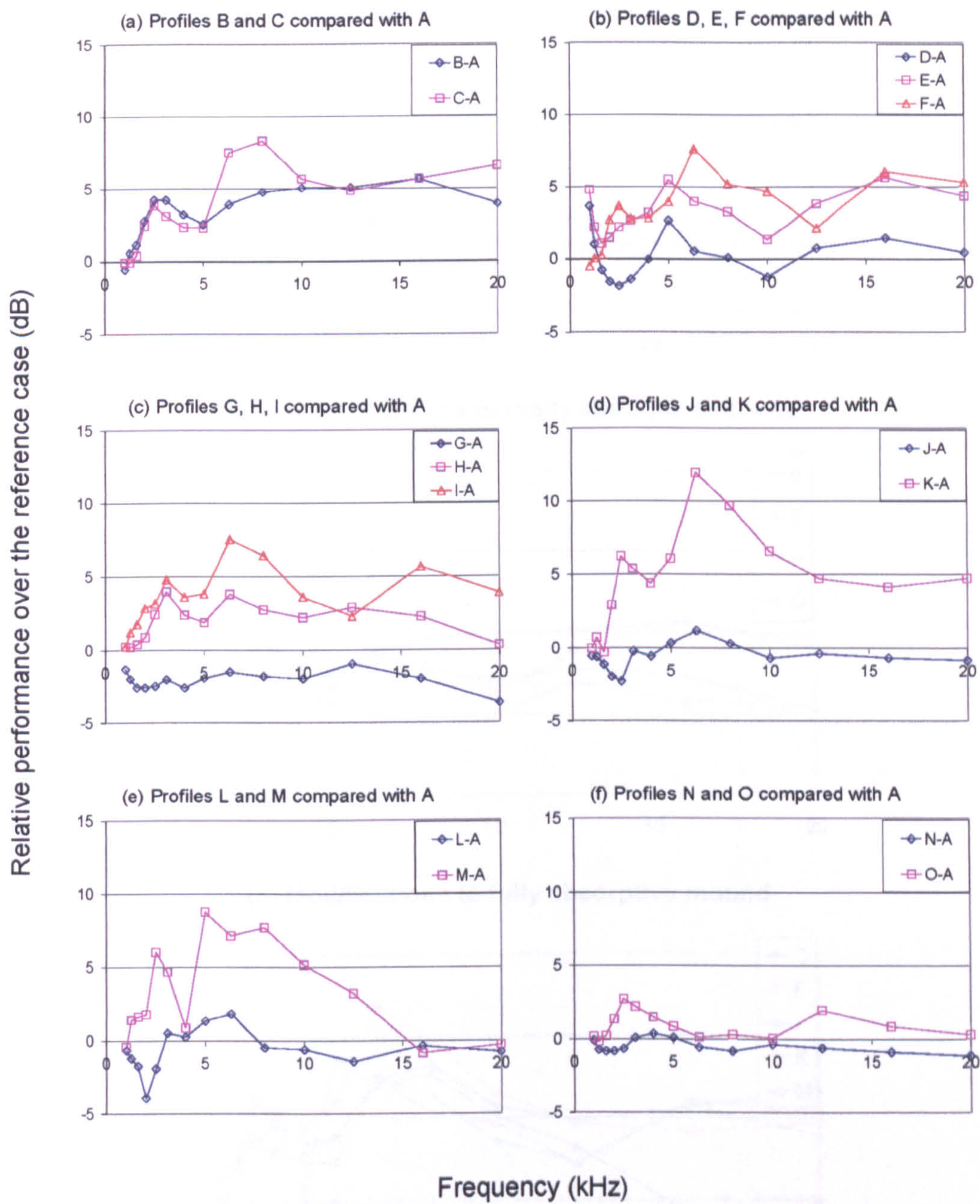
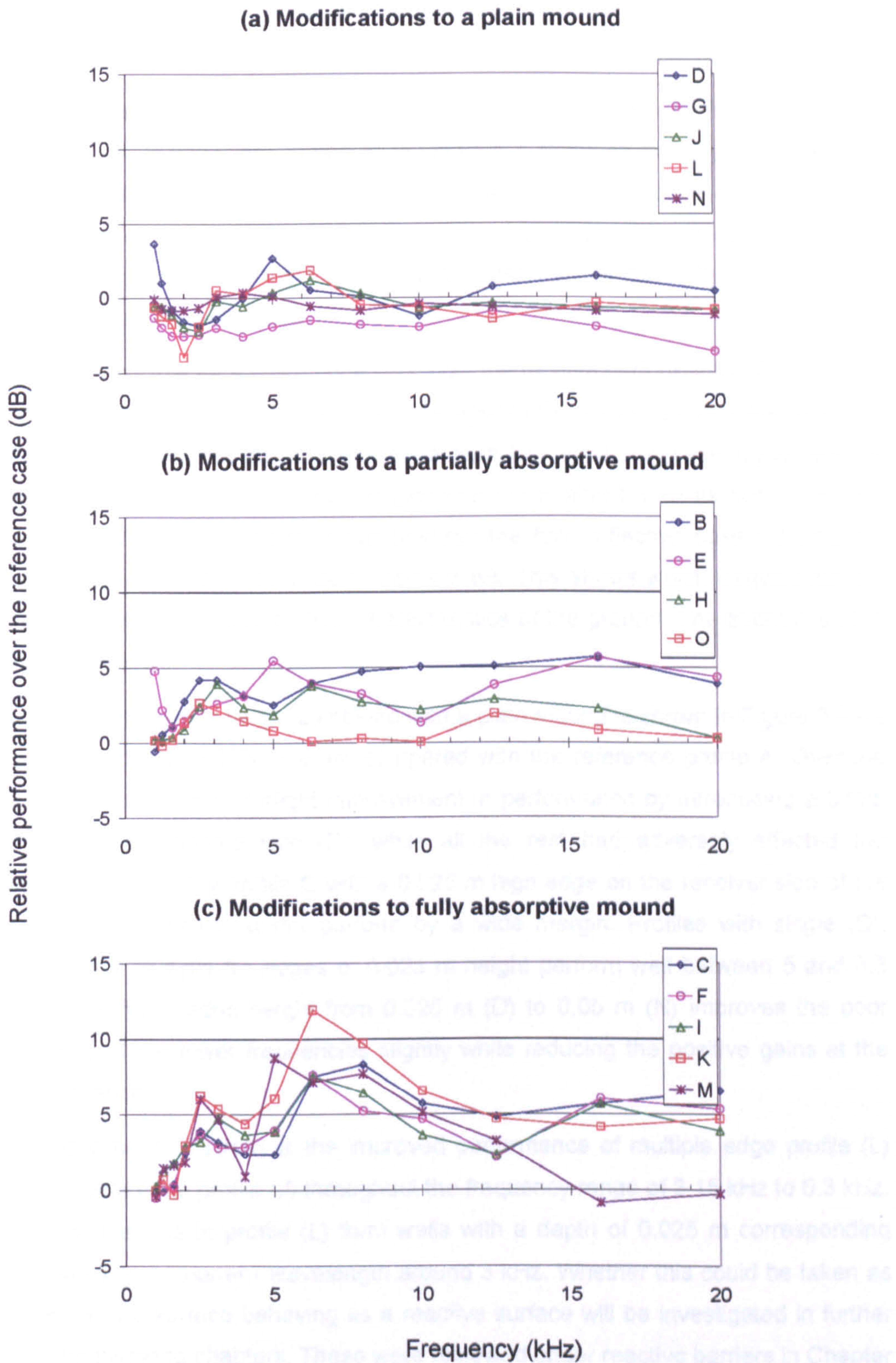


Figure 5.8 : Comparison of the effects of different absorption characteristics over the performance for given edge conditions.





**Figure 5.9 : Comparison of the effects of different edge conditions over the performance for given absorption characteristics.**



### **5.6.4 Discussion**

In order to illustrate the effect of the absorbing material on the performance of the mound, cases A, B and C are compared in Figure 5.7. Between the fully reflective case (A) and the fully absorptive case (C), there is a 3.8 dB difference over the whole spectrum. Placing absorptive material only on the source side (B) provides most of the beneficial effect caused by the fully absorptive case (C), as case (B) is only 0.5 dB short of the fully absorptive case.

Figure 5.8 shows that for a given edge condition, the relative performance of any profile has a tendency to improve with increased absorption of the ground cover. Between 6.3 and 10 kHz, reducing the absorptive material from fully absorbing case (C) to partially absorptive case (B) yields reductions in performance of about 4 dB as seen in Figure 5.8 (a). This is the intermediate stage towards the fully reflective case (A) and the reductions in performance increase to about 8 dB. This shows which frequencies are affected most through the absorbing characteristics of the ground. The effect is visible especially at 8 kHz.

The effect of any barrier height combined with a plain mound is shown in Figure 5.9 (a) where profiles D, G, J, L and N are compared with the reference profile A. Over the whole spectrum, there was slight improvement in performance by introducing a 0.025 m screen on the source side (D), while all the rest had adversely affected the performance. Especially profile G with a 0.025 m high edge on the receiver side of the horizontal top is seen to under perform by a wide margin. Profiles with single (D), double (J) and multiple (L) edges of 0.025 m height perform well between 5 and 6.3 kHz. Increasing the edge height from 0.025 m (D) to 0.05 m (N) improves the poor performance at the lower frequencies slightly while reducing the positive gains at the higher frequencies.

Perhaps one point to stress is the improved performance of multiple edge profile (L) over the double edge profile (J) throughout the frequency range of 3.15 kHz to 6.3 kHz. The series of edges in profile (L) form wells with a depth of 0.025 m corresponding approximately to a quarter - wavelength around 3 kHz. Whether this could be taken as an evidence of a surface behaving as a reactive surface will be investigated in further detail in the following chapters. These were reviewed under reactive barriers in Chapter 3.

In Figure 5.9 (b) the mounds associated with the partial absorption case reveal that increasing the height of the edge on the source side diminishes the beneficial effects of the absorptive slope. In the presence of the 0.025 m high edge, frequency range of 8 to

12 kHz seem to be affected and rising the edge height to 0.05 m influences most of the frequencies except those at the lower end.

The fully absorptive cases in Figure 5.9 (c) show the distinctive increase in performance between 6 and 8 kHz. The multiple edge profile (M) still maintains its performance at around 3 kHz and at 5 kHz the possible reasons for which were speculated above, but fails to retain this trend and consecutively becomes the worst performing profile of the fully absorptive cases, at the higher frequencies. Profile K performs better than any other profile. This is prominent especially between 6 to 8 kHz.

The findings on small height barriers can be translated into reality by using the scale factor of 1:10. In the case of a plain mound, a very small edge, of height 0.25 m, can be slightly beneficial. As the ground absorption increases, installing a barrier can affect the performance adversely. Under these conditions, as the height of the edge increases, the reductions in performance increase. An exception seems to be the double edge case with 0.25 m high edges.

The observed differences between different profiles are very small, indicating perhaps to the shortcomings in the uniform field experiments. This will be the subject of detailed discussions in the forthcoming chapters. These experiments demonstrated the benefits of absorbing slopes in qualitative terms. However the performance of various edge conditions could not be conclusively confirmed.

## **5.7 TECHNIQUES AVAILABLE FOR THE INVESTIGATION OF BARRIERS**

The three main techniques available for investigating the performance of noise barriers were discussed in Chapter 3. These are numerical modelling, physical scale modelling, and on-site measurements. Preliminary investigations were described in this Chapter using on-site measurements and physical scale modelling. This section will highlight the advantages and limitations of these techniques which will lead to the methodology to be adopted for the purposes of this work.

### **5.7.1 Noise Measurements**

The preliminary noise survey undertaken to assess the feasibility of further site investigations revealed a number of limitations of this technique which would make it unsuitable for this work.

The preparations involved with this survey were considerable although it was a one-day noise measurement. Finding a convenient site, carrying out the relevant risk



assessments, satisfying the University safety requirements for site surveys, notifying the local police and monitoring the weather forecasts to identify the favourable conditions were some of the early preparations. The survey could only be undertaken by at least two people. Therefore arrangements had to be made with an appropriately qualified member of staff. The equipment which would be required on site had to be determined in advance. A vehicle had to be arranged for their mobilisation to and from the site. While on site, proper setting up of the equipment and monitoring of all variables was vital.

However, the survey was still interrupted towards the second half of the day due to worsening weather conditions. The data collected did serve the purpose of obtaining a typical traffic noise spectrum, and also obtaining a representative insertion loss value for the earth mound under investigation.

Consideration was given to the possibility of employing this technique in order to develop a novel shape. The costs and time involved with the fabrication and installation of a number of different shapes of barrier profiles would have been an immense task. In order to quantify the effect of the modification, extensive before and after tests would have been essential. All tests would need to be normalised to the same reference atmospheric conditions in order to have statistically meaningful comparisons. This would imply careful monitoring of all variables including traffic conditions. The monitoring equipment would need to be different than conventional sound level meters used in this survey, if continuous on-site monitoring was to be undertaken.

In the light of this investigation, the prospects of any future on-site testing were ruled out. Before any full-scale tests can be justified, modelling work would need to indicate substantial acoustical gains over a plain mound.

### **5.7.2 Physical Modelling**

There is not a standard or widely accepted way of implementing physical modelling and hence one is usually forced to make certain choices based on availability as discussed in Chapter 3.

The modelling work described in this chapter was undertaken under uniform field conditions where mean squared pressure is assumed to be constant throughout the room volume. This method is likely to suffer from the reverberant build up of sound within the testing room due to the use of a continuous noise source. This would limit or under some circumstances totally eliminate the observed relative improvements between two barrier profiles.

Additional work would be required to quantify the contributions of reflections from room boundaries, and to determine whether an alternative testing arrangement would be essential for meaningful comparisons. This will be discussed in Chapter 6.

However it is considered that physical scale modelling would be very useful for investigating a large number of different barrier profiles cost effectively, in a short period of time and free from atmospheric effects.

### **5.7.3 Numerical Modelling**

The numerical models available for investigating the performance of barriers in homogeneous atmosphere but in presence of a ground surface were reviewed in Chapter 2.

Boundary element technique was identified as an accurate tool for being able to complex geometries. The software program called SYSNOISE will be used for this purpose. This is an established and commercially available software which is very versatile and can deal with the modelling of different edge conditions investigated earlier. The available geometrical diffraction models would not be suitable for these profiles where multiple diffraction and scattering mechanisms make the problem numerically complex.

Therefore numerical modelling, by boundary element methods, will be used to supplement the findings of physical scale modelling. There may be certain geometries which are difficult to fabricate as a scale model. Therefore once these methods provide consistent results with each other, the investigations will be extended further using numerical modelling.

## **5.8 CONCLUSIONS**

In this Chapter, the reasons for further research into earth mound type barriers were discussed. In order to promote their applications further, and to offset some non-acoustic limitations they have, the need for an enhanced acoustic performance was identified.

The preliminary work described in this chapter explored the possibility of using single and multiple edges on top of earth mounds to achieve this. This investigation did not provide any conclusive evidence in support or against the use of small height barriers on a plain earth mound. However there was limited evidence that a series of multiple edges on top of an earth mound type barrier could be beneficial at selected frequencies. The forthcoming chapters will investigate these diffraction and scattering

phenomena in greater detail both theoretically and experimentally and will seek to optimise the solution, if any.

Following the discussions on preliminary work, it was identified that modelling techniques, both physical and numerical, would be better suited for the purposes of this investigation. The physical scale modelling will be initially carried out in a large space with a uniform sound field. The boundary element technique will be applied, using the software SYSNOISE, to verify or otherwise the data collected using physical modelling.

The next chapter is a theoretical appraisal of the acoustic performance of the rib structures or multiple edges to be investigated in the forthcoming chapters. It aims to identify the physical parameters and mechanisms involved in their design, based on theoretical considerations used in the study of diffraction gratings and resonators.



## 5.9 REFERENCES

- 
- <sup>1</sup> JONASSON, H.G., Diffraction by wedges of finite acoustic impedance with applications to depressed roads, *J.Sound Vib.*, 25(4), 577-585, 1972
- <sup>2</sup> PIERCE, A.D., Diffraction of sound around corners and over wide barriers, *J.Acoust.Soc.Am.*, Vol. 55, No. 5, 941-955, May 1974
- <sup>3</sup> KAWAI, T., Sound diffraction by a many-sided barrier or pillar, *J.Sound Vib.*, 79(2), 229-242, 1981
- <sup>4</sup> DE JONG, B.A., MOERKEREN, A. and VAN DER TOORN, J.D., Propagation of sound over grassland and over an earth barrier, *J.Sound Vib.*, 86(1), 23-46, 1983
- <sup>5</sup> RASMUSSEN, K.B., On the effect of terrain profile on sound propagation outdoors, *J.Sound Vib.*, 98(1), 35-44, 1985
- <sup>6</sup> FUJIWARA, K., ANDO, Y., and MAEKAWA, Z., Noise control by barriers - Part 1: Noise reduction by a thick barrier, *Applied Acoustics*, 10, 147-159, 1977
- <sup>7</sup> MAEKAWA, Z., and OSAKI, S., A simple chart for the estimation of the attenuation by a wedge diffraction, *Applied Acoustics*, 18, 355-368, 1985
- <sup>8</sup> HUTCHINS, D.A., JONES, H.W., and RUSSELL, L.T., Model studies of barrier performance in the presence of ground surfaces. Part II - Different shapes, *J.Acoust.Soc.Am.*, 75(6), 1817-1826, June 1984
- <sup>9</sup> HOTHERSALL, D.C., CHANDLER-WILDE, S. N., HAJMIRZAE, M.N., Efficiency of single noise barriers, *J.Sound Vib.*, 146(2), 303-322, 1991
- <sup>10</sup> HOTHERSALL, D.C., CHAPMAN, B.C., and CHANDLER-WILDE, S.N., The propagation of road traffic noise over earth mounds, I.O.A. meeting on "Barriers for Noise Control", London, October 1985, *Proceedings of Institute of Acoustics*, 1(1), 135-142, 1985
- <sup>11</sup> CHEW, C.H., Effectiveness of grass embankments in screening high-rise buildings from highway traffic noise, *Applied Acoustics*, 37, 251-260, 1992
- <sup>12</sup> DAIGLE, G.A., Report by the International Institute of Noise Control Engineering Working Party on the Effectiveness of Noise Walls, *Noise/News International*, 13-35, March 1998

- 
- <sup>13</sup> Environmental Noise Barriers - A Guide to Their Acoustic and Visual Design, Bentz Kotzen and Colin English, E & FN Spon, 1999
- <sup>14</sup> Organisation for Economic Co-operation and Development (OECD), Roadside Noise Abatement, IRRD No. 870922, Chapter VI, Noise Barriers, 105-142, 1995
- <sup>15</sup> COHN, L.F., Highway noise barriers, National cooperative research program, synthesis of highway practice 87, Transportation Research Board, Washington D.C., December 1981
- <sup>16</sup> JOHNSON, P., Channel Tunnel Rail Link Section 1: Environmental Management During Construction, the Proceedings of Institution of Civil Engineering, Civil Engineering Special Issue, Volume 156, 16-20, November 2003
- <sup>17</sup> The New Civil Engineer, Magazine of the Institution of Civil Engineers, p 10, 6 November 2003
- <sup>18</sup> The Newsletter 'A3 Hindhead News', Issue 2, April 2002, detailed information can be found on the Highways Agency webpage dedicated to the project  
[http://www.highways.gov.uk/roads/area/03/works/a3\\_hindhead\\_scheme/news.htm](http://www.highways.gov.uk/roads/area/03/works/a3_hindhead_scheme/news.htm)
- <sup>19</sup> Volume 10 Environmental Design, Section 5, Environmental Barriers, Part 1 HA 65/94 Design Guide For Environmental Barriers, 1994
- <sup>20</sup> Volume 10 Environmental Design, Section 5, Environmental Barriers, Part 2 HA 66/95 Environmental Barriers – Technical Requirements, 1995
- <sup>21</sup> CRTN, Calculation of Road Traffic Noise, Department of Transport, Welsh Office, HMSO, 1988

## 6 THEORETICAL APPRAISAL OF THE ACOUSTICS OF RIB STRUCTURES

As discussed in Chapter 3, the terms '*rib structure*' and '*parallel ribs*' have been used by previous researchers to describe '*a series of parallel low-height walls on the ground*'. Therefore the term rib structure will be adopted as a generic term throughout this work to describe thin flat protrusions from a horizontal plane. Depending on the nature of rib structure under consideration, the term '*n-edge*' will also be used to refer to the specific number of edges comprising the structure to be able to distinguish one from another (i.e. 8-edge, single-edge, multiple edge etc.)

It should be noted that more recent work by others, on similar applications, used the terms '*reactive surface*', '*soft surface*' and '*pressure release surface*' when discussing these within theoretical context and referred to the terms '*wells*', '*tubes*', '*channels*' or '*quarter wavelength resonators*' when describing these physically. This work does not aim to coin new terms but rather uses the existing terminology as appropriate.

### 6.1 INTRODUCTION

This chapter, together with the previous one, forms part of the research methodology. The experimental work described in the previous chapter looked at the possibility of using single and multiple edges on top of earth mounds to improve their performance. It was found that a series of multiple edges on top of an earth mound type barrier could be beneficial at selected frequencies. It was concluded that further work would need to be undertaken to verify, or otherwise, these observations. This chapter undertakes a theoretical appraisal of the likely parameters and mechanisms involved in the design of a series of multiple edges, or rib structures. The theoretical approaches used are similar to those used in the study of resonators and diffraction gratings.

Recently, the use of '*acoustically soft pressure release surfaces*' on top of conventional barriers has been investigated. Barriers with horizontal<sup>1</sup> and cylindrical<sup>2</sup> caps have been studied with a series of tubes attached onto them which had depths corresponding to quarter-wavelength of the frequency to be controlled. These were shown to provide substantial noise reductions. An earlier research investigated the use of a similar concept for traffic noise reduction via exclusion of surface waves with a series of wells on the ground<sup>3</sup>.



In architectural acoustics Schroeder diffusers and quadratic residue diffusers on surfaces are used to scatter the sound waves in a manner to prevent unwanted reflections<sup>4</sup>. In building acoustics quarter-wave resonators have been used in ventilation systems and in industrial noise for fan noise applications<sup>5</sup>.

Acoustical effects due to periodic structures such as auditorium seating<sup>6</sup> and staircases were explained in terms of diffraction/interference gratings. Similarly, the use of street furniture and tree trunks as a possible means of scattering noise in urban environments has been proposed<sup>7</sup>.

This Chapter is concerned with noise attenuation mechanisms of periodic structures, however scattering from non-periodic surfaces have also been investigated. Some examples are underwater acoustic backscattering from ocean floor<sup>8</sup> and propagation over ground surfaces with small sized irregularities<sup>9</sup>.

The aim of this chapter is to present the findings of some of the related research in order to explain the mechanisms involved in noise attenuation by rib structures consisting of multiple edges or wells. Theoretical concepts used for the investigation of quarter-wave resonators and diffraction/interference gratings as well as surface wave generation mechanisms are suggested as the likely approaches which could explain these noise attenuations.

## **6.2 BACKGROUND**

This section provides a number of practical cases where noise attenuations have been reported using a series of wells, edges or roughness elements.

### **6.2.1 A series of edges on the ground**

A series of rib structures, consisting of low height brick walls, were investigated under soft and hard ground conditions. These were claimed to reduce the noise by surface waves exclusion<sup>3</sup>.

It was suggested that the impedance of the rib structure can be designed to provide optimum 'absorption' of traffic noise, taking into account the predominant frequencies of the traffic noise spectrum. This impedance matching would be achieved by choosing appropriate groove depths. The wall structure was modelled mathematically as an infinite homogeneous impedance boundary. This would be valid for sound with wavelengths greater than twice the distance between two walls, when no transverse wave modes were possible in the grooves. It was noted that for high frequencies a scattering and refraction approach would be necessary.

Outdoor measurements indicated that attenuations up to 20 dB between 125 Hz and 400 Hz and amplifications of up to 12 dB between 400 Hz and 1000 Hz were possible. This distinct effect observed at low microphone positions disappeared as the microphone was raised. It was found that the line below which a sound shadow exists for the surface waves and the ground must be less than 9 degrees. At an angle of 13 degrees, no significant effect was found. The absorption band would be expected to shift to higher frequencies with lower walls however no significant influence was observed. However the results showed that a rib structure offers a good method of attenuating the sound energy in the low frequencies produced mainly by trucks.

In the above measurements, there is no clear indication on the wall heights or the separation distances between the walls. The number of brick walls is given as 16 or 21 depending on the experiment. A combination of wall heights and separation distances appear to have been used. It is likely that different wall heights were achieved by using several bricks on top of each other and in differing alignments. For example, a 'standard' UK brick would have the dimensions of 215mm (L) x 102.5mm (W) x 65mm (D) however different sized bricks are also available. It could be deduced from the scale provided in the sketch of experimental set-up that the well depths were mainly 0.25m to 0.5m.

Based on theoretical considerations, the attenuation mechanism for the rib structures was shown to be surface wave exclusion. Further details on surface waves are given in forthcoming sections.

### **6.2.2 Noise barrier with a reactive cylindrical top**

A similar application was investigated on a noise barrier with radially arranged edges attached on its top (called 'Waterwheel'). It was suggested that at tube depths corresponding to quarter wavelength of the frequency under investigation, the barrier would approximate to a 'pressure release surface' or to a 'soft surface' where sound pressure at the surface would be zero. Theoretical considerations on these concepts are given in section 6.3. It was noted that the channels had to be sufficiently narrow when compared to the wavelength, so that the sound wave would only propagate in the direction parallel to the radius.<sup>2</sup>

Therefore at tube depths designed for attenuating 500 Hz, it was found that the surface sound pressure of the waterwheel vanished at around frequencies corresponding to  $(600 + 1000 n)$  Hz where  $n = 0, 1, 2$ , etc. However, in higher frequency range, no obvious relationship was observed between the frequencies that improve the sound shielding efficiency and those that make the surface soft. The Waterwheel increased the sound energy diffracted into the back of the barrier at frequencies in the range of

315 Hz to 400 Hz and the effect of the Waterwheel was negative by up to 5 dB. The Waterwheel was found to have no beneficial effect on the attenuations where the sound pressure levels were already small in its absence, for example due to destructive interference between direct and ground reflected sound paths.

The results of measurements using physical models showed smaller gains since in practice the soft surface would not be equally effective throughout the whole range of frequencies. The barrier with a Waterwheel on its top provided 10 dB average improvement at the receivers under consideration and in the frequency range where it was intended for.

This study demonstrated the relationship between the well depths and the lower limit of the frequency where improvements were to be expected. It also highlighted the need for an alternative approach to explain the attenuations observed at high frequencies.

### **6.2.3 Noise barrier with a reactive horizontal cap**

A T - profiled barrier with a theoretical soft upper surface for all frequencies was shown to produce an improvement of 8.3 dB in the mean insertion loss over that for a plane rigid screen of the same overall height. In practice this was attempted to be realised by a series of vertical wells on the horizontal cap.<sup>1</sup>

For the geometry under consideration the lowest frequency for which the impedance is zero was 900 Hz ( $f_1$ ). Between approximately 700 Hz and 1500 Hz, the measured insertion loss, using physical models, was found to be the same for a theoretical soft surface. There was a dip in the spectrum around 2000 Hz which was due to pressure maximum at the mouth of the wells corresponding to a frequency of  $2f_1$ . At lower frequencies, between 160 Hz and 500 Hz, the soft barrier produced lower values of insertion loss than the rigid barrier. This was explained as being due to increased impedance values and to surface wave generation below  $f_1$ . It was observed that a reduction in the number of wells tuned to a particular frequency affected the overall efficiency adversely in the range from 300 to 1500 Hz.

The primary mechanism of noise attenuation involved in both barrier applications above was explained as being scattering. These soft surfaces act like a perfectly reflective boundary but with a phase difference of  $180^\circ$ .

### **6.2.4 Use of quarter-wave resonators in building ventilation openings**

The theory and applications of quarter wave resonators were presented by Field and Fricke<sup>5</sup>. It was demonstrated by qualitative and quantitative derivations that resonance would be set up in the tube when the cavity length corresponds to odd multiples of the



quarter wavelength. The application described was for a building ventilation opening and the mechanism of attenuation was explained to be scattering.

The authors explained that the impedance in a quarter-wave resonator at resonance implies a condition of optimum absorption and scattering of incident sound at the frequency of resonance. The open mouth of a quarter-wave resonator at resonance can be considered as a pressure release surface relative to the surrounding medium due to low pressure at the tube entrance. At resonance reactive component disappears and the impedance at the open end of the resonator reduces to the sum of the internal resistance and radiation resistance of the open end. When the frictional (internal) resistance in the resonator cavities is sufficiently small, it will act primarily as an absorber. If the combined resonator resistances (internal resistance + radiation resistance) are sufficiently small the resonator will act as a scatterer. The optimum scattering and absorption condition at resonance allow the resonator to be used as a frequency dependent attenuator. Hence, it was argued, for a resonator to scatter incident sound well, it must be a strong absorber. The resonators contain no absorptive material within their cavities and have no perforate or lining covering the resonator mouths. Therefore both internal resistance and radiation resistance was kept low.

These resonators were experimentally tested with their cavities open and closed off. At frequencies other than the resonant frequencies, the attenuations and amplifications were attributed to reflections and diffractions off the resonator casing. This work demonstrated that the resonator approach does not fully explain the mechanisms involved throughout the testing frequency, especially at higher frequencies.

### **6.2.5 Seat dip effect in auditoria**

The seat dip effect in auditoria has been noted as being a low-frequency attenuation affecting sound travelling at grazing incidence over seating. This attenuation was described to be due to scattered sound from the seats interfering with sound travelling directly from the source on the stage. This idea was extended to environmental noise control. Multiple low barriers and bunds with trenches were investigated for situations when the source and receiver were in direct line of sight of each other. Use of a fractal array of different-sized barriers or trenches has been proposed to give improved insertion loss peaks at many frequencies.<sup>6</sup>

### **6.2.6 Diffusors**

Schroeder applied binary maximum-length sequence to a metal sheet having grooves with a depth of quarter wavelength to achieve diffusion of sound. These are said to be effective over a band of plus or minus one-half octave of the frequency to which the

wells are tuned. Using number theory sequences, commercially available products have been developed for applications in room acoustics. These have varying well depths and are effective over broadband frequencies and wider angles. The low frequency limit is mainly determined by well depth and the high frequency limit is mainly determined by well width. The application of fractals (i.e. diffusors within diffusors) are said to address the conflicting needs of the low and high frequency performance requirements in a more efficient manner.<sup>4</sup>

### **6.2.7 Propagation over ground having small-sized Irregularities**

Laboratory and outdoor measurements have been used to investigate the effects of different shaped scattering bodies over hard ground. It was shown that a rough boundary produces a distinct ground effect at lower frequencies on near-grazing sound propagation especially if the surface material is acoustically hard. This effect was noted to be different to that observed due to interference effects caused by path length difference. The findings were compared with a boundary element code and analytical results obtained by semi-cylindrical boss theory by Twersky. This investigation looked at periodic and random scatterer distributions, different shapes of scatterers as well as the interaction between these.<sup>9</sup>

Propagation from a point source over an impedance plane near grazing incidence was extended heuristically to include diffraction grating effects, and the resulting predictions were shown to be consistent with the data obtained over periodic roughness. In order to model the diffraction grating effect, an additional term proportional to the area occupied by the elements of the diffracting array was introduced. The additional wave component was considered to be reflected coherently by the 'grating' of roughness and had an extra path length  $\Delta = pb \sin \alpha$ , where  $p$  is an integer depending on the order of interference effect and  $b$  is the spacing between roughness elements.

The measurements have shown that there are considerable differences between the ground effects caused by periodically and randomly spaced roughnesses with the same packing density. Periodically spaced roughnesses yield additional diffraction grating effects and give greater relative sound pressure level minima. Incoherent scattering was reported to play an important role for the source-receiver geometries and roughness sizes reported.

## 6.3 PRESSURE RELEASE SURFACES

This section is on the theoretical considerations involved in approximating a series of edges on a hard surface as a pressure release surface.

### 6.3.1 Boundary Conditions

The definitions of the acoustic boundary conditions, which will be assumed for some aspects of this work, are described below. These are the hard, soft and absorbing boundary conditions, as applicable to the reflection of spherical waves at plane boundaries. The soft boundary conditions are also referred to as pressure - release boundaries or reactive surfaces.

Butler<sup>10</sup> explained that in reality both hard and soft boundary conditions imply perfect reflection of sound rays, with only the phase being different, whereas the absorbent condition would absorb the energy in the ray.

An account of the difference between the rigid and the pressure - release boundaries is provided by Junger and Feit<sup>11</sup>. Assuming an incident wave  $p_i$  is disturbed by the presence of a boundary to produce the reflected wave  $p_r$ , the resulting combined field  $p$  can be expressed as follows.

$$p = p_i + p_r \quad \text{Equation 6-1}$$

The rigid boundary is one over which the normal velocity component, or in other words, the pressure derivative vanishes.

$$\frac{\partial (p_i + p_r)}{\partial z} = 0 \quad \text{Equation 6-2}$$

This boundary condition is approximated when airborne sound impinges on a structural wall, causing pressure doubling to occur on the plane boundary, which corresponds to a 6 dB increase in the sound pressure levels.

On the other hand, pressure - release boundary is when the resultant pressure vanishes.

$$p_i + p_r = 0 \quad \text{Equation 6-3}$$

This boundary condition is approximated for waterborne sound by the free surface of the ocean. An ideal pressure - release boundary condition is satisfied when the particle velocity on the pressure - release surface is twice the particle velocity associated with the incident wave.



Rawlins<sup>12</sup> defined an acoustically hard surface as a perfectly reflecting one which has a vanishing admittance,  $\beta$ .

$$|\beta| \rightarrow 0 \quad \text{Equation 6-4}$$

An acoustically soft surface is where pressure fluctuation vanishes on the surface and the admittance,  $\beta$ , tends to infinity.

$$|\beta| \rightarrow \infty \quad \text{Equation 6-5}$$

A perfectly absorbing surface is defined by combining the solutions of the hard and soft surfaces and dividing the result by two. This solution gives no reflected wave and thus is as if all the energy of the incident wave is absorbed by the surface. Although this formulation is not appropriate mathematically, in practice agrees well with experimental measurements.

This boundary condition is approximated when an airborne sound impinges on a wall covered by a thick lining of cellular or fibrous material such as fibreglass and mineral wool.

Fujiwara et al.<sup>1</sup> in their boundary element modelling work undertaken to compare various forms of noise barriers adopted similar definitions above. The rigid boundary surface is defined as having a zero surface admittance.

$$\beta = 0 \quad \text{Equation 6-6}$$

This is the Neumann boundary condition where the normal component of the particle velocity is zero at the boundary. A soft surface is defined as having a zero surface impedance.

$$Z = 0 \quad \text{Equation 6-7}$$

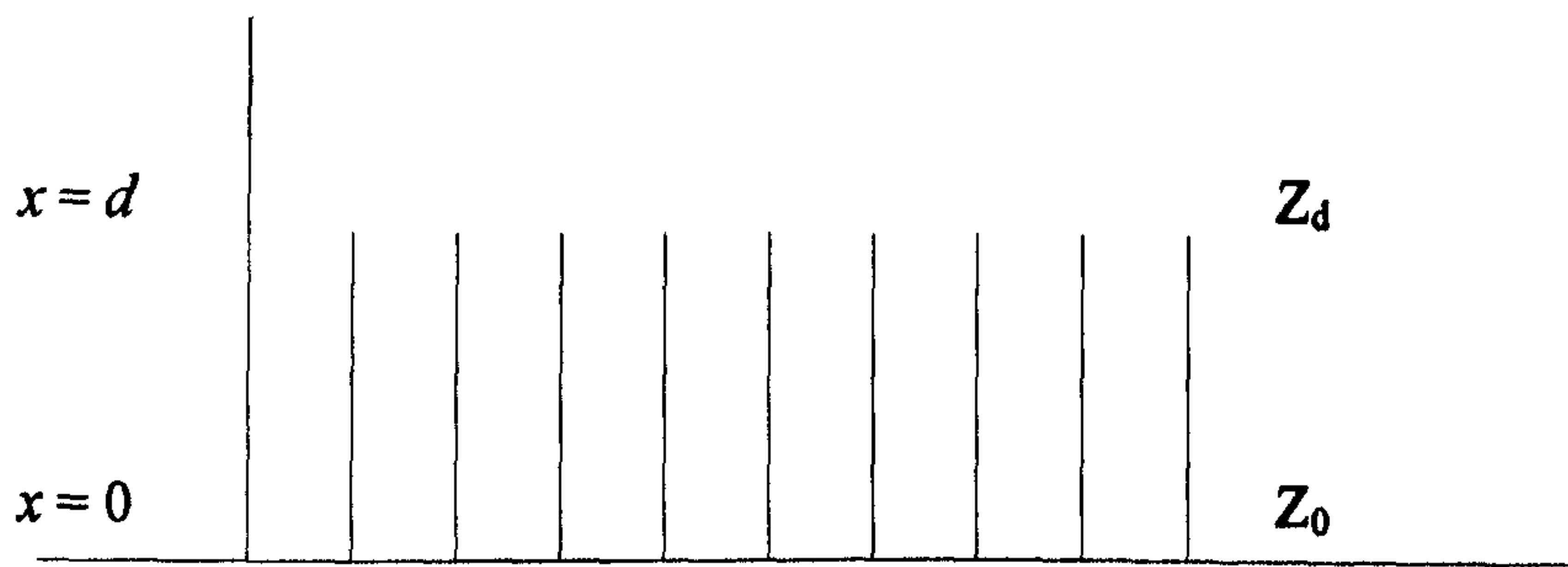
This corresponds to the Dirichlet boundary condition where the excess pressure is zero at the boundary.

### 6.3.2 Quarter-wave Resonators

A quarter-wave resonator can be thought of as a pipe, a tube or a well closed at one end and open at the other. The walls and the closed end of these cavities confine a body of air and under certain conditions this body of air can be brought to a state of resonance.

Therefore noise propagation over a series of rectangular channels is considered for explaining the underlying mathematical principles of resonators. It is assumed that the

walls and the closed end of the channels are rigid and they are sufficiently wide for viscous and thermal conduction effects to be negligible.



The acoustic impedance can be defined as follows<sup>5</sup>

$$Z = \frac{p}{U} = \frac{\rho_o c}{S} \tag{Equation 6-8}$$

where

- $p$  is the acoustic pressure
- $U$  is volume velocity
- $\rho_o c$  is the characteristic impedance of air
- $S$  is the cross-sectional area of the resonator cavity

For the cases when both the incident waves and reflected waves are present the above equation can be expressed as follows

$$Z = \frac{p_i + p_r}{U_i + U_r} = \frac{\rho_o c}{S} \cdot \frac{p_i + p_r}{p_i - p_r} \tag{Equation 6-9}$$

The incident and reflected acoustic pressures  $p_i$  and  $p_r$  can be given as follows

$$p_i = P_i e^{j(\omega t - k x)} \tag{Equation 6-10}$$

$$p_r = P_r e^{j(\omega t + k x)} \tag{Equation 6-11}$$

At resonance the reactive component of the impedance  $Z_d$  becomes zero and the input impedance of the resonator can be expressed as<sup>13</sup>

$$Z_d = \frac{\frac{\rho_o c}{S} \left( Z_o - j \frac{\rho_o c}{S} \tan kd \right)}{\frac{\rho_o c}{S} - j Z_o \tan kd} \tag{Equation 6-12}$$

where

$Z_o$  is the impedance of the rigid end

$Z_d$  is the impedance of the open end

Assuming rigid end termination ( $Z_o = \infty$ ) and substituting this into above equation gives

$$Z_d = -j \frac{\rho_o c}{S} \cot(kd) \quad \text{Equation 6-13}$$

The specific input impedance of the open side of a rigid rectangular channel has been represented approximately as<sup>1</sup>

$$Z_{in} = i \cot(kd) \quad \text{Equation 6-14}$$

where

$k$  is the wavenumber,

$d$  is the depth of the wells

$Z_{in}$  is the acoustic impedance at the surface.

The wavenumber can be written as follows.

$$k = \frac{2\pi}{\lambda} \quad \text{Equation 6-15}$$

For a surface which approximates to an acoustically soft surface, it has been shown above that

$$Z_{in} = 0 \quad \text{Equation 6-16}$$

Therefore substituting this into Equation 6-14 gives

$$i \cot(kd) = 0 \quad \text{Equation 6-17}$$

This could be rewritten as

$$i \frac{\cos(kd)}{\sin(kd)} = 0 \quad \text{Equation 6-18}$$

This equation would be true if

$$\cos(kd) = 0 \quad \text{Equation 6-19}$$

Solving for  $kd$  gives the following



$$kd = (2n + 1) \frac{\pi}{2} \quad \text{Equation 6-20}$$

Substituting Equation 6-15 into above, results in the following

$$\frac{2 \pi d}{\lambda} = (2n + 1) \frac{\pi}{2} \quad \text{Equation 6-21}$$

Simplifying and making  $d$  the subject of the formula gives

$$d = (2n + 1) \frac{\lambda}{4} \quad \text{Equation 6-22}$$

Therefore, at depths corresponding to odd multiples of the quarter wavelength of a sound field, a surface could be considered to be a pressure release or reactive surface.

However, in all practical cases some resistive component will exist. If this is small and is assumed to be constant with frequency, the specific input impedance can be represented as<sup>1</sup>

$$Z_{in} = r_s + i \cot(kd) \quad \text{Equation 6-23}$$

Therefore according to the above equation, the specific input impedance of the surface will depend on the nature of this resistive component, as well as the depth of the cavities and wavelength of sound. This approach does not take into account the width of the cavities, or the nature of edges. These are explained below by the diffraction grating approach.

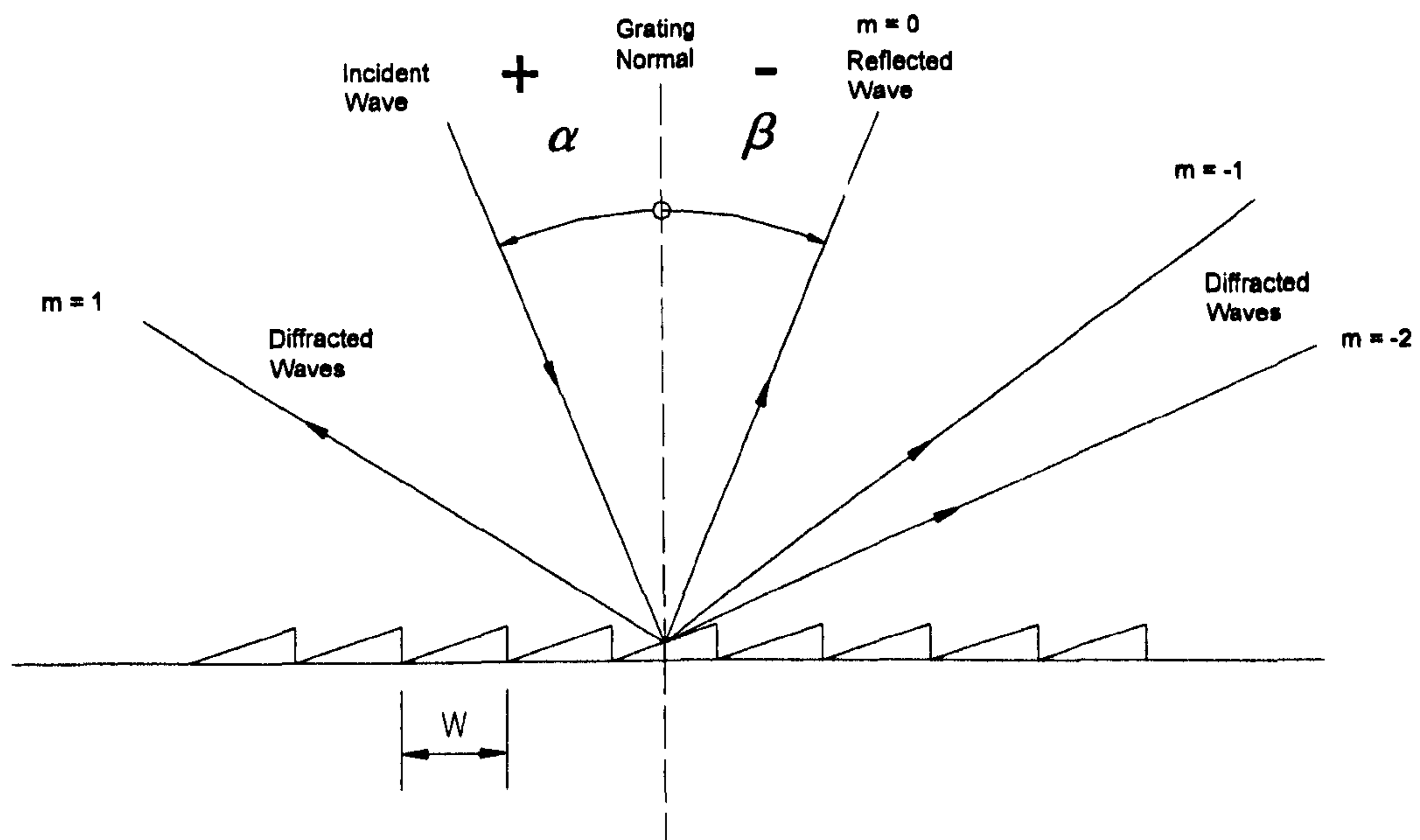
## 6.4 DIFFRACTION GRATINGS

This section looks at diffraction gratings and into how these could be used in explaining the noise attenuation mechanisms involved in the study of a series of edges situated on a hard surface.

A diffraction grating could be defined, in this context, as a collection of reflecting elements, separated by a distance comparable to the wavelength of sound wave under consideration. These gratings could be classified under two categories, namely reflection and transmission type gratings. A reflection grating could be realised when these reflecting elements are located on a reflective surface, such as hard ground. A transmission grating, on the other hand, could be thought of as a series of elements resting against a 'transparent' surface, such as air. The picket fence type barriers reviewed in Chapter 3 could be investigated under this category of gratings.

Therefore a sound wave incident on a grating will, upon diffraction, have its amplitude, or phase, or both, modified in a predictable manner. The theoretical concepts below are defined with specific reference to periodic reflection type gratings since these are also the subject of this research programme.

When mono frequency sound wave, with a wavelength of  $\lambda$ , is incident on a grating surface, it is diffracted into discrete directions. These can be discussed with reference to Figure 6.1<sup>14</sup>.



**Figure 6.1 – A typical diffraction grating**

Where;

$\alpha$  is the angle of incidence

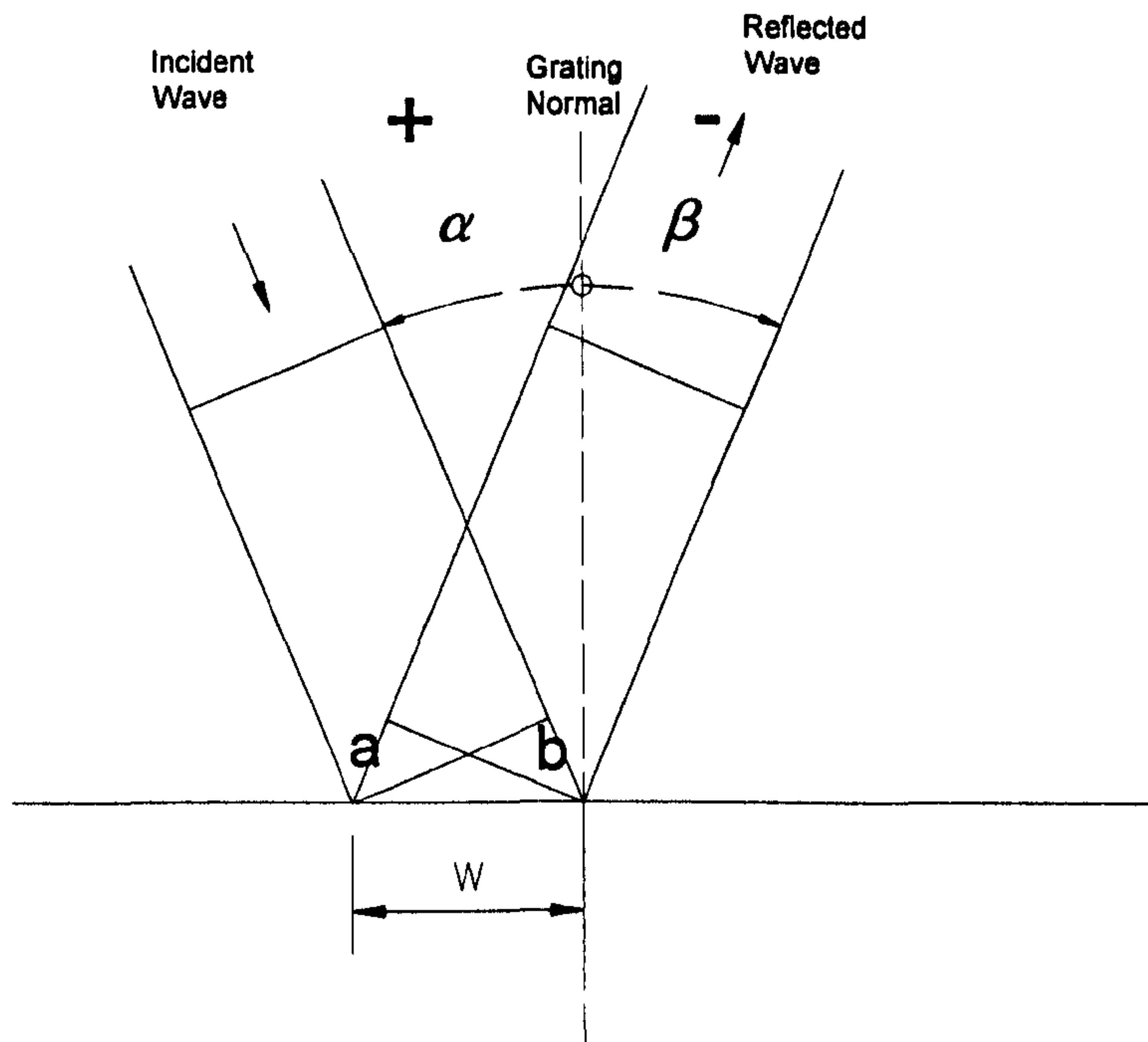
$\beta$  is the angle of diffraction

$m$  is the order of diffraction ( $= 0, \pm 1, \pm 2$ , etc)

$w$  is the horizontal spacing between diffracting elements

The angles are measured from the grating normal which is perpendicular to the grating surface at its centre. The angles are measured from the grating normal. The sign convention for these angles is that those to the left of the grating normal (anti-clockwise) are positive and the ones to the right (clockwise) are negative. The zero diffraction order ( $m = 0$ ) represents specular reflection. The positive diffraction orders appear at the same side of the normal as the incident wave and the negative orders lie on the opposite side.

The diffracted wave front is formed by contributions from individual diffracting elements, each of which acts as a point source. These contributions can yield constructive and destructive interference patterns at varying diffraction angles.



**Figure 6.2 – Path length difference for a plane wave**

The geometrical path difference,  $\delta$  between an incident and reflected plane wave from adjacent elements could be expressed as  $a - b$ , where  $a = \sin\alpha$  and  $b = \sin\beta$ . Since in accordance with the sign convention  $\beta$  is negative,  $\delta$  could be expressed as  $\sin\alpha + \sin\beta$ .

For constructive interference the diffracted rays from the adjacent elements should be in phase and therefore the path length difference should equal the wavelength or its integral multiples. At all other angles, there will be some measure of destructive interference between the wavelets originating from the groove facets. These relationships are expressed by the grating equation.

Constructive interference can be defined by

$$m \lambda = w (\sin \alpha + \sin \beta) \quad \text{Equation 6-24}$$

Since the maximum possible value of  $\sin\alpha + \sin\beta$  is 2, for a particular wavelength  $\lambda$ , all values of  $m$  for which  $|m\lambda/w| < 2$  would correspond to physically realizable diffraction orders.

The maximum value of destructive interference can similarly be expressed as appearing when



$$\frac{m \lambda}{2} = w (\sin \alpha + \sin \beta) \quad \text{Equation 6-25}$$

The grating equations above suggest that the diffraction pattern is independent of the shape of the diffracting elements. However in reality the intensity of a general grating is proportional to a diffraction factor and an interference factor<sup>15</sup>.

Diffraction factor  $F$  depends on the properties of the individual diffracting elements of the grating and on the angles of incidence,  $\alpha$ , and diffraction  $\beta$ . It specifies the broadband distribution of intensity in various orders of diffraction pattern. Different shapes of diffracting elements have been investigated as discussed earlier<sup>9</sup>.

Interference factor can be derived without the form of the diffraction factor and can be represented as<sup>15</sup>:

$$\left( \frac{\sin Nv}{N \sin v} \right)^2$$

where

$N$  is the number of diffracting elements

and  $v = w/2 (\sin \alpha + \sin \beta)$

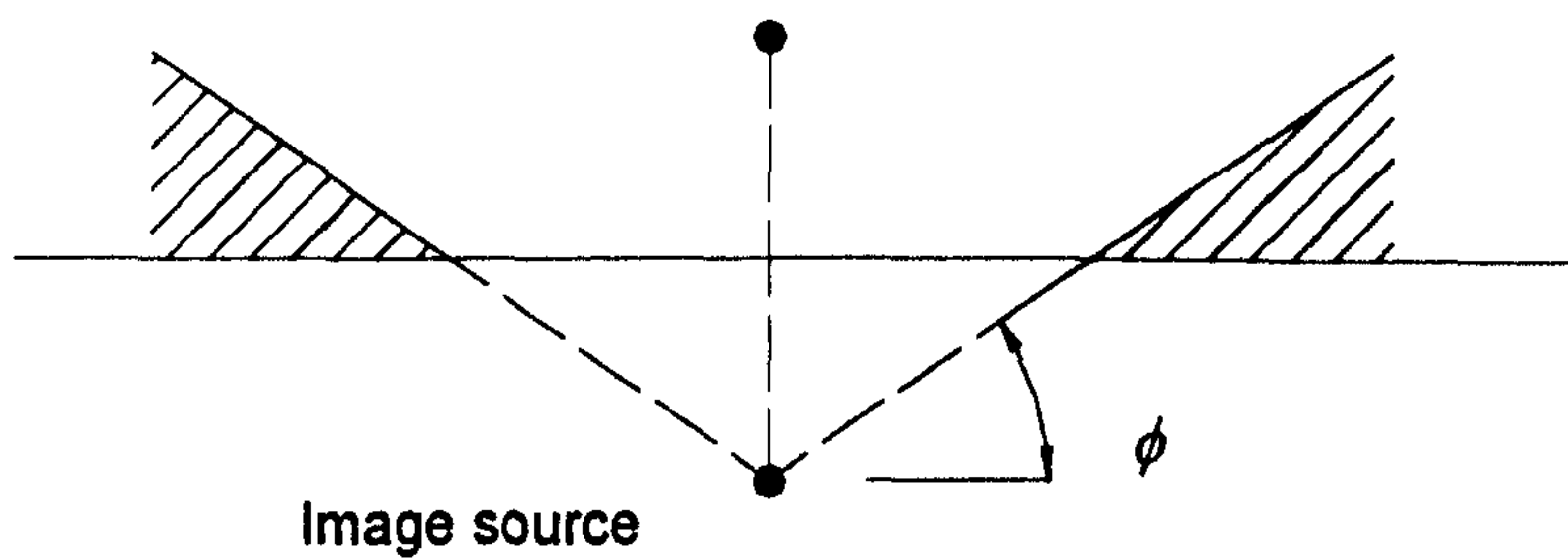
Whenever there exists a linear array of identical sources of waves having either identical phases or phases that progress linearly with position along the array, the relative wave intensity at a distance is given by a grating interference factor.

## 6.5 SURFACE WAVES

This section looks at how surface wave generation or exclusion mechanisms could play a role in determining the performance of a series of edges situated on the ground.

Surface waves can only exist between the flat ground and a conical surface (with an apex at the image source position) whose vertical projection defines the maximum value of the incidence angle for which a surface wave can occur<sup>16</sup>.

Source



In the diagram above, the hatched zone indicates the area where surface waves are possible. The value of the incidence angle  $\phi$  can be defined as follows

$$\sin(\phi) < \frac{[\text{Im}(Z_s) - \text{Re}(Z_s)]}{|Z_s|^2} \quad \text{Equation 6-26}$$

For grazing incidence wave with  $\phi = 0$ , this general condition requires only that the imaginary part  $\text{Im}(Z_s)$  of the surface impedance exceed the real part  $\text{Re}(Z_s)$ . This criterion also applies for the existence of surface waves for propagation of near-grazing incidence of plane waves travelling over an impedance ground.

The surface impedance  $Z_s$  of a thin homogeneous layer of thickness  $d$ , situated over a rigid semi-infinite backing, can be written in terms of characteristic impedance  $Z_c$  as follows

$$Z_s = Z_c \coth(-ik_b \cdot d) \quad \text{Equation 6-27}$$

where  $k_b$  is the acoustic propagation constant for layer media. According to this 'thin layer model' approach, increasing the height of the edges would effectively increase the thickness of the layer.

The significant effect of surface waves can be seen at low frequencies for the lowest flow resistivities due to greater reactive component (i.e. imaginary component) of surface impedance for a hard-backed layer model for the ground. As the source height becomes lower or as the number of edges becomes higher, the likelihood of generating surface waves would also increase. These would make the potential improvements due to a series of edges less apparent, or even negative, over certain frequencies.

In a series of model experiments designed to study the attenuation of surface waves, Donato<sup>17</sup> described that the ground consisted of 'panels made up of a lattice of ½ inch cubic apertures separated by thin plastic walls and having the appearance of a rectangular grille'. This would correspond to the reactive component of the ground impedance and the resistive component was simulated by covering the lattice with a thin layer of felt. The description of the resistive component of the ground model above

resembles that of the rib structures investigated as part of this work. Therefore surface wave generation also needs to be considered as a likely mechanism which affects the performance of rib structures.

## 6.6 CONCLUSIONS

The discussions above showed that based on theoretical considerations and practical applications of gratings and resonators, a number of physical parameters were likely to influence the attenuation of noise. These have been identified as follows.

- Wavelength of the incident wave,  $\lambda$
- Well depth,  $d$
- Total number of diffracting elements,  $N$
- Well width, or horizontal spacing between adjacent elements,  $w$
- Source location determining angle of the incident wave,  $\alpha$
- Receiver location, with respect to the order of diffracted wave,  $\beta$
- Nature of the individual diffracting element,  $F$
- Total distance covered by diffracting elements,  $L$
- Proportion of source-to-receiver distance ( $X$ ) to that covered by diffracting elements,  $X / L$

It was found that the low frequency limit of attenuations is mainly determined by well depth and the high frequency limit is influenced by well width. Long wave scattering effects were identified to be the main noise attenuation mechanism at lower frequencies and diffraction effects were likely to be the main mechanism at higher frequencies. The distinction between the definitions of 'diffraction' and 'scattering' phenomena is characterised by the ratio of sound wavelength to size of object. If the sound wavelength is larger than the object it encounters, this is defined as scattering (or Rayleigh scattering). Conversely, if the sound wavelength is smaller than the object, then it manifests itself as diffraction. Surface wave generation mechanisms were also shown to be applicable at low frequencies in certain situations. Therefore a combined 'grating/ resonator/ surface wave' approach could be more appropriate for explaining the noise attenuations by rib structures. However it is not the aim of this research project to produce an analytical model based on this combined approach. The parameters listed above will be investigated in more detail in the forthcoming chapters by physical and numerical modelling. This work may reveal that the combined approach is not sufficient in explaining all of the findings. Therefore it may need to be modified to include other mechanisms not considered in this chapter.



This chapter, together with the previous one, described the research methodology to be adopted, and identified the specific areas of research. Physical and numerical modelling techniques will be used to investigate the acoustic performance of multiple edges on the ground and on other earth mound type barriers.

The next chapter will describe an investigation into the general experimental set-up for physical modelling. It also aims to identify the likely limitations of the uniform field experiments and to explore the conditions under which this technique could be used.

**6.7 REFERENCES**

- 
- <sup>1</sup> FUJIWARA, K., HOTHERSALL, D.C. and KIM, C., Noise Barriers with Reactive Surfaces, *Applied Acoustics*, Vol. 53, No 4, 255-272, 1998
- <sup>2</sup> OKUBO, T. and FUJIWARA, K., Efficiency of A Noise Barrier on the Ground With An Acoustically Soft Cylindrical Edge, *Journal of Sound and Vibration*, 216(5), 771-790, Article No. sv981720, 1998
- <sup>3</sup> Van Der HEIJDEN, L.A.M. A and Martens, M.J.M., Traffic Noise Reduction by Means of Surface Wave Exclusion Above Parallel Grooves In The Roadside, *Applied Acoustics*, 15, 329-339, 1982
- <sup>4</sup> EVEREST, F.A., *Master Handbook of Acoustics*, Fourth Edition, McGraw Hill, 289-315, 2001
- <sup>5</sup> FIELD, C.D. and FRICKE, F.R., Theory and Applications of Quarter-wave Resonators: A Prelude to Their Use for Attenuating Noise Entering Buildings Through Ventilation Openings, *Applied Acoustics*, Vol. 53, No. 1-3, 117-132, 1998
- <sup>6</sup> DAVIES, W.J., From Concert Halls to Noise Barriers: Attenuation from Interference Gratings, *IoA Spring Conference*, 2002
- <sup>7</sup> Noise Management, *The Newsletter for Noise Professionals*, Issue 33, page 4, [www.noise-management.co.uk](http://www.noise-management.co.uk), February/March 2003
- <sup>8</sup> CHAPMAN, R.P., BLUY, O.Z. and HINES, P.C., Backscattering from Rough Surfaces and Inhomogeneous Volumes, pp 441-458, Chapter 40, *Encyclopaedia of Acoustics*, edited by Malcolm J. Crocker, ISBN 0-471-80465-7, John Wiley & Sons, Inc., 1997
- <sup>9</sup> BOULANGER, P., ATTENBOROUGH, K., TAHERZADEH, S., WATERS-FULLER, T., and MING LI, K., Ground Effect Over Hard Rough Surfaces, *J.Acoust.Soc.Am.*, 104(3), Pt 1, 1474-1482, September 1998
- <sup>10</sup> BUTLER, G.F., A Note on Improving the Attenuation Given by a Noise Barrier, *Journal of Sound and Vibration*, 32 (3), 1974, 367 - 369.
- <sup>11</sup> JUNGER, M.C., and FEIT, D., *Sound, Structures and Their Interaction*, Cambridge (Mass.), London: M.I.T. Press, ISBN 026210010x, Chapter 3 - Application of The Elementary Acoustic Solutions, 34-36, 1972
- <sup>12</sup> RAWLINS, A.D., Diffraction of Sound by a Rigid Screen With a Soft or Perfectly Absorbing Edge, *Journal of Sound and Vibration*, 45 (1), 1976, 53 - 67.



---

<sup>13</sup> KINSLER, L.E., FREY, A.R., COPPENS, A.B., and SANDERS, J.V., Fundamentals of Acoustics, Fourth Edition, John Wiley & Sons, Inc., ISBN 0-471-84789-5, 2000

<sup>14</sup> Diffraction Grating Handbook, Christopher Palmer (editor), Thermo RGL, Richardson Gratings Laboratory, fifth edition, 2002, on-line book address: <http://www.gratinglab.com/library/handbook/handbook.asp>

<sup>15</sup> ELMORE W.C. and HEALD M.A., Physics of Waves, ISBN 0-486-64926-1, Dover Publications, Inc., New York, 1985

<sup>16</sup> SUTHERLAND, L. C ., and DAIGLE, G .A., Atmospheric Sound Propagation, Chapter 28, Handbook of Acoustics, M. J. Crocker (Editor), 305-329, 1998

<sup>17</sup> DONATO, R.J., Model Experiments on Surface Waves, J. Acoust. Soc. Am., 63(3), March 1978, 700-703

## **7 AN INVESTIGATION INTO THE EXPERIMENTAL SET-UP**

The previous chapter identified the mechanisms and parameters involved in attenuation of noise by means of rib structures consisting of multiple edges. It was reported that the investigation into their performance using uniform field experiments could have some limitations.

The work described in this chapter is directed towards characterising the testing room, the sound source and the materials to be used for physical scale modelling investigation described in the forthcoming chapters. Reverberation time measurements are carried out to establish the suitability of the testing space for modelling work and to quantify the effects of the reverberant field. Directivity tests are undertaken to determine the source characteristics. These tests are used in the discussion of the potential limitations of the reverberant field on the experiments.

Impedance tube measurements are aimed at investigating the absorptive properties of the modelling materials used. These are supplemented by the findings of previous research using airflow resistivity measurements.

### **7.1 PHYSICAL SCALE MODELLING UNDER UNIFORM FIELD CONDITIONS**

#### **7.1.1 Background**

The main principles of physical scale modelling and the previous work undertaken on noise barriers using this technique were reviewed in Chapter 3.

It was demonstrated that there are no established rules as to how physical modelling can be put into practice. Occasionally, there may be ideal choices. However, various decisions on the choice of a scale factor, noise source, receiver, processing and displaying devices, model materials and even a testing medium are more frequently dictated by availability and practical convenience. Since all are inter-related, a decision on the use of one of them usually determines the choices to be made on the rest.

In the light of previous physical modelling work, the choices of physical model details for the purposes of present work are described below.

### 7.1.2 Testing Room

When investigating the performance of a barrier by physical modelling, only the direct component of the sound field needs to be considered. This could include the top diffracted waves, or in absence of a barrier, the rays propagating straight to the receiver. Reflections from the room boundaries could be a problem unless they can either be eliminated or identified and ignored. Therefore, the testing room should ideally be a purpose built anechoic (or semi-anechoic) chamber. These provide a testing space free of reverberant field, practically eliminating the reflections<sup>1</sup>.

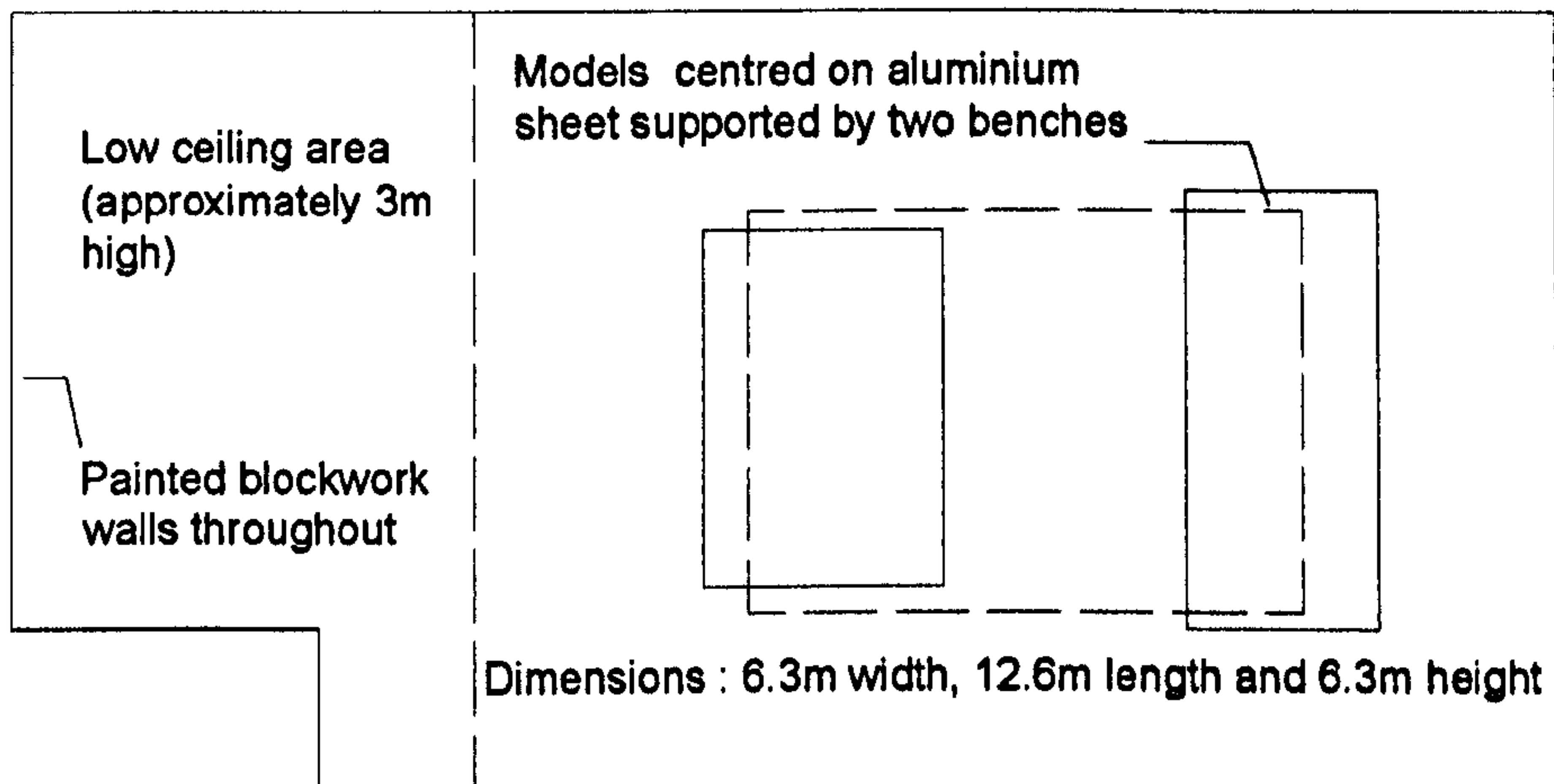


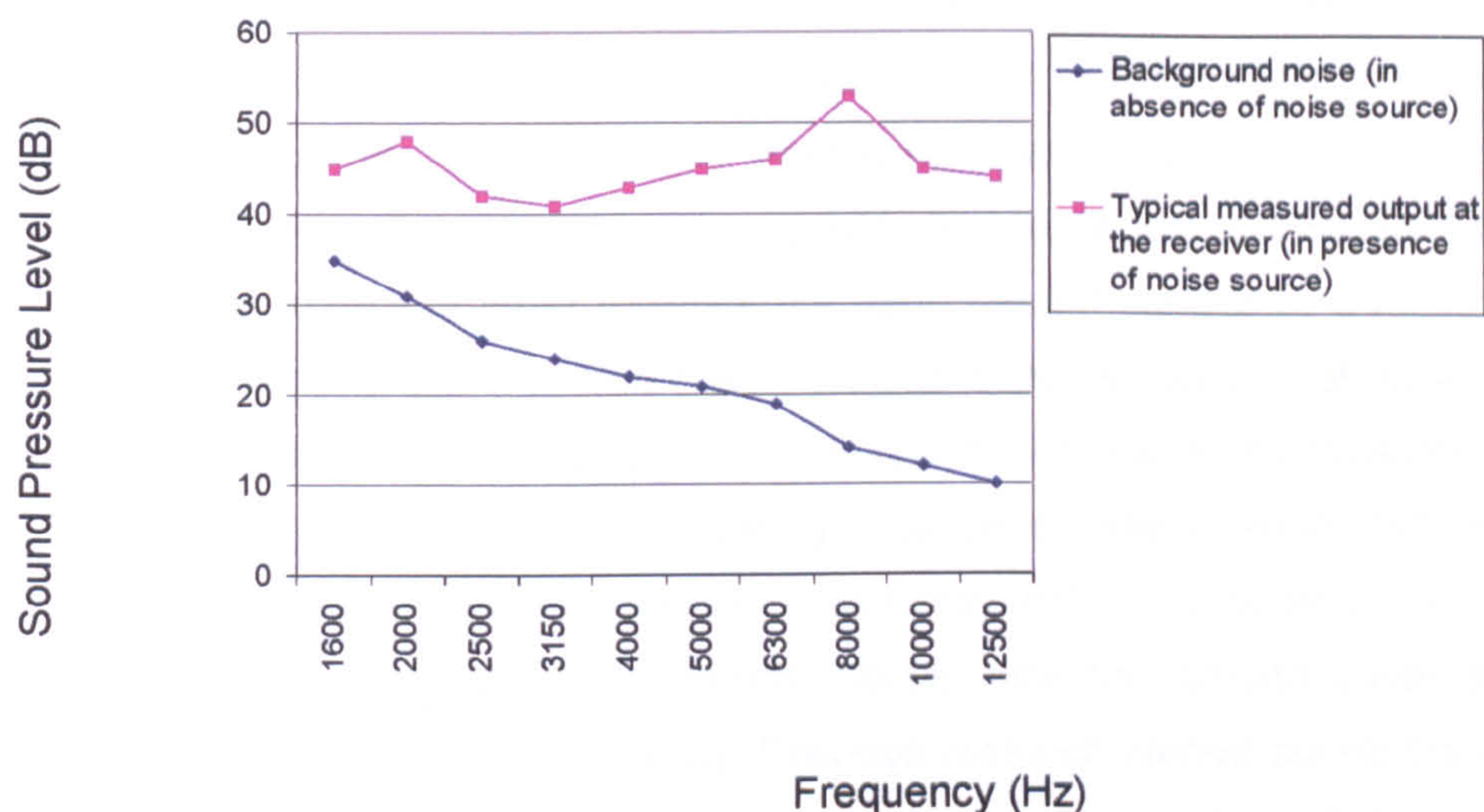
Figure 7.1 : Plan of testing room and the general location of models

However, the space available for the current physical modelling work was a large irregular shaped room with reflective walls. The length was 12.6 m in the direction of the source-to-receiver configuration and the width and height dimensions of the room were both 6.3 m. There is a part of the room where the ceiling height is approximately 3m above the floor. The barrier-source-receiver configuration was resting on an aluminium sheet supported by two benches. The benches are approximately 1m high measured from the room floor. The details of the testing room and the general experimental layout are shown in Figure 7.1. The lack of a purpose built room was a considerable limitation. Therefore further tests may need to be undertaken in an anechoic or semi-anechoic chamber as stated above. This will be decided following the findings of the work discussed in this chapter.

### 7.1.3 Background Noise

The typical background noise levels within the testing space are shown in Figure 7.2. These are compared with a measured sound pressure level at a typical receiver position in presence of the sound source. It can be seen that the background noise levels are lower than the measured levels by at least 10 dB or more.





**Figure 7.2 : The background noise levels within the uniform testing space**

The uniform field testing space is situated close to other laboratory facilities and this is the reason for high background noise levels especially at the lower end of the frequency spectrum of interest. In the instances when there were extraneous noise sources due to adjacent facilities, the experiments were repeated. Generally, the background noise levels did not have a major influence on the measured noise levels.

#### 7.1.4 Scale Factor

The equipment available for physical modelling dictated that the upper limit of the testing frequencies be around 20 kHz. Considering the A-weighted traffic noise spectrum is between 100 - 4000 Hz, with a peak at around 1000 Hz, the scale factor is limited to around 1:10 for obtaining a good representation of the traffic noise. The model frequencies of 2 kHz to 22 kHz will enable a scaled spectrum of 200 Hz to 2200 Hz to be investigated which approximates well to a typical traffic noise spectrum. However the compromise in the receiver distances will be considerable.

#### 7.1.5 Modelling Materials

The modelling materials used for constructing various physical models consist of aluminium, in sheet or angle form, medium density fibre and glass fibre quilt.

Aluminium sheets will be used for simulating a flat and reflective ground surface. It was considered that this could minimise the influence of the ground surface on the barrier performance. The phase change upon reflection would be limited and the dips in the spectra could be related mainly to interference effects due to path difference between direct and ground reflected rays. The rib structures will be constructed from aluminium angles of various dimensions depending on the experimental set-up.



The earth mound will be constructed from medium density fibreboards appropriately sealed at the junctions. The absorption characteristics of this material will be quantified via impedance tube measurements. Absorption coefficients will be related to flow resistivity values and these will be compared to typical values provided in the literature for a ground surface in order to relate the earth mound surface to a realistic ground surface. Glass fibre quilt was also briefly used as a model material, at the early stages of the investigation, as described in Chapter 5, in order to simulate "absorbing ground" cover. The absorptive property of this ground cover was exaggerated in order to maximise ground absorption. Therefore, this may not correspond to any particular surface treatment in reality, but helped identify how the ground cover affects the performance of different modifications. Previous research carried out on the glass fibre quilt, using airflow resistivity tests, will be used to supplement the findings of impedance tube measurements.

### **7.1.6 Noise Source and Receiver**

The types of sources available for modelling work were discussed in Chapter 3. The determining factors in the choice of an appropriate sound source are its directivity characteristics, the frequency content of the noise produced, maximum output that can be achieved, physical dimensions of the source, and availability. Initial attempts were made to use air jet as a noise source. The small sized nozzle was made even smaller by filling it by a resin and drilling another hole through it. The nozzle was used both directed towards the receiver and vertically upwards. However, the turbulence effects could not be eliminated and this noise source was not considered any further. Even though the spark source was clearly the ideal choice due the short duration of the sound burst and the high frequency content of the noise, this was ignored due to safety considerations (high voltage). No attempts were made to use ultrasonic whistle sources.

Therefore, due to immediate availability, small size, and its high frequency content a tweeter speaker was the preferred choice. The coil diameter of the speaker was 5 cm and it was enclosed in a box to avoid bipolarity in the source. An in series connected capacitor reduced the risk of damage from the low frequencies. The effective frequency range was 1.5 kHz to 20 kHz. For the frequency range under consideration a 1 / 2" microphone would be sufficient, even though 1 / 4" microphone was used for some of the modelling work described in the forthcoming chapters.

The use of a continuous sound source under uniform field conditions necessitated an investigation into the effects of reverberant field on the experimental results. Therefore reverberation time measurements were undertaken which were aimed at determining

to suitability of the testing room for the modelling work. The directivity characteristics of the noise source were also experimentally determined. These two parameters were used to estimate the reverberant field by reference to the room acoustic equation. The findings were compared with two test geometries selected from the literature. These were chosen such that they would provide an indication on the instances when the uniform field experiments would give reasonable results. These would also reveal the potential shortcomings of the method. Impedance tube measurements were carried out to quantify the absorptive properties of the model materials. The findings of these tests were compared with the flow resistivity values of known materials, both directly and using approximate relationships.

The reverberation time measurements aimed at determining to suitability of the testing room for the modelling work are described below.

## **7.2 REVERBERATION TIME MEASUREMENTS**

### **7.2.1 Background**

"The acoustic properties of a room are most commonly characterised by the reverberation time. This is the time required for a sound to decay in intensity to almost zero. This has been defined as the time required for the sound pressure level to decrease by 60 dB, or time for the mean-squared sound pressure (average sound energy intensity) to decay to one-millionth of its initial value"<sup>1</sup>.

The reverberation time, T60, based on the 60 dB decay can prove to be difficult to achieve in real rooms due to the presence of background noise. Therefore, the process of decay are usually analysed in smaller, defined periods of time, namely, t10, t20 and t30. Time required for a level decay of X dB from 5 dB down to (5 + X) dB below a reference level is defined as tX where X (dB) = 10, 20 and 30 in this case. These times are extrapolated to a range of 60 dB as follows:  $T10 = 6 \times t10$ ,  $T20 = 3 \times t20$ ,  $T30 = 2 \times t30$ . T10 is also known as Early Decay Time<sup>2</sup>.

Since the space available for physical modelling work is an "unconventional" room, reflections will influence the physical modelling work adversely. Therefore, preliminary work needs to be focused on quantifying the contribution of the reflections and to eliminate them if possible. Reverberation time measurements are carried out in order to serve this purpose. Some of the answers which will be sought will be how much the reverberant component of the sound affects the direct component, how can these effects be eliminated - either physically or mathematically - if desired and whether an optimum source-to-receiver distance exists in order to minimise these effects.



The inherent assumption in these experiments is that the testing space is uniform field for the frequencies of interest where mean squared pressure is constant throughout volume.

### **7.2.2 Aim of the Experiment**

The purpose of these experiments was to determine the reverberation times of the testing room using alternative approaches for various source and receiver configurations. The reverberation time measurements have been carried out by two different approaches.

The first one involved the use of a sound level meter and a level recorder as the recording equipment. Three different source combinations were used for these experiments. These were a starting pistol, single wedge speaker and double wedge speakers. Starting pistol is commonly used for reverberations time measurements however has a limited output capability. Therefore a wedge speaker is used to be able to obtain a higher sound pressure level output and also to be able to compare the results obtained by different noise sources. The use of a second speaker is intended to give a more uniform sound field within the testing room.

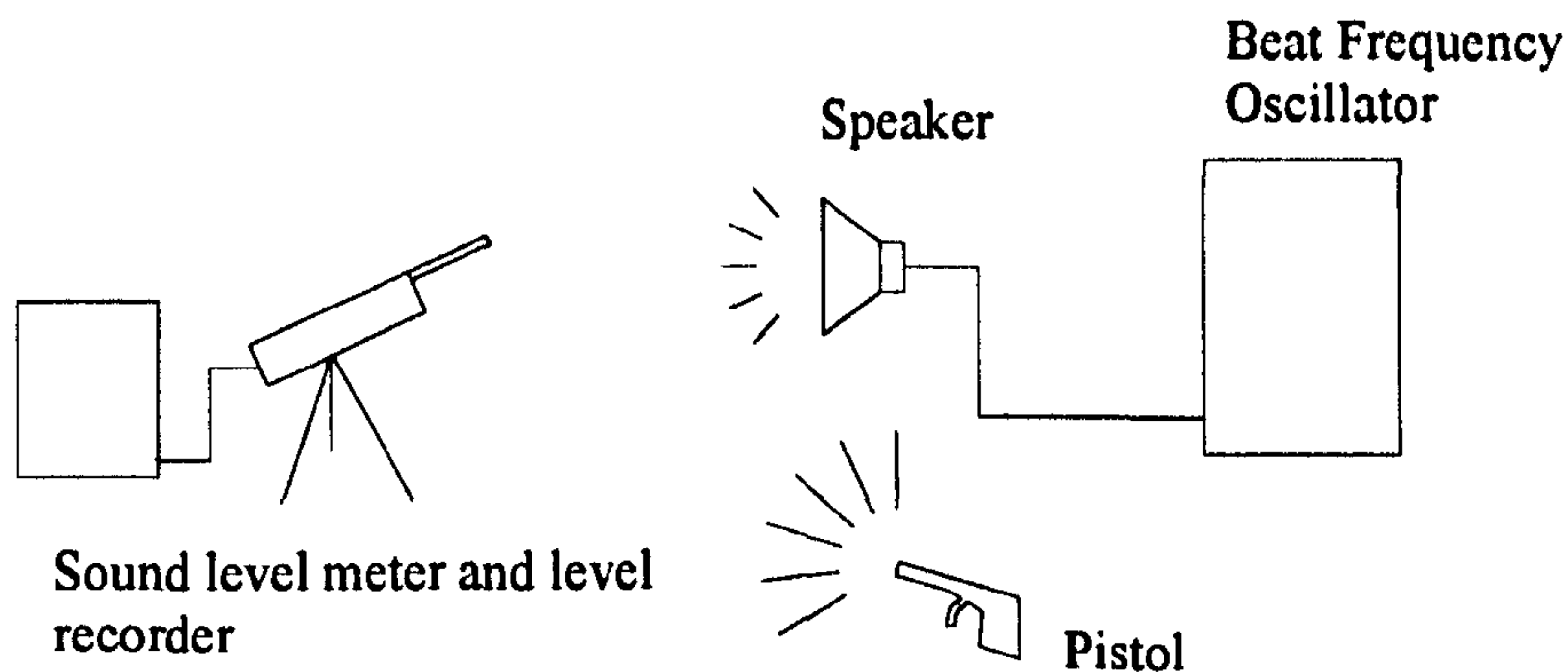
The second method involved the use of a purpose-built digital sound analyser with an in-built reverberation time analysis module, called NC10, as the recording equipment. A starting pistol and a single wedge speaker were both used as sources in these measurements. As above, two different noise sources are used to be able to identify if the results obtained by different sources are consistent.

This section will provide the details of the experiments involved with each method. The testing space is 12.6 m long and 6.3 m wide. The approximate height of the room is 6.3 m except in "the low ceiling area", where it is reduced to around 3 m. The dashed line in the plan views of the testing room from Figure 7.4 to Figure 7.16 represents this change of height, the low ceiling area being to the left.

### **7.2.3 The Level Recorder Experiments**

#### **7.2.3.1 Instrumentation**

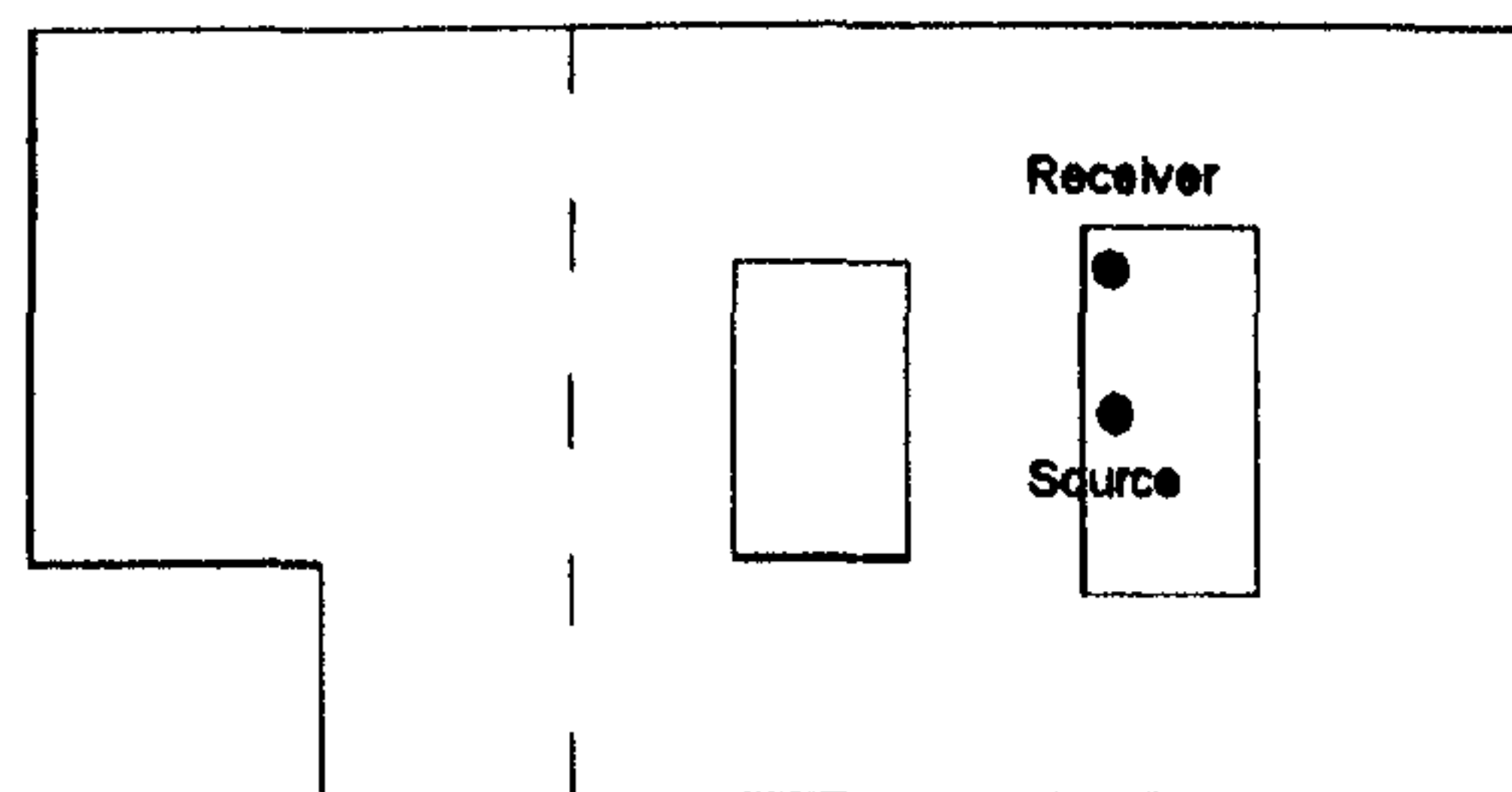
The noise recording equipment used in these experiments were a sound level meter with a filter set (B&K 2231) and a level recorder (B&K 2306) with a 25 dB potentiometer. The noise sources were a starting pistol or wedge speakers connected to a beat frequency oscillator (B&K 1022), as applicable.



**Figure 7.3 : Experimental set-up for level recorder tests**

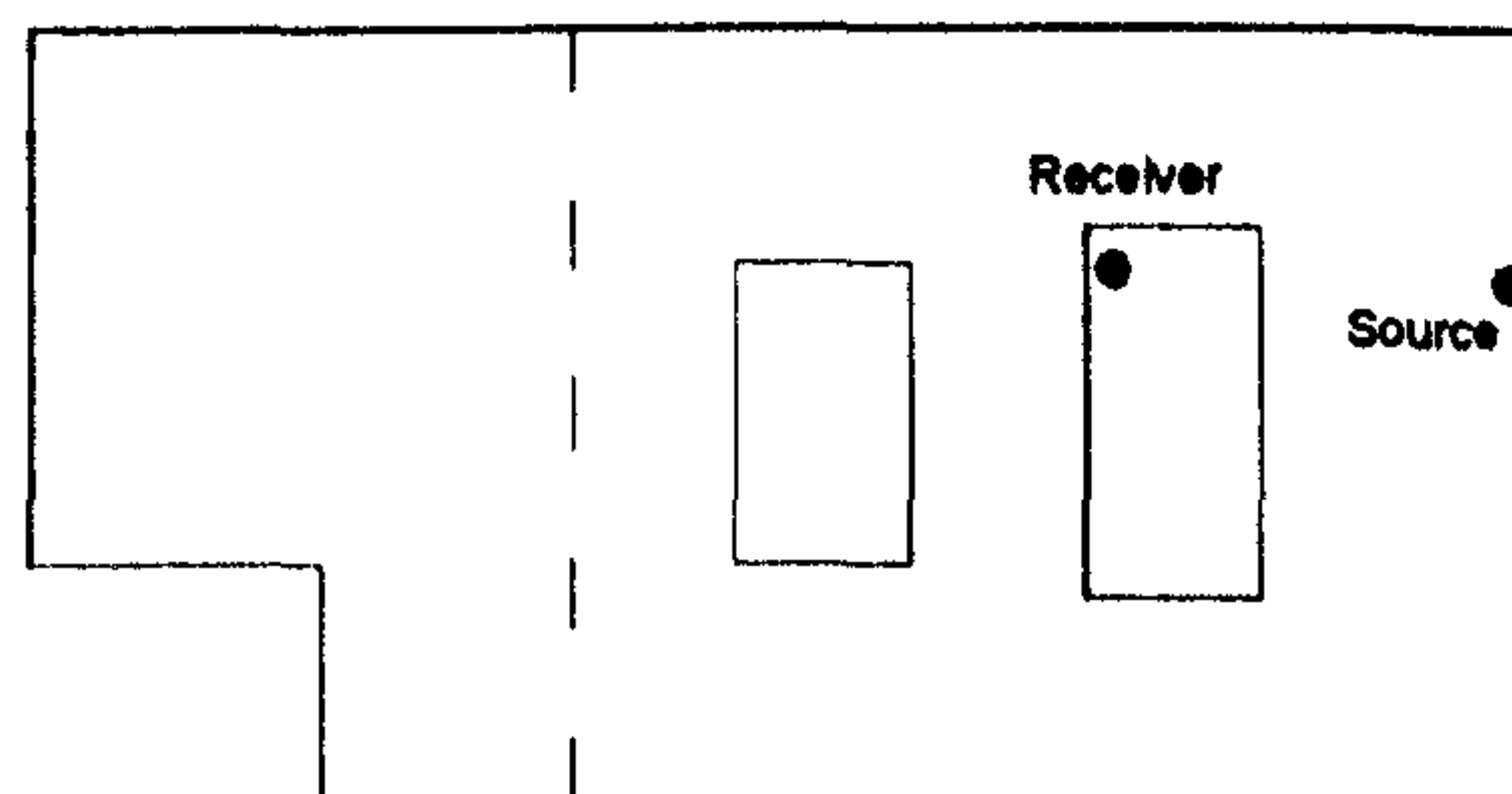
### 7.2.3.2 Source and Receiver Positions

The plan views below show the approximate locations of the source and receivers with respect to each other and the walls of the testing space. In the case of pistol tests, the receiver was positioned 0.30 m above the bench. The pistol was kept approximately 1.5 m from the receiver.



**Figure 7.4 : Plan view of the testing room showing the source-receiver configuration for the starting pistol tests.**

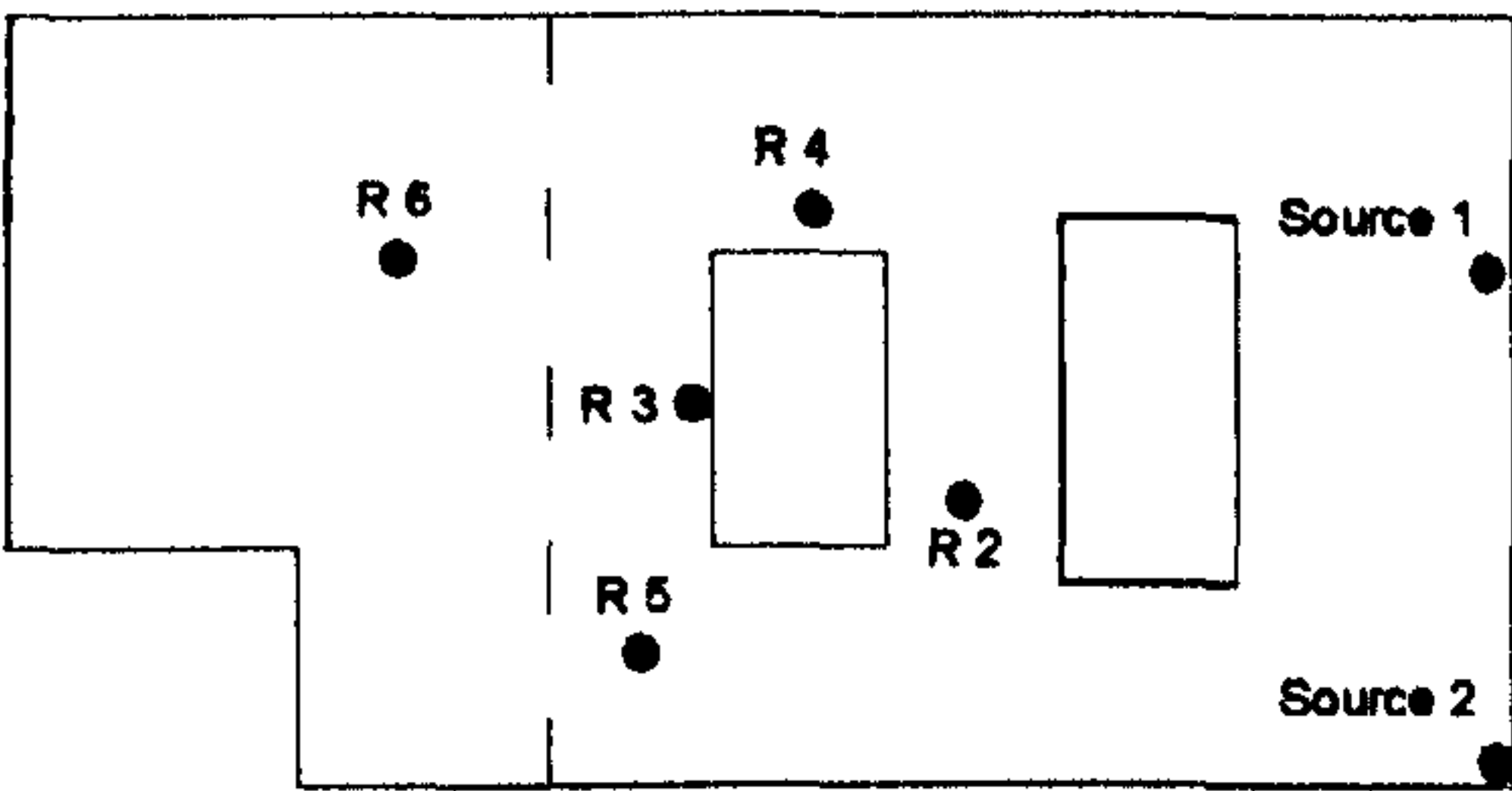
For the single wedge speaker tests, the receiver was at the same location as before and the wedge speaker was positioned against the wall 2.5 m from the receiver.



**Figure 7.5 : Plan view of the testing room showing the source-receiver configuration for the speaker tests.**

The double wedge speaker tests involved an additional speaker in one corner of the testing room, placed against the wall. This was expected to provide a more uniform sound field within the testing room and also to increase the output at the individual one-

third octave band frequencies. Five receiver positions were selected which were distributed throughout the testing room and were situated away from the walls as much as possible.



**Figure 7.6 : Plan view of the testing room showing the source-receiver configurations for the double-speaker tests**

These receiver positions are labelled R2 - R6, following the previous receiver position, R1. The dashed line above indicates "the low ceiling" area of the testing space, and receiver 6 was selected in that area.

### 7.2.3.3 Method

The details of the equipment and set-up are given above. The sound level meter was calibrated using a reference level of 94 dB at 1 kHz. The level recorder was calibrated to give a maximum deflection at 95 dB using the reference calibration level. The summary of measurement details for each source is given in Table 7-1.

Receiver	Source	Frequency Range (1/3 octave)	Number of tests	Number of receiver positions
Level recorder	Starting pistol	100Hz to 20kHz	3	1
Level recorder	Single speaker	800Hz to 4kHz	4	1
Level recorder	Double speakers	800Hz to 4kHz	1	5

**Table 7-1 : Summary of experiments carried out**

The paper speed of the level recorder was 30 mm / s. The sound level meter was adjusted to give a sound pressure level in linear scale. Once the paper was moving with the pen operational, the pistol was fired and following this the level recorder was switched off.

In the case of speaker tests, the output was adjusted such that maximum deflection of the pen was achieved. After allowing ample time for the sound pressure fluctuations to settle so that the pen movement would stabilise, the paper was switched on and the speaker output from the oscillator was instantaneously switched off to obtain a decay curve. A sample decay curve is shown below.



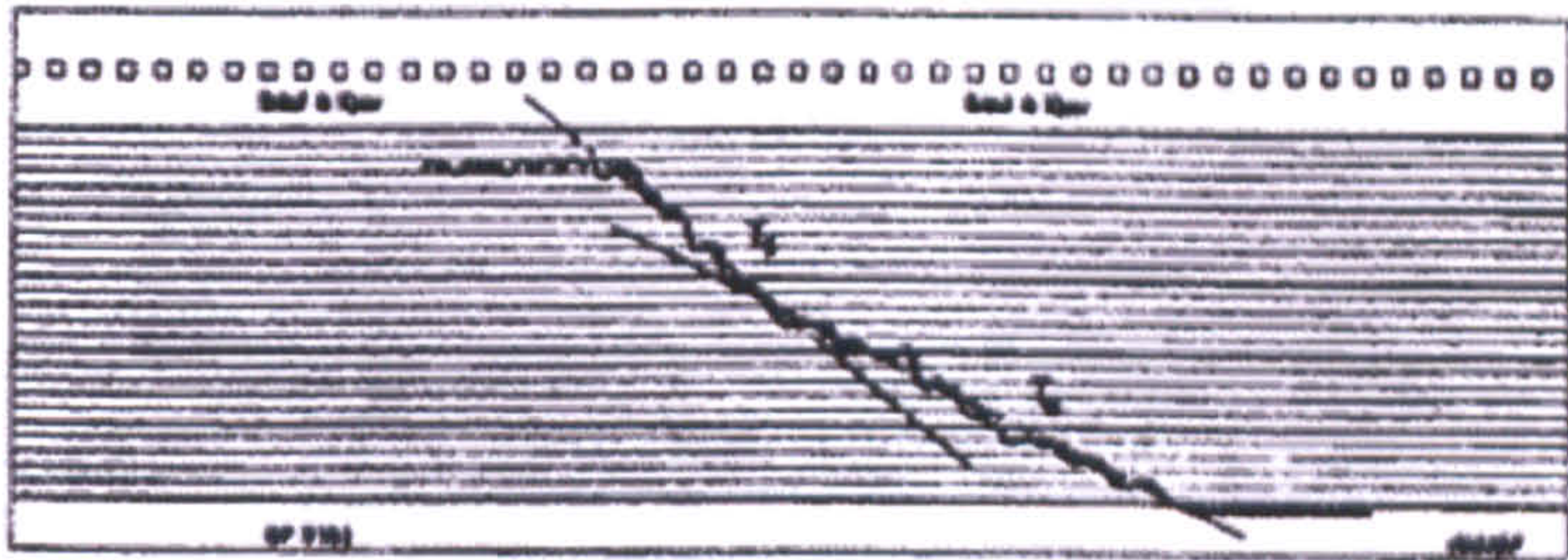


Figure 7.7 : Sample decay curve

In both the pistol and speaker tests, the time taken for the sound pressure level to decrease from the maximum to the minimum in seconds (x-axis) and the corresponding decay rate in dB (y-axis) were measured using a protractor and a ruler. The procedure was repeated for all the 1 / 3 octave band frequencies under consideration.

### 7.2.3.4 Results

Maximum sound pressure levels produced by the starting pistol throughout the spectrum are shown in Figure 7.8. In all three tests, the maximum output is centred at around 1kHz. The spectrum increases roughly linearly from the minimum sound pressure level at 100 Hz to a maximum around 1 kHz and back to the minimum at the 20 kHz. The maximum sound pressure level was around 92 dB and the minimum sound pressure was 75 dB.

Another point to note is the variability of the output from one test to another, given the same source-receiver configuration in all three tests. The largest variation occurs at the between 800 Hz - 5 kHz. Sound pressure levels at the lower and higher end of the spectrum are much more stable.

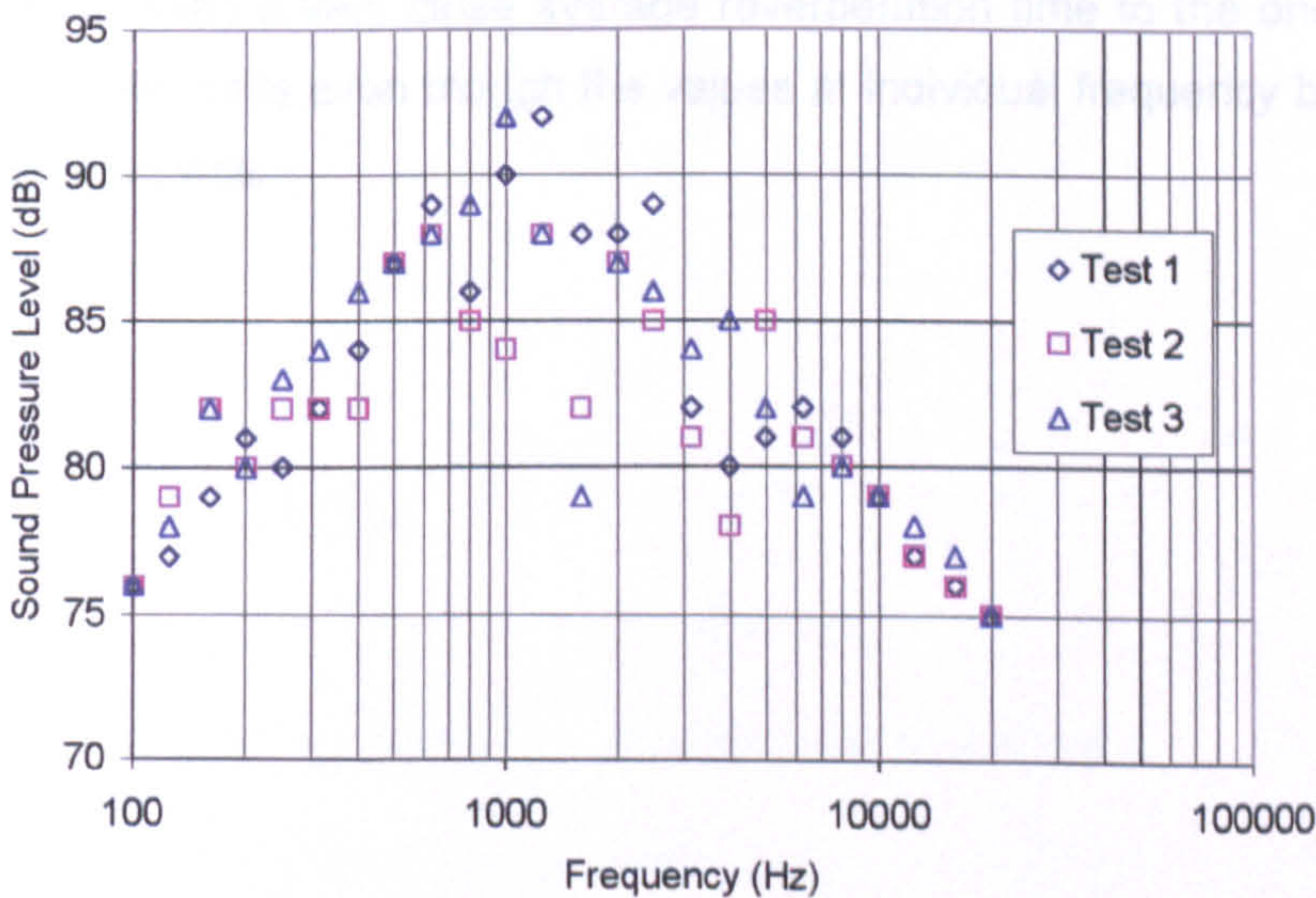


Figure 7.8 : Starting pistol sound pressure levels obtained for different tests throughout the testing range.



The reverberation times for the three tests obtained by the pistol can be seen in Figure 7.9. The vertical axis shows the reverberation times in seconds and the horizontal axis shows the frequency in Hz.

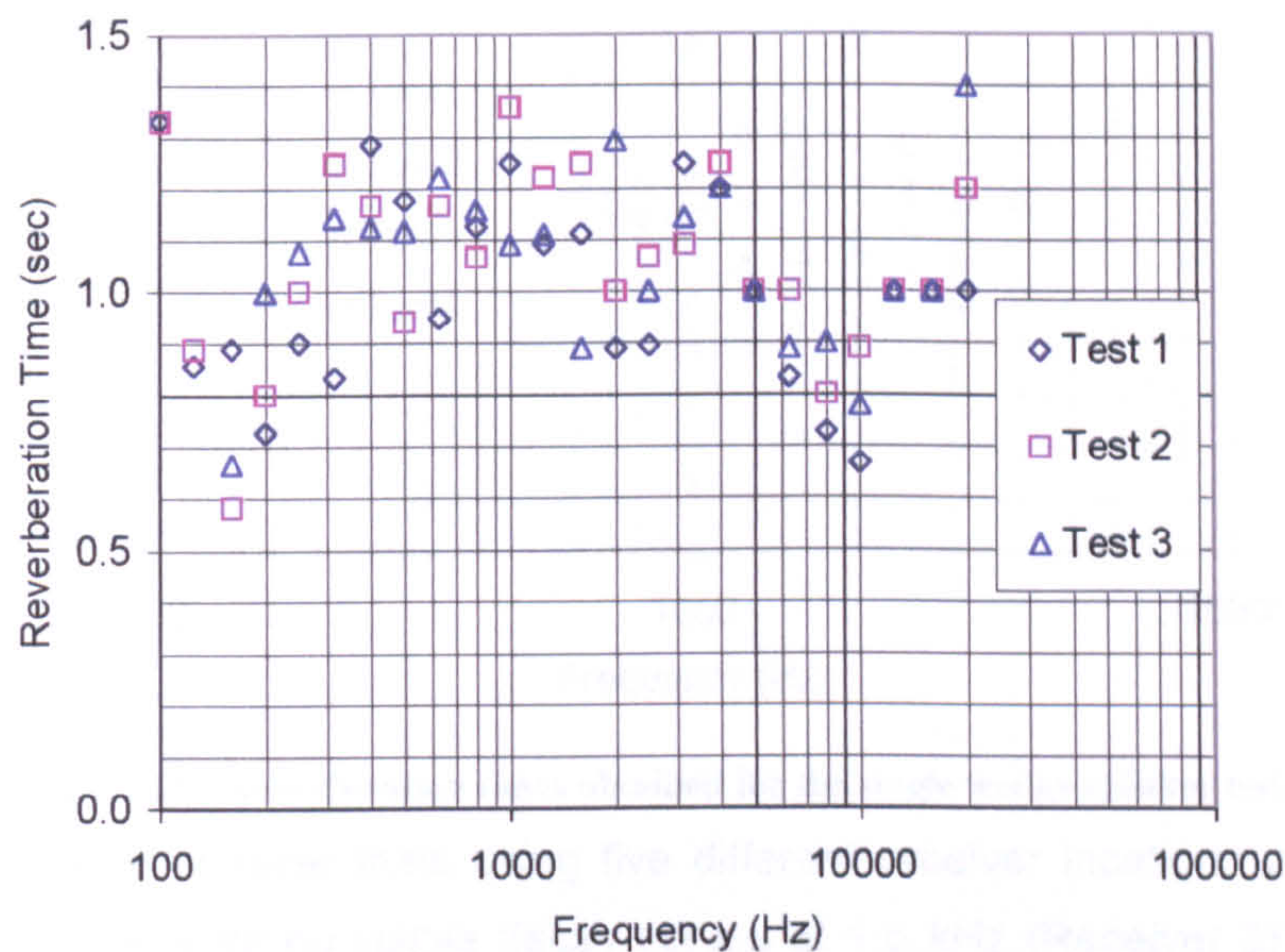
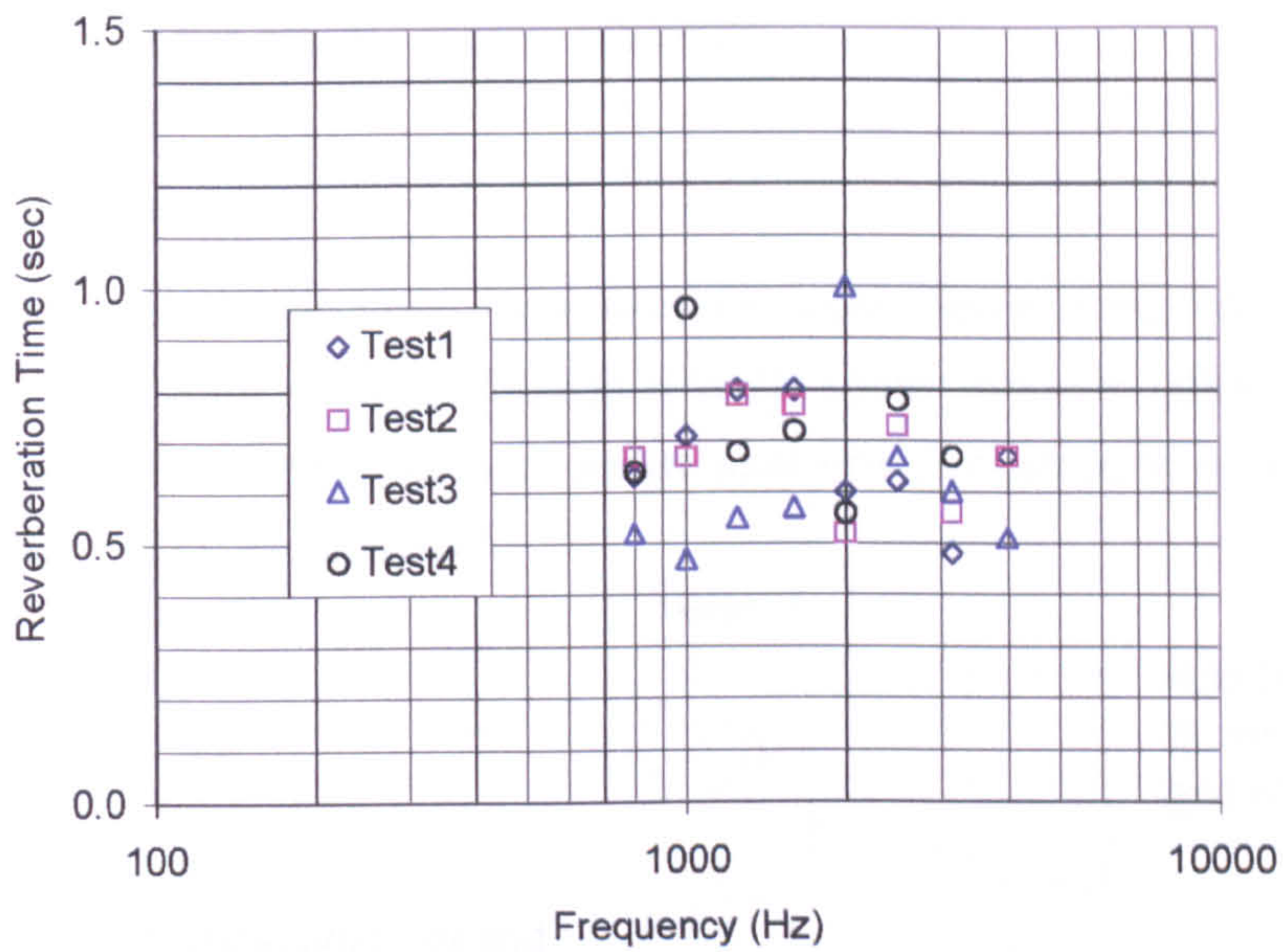


Figure 7.9 : Reverberation times obtained for the starting pistol tests

The results are highly variable and there does not appear to be general trend. The average reverberation times obtained by a pistol source lie close to each other with 1.00, 1.05 and 1.06 seconds respectively.

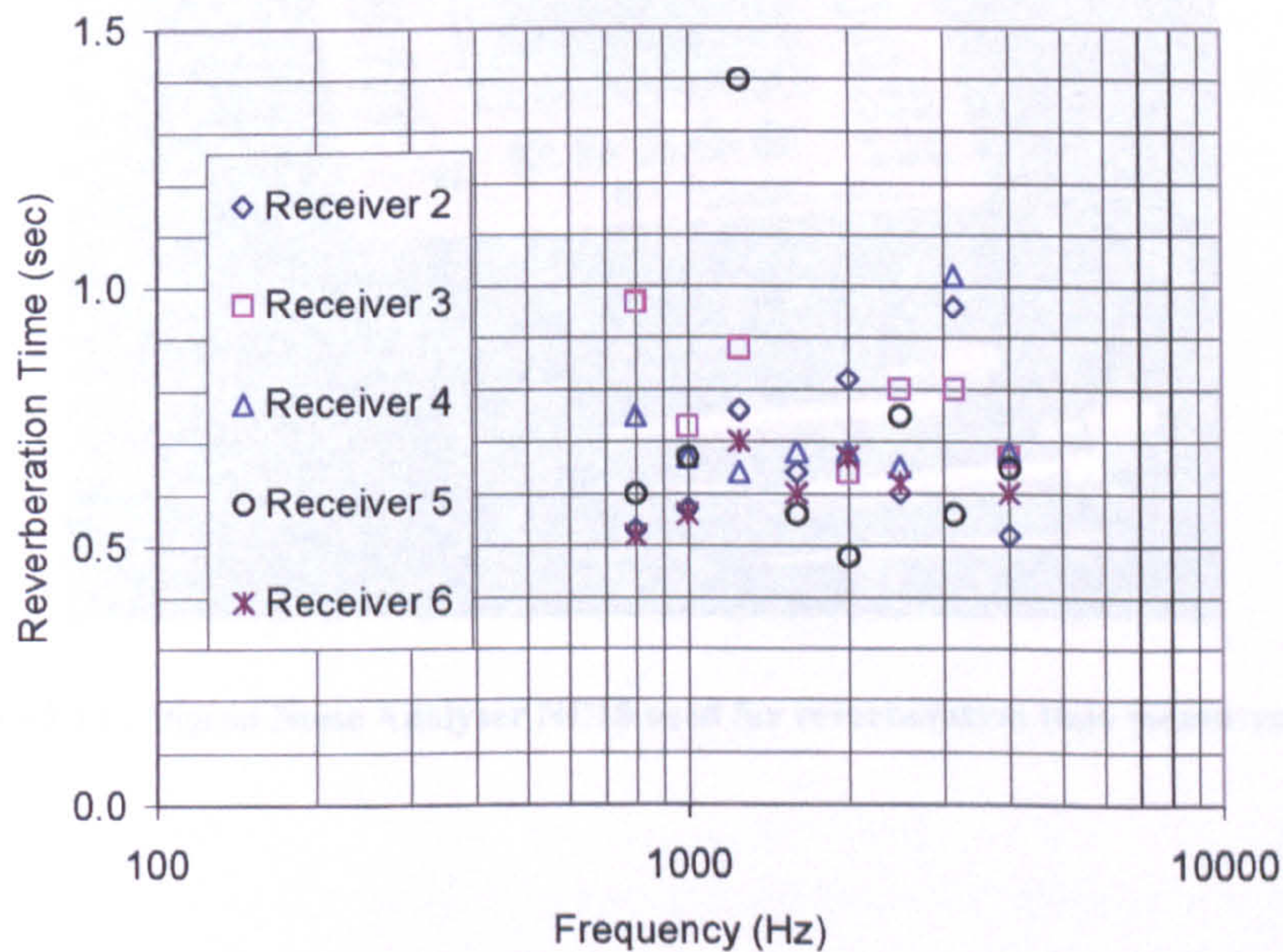
The results for the four tests undertaken using the single wedge speaker are shown in Figure 7.10. With the exception of test 3, correlation between the reverberation times are generally reasonable. Excluding the test 3 results, the average reverberation times for the spectrum under investigation have been calculated as 0.66, 0.67 and 0.72 seconds. Test 3 gives a very close average reverberation time to the ones observed above with 0.61 seconds even though the values at individual frequency bands do not appear to correlate well.





**Figure 7.10 : Reverberation times obtained for the single wedge speaker tests**

The double wedge speaker tests using five different receiver locations are shown in Figure 7.11. There were no visible decay curves at 1.6 kHz (Receiver 3) and at 3.15 kHz (Receiver 6), and these are excluded from the graph. Receiver 5 gives anomalies at more than one frequency band. The most prominent one occurs at 1.25 kHz, which is an excessively high reverberation time with 1.4 seconds. The reverberation times at 2 kHz and 3.15 kHz also seem to be below the average values.



**Figure 7.11 : Reverberation times obtained for the double wedge speaker tests**



## 7.2.4 The NC10 Experiments

### 7.2.4.1 Instrumentation

In order to obtain a more accurate representation of the nature of the reflections in the room, further tests were carried out using a digital sound analyser called NC10. The noise sources were a starting pistol or wedge speakers connected to a random noise generator (B&K 1402), as applicable.

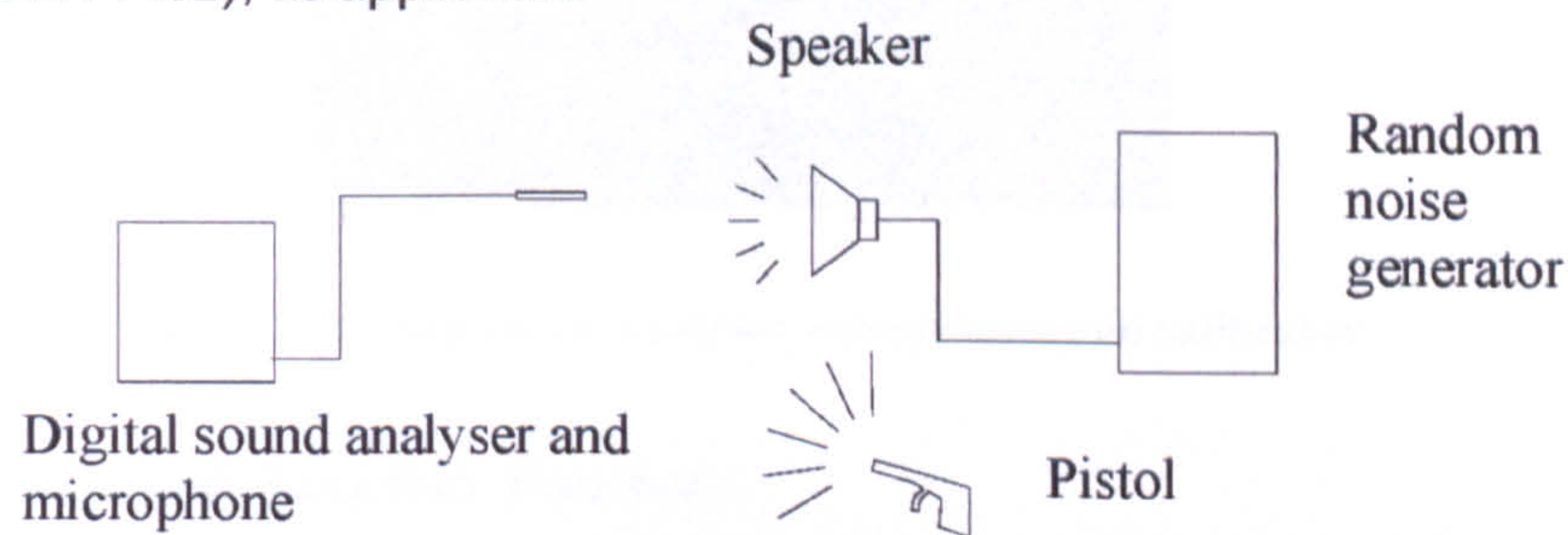


Figure 7.12 : Experimental set-up showing NC10 tests



Figure 7.13 : Digital Noise Analyser NC10 used for reverberation time measurements





Figure 7.14 : The NC10 Analyser, microphone and calibrator

### 7.2.4.2 Source and Receiver Positions

Two sets of tests were undertaken using the NC10. The first one consisted of wedge speaker tests which were repeated 5 times for the configuration shown in Figure 7.15. The second one was with a starting pistol as the sound source and was repeated twice for the set-up shown in Figure 7.16.

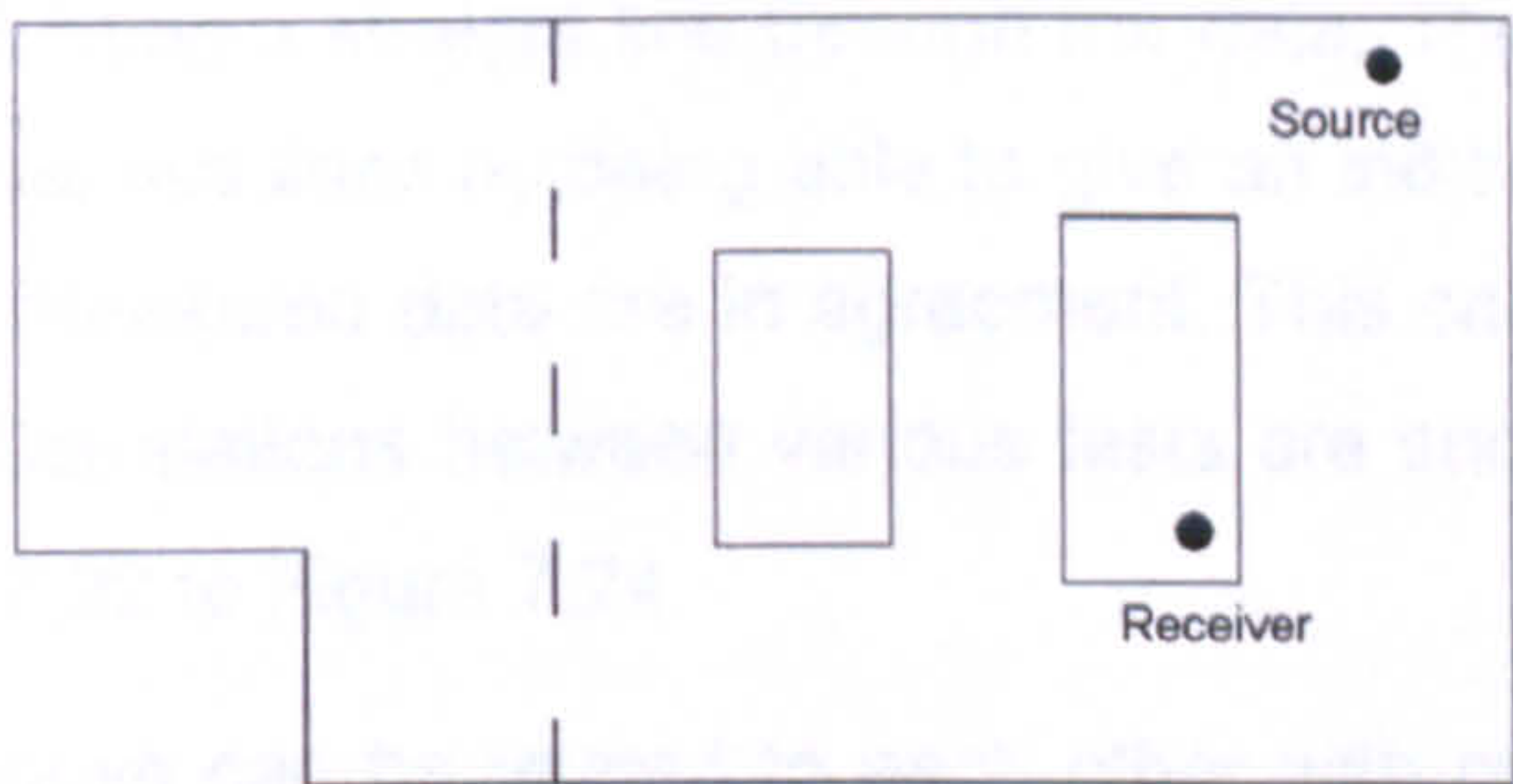


Figure 7.15 : Source-receiver configuration for the reverberation time tests undertaken by NC10 using a wedge speaker as the source.

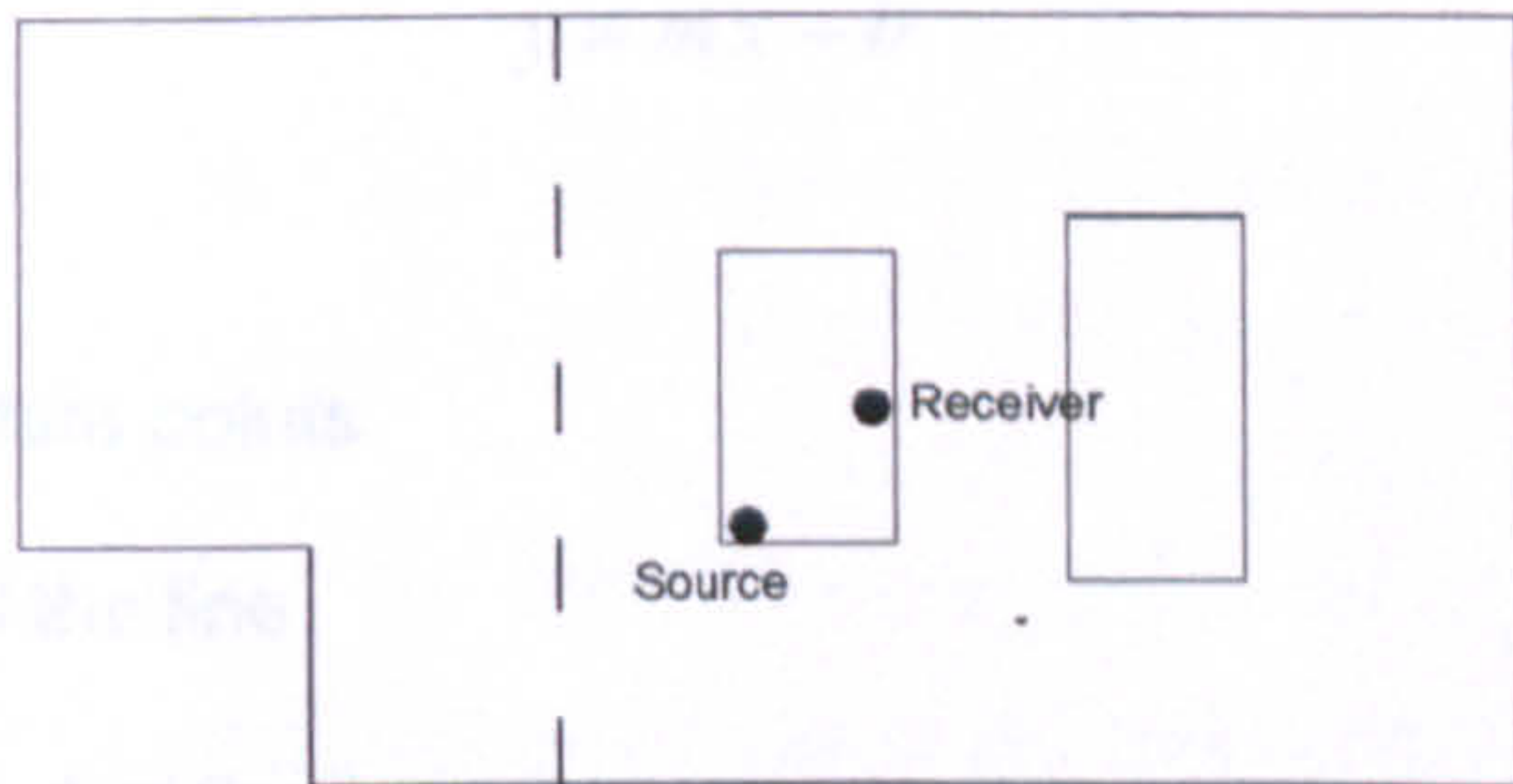


Figure 7.16 : Source-receiver configuration for the reverberation time tests undertaken by NC10 using a starting pistol as the source.

### 7.2.4.3 Method

The NC10 analyser records the signal decay behaviour in a room by using a parallel real-time third-octave analysis and automatically calculates the reverberation time for each third octave in accordance with ISO 354/ DIN52212 and ISO 3382/DIN 52216<sup>2</sup>.



The time scale can be read to a precision of 2.5 ms and the decay levels can be observed from 110 dB down to 20 dB. The frequency bands under investigation were the 1 / 3 octave bands between 500 Hz and 16 kHz inclusive. Also the averaging time can be adjusted.

During the calculation of the reverberation time, the ideal straight line is drawn through each decay curve. The method of the smallest error squares (linear regression) is applied. At the same time automatic checks are carried out on how strongly the measured curve fluctuates from the ideal straight line (regression line), or how well it correlates (empirical correlation).

For a given frequency band, the measured curve contains 280 data points as shown in Figure 7.25 and Figure 7.26. This is based on a total measurement time of 0.7s and a resolution of 2.5ms. Each data point on the graph is represented by an  $x$  value (time in ms) and a corresponding  $y$  value (sound pressure level in dB). However the extent of the data points used as part of regression line is determined by the definition of reverberation time under consideration (i.e. T30, T20 and EDT). Linear regression procedure fits a straight line through these points. The straight line is drawn such that the squared deviations of the observed points from the line are minimised. In practice, there are many ways of fitting a straight line through the data. Therefore it is important to distinguish between various lines by being able to give an indication on how well the regression line and the measured data are in agreement. This can be achieved by the correlation coefficient. Correlations between various tests are shown in Figure 7.18 to Figure 7.20 and Figure 7.22 to Figure 7.24.

The terms discussed above can be related to each other with reference to the linear regression line, which has the general form

$$y = mx + b$$

where,

$x$  and  $y$  are the data points

$m$  is the slope of the line

$b$  is the y-intercept of the line

The constants  $m$  and  $b$  can be determined from statistical approach called linear regression. Given a set of data  $(x_i, y_i)$  with  $n$  data points, the slope,  $m$ , the y-intercept,  $b$  and the correlation coefficient,  $r$ , can all be related as follows



$$m = \frac{n\sum(xy) - \sum x \sum y}{n\sum(x^2) - (\sum x)^2}$$

$$b = \frac{\sum y - m \sum x}{n}$$

$$r = \frac{n\sum(xy) - \sum x \sum y}{\sqrt{[n\sum(x^2) - (\sum x)^2][n\sum(y^2) - (\sum y)^2]}}$$

The denominator in the above equation describing the correlation coefficient is a measure of the degree to which x and y vary together. The numerator, on the other hand, indicates the degree to which x and y vary separately.

The reference level for the start of the decay curve is defined by using a trigger function which can be modified according to the nature of the source being used. When the starting pistol was used as the source, the trigger level was set as 70 dB (A) on the rising edge of the trigger so as to capture the peak sound pressure level fully. In the case of the wedge speaker, the trigger occurred when the sound pressure level was falling and reached past 75 dB (A). The pretrigger was set as 10% of the duration of the measurement which meant the logger recorded 10% of the time frame before the trigger condition was met.

The main advantage of the NC10 method is the automated nature of the trigger and the decay curve production, reducing manual intervention, which is prone to error. The following are the findings using these two methods of measuring reverberation times.

#### 7.2.4.4 Results

The reverberation times for the wedge speaker and the starting pistol tests using the NC10 are shown in Figure 7.17 to Figure 7.26. The average reverberation times for the speaker tests based on T30, T20 and EDT are shown in Figure 7.17. Figure 7.18 to Figure 7.20 give the corresponding correlations obtained for the T30, T20 and EDT. The average reverberation times for the pistol tests based on T30, T20 and EDT are given in Figure 7.21 and the corresponding correlations are shown in Figure 7.22 to Figure 7.24. Two selected decay curves, as captured by the NC10, are included for each source in Figure 7.25 and Figure 7.26.



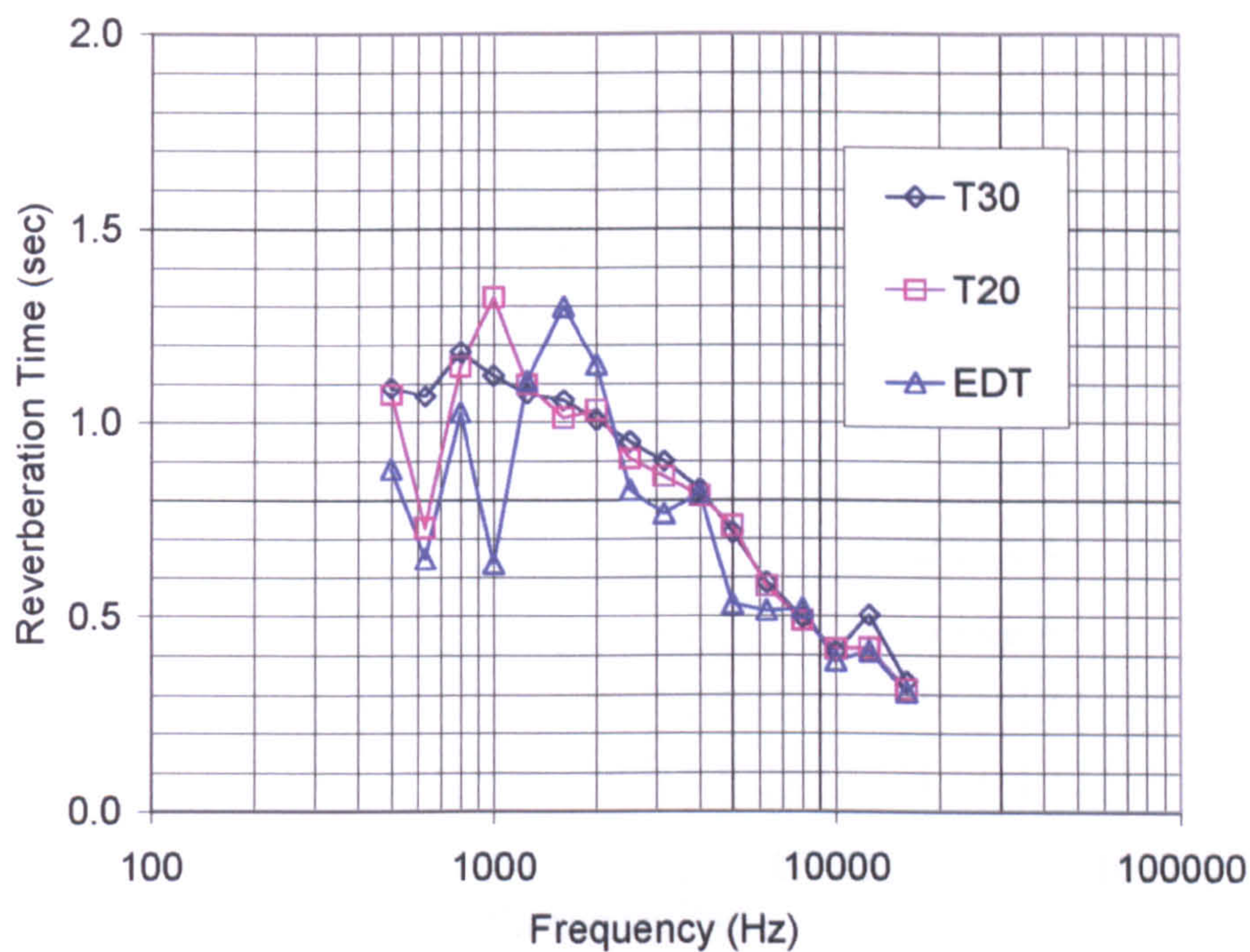


Figure 7.17 : Average reverberation times for the NC10 tests using the wedge speaker as the source.

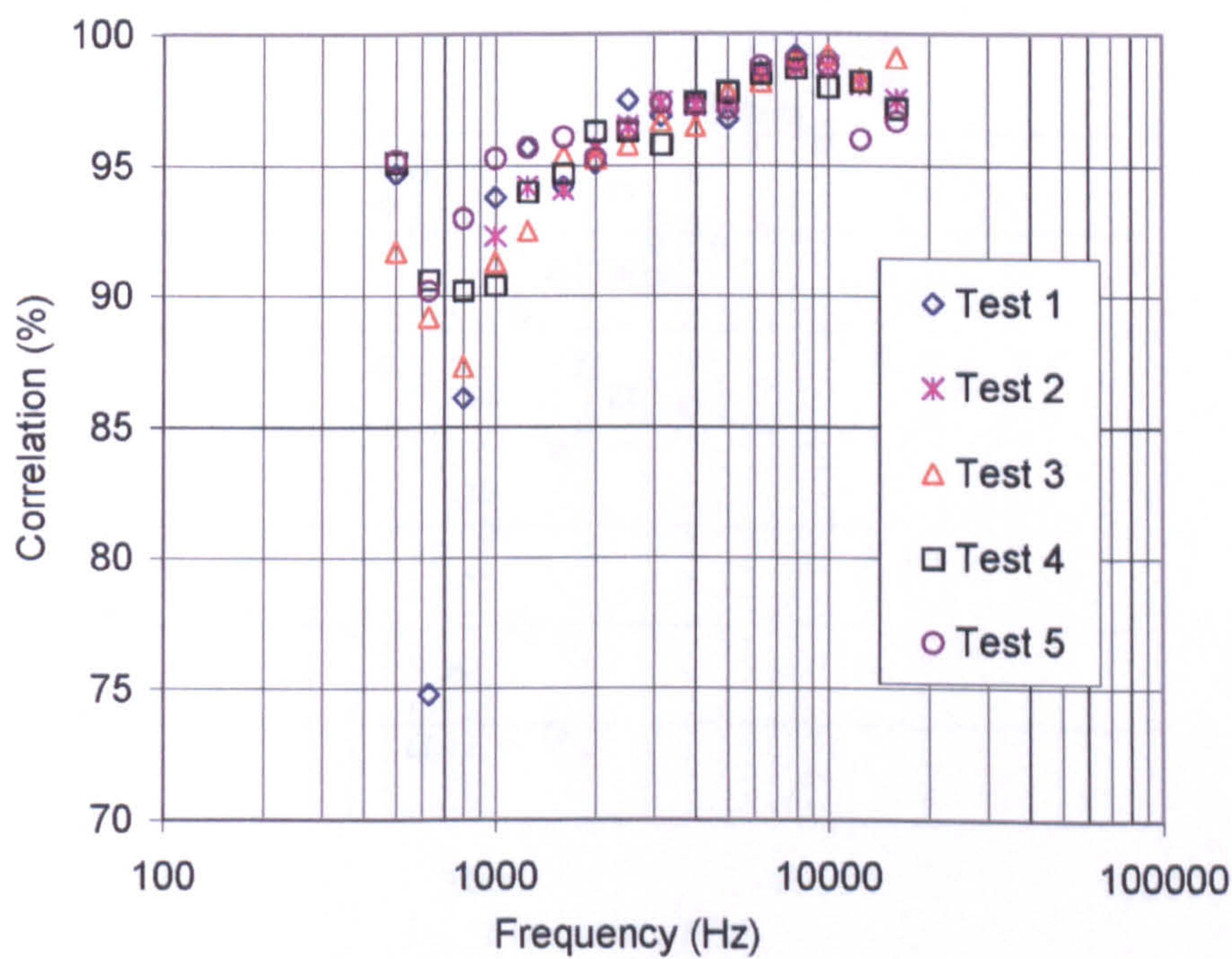


Figure 7.18 : Correlation of the T30 test results using the wedge speaker.



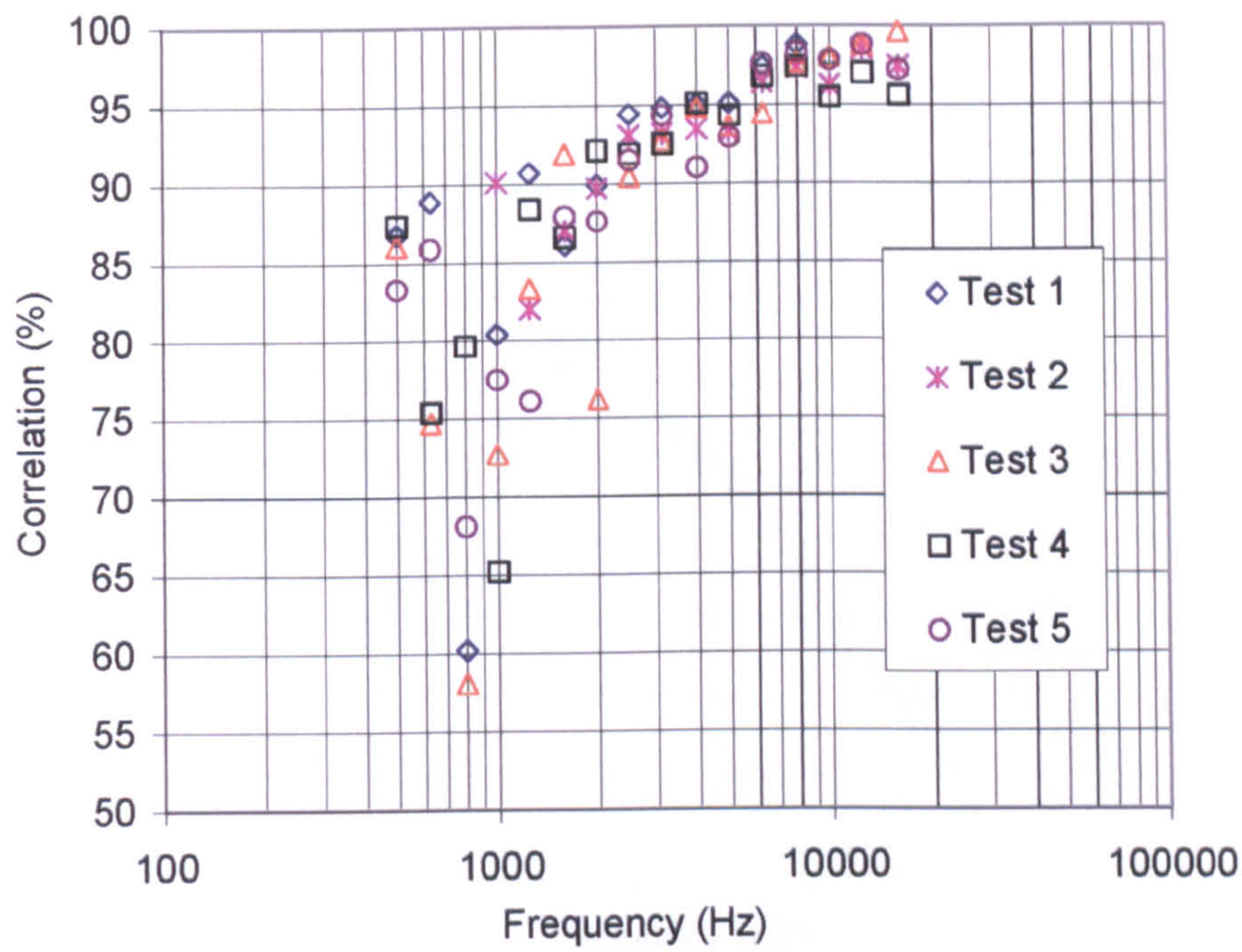


Figure 7.19 : Correlation of the T20 test results using the wedge speaker.

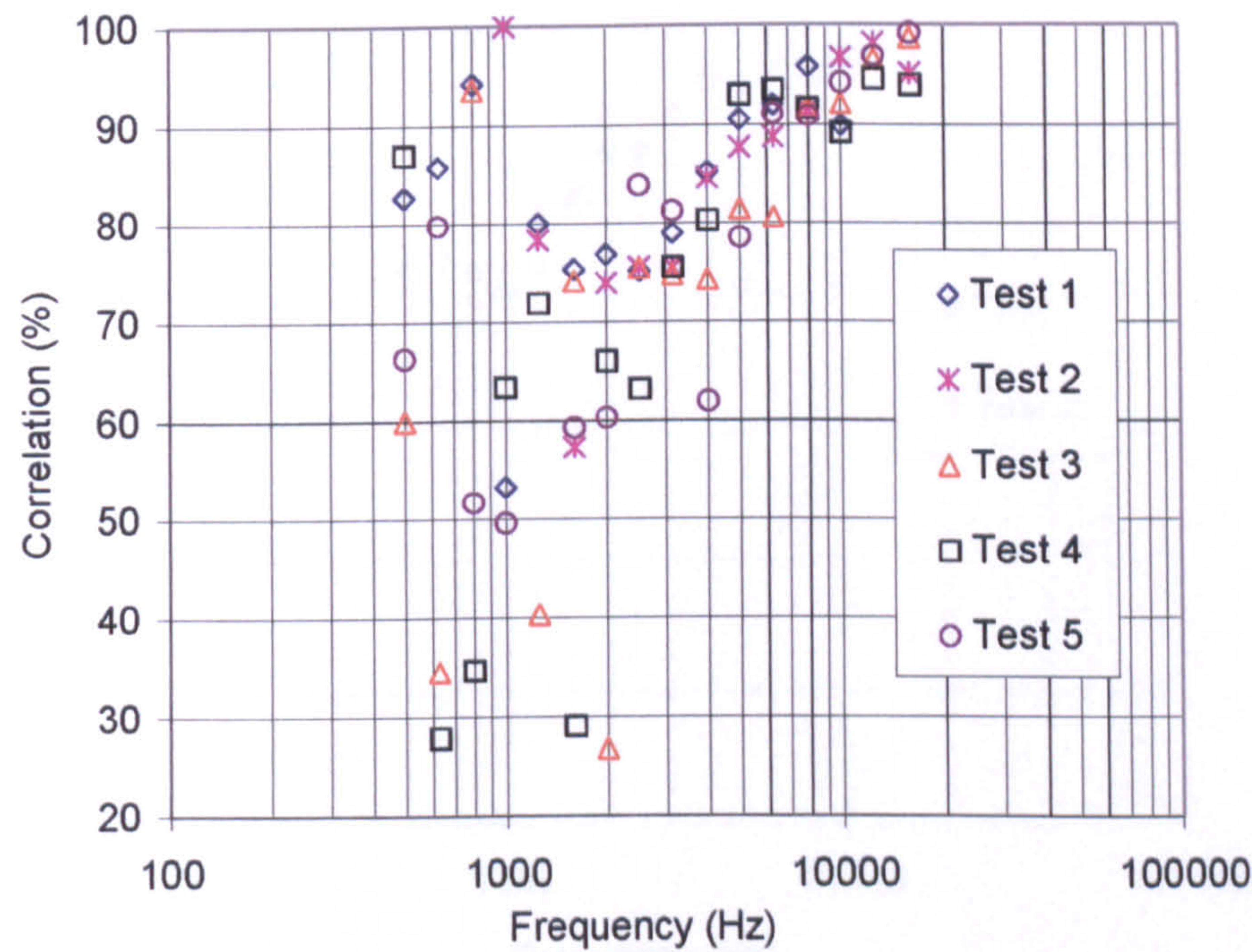


Figure 7.20 : Correlation of the early decay times (EDT) using the wedge speaker.



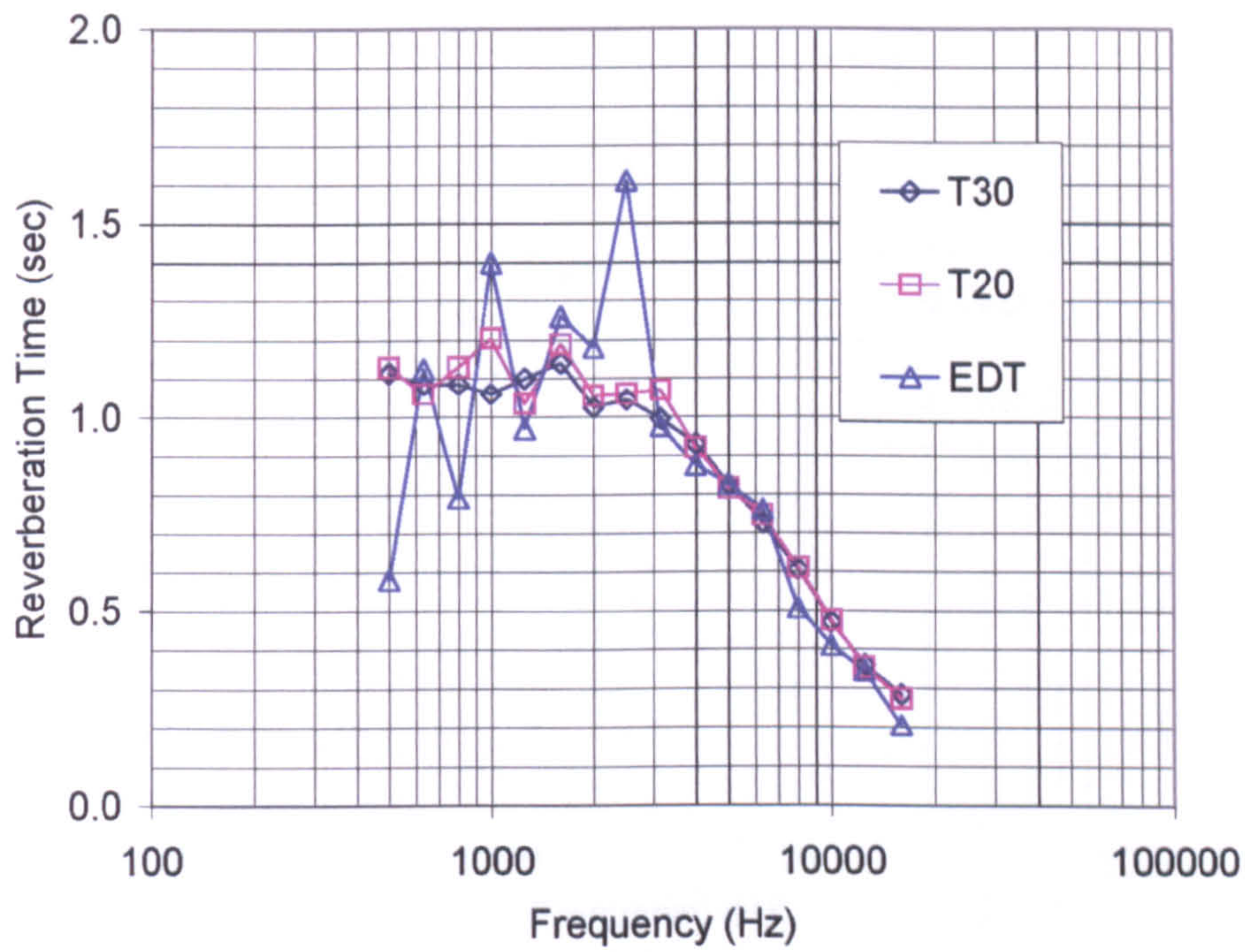


Figure 7.21 : Average reverberation times for the pistol tests.

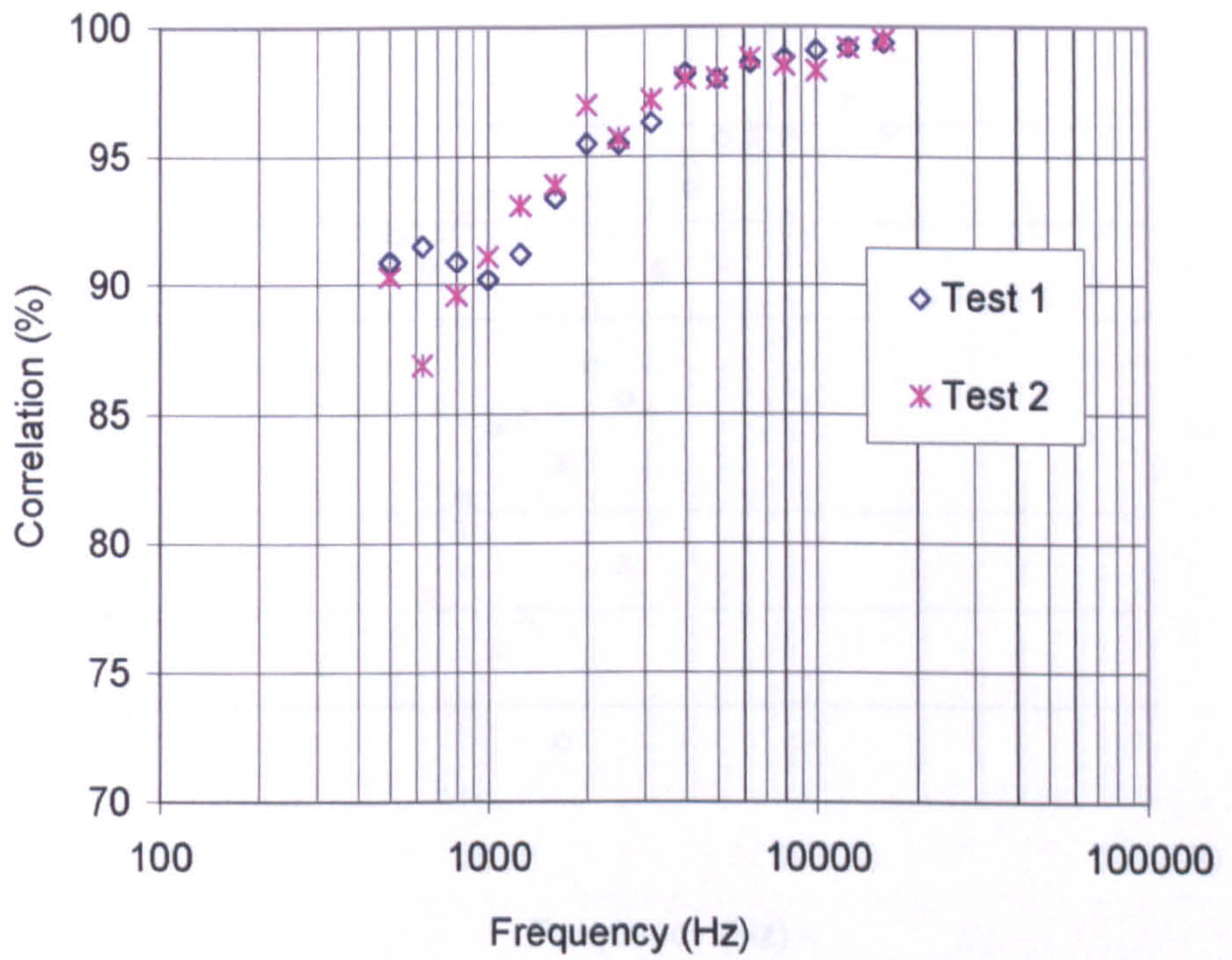


Figure 7.22 : Correlation of the T30 test results using the starting pistol.



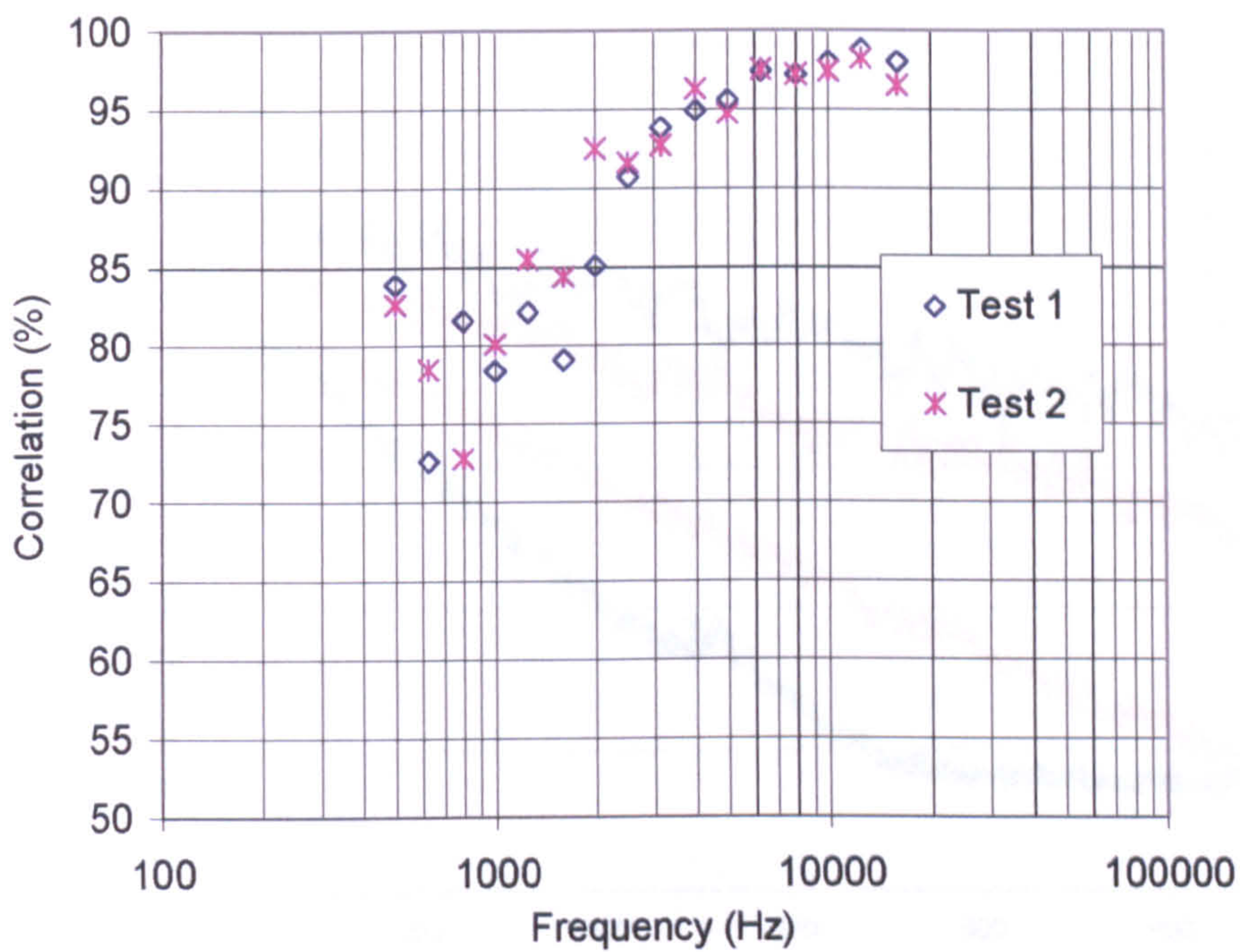


Figure 7.23 : Correlation of the T20 test results using the starting pistol.

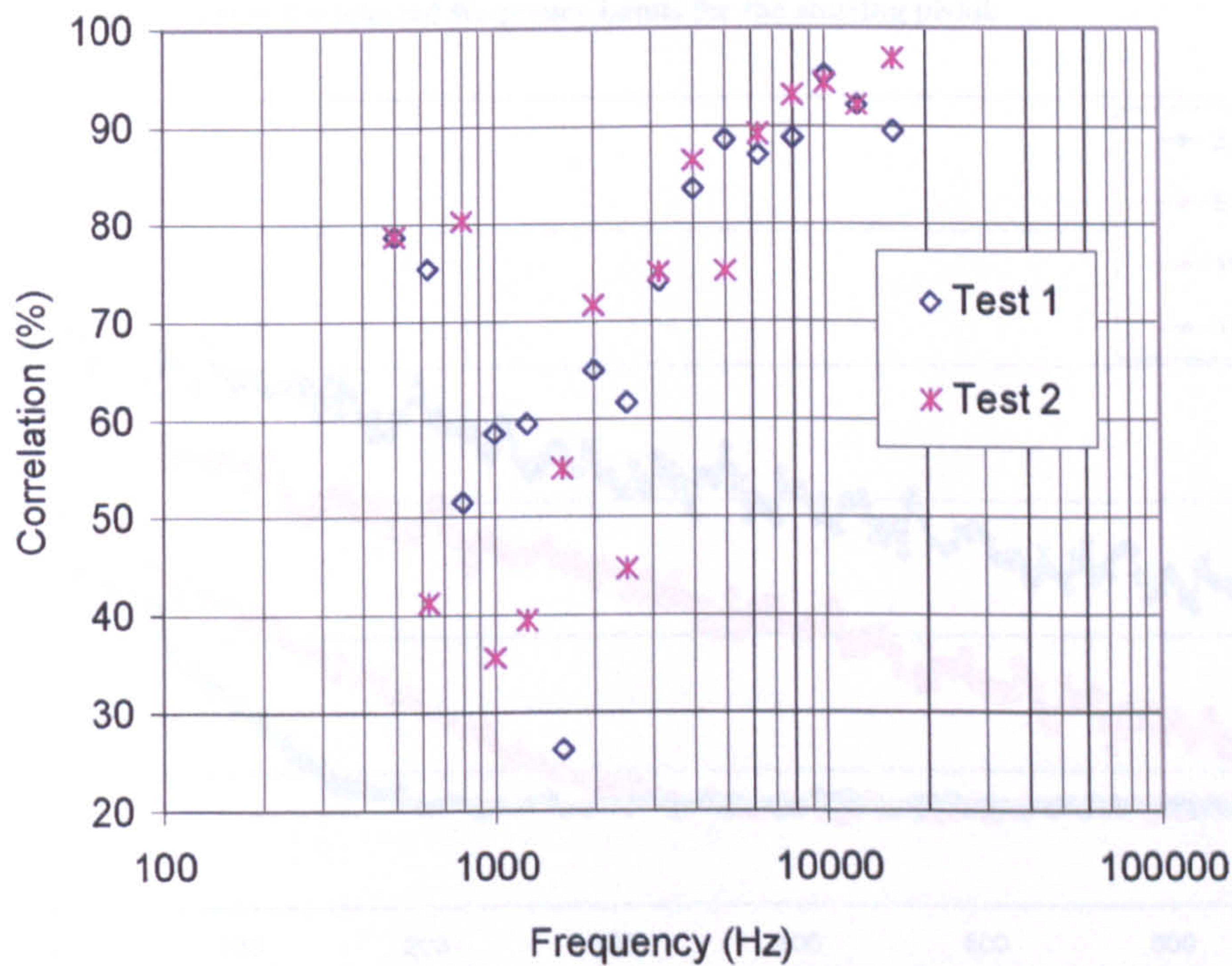


Figure 7.24 : Correlation of the early decay times (EDT) using the starting pistol.

Table 7.2 shows the selected frequency bands for the wedge speaker. The results obtained by the NC10 yielded very consistent results for both the 2 tests with the starting pistol and the 5 tests with the wedge speaker. As the amount of decay is small, from 10 dB to 30 dB, there is a progressive settling of the fluctuations in the correlation, leading to the correlation.



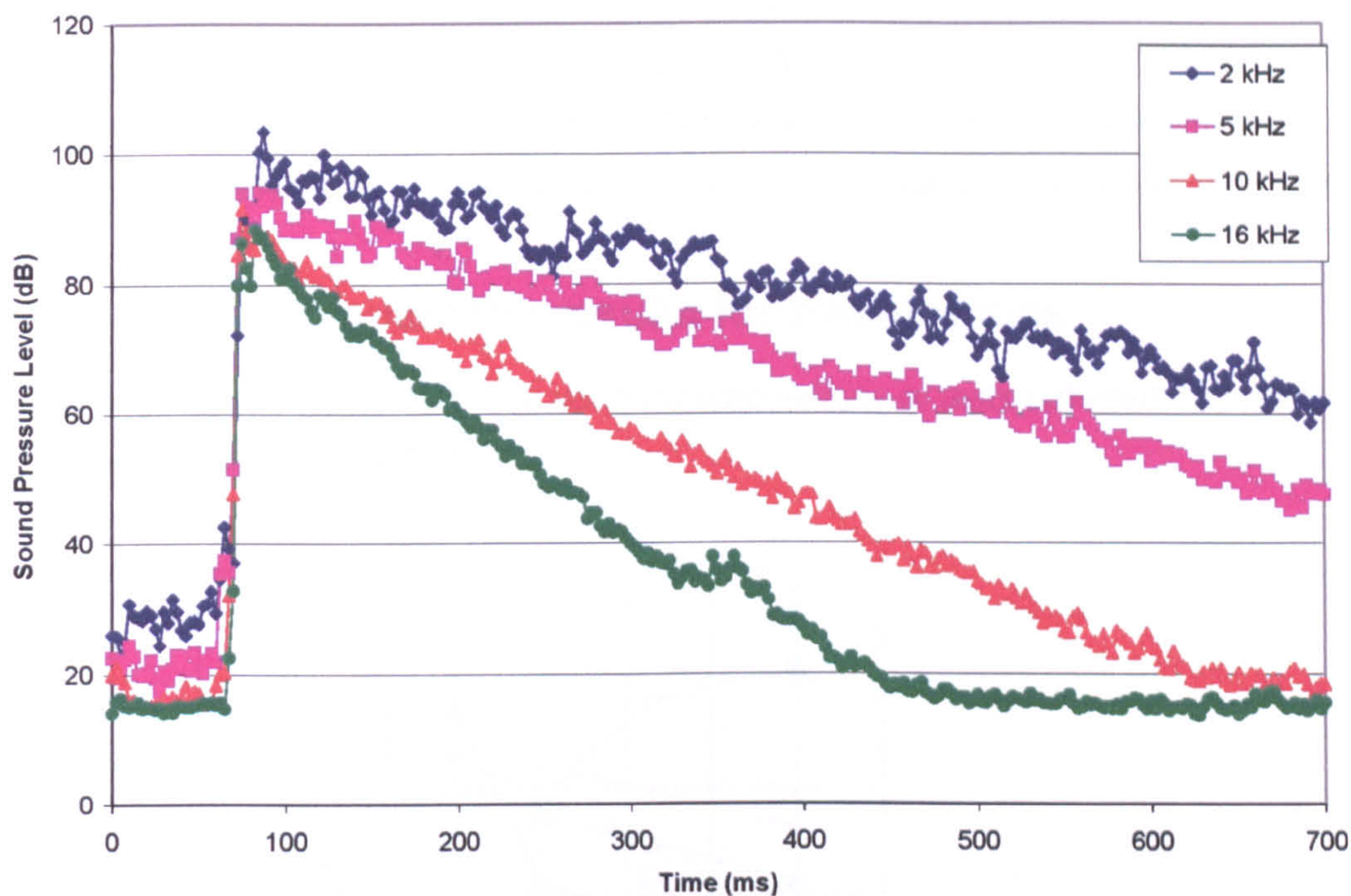


Figure 7.25 : Decay curves for selected frequency bands for the starting pistol.

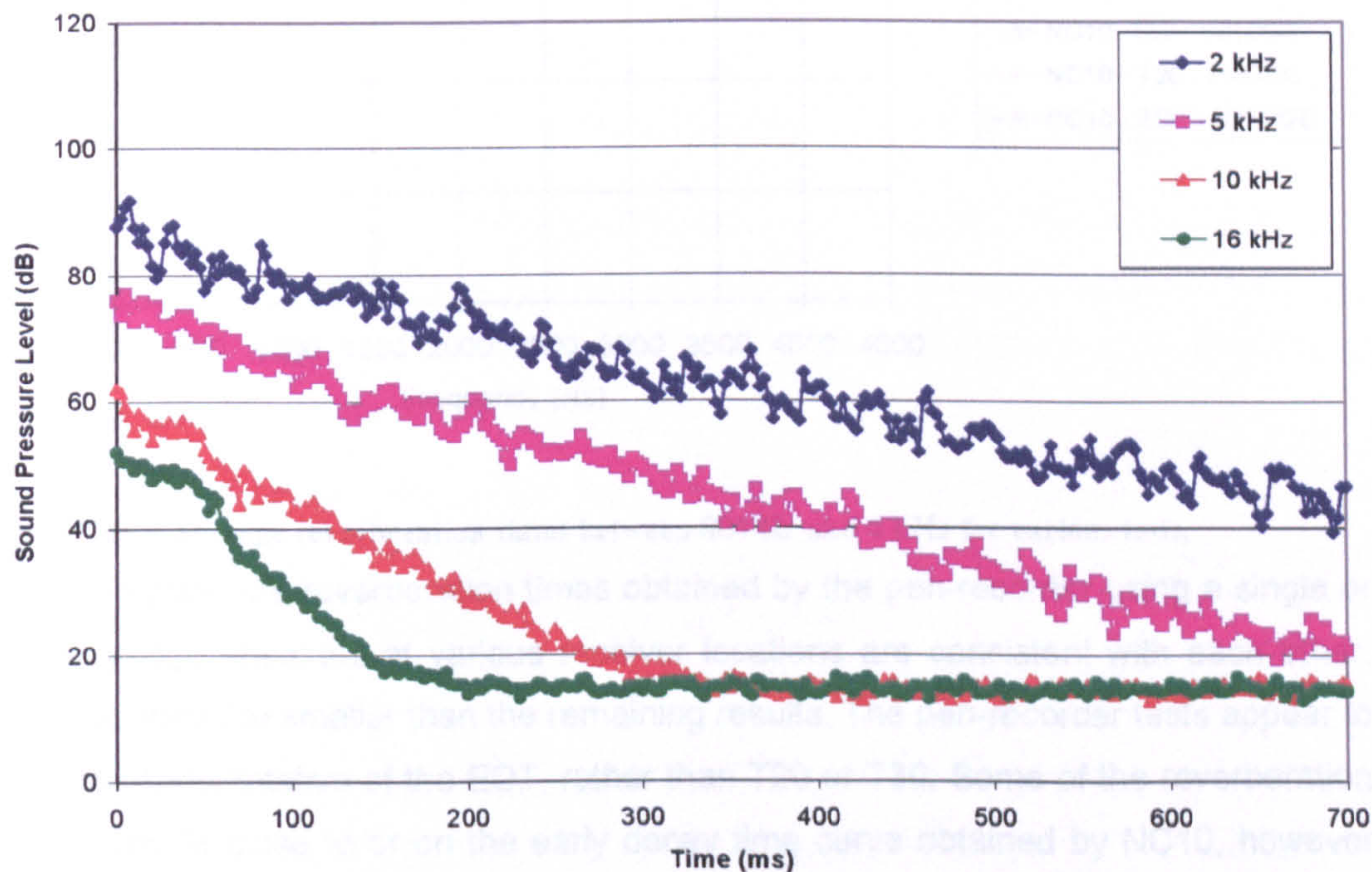


Figure 7.26 : Decay curves for selected frequency bands for the wedge speaker.

The tests carried out by the NC10 yielded very consistent results for both the 2 tests with a starting pistol and the 5 tests with the wedge speaker. As the amount of decay is increased from 10 dB to 30 dB, there is a progressive settling of the fluctuations in the results and an increase in the correlations.



As would be expected, the reverberation times are reduced as the frequency increases. Reverberation times are between 1.0 and 1.1 seconds from 500 Hz up to 3.15 kHz. From this point onwards, they start decreasing in a linear fashion under a logarithmic frequency scale. The minimum reverberation time is 0.3 seconds at 16 kHz.

### 7.2.5 Comparative results for two methods

The average reverberation times for various combinations of tests between 800 Hz and 4 kHz are shown in Figure 7.27.

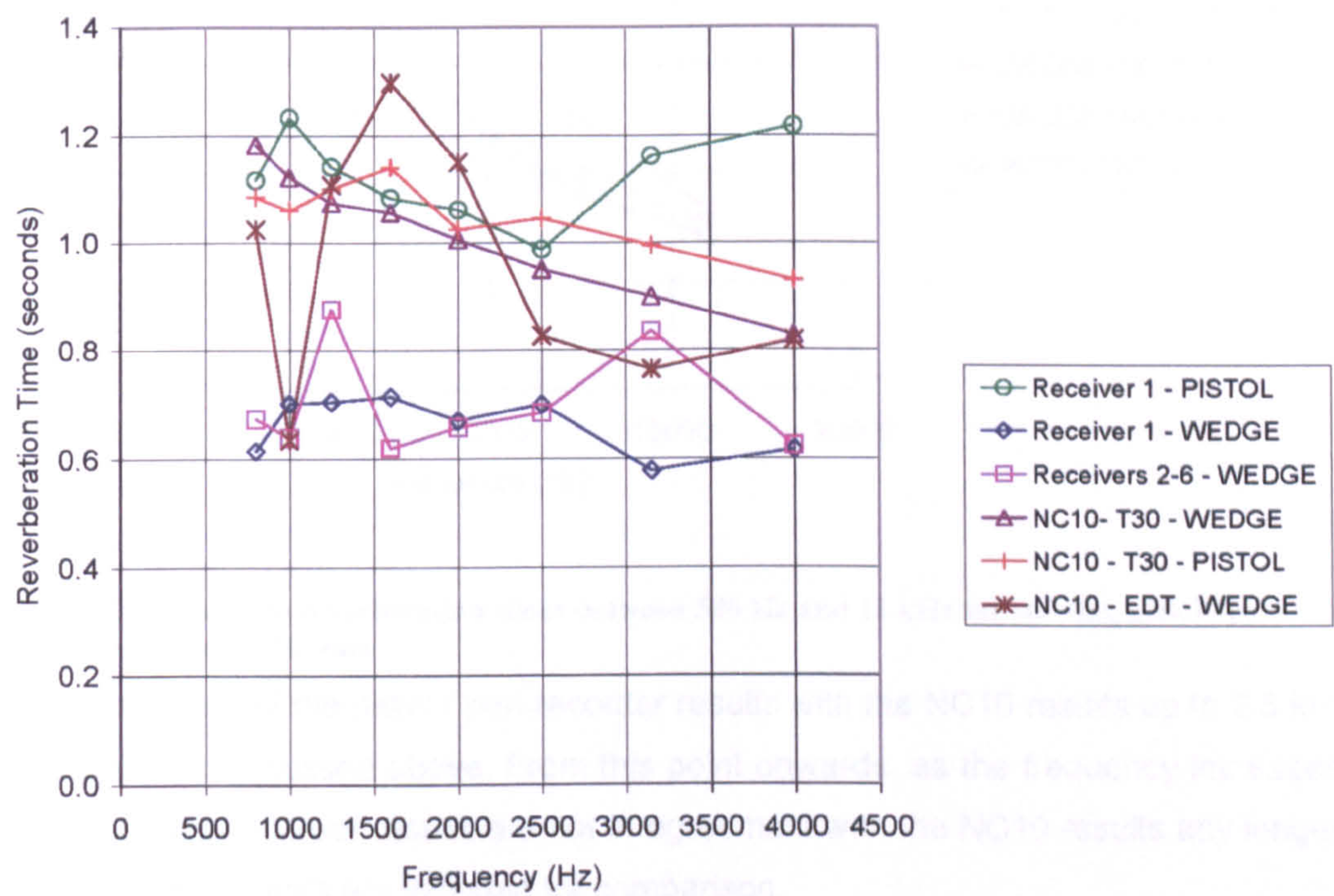


Figure 7.27 : Average reverberation times between 800 Hz and 4 kHz for various tests.

As seen above, the reverberation times obtained by the pen-recorder using a single or double wedge speakers at various receiver locations are consistent with each other. However, they are smaller than the remaining results. The pen-recorder tests appear to be more representative of the EDT, rather than T20 or T30. Some of the reverberation time values lie close to or on the early decay time curve obtained by NC10, however these are mainly smaller than the early decay times.

The T30 results obtained by either the wedge speaker or the starting pistol using the NC10 are within 0.1 seconds of each other. The starting pistol tests obtained by the pen recorder lie in between these two curves with an exception at higher frequencies.

Since there was no data above 4 kHz for the wedge / pen-recorder tests, the comparisons above have been limited to 4 kHz. The reverberation times between 500



Hz and 16 kHz for the pistol / pen-recorder tests and the various results obtained by NC10 are seen below.

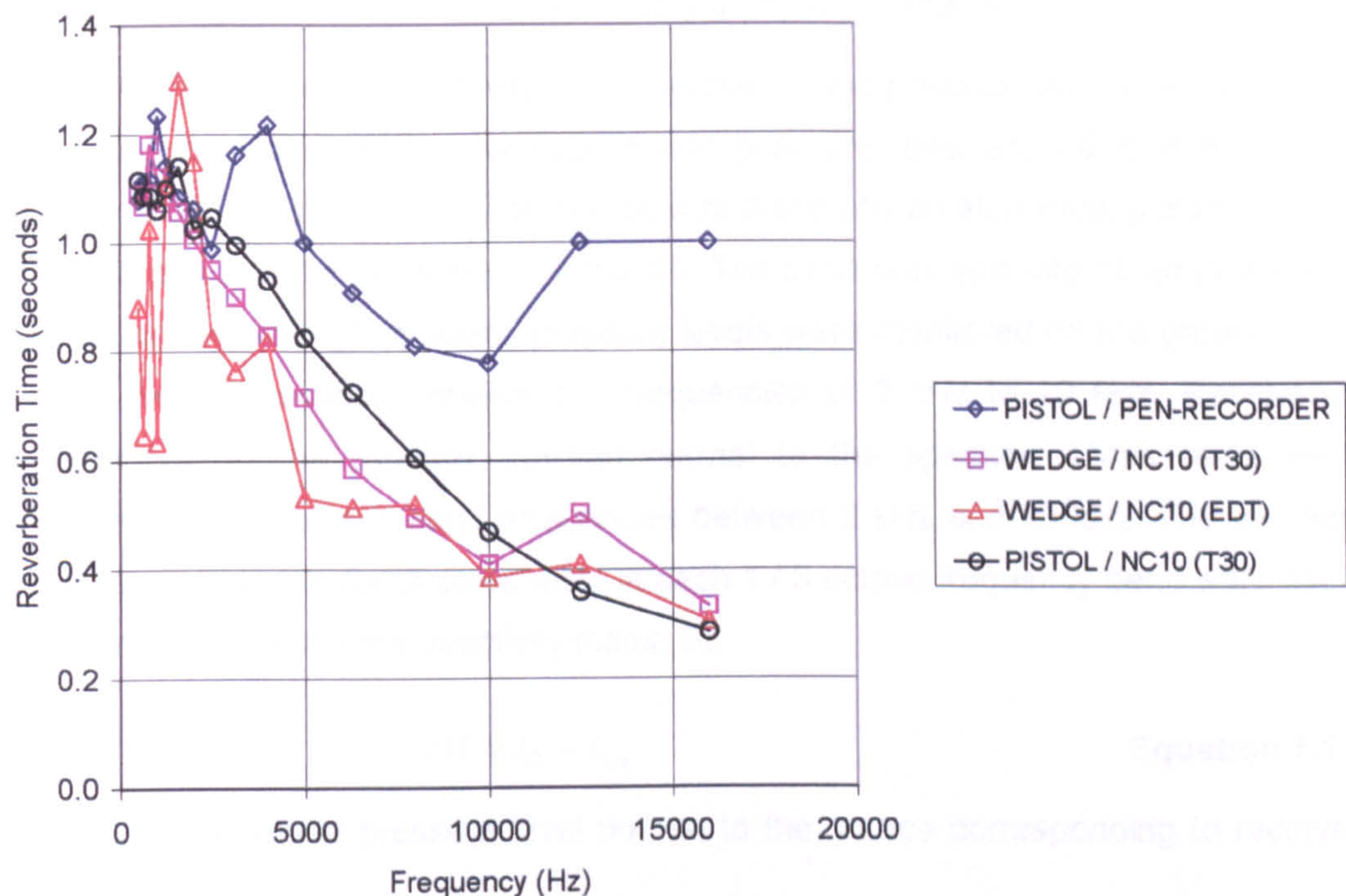


Figure 7.28 : Average reverberation times between 500 Hz and 16 kHz for starting pistol / pen-recorder and the NC10 tests.

The consistency of the pistol / pen-recorder results with the NC10 results up to 2.5 kHz are visible, as discussed above. From this point onwards, as the frequency increases, the pistol / pen-recorder results are not in agreement with the NC10 results any longer. The early decay times are included for comparison.

These experiments have shown that the T30 results obtained by NC10 are likely to be representative of the reverberation times within the testing space. These will be used in the forthcoming sections for estimating the reverberant field.

### 7.3 SOURCE DIRECTIVITY

Another parameter required for estimating the reverberant levels is the directivity of the source. These are determined in this section.

#### 7.3.1 Aim of the Experiment

The aim of this experiment is to determine the directivity characteristics of the source to be used at the frequency bands of interest.



### 7.3.2 Experimental Apparatus, Set-up and Procedure

The experimental apparatus consisted of the source connected via an amplifier to a random noise generator and the receiver connected to an analyser.

In order to determine the directivity of the source, sound pressure level in the direction of the source relative to the average sound pressure level around it at the same distance had to be determined. The source was placed on an aluminium platform and a circle of a radius of 1 m was drawn around it. The circle was split into 16 equal sectors of 22.5 degrees each. The sound pressure levels were monitored on the ground level at each receiver location between the frequencies of 2 kHz to 20 kHz. Receiver 1 corresponded to the receiver position normal to the speaker. Three tests were performed at 1 / 3 octave band frequencies between 2 kHz and 20 kHz. The average sound pressure levels for all three tests at each 1 / 3 octave frequency band were used as follows to determine the directivity index, DI.

$$DI = L_1 - L_{av} \quad \text{Equation 7.1}$$

where  $L_1$  is the sound pressure level normal to the source corresponding to receiver number 1

and  $L_{av}$  is the space average sound pressure level determined as follows

$$L_{av} = 10 \log \left( \frac{10^{\left(\frac{L_1}{10}\right)} + \dots + 10^{\left(\frac{L_{16}}{10}\right)}}{16} \right) \quad \text{Equation 7.2}$$

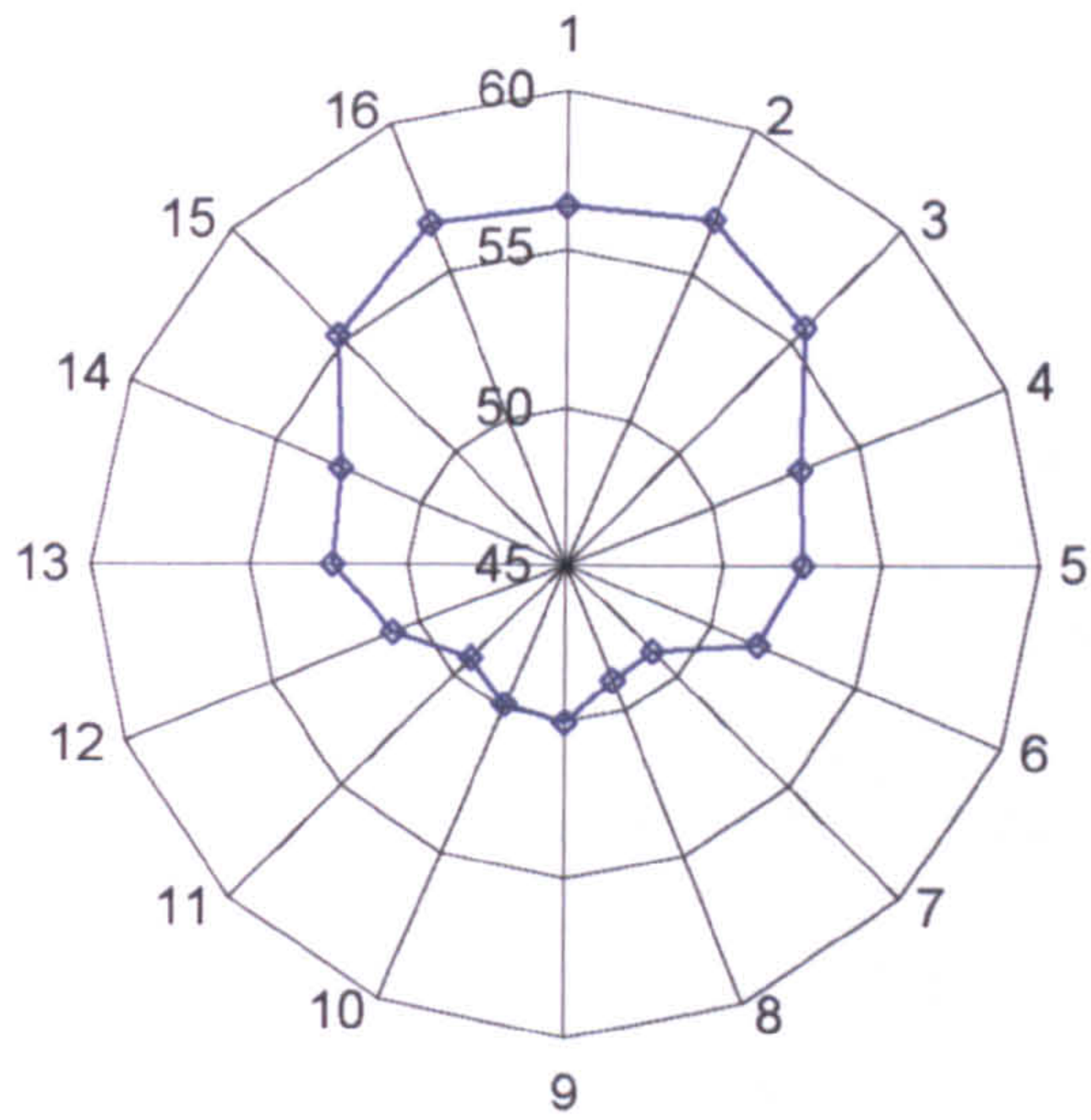
Then the directivity factor, Q, was found according to the formula

$$Q = 10^{\left(\frac{DI}{10}\right)} \quad \text{Equation 7.3}$$

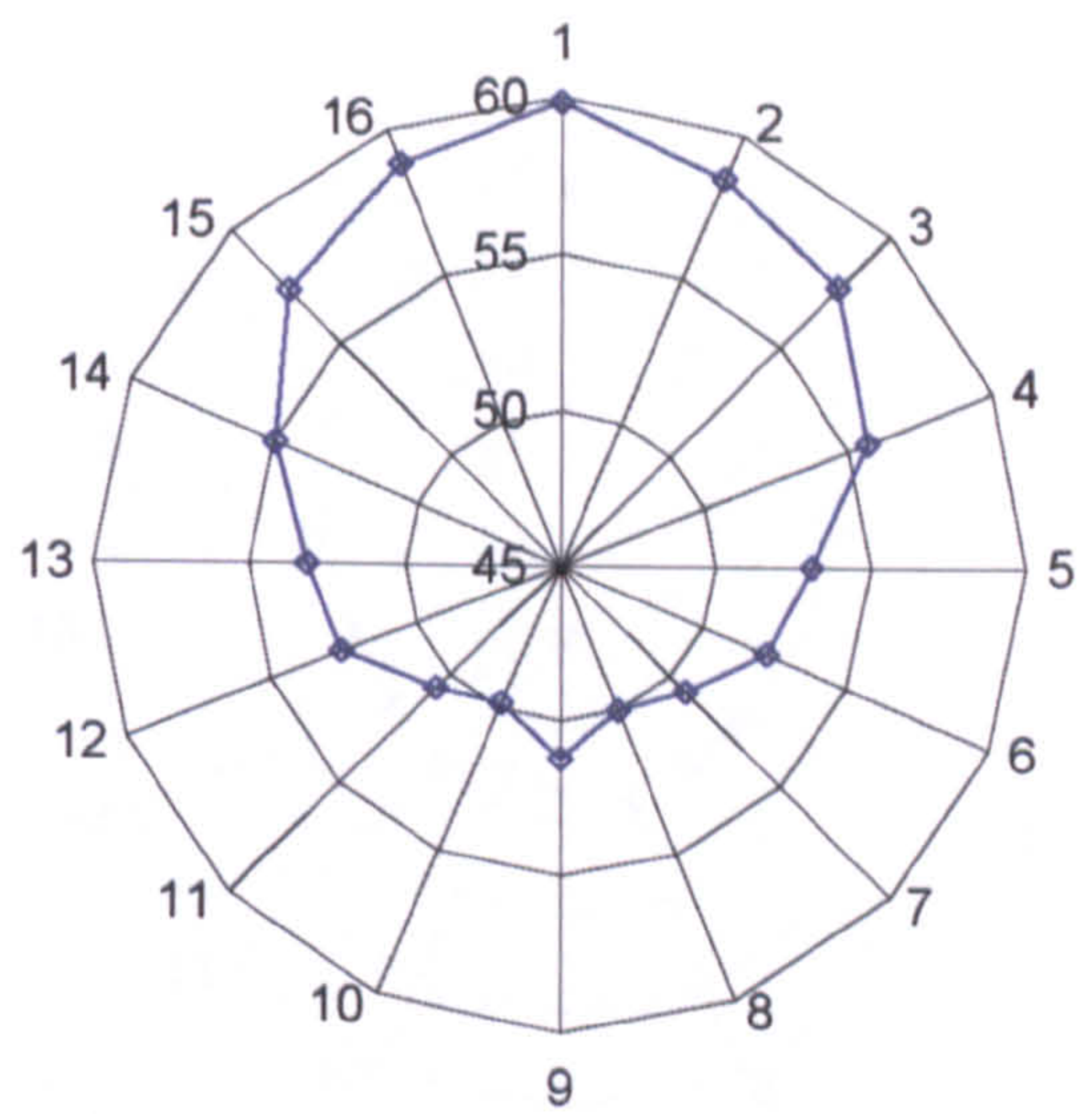
### 7.3.3 Results

The results are summarised in Figure 7.29 to Figure 7.31. The sound pressure levels are plotted in the form of a polar graph. The numbers 1-16 correspond to the receiver positions located 22.5 degrees clockwise of each other, where receiver 1 indicates the normal to the source.

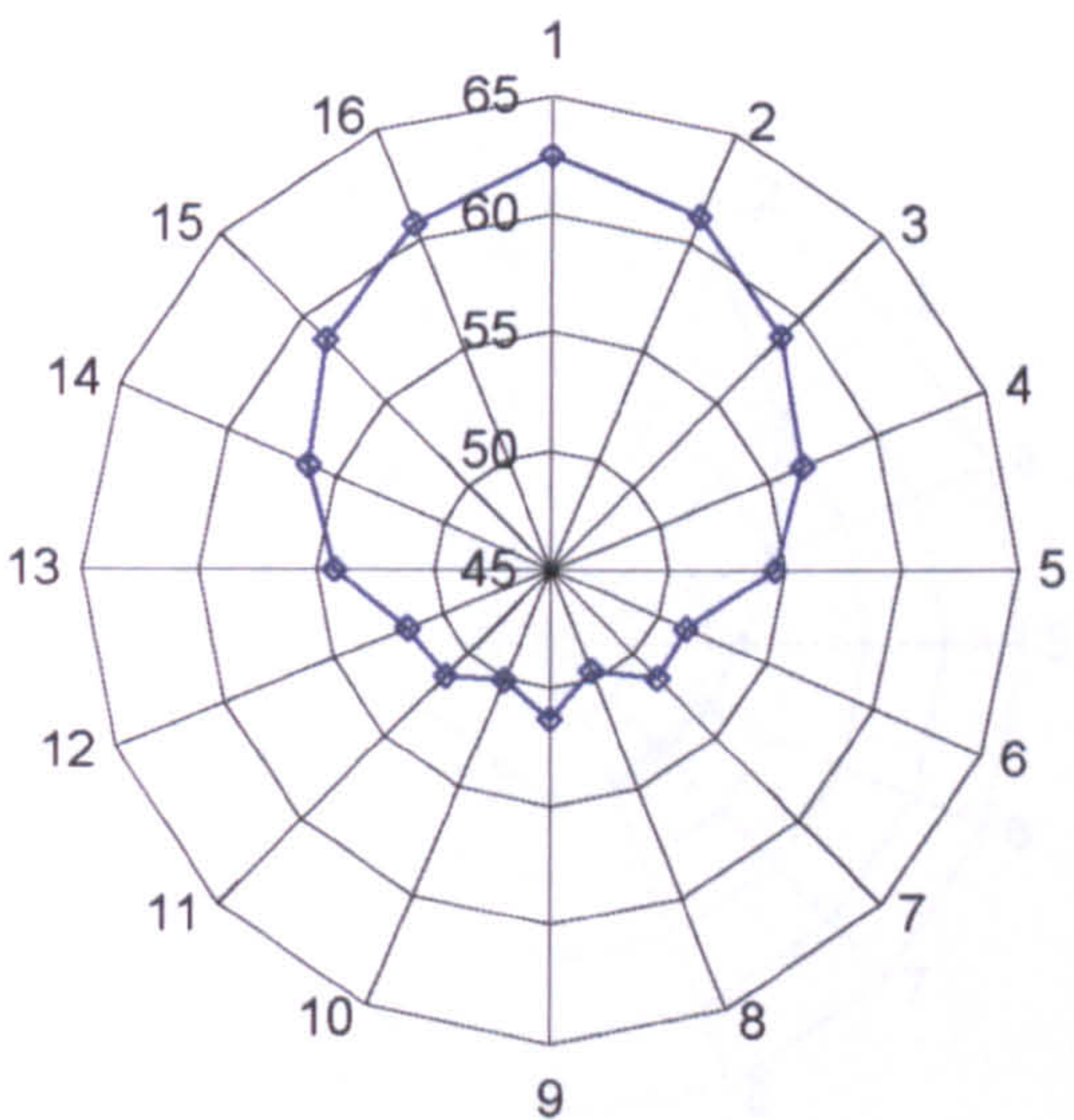




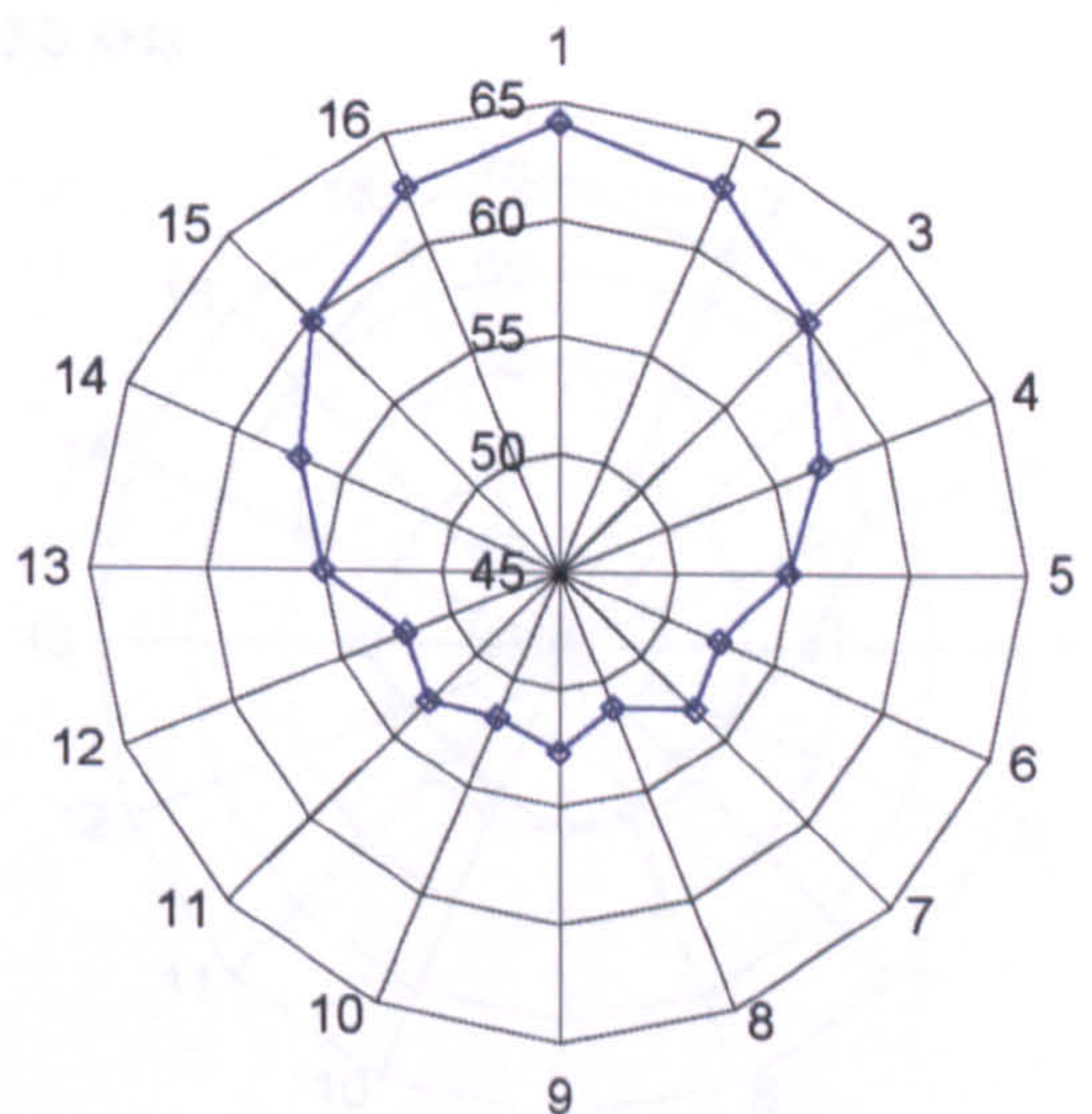
2 kHz



2.5 kHz



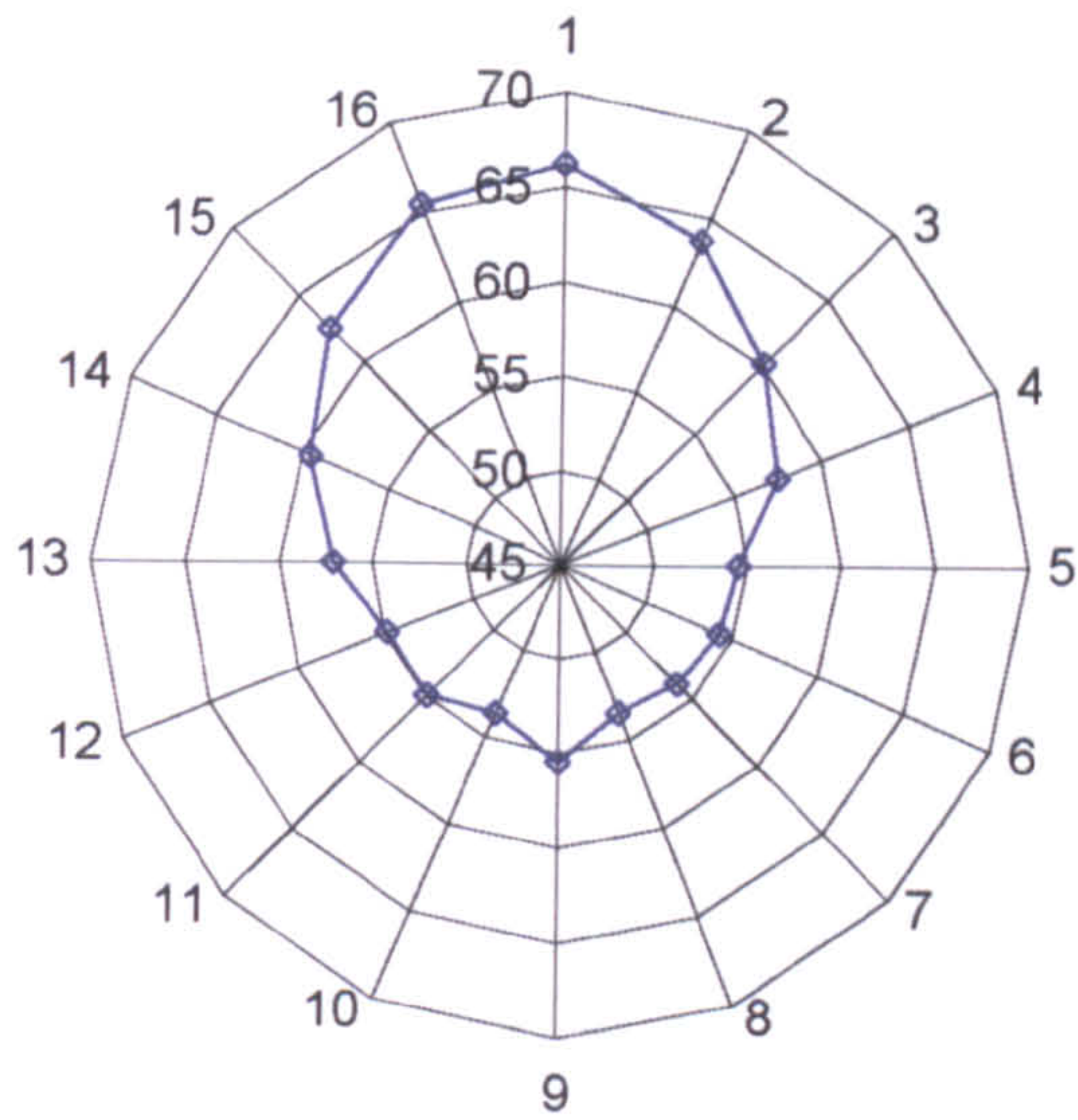
3.15 kHz



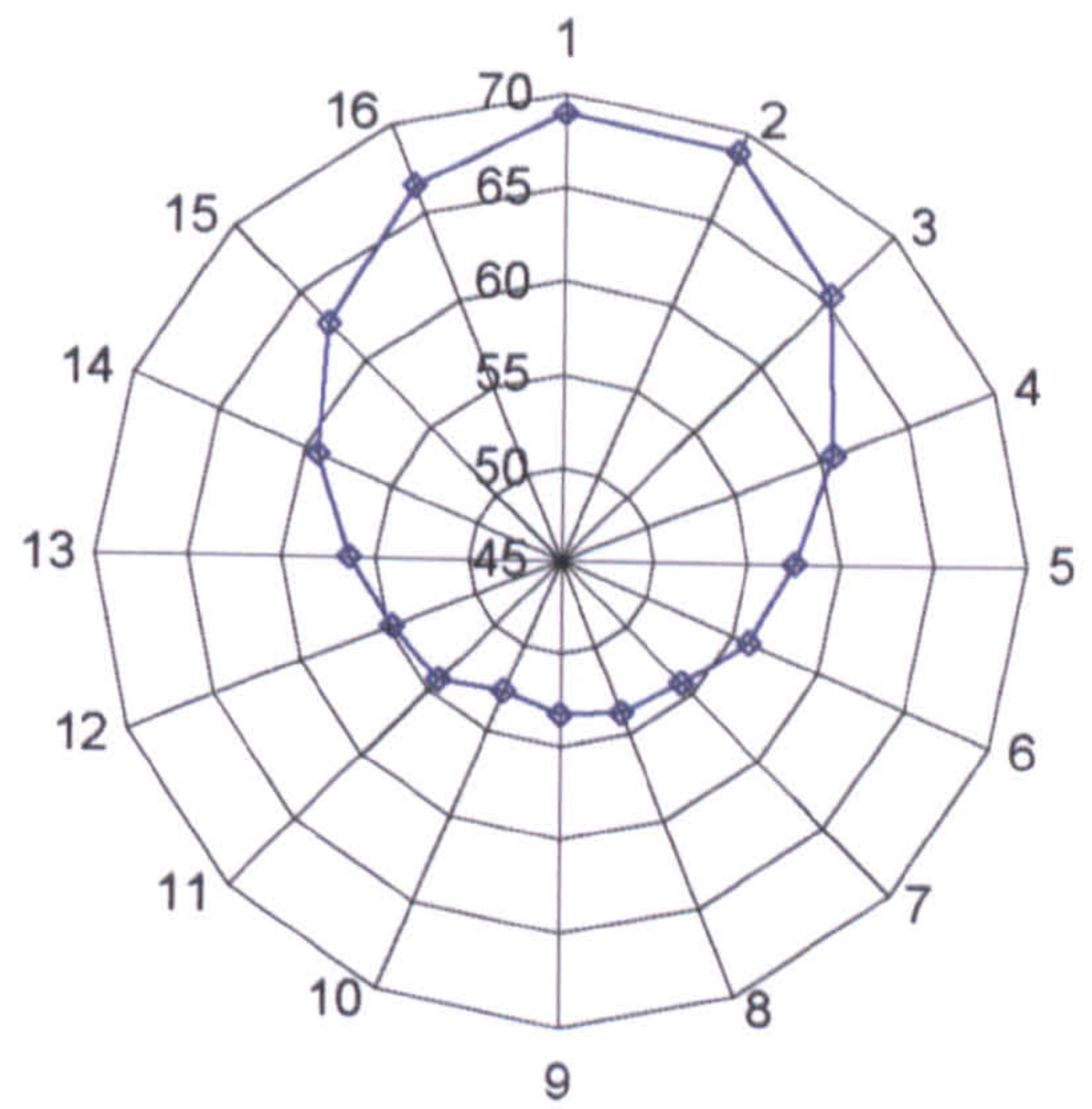
4 kHz

Figure 7.29 : Polar plot of sound pressure levels for 2, 2.5, 3.15 and 4 kHz

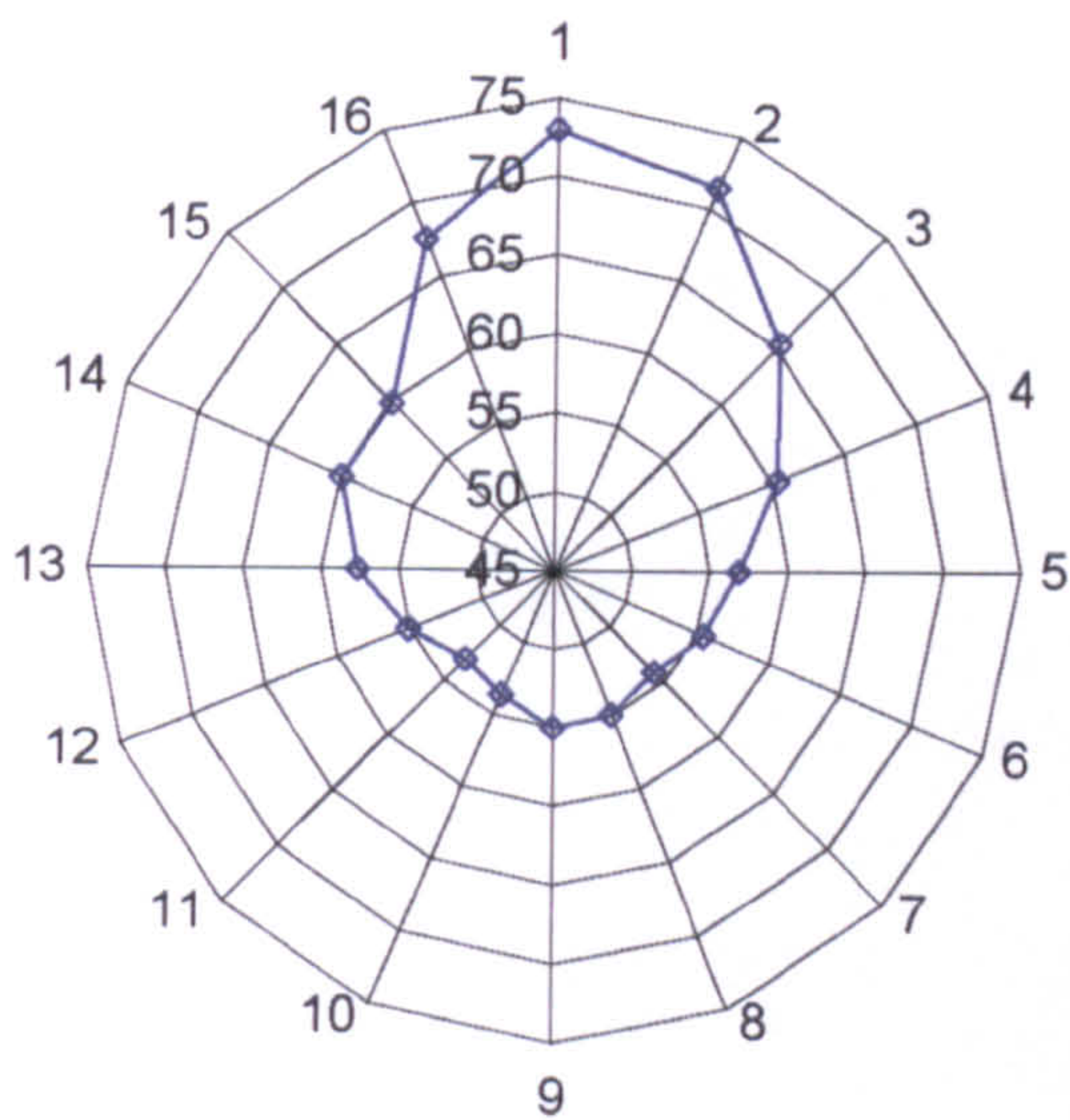




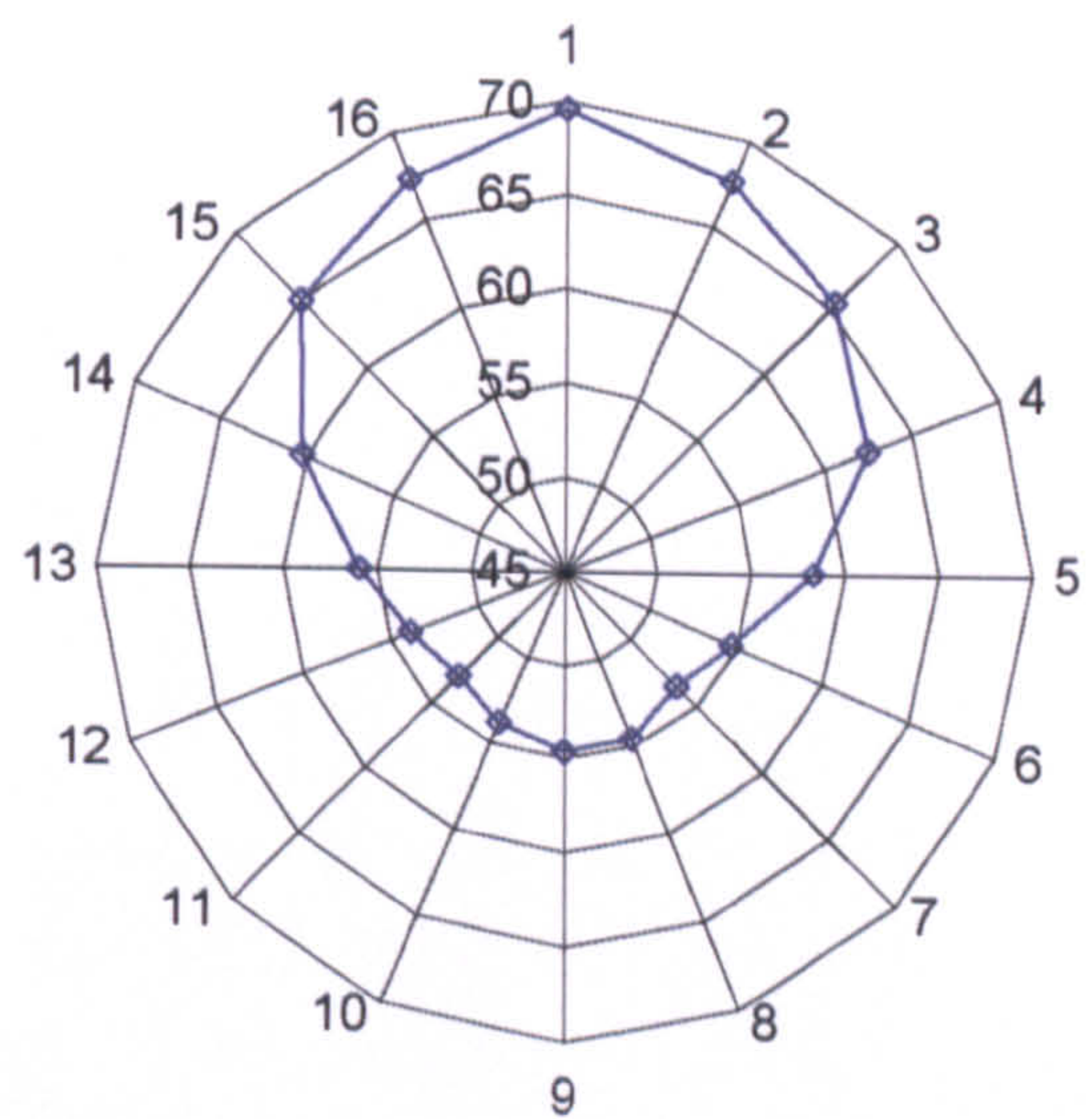
5 kHz



6.3 kHz



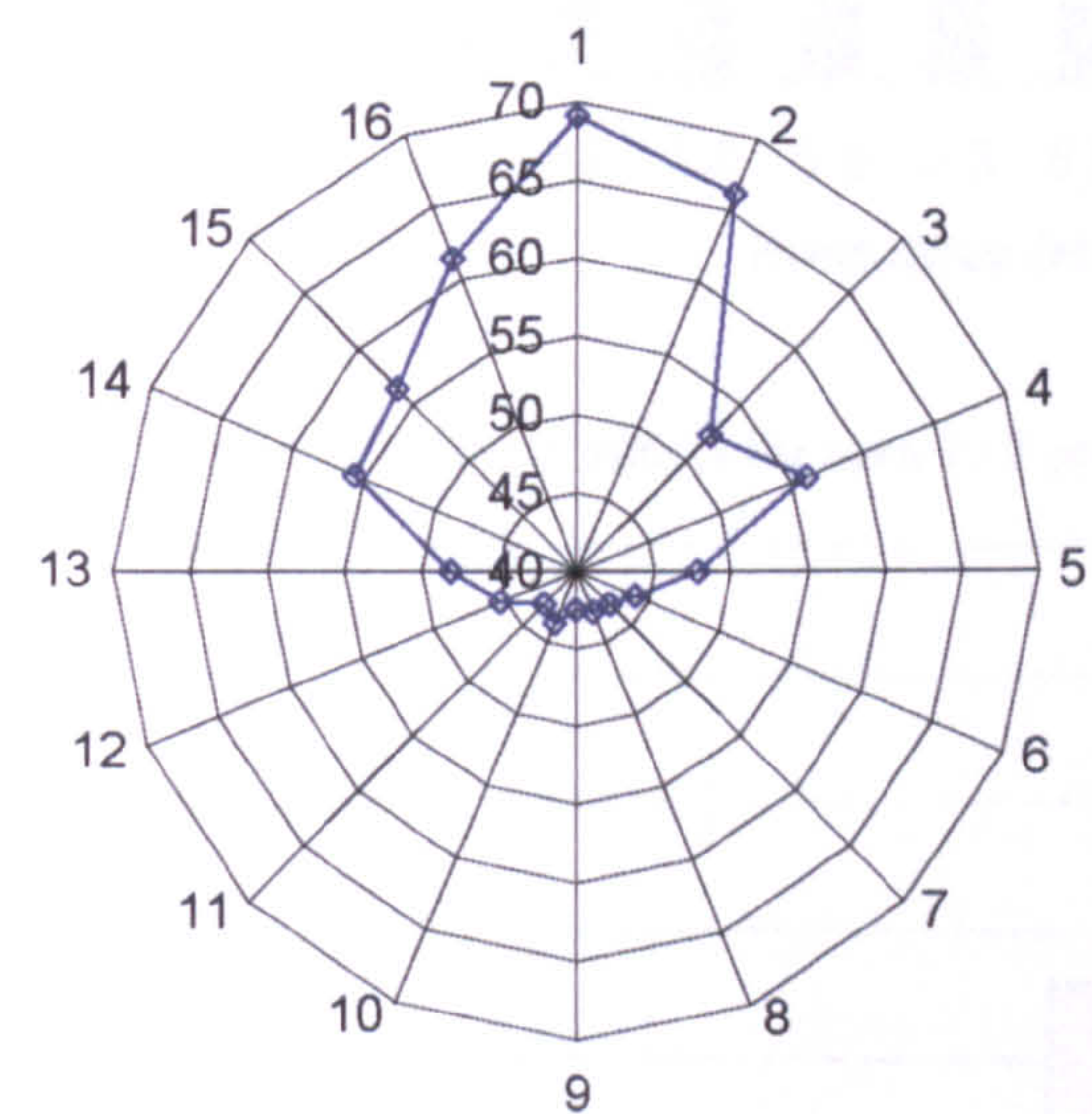
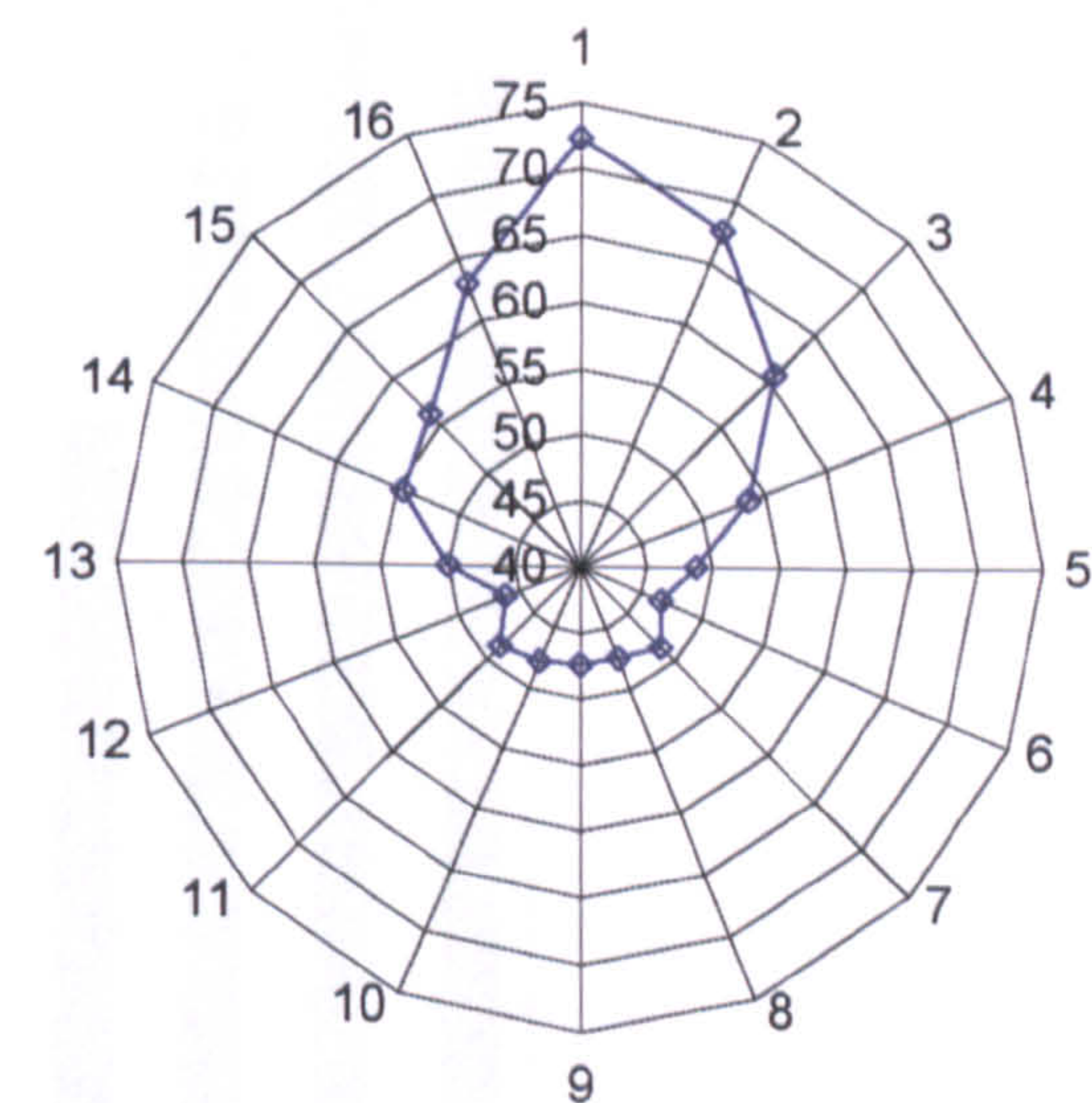
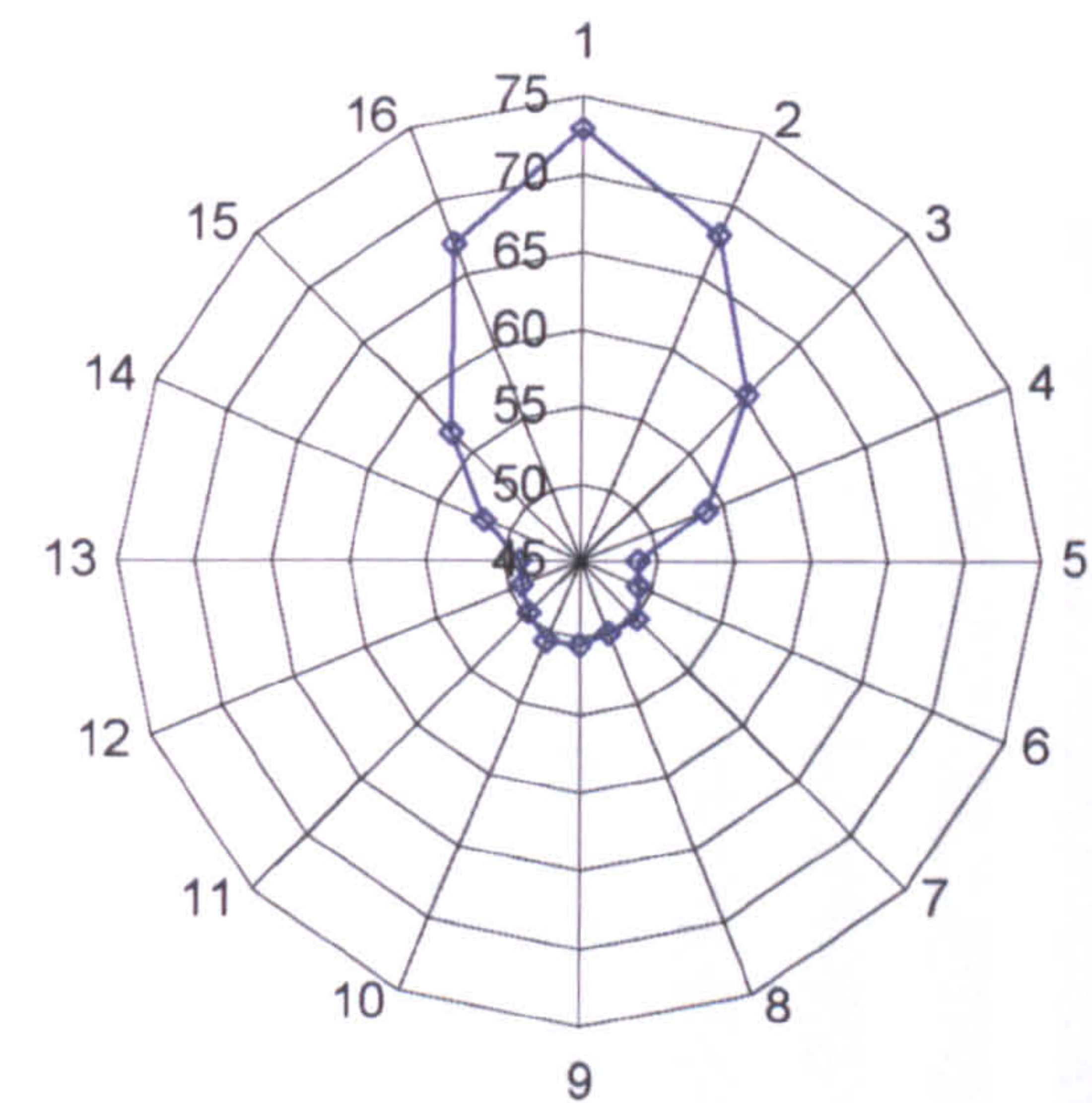
8 kHz



10 kHz

Figure 7.30 : Polar plot of sound pressure levels for 5, 6.3, 8 and 10 kHz





**Figure 7.31 : Polar plot of sound pressure levels for 12.5, 16 and 20 kHz**  
 The following are the summary results for all one-third octave frequency bands showing the directivity index, DI in dB and the directivity factor Q.



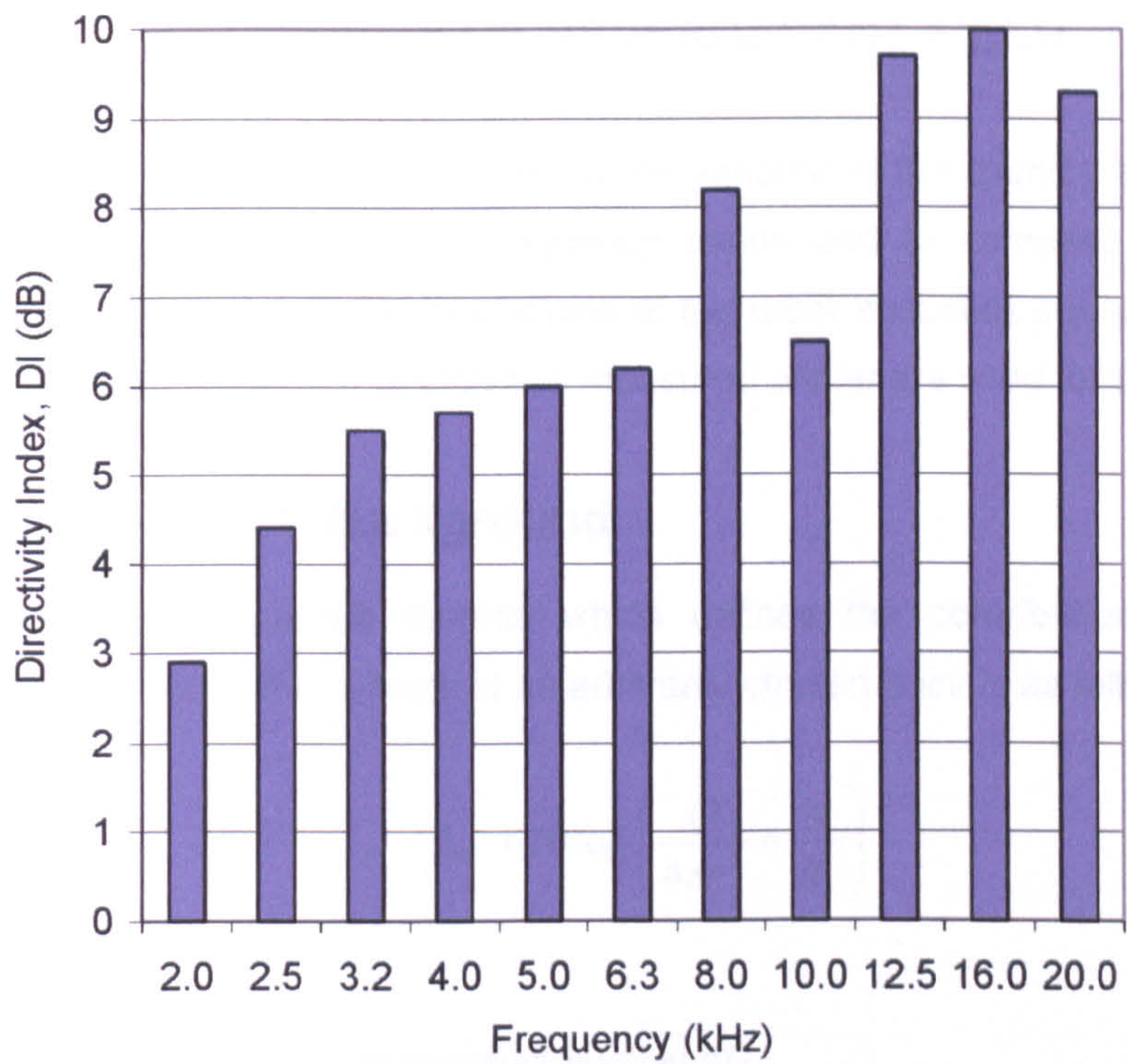


Figure 7.32 : Directivity indices for each 1 / 3 octave band frequency between 2 - 20 kHz

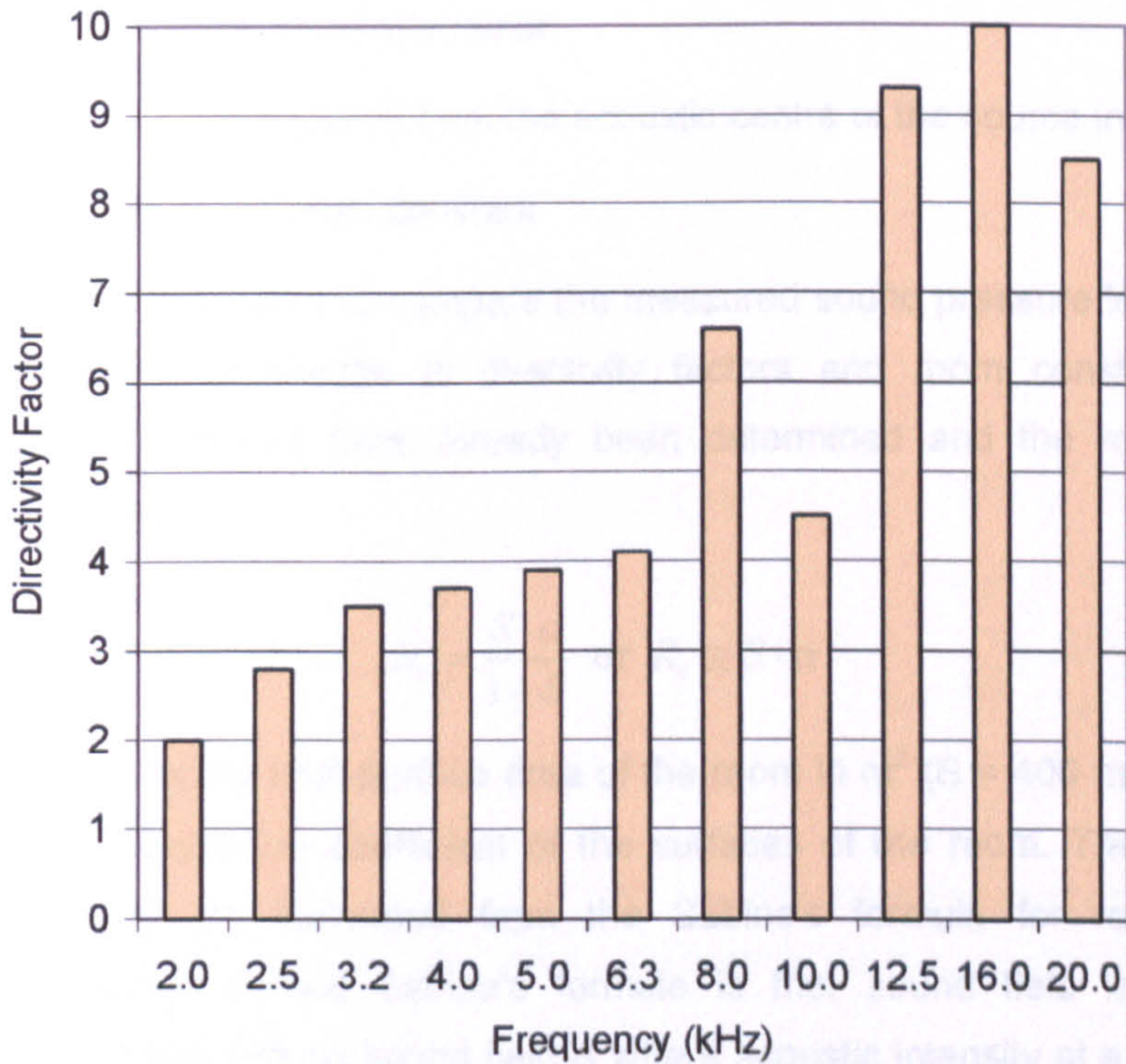


Figure 7.33 : Directivity factors for each 1 / 3 octave band frequency between 2 - 20 kHz.



## 7.4 ESTIMATION OF REVERBERANT FIELD

The aim of this section is to assess the variation of the sound pressure levels within the testing space at different frequency bands and to compare sound pressure level measurements with the predictions of the room acoustics equation. The reverberation times and the source directivities measured earlier are used for this purpose.

### 7.4.1 Background

The room acoustics formula which defines the contributions from a direct and reverberant field in a room at an arbitrarily chosen point is as follows.

$$L_p = L_w + 10 \log \left( \frac{Q}{4\pi r^2} + \frac{4}{R_c} \right) \quad \text{Equation 7.4}$$

where

$L_p$  is the sound pressure level in dB

$L_w$  is the sound power level in dB

$Q$  is the directivity factor

$r$  is the distance from the acoustic centre of the source in meters

$R_c$  is the room constant

In order to be able to compare the measured sound pressure levels with the predicted ones, the knowledge of directivity factors and room constants is required. The directivity factors have already been determined and the room constants can be estimated.

$$R_c = \frac{S \cdot \alpha}{1 - \alpha} \quad \text{or} \quad R_c \cong S \cdot \alpha \quad \text{Equation 7.5}$$

where  $S$  is the total surface area of the room in  $\text{m}^2$  ( $S = 400 \text{ m}^2$ ) and  $\alpha$  is the average sound absorption coefficient of the surfaces of the room. The absorption coefficient itself can be estimated from the Sabine's formula for reverberation time. The assumption behind Sabine's formula is that sound field is diffuse, uniform and reverberant. Diffuse sound field is where acoustic intensity at a point is independent of direction. The meaning of uniform field has been defined earlier as mean squared pressure being constant throughout volume. Reverberant field is where all waves have undergone reflection, hence they are at random incidence and diffuse.



$$T = \frac{0.161 \cdot V}{S \cdot \alpha} \quad \text{Equation 7.6}$$

where, T is the reverberation time in seconds and V is the room volume in m<sup>3</sup> (V = 500 m<sup>3</sup>). Having established the reverberation times at each 1 / 3 octave frequency band in the previous sections, the absorption coefficient can be obtained by re-arranging the Sabine formula.

$$\alpha = \frac{0.161 \cdot V}{S \cdot T} \quad \text{Equation 7.7}$$

Various measured and estimated parameters in 1 / 3 octave frequency bands between 2 kHz and 20 kHz are shown in Table 7-2.

Frequency (kHz)	Reverberation Time (seconds)	Absorption Coefficient (α)	Room Constant (R <sub>c</sub> )	Directivity Factor (Q)
2	1.03	0.20	100	2
2.5	1.05	0.20	100	2.8
3.15	1.00	0.20	100	3.5
4	0.93	0.22	112.8	3.7
5	0.83	0.25	133.3	3.9
6.3	0.73	0.27	147.9	4.1
8	0.61	0.33	197.0	6.6
10	0.47	0.40	266.7	4.5
12.5	0.36	0.57	530.2	9.3
16	0.29	0.67	812.1	10.0
20	0.21	0.95	7619	8.5

Table 7-2 : Parameters to be used for estimating the sound pressure levels. These parameters will be used for comparing the measurements to be undertaken with the predictions of the room acoustics equation.

### 7.4.2 Experimentation

Sound pressure level measurements were undertaken to verify that the measurements agree with the theoretical predictions. This experiment is intended to serve two

purposes. It is expected to show that the parameters obtained earlier are reliable and to help determine the source characteristics.

The source was positioned on an aluminium platform and the sound pressure levels were monitored normal to the source at 5 cm intervals up to 300 cm away from the source with the same output. In order to account for any variations in the output, a reference point was chosen 5 cm from the source. The sound pressure levels at the reference point were monitored with each receiver location and corrections performed to account for any fluctuation in the output levels. The frequencies under investigation were 1/24 octave band frequencies between 2 kHz and 22 kHz.

The variation of sound pressure levels with distance from the source was also predicted by using the room acoustics equation. The measurements and the predictions were compared and conclusions drawn concerning the optimum source-receiver configuration where the effects of the reflections will be minimised.

### **7.4.3 Results**

The measurements at selected individual 1 / 24 octave band frequencies are compared with predictions of the room acoustics equation. The directivity factor values and the room constants are those predicted in the previous sections for the nearest 1 / 3 octave frequency bands.

The variation of the sound pressure levels with frequency and distance from the source is provided in Figure 7.34. Sound pressure level differences are relative to a reference point 0.05 m away from the source. The frequencies are those between 2 kHz and 20 kHz in 1 / 24 octave band intervals. The distances are in cm up to 300 cm from the source. Between 2 kHz and 7 kHz, the source behaves similar for all frequencies and higher frequencies show fluctuations. Throughout the frequency range of interest, the source does not have a linear response. When considering insertion loss of a barrier, it should be more representative to compare each individual frequency on its own, rather than assessing broadband insertion losses which will be biased towards certain frequencies.



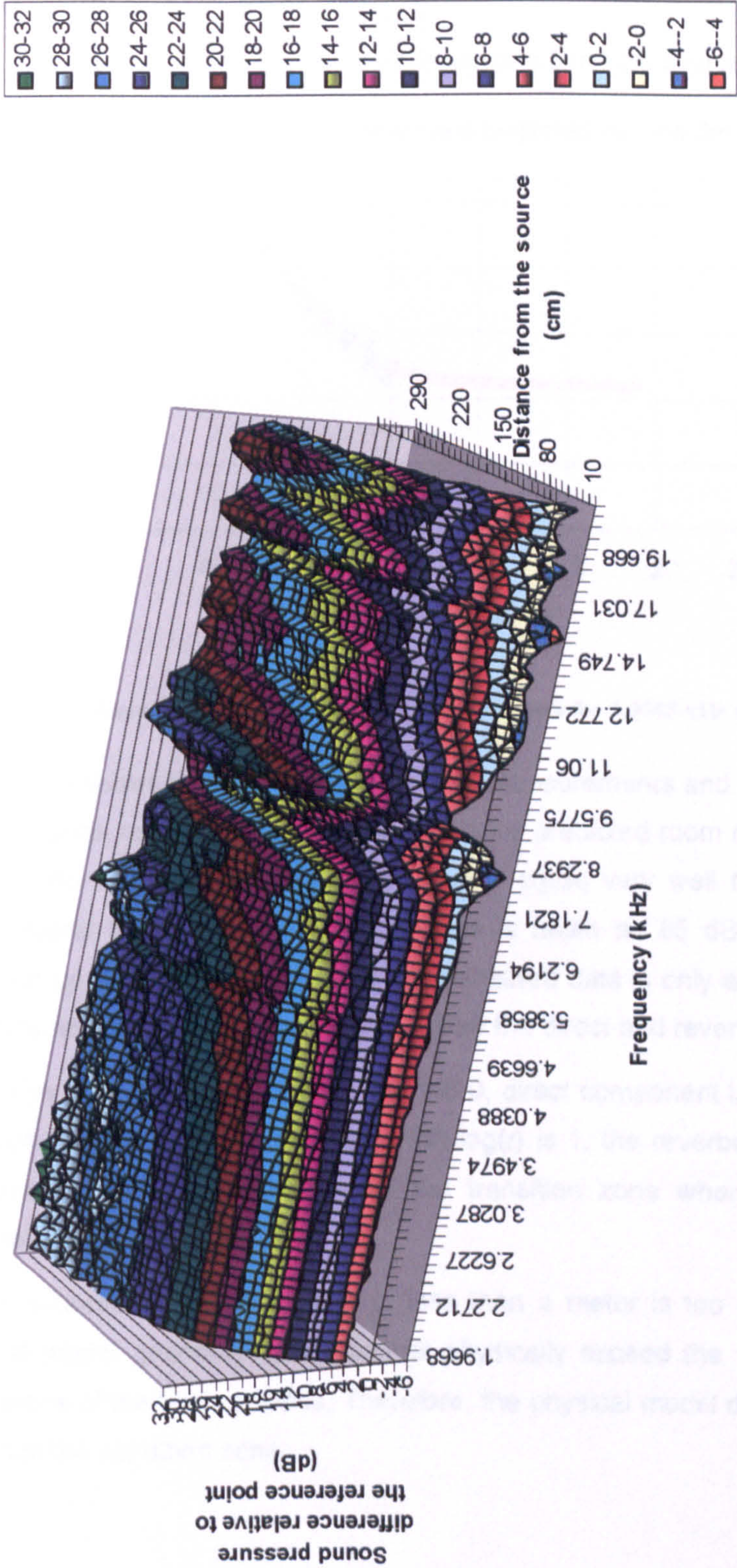
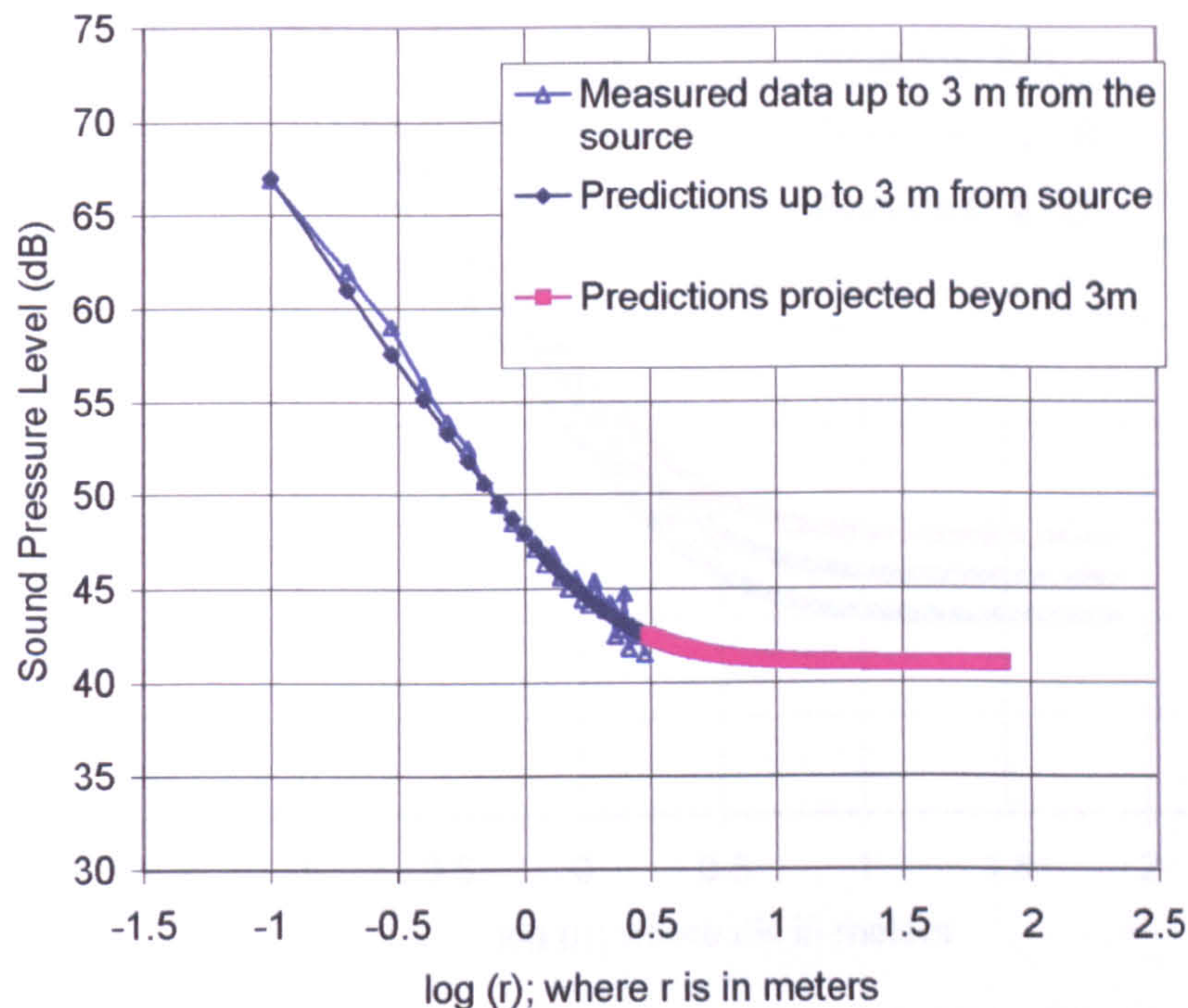


Figure 7.34 : Variation of sound pressure levels



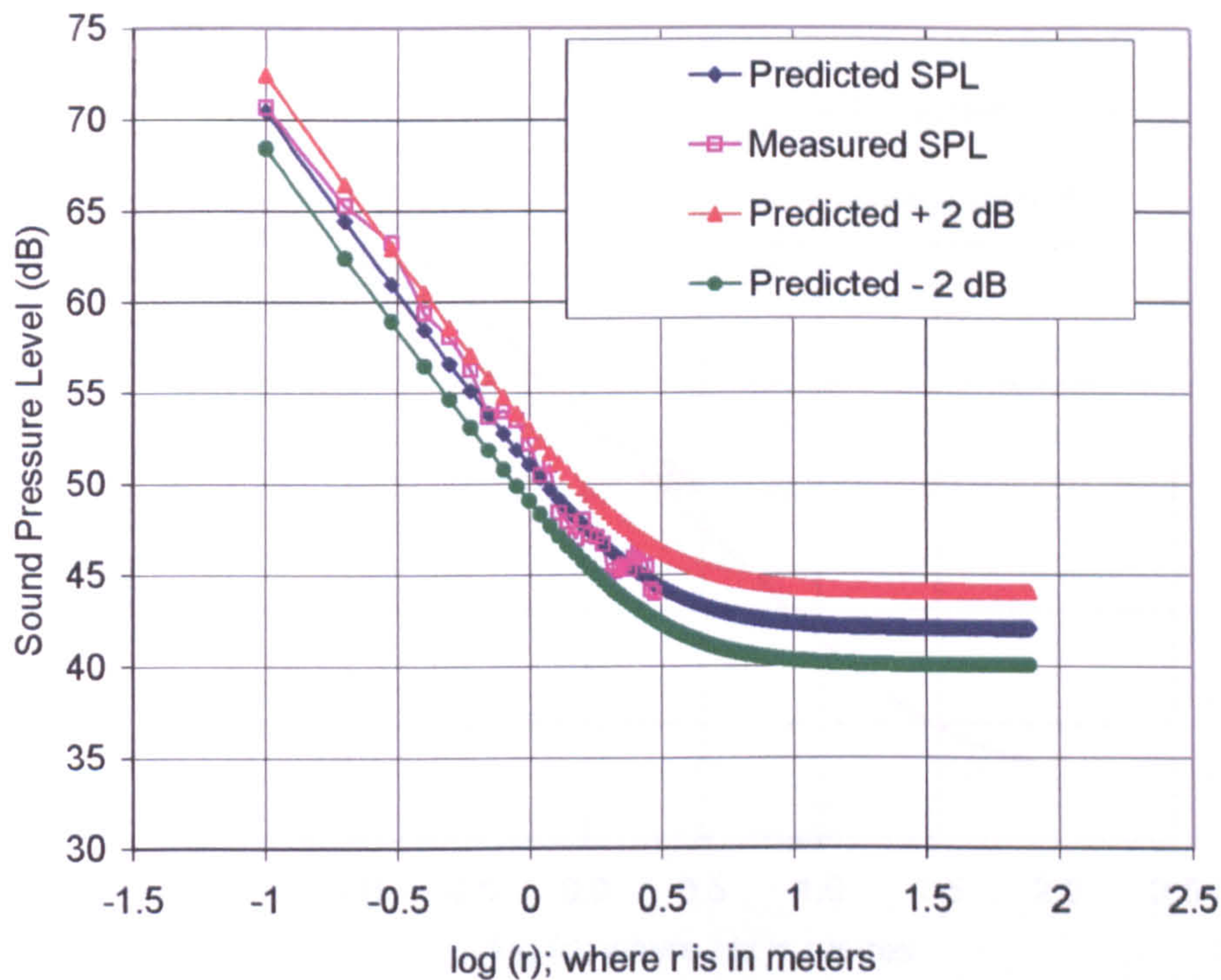


**Figure 7.35 : Measured and predicted sound pressure levels for 1.9668 kHz ( $Q = 2$ ,  $R_c = 100$ ; assumed  $L_w = 55$  dB)**

Figure 7.35 shows the sound pressure level measurements and predictions for 1.9668 kHz, for measured directivity factor of 2 and the predicted room constant of 100. It can be seen the measured and predicted values agree very well for the right choice of sound power level,  $L_w$ , which in this case is taken as 55 dB. The predictions are projected up to 77.5 m even though the measured data is only available for up to 3 m. This is to have a better understanding of how the direct and reverberant levels interact. Up to 1 m from the source, where  $\log(r)$  is 0, direct component is the only contributing field and beyond around 10 m, for which  $\log(r)$  is 1, the reverberant levels dominate. The zone in between is known as the transition zone where the direct and the reverberant fields interact.

A source-to-receiver configuration of less than a meter is too small for any realistic physical model geometry and it cannot physically exceed the 10 m limit due to the dimensions of the testing space. Therefore, the physical model distances are bound to remain in the transition zone.



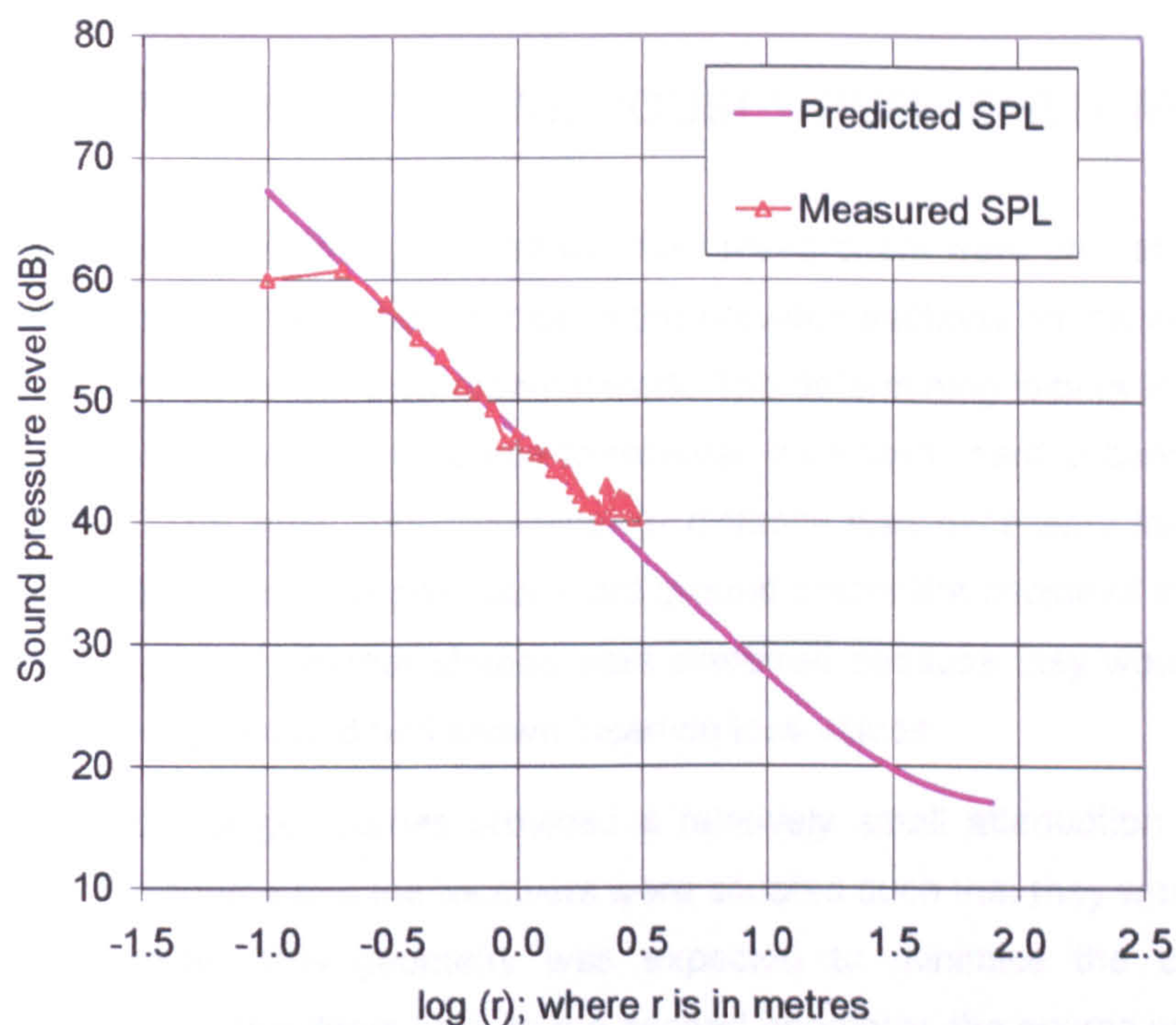


**Figure 7.36 : Measured and predicted sound pressure levels for 3.2081 kHz ( $Q = 3.5$ ,  $R_c = 100$ ; assumed  $L_w = 56$  dB)**

A similar graph is shown Figure 7.36 for 3.2081 kHz for a measured directivity factor of 3.5 and a predicted room constant of 100. The predictions of the sound pressure level are based on an assumed sound power level,  $L_w$ , of 56 dB. This graph shows how the choice of a 2 dB higher or lower  $L_w$  will affect the position of the predicted line.

It can be deduced from the above graph that estimation of the contribution of the reverberant field on the direct field is possible provided a reasonable choice of sound power level is made. The predictions of room constant and the measurements of directivity factor appear reasonable.





**Figure 7.37 : Measured and predicted sound pressure levels for 22.067 kHz ( $Q = 8.5$ ,  $R_c = 7619$ ; assumed  $L_w = 49$  dB)**

Figure 7.37 shows the predictions and measurements for 22.067 kHz. Measurements are seen to deviate from the predictions as the distance from the source is increased. The reason for this is likely to be the inaccurate prediction of the room constant, which pushes the reverberant part of the predictions too low. The room constant and the directivity factor used is that for the 20 kHz. The predictions of the room constant at 20 kHz were based on the predicted reverberation time, since no measured reverberation time data were available at that frequency band.

All 1 / 3 octave band frequencies show similar trends. These follow the predictions of the room acoustics equation reasonably well when appropriate values of the measured directivity factors and the predicted room constants are used in conjunction with suitable choice of sound power levels. The appropriate choices for the  $L_w$  seem to be around 55 dB for lower frequencies under investigation and at around 50 dB for the highest frequency bands.

This section showed that the experimental results are likely to be influenced by the reverberant field. The extent of this influence will be discussed in the forthcoming sections.



## 7.5 COMPARISON TO PREVIOUSLY PUBLISHED WORK

Two configurations previously studied by other researchers were chosen as reference cases to test the validity of the findings of the previous sections on the likely effects of the reverberant field on the experimental work. The determining factors in the choice of these geometries were small source-to-receiver distances, hard ground and simple barrier shapes. The small source-to-receiver distance was necessary for avoiding the reverberant field as much as possible. Hard ground meant the choice of model material would be easy. Simple barrier shapes were preferred because they would have been commonly investigated and had known insertion loss values.

The first one of the geometries provided a relatively small attenuation on the direct levels since the source and the receivers were situated such that they were grazing the top of the barrier. This geometry was expected to minimise the effects of the reverberant field on the direct field. In the second geometry, the source was situated in the deep shadow zone behind the barrier. The direct field would be attenuated considerably, exposing it to the adverse effects of the reverberant field. These two geometries were expected to provide an indication on the extent of the effects of reverberant field on the findings of the physical modelling.

### 7.5.1 De Jong et al.'s Model

The first geometry was that of De Jong et al.'s<sup>9</sup>. They included the actual dimensions of their model which was used to test the validity of a mathematical model. The barrier height was 0.03 m and was resting on an aluminium surface. A point source was positioned at a height of 0.01 m resting 0.2 m away from the barrier. The authors do not give further details on the source type. The receiver height was fixed at 0.08 m and at a distance 0.8 m from the barrier. The details are as shown below.

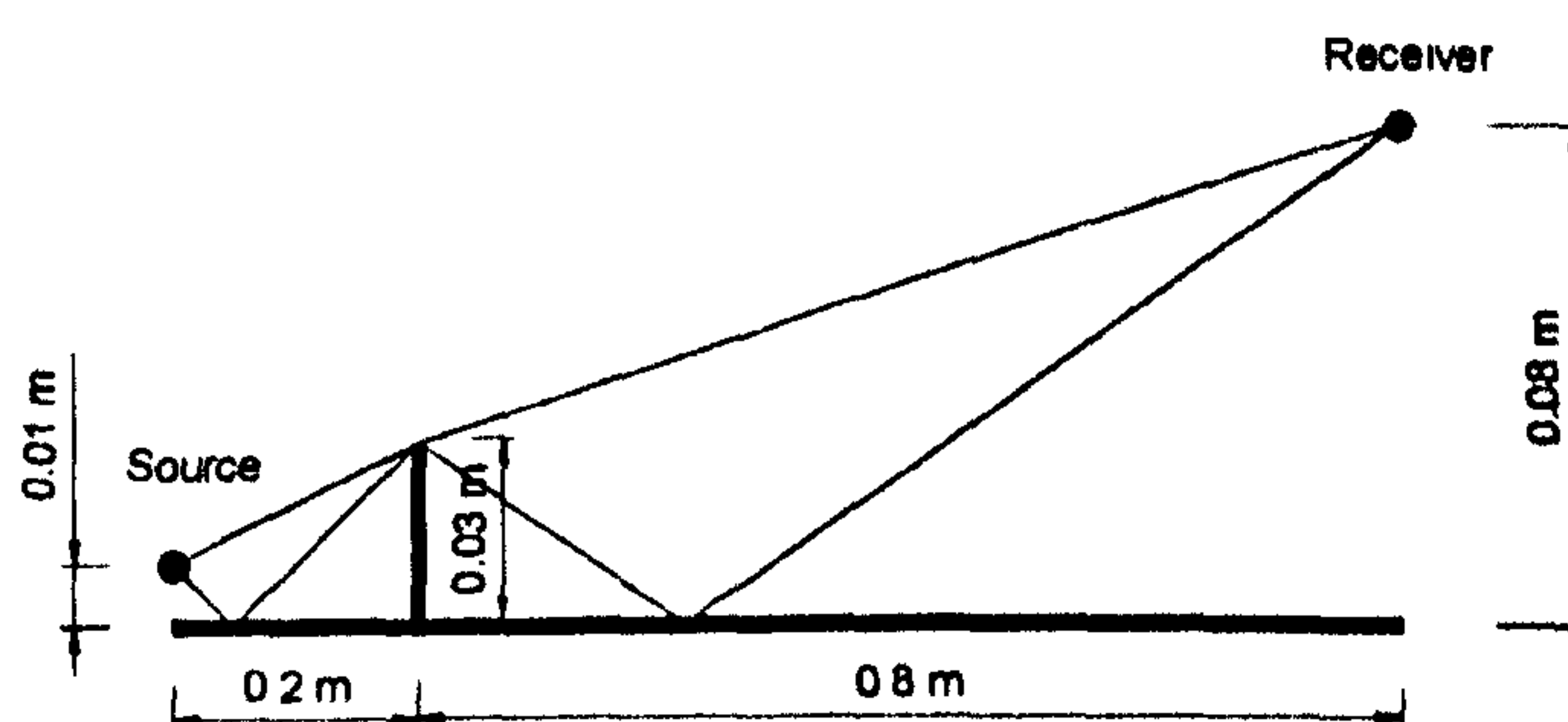


Figure 7.38 : De Jong et al.'s geometry.



This geometry had to be slightly adjusted by a scale factor of 1.7 to bring the barrier height to the height of the already available 0.05 m high aluminium angle to be used as the barrier. The sketch of the geometry under investigation with all the dimensions scaled accordingly is shown in Figure 7.39.

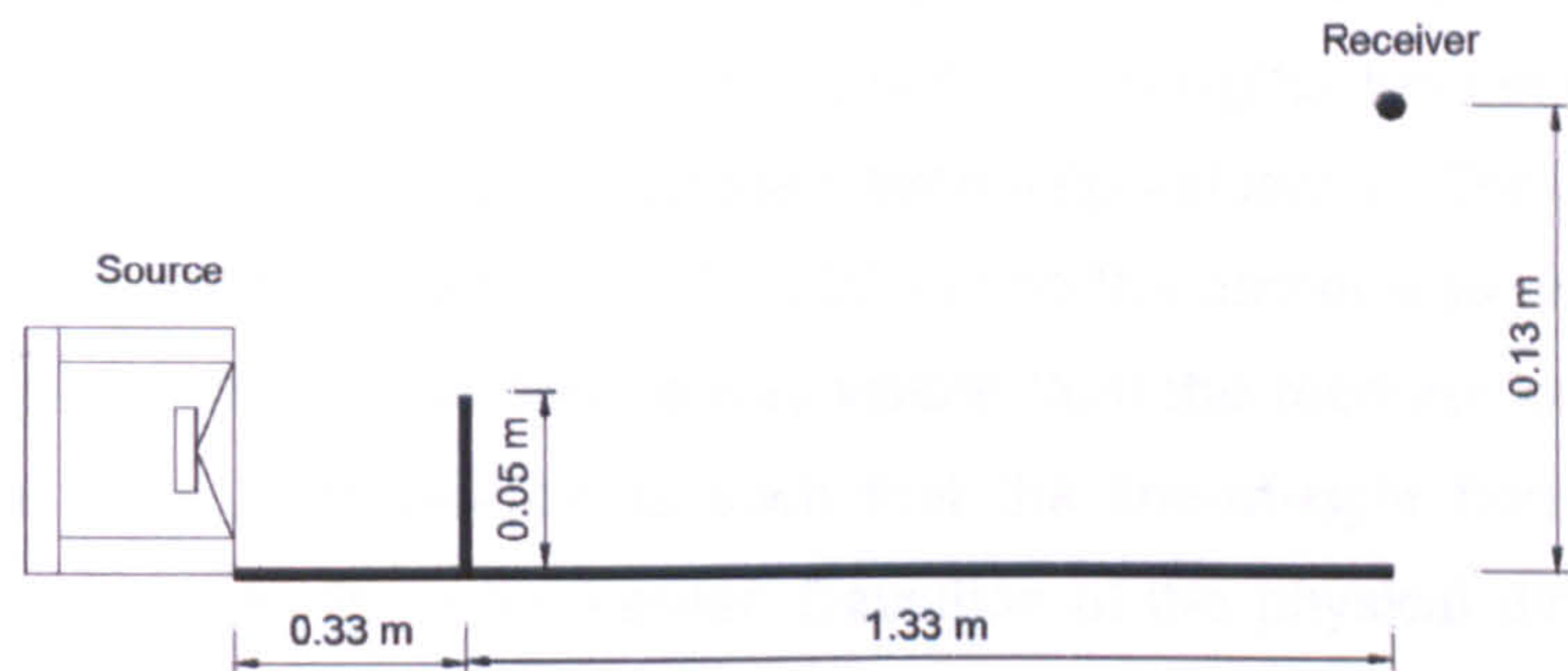


Figure 7.39 : The testing geometry obtained by scaling the reference geometry by 1.7.

Since the dimensions involved were very small, it could be tested in the testing space available. It was determined that up to around 1 m from the source, the sound field would be completely dictated by the direct field. The overall source-to-receiver distance was 1.7 m which meant it was reasonable to assume the effects of the reverberant field would be very small. In addition, "close to zero" path length difference ensured rays both in the presence and the absence of the barrier would be equally affected from a possible influence of the reverberant field.

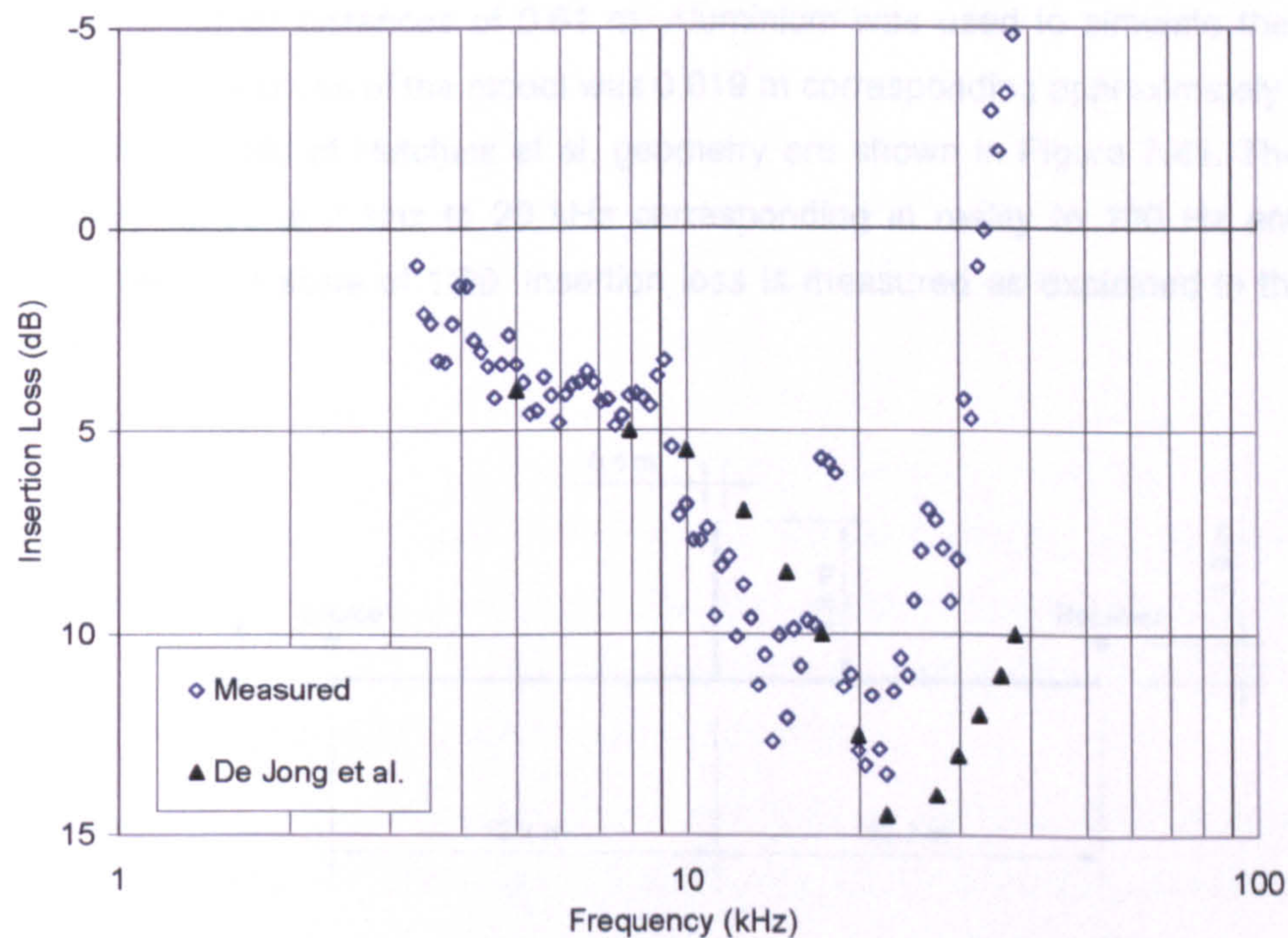


Figure 7.41 : Distribution of all geometry.

Figure 7.40 : Comparison of the measured insertion losses with those of De Jong et al.



Insertion losses are measured by monitoring the sound pressure levels with and without the barrier and finding their difference. The testing frequency is between 2 kHz and 22 kHz corresponding to 3.4 kHz and 37.4 kHz respectively in De Jong et al.'s model. The measured insertion values are compared with those reported by De Jong et al. as seen in Figure 7.40. The correlation is good up to higher frequencies where, it is thought, the dimensions of the source start becoming influential. The overall physical dimensions of the source reached 0.07 - 0.08 m and the barrier was only 0.05 m high. This meant the top part of the source was visible from the receiver location, whereas the geometry under consideration is such that the line-of-sight from source to the receiver is grazing the top of the barrier. Deviation of the physical dimensions of the source from a point source, and the uncertainty of the acoustic centre of the source are thought to be responsible for the discrepancies observed at higher frequencies.

### 7.5.2 Hutchins et al.'s Model

The second geometry used was that of Hutchins et al.<sup>3</sup>. They used 1:80 scale factor to test a geometry with a barrier height of 4.9 m with symmetrical source-to-barrier and receiver-to-barrier distances of 12.2 m and source and receiver heights of 1.2 m. The ground on either side of the barrier was asphalt. For the purposes of this work, a scale factor of 1:20 was used to simulate the geometry described above. This required a model height of 0.25 m, source and receiver height of 0.06 m and source-to-barrier and receiver-to-barrier distances of 0.61 m. Aluminium was used to simulate the asphalt ground. The thickness of the model was 0.019 m corresponding approximately to 0.4 m in real life. Details of Hutchins et al. geometry are shown in Figure 7.41. The testing frequency range is 2 kHz to 20 kHz corresponding in reality to 100 Hz and 1 kHz respectively at a scale of 1:20. Insertion loss is measured as explained in the model above.

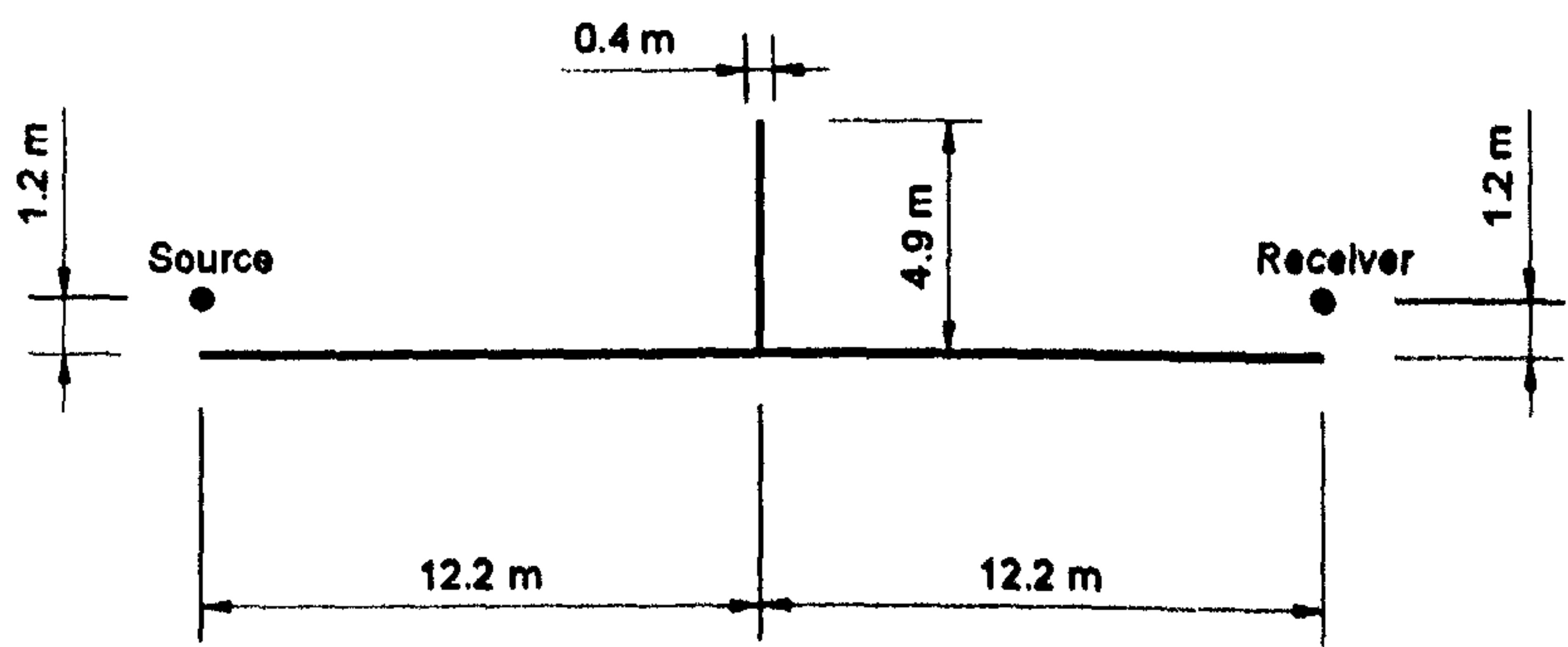


Figure 7.41 : Hutchins et al. geometry.



The insertion loss values reported by the authors are interpolated at the selected frequency bands such that the whole shape of the graph is shown between 100 Hz and 1 kHz. The results obtained as a result of the physical modelling at the real frequencies are plotted onto the same graph to enable direct comparison. As seen in Figure 7.42, only the interference minima values are measured accurately.

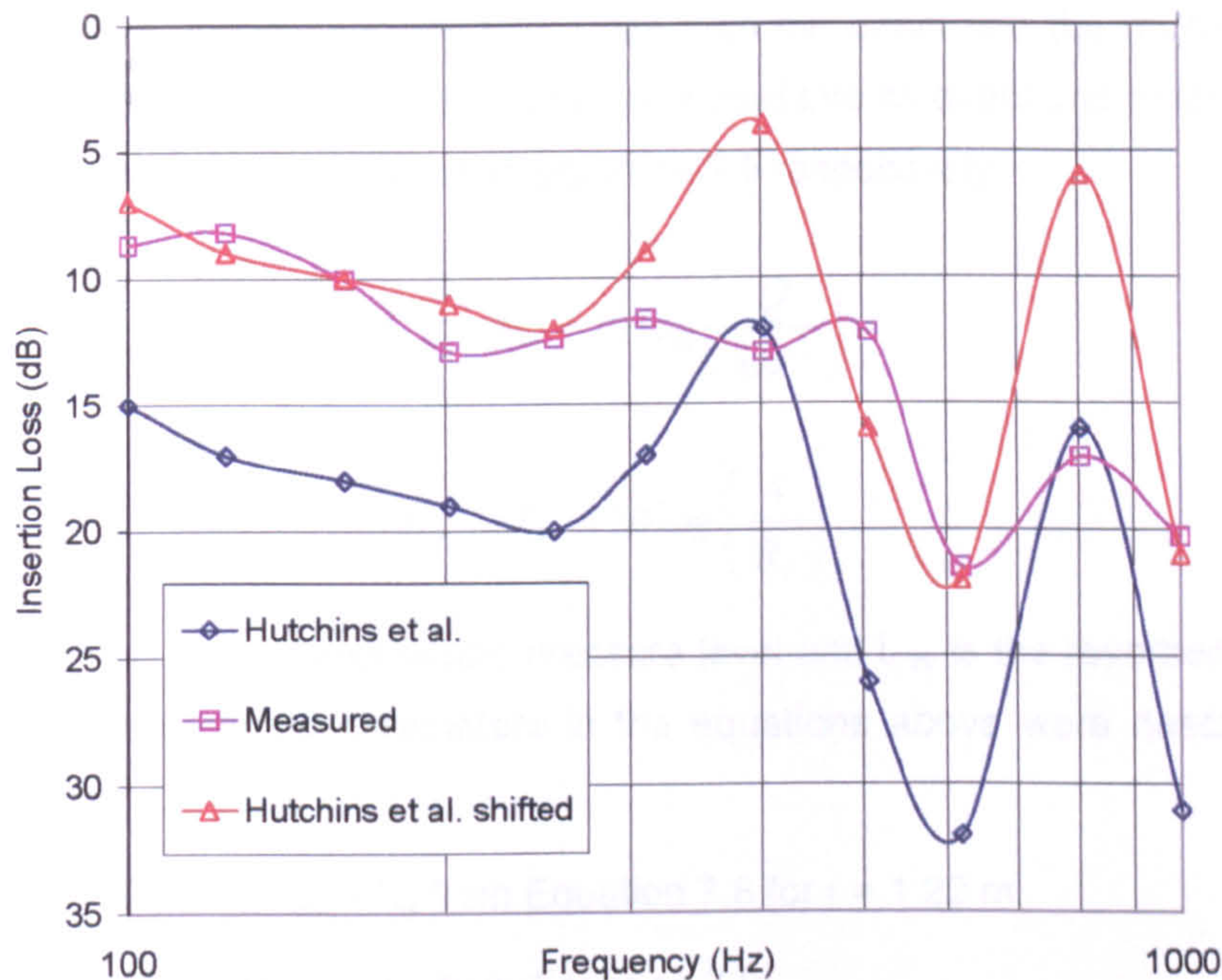


Figure 7.42 : Comparison of the measured insertion losses with those of Hutchins et al.

The insertion loss values throughout the remaining of the spectrum are consistently under estimated. The location of the interference maxima values on the frequency axis are very similar to the reference case. These observations about the interference maxima and minima point towards a possible qualitative agreement between the two curves, leading to the "shifted" curve seen in Figure 7.42. It can be seen that a reduction of the actual insertion loss values by 8 dB for frequencies up to 400 Hz and by 10 dB at the higher frequencies reveal the shape of the measured curve with the exception at the minima points. Therefore the measured insertion losses are 8 - 10 dB less than the actual ones except at the interference minima which are accurately predicted. This discrepancy is very large and further consideration needs to be given to the magnitude of the effects due to reverberant field.

A simple experiment was carried out to observe how well the actual sound pressure levels can be predicted. Since this is based on estimated direct and reverberant levels, any successful outcome would also verify the magnitudes of the direct and reverberant levels.



Sound pressure level values at the receiver location under consideration were monitored both in the presence and in the absence of the barrier. Predictions of the sound pressure levels obtained in the presence of barrier were made based on the sound pressure levels obtained without the barrier. The direct and reverberant levels needed to be estimated in order to achieve that. The exact process of obtaining predicted sound pressure levels is as follows.

The room acoustics formula includes both the direct and the reverberant components of the sound. This formula can be separated into its direct and reverberant components as shown in Equation 7.8 and Equation 7.9 respectively.

$$L_{dir} = L_w + 10 \log \left( \frac{Q}{4\pi r^2} \right) \quad \text{Equation 7.8}$$

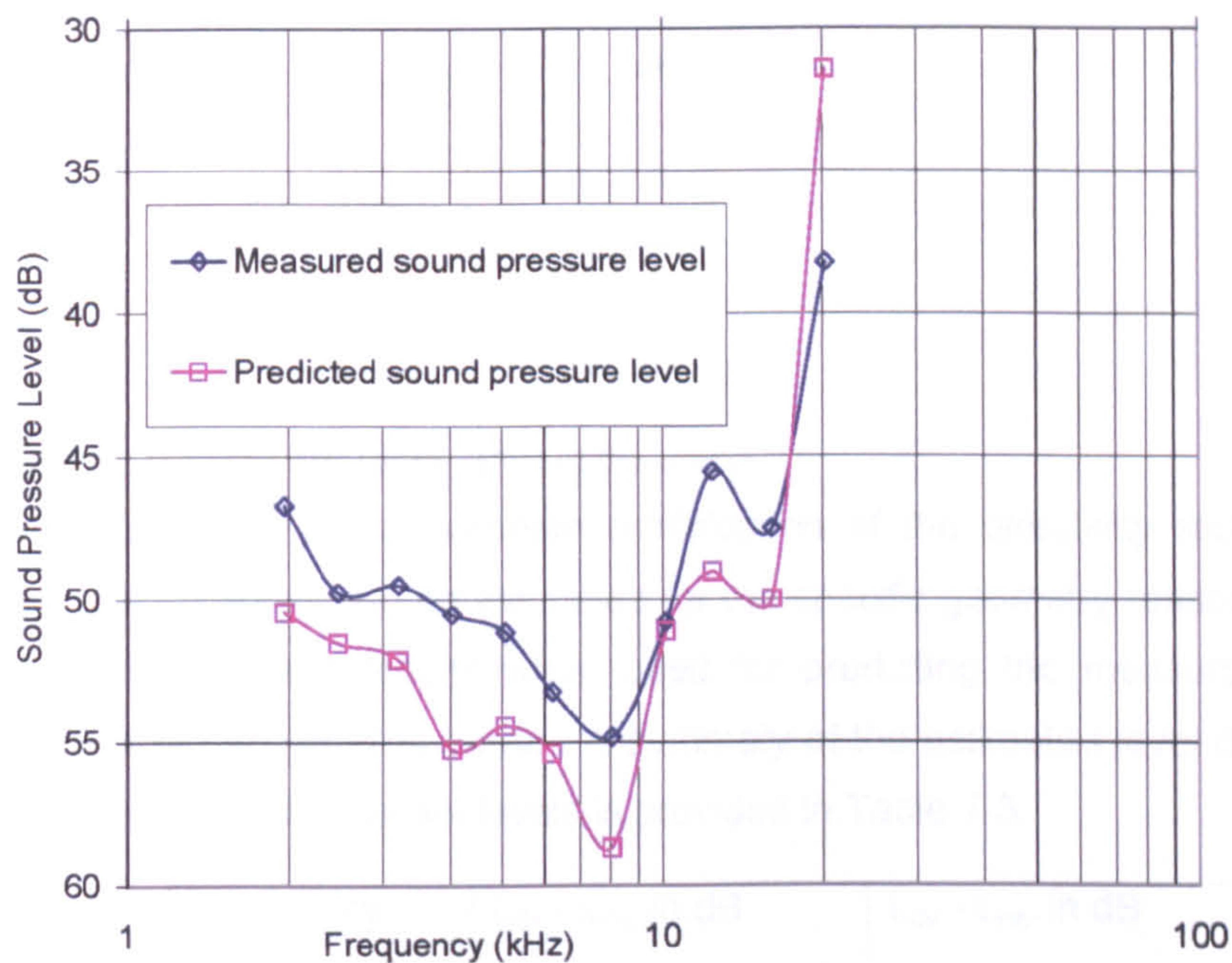
$$L_{rev} = L_w + 10 \log \left( \frac{4}{R_c} \right) \quad \text{Equation 7.9}$$

where  $L_{dir}$  is the direct sound pressure level and  $L_{rev}$  is the reverberant sound pressure level. The various parameters in the equations above were described earlier in this chapter.

- [1] Estimate  $L_{dir} - L_w$  from Equation 7.8 for  $r = 1.22$  m.
- [2] Estimate  $L_{rev} - L_w$  from Equation 7.9.
- [3] Find  $L_{dir} - L_{rev}$  by subtracting SPL in [2] from SPL in [1].
- [4] Measure the SPL in the absence of barrier.
- [5] Estimate the direct and reverberant components of the measured levels with the aid of information provided in [3].
- [6] Check the estimated levels by adding these logarithmically and comparing with the levels obtained in [4].
- [7] Measure the SPL in the presence of barrier.
- [8] Subtract the insertion loss obtained by Hutchins et al. (in Figure 7.42) from the direct component of sound obtained in [5].
- [9] Add the new direct level obtained above with the reverberant component of sound (obtained in [5]) logarithmically.
- [10] Plot these levels in Figure 7.43 to compare the estimated SPL in [9] with those in [7] which were obtained by measurements.



The estimated and the measured sound pressure levels at the receiver position in the presence of barrier are shown in Figure 7.43. The estimated levels are 2 - 4 dB more than the actual levels.

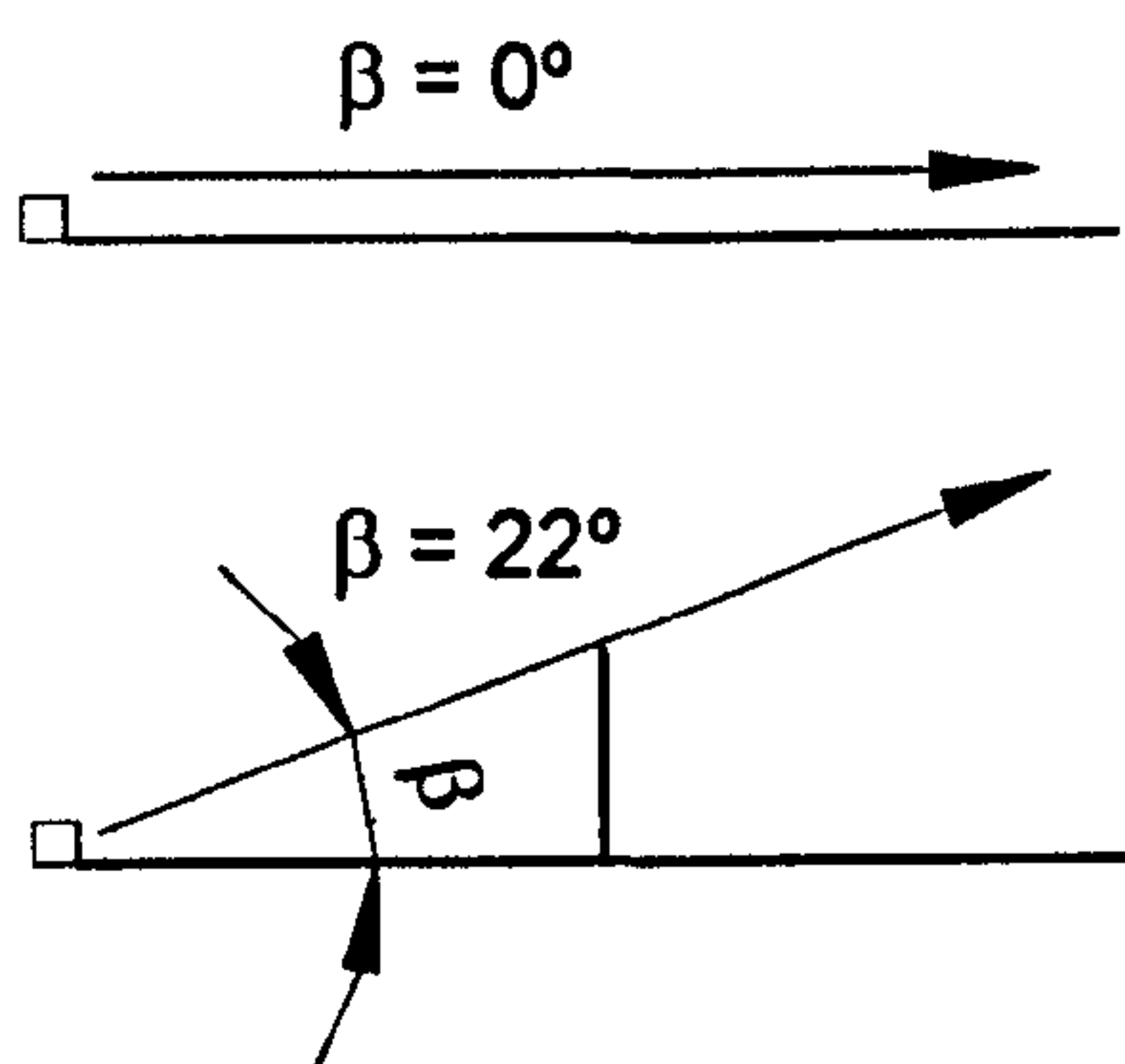


**Figure 7.43 : Measured and predicted sound pressure levels at a specific receiver location in the presence of barrier.**

This can only be explained by possible over-predictions in the reverberant component of the sound field at the receiver location. The two parameters that were used in the prediction of the reverberant sound were the directivity factor,  $Q$ , and the room constant,  $R_c$ , as discussed previously. The room constant is a function of the absorption coefficient,  $\alpha$ , which in turn is mainly determined by the reverberation time (room volume and the surface area are constant). Extensive reverberation time measurements were undertaken as discussed earlier. Therefore the room constants determined at the individual frequency bands are considered to reflect the reality and these are not thought to be responsible for the over-predictions in the reverberant field.

One possible way of eliminating the discrepancy is by assuming lower directivity factor values than those determined in the previous chapter. The directivity factors were measured for the cases normal to the source in the horizontal plane. However the consideration is the vertical plane and when there is a barrier in between, the directivity of the source in the direction of the top edge of the barrier will definitely be different, and most probably smaller than that determined previously. Since the source is non-directional in horizontal plane, there is no reason why it should be in the vertical plane. Hence, as explained elsewhere<sup>4</sup>, the top diffracted wave will not have the same intensity as the direct wave taken as a reference.





**Figure 7.44 : The directivity effect of the source**

Therefore, with the appropriate modification of the directivity factor, the direct and reverberant levels can be estimated for the specific geometry reasonably well and they provide consistent results when used for predicting the measured sound pressure levels obtained with the barrier. A summary of the estimated level differences between the direct and reverberant levels is provided in Table 7-3.

Frequency (kHz)	$L_{dir} - L_{rev}$ in dB as estimated by [3] (without a barrier)	$L_{dir} - L_{rev}$ in dB estimated after a modification of directivity factors (with barrier)
2	4.3	8.6
2.5	5.8	7.7
3.15	6.7	9.6
4	7.5	12.9
5	8.4	12.1
6.3	9.1	11.7
8	12.2	32.2
10	12	12
12.5	18.2	21.7
16	20.4	28.4
20	29.4	20.7

**Table 7-3 : Estimation of the difference between the direct and reverberant levels.**

The two reference geometries investigated above showed the likely limitations of the testing method. In the cases where the direct sound is not already attenuated too much, reasonable insertion values could be obtained. In the cases where the direct sound has been reduced to levels comparable to reverberant levels, it may not be

possible to obtain the true performance of a configuration. In this case, a relative performance investigation is thought to be possible. In the extreme case where the direct field has been reduced by 10 dB more than the reverberant field no gains of any magnitude would be recorded. This will be the subject of further discussions in the forthcoming chapters.

It is considered that uniform field experiments should be undertaken in a progressive fashion, starting with the smallest geometries and gradually moving towards the largest geometries such that the likely effects of reverberant field could be identified. This approach would determine whether there is a need for repeating certain experiments in a semi-anechoic chamber.

## **7.6 IMPEDANCE TUBE MEASUREMENTS**

### **7.6.1 Aim of the Experiment**

The objective of this experiment is to measure the sound absorption of the two different materials to be used during physical modelling, for normally incident sound, by means of the standing - wave tube method. The materials under investigation will be the absorptive lining used to simulate the absorbing ground cover and the medium density fibre (m.d.f.) which was used as the model material. These values will be related to the flow resistivity values with reference to values provided in the literature.

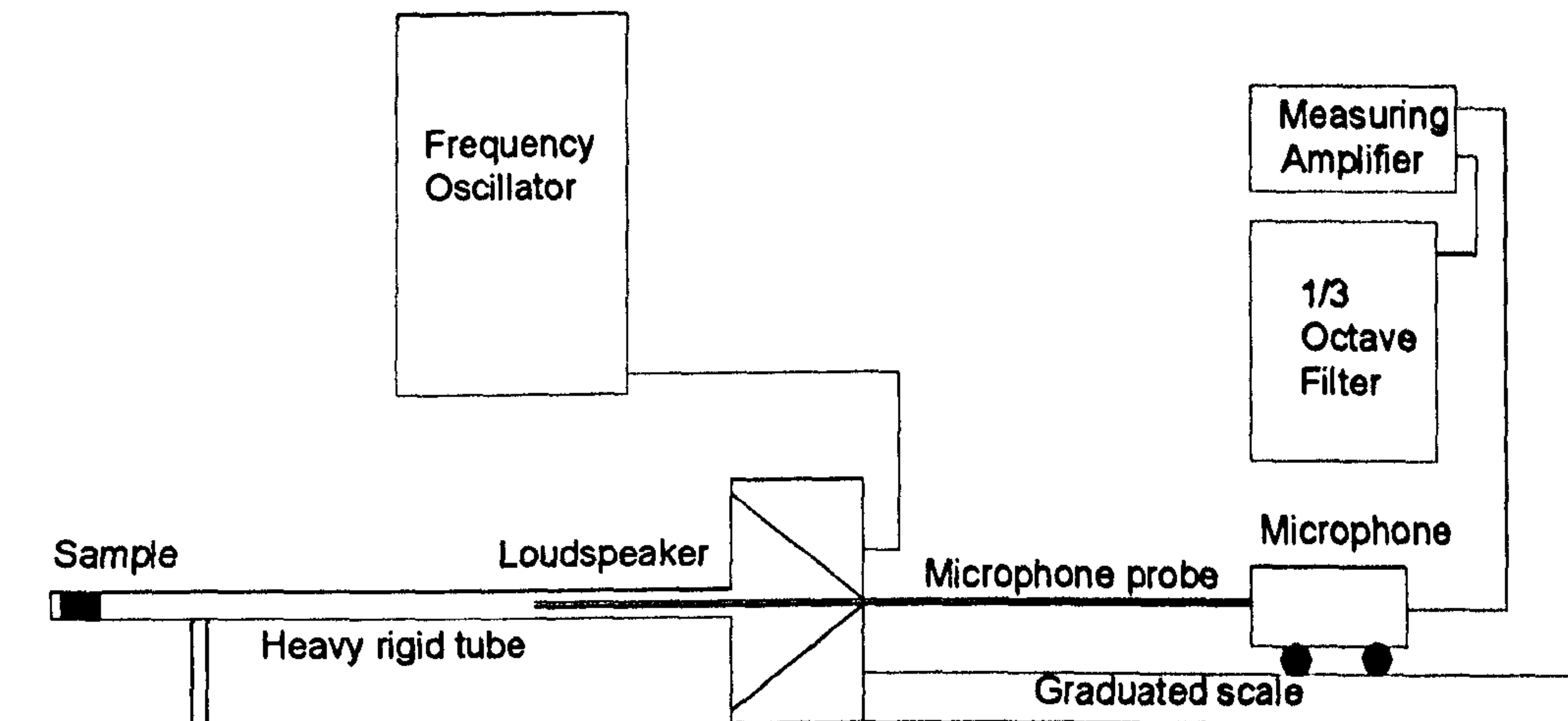
### **7.6.2 Experimental Apparatus Set-Up and Procedure**

The apparatus can be summarised as follows: Loudspeaker, 30 mm diameter measuring tube, Microphone and the probe, Pure-tone oscillator - B&K 1022, Measuring amplifier - B&K 2610, Third-octave filter - B&K 1612

The experimental set-up is as shown in Figure 7.45. The sine wave generator is connected to the loudspeaker which is used to generate the sound wave at the desired frequency, at one end of the measuring tube. The absorbent material is located at the opposite end of the tube. The microphone and the probe can be easily moved



backwards and forwards via the wheels and the rail system. The microphone is connected to the measuring amplifier and the 1/3 octave band filter.



**Figure 7.45 : Experimental set-up and apparatus for the impedance tube measurements**

A 30 mm diameter sample of the absorbent material is inserted in the end of the measuring tube by means of the holder. The required frequency is selected on the signal generator and the band-pass filter. Then the output of the signal generator is adjusted to give a reasonable signal. The same adjustments are made to the sensitivity of the measuring amplifier to give a deflection of the needle. The maximum (A + B) and minimum (A - B) voltage values are read. The ratio of the maximum signal to the minimum signal gives the standing wave ratio, SWR.

$$SWR = \frac{A + B}{A - B} \quad \text{Equation 7.10}$$

This can be used to determine the absorption coefficient  $\alpha$  as follows.

$$\alpha = 1 - \left( \frac{SWR - 1}{SWR + 1} \right)^2 \quad \text{Equation 7.11}$$

The use of an alternative scale enables a direct reading of the absorption coefficient as a percentage. The maximum signal is adjusted to give 100%. Then, the minimum needle deflection reading gives the absorption coefficient directly, without any adjustments.

### 7.6.3 Results

Two different materials were investigated and compared to the no sample case. The two materials were the medium density fibre (m.d.f.) used to construct the physical model and the glass fibre quilt used on the slopes of the model to simulate absorbing ground conditions. No sample case was intended to give an indication as to what the absorption characteristics of the reflective aluminium would be. It was assumed that



both the end cap of the impedance tube and the aluminium ground surface are reflective.

The thickness of the m.d.f. material was 4 mm and the thickness of the glass fibre quilt was 8 mm. Three samples of each material were selected randomly. These were tested for the 1 / 3 octave frequency bands between 1 kHz and 6.3 kHz inclusive. Each test was carried out 8 times for each sample. Figure 7.46 shows the results obtained for the glass fibre quilt.

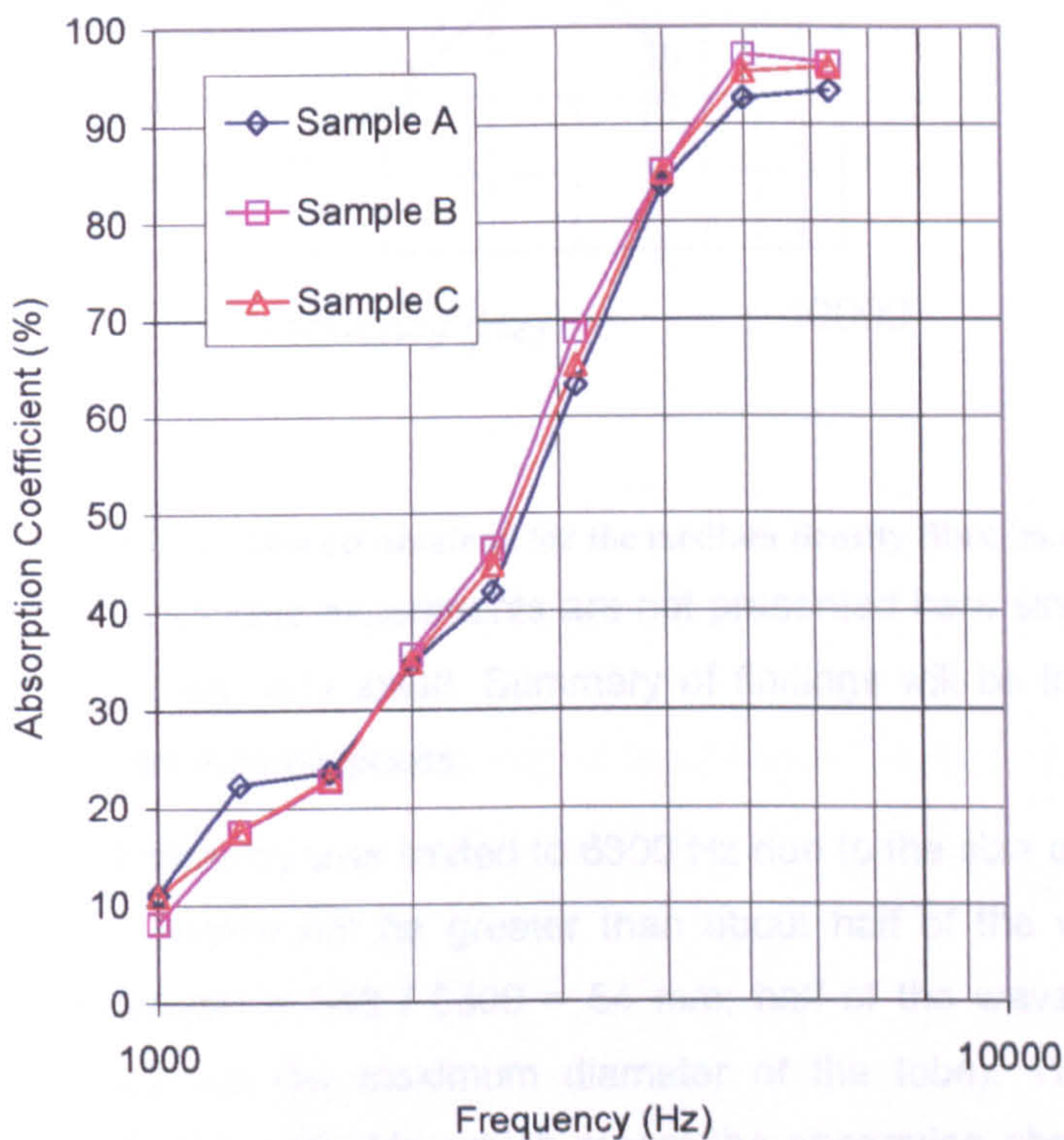


Figure 7.46 : Absorption coefficients obtained for glass fibre quilt.

The absorption characteristics of the three samples are very similar to each other which imply the uniformity of the material. The shape of the absorption coefficient graph resembles that of a porous absorber, the absorption coefficient increasing with the frequency. The results from the standing wave tube, though reproducible, are less than those from the reverberation chamber<sup>5</sup>. Therefore, higher absorption coefficients are expected in random incidence.

The model material was constructed from medium density fibreboard. The absorption coefficient of this material was small compared with the absorbing material as expected. However, it could not be considered to be reflective because it did possess some degree of absorption. In order to quantify this, three samples were tested, as above. Figure 7.47 shows the average results of eight tests for each of the three samples.



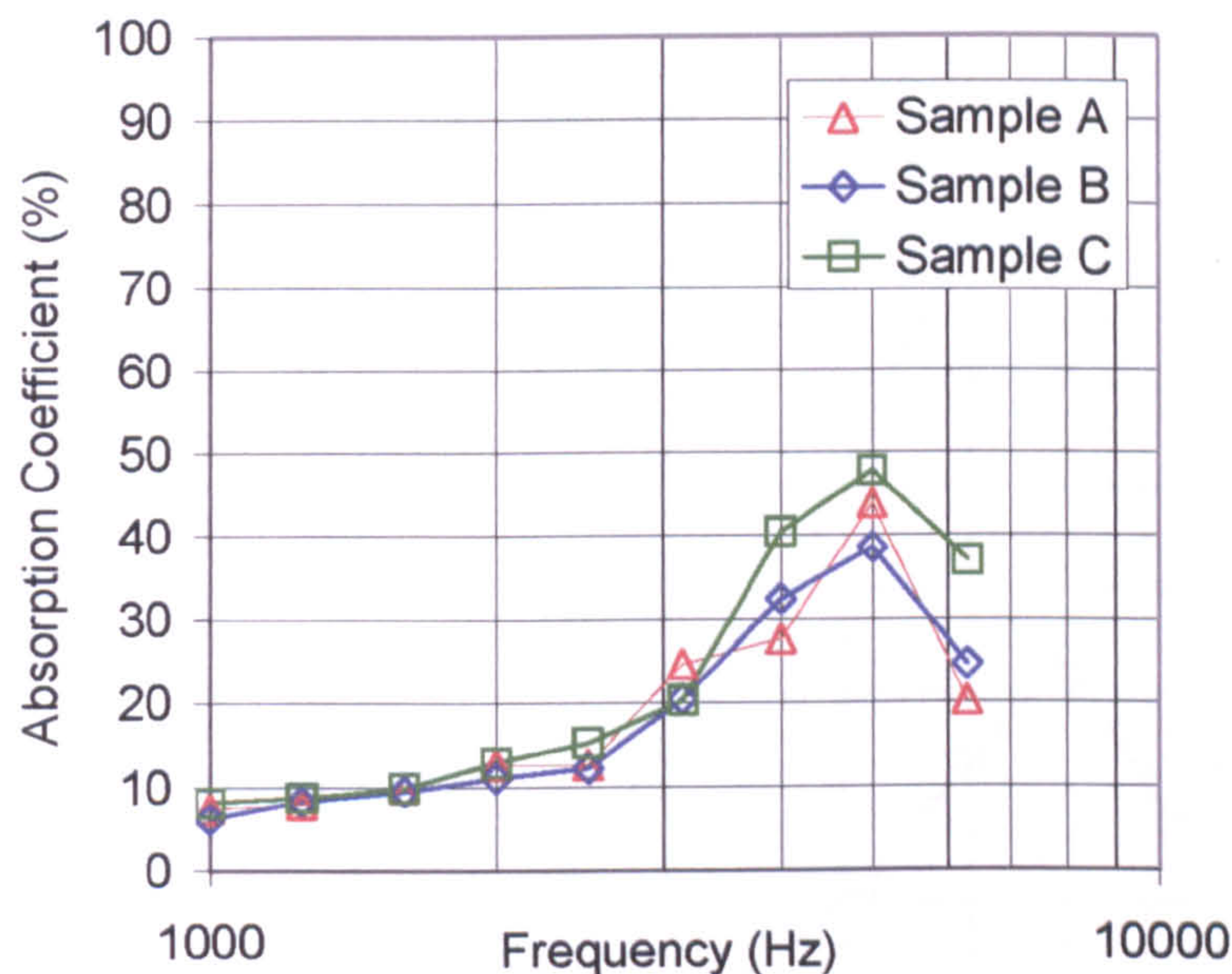


Figure 7.47 : Absorption coefficients obtained for the medium density fibre (m.d.f.)

The details of the no sample experiments are not presented here since the absorption coefficients recorded are very small. Summary of findings will be included below for discussion and comparison purposes.

The upper testing frequency was limited to 6300 Hz due to the size of the tube, whose maximum diameter should not be greater than about half of the wavelength under investigation (wavelength =  $340 / 6300 = 54$  mm; half of the wavelength = 27 mm; therefore that should be the maximum diameter of the tube). The frequencies of interest were between 2 - 22 kHz, which meant the absorption characteristics of the material between 8 - 22 kHz could not be determined.

The average values for the absorptive lining and the model material are seen Figure 7.48. The absorption coefficient values obtained when there is no sample in the sample holder are also included for comparison purposes. The "no sample" case is theoretically expected to give zero absorption coefficients due to the fact that the sample holder is a hard and reflective metal. However, in practice some absorption values are recorded due to reflections from not only the sample holder but from the sides of the tube as well. These are around 3-5 %.



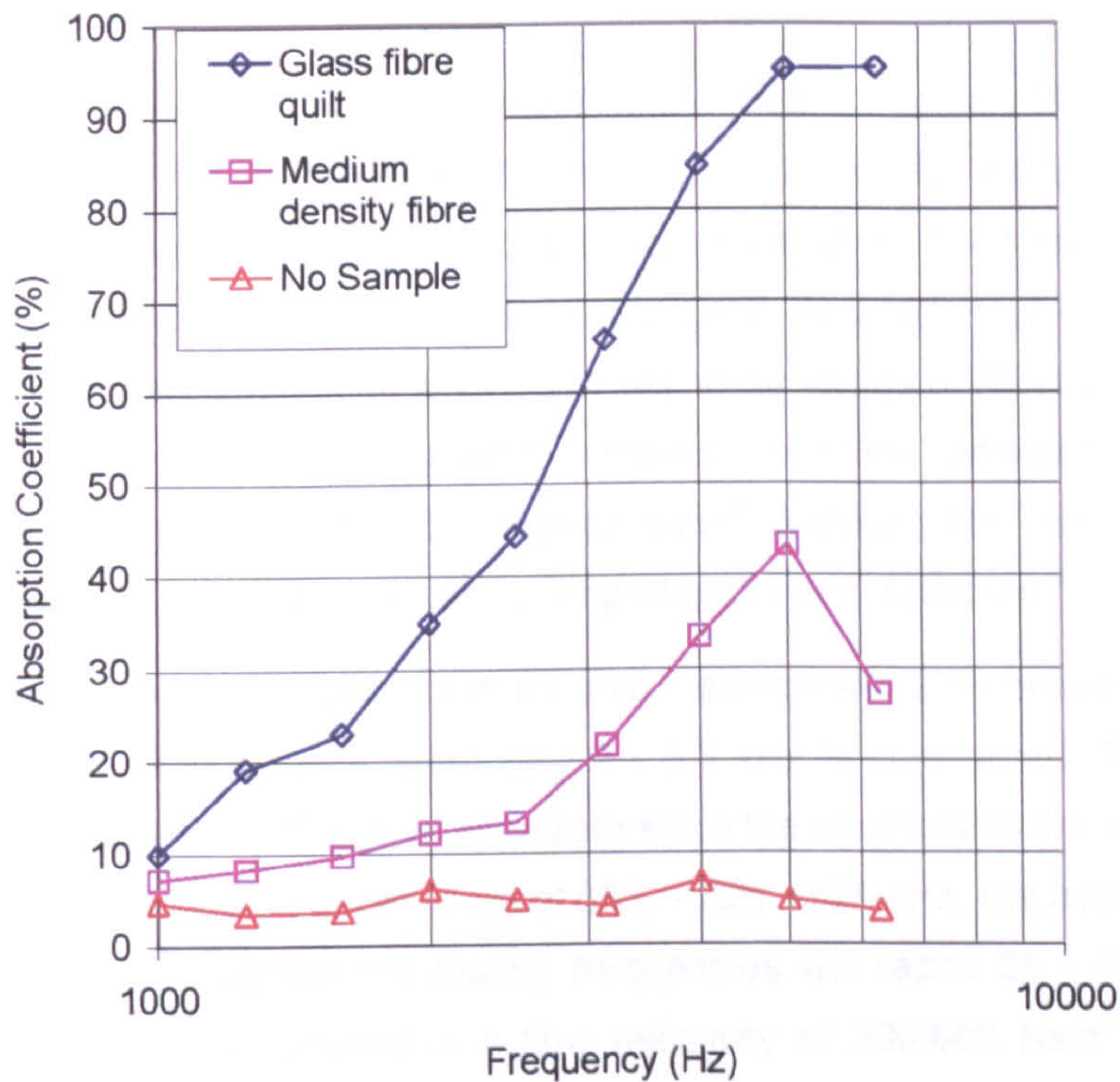


Figure 7.48 : Summary of absorption coefficients obtained for the three cases.

The average absorption coefficient value for the frequency range between 2 kHz and 6.3 kHz is 25 % for the medium density fibre (m.d.f.) and 70% for the glass fibre quilt. These values are expected to become higher when the whole testing frequency range of 2 kHz to 22 kHz is to be considered.

The average absorption coefficient of the glass fibre quilt between 1 kHz and 6.3 kHz was 52%. When the lower frequencies of 1, 1.25 and 1.6 kHz were discarded, this value rose to 70%. The absorption coefficients in the frequency bands above 6.3 kHz are expected to be similar to those obtained for 5 kHz and 6.3 kHz or higher, since these values are already 95% or above. This means the average absorption coefficient of the material within the frequency range of 2 kHz to 22 kHz will rise to about 80% to 85%.

Using the approximate relationship between the absorption coefficient,  $\alpha$ , and flow resistivity,  $\sigma$ , as indicated elsewhere<sup>6, 7</sup>, the corresponding flow resistivity can be quoted as around 20,000 Nsm<sup>-4</sup>. This flow resistivity value can be related to the published flow resistivity values for a realistic surface. This value corresponds to " 0.1 m new fallen snow over older snow"<sup>18</sup>. The main objective in using a material possessing extreme absorption characteristics is obviously not for simulating a snow covered ground surface. Objective is to enhance the absorptive properties of the model ground cover



such that its effects will be clearly identifiable even in the presence of a reverberant field discussed in the earlier sections within this chapter.

A similar way of thinking can be extended to the medium density fibre (m.d.f.). Since the model is intended as "an earth mound" the choice of the model material is very important and it has to correspond to a typical surface for such an application. It is reported that  $100,000 \text{ Nsm}^{-4}$  is a reasonably good description of the attenuation of sound due to ground absorption where flow resistivity values of  $50,000$ -  $200,000 \text{ Nsm}^{-4}$  have been given for various ground surfaces, including different grass covered grounds, bare sandy ground and ploughed sand<sup>9</sup>. Similarly flow resistivity values of  $150,000$  -  $300,000 \text{ Nsm}^{-4}$  correspond to "airport grass or old pasture"<sup>8</sup>.

The average absorption coefficient of the m.d.f. samples is 20% between 1 kHz to 6.3 kHz. This value rises to 25% when only 2 - 6.3 kHz is considered. The frequencies above 6.3 kHz are more difficult to speculate since the possibilities are more. Assuming the absorption reaches an upper value of 65% - 70% at 20 kHz, the average absorption coefficient value throughout the testing frequencies will reach 35 - 45%. This value could be roughly approximated to a flow resistivity of  $200,000 \text{ Nsm}^{-4}$  from the data provided by other researches<sup>6,7</sup>. The values of " $\alpha = 0.33$  and  $\sigma = 250,000 \text{ Nsm}^{-4}$ " are "typical of grassland surfaces"<sup>6</sup> and hence it is reasonable to relate the model material to a ground surface.

## **7.7 FLOW RESISTIVITY OF THE ABSORBING MATERIAL**

The reasons for choosing the particular absorbing material described above were partly due to extensive previous research carried out at Hallam University using this material. The background theory, the methodology and the apparatus used for flow resistivity measurements have been previously described by Hall et al<sup>10</sup>. This work details the calibration of the apparatus by comparing the results to those obtained by a different apparatus at the Building Research Establishment (BRE).

Consequently the airflow resistivity of the absorptive material under consideration was identified to be less than  $10 \text{ kPa.s/m}^2$  ( $=10,000 \text{ Ns/m}^4$ ). This value is lower than that reported in the previous section, determined by impedance tube measurements. However it is close to the range quoted in the literature for a '0.1m new fallen snow, over older snow'.

Both the impedance tube measurements and flow resistivity tests are consistent in classifying the material as 'a highly absorbent' ground surface. In the case of impedance tube measurements this is true for the frequencies and the physical scale

under consideration. It should be noted that the use of this material was restricted to the preliminary investigations in Chapter 5.

## **7.8 GENERAL DISCUSSION**

The work undertaken in this chapter was directed towards characterising the testing space, the sound source and the modelling materials to be used for physical scale modelling purposes.

The use of a continuous noise source under uniform field conditions necessitated an investigation into the potential effects of the reverberant field on the experimental results. Therefore reverberation time measurements and directivity tests were undertaken which were aimed at estimating the magnitude of the reverberant field. The findings were compared with the two test geometries selected from the literature. Impedance tube measurements were undertaken to characterise the model materials. The findings were supplemented by direct and approximate relationships to flow resistivity values of known ground surfaces. These are discussed below.

### **7.8.1 Reverberant Field within Testing Space**

Accurate representation of reverberation times at a frequency range of 2 to 20 kHz were essential for characterising the influence of reflections on the physical scale modelling results. Two different methods were used in order to have an understanding of the room behaviour at the testing frequencies. These used different sound source combinations in conjunction with a "traditional" pen-recorder (or level recorder), and a purpose built digital sound analyser called NC10. This highlighted how the traditional and modern methods yield differing results depending on practical difficulties and the operator influence.

Starting pistol is commonly used as a noise source in reverberation time measurements. The fact that it produces a tone burst of short duration and its small size makes it suitable for these experiments. The pistol was kept close to the receiver to maximise the output, but even so, only the frequencies centred around 1.25 - 1 kHz exceeded the 90 dB level. The tone burst due to the pistol provided a roughly constant spectrum which peaked around 1 kHz and decreased linearly to around 75 dB at the higher and the lower ends of the spectrum.

The fastest paper speed available on the level recorder was 30 mm/s. The reason for choosing the fastest paper speed possible was to maximise the length of the x-axis (time) in the decay curve such that its measurement would be easier and more



accurate. However the time axis was bound to remain too small because the peak sound pressure levels did not reach the maximum allowable deflection of 95 dB. Hence the decay rates were not sufficient to give a reasonable time axis dimension. This was reflected in the reverberation times obtained.

Theoretically, both the time axis (x-axis) and the sound pressure level axis (y-axis) could be extended by increasing the output from the source. However, the source was already close to the receiver and its output was more or less steady, with small variations in the sound pressure levels from one blast to another.

Another way of maximising the scales involved would be via the pen-recorder itself. This could be achieved by calibrating the pen-recorder such that the maximum sound pressure level occurring on the chart would be much less than 95 dB (say 15 dB lower) to utilise full decay of 25 dB. Since the smallest calibration level available was 94 dB, the chart could not be calibrated to give the maximum deflection at a smaller sound pressure level. Even if an appropriate calibrator were available, sensitivity setting of the pen-recorder would not allow this to be realised on the chart. The sensitivity of the level recorder was already at the maximum allowable setting and lowering the sensitivity would only lower where the peak sound pressure levels occur on the chart. If a calibrator with a higher reference sound pressure level was used in conjunction with a lower sensitivity setting in the pen-recorder, this time the output from the pistol source would not be sufficient.

The pistol source used in conjunction with a pen-recorder having a 25 dB potentiometer posed practical difficulties. Therefore the noise output was increased by using a speaker. Single wedge speaker tests were restricted to 1 / 3 octave band frequencies between 800 Hz and 4 kHz. Above 4 kHz, the maximum achievable sound pressure level at the receiver location was 80-85 dB, enabling only 10-15 dB of decay, and not providing a representative decay curve. Frequencies below 800 Hz were of no interest.

Between 800 Hz and 4 kHz, the maximum sound pressure levels reached 92 dB to 95 dB and hence the decay rates were maximised to 22-25 dB. As a result, the time axis became relatively larger in size and its measurement was easier. Since reverberation times were small, the resulting x-axis in mm was still not large enough to enable a very comfortable or precise manual measurement using a ruler or a protractor.

In order to determine whether the reverberation times obtained at a single receiver location were representative of the whole testing space, tests were repeated at a number of receivers. Two wedge speakers were placed in the corners of the room with the intention of obtaining a uniform sound field across the testing space and sufficiently high output sound pressure levels throughout. It was found that the average

reverberation values obtained throughout the testing space for wedge speaker tests were in agreement with each other. This indicated it would be reasonable to assume the testing space represented uniform field conditions.

The lack of data at the frequencies above 4 kHz was a concern since most of the physical scale modelling would be concentrated at frequencies above 2 kHz up to 22 kHz. The distinctive conflict between the reverberation times obtained by the starting pistol and the wedge speaker sources meant the reverberation times had to be measured with an alternative technique. A digital sound analyser was employed as a fully integrated system to measure the reverberation times. This removed operator influence and the practical difficulties associated with the manual measurement of the decay curve gradients. Larger decay levels eliminated the problem of not being able to produce a representative straight decay line, removing the possible errors due to the measurement of the gradient of the decay curves. The small sampling times of the sound pressure levels meant the times involved could be assessed reliably.

The correlations obtained by the digital sound analyser NC10 were shown to be very high, exceeding 95% in the case of T30 results above 2 kHz. These were between 90% and 95% for the lower end of the frequency spectrum under investigation. The correlations deteriorated as the decay level diminished (i.e. for T20 and EDT). The correlation of T20 results still lie between 90-95% above 2 kHz, however at the lower end of the spectrum, they are lower than 90% varying greatly from test to test. Even though the correlation figures for the T20 were not as good, the average reverberation time values followed the average T30 values reasonably well. Early decay times (EDT) varied greatly fluctuating up or down relative to the T30 curves up to 3 kHz. After this point, all three parameters follow very similar trends. These observations are valid in both cases when a starting pistol or a speaker is used as the sound source. Therefore the discrepancies obtained in the tests carried out by the level recorder using two different sound sources were mainly due to the manual method of measuring the decay curve gradients.

The T30 values obtained by the pistol and speaker tests were found to be within 0.1 seconds of each other at all frequency bands showing the consistency of the results. Therefore, T30 values were considered to be representative of the reverberation times due to the high correlation values obtained within each test for each 1 / 3 octave band frequency band for both sound sources.

Another parameter required for estimating the reverberant field levels was the directivity characteristics of the sound source. The directivity indices and directivity factors were determined by experiments at 1/3 octave band frequencies between 2 kHz and 20 kHz. The reverberant fields were estimated using the reverberation times and



the source directivities. It was found that the source to receiver distances would remain in the transition zone between the direct and reverberant field dominated zones. Therefore the reverberant fields would be expected to influence the experimental results. The extent of this influence would depend on how much the direct field would be attenuated due to the presence of a barrier.

Two reference geometries previously studied by other researchers were chosen as reference cases to test the validity of the above findings. The first one of the geometries provided a relatively small attenuation on the direct levels since the source and the receivers were situated such that they were grazing the top of the barrier. This geometry was expected to minimise the effects of the reverberant field on the direct field. In the second geometry, the source was situated in the deep shadow zone behind the barrier. The direct field would be attenuated considerably, exposing it to the adverse effects of the reverberant field.

These two geometries showed the likely limitations of the testing method. In the cases where the direct sound is not already attenuated too much, reasonable insertion values could be obtained. In the cases where the direct sound has been reduced to levels comparable to reverberant levels, it may not be possible to obtain the true performance of a configuration. In this case, a relative performance investigation is thought to be possible. In the extreme case where the direct field has been reduced by 10 dB more than the reverberant field no gains of any magnitude would be recorded.

It was considered that uniform field experiments should be undertaken in a piecemeal fashion starting with the smallest geometries and gradually moving towards the largest geometries such that the likely effects of reverberant field could be identified. This approach would determine whether there is a need for repeating certain experiments in a semi-anechoic chamber.

### **7.8.2 Absorptive Properties of Model Materials**

Impedance tube measurements were carried out at normal incidence to determine the absorption coefficients of two of the model materials. The first material, which is aluminium, is used to simulate "reflective ground surface" and data available in literature on aluminium is considered to be reliable to safely categorise it as a reflective surface without the need for further testing. Aluminium angles of various dimensions were used to simulate multiple diffracting edges. The other two materials used were the medium density fibre model material and the absorptive ground cover. Their average absorption coefficient values within the testing frequency range were related to airflow resistivity values from the published data in the literature. Accordingly, the model material (medium density fibre) and the absorptive cover (glass fibre quilt)

corresponded to a grass covered ground surface with  $\sigma = 200,000 \text{ Nsm}^{-4}$  and a surface covered with freshly fallen snow with  $\sigma = 20,000 \text{ Nsm}^{-4}$  respectively. These values obtained for the absorptive cover were compared with the findings of airflow resistivity tests carried out previously at Hallam University. It was found that the approximate relationship between the absorption coefficients and the airflow resistivities yielded consistent results when compared with the direct measurements of airflow resistivity. It was considered that for the purposes of this work, the approximate relationship between absorption coefficients and flow resistivity provided a reasonable idea on the general absorptive characteristics of the materials used for modelling.

## 7.9 CONCLUSIONS

The requirements of physical scale modelling were identified by looking at the work carried out by previous researchers. It was realised that there is not a standard way of carrying out physical modelling. According to the availability of space and equipment, the best possible choices were made in order to minimise adverse effects of these on the physical modelling to be undertaken in the next chapter.

A large room with a high ceiling and an assumed uniform field was used as the testing room. The modelling scale was chosen as 1:10. The sound source was a 2" tweeter speaker enclosed in a box. A capacitor eliminated the low frequency component of the noise, which could damage the speaker. The speaker itself was connected to a random noise generator and an amplifier. The testing frequency range was 2 kHz to 22 kHz and the frequency band investigated was 1 / 24 octave band intervals. The receiver was a 1 / 4" microphone connected to a dual channel analyser which was used to monitor the sound pressure levels at the receiver point of interest and at the reference point. Three different model materials were used to model hard, absorbing and typical ground conditions.

The testing space, the sound source and the modelling materials to be used for physical scale modelling purposes were characterised. Reverberation time measurements were carried out to find out the suitability of the testing space for modelling work and to quantify the effects of the reverberant field. Directivity tests helped determine the source characteristics.

Having determined the source and room characteristics, variation of sound pressure levels with distance from the source was monitored. Measured data up to 3 m from the source were compared with the predictions made by the room acoustics equation. The predicted graphs themselves were based on measured directivity factors and predicted



room constants determined for each 1 / 3 octave frequency band of interest. The predictions and the measurements agreed well.

The main outcome of this comparison was that any realistic source-to-receiver configuration would be likely to remain in the transition zone between the zones dominated by direct and reverberant fields. This implied the physical scale modelling results would be influenced by the presence of reverberant field. However, a relative performance study of different barrier configurations could be possible if the source-to-receiver distances were carefully selected in order to minimise the effects of the reverberant field.

Scale modelling using two different test geometries selected from the literature showed that the magnitude of these effects depended on how much the direct component of the sound field would be attenuated in relation to the reverberant component. This would be governed by the choice of source - to - receiver distance and the size of the geometry to be investigated.

It was considered that uniform field experiments should be undertaken in a piecemeal fashion starting with the smallest geometries and gradually moving towards the largest geometries such that the likely effects of reverberant field could be identified. This approach would determine whether there is a need for repeating certain experiments in a semi-anechoic chamber.

Impedance tube measurements were undertaken to determine the absorptive behaviour of the modelling materials. Absorption coefficients were related to flow resistivity of known materials by an approximate relationship. The values obtained for the absorptive ground cover were compared with the findings of airflow resistivity tests carried out previously at Hallam University. It was found that the approximate relationship between the absorption coefficients and the airflow resistivities yielded consistent results when compared with the direct measurements of airflow resistivity. It was considered that for the purposes of this work, the approximate relationship between absorption coefficients and flow resistivity provided a reasonable idea on the general absorptive characteristics of the materials used for modelling.

This investigation into the experimental set-up showed that it could be possible to undertake relative performance investigations of various barrier profiles using this method under uniform field conditions, subject to certain limitations. These limitations are explored further in the next chapter using various models consisting of multiple edges, or rib structures, both on their own and on other earth mound type barriers.

## 7.10 REFERENCES

- 
- <sup>1</sup> ANDERSON, J.S., BRATOS-ANDERSON, M., Noise Its Measurement, Analysis, Rating and Control, ISBN 0 291 39794 8, Published by Avebury Technical, 1993, 246-252
- <sup>2</sup> NC10 User Manual, Reverberation Time Analysis V 1.0, by Neutrik Cortex Instruments (NCI), 1997
- <sup>3</sup> HUTCHINS, D.A., JONES, H.W., RUSSEL, L.T., Model studies of barrier performance in the presence of ground surfaces. Part II - Different shapes, J.Acoust.Soc.Am., 75 (6), June 1984, 1817 - 1826.
- <sup>4</sup> NICOLAS, J., EMBLETON, T.F.W., PIERCY, J.E., Precise model measurements versus theoretical prediction of barrier insertion loss in presence of the ground, J.Acoust.Soc.Am., 73(1), January 1983, 44 - 54.
- <sup>5</sup> SMITH, B.J., PETERS, R.J., and OWEN, S., Acoustics and Noise Control, Addison Wesley Longman Limited, Second Edition, ISBN 0-582-08804-6, p. 45, 1996
- <sup>6</sup> FYFE, K.R., and HARRISON, C.C., Modelling of Road Noise Optimal Barrier Design, Canada Mortgage and Housing Corporation, CMCH CR File 6585-F039, March 1995
- <sup>7</sup> HOTHERSALL, D., Modelling The Performance of Noise Barriers, Eurosymposium 1992, The Mitigation of Traffic Noise In Urban Areas, Nantes, France, 12-15 May, 1992, 247-258
- <sup>8</sup> EMBLETON, T.F.W., Tutorial on Sound Propagation Outdoors, J.Acoust.Soc.Am. 100(1), July 1996, 31-48
- <sup>9</sup> DE JONG, B.A., MOERKERKEN, A., and VAN DER TOORN, J.D., Propagation of Sound Over Grassland And Over An Earth Barrier, Journal of Sound and Vibration, 86(1), 23-46, 1983
- <sup>10</sup> HALL, R., BOUGDAH, H., and MACKENZIE, R., A Method for Predicting  $L_{nT,w}$  for Light Weight Floating Floors Comprising Low Density Flexible Polyurethane Foam on Concrete Supporting Floors, Journal of Building Acoustics, 3(2), 1996, 105-117



# 8 PHYSICAL SCALE MODELLING: UNIFORM FIELD TESTS

The suitability of the testing method and the choices of various modelling materials and equipment have been discussed in Chapter 7. The main aim of this chapter is to investigate the performance of various barrier configurations using this method. The work undertaken also aims to identify potential limitations of the method. The forthcoming sections will investigate how a reactive earth mound could be realised in practice. The barrier profiles to be studied consist of a series of edges on a hard reflective ground and on earth mound type barriers.

## 8.1 EXPERIMENTAL METHOD

The uniform field experiments were carried out in an irregular shaped room with approximate dimensions of 12.6 x 6.3 x 6.3 metres (excluding the irregularities), the longer dimension corresponding to the length of the room, with which the source and the receivers were aligned. A three dimensional sketch of the testing room can be seen below.

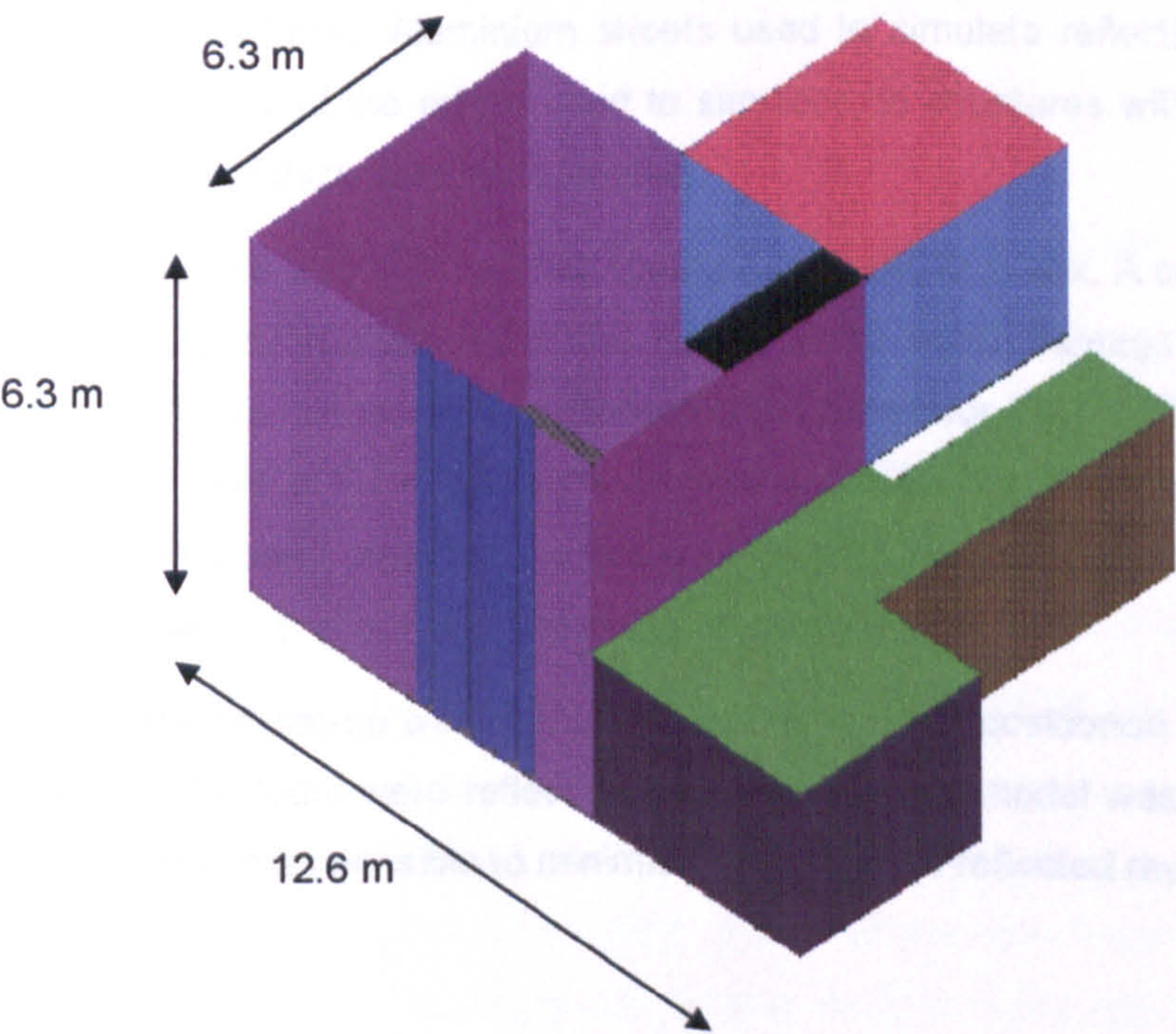
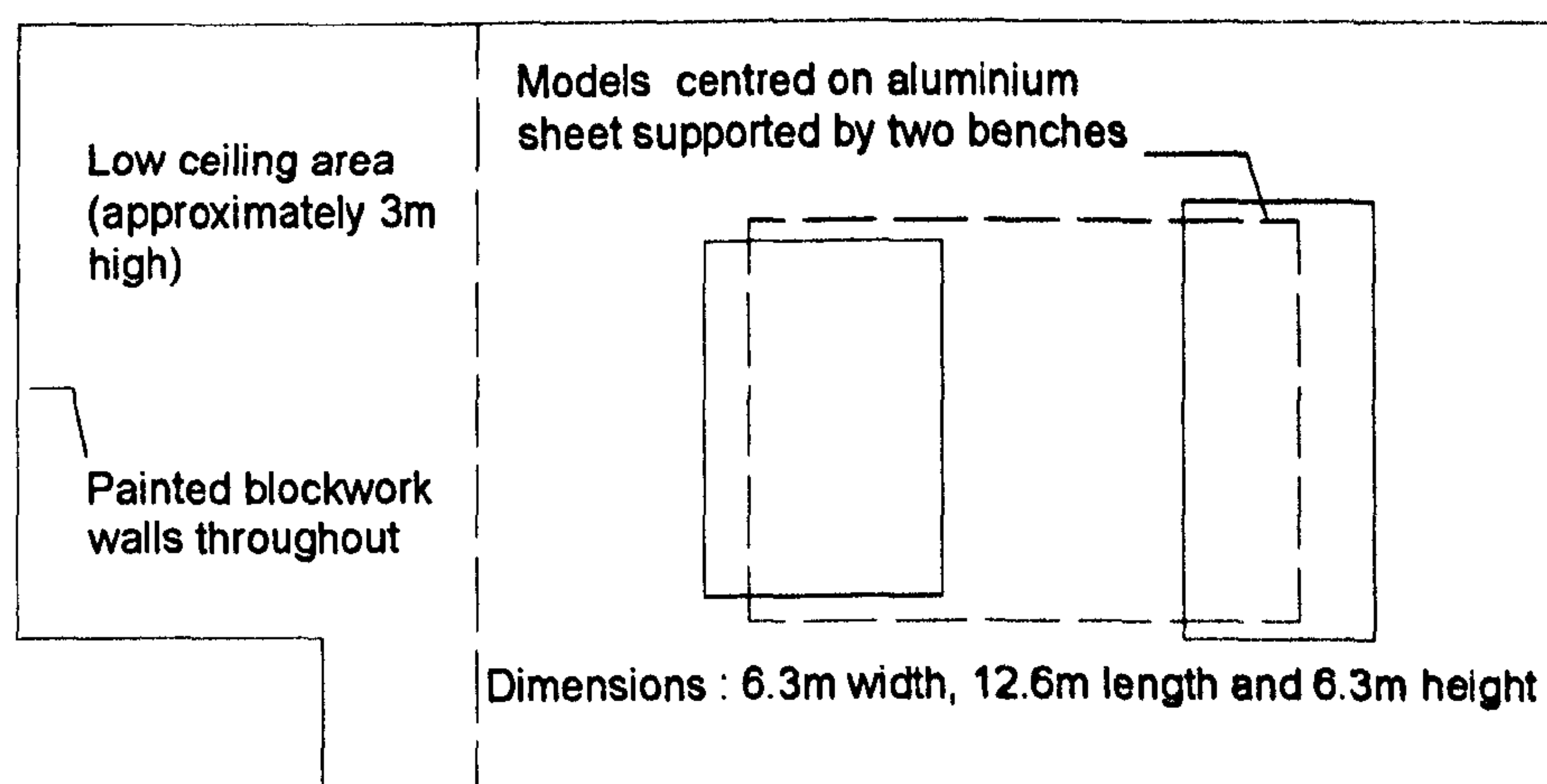


Figure 8.1 : A 3D sketch showing the testing room





**Figure 8.2 : The plan view of the testing room**

The modelling scale is 1:10 throughout the experiments. Testing frequencies are limited to a range of 2 kHz to 22 kHz, at 1 / 24 octave band intervals, corresponding to 100 Hz and 2200 Hz respectively at 1:10 scale. However, the dimensions and frequencies reported throughout will be those of the model. The real dimensions and frequencies will be considered when discussing potentially successful profiles in the forthcoming chapters.

Two main modelling materials were used to model hard ground and the earth mound barrier surface. The earth mound model was constructed from 4mm thick MDF (medium density fibre). Aluminium sheets used to simulate reflective ground surface were 2mm thick, and the edges used to simulate rib structures with reactive surfaces consisted of 1mm thick aluminium angles.

The sound source was a 2" tweeter speaker enclosed in a box. A capacitor eliminated the low frequency component of the noise, which could damage the speaker. The speaker itself was connected to a random noise generator (B&K1402) and an amplifier. The receiver was a 1 / 4" microphone connected to a dual channel analyser (B&K 2144) with an 8 band pass filter, which was used to monitor the sound pressure levels at the receiver point of interest and at the reference point.

The experimental set-up was in the centre of the room, positioned on top of a bench. The walls of the room were reflective and therefore the model was placed away from the walls as much as possible to minimise the effects of reflected rays.



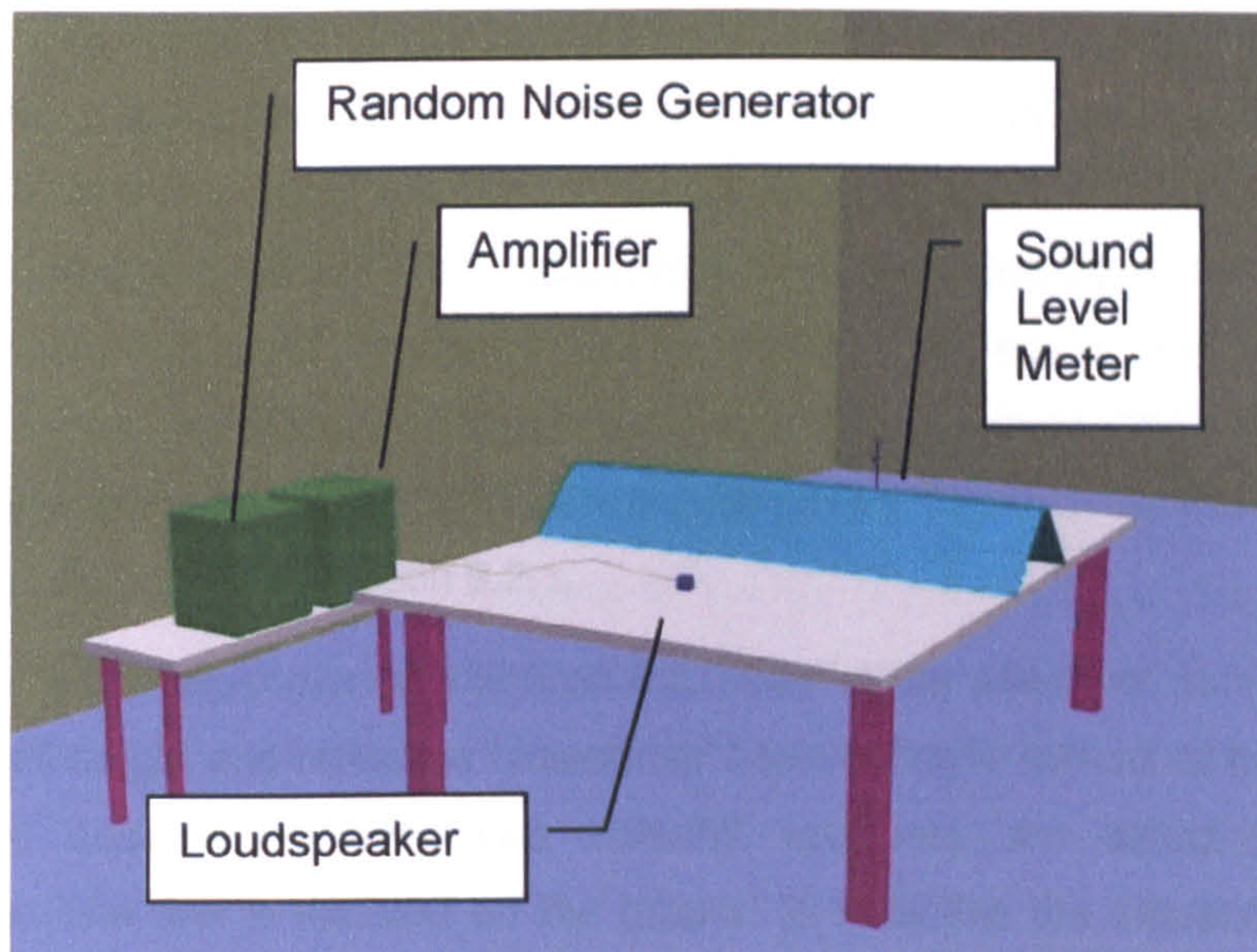


Figure 8.3 : General test arrangement

The reference levels were monitored 0.30 m from the source at the ground location. Single receiver location was monitored at a time with a single microphone for 40 seconds. For each receiver location, the sound pressure levels in dB were monitored for the reference point and the receiver and the difference between the levels was used to relate the receiver location to others. It is reasonable to assume the output of the noise does not vary between the measurements at the reference location and the receiver (80 seconds in total), even though it would have been ideal to be able to monitor both the reference and the receiver locations simultaneously with two microphones.

As discussed in the previous chapter the background noise levels were found to be lower than the measured levels at a typical receiver by at least 10 dB or more. In the instances when there were extraneous noise sources due to adjacent laboratory facilities, the experiments were repeated. Generally, the background noise levels did not have a major influence on the measured noise levels.

The geometries are intended to investigate the effects of different edge configurations progressively so that potential limitations in the experimental method can be identified.

In the first set of tests, the effects of multiple edges situated on the ground are studied. Initially the progressive increase in the number of edges is investigated at a single receiver location. This receiver is chosen such that the line-of-sight from the physical centre of the source to the receiver is grazing the top of the edge. This ensures the subsequent addition of edges in the direction of the receiver do not affect the path length of the sound. Having established the potential benefits of progressive increase



in the number of edges, the effects of doubling the number of wells and the width of the reactive surface are investigated. An array of six receiver locations is used to provide evidence on how the spectrum behind the reactive surface is affected at various distances and heights. Two of these receivers are in the shadow zone, two are situated along the line-of-sight from the source grazing the top of the edges, and the remaining two are in the illuminated zone. These experiments also use three different well depths to identify the effect of these on the lowest frequency at which attenuations occur. These will be discussed in section 8.2.1.

The second set of experiments in section 8.2.2 look at the effects of multiple wells on top of a small height and reflective rectangular barrier. These consist of three different well depths described above. Two different receivers are selected for these experiments. The first is situated on the ground to minimise the influence of ground reflected paths. It was shown in chapter 6 that a series of edges are likely to provide the maximum attenuation when sound is grazing the surface. Therefore, the second receiver is situated at the same height as the height of the barrier, to maintain a near grazing incidence angle over the series of edges.

The third set of experiments investigates the influence of multiple wells placed on top of an earth mound. The large size of this geometry and the increased path length means the direct field would be attenuated as much as possible and the adverse contributions from the reverberant field would be maximised. This geometry is expected to provide some indication on the shortcomings of the method. It will also determine if the reactive surfaces are able to provide additional attenuations when the existing attenuations due to presence of a large sized barrier are substantial. Two receivers are selected for these tests both of which are in deep shadow zone. The first one is resting on the ground, as before, to minimise ground influence. The second one is situated above the ground and represents the height of a typical receiver. These are discussed in section 8.2.3.

The following are the findings of the uniform field experiments carried out for the geometries described above.



# 8.2 RESULTS

## 8.2.1 Multiple Edges on the Ground

### 8.2.1.1 Progressive Increase in the Number of Edges

The basic geometry is shown in Figure 8.4. The source was resting on an aluminium sheet which was used as the ground surface. The height of the receiver was 0.04 m. A single edge consisting of a 90 degree aluminium angle with dimensions 0.025 m x 0.025 m was installed in between the source and the receiver. Both the source and the receiver were positioned 0.5 m from the edge, situated on opposite sides. The horizontal leg of the first aluminium angle was tagged underneath the aluminium sheet on which the source was resting, to prevent noise from travelling underneath the interface between the edge and the platform.

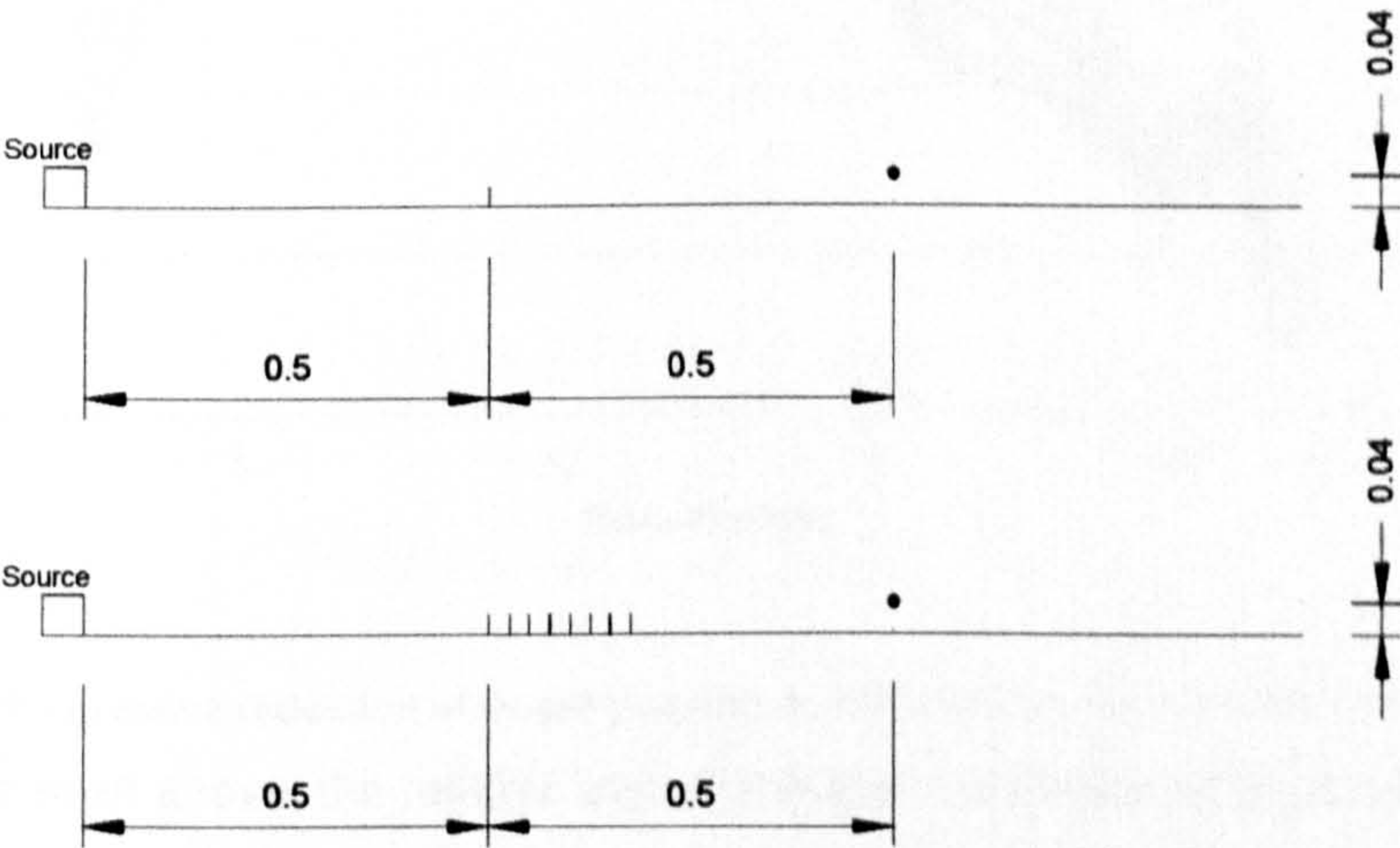


Figure 8.4 : Experimental set-up for investigating effect of up to 8 edges

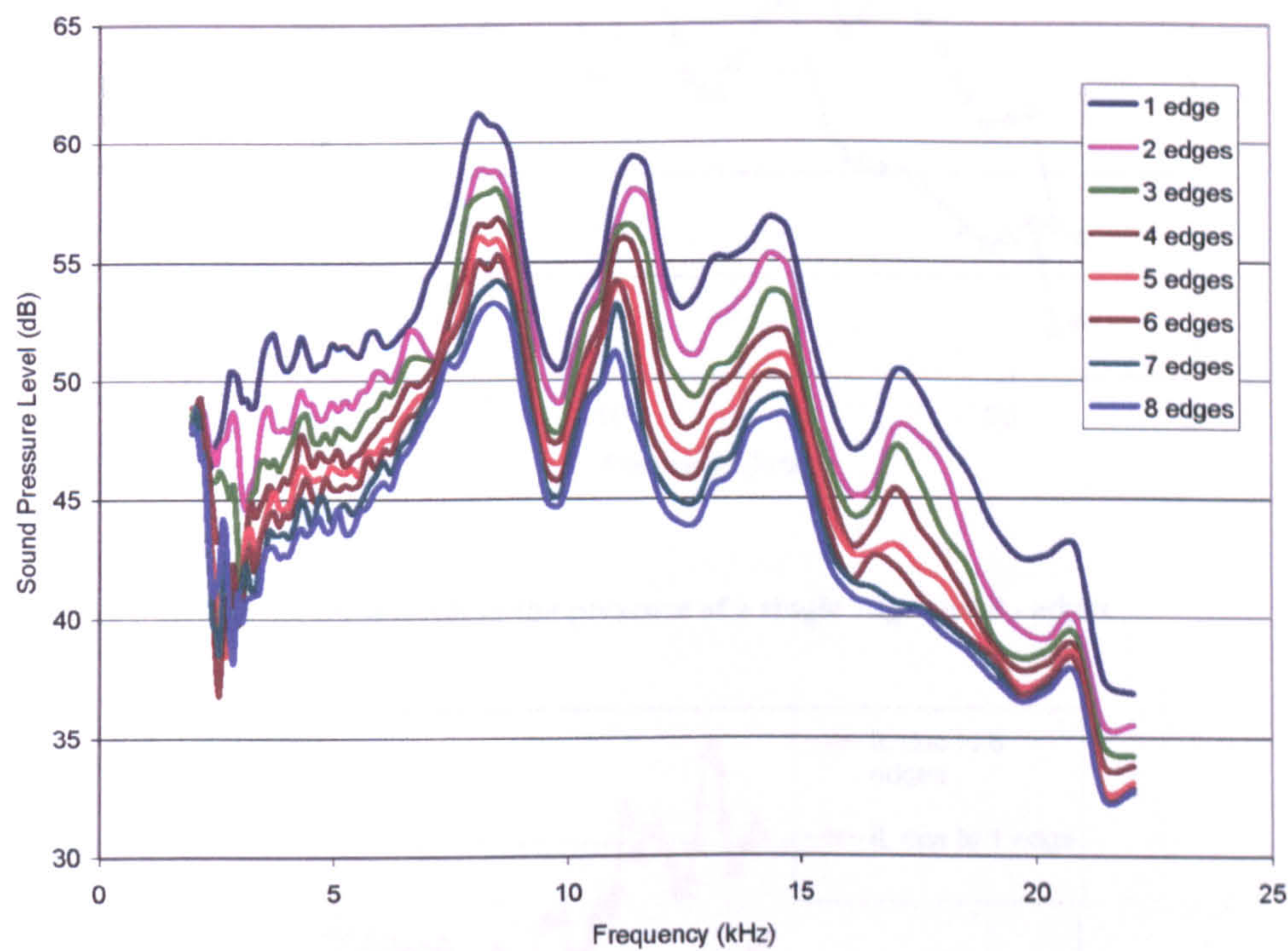
The receiver position was selected such that the direct path from the physical centre of the source to the receiver would be grazing the top of the first edge and a further increase in the number of edges would not cause any change in the path length difference. Hence, any attenuation would be due to the effect of the edges and not to a change in path length difference.

A constant noise output was generated and the sound pressure levels monitored at the receiver position for testing frequencies of 2 kHz to 22 kHz. The process was repeated for up to 8 edges, every time adding one more angle in the direction of the receiver. Since the edges comprise angles of 0.025 m x 0.025 m, the spacing between the edges was determined by the length of the horizontal leg which was 0.025 m. The



sound pressure levels in the absence of the single edge were also monitored such that the insertion loss of the single edge alone and consequently that of the 8 -edges could be determined.

Sound pressure levels observed with a constant noise output, for a single edge progressively increased to 8 edges, are shown in Figure 8.5.



**Figure 8.5 : Progressive reduction of sound pressure levels with increased number of edges.**

As it can be seen above, the relative sound pressure levels are reduced with increased number of edges. More interesting is the direct comparison of a single edge with 8 edges in Figure 8.6. This curve also shows that the performance of the 8-edges is clearly superior to that of the single edge with the exception at the lower end of the frequency bands under investigation.



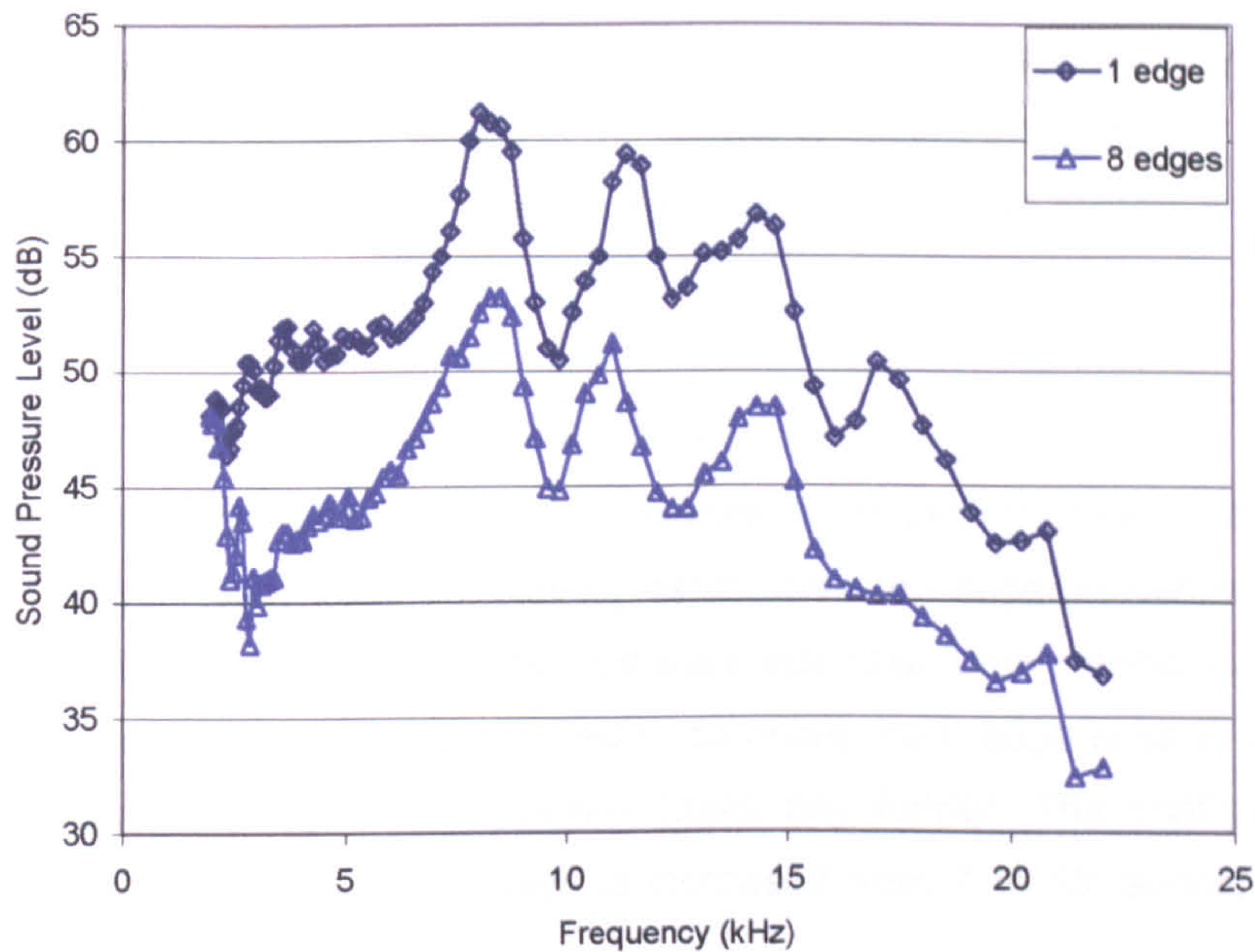


Figure 8.6 : Sound pressure levels in the presence of a single edge and 8 - edges.

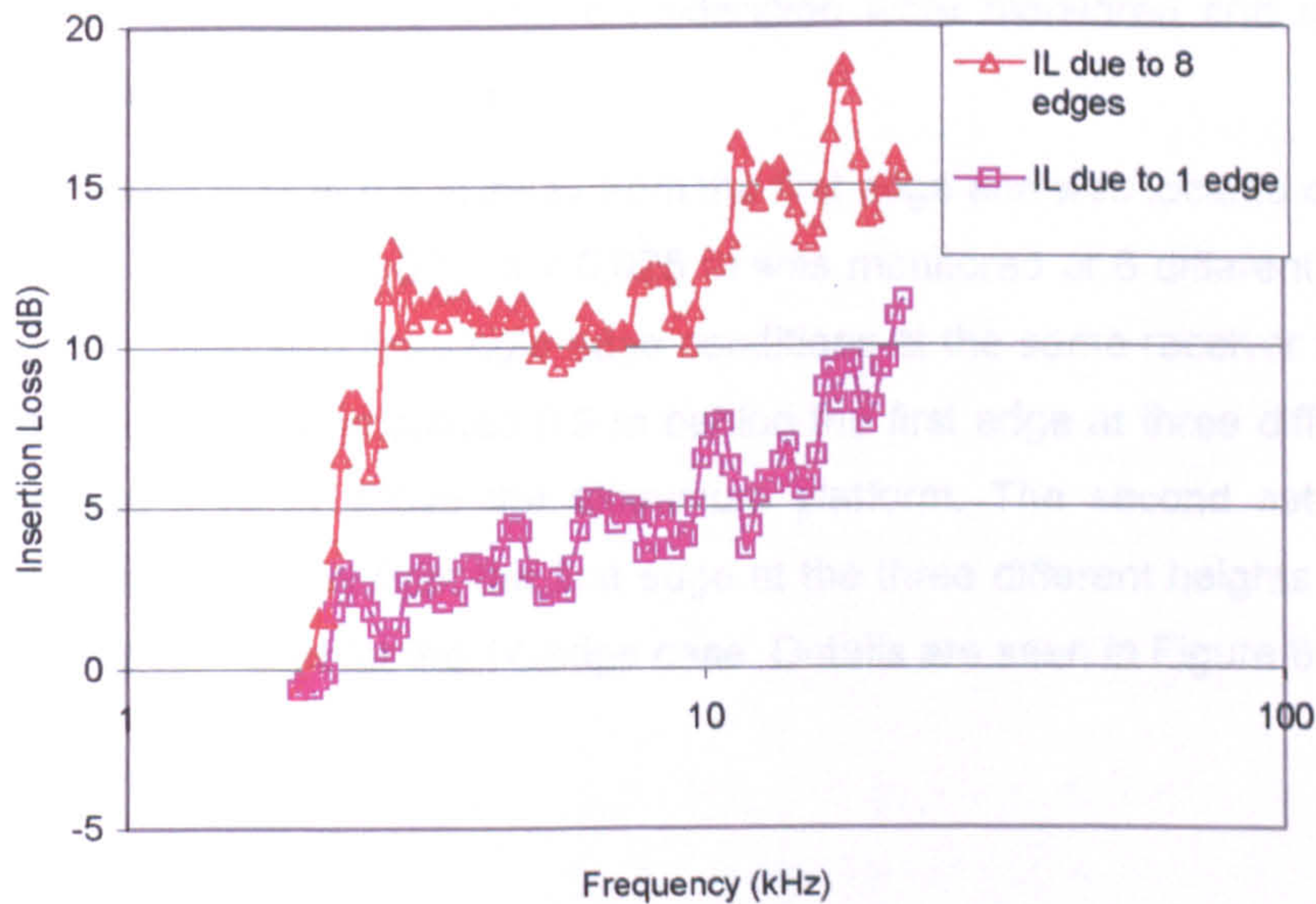


Figure 8.7 : Insertion loss values for a single edge and for 8 - edges.

Insertion loss values for a single edge and for 8 edges are shown in Figure 8.7. The insertion loss values for a single edge increased linearly from around 0 dB at 2 kHz to around 10 dB at 22 kHz. Insertion loss due to 8 edges shows a distinctive jump at around 3 kHz to 13 dB, remaining constant until 10 kHz and then increasing further. The insertion loss provided by the 8-edge case is higher by 5 to 10 dB than the single edge case. The linear average insertion loss value due to the single edge is 4.5 dB and linear average insertion loss due to 8 edges is 11.4 dB. The improvement in the



insertion loss is 6.9 dB. A simplistic path length difference approach dictates that the insertion loss is 5 dB when the line-of-sight from source to receiver is intercepted. The exact location of the acoustic centre of the source is not known, however, the insertion loss of 4.5 dB in the case of the single edge is good supportive evidence of the above statement.

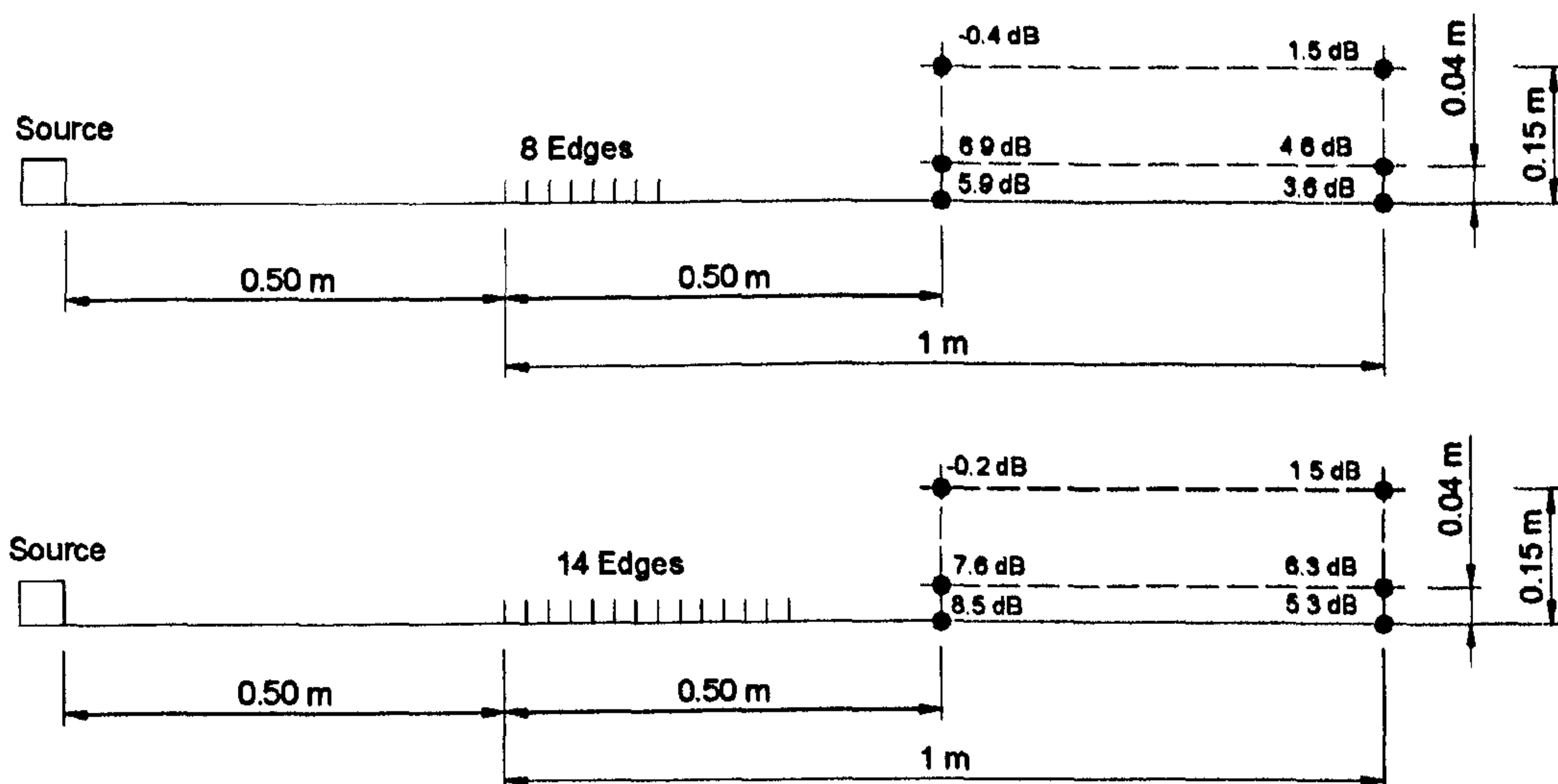
#### 8.2.1.2 Doubling of the Number of Wells

In the tests above, the progressive improvement in the performance by the increased number of edges was observed. Having established the superior performance of 8-edges over a single edge, the experiments were extended further to the investigation of the effect of more edges. It was decided to compare the 8-edge case to the 14-edge case, without examining the in-between cases any further. The configurations are chosen such that the number of wells is increased from 7 to 13, almost doubling in number.

The equipment used was the same as above. Random noise generator was connected to an amplifier and the noise output was kept constant throughout the test. The SPL with the configurations under consideration were monitored and compared with the SPL for a single edge case.

Source was kept at 0.5 m away from the first edge and was located on the ground. The case of 8 edges of 0.025 m x 0.025 m was monitored at 6 different receiver locations and compared with the single edge conditions at the same receiver locations. The first three receivers were placed 0.5 m behind the first edge at three different heights of 0, 0.04 and 0.15 m above the aluminium platform. The second set of receivers was placed at 1 m away from the first edge at the three different heights mentioned above. This was repeated for the 14-edge case. Details are seen in Figure 8.8.





**Figure 8.8 : The two configurations investigated showing the source and the receiver locations. The dB values included give the relative improvements over a single edge situated 0.5 m from the source.**

Relative improvement over a single edge (dB)		
Receiver co-ordinates	8 – edge case	14 – edge case
(50,0)	5.9	8.5
(50,4)	6.9	7.6
(50,15)	-0.4	-0.2
(100,0)	3.6	5.3
(100,4)	4.6	6.3
(100,15)	1.5	1.5

**Table 8-1 : Relative improvements of both configurations over a single (where the well depth and spacing are 0.025 x 0.025 m)**

The spectrums for the relative differences in sound pressure levels compared with the single edge case for both configurations are shown Figure 8.9 to Figure 8.12.



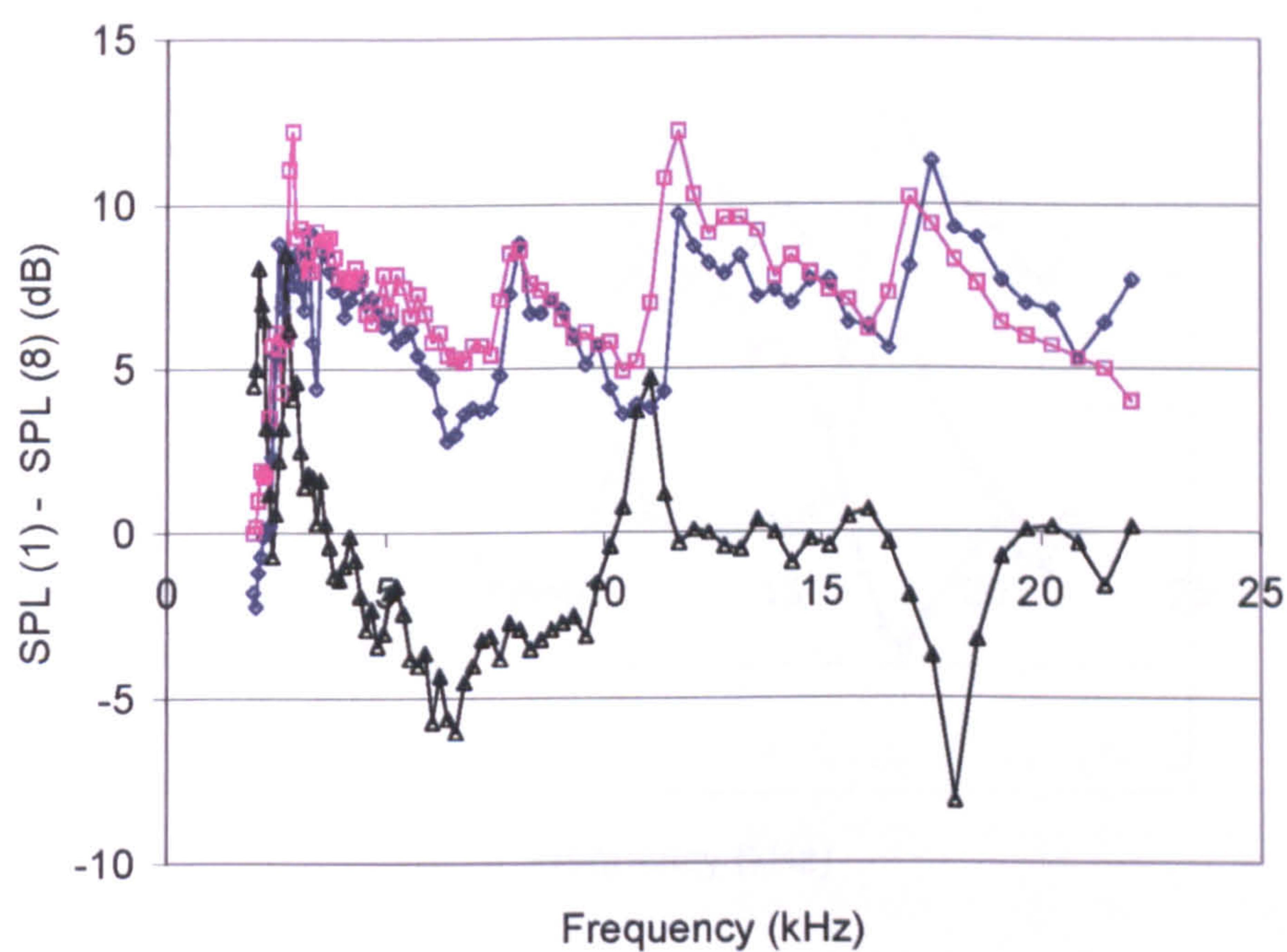


Figure 8.9 : Relative performance of 8 edges over a single edge (receiver distance = 0.5 m).

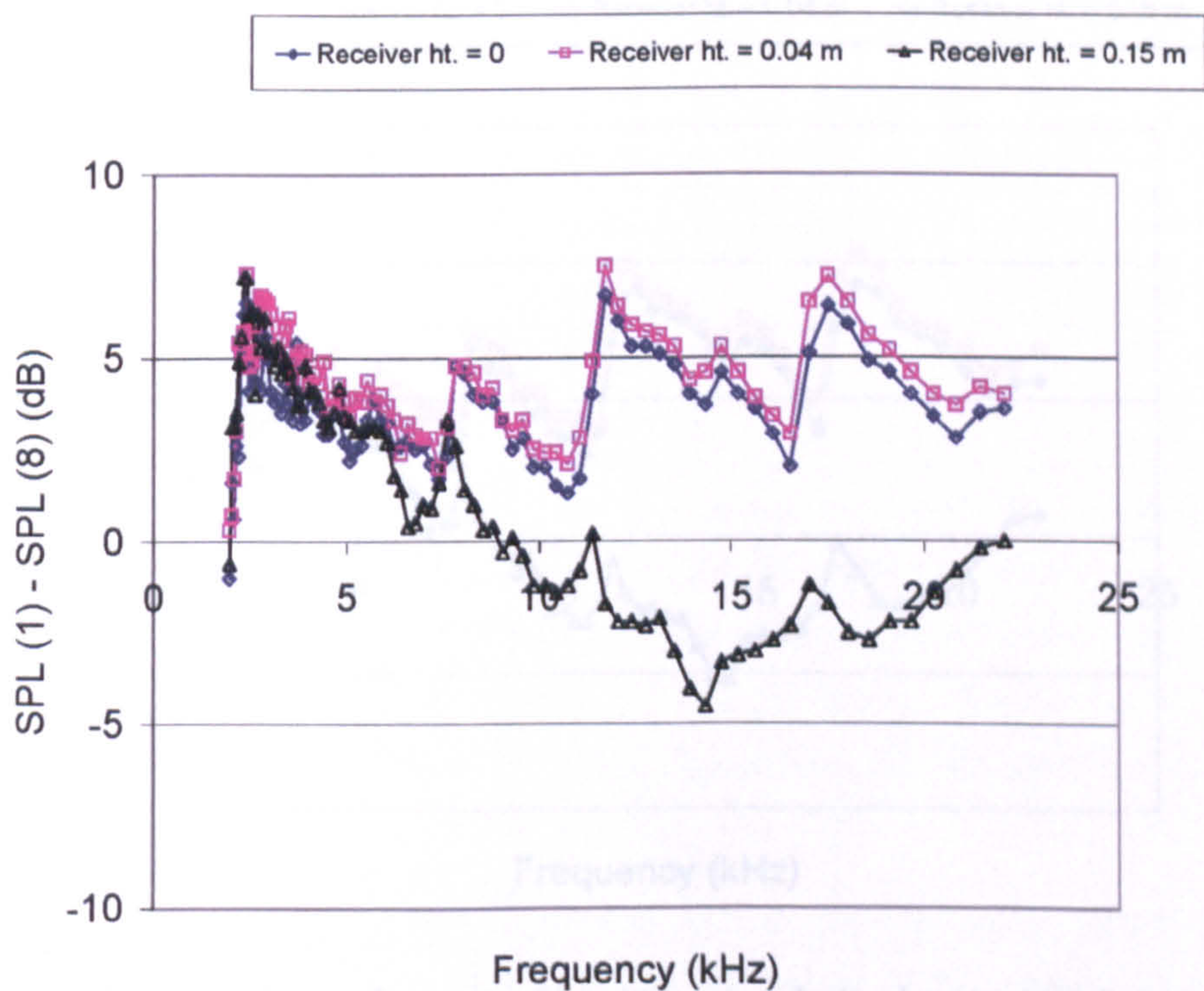


Figure 8.10 : Relative performance of 8 edges over a single edge (receiver distance = 1 m)



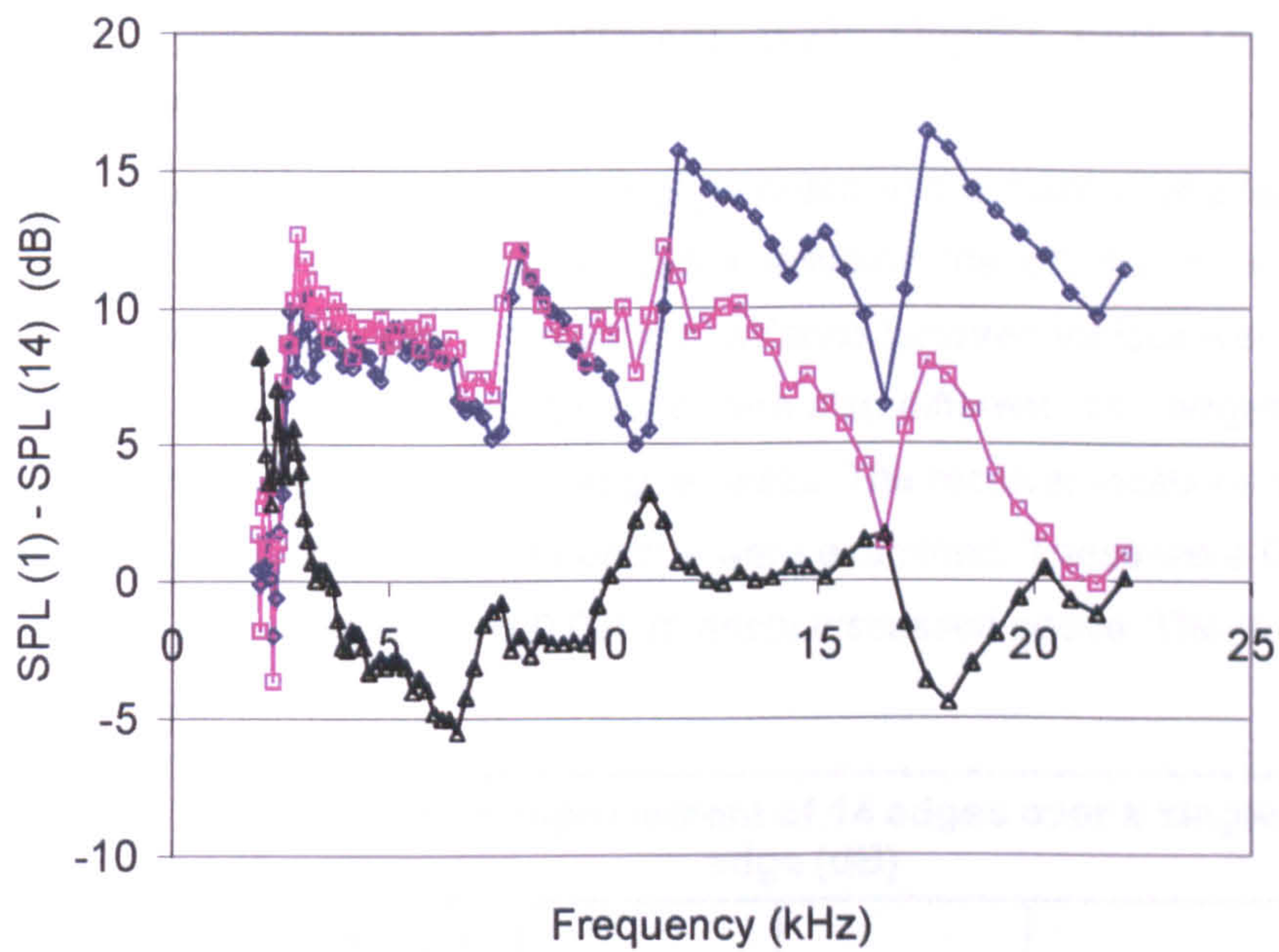


Figure 8.11 : Relative performance of 14 edges over a single edge (receiver distance = 0.5 m)

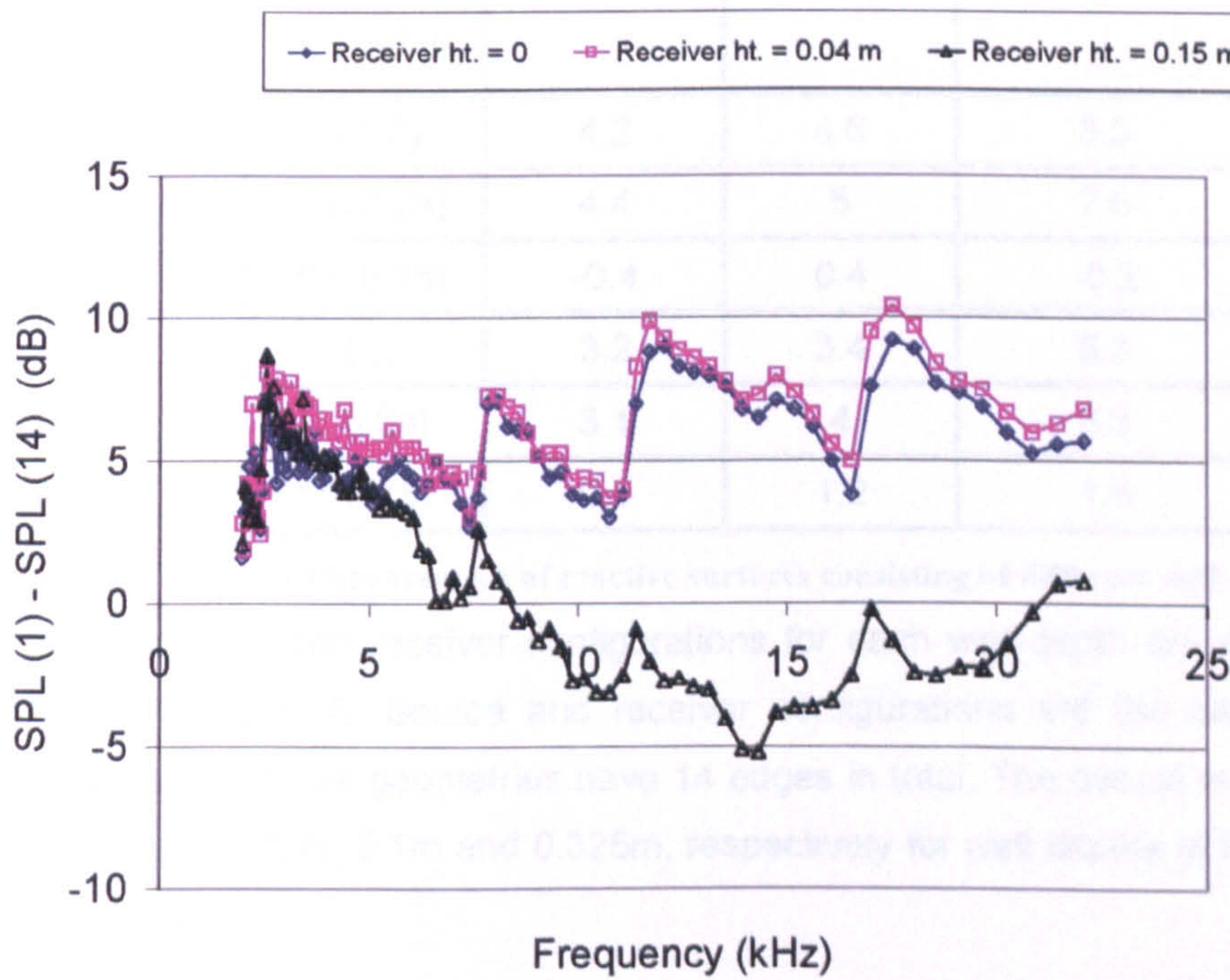


Figure 8.12 : Relative performance of 14 edges over a single edge (receiver distance = 1 m).



8.2.1.3 Comparison of Different Well Depths with Dissimilar Overall Widths

After realising the benefits of gradually increasing the number of edges, it was decided to fix the edge numbers at 14, and investigate the effects of various well depths. However the differences in separation distance between various well depths meant the overall width of the reactive surfaces were also different. 14 - edges were placed in a manner to form a series of rectangular wells. The receiver locations were the same six investigated above. Three well depths were examined. These were 0.017 m and 0.008 m depths compared with the 0.025 m depth discussed above. The results are tabulated in Table 8-2.

Relative improvement of 14 edges over a single edge (dB)			
Receiver co-ordinates (x, y) in m	D = 8mm	D = 17 mm	D = 25 mm
(0.5,0)	4.2	4.6	8.5
(0.5,0.04)	4.4	5	7.6
(0.5,0.15)	-0.4	0.4	-0.2
(1,0)	3.2	3.4	5.3
(1,0.04)	3.1	4	6.3
(1,0.15)	0.5	1.2	1.5

Table 8-2 : Relative improvement of reactive surfaces consisting of different well depths.

The geometries and receiver configurations for each well-depth are shown in Figure 8.13 to Figure 8.15. Source and receiver configurations are the same in all three geometries. All three geometries have 14 edges in total. The overall widths of reactive surfaces are 0.22m, 0.1m and 0.325m, respectively for well depths of 0.008m, 0.017m and 0.025m.

There were gains recorded in excess of that provided by a single edge for lower receiver locations. These diminished as the height of the edges were reduced. The edges became smaller than the physical centre of the source itself. This meant the line of sight from source to receiver was not grazing the top of the edges, nor was the receiver in the shadow zone. Therefore, it was decided to raise the edges above the ground sufficiently so that these conditions would be met for the lower receiver locations.



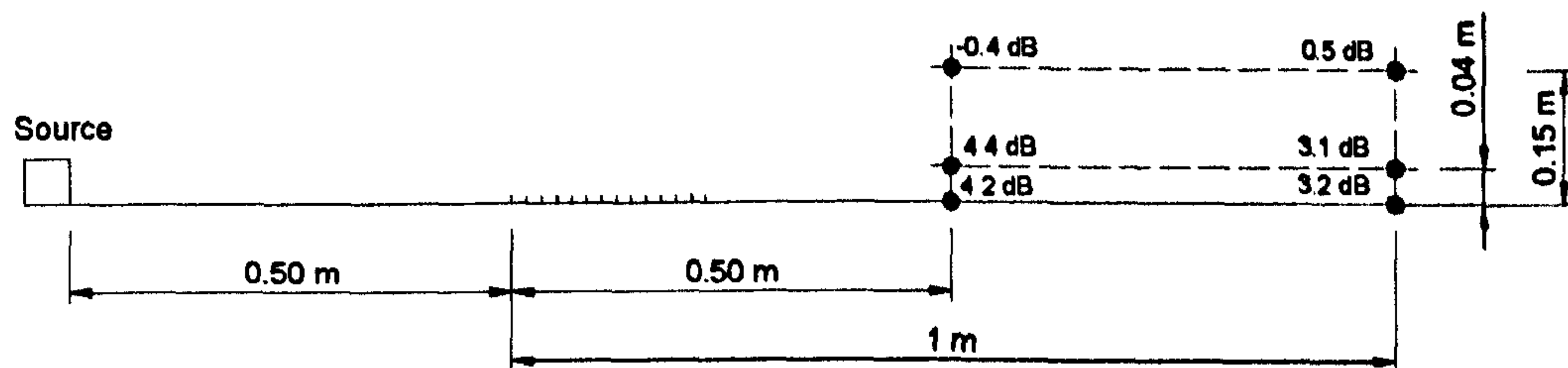


Figure 8.13 : The height of the wells is 0.008 m. The spacing between the edges is 0.017 m. Total width of the reactive surface is approximately 0.22 m.

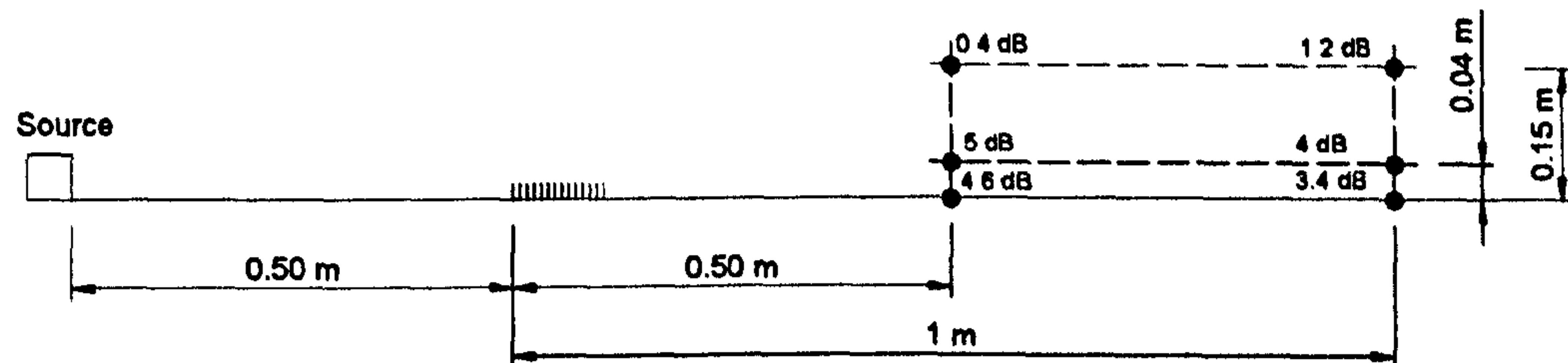


Figure 8.14 : The height of the wells is 0.017 m. The spacing between the edges is 0.008 m. Total width of the reactive surface is approximately 0.10 m.

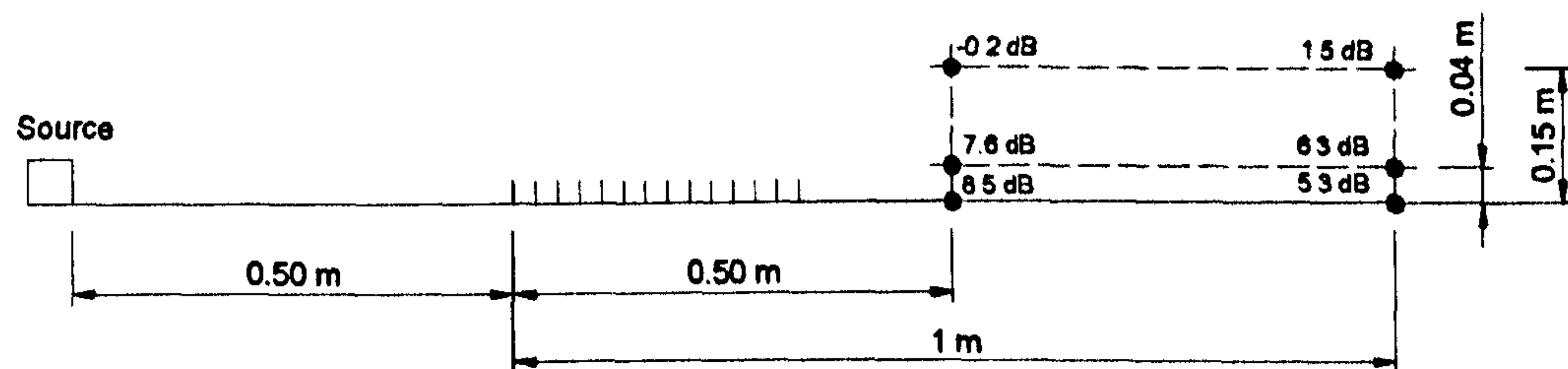


Figure 8.15 : The height of the wells is 0.025 m. The spacing between the edges is 0.025 m. Total width of the reactive surface is approximately 0.325 m.

The spectrums for the 0.008 m and 0.017 m deep edges are shown below.



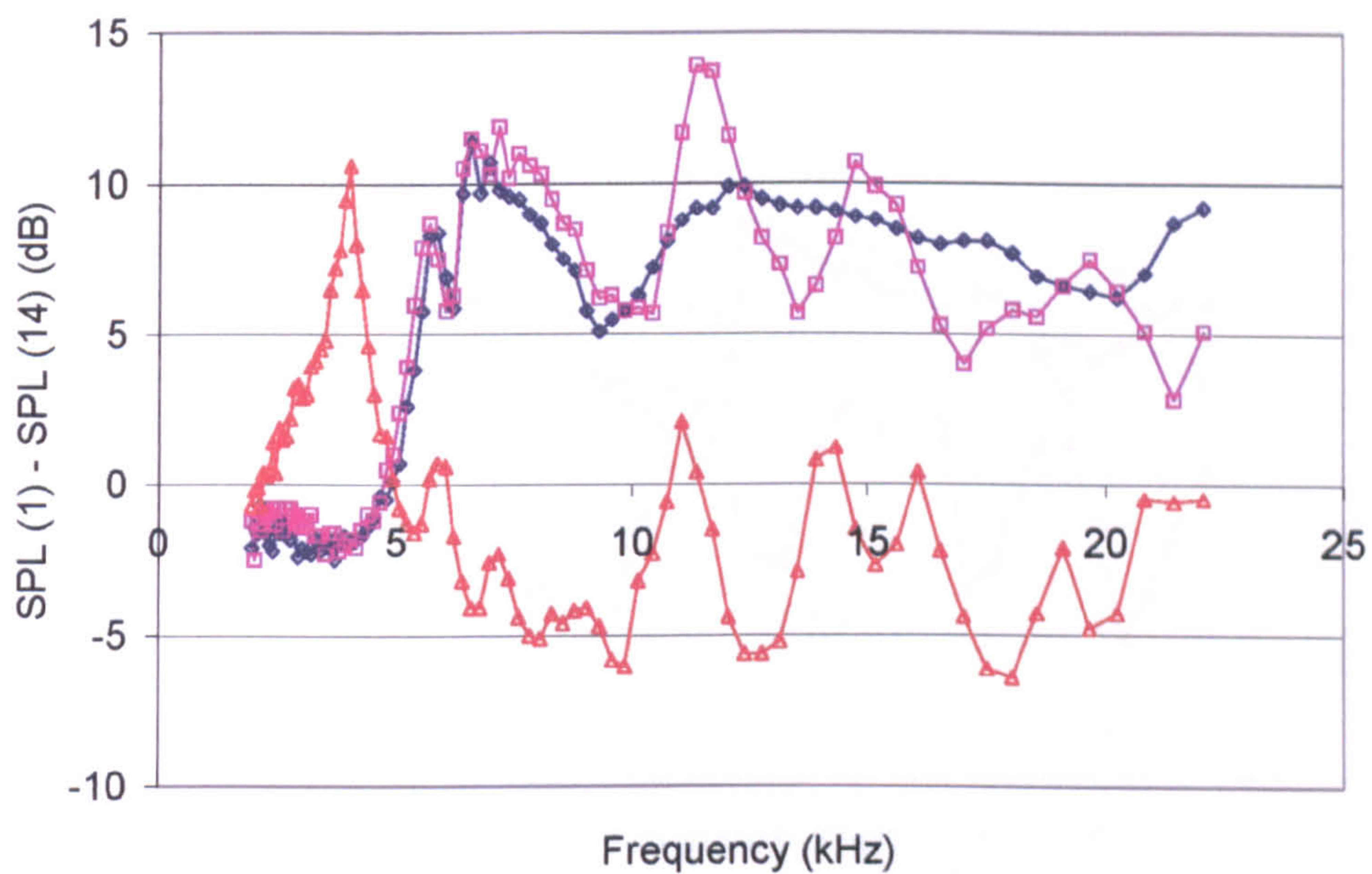


Figure 8.16 : Relative improvement of 14-edges over a single edge (edge height 0.008 m, edge spacing 0.017 m, receiver 0.50 m from first edge)

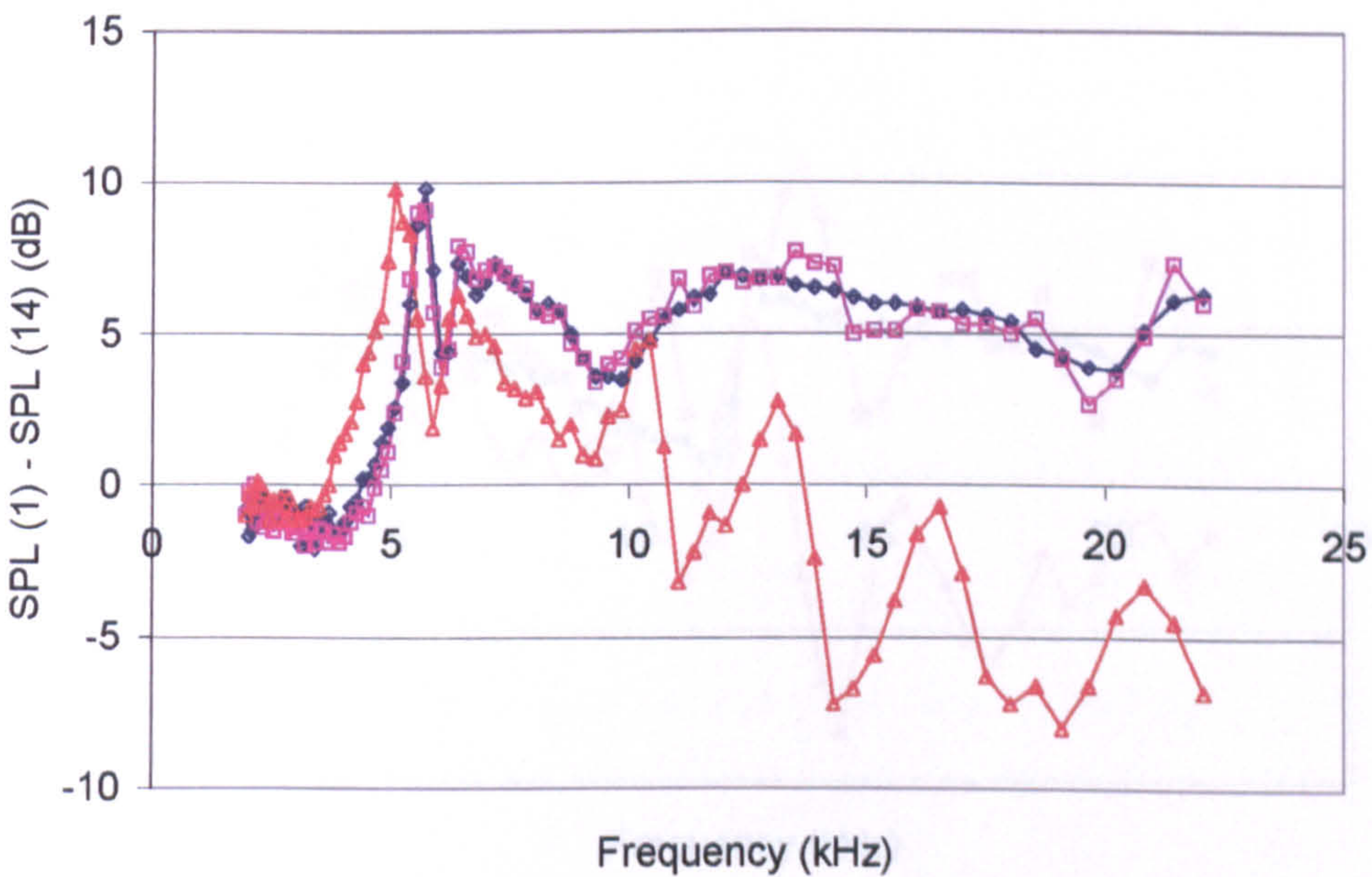
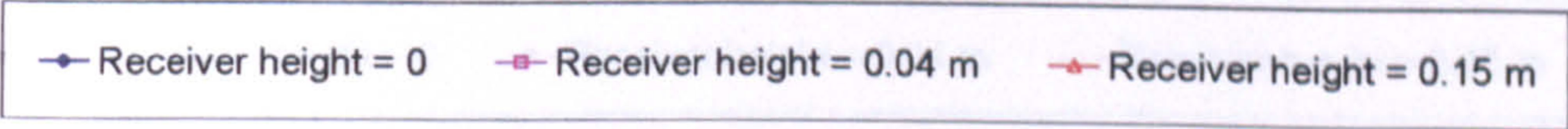


Figure 8.17 : Relative improvement of 14-edges over a single edge (edge height 0.008 m, edge spacing 0.017 m , receiver 1 m from first edge)





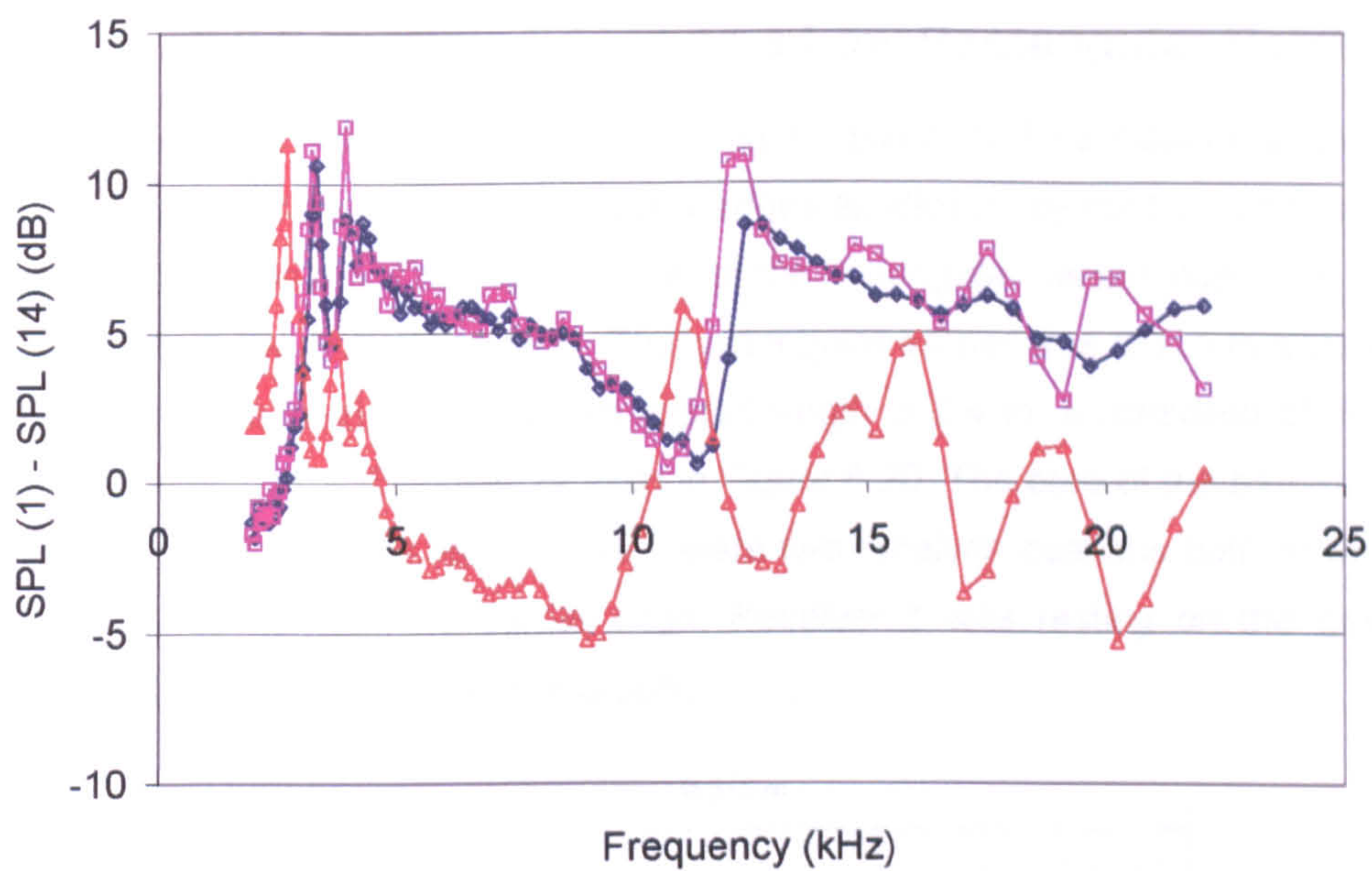


Figure 8.18 : Relative improvement of 14-edges over a single edge (edge height 0.017 m, edge spacing 0.008 m, receiver 0.5 m from first edge)

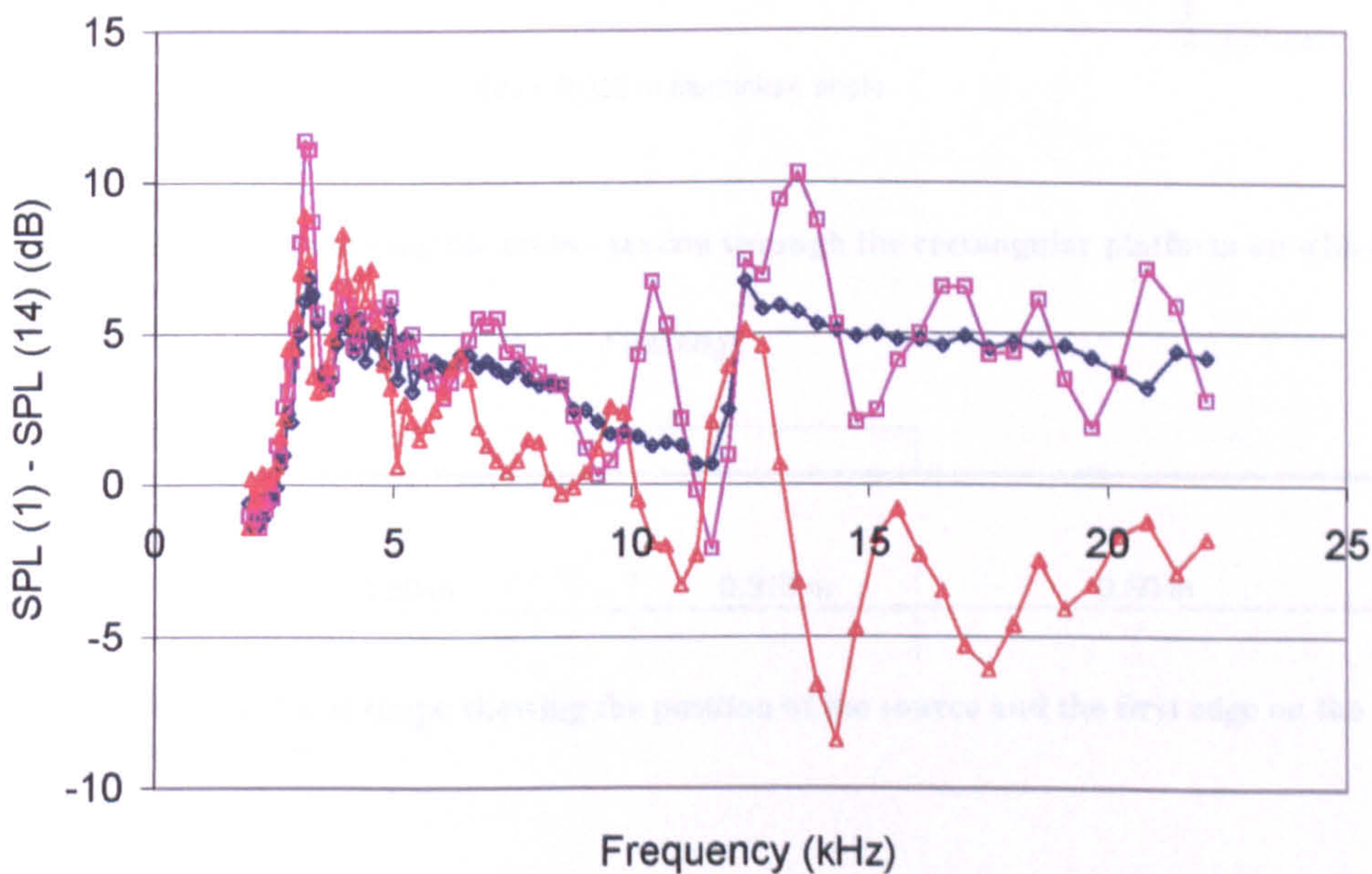
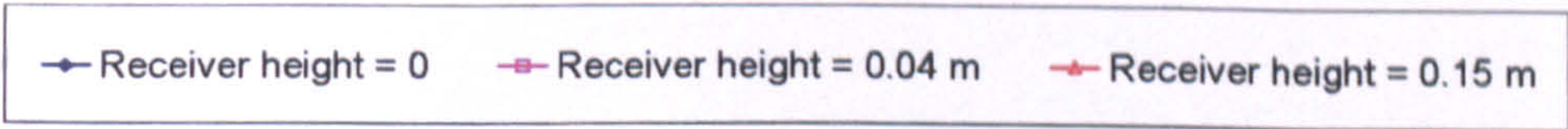


Figure 8.19 : Relative improvement of 14-edges over a single edge (edge height 0.017 m, edge spacing 0.008 m, receiver 1 m from first edge)





### 8.2.2 Multiple Edges on a Low Rectangular Barrier

The edges were set up on top of a rectangular platform. This meant that the width of the platform was fixed and only as many edges as allowed by the top horizontal section could be fitted on top. The insertion loss of the rectangular section itself was measured separately at the end of the tests. The rectangular barrier was 0.315 m wide and 0.05 m high in cross-section and had an overall length of 2.4 m. It consisted of interlocking aluminium sheets and angles as seen in Figure 8.20. The core of the barrier was filled with hardwood along its length. There were two receiver locations both of which were situated 0.50 m from the barrier edge. Receiver 1 was resting on the ground and receiver 2 was 0.04 m above the ground.

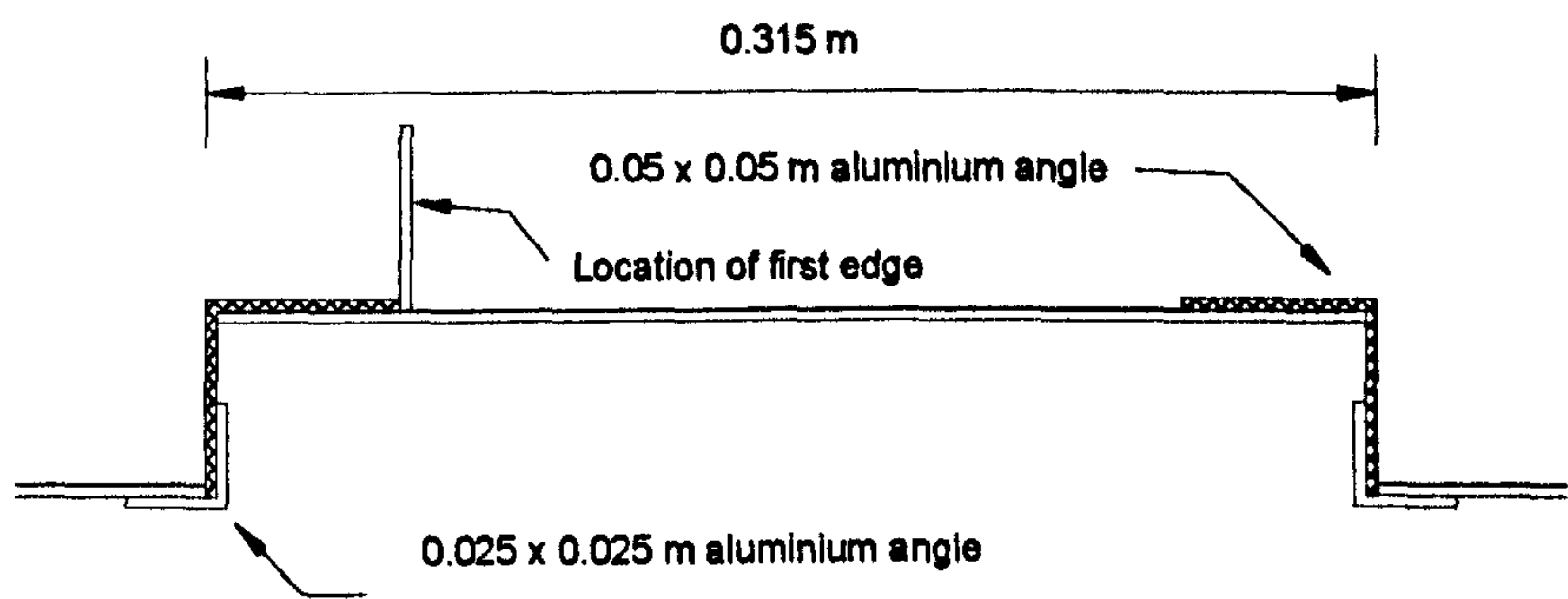


Figure 8.20 : Detail showing the cross - section through the rectangular platform on which the edges were placed.

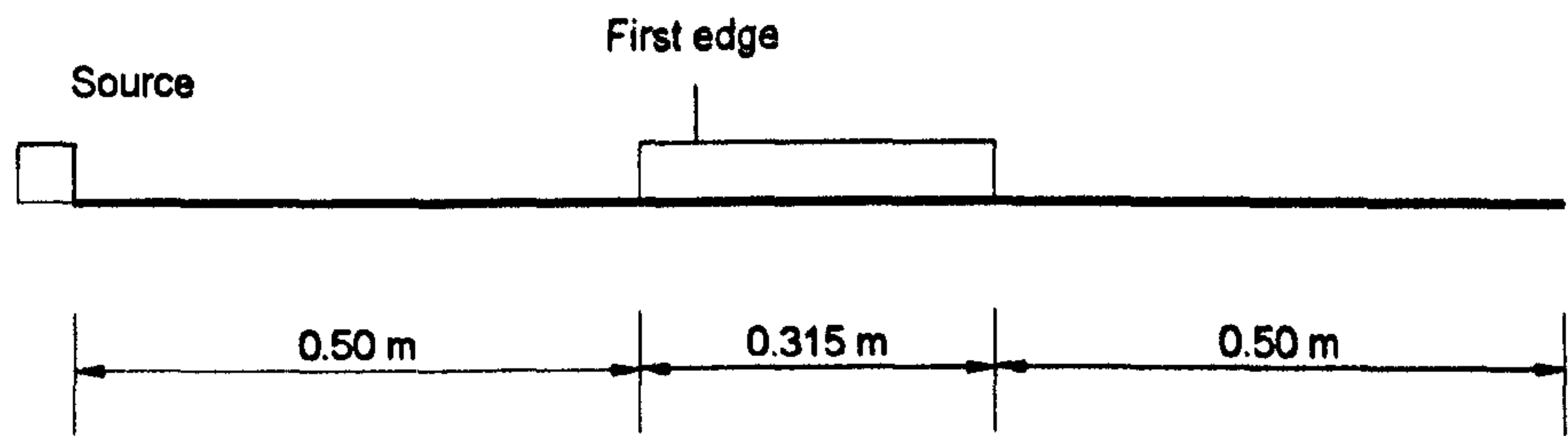
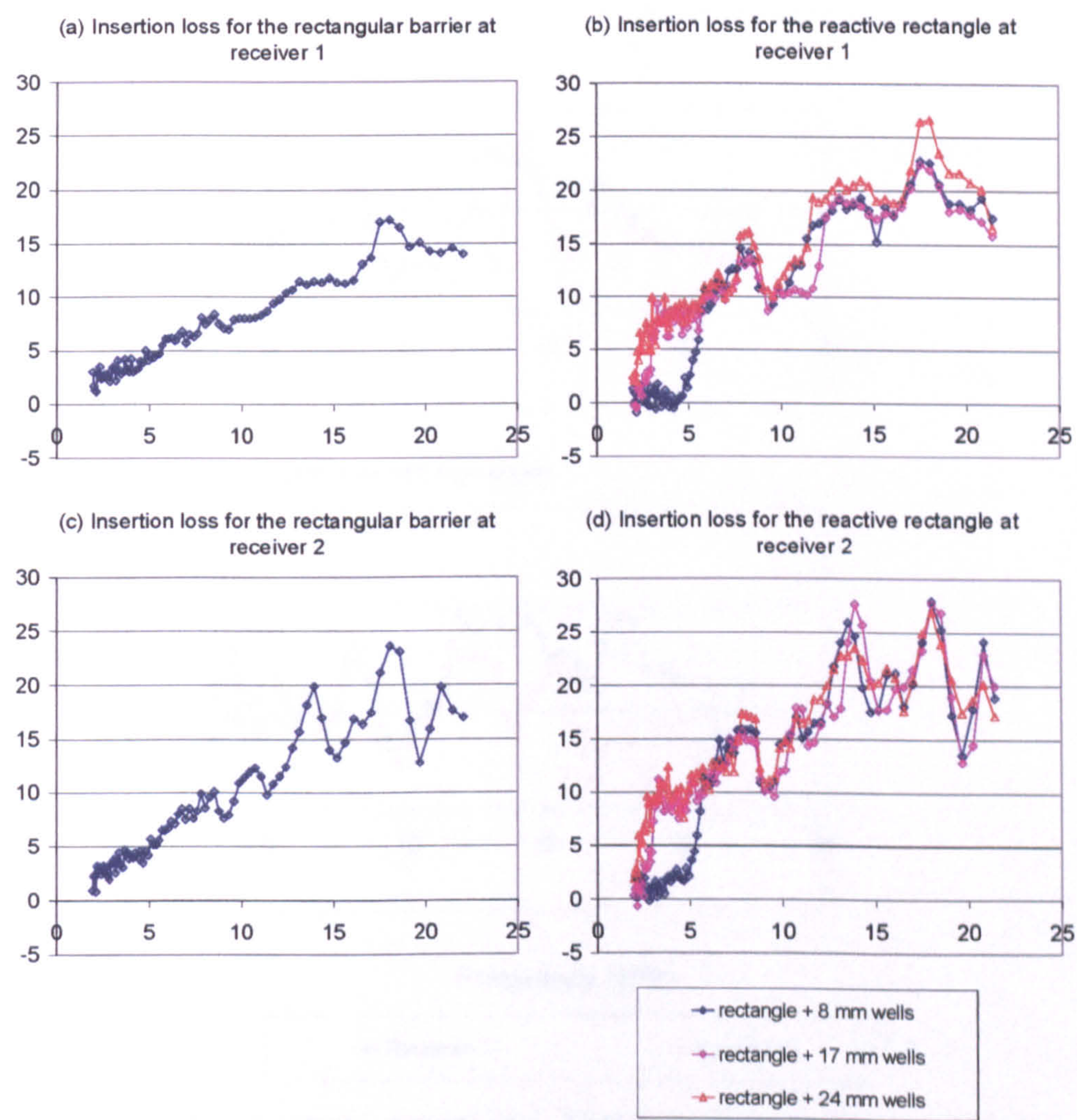


Figure 8.21 : The basic shape showing the position of the source and the first edge on the rectangular platform.



		Receiver (50, 0)		Receiver (50, 4)	
	Insertion loss of rectangular barrier (dB)	7		8.6	
	Additional effect of edges (dB)	Single Edge	Multiple Edges	Single Edge	Multiple Edges
Depth of the Edge	D = 50 mm	2.6	N / A	2.7	N / A
	D = 25 mm	1.5	5.2	1.3	4.7
	D = 17 mm	0.7	3.3	0.8	3.4
	D = 8 mm	0	1.9	0.1	1.7

**Table 8-3 :** The improvement due to the multiple edges over the basic shape.



**Figure 8.22 :** Comparison of the insertion loss values for the rectangular barrier alone and the reactive rectangular barriers with various well depths

The effects of the single edges of 50 mm, 25 mm, 17 mm and 8 mm edges have been investigated. Also, effect of multiple edges was examined. This was in the shape of 14



edges in the case of 8 mm edges, 15 edges for 17 mm edges and 11 edges for the 25 mm edges. Multiple edge configurations for the 50 mm edge were not investigated.

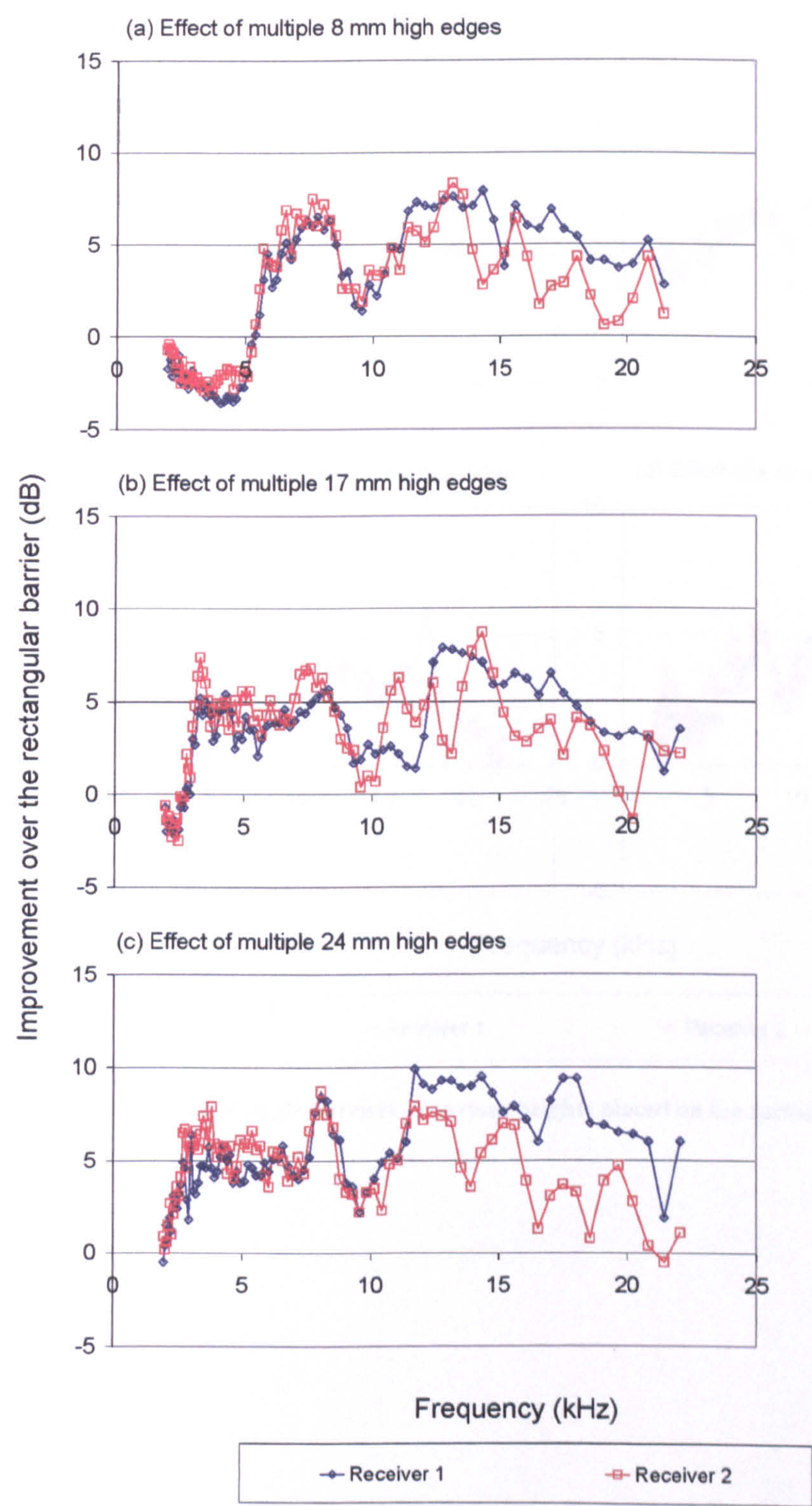


Figure 8.23 : Effect of multiple edges of various heights placed on the rectangular barrier



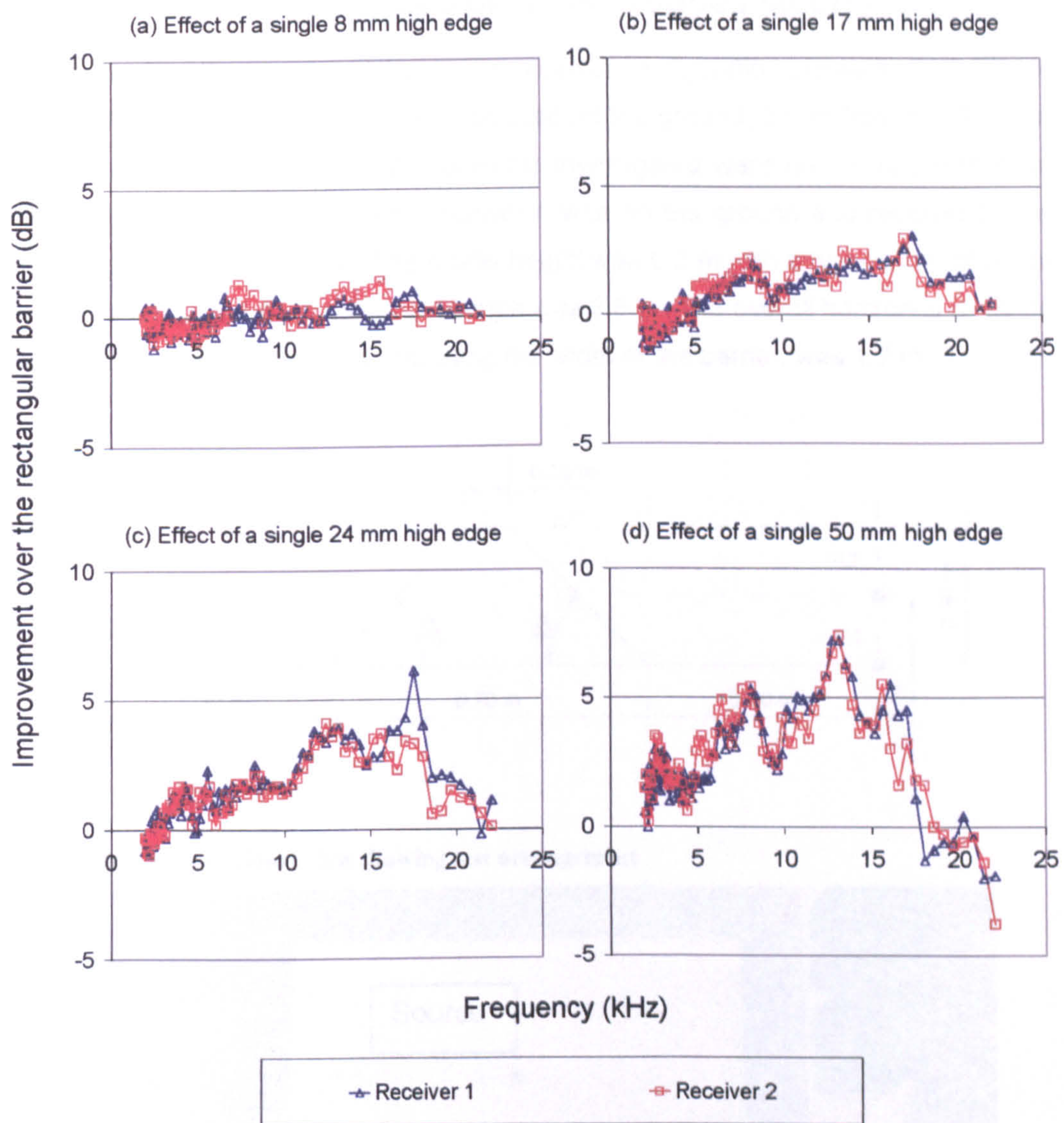


Figure 8.24 : Effect of single barriers of various heights placed on the rectangular barrier.



### 8.2.3 Multiple Edges on a Flat-Topped Mound

The details of earth mound and the source-receiver configuration are as seen in Figure 8.25 and Figure 8.26. The source was situated on the ground, 0.5 m from the "foot" of the earth mound. The two receiver locations investigated were on the opposite side, positioned 0.5 m from the barrier. Receiver 1 was on the ground and receiver 2 was 0.15 m high above the ground. The model height was 0.3 m with a base width of 0.7 m and a top width of 0.1 m. Total model length was 3.6 m. The overall horizontal distance from the source to the receivers, including the width of the barrier, was 1.7 m.

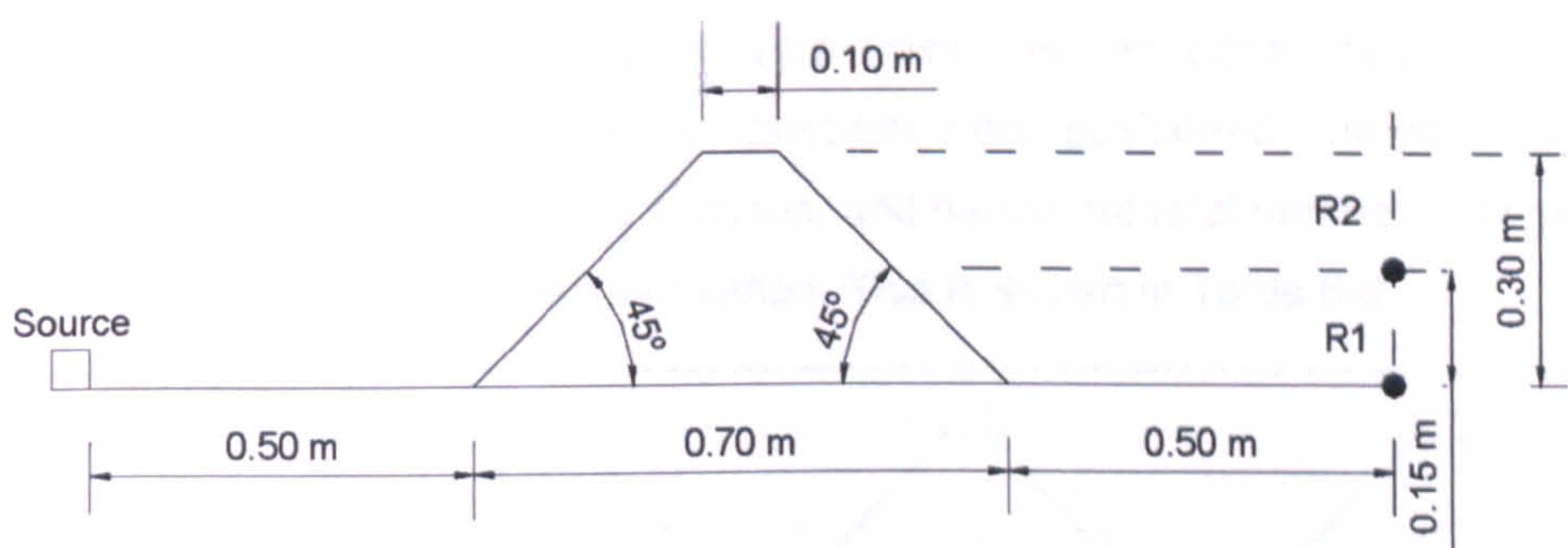


Figure 8.25 : Cross-sectional view showing test arrangement.

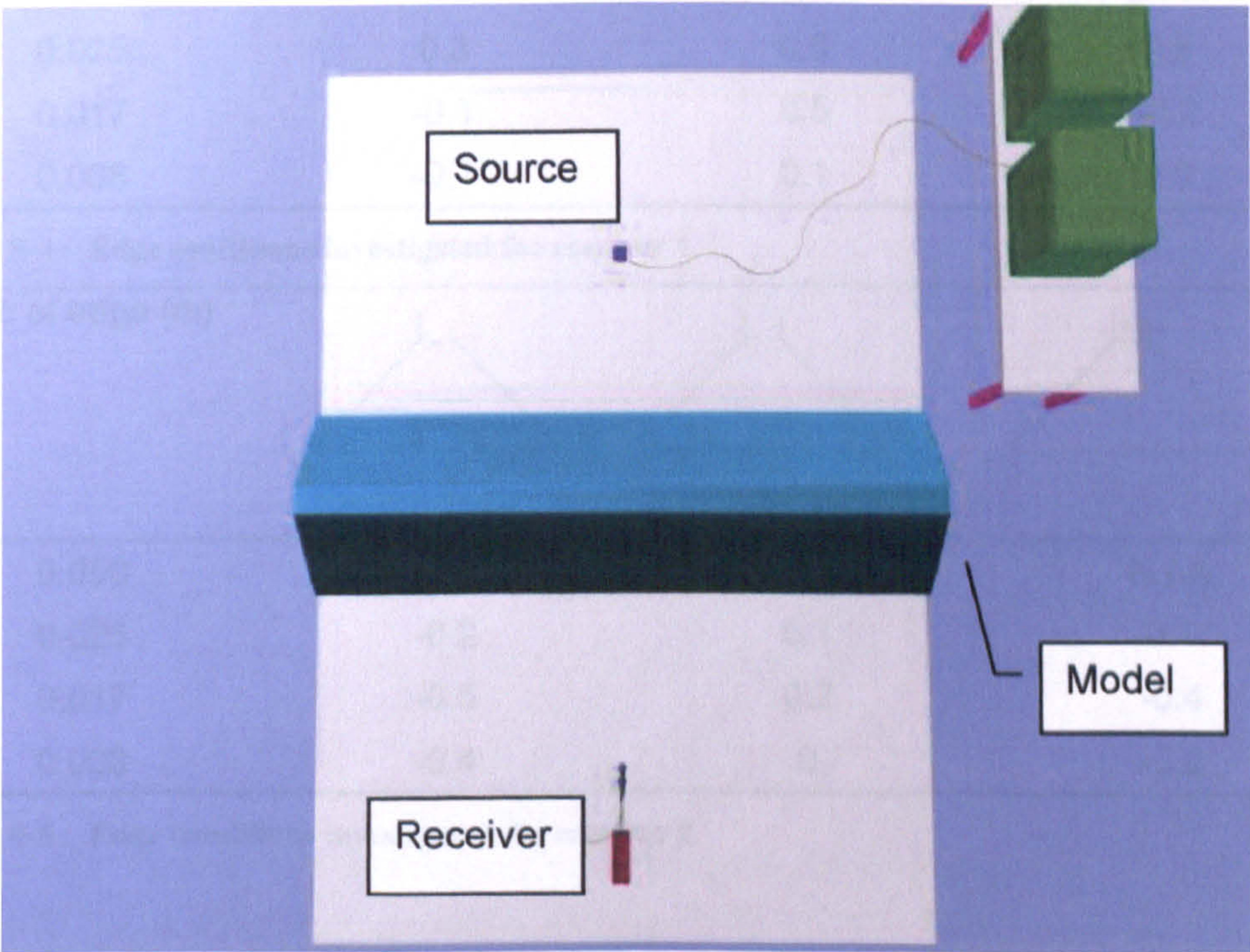


Figure 8.26 : Plan view of flat-topped earth mound configuration



Sound pressure levels at the receiver locations were monitored together with the sound pressure levels at a reference point of 0.30 m from the source situated on the ground. The total averaging time was 40 seconds for each measurement and 1/24 octave band frequencies were monitored with an 8-pass frequency analyser.

The experiments were carried out for 11 different configurations details and relative performances of which are shown in Table 8-4 and Table 8-5. Frequency range investigated varied from 2 kHz to 22 kHz. Five tests were carried out for each receiver position for every configuration. In addition to the single and multiple edge conditions, the double edge configurations were also investigated. The edges consisted of aluminium angles. The single edges were all placed on the source side of the top horizontal section, and double edges were positioned on either sides of the top horizontal section. As many edges as possible were positioned one after another, depending on the width of the angle sections, and hence the total number of edges and the separation distance between them varied. This is shown in Table 8-6.

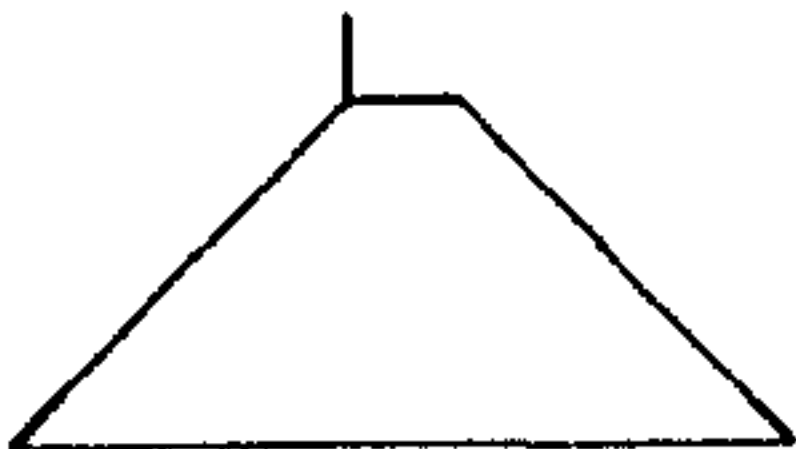

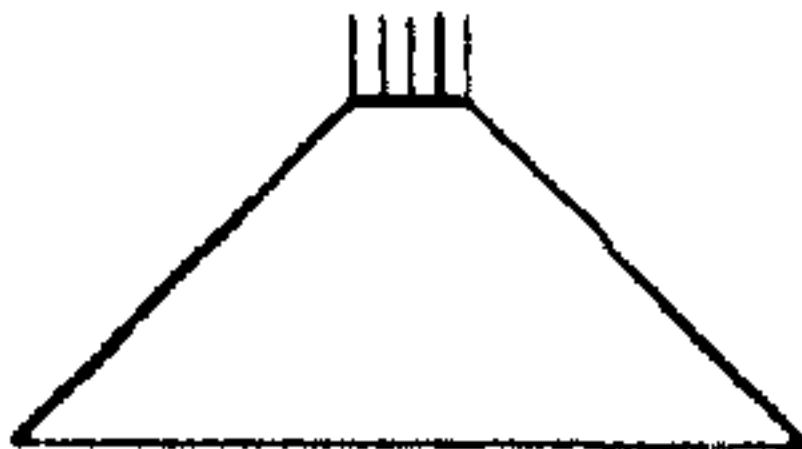
Depth of edge (m)			
0.050	0.4	0.3	N / A
0.025	0.3	0.5	0.5
0.017	-0.1	0.5	-0.2
0.008	-0.1	0.1	0.3

Table 8-4 : Edge conditions investigated for receiver 1.

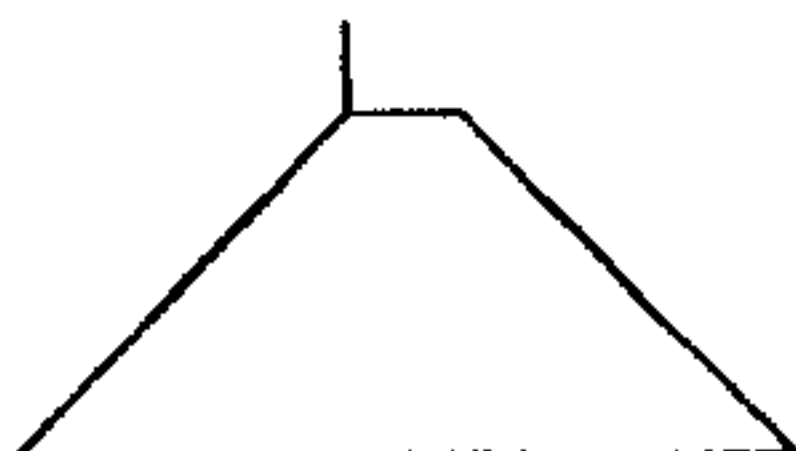
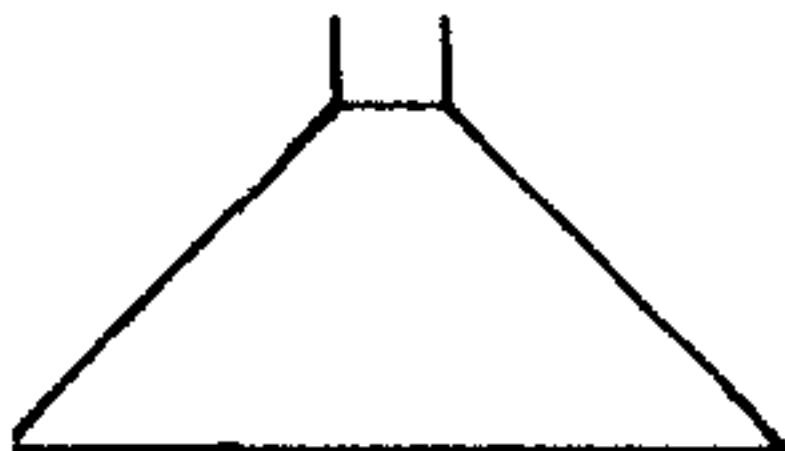
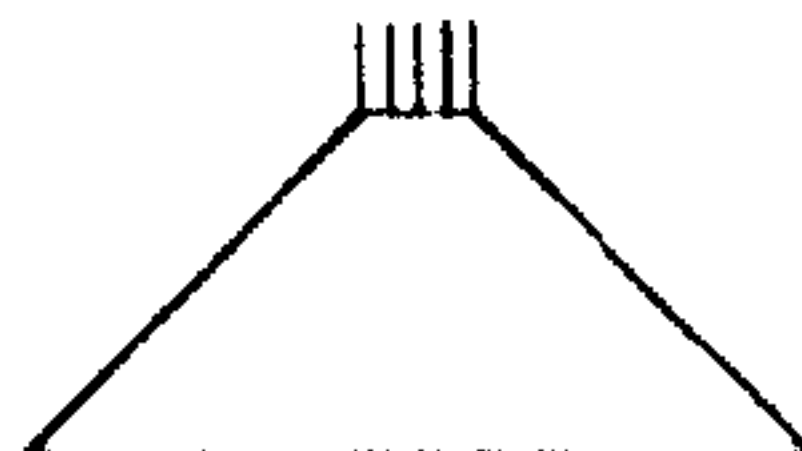
Depth of edge (m)			
0.050	0.5	0.4	N / A
0.025	-0.2	0.1	0.1
0.017	-0.5	0.2	-0.4
0.008	-0.4	0	-0.2

Table 8-5 : Edge conditions investigated for receiver 2.



Depth of edge (m)	Multiple Edges
0.050	n/a
0.025	total of 5 (separation = 0.025m)
0.017	total of 10 (separation = 0.008m)
0.008	total of 5 (separation = 0.017m)

Table 8-6 : The details of the reactive configurations.

The recorded differences were negligible. This is due to the masking effect of the reverberant field. The direct field is now subjected to much larger attenuation due to the size of the obstacle and hence the length of the path difference. Therefore, small modifications on top are not providing any contributions. The spectra of gains are shown in Figure 8.27.

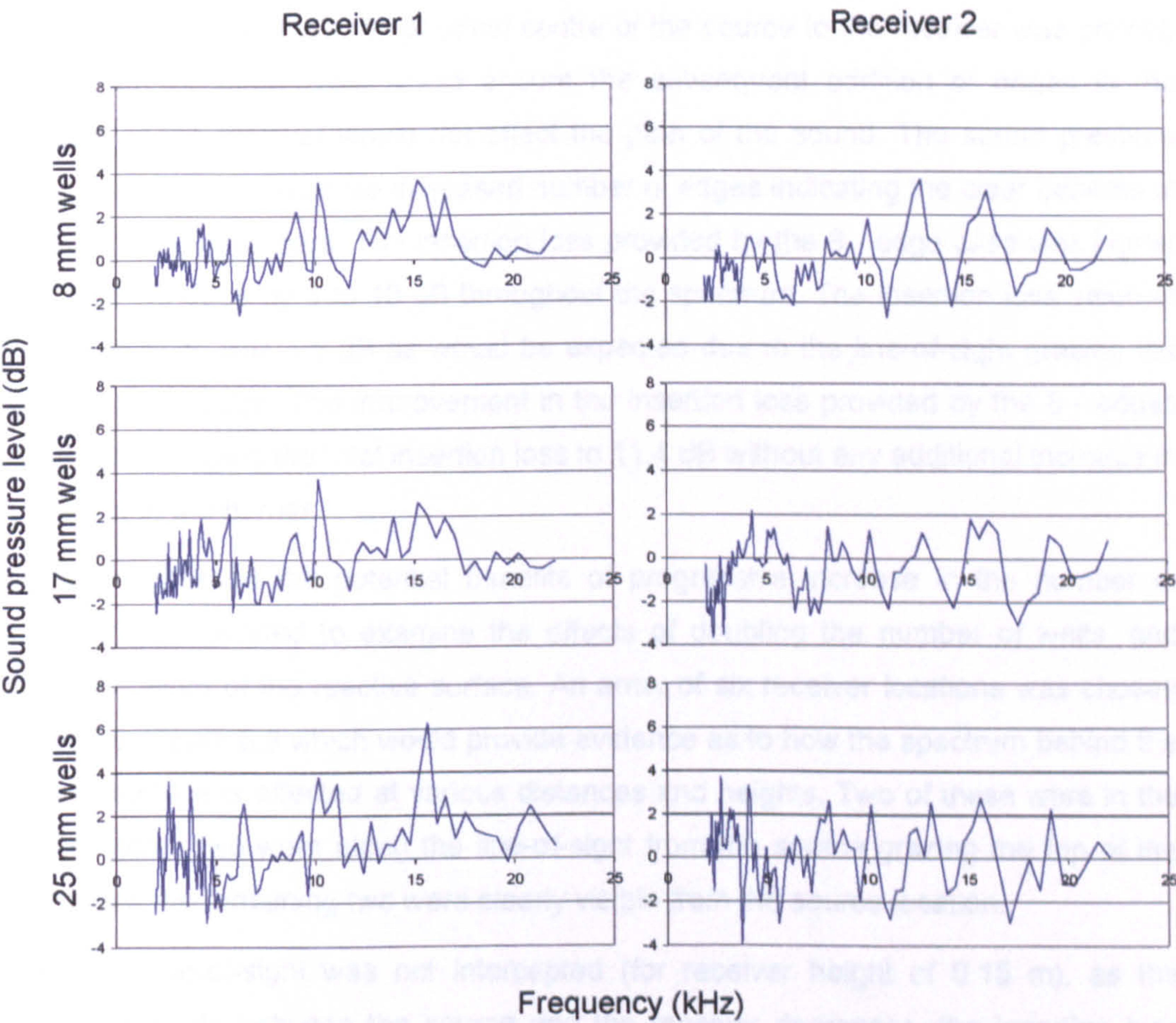


Figure 8.27 : The frequency spectrum of gains for various reactive configurations.

The differences between the various configurations and the basic mound shape were found to be very small. The insertion loss of the basic shape was measured as 9.3 dB for receiver 1 and 10.6 dB for receiver 2. Due to the high initial reduction of the direct sound, it is thought any contributions are completely masked by the reverberant sound,



and hence no change of any sort is recorded (either overall or in any individual frequency band).

### 8.3 DISCUSSION

This chapter looked at experimental investigation of reactive surfaces consisting of a series of wells on the ground and on top of earth mound type barriers. Instead of testing the modifications straightaway on top of a mound, the process has been split into stages where a series of wells were tested on their own. Since the geometry involved was small, it was considered the effects of reverberant sound would be small.

Initially, the progressive increase in the number of edges was investigated. The sound pressure levels were monitored at a single receiver location which was chosen such that the line-of-sight from the physical centre of the source to the receiver was grazing the top of the edge. This would ensure the subsequent addition of edges in the direction of the receiver would not affect the path of the sound. The sound pressure levels were reduced with the increased number of edges indicating the clear benefits of increased edge numbers. The insertion loss provided by the 8 - edge case was higher than a single edge by 5 to 10 dB throughout the spectrum. The insertion loss value of the single edge was 4.5 dB as would be expected due to the line-of-sight grazing the top part of the edge. The improvement in the insertion loss provided by the 8 - edges was 6.9 dB bringing the total insertion loss to 11.4 dB without any additional increase in the height of the barrier.

Having established the potential benefits of progressive increase in the number of edges, it was decided to examine the effects of doubling the number of wells, and hence the width of the reactive surface. An array of six receiver locations was chosen as seen in Figure 8.8 which would provide evidence as to how the spectrum behind the reactive surface is affected at various distances and heights. Two of these were in the shadow zone, two were along the line-of-sight from the source grazing the top of the edges, and the remaining two were clearly visible from the source location.

When the line-of-sight was not intercepted (for receiver height of 0.15 m), as the subtended angle between the source and the receiver decreases, the insertion loss increases. Even though the line-of-sight is not intercepted, the insertion loss still appears to be positive on average, for the receiver at 1 m away. This could be due to the line-of-sight being closer to reactive surface than for the receiver at 0.5 m away. Increasing the number of edges when the receiver is visible from the source position has no effect. When the receiver height is 0.15 m reduction in performance occurs between 3.5 kHz - 10 kHz and between 17 kHz - 20 kHz for the receiver situated 0.5 m



away (see Figure 8.9 and Figure 8.11) and at all frequencies above 9 kHz for the receiver situated 1 m away (see Figure 8.10 and Figure 8.12)

Provided the line-of-sight from the source to the receiver is intercepted, the improvement in performance is enhanced by the increased number of edges. For receiver positions which are in the shadow zone, tendency is a decrease in performance (for a given receiver height) as the receiver position is further away from the edges and a decrease in performance (for a given horizontal distance) as the receiver position is more in the shadow zone.

When the receiver is situated 1 m away from the 1st edge, the frequency signature of all receiver heights is similar. Moving from "8 edges" to "14 edges", increase in performance is pushed upwards (compare Figure 8.10 to Figure 8.12).

When the receiver is situated 0.5 m away from the 1st edge, for the 14 - edges case as seen in Figure 8.11, the performance of 0.04 m high receiver is less than that of the receiver on the ground, especially at higher frequencies above 11.5 kHz.

The spectra of the improvements relative to the single edge case for the receivers in the shadow zone have shown a distinctive "stepped" shape, where the distinctive peaks are followed by linear reductions in the gains. When we examine the difference between the single edge and the 8 - edge cases closer in Figure 8.28, an interesting observation can be made concerning the location of these peaks. This graph is for the well depth of 0.025 m where the receiver height is 0.04m above the ground and horizontally it is situated 0.5 m from the first edge.

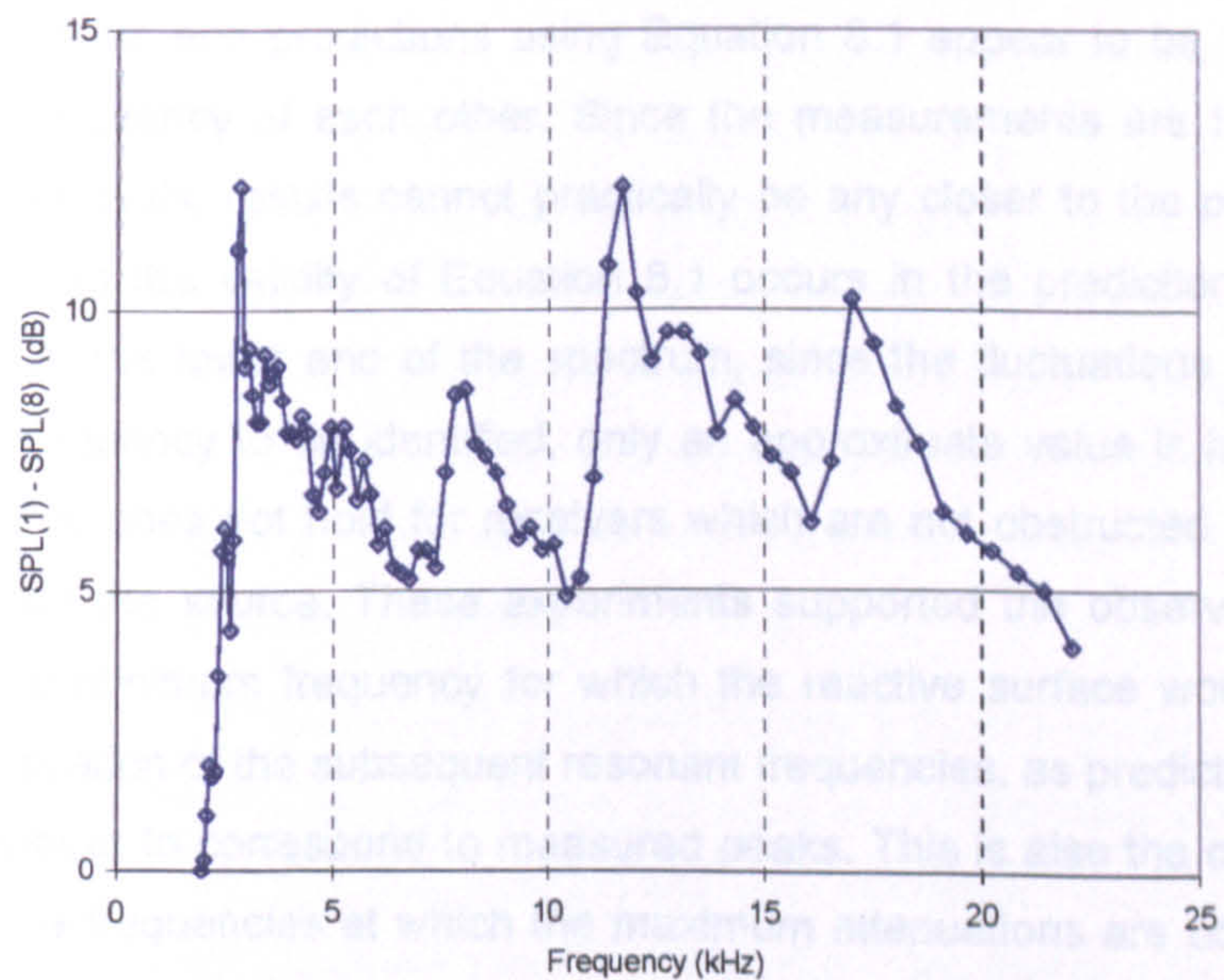


Figure 8.28 : Difference between the sound pressure levels in the presence of a single edge SPL (1) and 8-edges SPL (8).



In the experiments under consideration the channel depth was 0.025 m, which meant the corresponding lowest resonant frequency would be 3.4 kHz. The peaks appear to be 1.5 times the previous peak frequency. This observation can be summarised in the following form.

$$f_i = f_1 \left(\frac{3}{2}\right)^{(i-1)}$$

Equation 8.1

where  $i = 2, 3, 4...$ etc. The relationship identified in Chapter 6, regarding the location of the resonant frequencies is as follows.

$$d = (2n + 1) \frac{\lambda}{4}$$

Equation 8.2

The resonant frequencies can be predicted from above equation by substituting  $\lambda = v/f$ , where  $v = 340$  m/s. The predictions using Equation 8.1 and Equation 8.2 as well as the measured peaks from Figure 8.28 are summarised in Table 8-7.

Peak frequencies (kHz)	$f_1$	$f_2$	$f_3$	$f_4$	$f_5$
Predictions from Equation 8.1	3.4	5.1	7.65	11.475	17.213
Predictions from Equation 8.2	3.4	10.2	17	23.8	30.6
Readings from Figure 8.28	$\approx 3.00$	5.233	8.058	11.715	17.529

Table 8-7 : Predicted and measured peak frequencies.

The measurements and predictions using Equation 8.1 appear to be within a 1 / 24 octave band frequency of each other. Since the measurements are taken in 1 / 24 octave band intervals, results cannot practically be any closer to the predictions. The only exception to the validity of Equation 8.1 occurs in the prediction of the lowest frequency  $f_1$ . At the lower end of the spectrum, since the fluctuations do not allow a clear "peak" frequency to be identified, only an approximate value is included above. This relationship does not hold for receivers which are not obstructed from a straight line drawn from the source. These experiments supported the observation of others concerning the minimum frequency for which the reactive surface would be realised however the location of the subsequent resonant frequencies, as predicted by Equation 8.2, do not appear to correspond to measured peaks. This is also the case for the 14-edge case. The frequencies at which the maximum attenuations are observed remain similar to those for the 8-edge case. An alternative explanation for the location of the maximum attenuations could be the diffraction grating effects.

The maximum value of destructive interference would be expected to appear when



$$\frac{m \lambda}{2} = w (\sin \alpha + \sin \beta) \quad \text{Equation 8-3}$$

Where;

$\alpha$  is the angle of incidence

$\beta$  is the angle of diffraction

$m$  is the order of diffraction (= 0, 61, 62, etc)

$w$  is the horizontal spacing between diffracting elements

For the configuration considered, the angles of incidence and diffraction are both approximately 90 degrees. Due to the sign convention described in chapter 6, the angle of diffraction has a negative value. Therefore substituting these into above equation gives zero on the right hand side of the equation. This would only be valid for zero diffraction orders ( $m = 0$ ) (i.e. specular reflection) for all frequencies. At diffraction angles other than at grazing incidence (i.e. the receiver 1.5m high), the grating separation is too small to give any physically realisable diffraction orders within the range of frequencies considered.

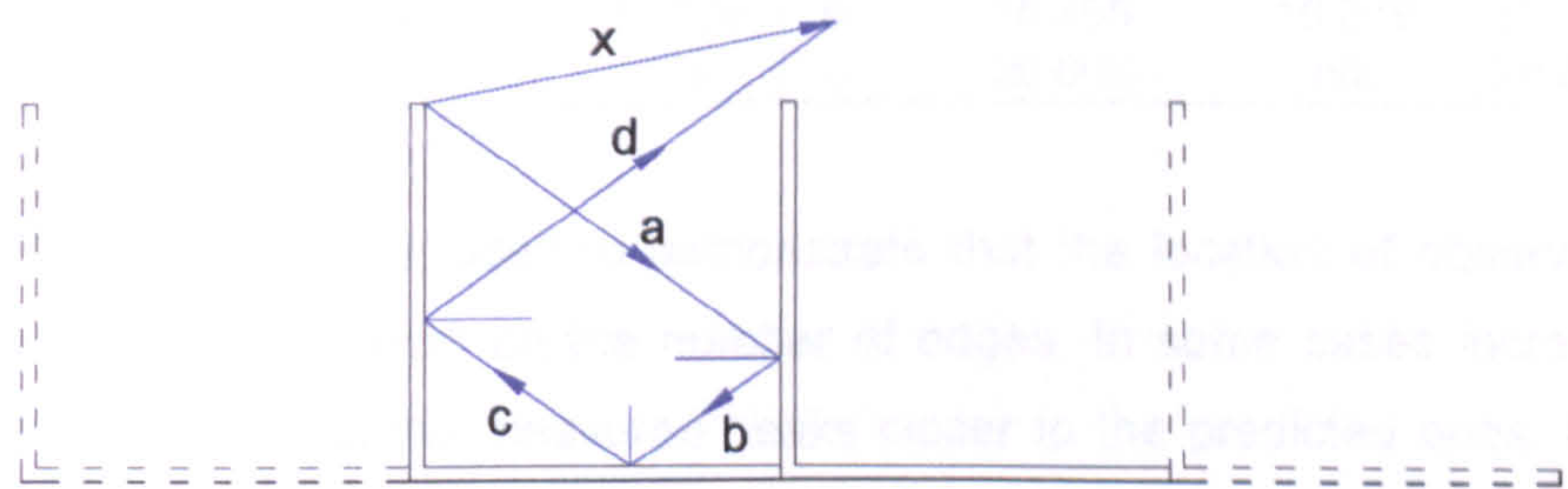
The investigation was extended to different well depths to identify whether the observations on the maximum attenuations would be valid. The gains recorded in the case of well depths of 0.008 m (see Figure 8.16 and Figure 8.17) and 0.017 m (see Figure 8.18 and Figure 8.19) were still substantial even though any potential peak frequencies are less readily identifiable. The lowest resonant frequencies for these two well depths are around 10.625 kHz and 5 kHz respectively. The experimental results indicated that these are more likely to be situated around 5.7 kHz and 3.2 kHz. The readings are 1 / 2 and 2 / 3 times the predicted peaks. Therefore the empirical relationship above relating the peak frequencies does not hold for different well depths. It should be noted that the total width of reactive surfaces are not equal. There is a possibility that different aspect ratios of well depth to separation distance in conjunction with different reactive surface widths could reveal a more conclusive relationship. This would require further parametric studies.

The negative performance at low frequencies (Figure 8.16 to Figure 8.19) should also be noted. These were not so prominent in the case of 0.025m wells discussed earlier. The surface wave generation mechanisms identified in Chapter 6 could be responsible for the reductions in performance and these become more visible with decreased well heights.

Quarter wavelength resonance, diffraction effects (but not necessarily the 'grating' effects) and surface wave generation mechanisms all offer partial explanations for the



experimental results. It may be recalled from Chapter 6 that these were identified as the three likely noise attenuation mechanisms for multiple-edges. The relative sizes of the peaks (maxima and minima) in Figure 8.28 could offer some additional clues towards explaining the experimental results better. One likely mechanism would be interference effects between direct and multiply reflected (within the wells) ray paths as represented in the following diagram.



For clarity only a single well comprising two adjacent aluminium angles is shown. Each angle has the dimensions 0.025 x 0.025 m. The direct path is represented by path x and the multiple reflections are indicated by the path a, b, c and d. This particular diagram shows only 3 reflection paths within the well. However a number of alternative path diagrams would be possible for this geometry depending on the choice of the path a.

It is possible to obtain a path length difference,  $\delta_x$ , of 0.066m between the direct and multiple diffracted paths by assuming the above edge dimensions and the path diagram.

Over a hard ground, attenuation maxima (destructive interference) would occur at frequencies corresponding to path length differences,  $\delta_x$ , which are odd multiples of half-wavelength. These frequencies can be represented as follows

$$\delta_x = (2n + 1) \frac{\lambda}{2} \text{ where } n = 0, 1, 2 \text{ etc}$$

Similarly, an attenuation minimum (constructive interference) would be expected to occur at frequencies corresponding to path length differences,  $\delta_x$  which are even multiples of half-wavelength. This can be represented as shown below

$$\delta_x = (2n) \frac{\lambda}{2} \text{ where } n = 0, 1, 2 \text{ etc}$$

The following table shows the peak frequencies (maxima and minima) as predicted from above equations assuming a path length difference of 0.066m, compared with the peaks observed in Figure 8.28 and Figure 8.12.



n	Maxima (kHz)				Minima (kHz)			
	(2n+1)	Calculated	Observed (Figure 8.28)	Observed (Figure 8.12)	(2n)	Calculated	Observed (Figure 8.28)	Observed (Figure 8.12)
0	1	2.576	2.850	2.548	0	0	n/a	n/a
1	3	7.727	8.058	7.830	2	5.152	6.780	7.390
2	5	12.879	11.715	11.715	4	10.303	10.441	10.746
3	7	18.030	17.031	17.529	6	15.455	16.079	16.548
4	9	23.182	n/a	n/a	8	20.606	n/a	20.833

Figure 8.12 results are included to demonstrate that the location of observed peaks may slightly vary depending on the number of edges. In some cases increasing the number of edges brings the measured peaks closer to the predicted ones. Overall, it can be seen that there is a good agreement between the predicted and measured constructive and destructive interference peaks. These observations would be applicable to results shown in Figures 8.9 to 8.12, for near-grazing propagation. However for the receiver height of 0.15m, there are no clear patterns.

Similarly, the approach of interference peaks does not appear to be applicable to the results for well depths of 0.017m and 0.008m (shown in Figure 8.16 to Figure 8.19). These graphs do not show any evident trends which are comparable to those discussed above. It is possible that the interference mechanisms are more complex and therefore do not conform to an obvious pattern. This would require further investigations to verify. One possibility for investigating this mechanism could be by applying absorbent materials within the wells and observing the relative sizes of the resulting peaks. However this is beyond the scope of this research project.

Comparing the single value indicators in Table 8-2, the relative performance of a reactive surface at any given receiver location diminishes with reduced well depth. Excluding the receiver locations which are visible from the source, the gains over the single - edge cases on average are 3.7 dB, 4.3 dB and 6.9 dB for well depths of 0.008 m, 0.017 m and 0.025 m respectively.

The reactive surfaces were also tested on top of a low rectangular barrier as shown in Figure 8.20 and Figure 8.21. The summary of results in Table 8-3 show that the reactive configurations including the edges and the reflective rectangle provide gains in excess of that offered by the rectangle alone or a rectangle with a single edge on top. When the edge heights are translated into real dimensions by using 1:10 scale, these gains are more readily appreciated. The reactive configuration consisting of 0.17 m wells will match the performance of a single barrier of 0.5 m height, even though it is shorter by a threefold.



In Figure 8.22 the insertion loss of the rectangle and the reactive rectangle with three well depths are compared for receivers 1 and 2. In Figure 8.22 (a), for receiver 1, which is resting on the ground, the insertion loss increases from 2 dB to around 15 dB almost in a linear fashion. Slight deviation from linearity occurs at the higher end of the frequency spectrum, possibly due to the acoustic centre of the source not being located exactly on the ground (interference occurs between the direct rays and the ground reflected rays on the source side meeting on the barrier top). In Figure 8.22 (b), all three reactive rectangle systems perform better than the plain rectangle except at low frequencies. As the well depth is increased, the low frequency performance is clearly enhanced while the rest of the spectrum remains similar for all systems. Insertion loss of rectangle at receiver 2, as shown in Figure 8.22 (c) exhibits peaks and troughs due to the interference phenomena. The first one appears at around 13 kHz, which corresponds to the quarter wavelength of length of the path difference (on receiver side,  $\delta = 0.79$  cm and  $f = 10711$  Hz.  $\delta$  should be 0.65 cm to obtain 13000 Hz. Approx. 15 mm difference due to geometrical imperfections). In Figure 8.22 (d), reactive rectangle systems at receiver 2 show similar tendencies as discussed earlier for receiver 1. Compared with the plain rectangle at this receiver location, the low frequency performance decreases for all three well depths and the remaining of the spectrum are superior to that of the plain rectangle, being similar for all three systems.

Comparing the performance of reactive rectangle systems in Figure 8.22 (b) and (d) for the two receiver locations, it can be deceptive to realise the insertion losses at receiver 2 are greater than those for receiver 1. The reason is the initial higher insertion loss values of the receiver 2 compared with receiver 1 as seen in Figure 8.22 (c) and (a) respectively.

The “relative effects” of the reactive tops should hence be compared at the two receiver locations in isolation from the effects of the rectangular barrier. This can be seen in Figure 8.23 (a) to (c) where the effects of the multiple edges at the two receiver positions for three different well depths are shown. The effects of the reactive surfaces appear to be exactly the same up to around 12 kHz for both receivers. The performance of receiver 2 diminishes at higher frequency for all three well depths compared with receiver 1. The negative contributions of the 8 mm wells at frequencies below 5 kHz are immediately noticeable. These are likely to be due to surface wave generation at low frequencies. As the well depth is increased, this negative effect is shifted to as low as 2.5 kHz for 17 mm wells, disappearing completely for 25 mm wells. As it was discussed earlier, increasing the depth of the reactive surface reduces the lowest frequency for which the surface can be considered reactive. Therefore there will be an optimum depth where the low frequency performance will be positive. In this case, this depth seems to 25 mm for the specific geometry investigated.



The high frequency performance for all three well depths at both receivers is disappointing, the contributions to the performance approaching zero at around 20 kHz. Positive contributions at mid-frequencies for all three systems at both receivers (except at 10 kHz) are prominent. The frequency range of 5 – 15 kHz where favourable contributions were noted would represent the peak of the A-weighted traffic noise spectrum corresponding to a range of 500 Hz to 1500 Hz at the scale factor of 1:10.

Figure 8.24 show the effects of single edges when placed on top of the rectangular barrier on their own. As it is shown in (a), the contribution of the 8 mm edge is very small and these contributions increase as height of the single edge increases. This effect is prominent between frequencies 10 – 20 kHz, peak of the spectrum moving towards the lower frequencies with increased edge height and hence path length difference. The 50 mm edge has been additionally investigated in this case to observe the trends. The negative effect on the contribution at 20 kHz is worth noting.

When the effects of the series of wells were segregated from the whole system the favourable contributions were encouraging and hence the wells were placed on top of an earth mound. Increased path length meant the contributions from the reverberant sound were possibly masking any potential gains that might have been present. The predicted lowest frequencies for the reactive surface to be realised are not clearly visible as before. However, for the 25 mm wells there are gains up to 4 dB around 3-4 kHz which is not matched by the other well depths. The peak of these gains seems to drift towards 5 kHz but the gains are not conclusive. On the other hand, 8 mm wells show almost no gains around these frequencies. Around 11-12 kHz and beyond, the 8 mm wells perform slightly better than the other two well depths. Even though there are slight gains at around what appears to correspond to the lowest resonant frequency, these are very small. The overall performances do not show any particular trend. The reactive surface is not realised due to several reasons. The limitations of the testing space is one possibility. A second one could be the insufficient number of wells on top of the mound, due to the width of the top horizontal section, for the reactive surface to be realised.

The absorbing characteristics of the earth mound model could also have been responsible for some of this since the model material corresponded to a ground surface as opposed to a perfect reflective surface investigated above. The practical difficulty of fitting the series of wells on top of the mound and sealing any gaps to make the modification integral part of the model also played a role. Since the horizontal top part of the model was only 0.1 m wide, this limited the maximum number of wells which could be positioned on top. Consequently, this would have affected the realisation of the reactive surface. Also the overall width of the reactive surface in relation to the



wavelength of the sound wave would be important. Some of these factors will be investigated in more detail in the next chapter.

The physical scale modelling undertaken by uniform field experiments confirmed the benefits of a series of wells for small geometries but failed to provide any concrete evidence in the case of large geometries, even though very small gains have still been reported. It was decided to repeat these experiments in semi-anechoic chambers to further test the validity of the measurements. This would provide a better indication on the relative performance of different profiles and any practical design guidance that might accompany.

## **8.4 CONCLUSIONS**

In this chapter the performance of various barrier configurations was investigated. It was found that, for the small geometries where the path length difference is small and where the overall source - to - receiver distance remains within the direct field range as much as possible, a reasonable representation of the actual insertion loss values would be obtained using uniform field experiments. For larger geometries where the path length difference becomes larger and when larger insertion loss values are to be expected, the attenuations that can be achieved will be limited. A good qualitative agreement may be obtained for potentially high insertion losses however this depends on the choice of geometry size and source / receiver configuration.

A detailed investigation into the reactive surfaces was undertaken. These were tested initially on their own, and having confirmed their performance, on a small and large size barrier respectively. A series of wells situated on the ground provided considerable improvements over an equal height single edge. Similarly favourable gains were recorded when reactive surfaces of various well depths were installed on top of a low reflective barrier. These configurations clearly demonstrated the merits of using multiple edges on the ground and on low reflective barriers.

It was also shown that quarter-wavelength resonance and surface wave generation play a significant role in determining their performance at lower frequencies. At high frequencies diffraction effects were shown to be the likely mechanism responsible for the attenuations. However the geometries investigated did not allow these attenuations to be related to diffraction grating effects. In addition, interference between direct and multiply reflected (within the grooves) paths was shown to be a possible explanation for the measured peaks (maxima and minima) in attenuation spectra. However, these observations did not hold for some of the configurations with smaller edge heights.



When tested on top of earth mound type barriers, the reactive surfaces did not provide substantial improvements. There was inconclusive evidence that different well depths performed slightly better around the frequencies observed for other configurations. The possible reasons were thought to be either the limitations of the uniform field experiments or the insufficient number of wells required for this type of surface to be realised.

The next chapter will attempt to resolve this issue by presenting the results of repeat-tests carried out in semi-anechoic chambers. It is envisaged this would avoid the unwanted reverberant build-up of sound and help identify the limitations of the current method.



# 9      **PHYSICAL SCALE MODELLING: SEMI-ANECHOIC CHAMBER EXPERIMENTS**

The previous chapter provided details of a number of models and experiments under uniform field conditions. The discussions indicated that this method could have its shortcomings due to the reverberant build-up in the room, under certain situations.

This chapter presents the findings of the repeated tests in two different semi-anechoic chambers, and aims to identify the limitations of the method previously discussed. The direct comparison of the results obtained by both methods will be undertaken in the forthcoming chapters.

Additional experiments are also undertaken to supplement the findings of Chapter 8 and to understand the likely mechanisms of noise attenuation involved in the case of rib structures consisting of a series of edges or wells.

It should be noted that the format of presentation in this chapter follows closely that of the Chapter 8, where applicable, for ease of comparison.

## 9.1      **EXPERIMENTAL METHOD**

The experiments described in this chapter have been carried out in two different semi-anechoic chambers of the Sheffield University, School of Architecture. The smaller one is situated in the University campus, in the 16<sup>th</sup> floor of the Arts Tower and the second one is situated near Buxton, in Harpur Hill. Both of these facilities are currently used extensively for research and teaching by the Sheffield University. The approximate effective dimensions of the chambers are tabulated below.

Chamber location	Width (m)	Length (m)	Height (m)
Sheffield	3	3	2.75
Buxton	5.9	9.3	2.75

Due to its proximity to Hallam University, the initial experiments were carried out in the Sheffield chamber. The size and the location of this chamber meant only the smaller geometries could be tested here. Therefore for the experiments related to earth mounds, the Buxton facilities were used.



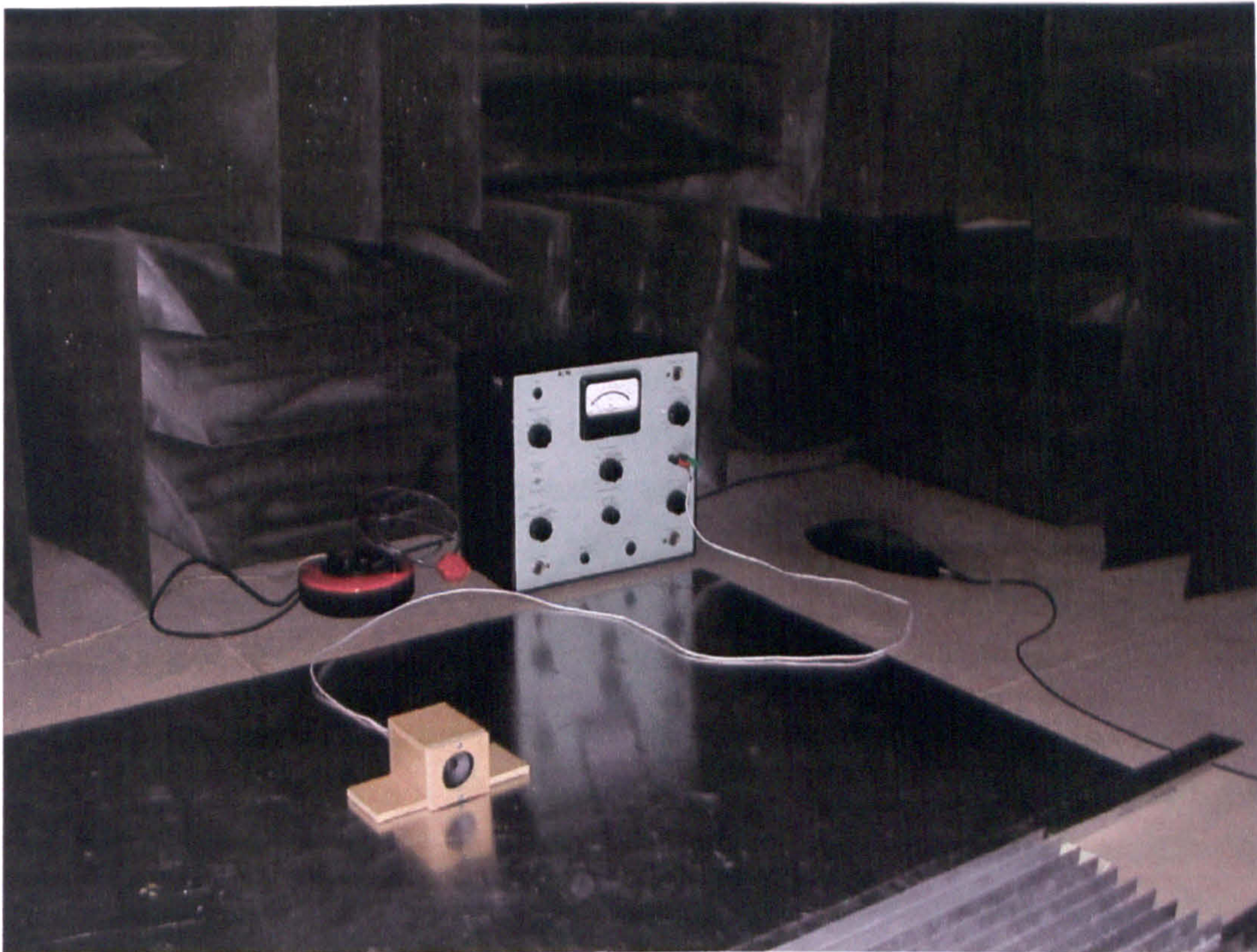


Figure 9.1 : General experimental set-up in Sheffield chamber

The instrumentation has been supplied by the Hallam University and the details of these were discussed previously, in Chapters 7 and 8. The noise source was a small sized tweeter speaker and was connected to a random noise generator. The receiver used was ½ inch type microphone connected to a B&K 2260 sound level meter. The 1/3 - octave band frequencies between 2 kHz and 12.5 kHz have been investigated.

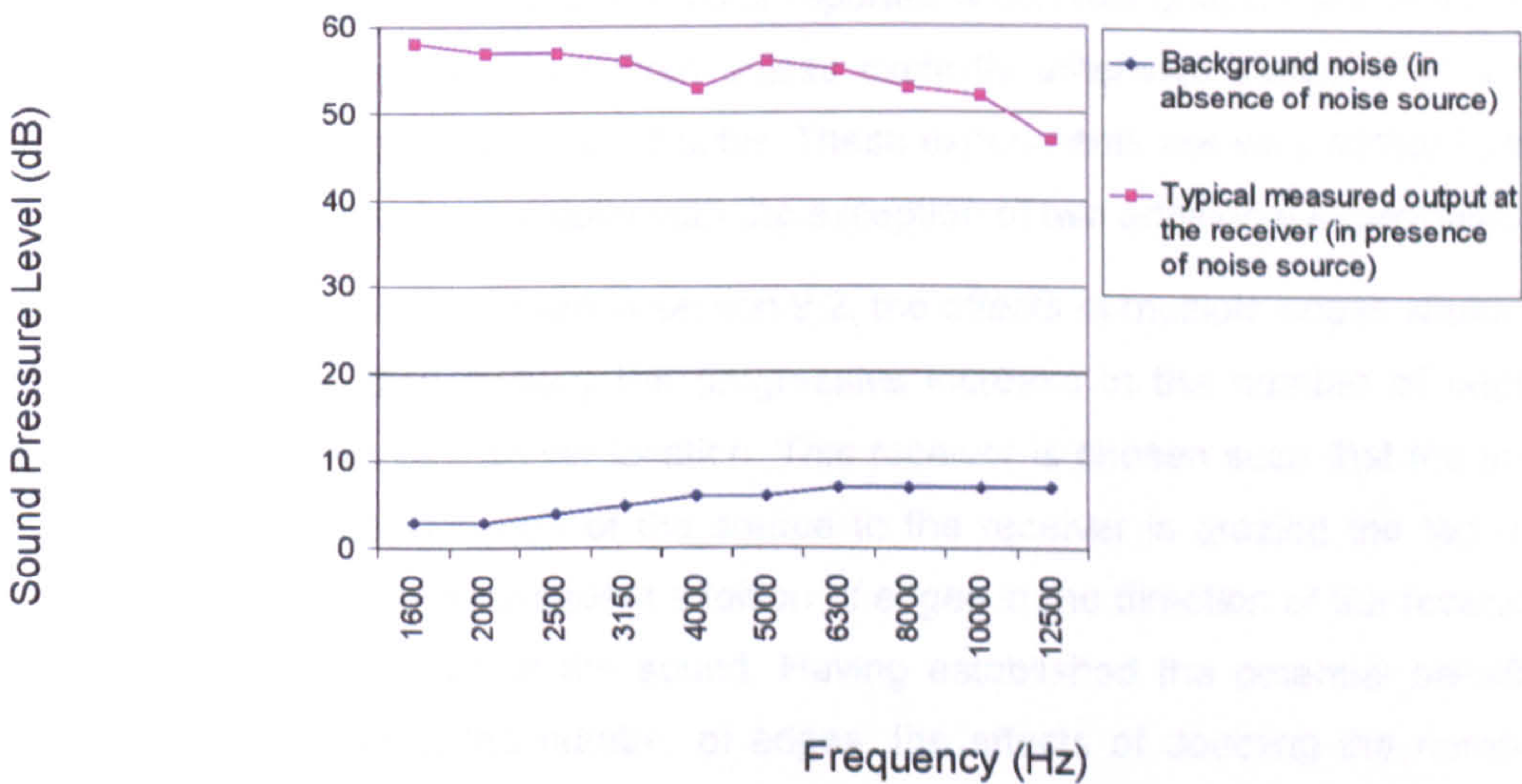


Figure 9.2 : The background noise levels at the semi-anechoic chambers



The background noise levels at both of the facilities were measured to be less than 10 dB, as shown in Figure 9.2. These were found to be substantially lower than sound pressure levels at a typical receiver in presence of the sound source and have no influence on the measurements.

The testing frequency range is one of the main differences from previous tests. Since the chambers are in extensive use by others throughout the year, these tests were carried out mainly over the weekends or bank holidays. The equipment at the Hallam University could not remain away from the laboratory for extended amounts of time and therefore the B&K 2260 sound level meter was identified as being small enough to be transported to and from the chambers every time testing was required. The compromise was the reduced testing range, however these tests are expected to provide meaningful data up to 12.5 kHz for comparison and validation purposes.

As explained in Chapter 8, the noise levels were monitored at the receiver positions under consideration and at a reference point. The reference point was 0.3m from the source and remained the same in all tests to enable comparisons between different configurations. A random noise generator was connected to an amplifier and the noise output was kept constant throughout the test. The sound pressure levels with the configurations under consideration were monitored and compared with the sound pressure levels for a single or no edge cases, as appropriate.

These experiments are an investigation into a number of rib structures consisting of multiple edges situated both on the ground and on earth mound type barriers. The experiments are extended to include a more detailed study of the effect of additional edges at various receivers and also the effect of a rib structure at different receiver heights. The frequencies and dimensions reported within this chapter are those of the model. All dimensions are in metres unless explicitly otherwise stated. Five sets of experiments are described in this chapter. These experiments are very similar to those undertaken in the previous chapter with the exception of two additional experiments.

In the first set of tests described in section 9.2, the effects of multiple edges situated on the ground are studied. Initially the progressive increase in the number of edges is investigated at a single receiver location. This receiver is chosen such that the line-of-sight from the physical centre of the source to the receiver is grazing the top of the edge. This ensures the subsequent addition of edges in the direction of the receiver do not affect the path length of the sound. Having established the potential benefits of progressive increase in the number of edges, the effects of doubling the number of wells and the width of the reactive surface are investigated. An array of six receiver locations is used to provide evidence on how the spectrum behind the reactive surface is affected at various distances and heights. Two of these receivers are in the shadow



zone, two are situated along the line-of-sight from the source grazing the top of the edges, and the remaining two are in the illuminated zone. In order to have a better appreciation of the relationship between attenuations and amplifications at various frequencies and receiver positions the effect of progressive addition of up to 17 edges at six receivers is studied simultaneously. These experiments can be considered to be a combination of the previous two. This test is first one of the additional experiments undertaken in this chapter

The second set of experiments consists of the second additional experiment. This investigates the effects of a rib structure at a number of receivers with different vertical heights. This geometry is intended to look at the effect of attenuations or amplifications at different diffraction angles. Before looking at the effects of different well depths, it was considered that more insight was required into the diffraction grating effects. These tests are discussed in section 9.3.

The third set of experiments use three different well depths to identify the effect of these on the lowest frequency at which attenuations occur. These will be discussed in section 9.4.

The fourth set of experiments in section 9.5 look at the effects of multiple wells on top of a small height and reflective rectangular barrier. These consist of three different well depths described above. Two different receivers are selected for these experiments. The first is situated on the ground to minimise the influence of ground reflected paths. The second receiver is situated at the same height as the height of the barrier, to maintain a near grazing incidence angle over the series of edges.

The fifth and the last one of the experiments investigate the influence of multiple wells placed on top of an earth mound. The large size of this geometry and the increased path length means the direct field would be attenuated as much as possible and the adverse contributions from the reverberant field would be maximised. This geometry is expected to provide some indication on the shortcomings of the method. It will also determine if the reactive surfaces are able to provide additional attenuations when the existing attenuations due to presence of a large sized barrier are substantial. Two receivers are selected for these tests both of which are in deep shadow zone. The first one is resting on the ground, as before, to minimise ground influence. The second one is situated above the ground and represents the height of a typical receiver. These are discussed in section 9.6.



## 9.2 MULTIPLE EDGES ON THE GROUND

### 9.2.1 Progressive Increase in the Number of Edges

This experiment was carried out to investigate the effects of progressive addition of extra edges, at a selected receiver. The basic geometry is shown below.

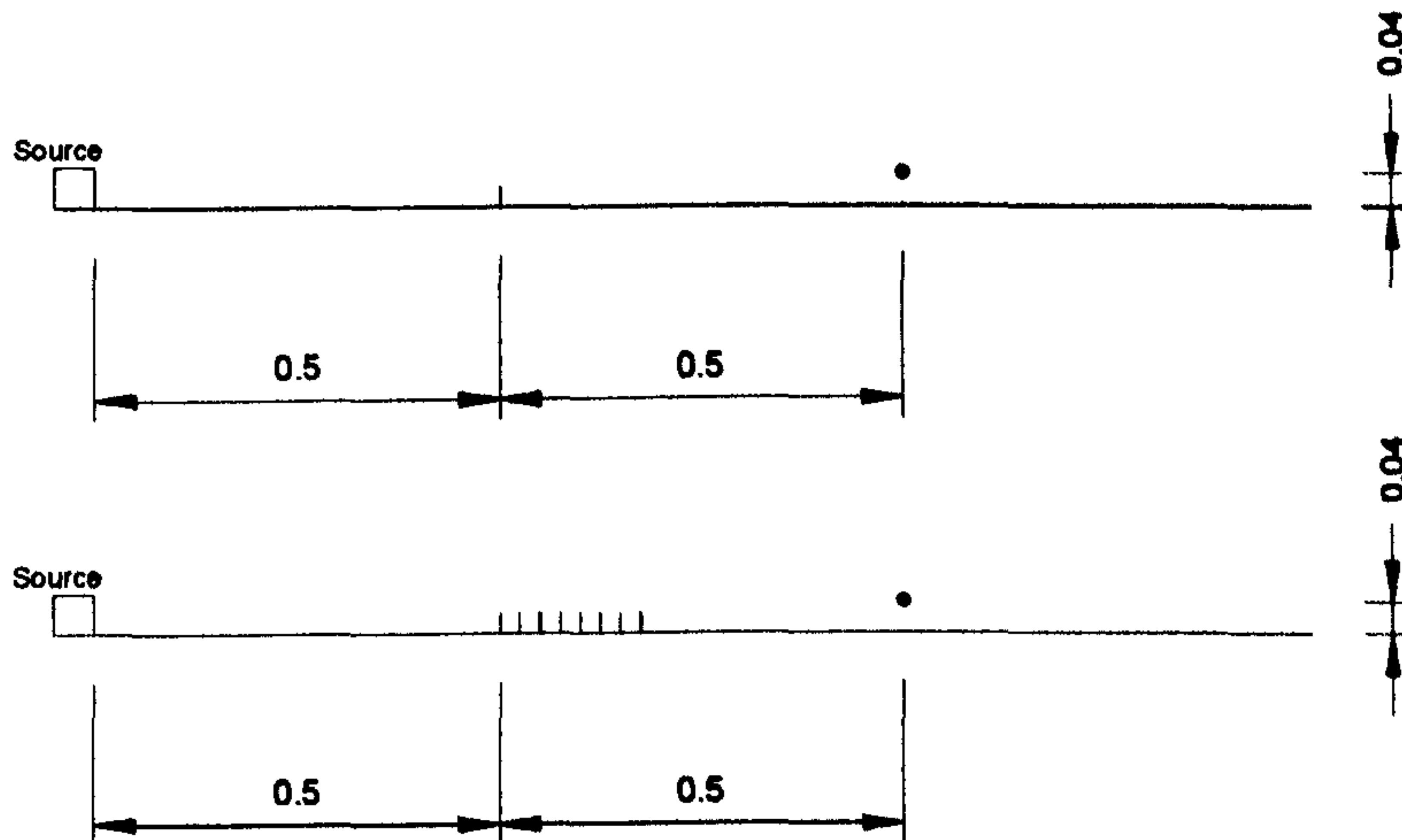


Figure 9.3 : Experimental set-up for investigating effect of up to 8 edges

The source was resting on an aluminium sheet which was used as the ground surface. The height of the receiver was 0.04 m. A single edge consisting of a 90 degree aluminium angle with dimensions 0.025 m x 0.025 m was placed between the source and the receiver. Both the source and the receiver were positioned 0.5 m from the edge, situated on opposite sides. A constant and continuous noise output was generated and the sound pressure levels monitored at the receiver position for testing frequencies of 1.6 kHz to 12.5 kHz. The sound pressure levels in the absence of the single edge were also monitored such that the insertion loss of the single edge and that of the 8 -edges could be determined. Sound pressure levels observed with a constant noise output, for a single edge progressively increased to 8 edges, are shown in Figure 9.4. The insertion loss values for a single edge and for 8 edges are compared in Figure 9.5.



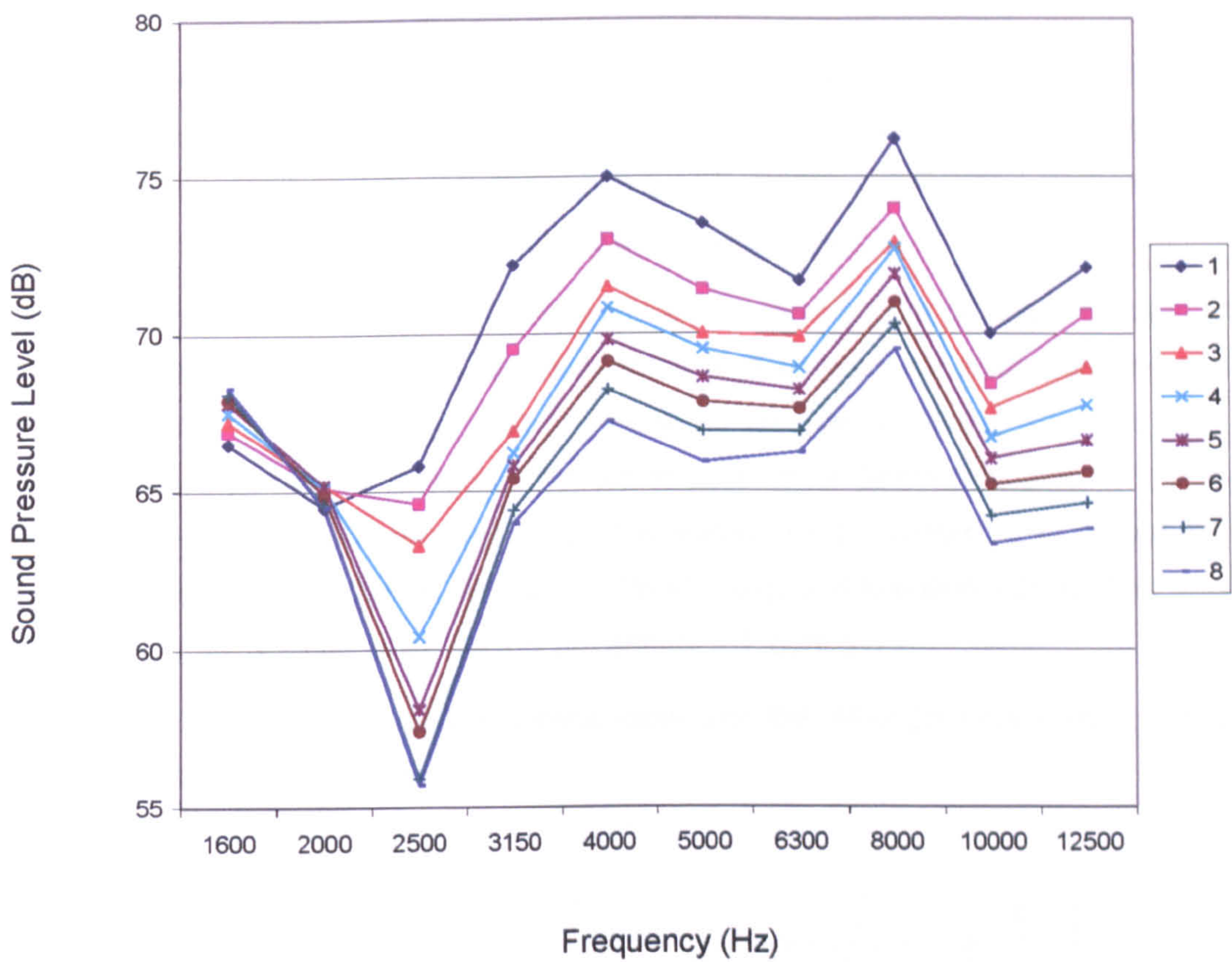


Figure 9.4 : Progressive reduction of sound pressure levels with increased number of edges

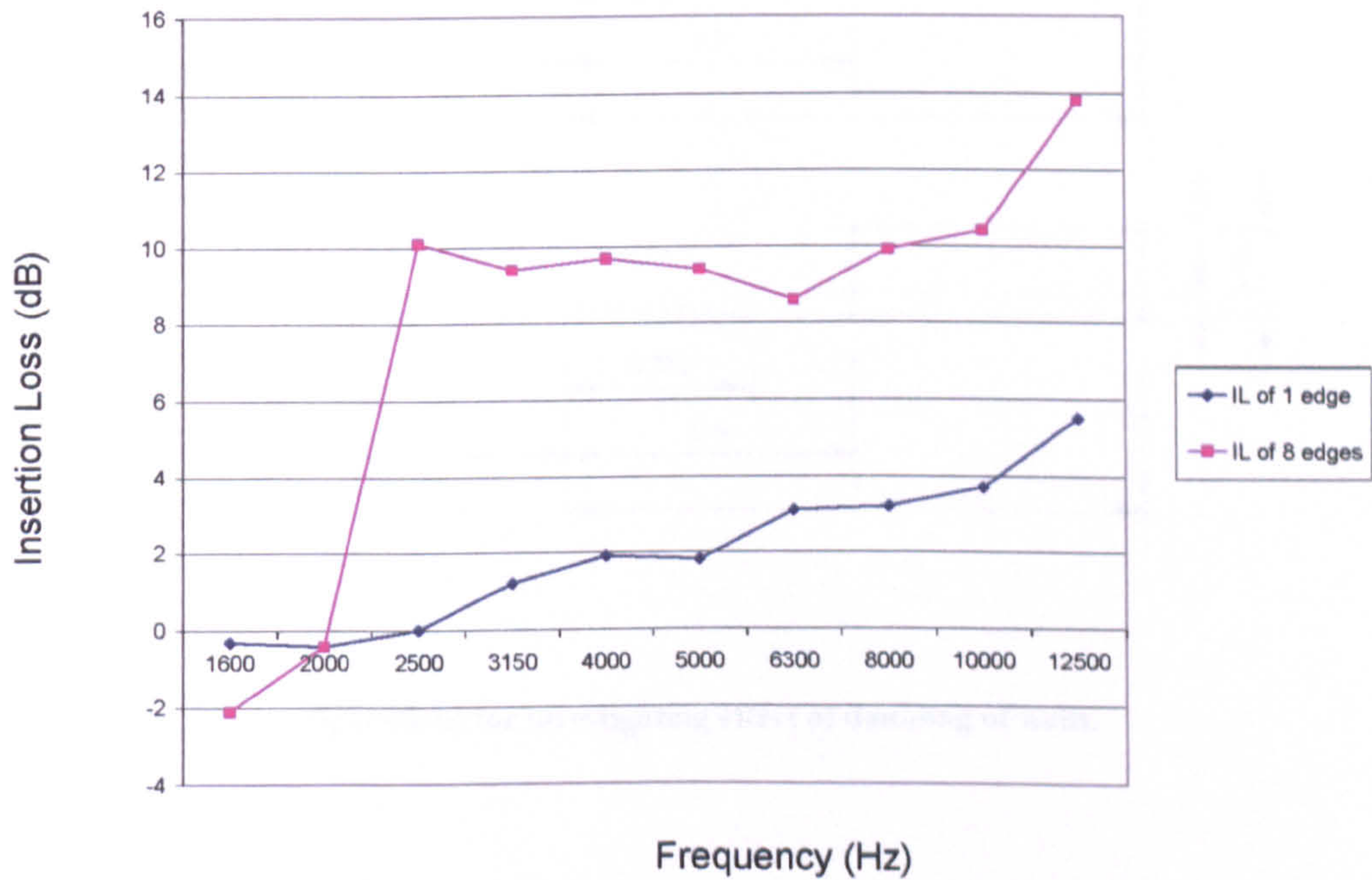


Figure 9.5 : Insertion loss values for a single edge and for 8 – edges.



### 9.2.2 Doubling of the Number of Wells

The tests above verified the progressive improvement in performance by the increased number of edges as observed previously. The experiments were extended further to the investigation of the effect of doubling of the wells at different receiver positions. The following tests compare the 8-edge case to the 14-edge case.

The source was 0.5 m from the first edge and was located on the ground. The case of 8 edges of 0.025 m x 0.025 m was monitored at 6 different receiver locations and compared with the single edge case at the same receiver locations. The first three receivers were placed 0.5 m behind the first edge at three different heights of 0, 0.04 and 0.15 m above the aluminium platform. The second set of receivers was placed at 1 m away from the first edge at the three different heights mentioned above. This was repeated for the 14-edge case. Details are shown in Figure 9.6.

The relative improvements of the 8-edge case and the 14-edge case over a single edge case are shown in Table 9-1.

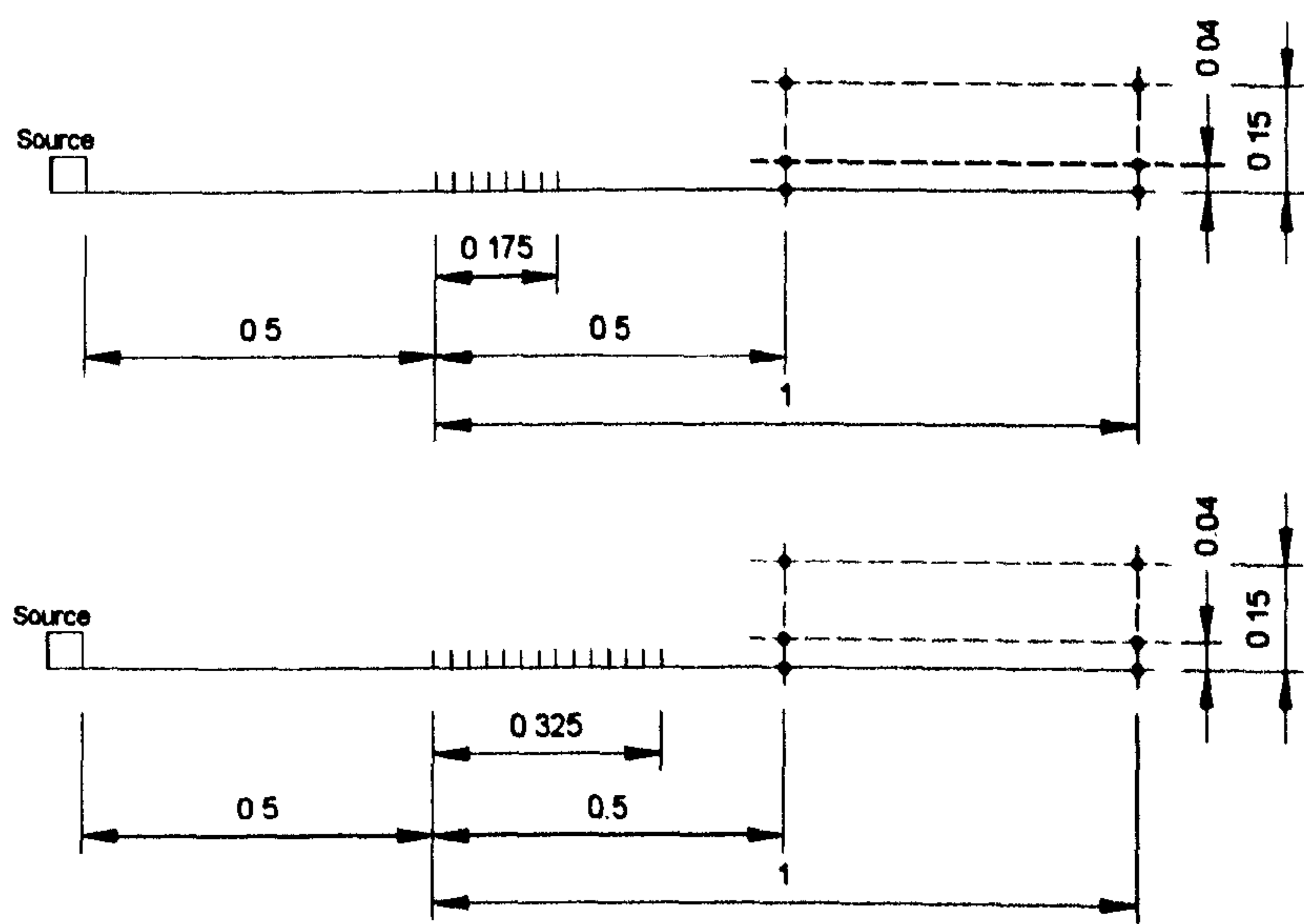


Figure 9.6 : The configurations for investigating effect of doubling of wells.



Relative improvement over a single edge (dB)		
Receiver co-ordinates	8 – edge case	14 – edge case
(0.5, 0)	5.3	8.3
(0.50, 0.04)	5.9	8.3
(0.5, 0.15)	2.4	1.1
(1, 0)	3.9	6.2
(1, 0.04)	4.7	6.9
(1, 0.15)	2.4	2.9

Table 9-1 : Relative improvements of both configurations over a single (where the well depth and spacing are 0.025 x 0.025 m)

The spectrums for the relative differences in sound pressure levels compared with the single edge case for both configurations are shown in Figure 9.7 to Figure 9.10.

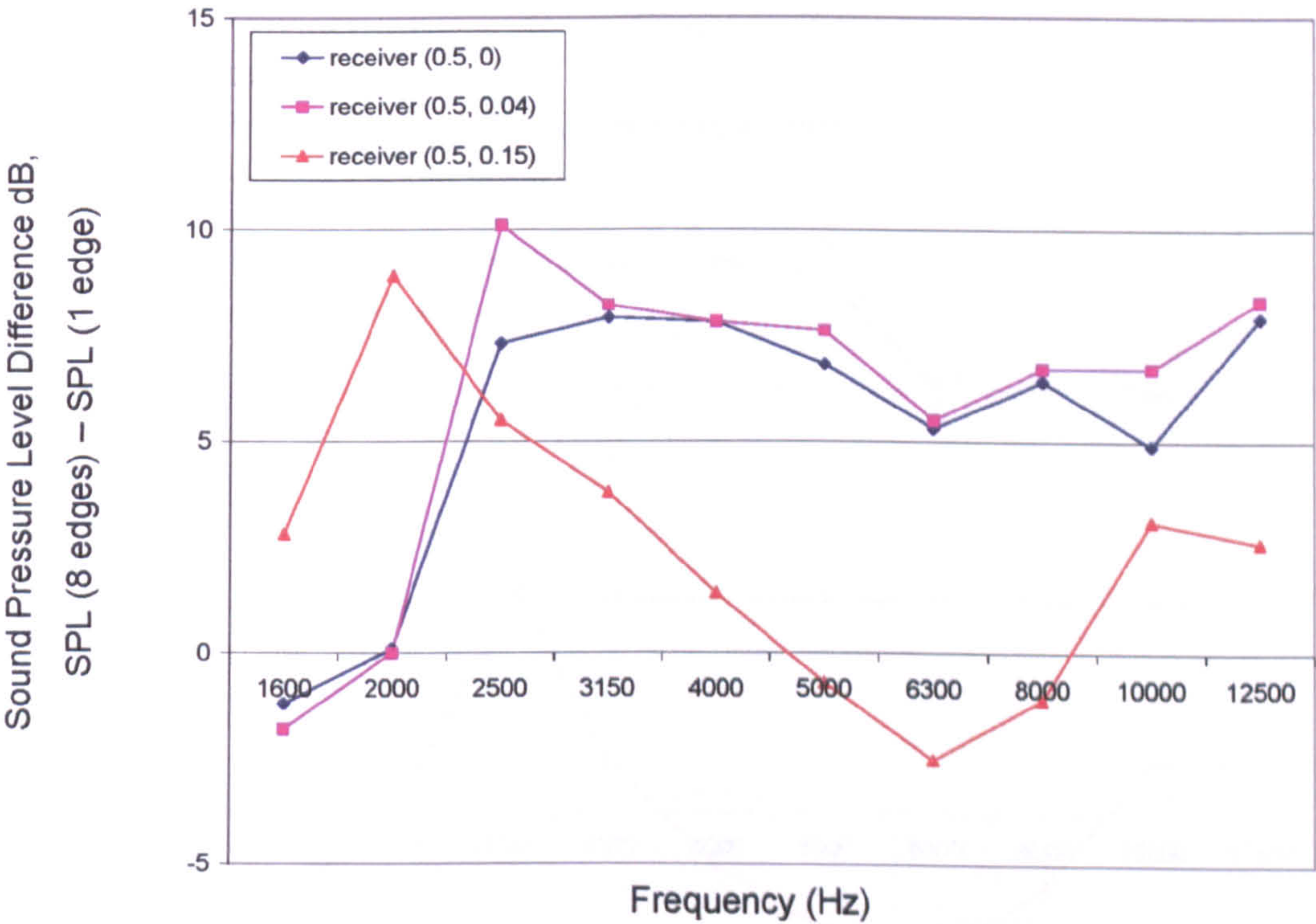


Figure 9.7 : Relative performance of 8 edges over a single edge.



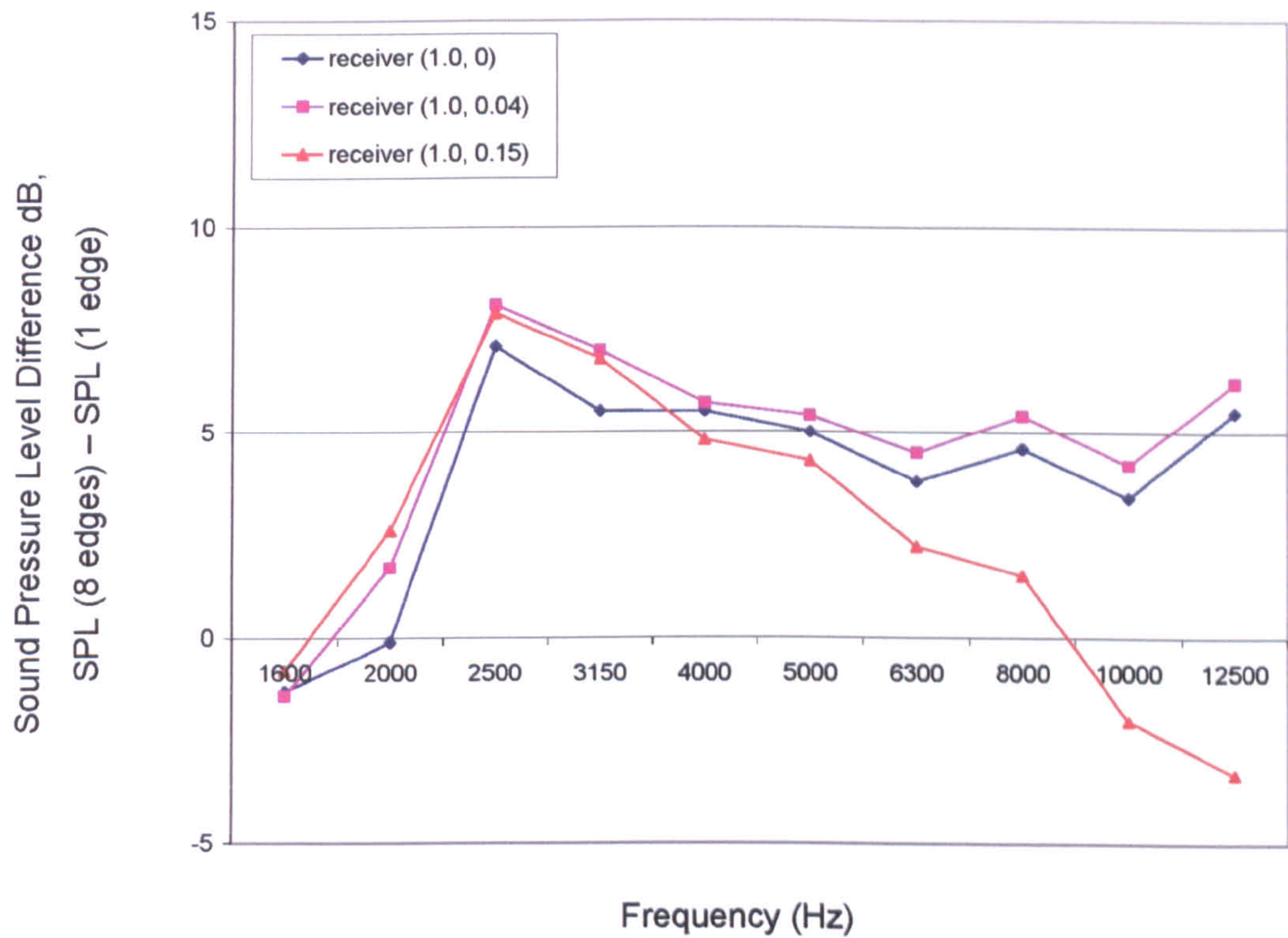


Figure 9.8 : Relative performance of 8 edges over a single edge

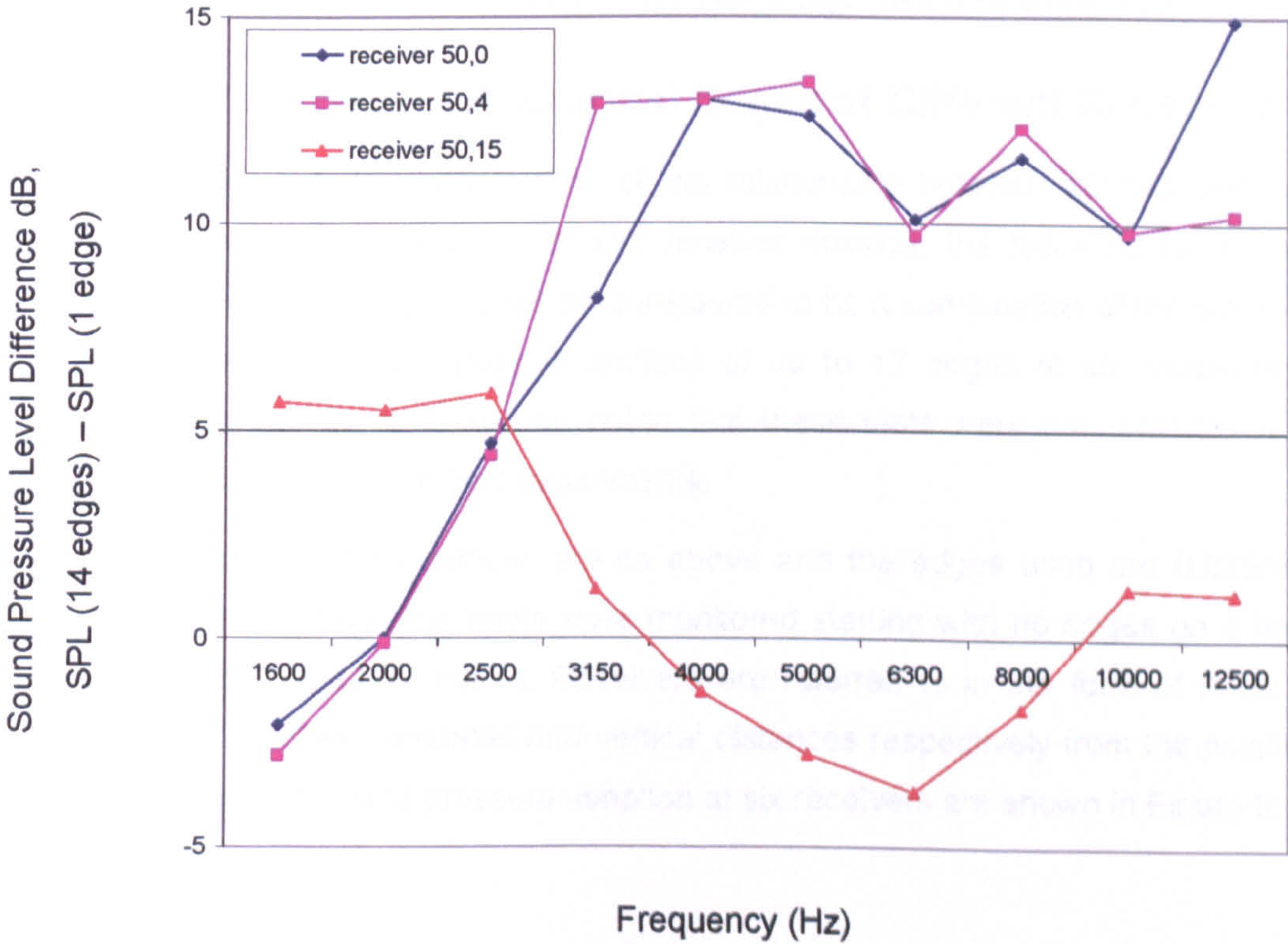


Figure 9.9 : Relative performance of 14 edges over a single edge (receiver distance = 0.5 m)



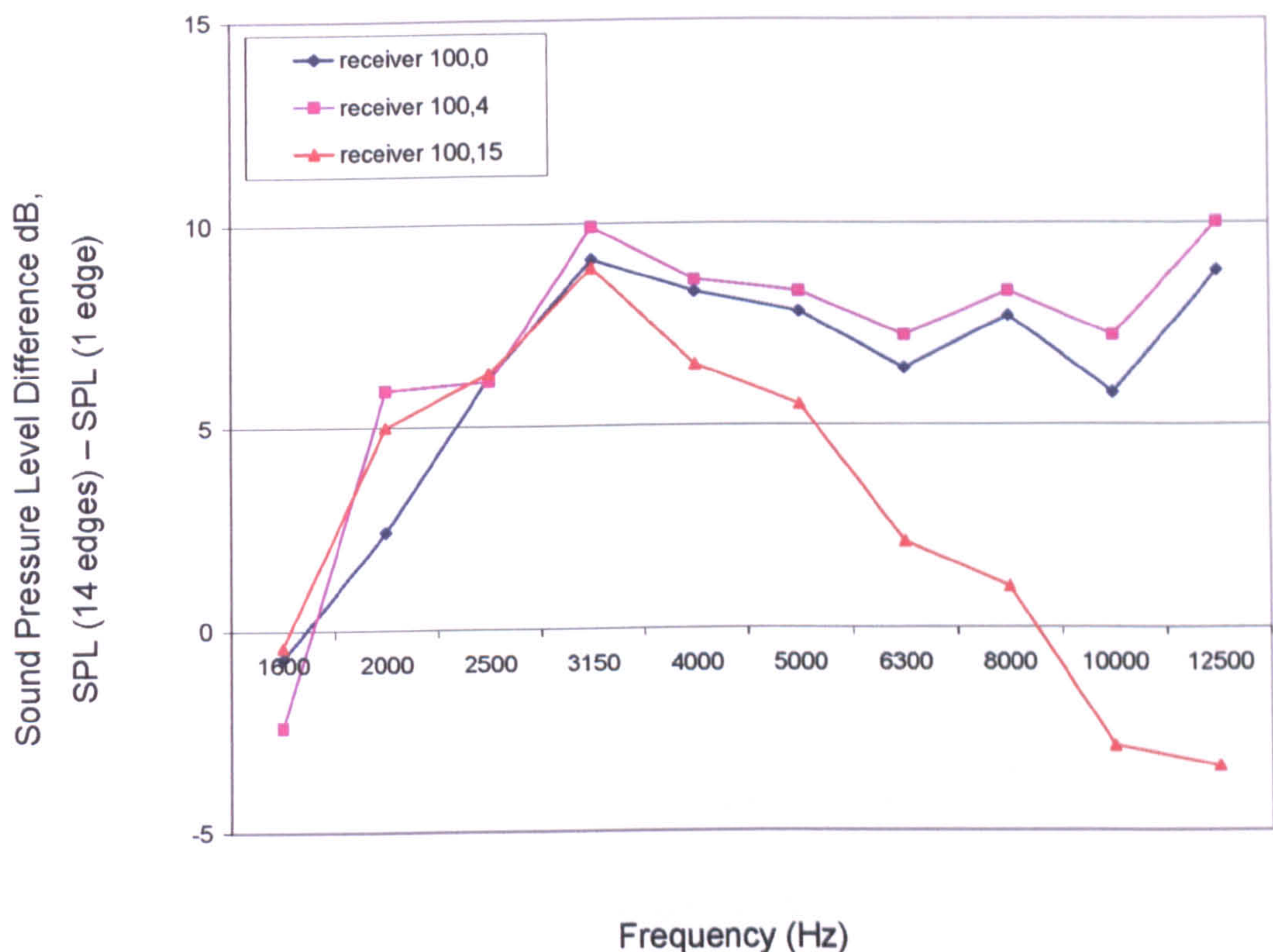


Figure 9.10 : Relative performance of 14 edges over a single edge (receiver distance = 1 m).

### 9.2.3 Effect of Additional Edges at Different Receivers

In order to have a better appreciation of the relationship between attenuations and amplifications at various frequencies and receiver position, the following tests were undertaken. These experiments can be considered to be a combination of the previous two where the effect of progressive addition of up to 17 edges at six receivers is studied simultaneously. It should be noted that these tests were not undertaken in previously described uniform field experiments.

The source-receiver configurations are as above and the edges used are 0.025m x 0.025m. The sound pressure levels were monitored starting with no edges on a hard reflective ground, up to 17 edges. Receivers are referred to in the form of R (x, y) where x and y are their horizontal and vertical distances respectively from the position of the first edge. The sound pressure variation at six receivers are shown in Figure 9.11 to Figure 9.16.



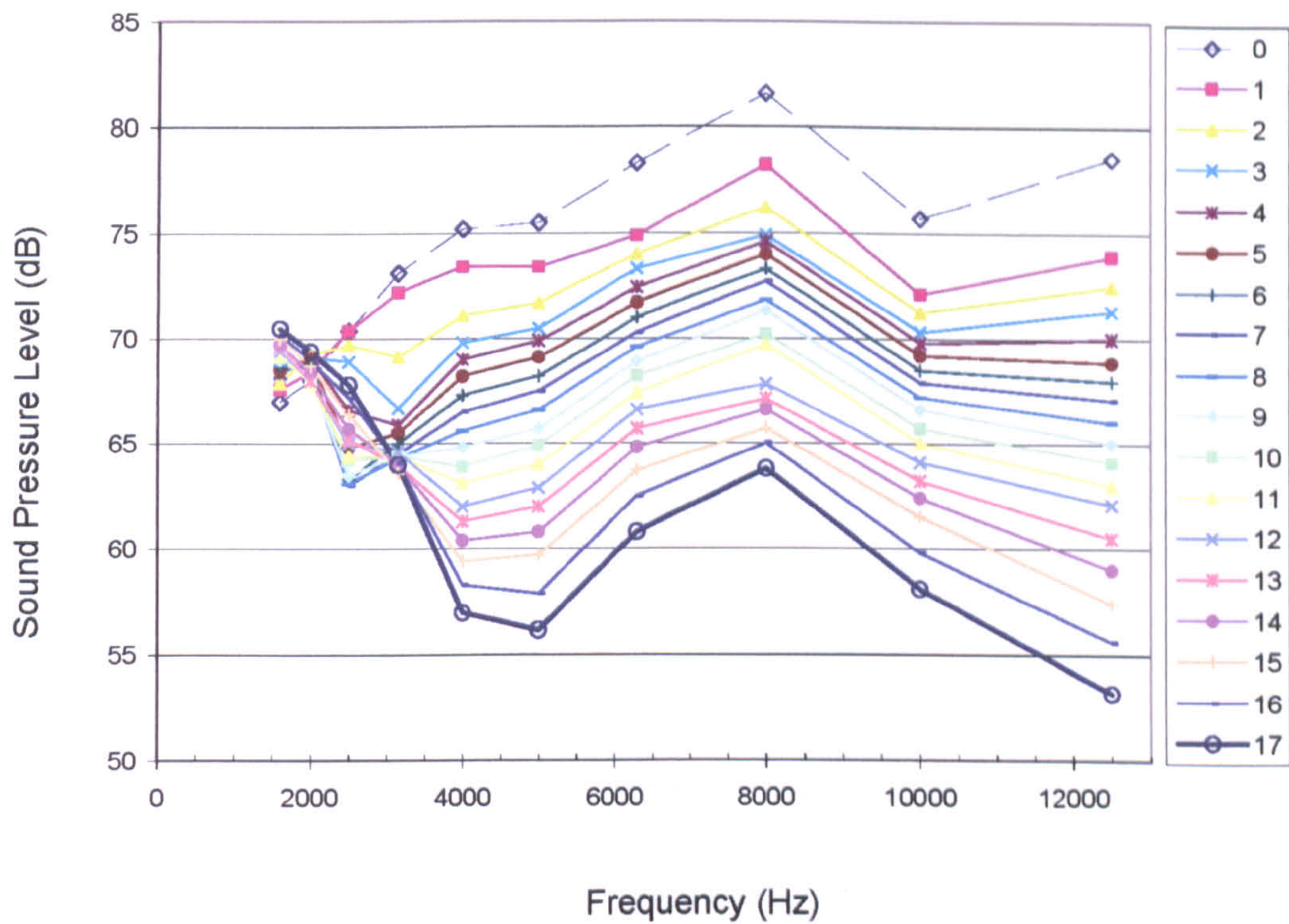


Figure 9.11 : Variation in SPL with increased number of edges, Receiver (0.5, 0)

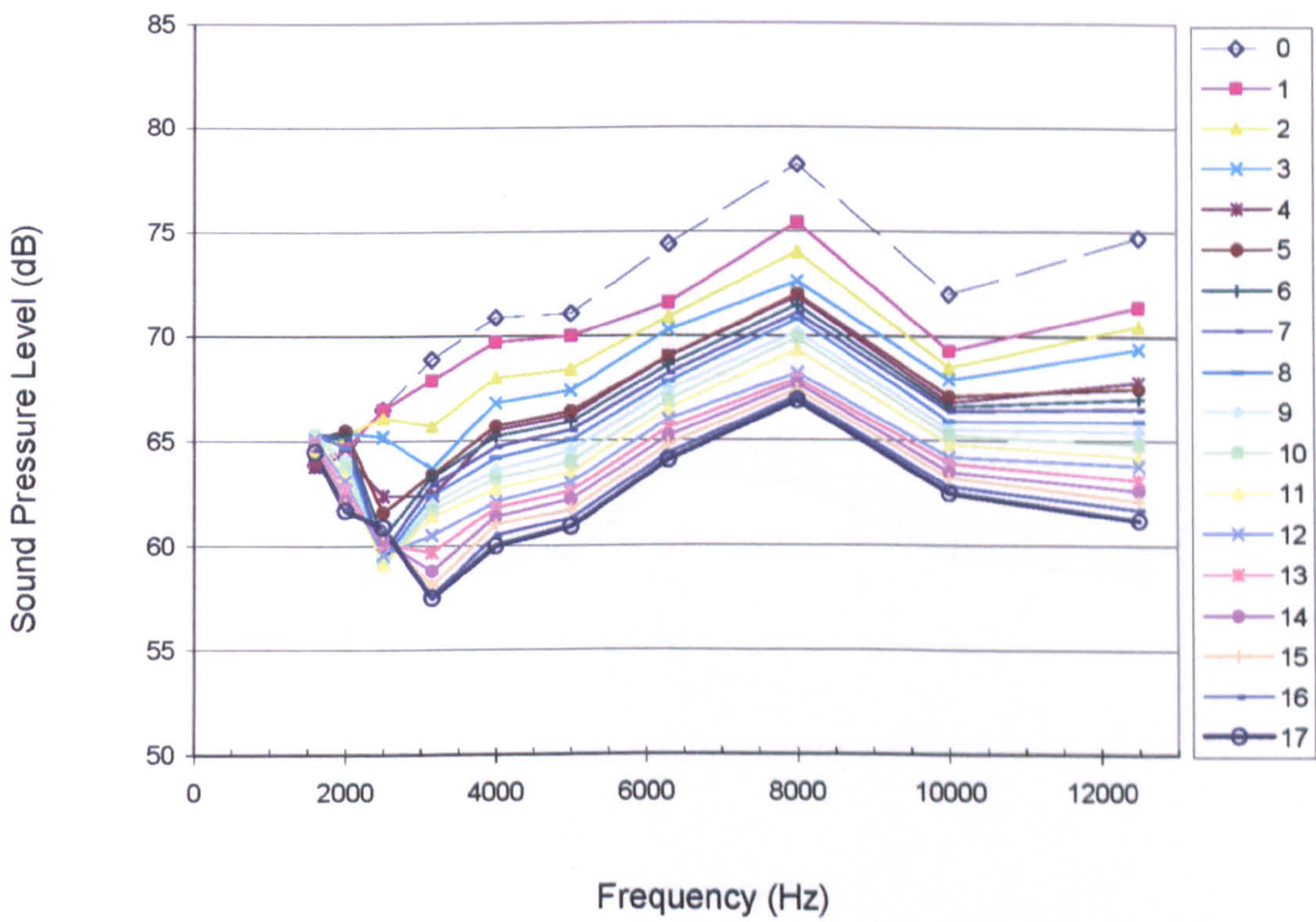


Figure 9.12 : Variation in SPL with increased number of edges, Receiver (1, 0)



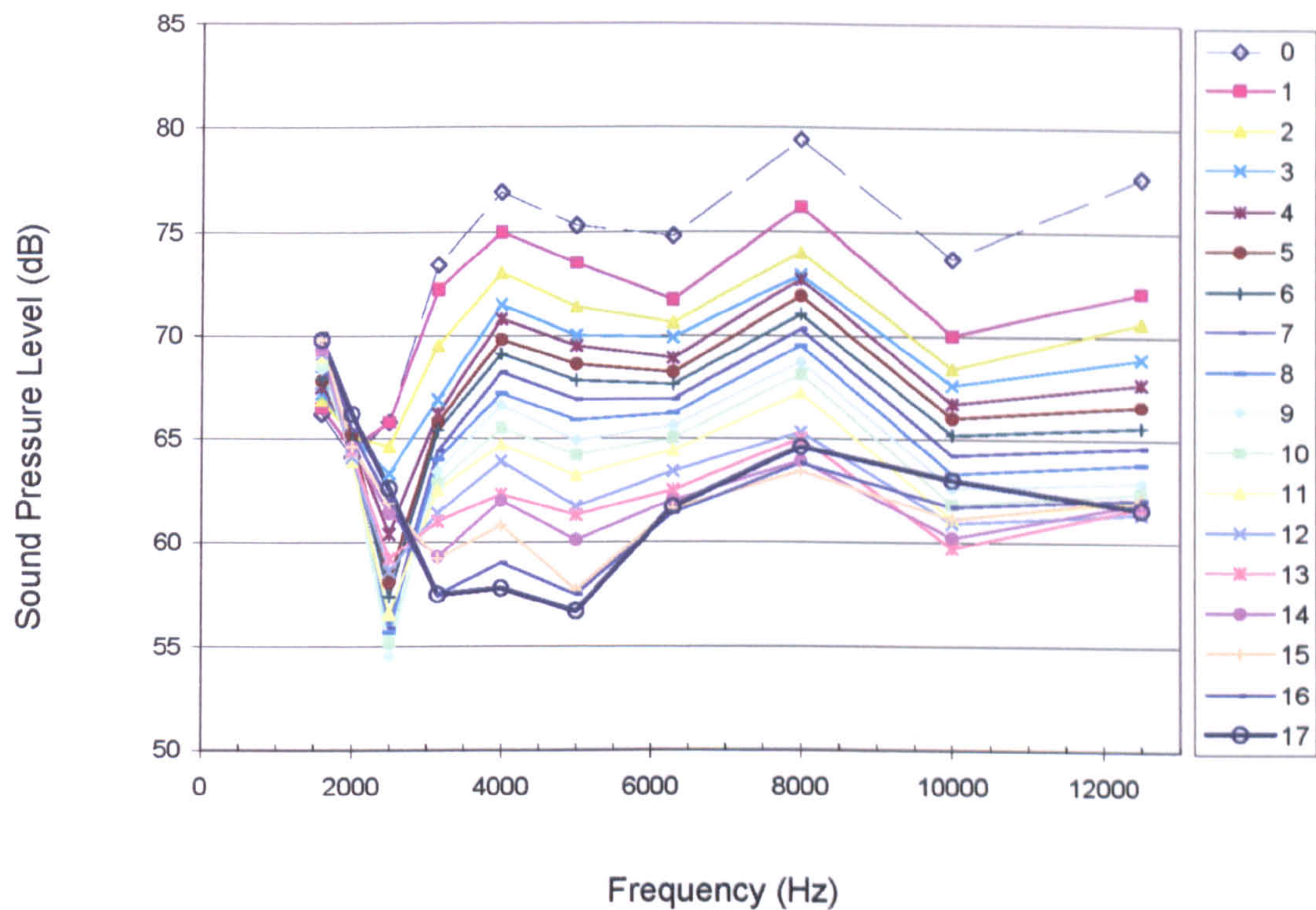


Figure 9.13 : Variation in SPL with increased number of edges, Receiver (0.5, 0.04)

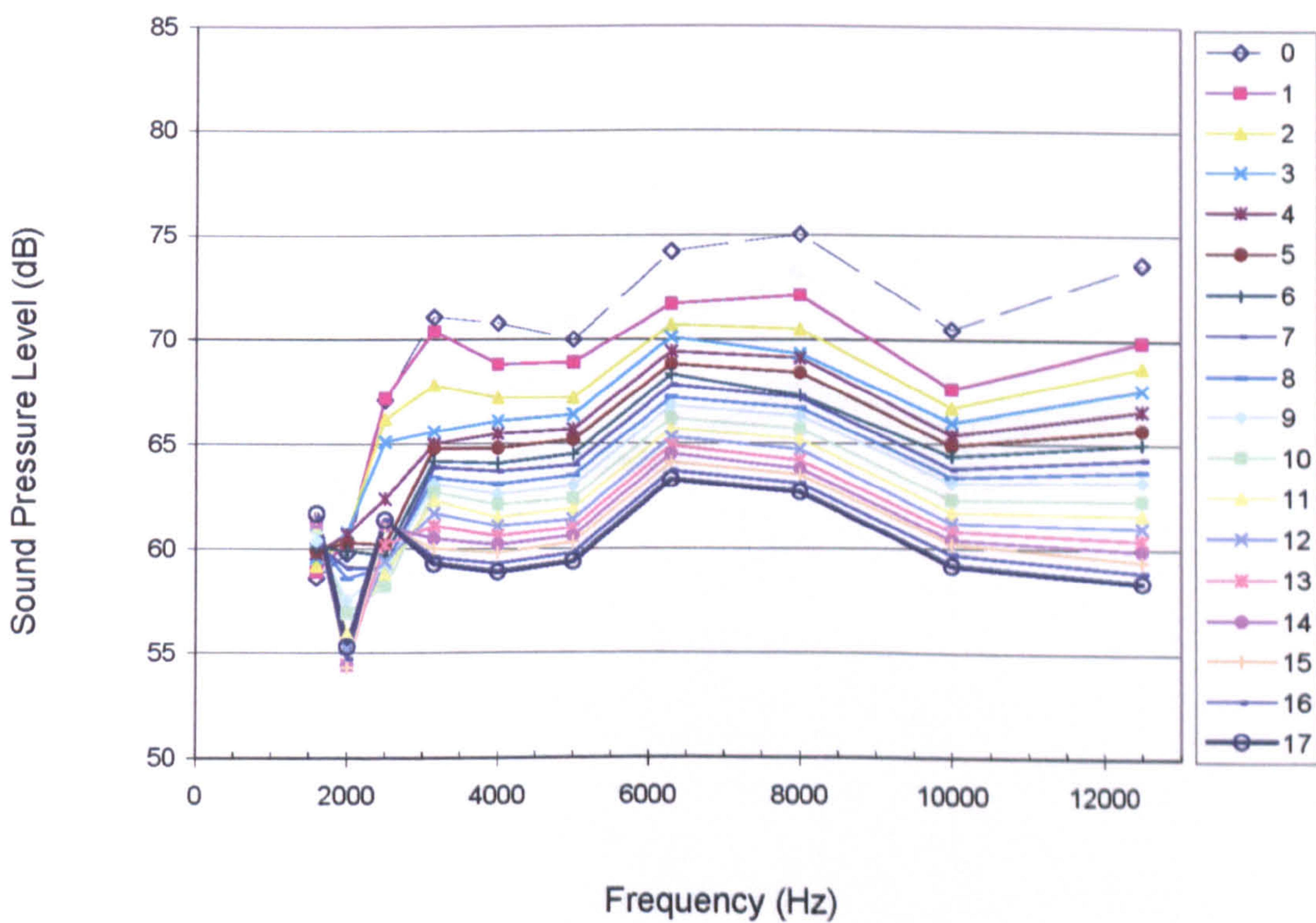


Figure 9.14 : Variation in SPL with increased number of edges, Receiver (1, 0.04)



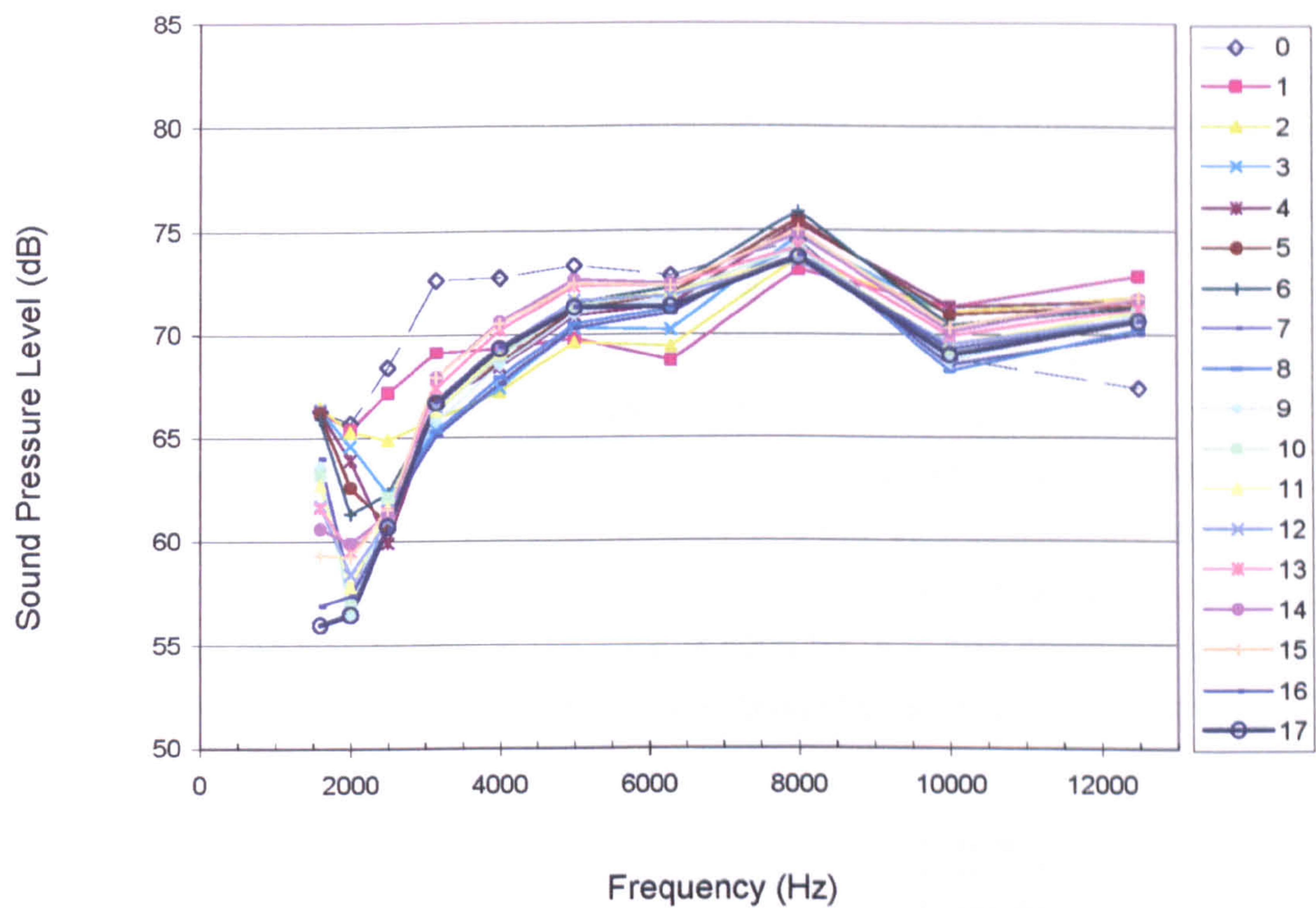


Figure 9.15 : Variation in SPL with increased number of edges, Receiver (0.5, 0.15)

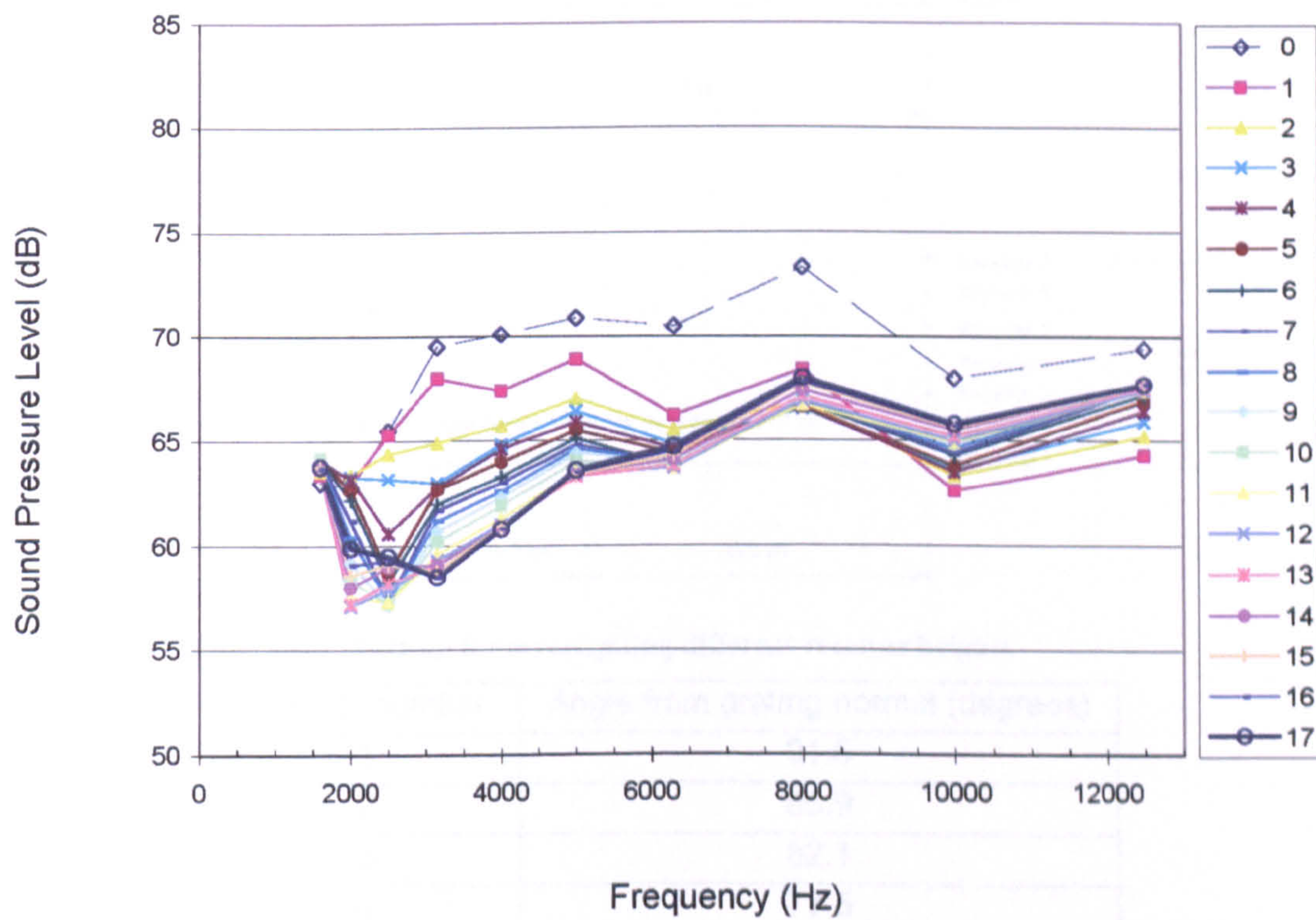


Figure 9.16 : Variation in SPL with increased number of edges, Receiver (1, 0.15)



9.3 ADDITIONAL EXPERIMENTS ON RECEIVER HEIGHT

Additional tests were undertaken to determine the effect of the rib structure at different receiver heights (i.e. diffraction angles). The receivers 1 to 7 are horizontally situated 1.2 m from the source, located 0m to 0.3m above the ground and spaced at 0.05m increments above each other. Their horizontal distance from the source is fixed as shown in the diagram below. Sound pressure levels were monitored at each receiver location with the single edge case and with 21 edges respectively. The height of edges was 0.017m and the separation distance between the edges was 0.008m. The resulting improvements and the insertion loss of each configuration are shown in Figure 9.18 to Figure 9.24. The frequency, which corresponds to the quarter-wavelength of the well depths, in this case is 5000 Hz. It is also noted that the only diffraction order physically realisable for this geometry is zero-order (occurring at around receivers 1 and 2).

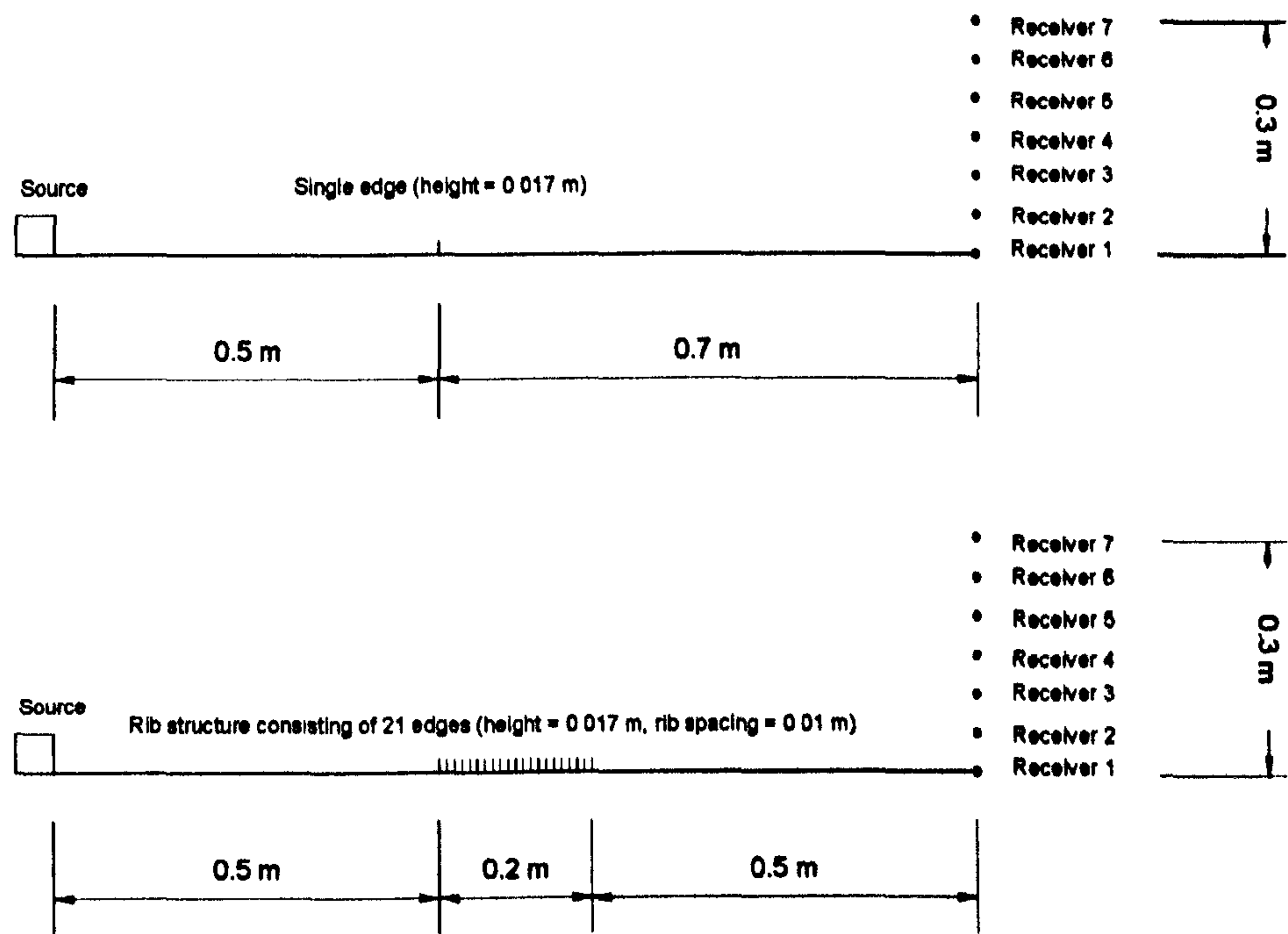


Figure 9.17 : Experimental set-up for investigating different receiver heights

Receiver number	Angle from grating normal (degrees)
1	91.6
2	86.9
3	82.1
4	77.5
5	73.0
6	68.8
7	65.0

Table 9-2 : Diffraction angles for various receivers



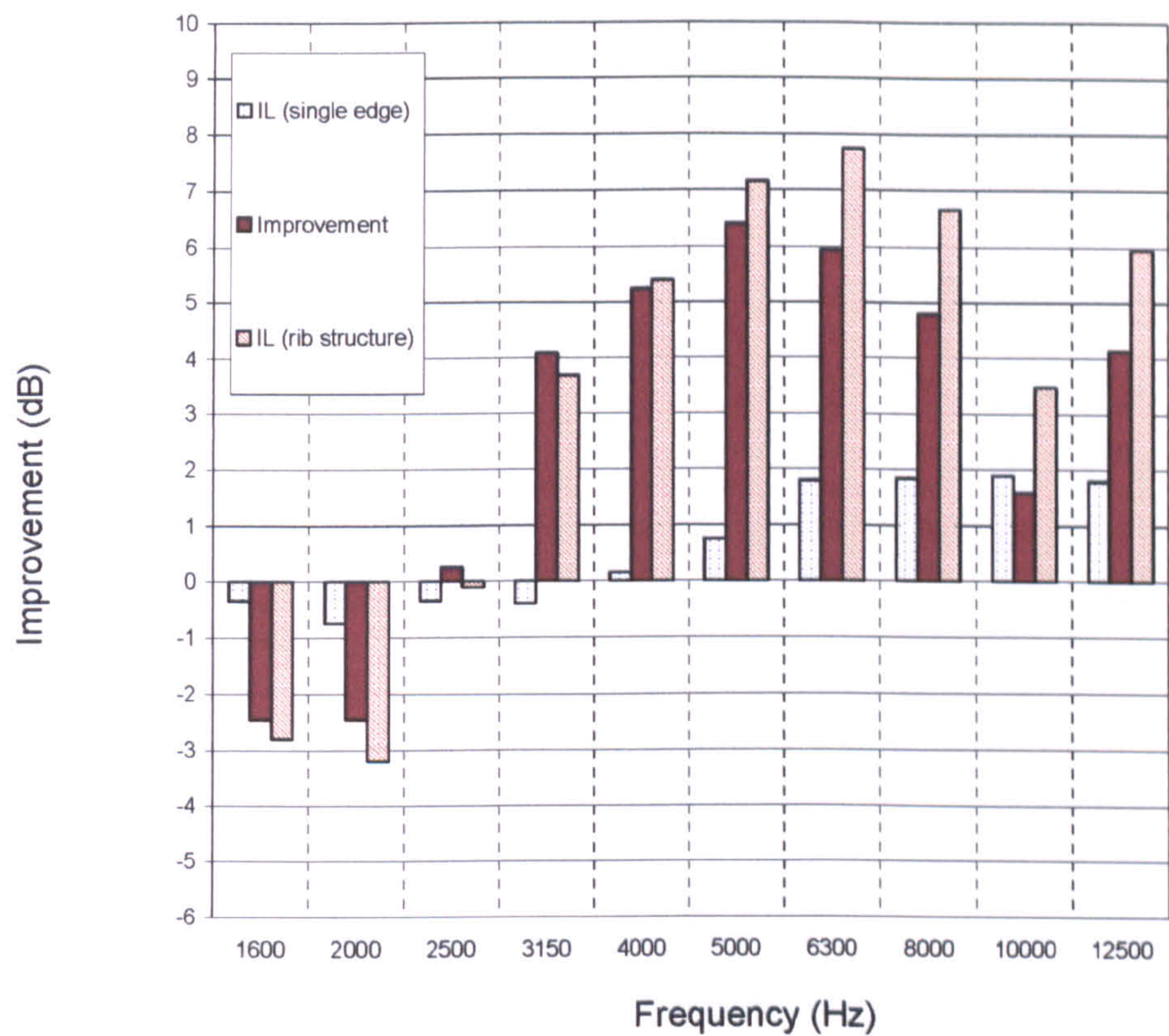


Figure 9.18 : Receiver height = 0m

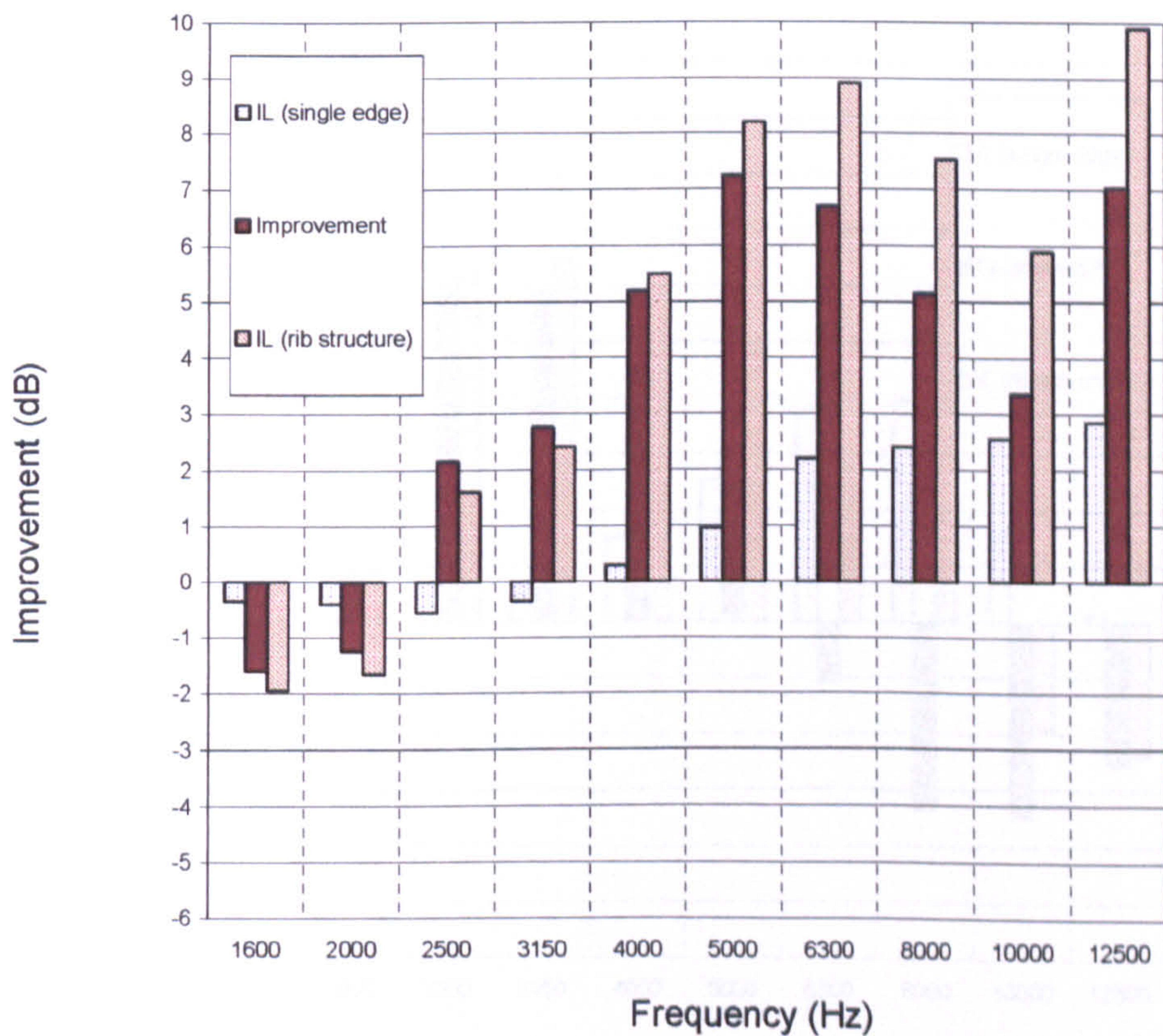


Figure 9.19 : Receiver height = 0.05m



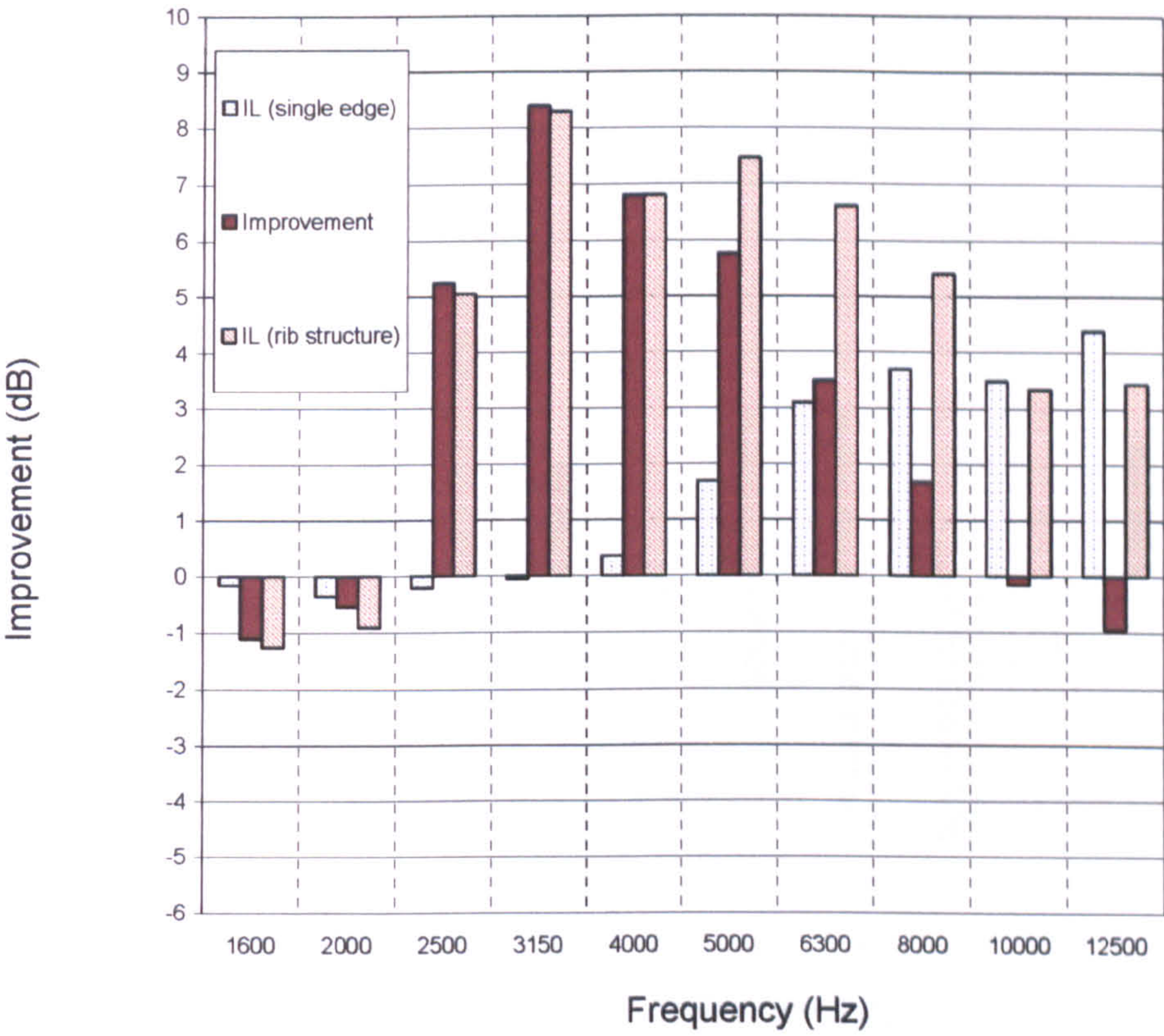


Figure 9.20 : Receiver height = 0.1m

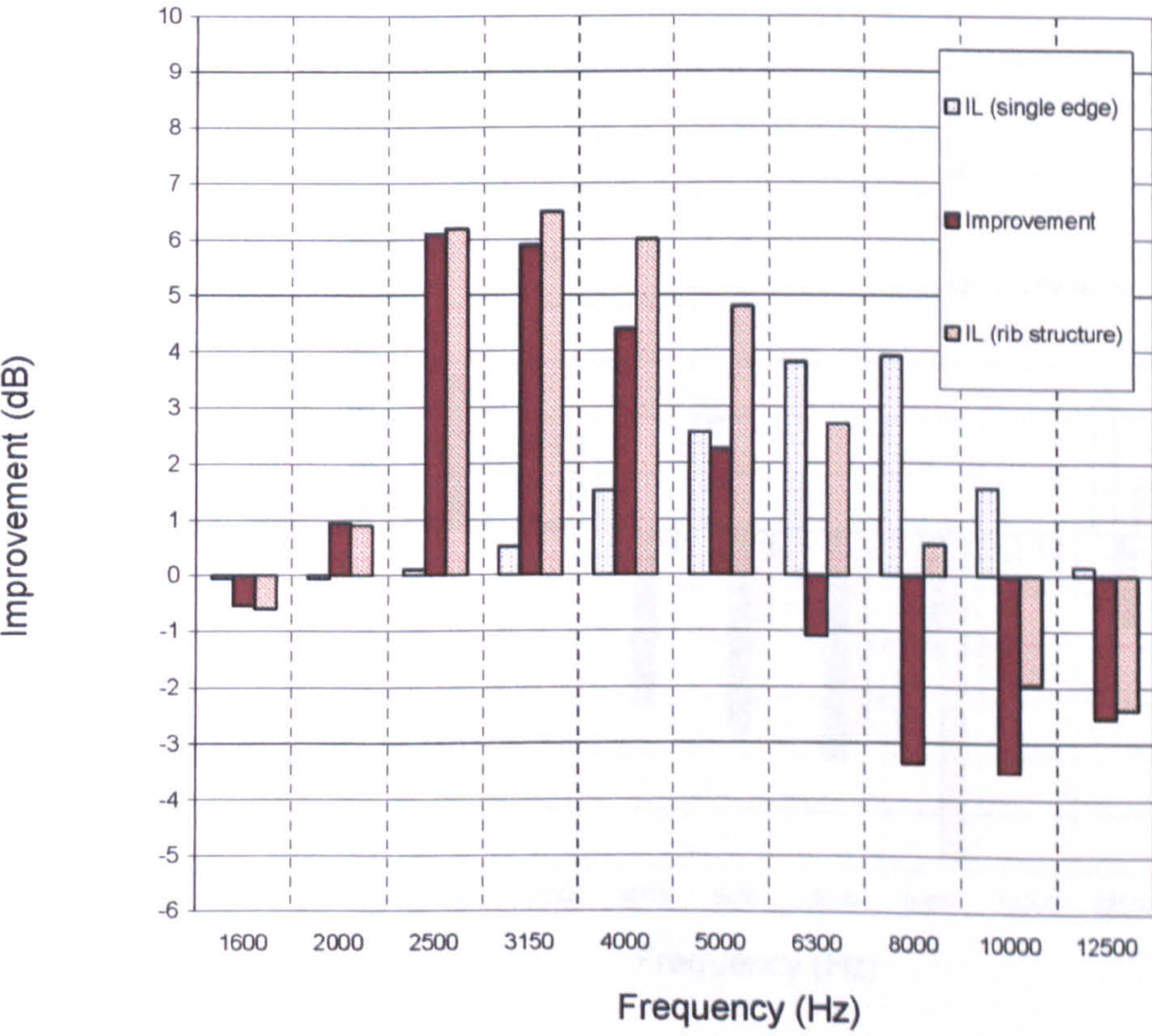


Figure 9.21 : Receiver height 0.15m



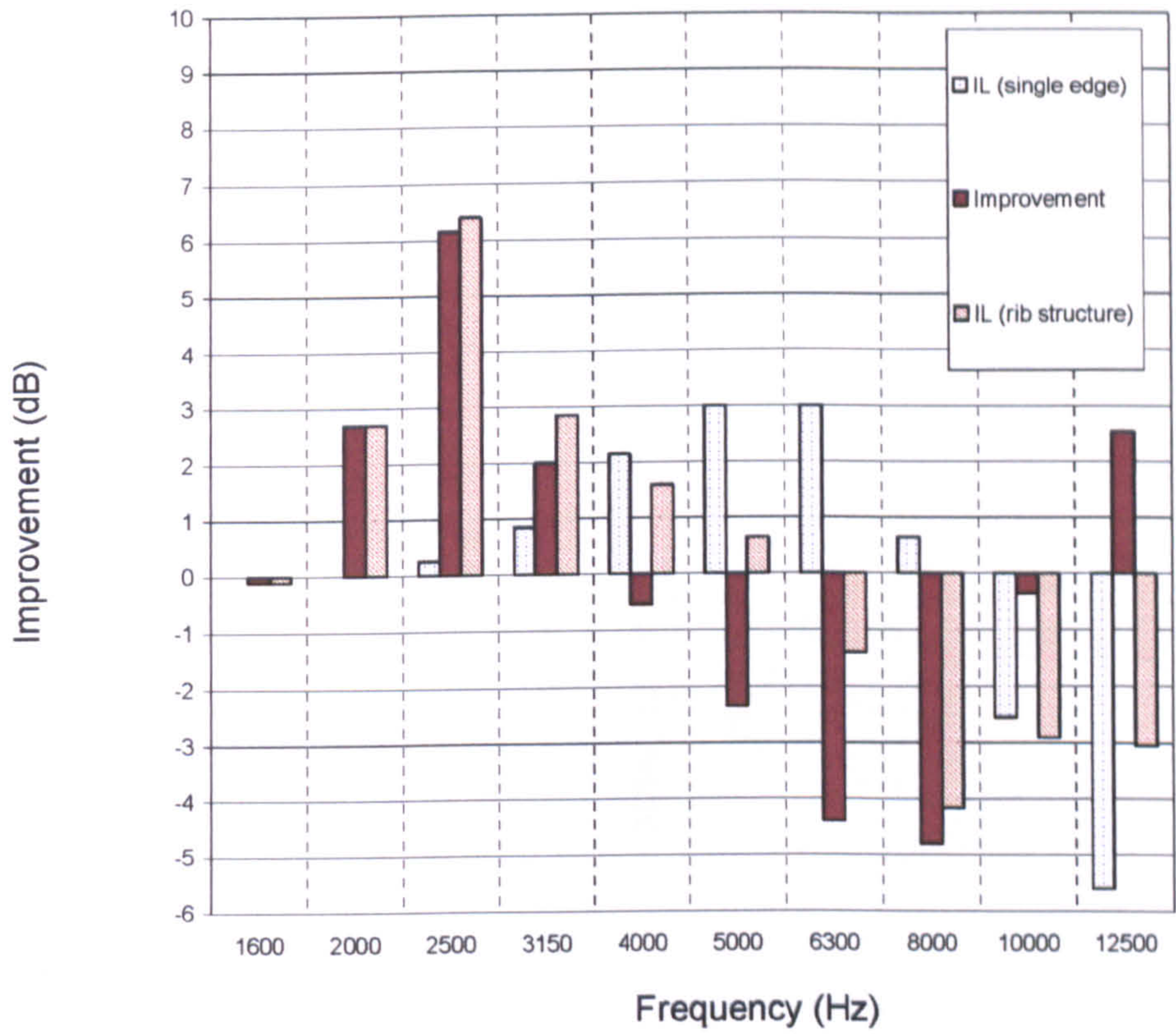


Figure 9.22 : Receiver height = 0.2m

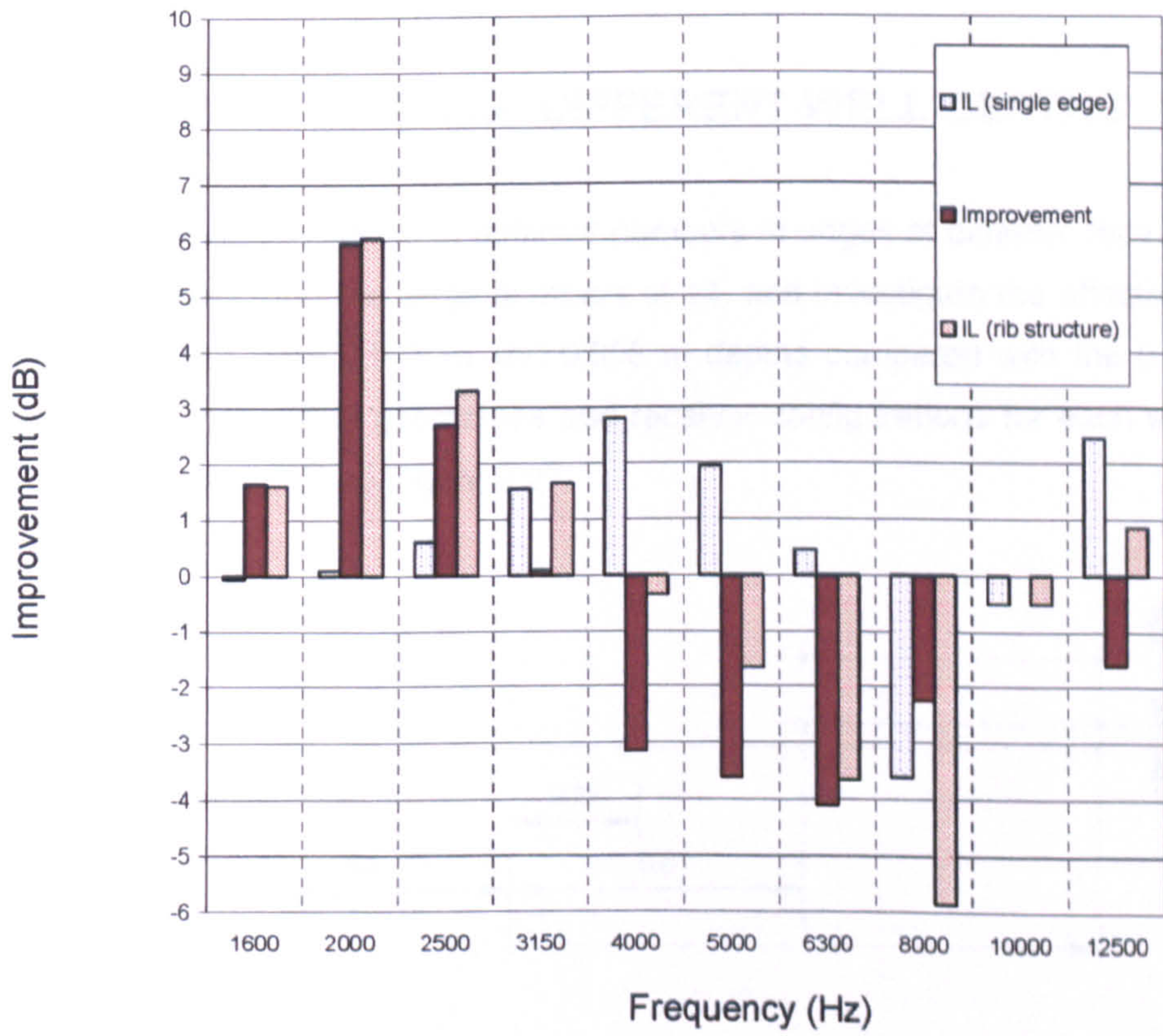


Figure 9.23 : Receiver height = 0.25m



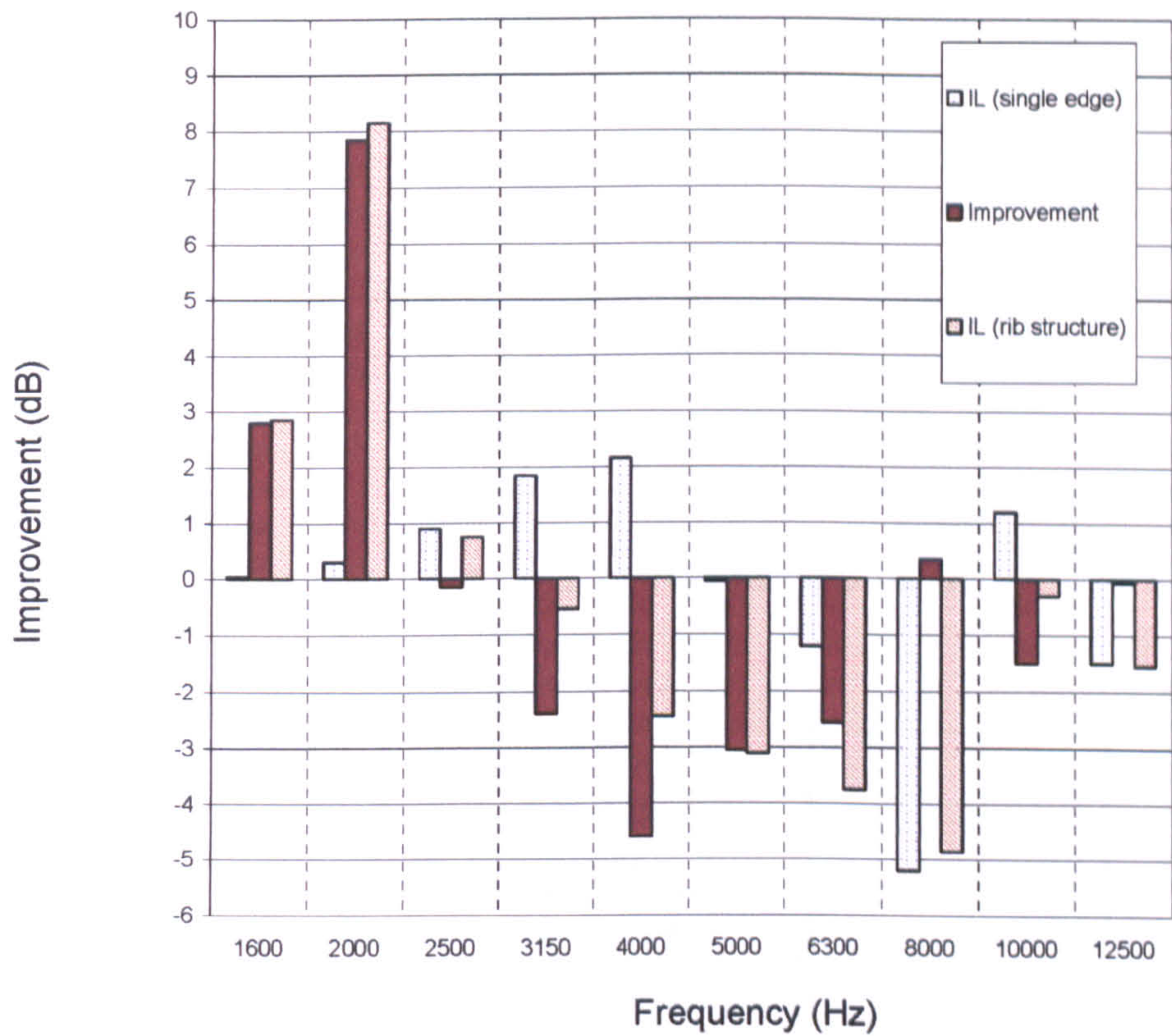


Figure 9.24 : Receiver height = 0.30m

### 9.4 COMPARISON OF DIFFERENT WELL DEPTHS

After observing the effects of different numbers of edges at different receiver positions, it was decided to fix the edge numbers at 14, and investigate the effects of three well depths. These were 0.017 m and 0.008 m depths compared with the 0.025 m depth discussed above. The geometries and receiver configurations for each well-depth are shown in Figure 9.25 to Figure 9.27.

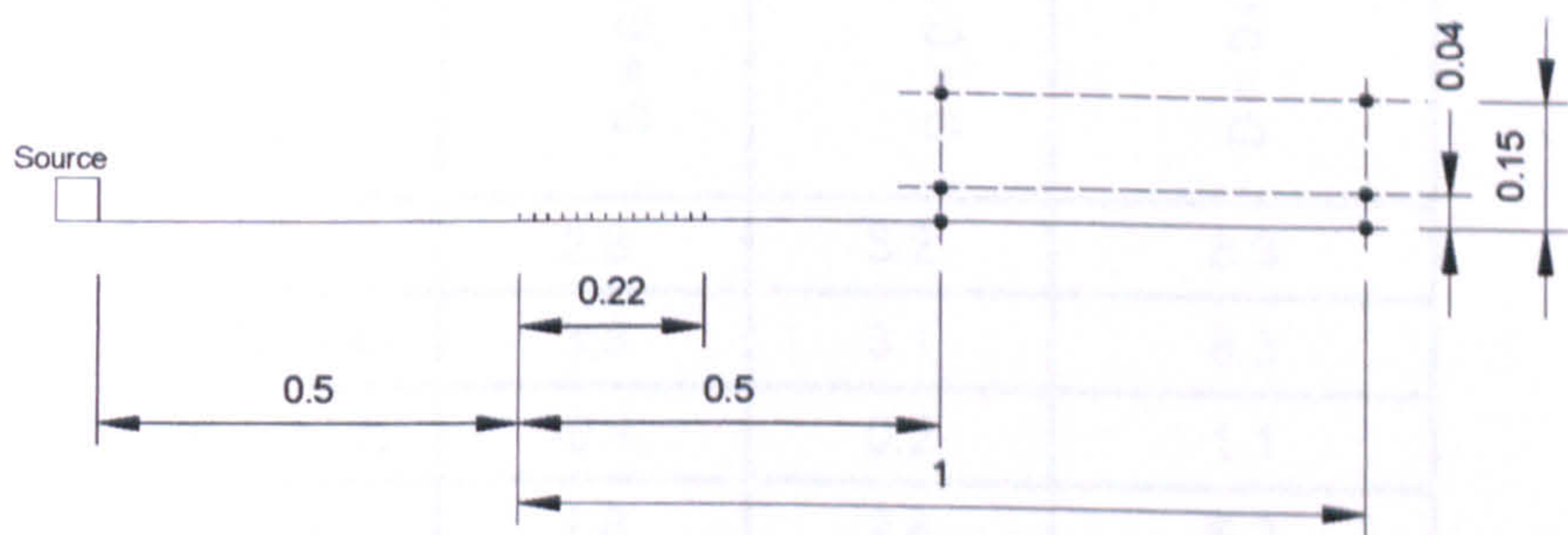


Figure 9.25 : The height of the wells is 0.008 m (well spacing is 0.017 m).



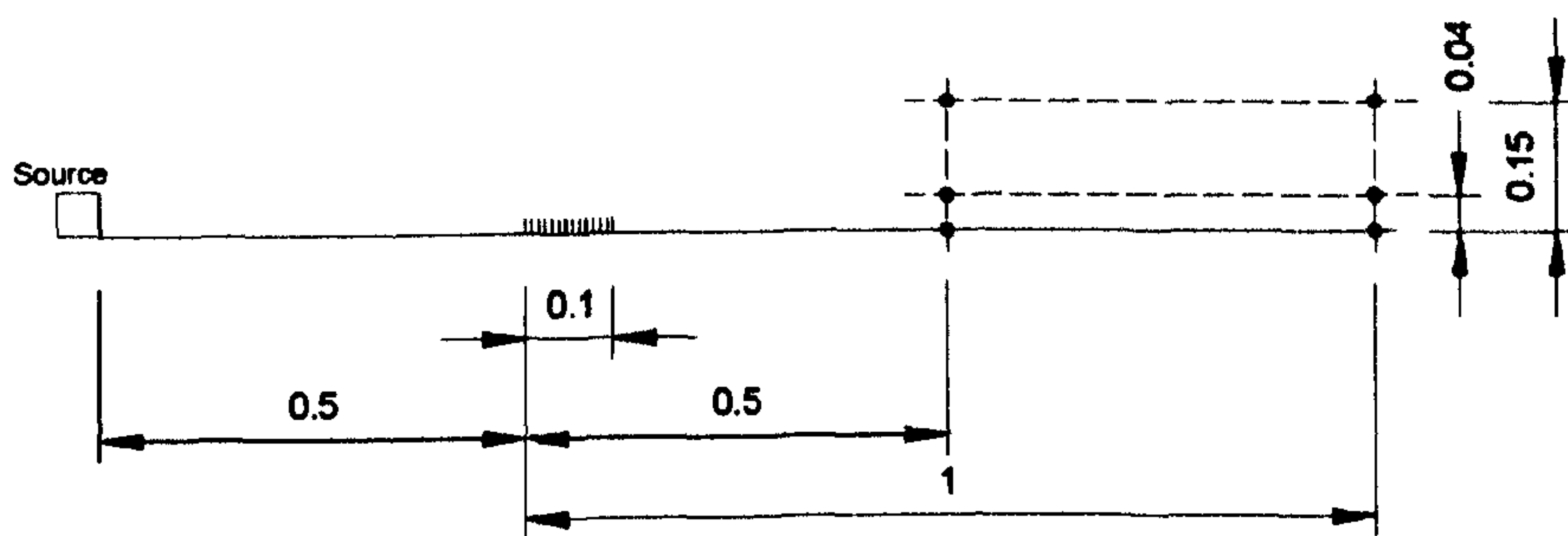


Figure 9.26 : The height of the wells is 0.017 m (well spacing is 0.008 m).

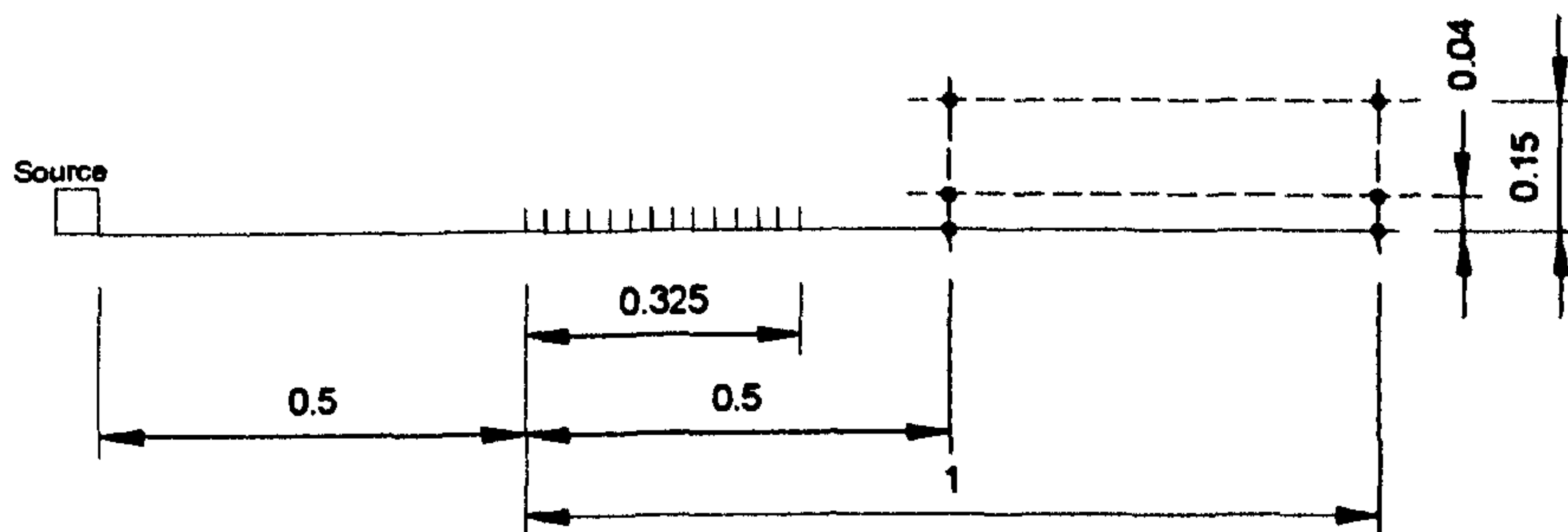


Figure 9.27 : The height of the wells is 0.025 m (well spacing is 0.025 m).

Source and receiver configurations are the same in all three geometries. All dimensions above are in metres. All three geometries have 14 edges in total. The relative improvements of different reactive surfaces over that of a single edge are tabulated in Table 9-3.

Relative improvement of 14 edges over a single edge (dB)			
Receiver co-ordinates (x, y) in m	D = 0.008m	D = 0.017 m	D = 0.025 m
(0.5,0)	2.8	3.2	8.3
(0.5,0.04)	3.3	3.1	8.3
(0.5,0.15)	-0.1	0.2	1.1
(1,0)	1.8	2.8	6.2
(1,0.04)	2.5	2.7	6.9
(1,0.15)	0.9	2.0	2.9

Table 9-3 : Relative improvement of reactive surfaces consisting of different well depths.



The spectrum of insertion loss and relative improvements obtained for the well depths of 0.008 m, 0.017 m and 0.025 m are shown in Figure 9.28 to Figure 9.33. In general it could be observed that gains obtained for lower receiver locations diminished as the height of the wells were reduced.

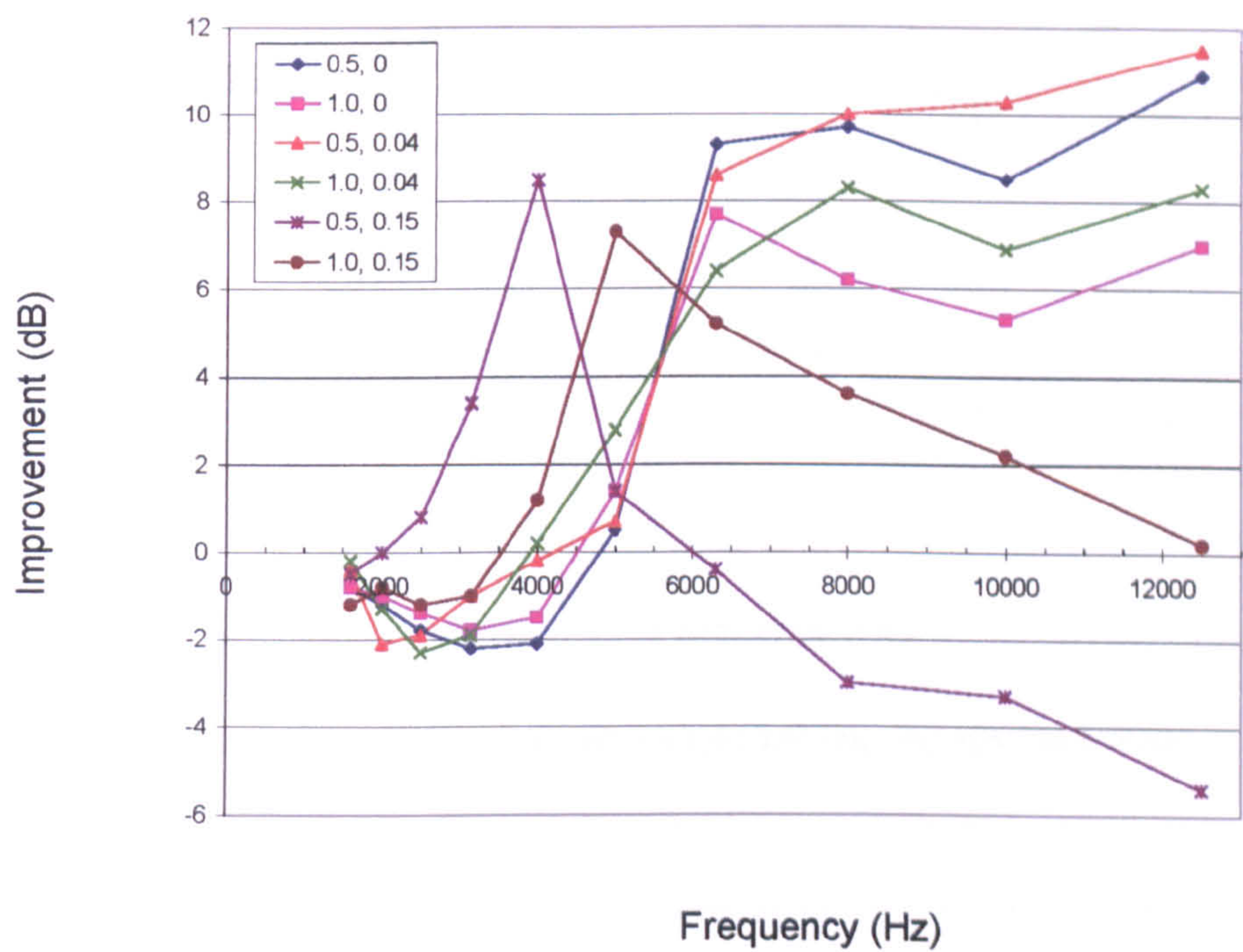


Figure 9.28 : Insertion Loss of 14-edges (edge height 0.008 m, edge spacing 0.017 m)

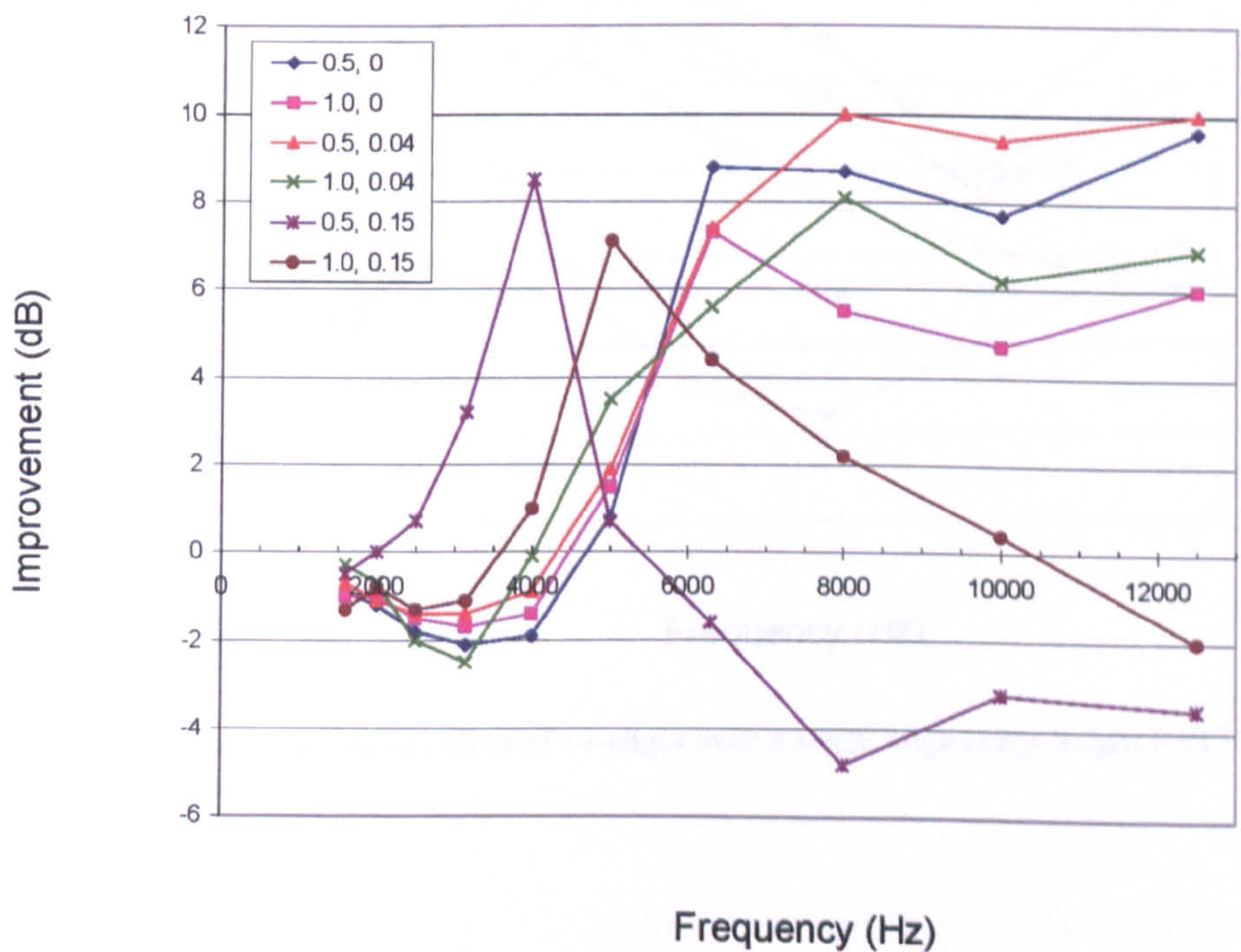


Figure 9.29 : Relative improvement of 14-edges over a single edge (edge height 0.008 m, edge spacing 0.017 m)



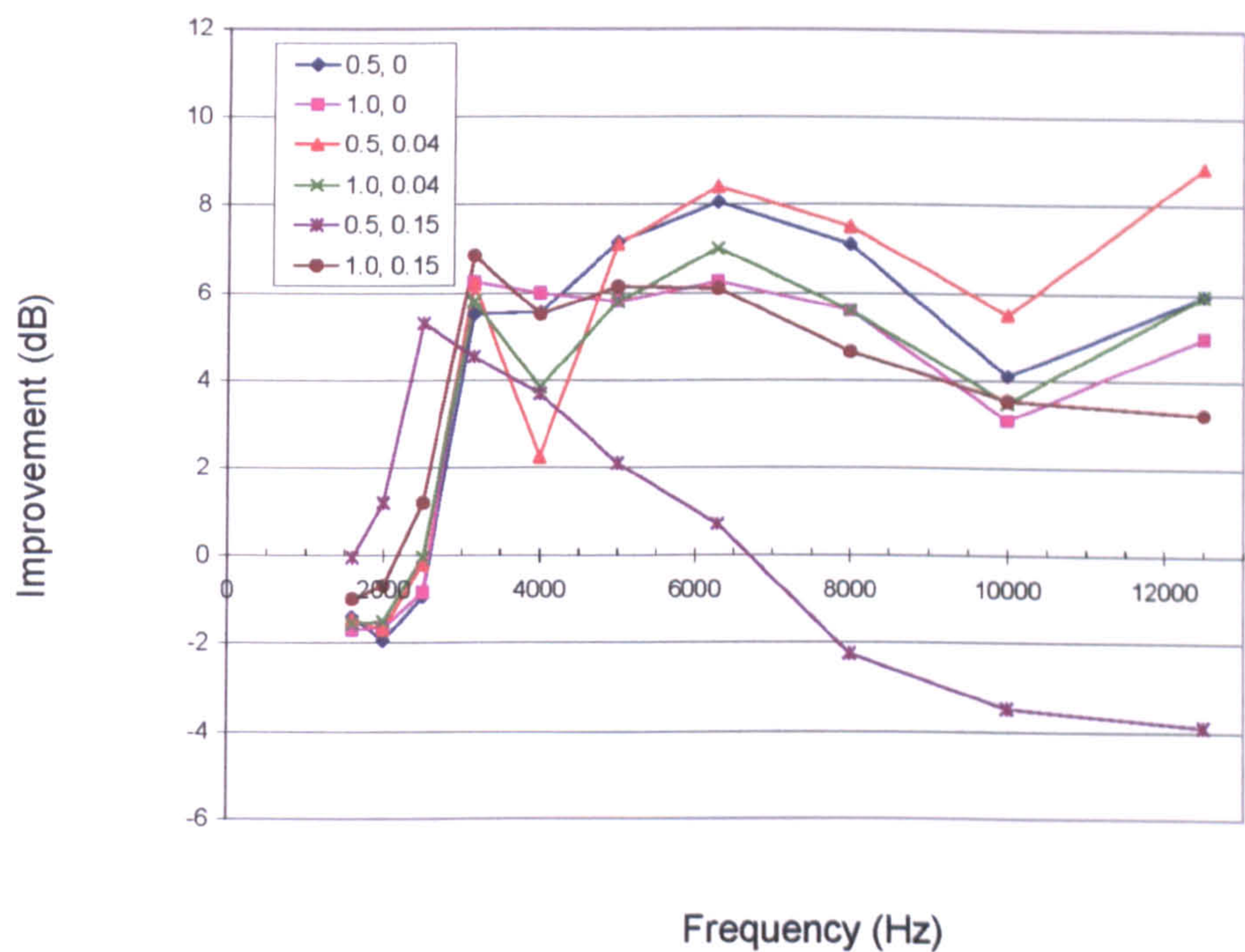


Figure 9.30 : Insertion Loss of 14-edges (edge height 0.017m, edge spacing 0.008m)

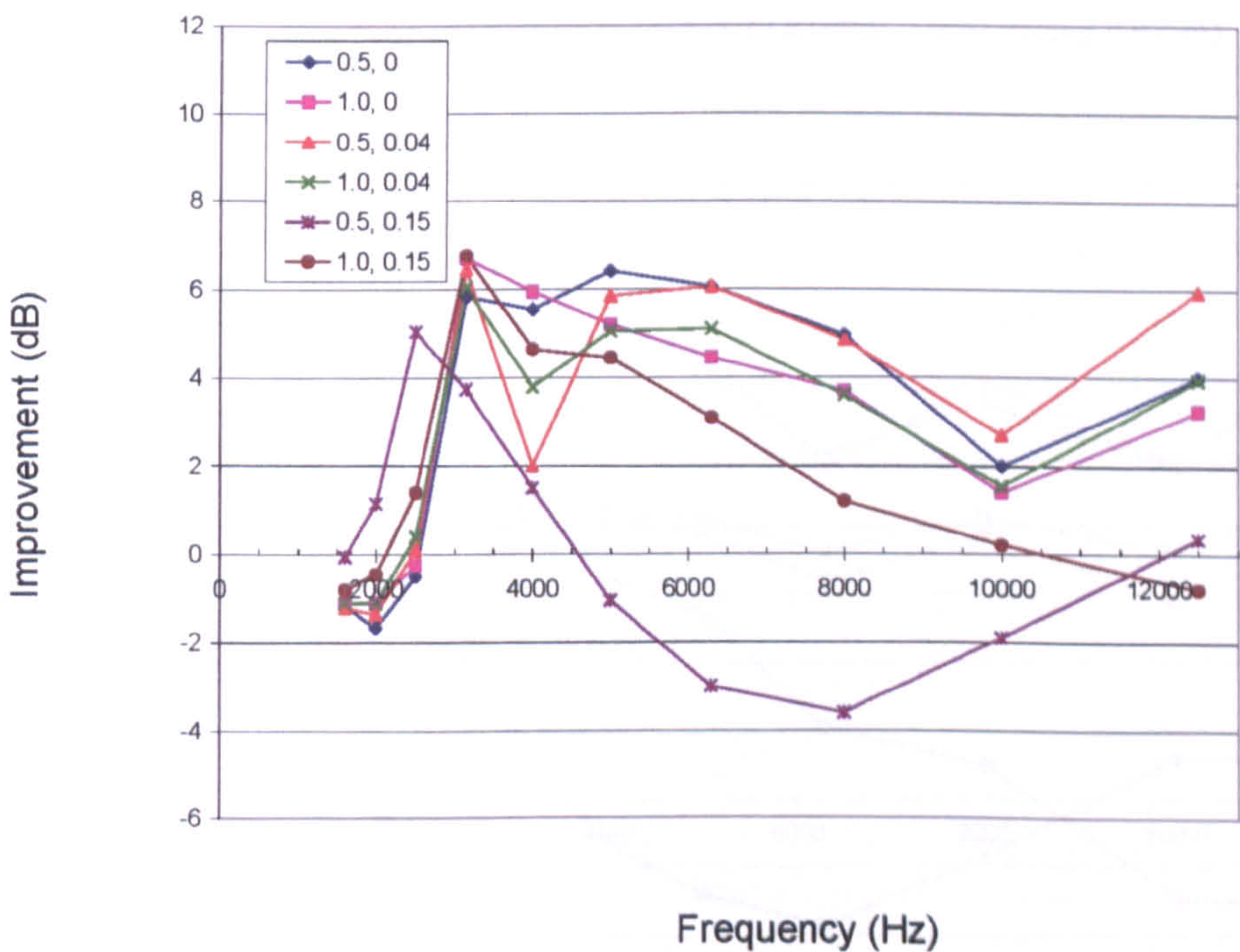


Figure 9.31 : Relative improvement of 14-edges over a single edge (edge height 0.017 m, edge spacing 0.008 m)



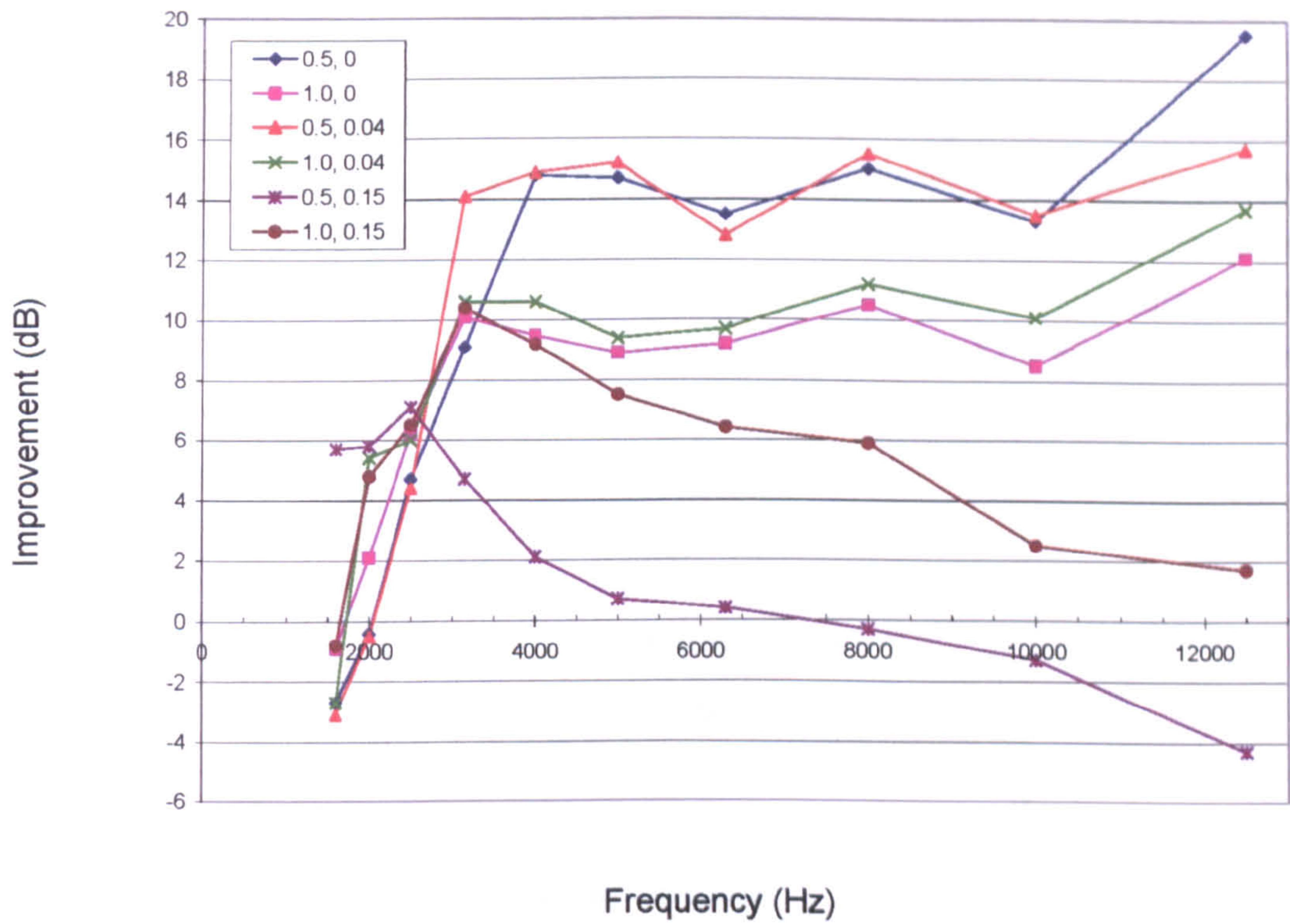


Figure 9.32 : Insertion Loss of 14-edges (edge height 0.025m, edge spacing 0.025m)

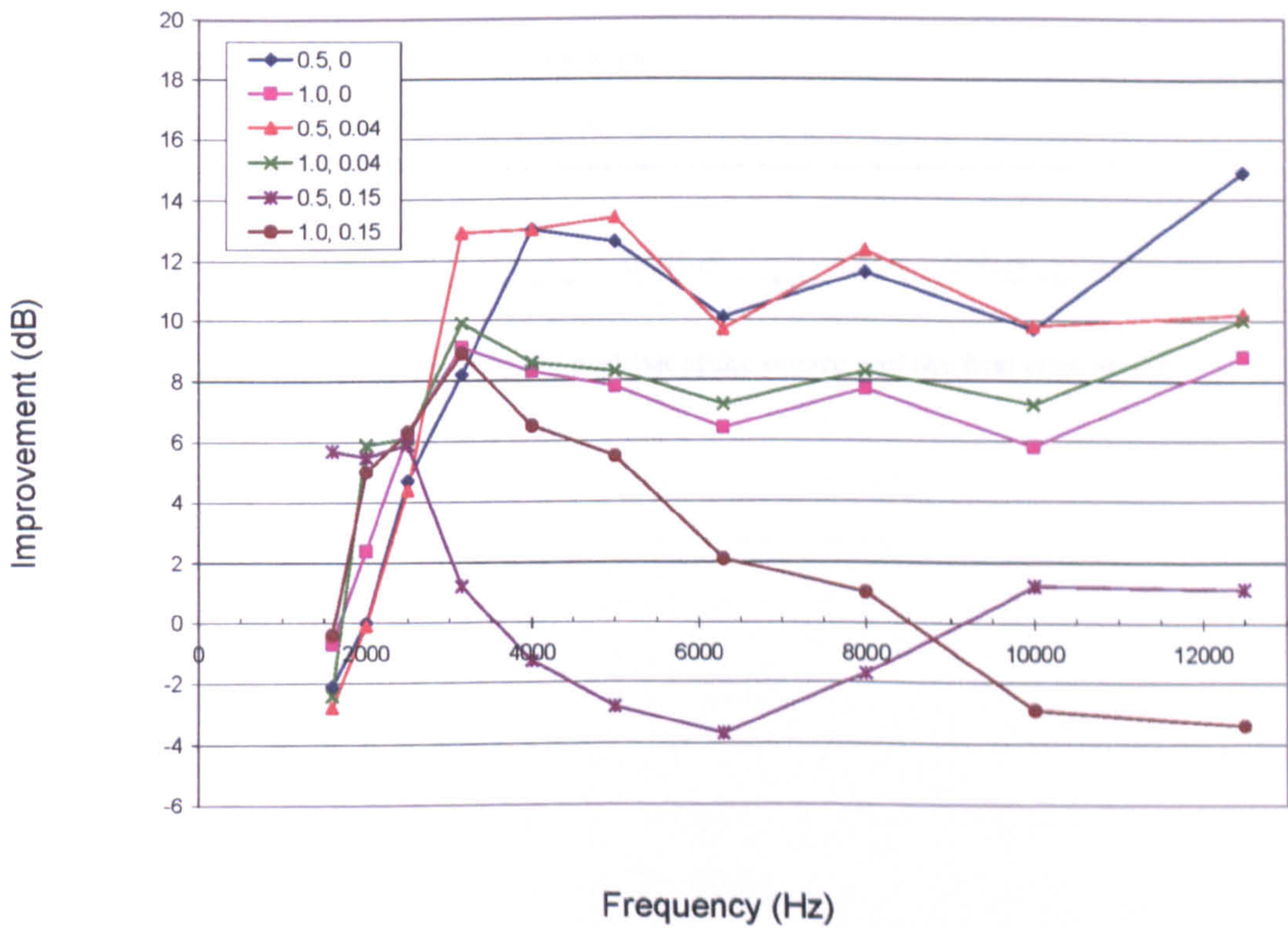


Figure 9.33 : Relative improvement of 14-edges over a single edge (edge height 0.025m, edge spacing 0.025m)



# 9.5 MULTIPLE EDGES ON A LOW RECTANGULAR BARRIER

These experiments investigated the effects of multiple edges on low rectangular barriers. These aim to establish if the improvements in performance would still be applicable and if these would reinforce the performance of the plain rectangular barrier. The edges were set up on top of a rectangular platform as shown in Figure 9.34 to Figure 9.36. The rectangular barrier was 0.315 m wide and 0.05 m high in cross-section and had an overall length of 2.4 m. Further details on this experimental set-up have been provided in Chapter 8.

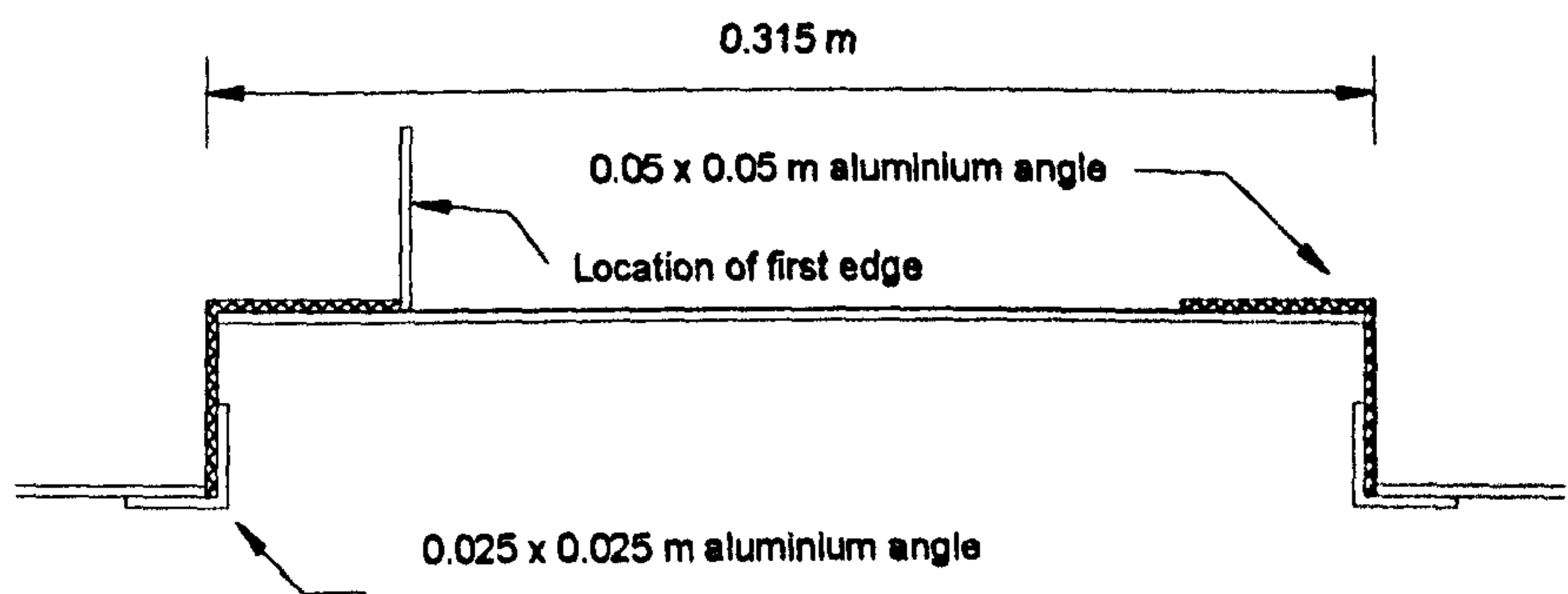


Figure 9.34 : Detail showing the cross - section through the rectangular platform on which the edges were placed.

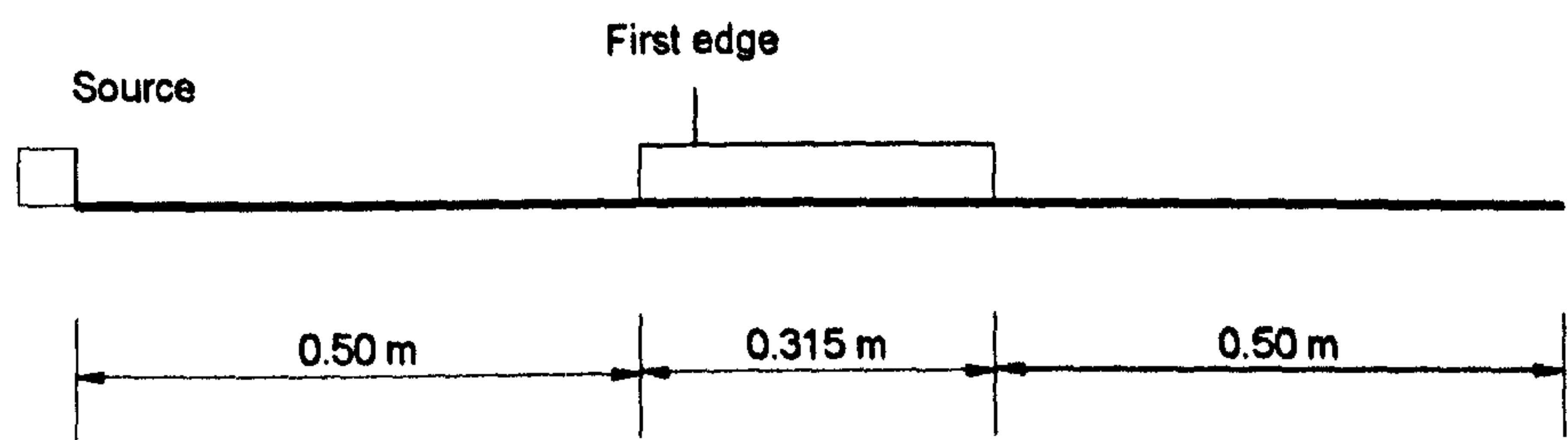
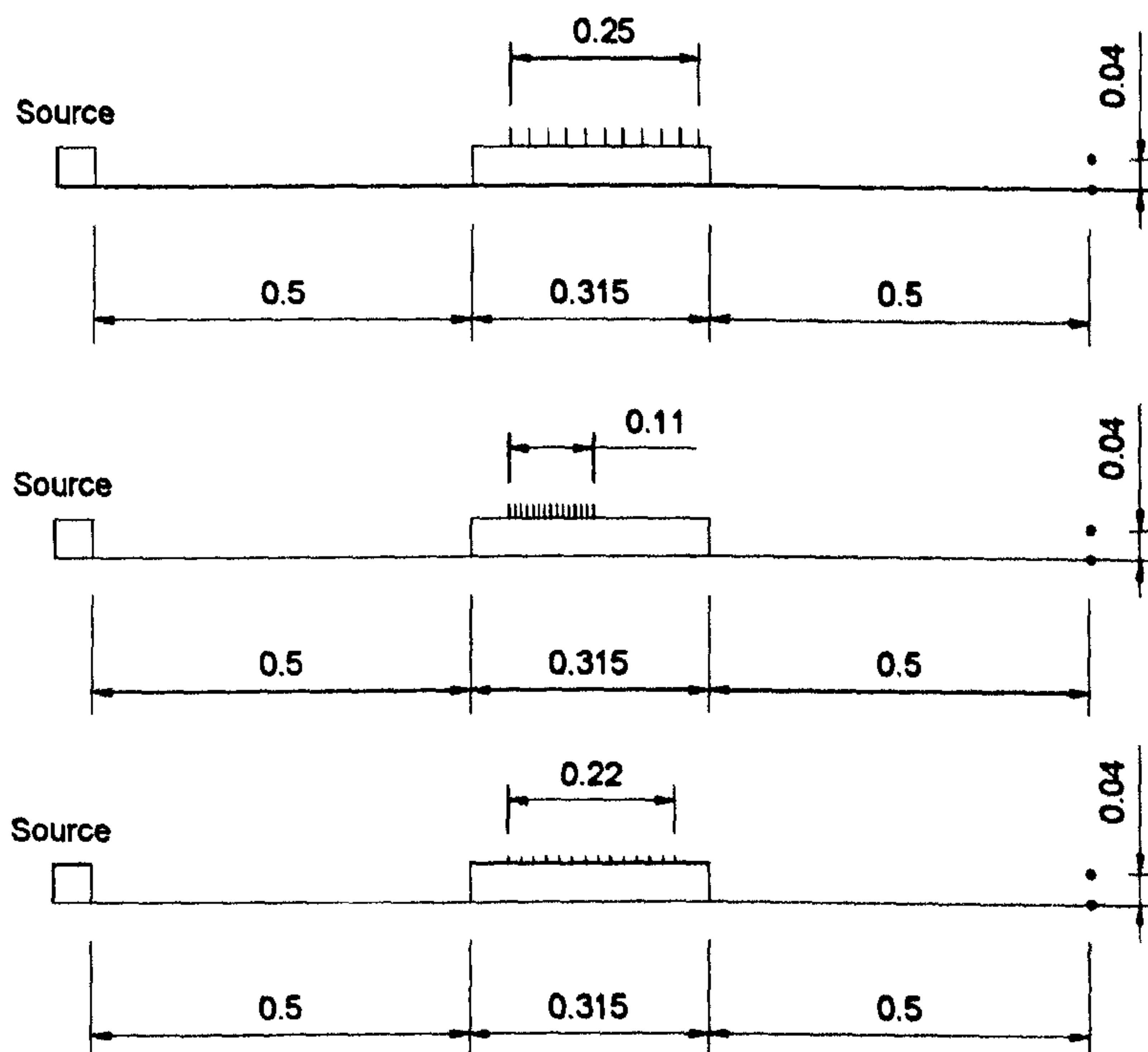


Figure 9.35 : The basic shape showing the position of the source and the first edge on the rectangular platform.





**Figure 9.36 : Experimental set-up for the reactive rectangles**

The insertion loss of the rectangular barrier and the relative improvement of single and multiple edges over a plain rectangle at the two receivers are summarised in Table 9-4.

		Receiver (0.5, 0)		Receiver (0.5, 0.04)	
	Insertion loss of rectangular barrier (dB)	7.6		8.4	
	Additional effect of edges (dB)	Single Edge	Multiple Edges	Single Edge	Multiple Edges
Well Depth	D = 0.025m	1.5	5.0	2.0	6.2
	D = 0.017m	0.4	3.2	0.6	3.5
	D = 0.008m	0.2	2.7	0.2	2.7

**Table 9-4 : The improvement due to the multiple edges over the basic shape.**

The spectra of improvements over a plain rectangle for receivers (0.5, 0) and (0.5, 0.04) are shown in Figure 9.37 and Figure 9.38 respectively. The insertion losses due to the plain rectangle and the reactive rectangles are shown in Figure 9.39 and Figure 9.40 for receivers (0.5, 0) and (0.5, 0.04) respectively.



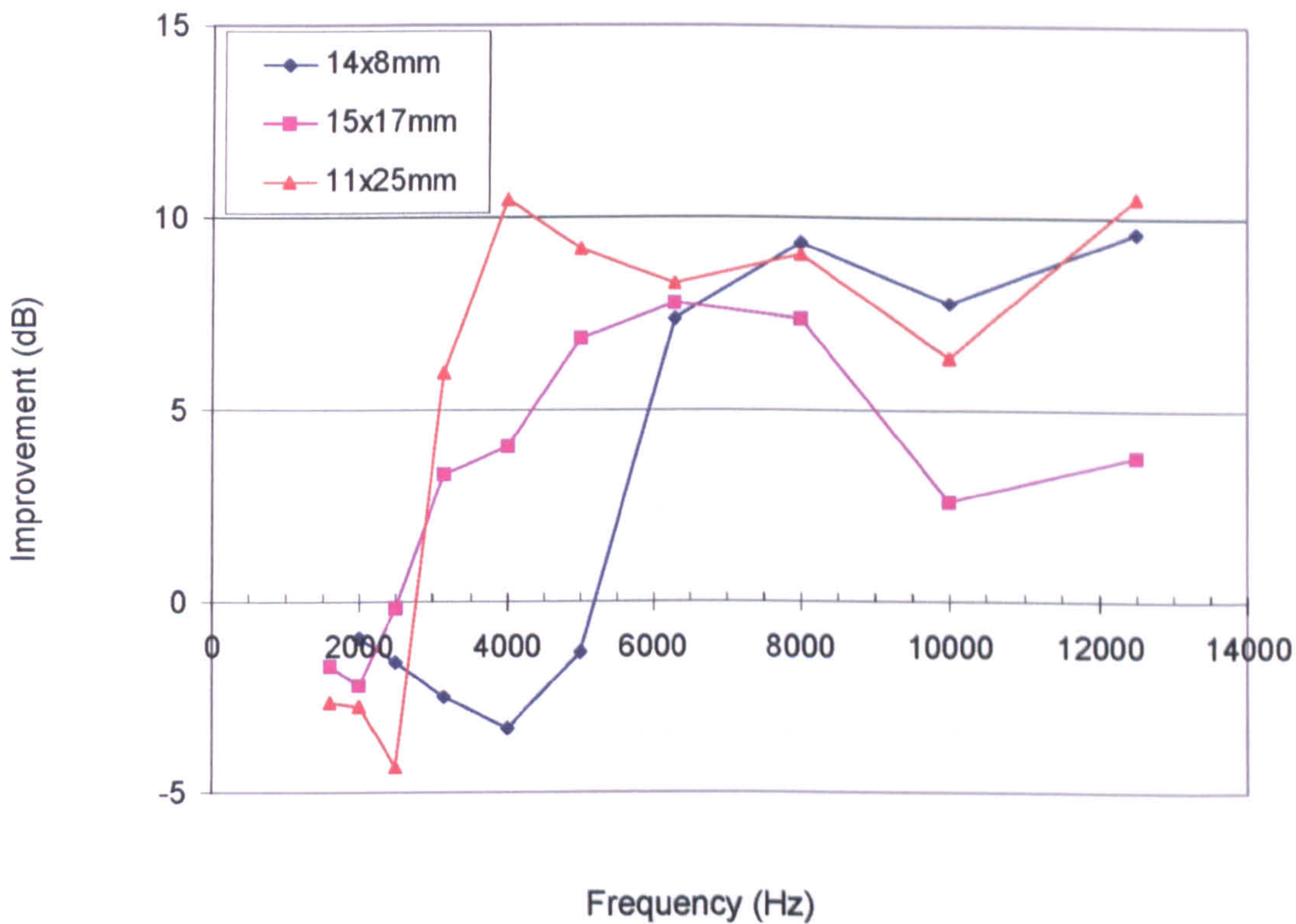


Figure 9.37 : Improvement in performance over plain rectangles by different edge heights (Rec. ht = 0.5, 0).

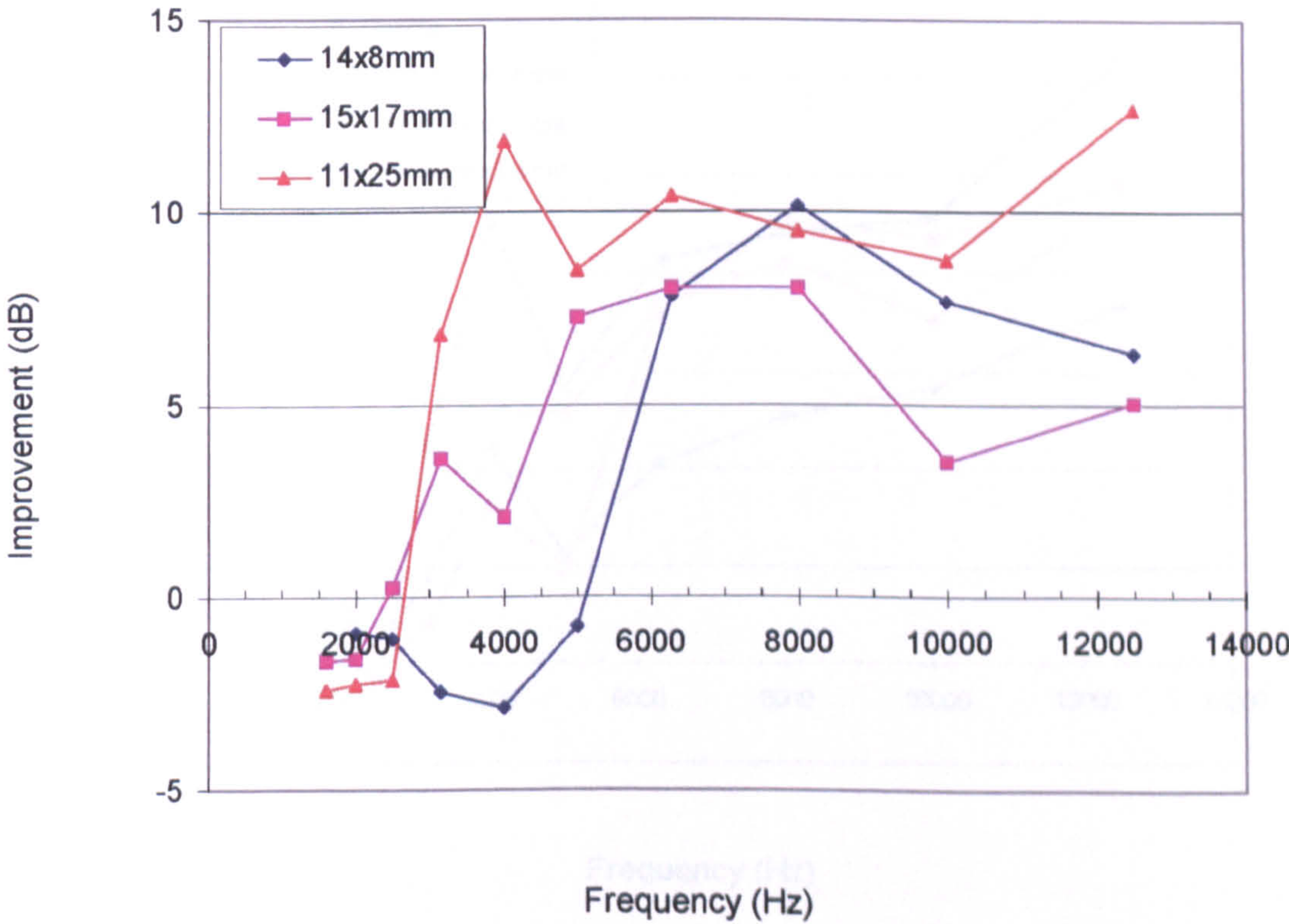


Figure 9.38 : Improvement in performance over plain rectangles by different edge heights (Rec. ht = 0.5, 0.04).



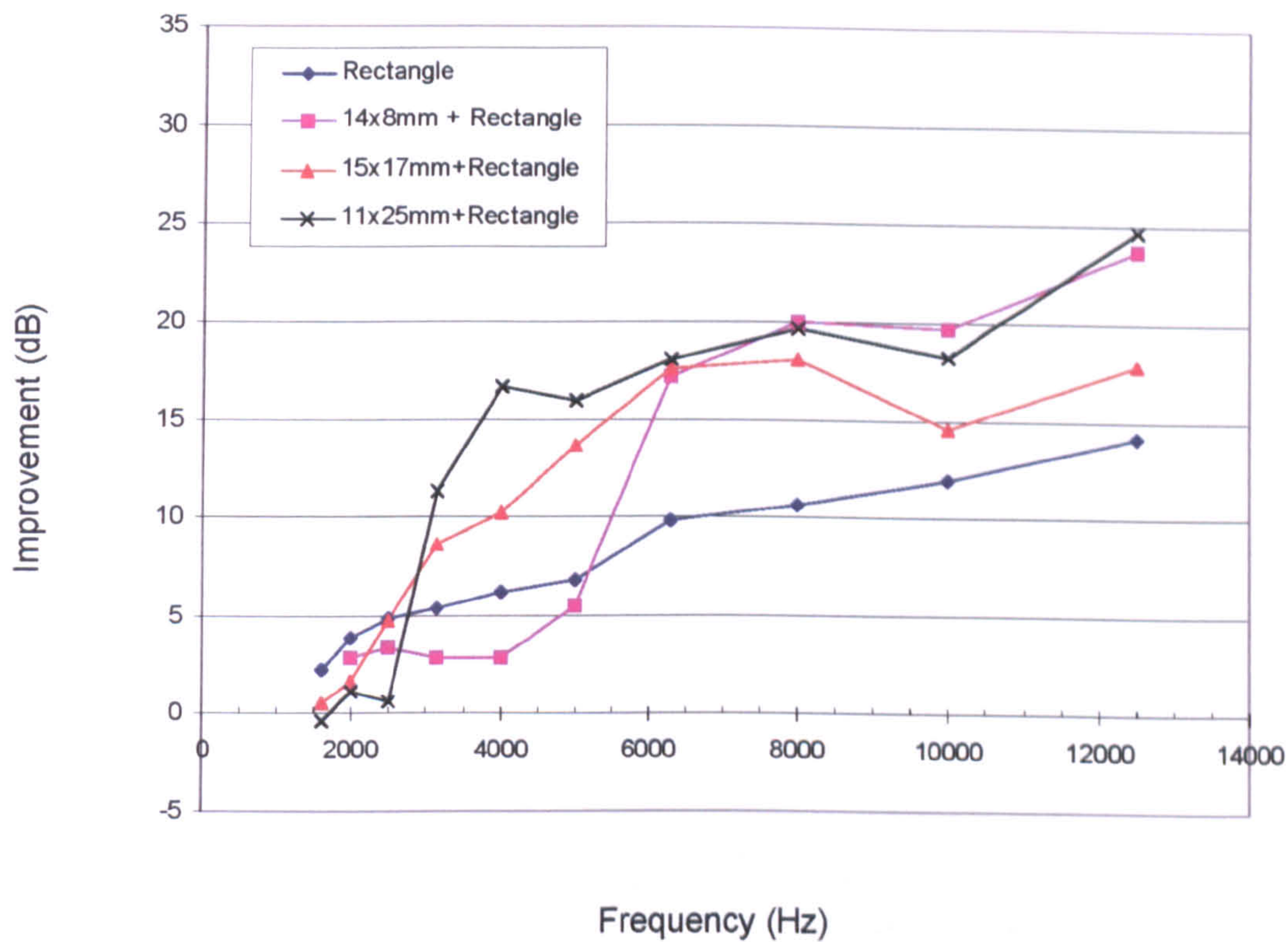


Figure 9.39 : Insertion loss of plain rectangle and combined edges plus rectangle (Rec. ht = 0.5, 0)

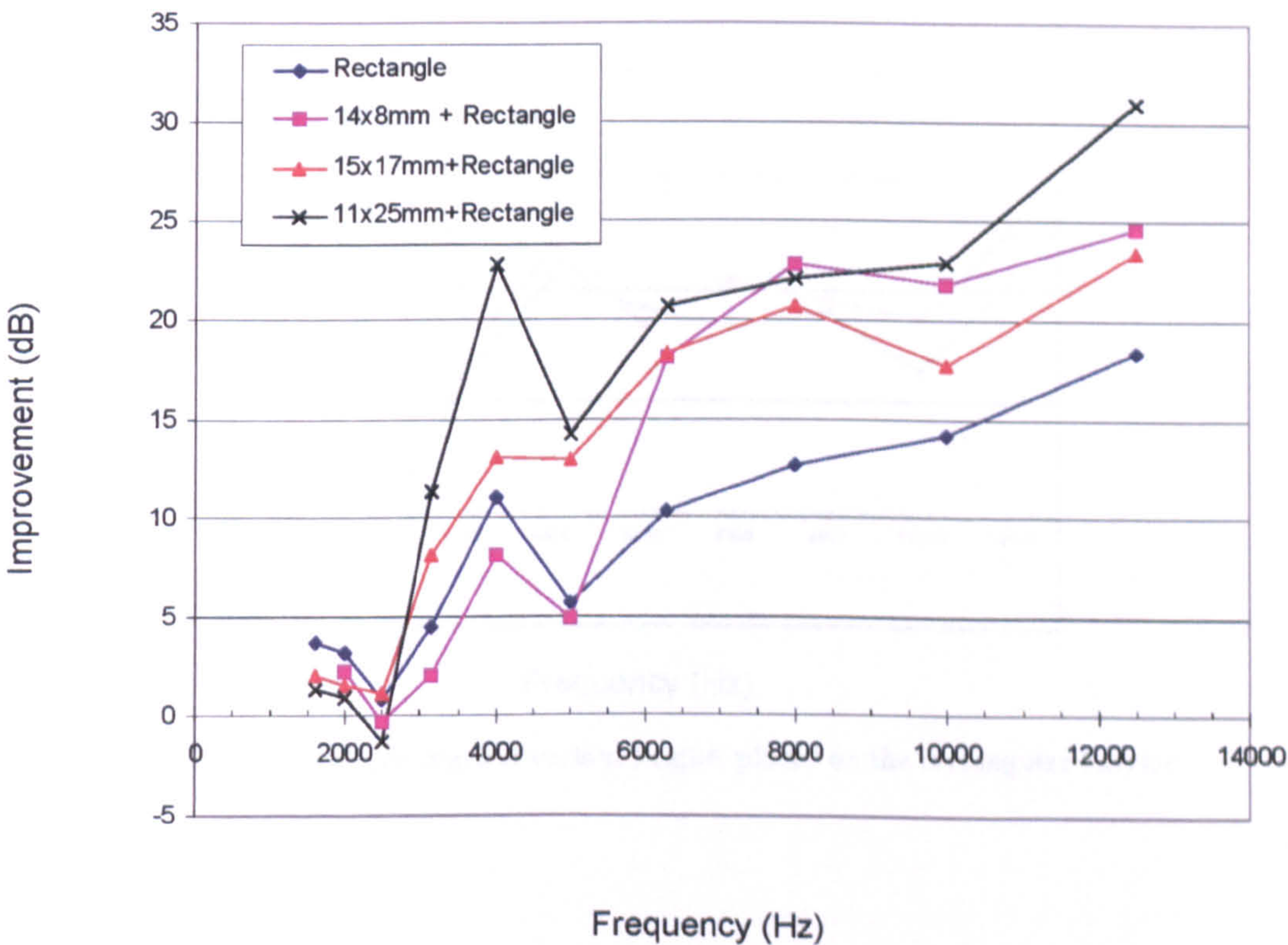


Figure 9.40 : Insertion loss of plain rectangle and combined edges plus rectangle (Rec. ht = 0.5, 0.04)



Improvement over the rectangular barrier (dB)

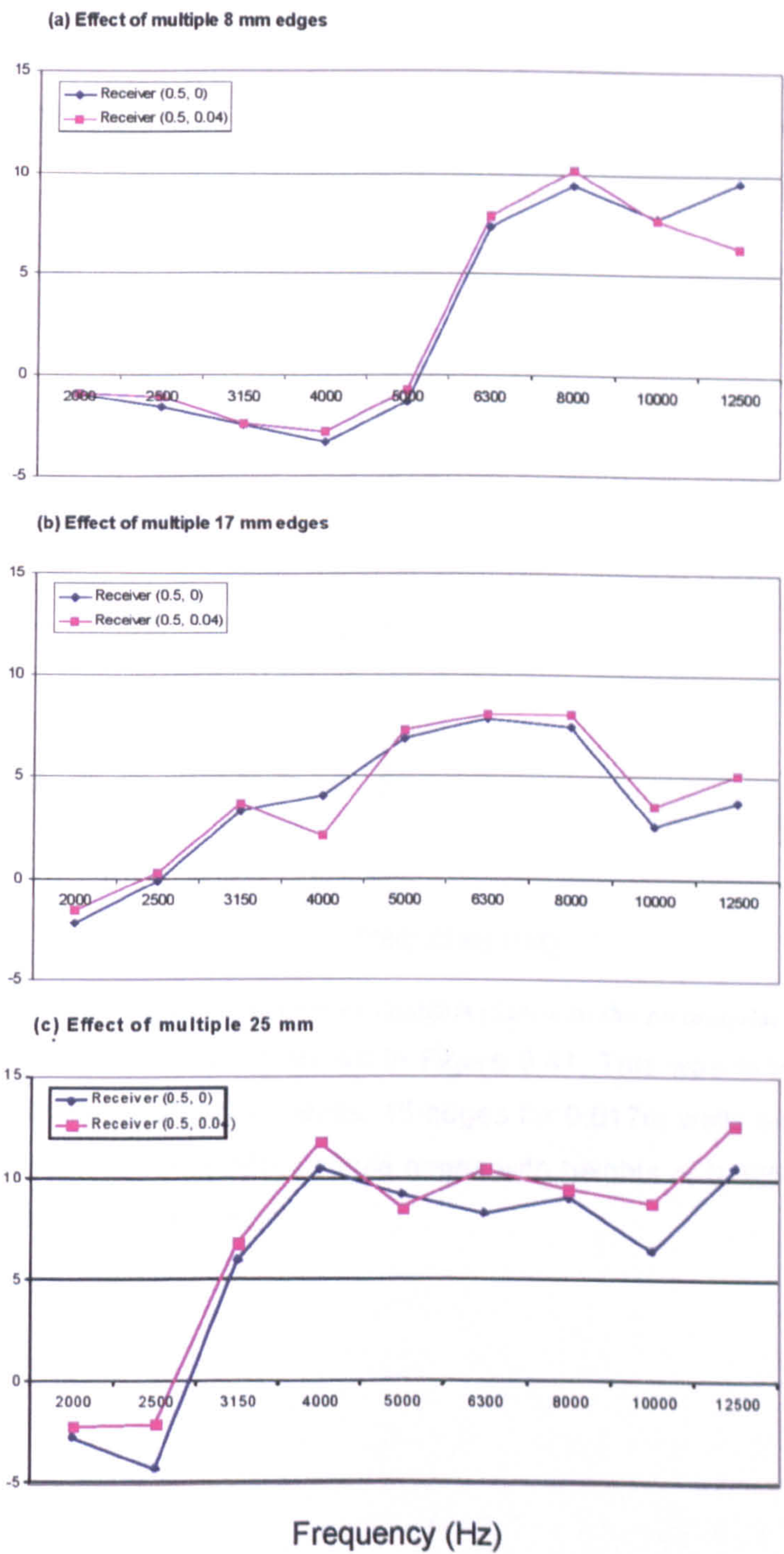
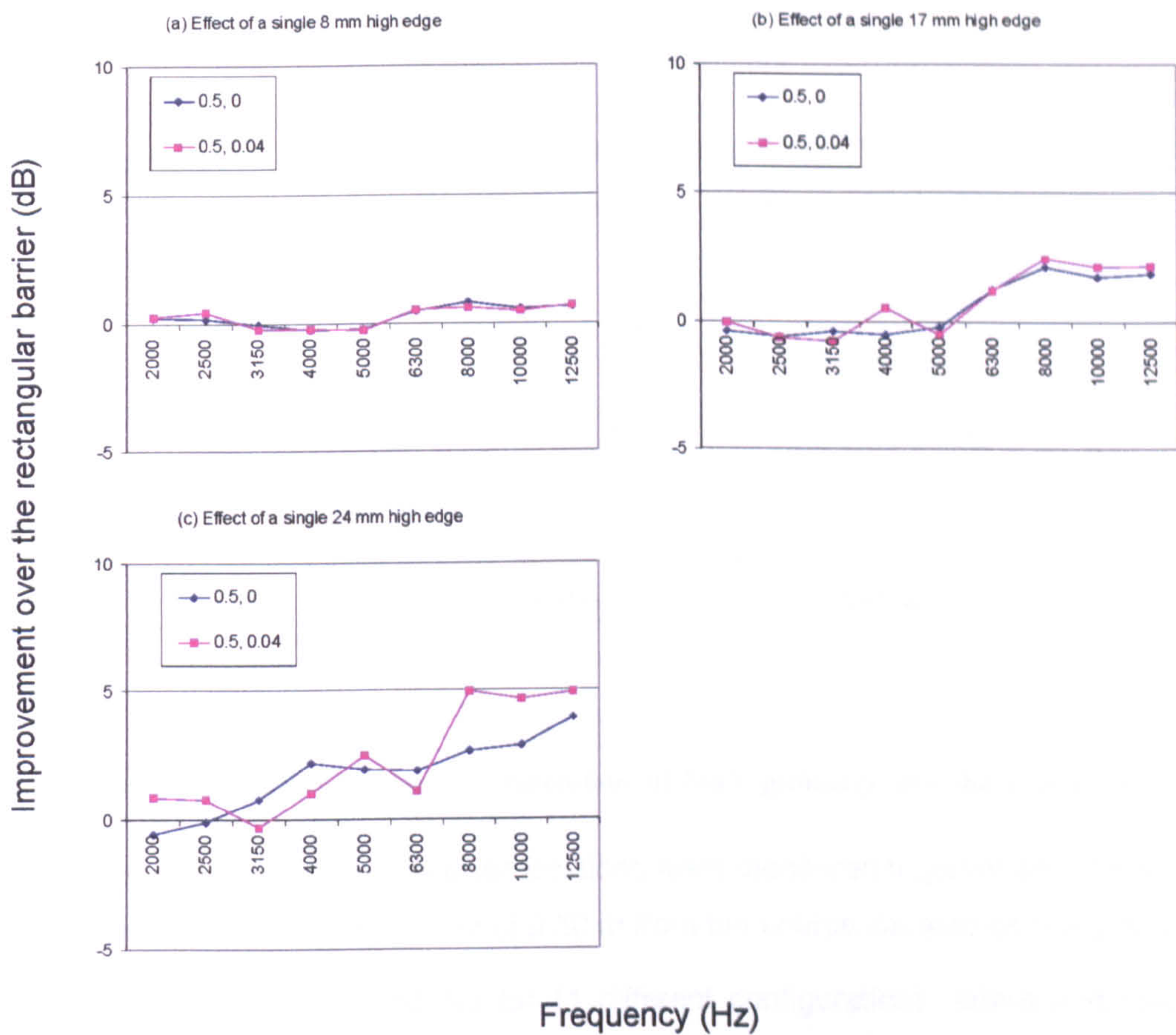


Figure 9.41 : Effect of multiple edges of various heights placed on the rectangular barrier





**Figure 9.42 : Effect of single barriers of various heights placed on the rectangular barrier.**  
 The effects of multiple edges are shown in Figure 9.41. This was in the shape of 14 edges in the case of 0.008m deep wells, 15 edges for 0.017m wells and 11 edges for the 0.025m wells. The effects of the single edges with heights of 0.025m, 0.017m and 0.008m are shown in Figure 9.42.



9.6 MULTIPLE EDGES ON A FLAT-TOPPED MOUND

The basic earth mound and the source-receiver configuration is as seen in Figure 9.43. Total model length was 3.6 m. Further details have been provided in Chapter 8.

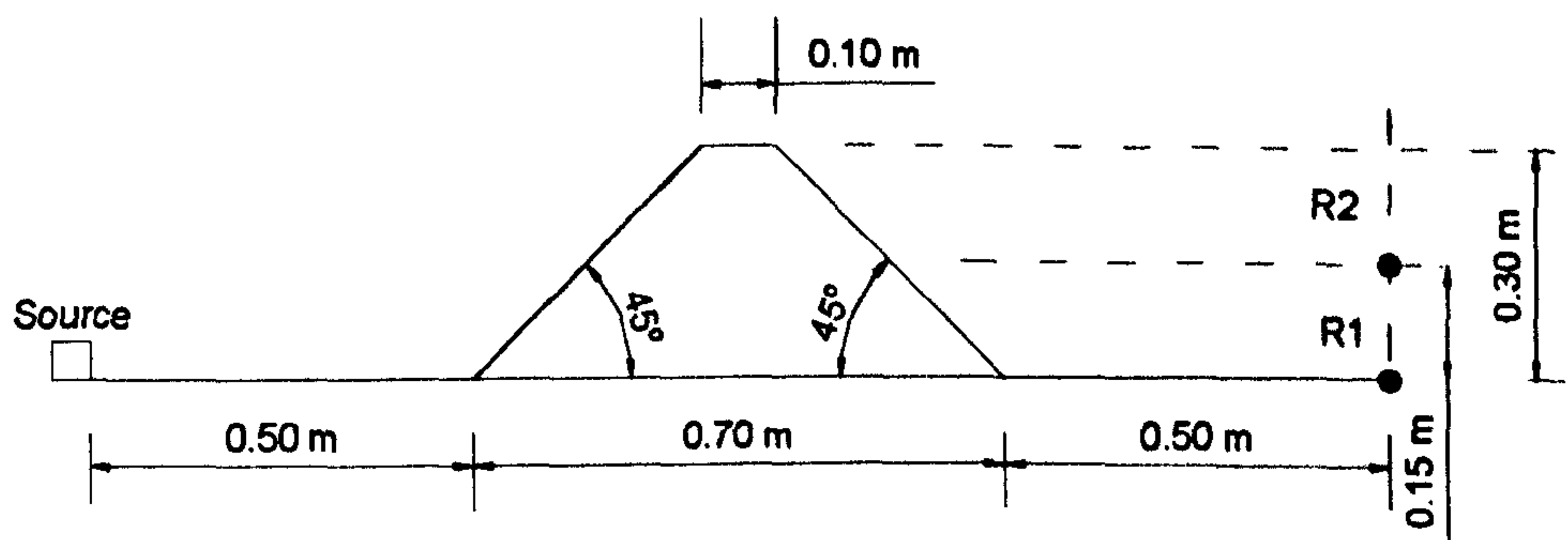


Figure 9.43 : Reference case showing dimensions of basic geometry and the source / receiver locations.

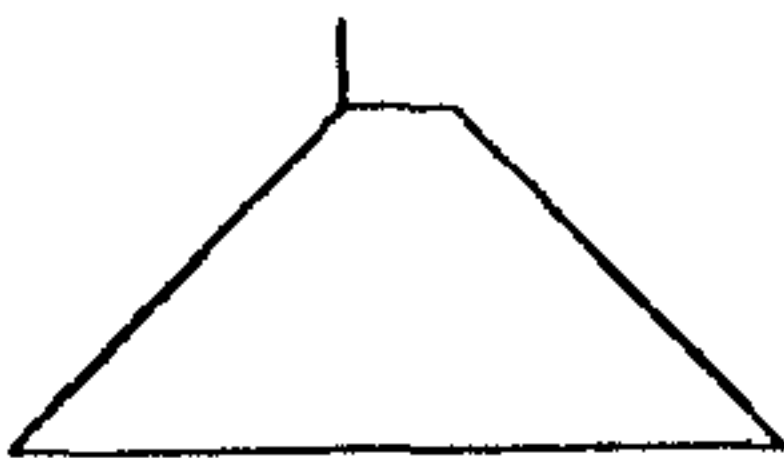

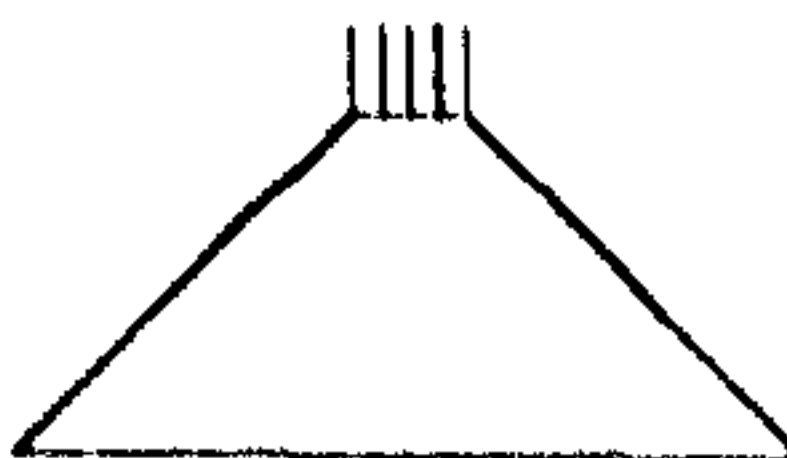
Sound pressure levels at the receiver locations were monitored together with the sound pressure levels at a reference point of 0.30 m from the source situated on the ground.

The experiments were carried out for 11 different configurations details and relative performances of which are shown in Table 9-5 and Table 9-6. In addition to the single and multiple edge conditions, the double edge configurations were also investigated. The single edges were all placed on the source side of the top horizontal section, and double edges were positioned on either sides of the top horizontal section. As many edges as possible were positioned one after another, depending on the width of the angle sections, and hence the total number of edges and the separation distance between them varied. This is shown in Table 9-7.

Edge height (m)			
0.050	0.4	1.9	N / A
0.025	0.2	0.7	0.3
0.017	0.0	0.3	0.1
0.008	-0.3	-0.6	0.0

Table 9-5 : Relative performance of various edge conditions investigated for receiver 1.



Edge height (m)			
0.050	1.0	2.9	N / A
0.025	0.6	1.6	1.9
0.017	0.2	0.8	1.1
0.008	-0.3	-0.3	0.3

**Table 9-6 : Relative performance of various edge conditions investigated for receiver 2.**

Edge height (m)	Multiple Edges
0.050	n/a
0.025	total of 5 (separation = 0.025m)
0.017	total of 10 (separation = 0.008m)
0.008	total of 5 (separation = 0.017m)

**Table 9-7 : The details of the reactive configurations.**

The spectra of gains are shown in Figure 9.44.



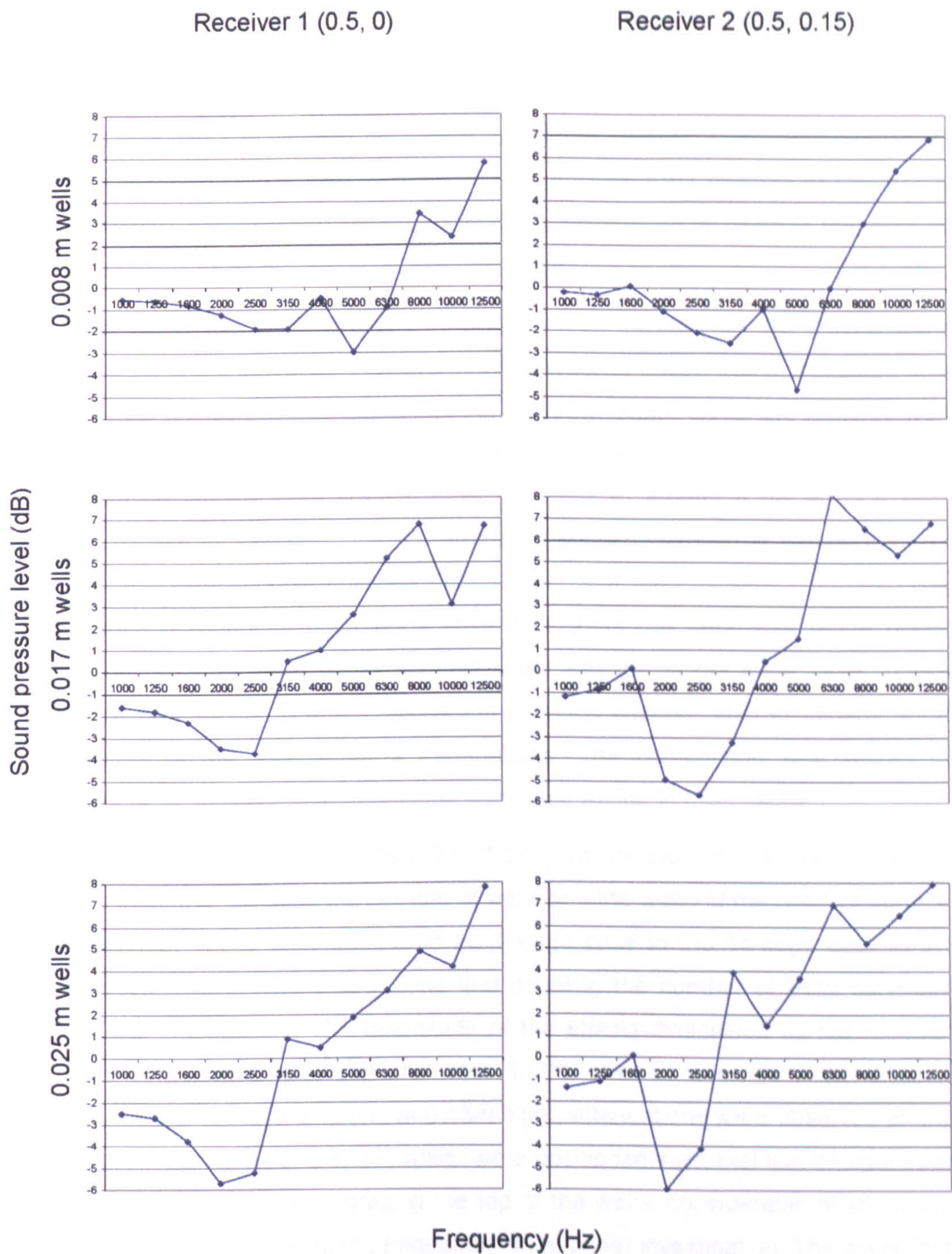


Figure 9.44 : The frequency spectrum of gains for various reactive configurations.



## 9.7 DISCUSSIONS

This chapter presents the findings of the repeated tests in two different semi-anechoic chambers, and aims to identify the limitations of the method previously discussed. Additional experiments are also undertaken to supplement the findings of Chapter 8 and to understand the likely mechanisms of noise attenuation involved in the case of rib structures consisting of a series of edges or wells.

In the first set of tests, the effects of multiple edges situated on the ground were studied. Initially the progressive increase in the number of edges was investigated at a single receiver location. It was found that the sound pressure levels are reduced with increased number of edges, except at 1600 Hz. The insertion loss values for a single edge increased linearly from around 0 dB at 2 kHz to around 6 dB at 12.5 kHz. Insertion loss due to 8 edges showed a distinctive sudden increase at around 2.5 kHz to 10 dB, remaining roughly constant until 10 kHz and then increasing further. The insertion loss provided by the 8-edge case throughout the frequency range under investigation is higher by 5 to 10 dB compared with the single edge case. These findings are very similar to those reported in previous chapter, both in general trend and in terms of the magnitude of attenuations. The comparison was limited to frequencies up to 12.5 kHz due to reasons discussed earlier in this chapter.

Having established the potential benefits of progressive increase in the number of edges, the effects of doubling the number of wells and the width of the reactive surface are investigated. These tests compared the 8-edge case to the 14-edge case at six different receiver locations. It was found that doubling the number of wells generally increased the attenuations. The magnitude of the effects diminished as the receiver was horizontally further away from the wells. In the case of receivers which were in direct line-of-sight of the source (i.e. at 0.15m high), attenuations were observed at low frequencies. In the case of receivers which were positioned such that line-of-sight from the source to the receiver was grazing the top of the wells, considerable attenuations were observed at higher end of the frequency range under investigation. The lower limit of these frequencies corresponded approximately to the quarter-wavelength of the wells discussed earlier, which is around 3400 Hz. Increasing the number of edges appears to have shifted the lower limiting frequency at which substantial reductions occur closer to this frequency. These reductions occurred at 2500 Hz for the 8-edge case and 3150 Hz for the 14-edge case.

In order to have a better appreciation of the relationship between attenuations and amplifications at various frequencies and receiver positions, additional tests were



carried out. These experiments can be considered to be a combination of the previous two where the effect of progressive addition of up to 17 edges at six receivers is studied simultaneously.

As shown in Figure 9.11 significant reductions have been achieved in the sound pressure levels (referred to as SPL) for receiver (0.5, 0), with increased number of edges. Between 4000 Hz and 12500 Hz, the reductions due to 17-edge case are between 17 dB and 26 dB. At lower frequencies, addition of further edges makes the situation worse, increasing the SPL by up to 4 dB. At 2500 Hz, 8-edge situation achieved the maximum sound reduction and the addition of the subsequent edges increased the SPL. At 3150 Hz addition of 4 edges achieved most of the reductions and the remaining edges up to 17 did not contribute substantially to the overall noise reduction at this frequency band. This receiver is situated on the ground and the addition of the first edge obstructs the line of sight from the source to the receiver as much as is possible in this configuration. The subsequent addition of edges does not affect the path length difference significantly and therefore it would be reasonable to assume that these gains are not a function of the path length difference. From the trend in the SPL reductions, further substantial reductions by the addition of even more edges appear achievable.

As shown in Figure 9.12, compared with the SPL reductions at receiver (0.5, 0), improvements at receiver (1, 0) are more modest at 9 to 14dB between 3150 Hz and 12500 Hz. The rate of SPL reductions is also smaller indicating that the additional substantial reductions may not be possible. The 11 dB improvement at 3150 Hz is noted. As recalled above, at receiver (0.5, 0) a similar performance was achieved by less fewer edges. At 2500 Hz the lowest SPL is achieved by 11-edge configuration and further addition of edges increases the SPL. The general SPL reduction pattern at receiver (1, 0) is similar to that of (0.5, 0). However the magnitudes of these reductions are much smaller even though both receivers are in the shadow zone. The main difference between these two configurations is the proportion of the source-to-receiver distance covered by edges, indicating that the smaller the proportion of area, lesser the reductions in SPL.

Figure 9.13 shows reductions for receiver (0.5, 0.04) which is at grazing incidence from physical centre of the source over the series of edges. Between 3150 Hz and 12500 Hz maximum reductions achieved are between 13 dB and 18 dB. However, this is not achieved by the 17-edge configuration, as was the case in the previous two receivers. The best performing configurations are 13-edge and 15-edge cases at 8000 Hz and 10000 Hz respectively.



At frequencies above 5000 Hz, attenuations due to the 17-edge case show that sound pressure levels either stopped decreasing or started increasing. This is the case also at 2500 Hz where the 9-edge configuration achieved 11 dB reductions and the 17-edge case performed as well as the 3-edge case.

Figure 9.14 shows that SPL reductions for the receiver (1, 0.04) are around 11 to 16 dB between 3150 Hz and 12500 Hz. Although the improvements around 4000 Hz are almost half the previous case, the high frequency performance at 12500 Hz remains largely unaffected. Increasing the horizontal distance of the receiver appears to limit the achievable reductions in SPL.

At 2000 Hz and 2500 Hz the diminishing returns are observed as before, as the SPL reaches its minimum with 14-edge and 10-edge configurations respectively. At 1600 Hz, the SPL is increased by 3 dB by the 17-edge case. None of the in-between cases at 1600 Hz reduces the SPL. The increase in SPL (or decrease in performance) at low frequencies could be due to surface wave generation mechanisms discussed in earlier chapters. Initially, increasing the number of edges appears to reduce the SPL at 2000 Hz and 2500 Hz. However subsequent addition of edges starts offsetting these improvements due to surface generation. In lower frequencies such as 1600 Hz, where surface waves may already be dominant, addition of more edges continues to support this mechanism, increasing the SPL. This observation applies to Figure 9.11 to Figure 9.14, indicating that at near grazing propagation over the edges, and at low receiver heights, an increase in the number of edges increases the likelihood of surface wave generation especially at lower frequencies.

At higher frequencies the general trend is a decrease in SPL with increased number of edges. The diminishing returns observed at receiver (0.5, 0.04) (see Figure 9.13 at 8 kHz and 10 kHz) at some of the higher frequencies are not noted here.

Receiver (0.5, 0.15) is of particular interest, since it is in direct line of sight of the source. The 17-edge configuration reduces SPL at low frequencies around 1600 to 2000 Hz, by 10 dB as shown in Figure 9.15. This is the reverse of the situation of previous cases where SPL increases were observed at receivers at grazing incidence or lower. At 2500 Hz 4-edge case performs the best with 8 dB reduction in SPL. In mid frequencies, between 5000 Hz and 8000 Hz, it should be noted that 1-edge case reduces the SPL by 3 to 4 dB and the subsequent addition of edges increases the SPL. At 12500 Hz, all configurations increase the SPL. Where the receiver is in direct line of sight, with the exception of frequencies less than 2000 Hz, subsequent addition of edges continue increasing (at higher frequencies) or decreasing (at lower frequencies) the SPL up to a point after which addition of further edges appear to reverse the situation.



In general, for the receivers in direct line of sight of the source, attenuations have been noted at lower frequencies and the high frequency performance deteriorates. At receiver (1, 0.15), as shown in Figure 9.16, the 17-edge case performs better than any other configuration between approximately 3150 Hz and 5000 Hz. At lower frequencies than these, various other configurations performed better in reducing the SPL and additional edges tend to increase the SPL. At frequencies greater than 10000 Hz, the single edge case is the most beneficial configuration reducing the SPL by up to 5dB. Addition of edges at around these frequencies increases the SPL back towards the situation where there were no edges. Although this receiver is horizontally further away from the edges, it appears to perform better than the receiver (0.5, 0.15). This may be due to closer propagation angles to the reactive surface.

As the propagation angle becomes closer to the surface of the rib structure attenuations increase at around frequencies corresponding to quarter wavelength of the well depth. The effectiveness of this pressure release surface may be limited to the vicinity of the wells and as propagation angle is further away from the surface, the reductions in SPL disappear. At higher frequencies the reductions depend on the receiver location and may be related to diffraction angles.

Additional experiments were undertaken to determine the effect of the rib structure at different receiver heights (i.e. diffraction angles). The rib structure consisted of 21 edges having 0.017m high wells. Seven different receiver locations were investigated. The frequency, which corresponds to the quarter-wavelength of the well depths, in this case is 5000 Hz. It is also noted that the only diffraction order physically realisable for this geometry is zero-order (occurring at around receivers 1 and 2).

At receiver heights of 0m and 0.05m the largest improvements occurred at 5000 Hz. As the height of the receiver is increased, this maximum benefit shifts to lower frequencies. This coincides with 3150 Hz at 0.1m high receiver, with 2500 Hz at 0.15m high receiver and with 2000 Hz at higher receivers.

At 1600 Hz, decreasing the height of the receivers reduces the performance. The receiver at 0.3m above the ground has +3 dB Insertion loss whereas the receiver at ground level, which is also the only receiver partially in the shadow zone, has -3 dB insertion loss, i.e. the rib structure has actually increased the sound pressure levels. The influence of the single edge is negligible at this frequency and therefore these effects can be attributed to the rib structure.

At around 6300 Hz, the situation appears to reverse. As the height of the receiver increases, the noise levels at the receiver increase hence the insertion loss decreases. The exception is the 0.05m high receiver at grazing incidence which possesses a



higher insertion loss than the receiver on the ground, which is partially in the shadow zone. At 12500 Hz, situation is similar to that described above.

Depending on the receiver height and the wavelength of the sound under consideration, insertion loss can vary. Based on the testing frequency range of 1600 Hz to 12500 Hz and the grating separation distance of approximately  $w = 0.01\text{m}$ , the only mode permitted by the grating equation at incidence and diffracted angles of 90 degrees, is  $m = 0$ . Therefore with the present set-up it may prove difficult to identify the diffraction angles at which these effects may be taking place.

After observing the effects of different numbers of edges at different receiver positions, it was decided to fix the edge numbers at 14, and investigate the effects of various well depths at six receivers described earlier. Three well depths were examined. These were 0.017 m and 0.008 m depths compared with the 0.025 m depth discussed above. In general it could be observed that gains obtained for lower receiver locations diminished as the height of the wells were reduced.

The maximum attenuations at the 0.025m wells correspond to the quarter-wavelength of the well depth. This was not observed for other two well depths. It should be stressed that the proportion of area covered by the 0.017m and 0.008m edges is much smaller than that covered by the 0.025m edges, even though the total number of wells is identical for all three cases.

In the case of 0.17m wells, the magnitudes of peaks are less pronounced. This may be due to the fact that, for the maximum attenuations at resonant frequencies to be realised, the wavelength of the sound wave has to be smaller than the half the overall width of the reactive surface. The 0.017m wells do not meet this requirement as shown below.

Well depth (m)	Approximate resonant frequency (Hz)	Corresponding wavelength (m)	Half the overall width of surface (m)
0.025	3400	0.1	0.163
0.017	5000	0.068	0.05
0.008	10750	0.032	0.11

As the well depths became smaller than the physical centre of the source itself (approximately at 0.025m above ground), the line of sight from source to receiver ceased to be grazing the top of the edges. This meant the receivers were in the shadow zone and some of the differences might have been due to the attenuations due



to line-of-sight being intercepted. Therefore, it was decided to raise the edges above the ground sufficiently so that these conditions would be met for all receiver locations.

In the second set of experiments, the multiple edges were installed on top of a low rectangular barrier. These experiments aim to establish if the improvements in performance would still be applicable and if these would reinforce the performance of the plain rectangular barrier.

The maximum attenuations for 0.025m and 0.008m wells appear to roughly correspond to quarter wavelength of the well depths. Although the 0.017m wells perform better than the 0.008m wells at lower frequencies, as would be expected from the deeper wells, this is not reflected in the overall performance, especially at higher frequencies. This may be related to the overall length of the reactive surface, which is half that covered by 0.025m and 0.008m wells. Although the 0.017m case has the largest number of edges, since these are confined to a smaller surface area, they do not perform as would be expected. The 0.025m and 0.008m cases perform similar to each other at higher frequencies. Therefore it could be concluded that similar reactive surface area ensures similar high frequency performance. However the well depth governs the low frequency performance and this would appear to be the main reason why the 0.025m wells performed substantially better than 0.008m wells by up to 15 dB at around 4000 Hz.

Table 9-4 shows that in terms of single figures all three well depths provided improvements of 3 dB to 6 dB over the insertion loss of the rectangular barrier, which is around 8 dB. This is potentially a substantial improvement but these observations need to be extended to other receiver locations.

The insertion loss values indicated that 10 dB improvements over a plain rectangle throughout the frequency spectrum are achievable with the appropriate choices of well depth and the total reactive surface area. The depth of the wells would determine the lower limit of the frequencies at which favourable attenuations are required. At lower frequencies than this, degradation in performance may be expected. The high frequency performance would be determined by the total surface area and the number of wells.

The third and last set of experiments looked at the effects of multiple edges on top of a flat-topped earth mound. It is recalled that previous experiments under uniform field conditions did not indicate substantial improvements for the geometries associated with earth mounds. Current tests, however, as shown in Figure 9.44, indicated that attenuations of up to 8 dB and amplifications of up to 6 dB are likely for the frequencies under consideration. The transition from negative to positive gains appears at higher frequencies for shallower well depths as would be expected. However apart from this,



there is not a conclusive relationship between the maximum attenuations and the quarter-wavelength of the well depths. The spectra in Figure 9.44 show large frequency dependence in noise attenuations. As noted earlier, surface wave generation mechanism could be a factor in limiting the achievable noise reductions at low frequencies. The single value performance indicators did not give substantial reductions at the receivers under investigation, since the attenuations and amplifications cancel each other. In addition, the limitations in the maximum number of wells practically achievable on top of the earth mound could also be a limiting factor in the performance. As discussed earlier, the overall surface area as well as the total number of edges plays an important role in determining the magnitude of attenuations.

The repeat tests under semi-anechoic chambers showed that substantial noise attenuations could be achieved by the application of rib structures. These can be used both on the ground and on other earth mound type barriers. The tests also verified the applicability of uniform field experiments in conjunction with a continuous sound source, subject to some limitations. It was shown that the main limitation would be realised at large sized geometries where the attenuations are expected to be largest.

## **9.8 CONCLUSIONS**

This chapter provided a discussion of the results of the experiments carried out in two different semi-anechoic chambers on rib structures consisting of multiple edges. It was found that mainly the depth of the wells determined the lower frequency limit of attenuations. At frequencies lower than the limiting frequency, the insertion loss of the rib structures were found to be negative. This is likely to be due to surface wave generation. The effectiveness of the pressure release surface appeared to be restricted to the vicinity of the wells and the attenuations were greatest for receivers which were situated at propagation angles and horizontal distances close to the reactive surface. The high frequency performance appeared to be dependent on diffraction effects characterised by the overall surface area of the wells and the total number of edges. This was not necessarily the case for receivers which were in direct line of sight of the source. It was found that there was an optimum number of edges for the most favourable attenuations. However this depended on the diffraction angles and the frequencies. Interference patterns, observed in Chapter 8, between the direct paths and the multiply reflected (within grooves) paths were not evident in the results obtained in this chapter. The reason is the differences between the frequency bandwidths of the two experiments. It is recalled that Chapter 8 experiments were carried out at 1/24 octave bands and this provided a higher resolution for identifying frequency



dependent peaks. The results presented in this chapter are limited to 1/3 octave bands as discussed earlier.

As the diffraction angles as measured from the grating normal were reduced, the attenuations were observed to shift to lower frequencies. The high frequency gains at these receivers were negative. For the maximum attenuations at resonant frequencies to be realised, the wavelength of the sound wave has to be smaller than half the overall width of reactive surface.

The geometries considered did not enable a clear relationship to be established for attenuations at various diffraction angles. The separation distance between the edges and the nature of the scattering objects have not been investigated as part of this work.

The semi-anechoic chamber experiments verified the usefulness of uniform field experiments under certain conditions. At smaller geometries (edges on the ground), good qualitative and quantitative agreements were obtained. At medium sized geometries (rectangular barriers) good qualitative agreements were obtained although the magnitude of some of the improvements at certain frequencies were somewhat limited by the presence of the reverberant field. At large geometries (earth mounds) single performance indicators were similar partly because the earth mound configurations did not provide substantial additional attenuations at the receivers under consideration. The frequency spectra obtained by semi-anechoic chamber measurements for large geometries showed that at higher frequencies, uniform field experiments failed to realise the substantial attenuations.

The next chapter provides the details of the numerical model using boundary element methods and presents a discussion of its findings. These will be used in the forthcoming chapters for comparing and validating the physical modelling undertaken in the room with a uniform field and in the semi-anechoic chambers.



# **10 NUMERICAL MODELLING USING BOUNDARY ELEMENT METHODS**

In Chapters 8 and 9, physical scale modelling technique was used to investigate the potential benefits of reactive configurations on their own and on earth mound type barriers. This work showed that substantial reductions were achievable by the use of multiple diffracting edges.

This chapter provides the details of the numerical modelling carried out by SYSNOISE. The indirect boundary element methods form the basis of the mathematical model. The findings of numerical models are used in the forthcoming chapters to aid the validation of the physical modelling results and to extend acoustic design guidance on earth mounds.

## **10.1 BACKGROUND**

Boundary element methods as applicable to the modelling of barriers were reviewed in Chapter 2. This section undertakes an account of the method specific to the analytical model to be used.

The last two decades have seen the emergence of a versatile and powerful method of computational engineering mechanics, namely boundary element method<sup>1</sup>. The mathematical background of the boundary element method has been known for nearly one hundred years. Indeed some of the boundary integral formulations for the elastic, elastodynamic wave propagation and potential wave equations have existed in the literature for at least fifty years. With the emergence of digital computers the method had begun to gain popularity as 'the panel method', 'the boundary integral equation method', and 'the integral equation method' during the sixties. The name was changed to 'the boundary element method' (BEM) by Banarjee and Butterfield in 1975, so as to make it more popular in engineering analysis community.

The propagation of acoustic waves is governed by the scalar wave equation or, if harmonic excitations are considered, by the Helmholtz equation, where reflections, scattering and diffractions are correctly characterised by boundary conditions. Helmholtz equation is as follows.



$$\nabla^2 p + k^2 p = 0 \quad \text{Equation 10.1}$$

where  $p$  is acoustic pressure and  $k$  is the wave number. The two-dimensional problem of a barrier resting on a flat ground is represented as follows where  $X$  and  $Y$  are the receiver and source positions respectively and  $s$  represents the barrier surface.

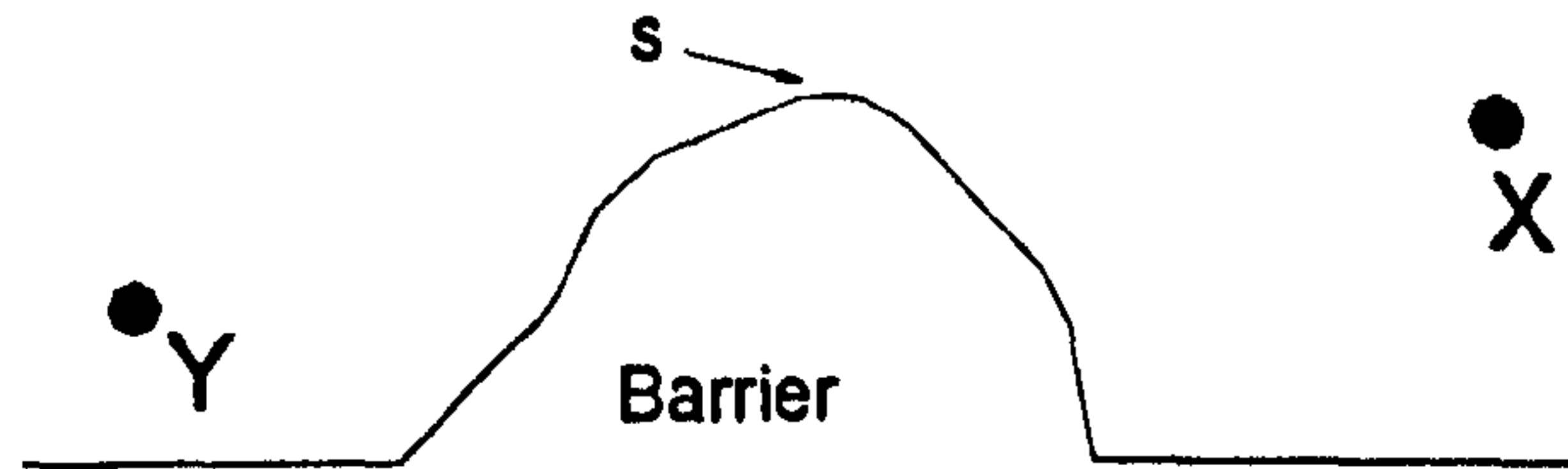


Figure 10.1 : Two - dimensional barrier problem.

By applying Green's theorem to the boundary value problem, with the appropriate choices of boundary conditions at the barrier surface, on the ground and at infinity, the following boundary integral equation has been obtained<sup>2, 3, 4</sup>.

$$p(x) = \int_s \left[ p(Y) \frac{\partial G(X, Y)}{\partial \nu} - G(X, Y) \frac{\partial p(Y)}{\partial \nu} \right] dS(Y) \quad \text{Equation 10.2}$$

where  $G(X, Y)$  is the Greens's function and has the following form for two dimensional geometries.

$$G(X, Y) = \frac{j}{4} H_0^{(1)}(kR) \quad \text{Equation 10.3}$$

$H_0^{(1)}$  is the Hankel function of the first kind and order zero and,  $R$  is the distance between the source and the receiver.

Since noise radiation or scattering mostly involve solutions over finite radiators or scatterers in "infinite" domains of homogeneous media, boundary integral equations are the almost perfect methodology for solving such problems<sup>5</sup>.

The boundary element method has two different approaches in formulating a problem. These are the direct collocation method and the indirect variational methods<sup>6</sup>. In the direct collocation method, the following system of *non - symmetric* equations must be created and solved for each selected analysis frequency.

$$[A(\omega)]\{p\} = [B(\omega)]\{v_n\} \quad \text{Equation 10.4}$$

where;

$\{p\}$  vector of nodal pressures on the BEM surface



$\{v_n\}$  vector of normal velocities on the BEM surface

The nodal pressure and nodal normal velocity on the BEM surface are also called primary surface results or potentials. From these pressure, velocity and intensity values are automatically calculated if field points are defined before the analysis.

In the indirect variational method the following system of *symmetric* equations must be created and solved for each selected analysis frequency.

$$\begin{bmatrix} B & C' \\ C & D \end{bmatrix} \begin{Bmatrix} \sigma \\ \mu \end{Bmatrix} = \begin{Bmatrix} f \\ g \end{Bmatrix} \quad \text{Equation 10.5}$$

where

$\sigma$  vector of single layer potentials (jump of velocity)

$\mu$  vector of double layer potentials (jump of pressure)

$f, g$  excitation vectors

The single layer potential (or jump of velocity) and double layer potential (or jump of pressure) on the BEM surface are also called primary surface results.

From the primary surface results in both the direct and indirect methods, pressure, velocity and intensity values can be calculated at field points (receiver location). The pressure at an arbitrary field point  $P$  is obtained from these potential values by field point postprocessing, using the expression

$$P_p = \{a\}' \{p\} + \{b\}' \{v_n\} \quad \text{Equation 10.6}$$

Seznec<sup>2</sup> presented a boundary elements technique for the diffraction of sound around barriers. He showed that this technique is well suited to complicated geometries, or acoustical models of the ground and barriers. Accuracy of the model depended on the number of elements, however, 6 elements per wavelength was found to be sufficient and 8 - 10 elements per wavelength ensured practically full convergence. He discussed that typical accuracies did not depend strongly on barrier shape or receiver location.

Hothersall et al.<sup>3</sup> observed large differences due to the effect of the problem of non-uniqueness of solution, and they showed that the large differences occur at one-third octave centre frequencies which happen to be close to eigenfrequencies of the boundary element value problem. These eigenfrequencies depend upon the shape and area of the cross-section, but increase in density with increasing frequency. At the lower frequencies inaccurate results due to the coincidence of an eigenfrequency with a one-third octave band centre frequency occur very rarely and are easily identified. At higher frequencies it appears that the density of eigenfrequencies is introducing



significant errors. They concluded that maximum element length of not more than  $\lambda / 5$ , where  $\lambda$  is the wavelength, was necessary.

Boundary element methods were identified as the most appropriate analytical tool for the investigation of the relative configurations of various barrier profiles consisting of rib structures. A brief summary of the theory behind the technique and the work done by other researchers shows that consideration should be given to the choice of problem formulation and mesh size selection. The findings should be interpreted with care due to the problem of non-uniqueness of the solution. The details of the model to be used in SYSNOISE are presented in the following sections.

## 10.2DETAILS OF THE NUMERICAL MODEL

### 10.2.1 Process of Modelling

This section provides a detailed account of the process by which a typical model was generated. The main steps are summarised in the block diagram shown in Figure 10.2.

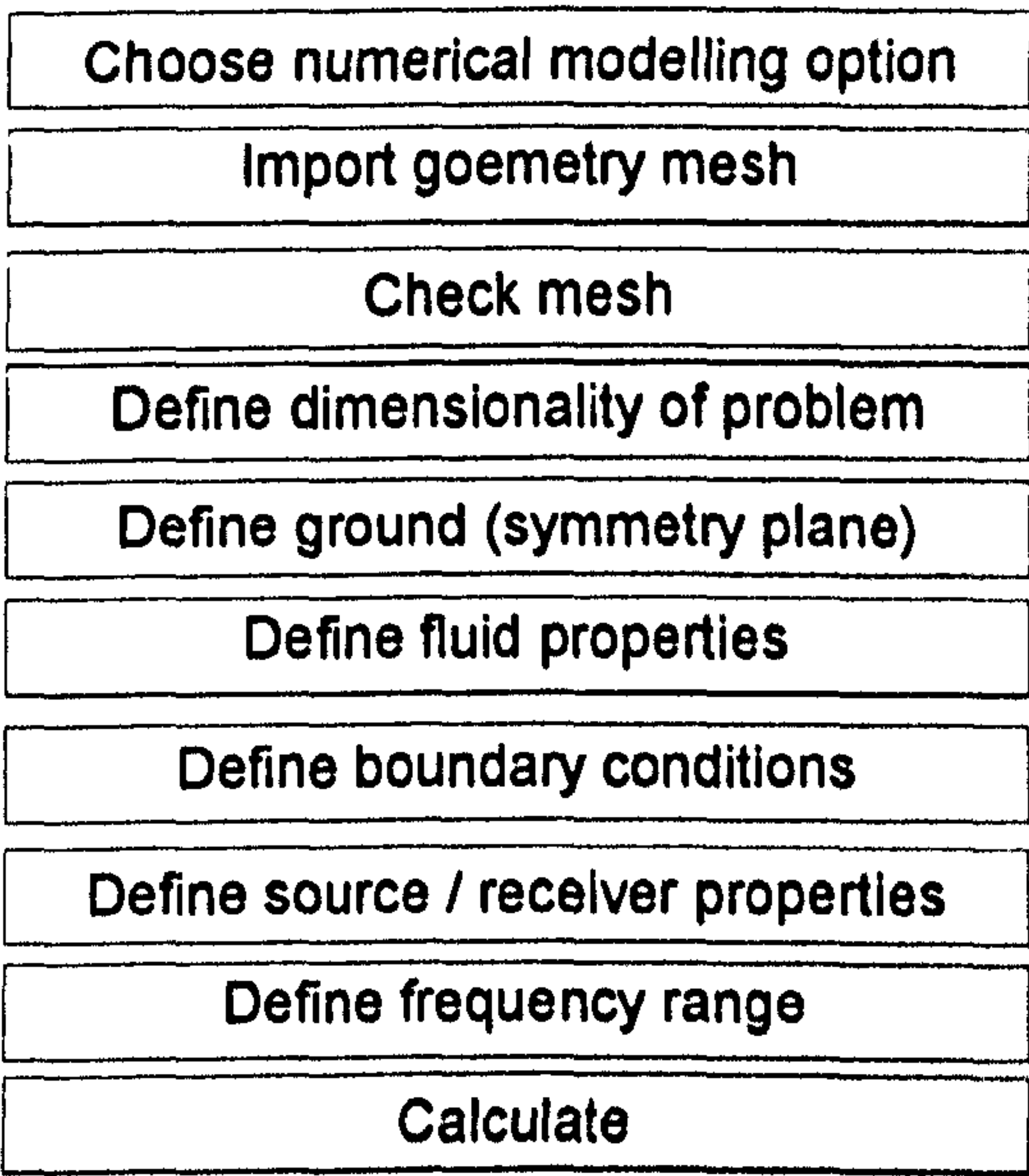


Figure 10.2 : Block diagram showing the numerical modelling process

The first step in the modelling was selecting the appropriate numerical modelling option. Indirect boundary element methods is used as the mathematical basis of all numerical models. The main difference between the Direct and Indirect formulation is the ability of the Indirect method to consider open structures or complex surfaces with junctions due to its use of pressure discontinuity and normal velocity discontinuity



through the boundary surface as boundary unknowns<sup>7</sup>. Therefore this option was particularly essential for the type of geometries under consideration.

The next step was importing an already existing geometry mesh. The model meshes are generally prepared in external mesh generators when the geometries are complex. The models considered in this research programme consist of two dimensional linear elements. Therefore SYSNOISE itself could be used for the pre-processing of the model geometry mesh. A sample geometry which has been pre-processed as field points (i.e. receiver locations) is given below.

*Point Line 0 0 0 To 3 3 0 Divide 170 Return*  
*Point Line 3 3 0 To 4 3 0 Divide 40 Return*  
*Point Line 4 3 0 To 7 0 0 Divide 170 Return*  
*Point Line 3 3 0 To 3 3.17 0 Divide 7 Return*  
*Point Line 3.075 3 0 To 3.075 3.17 0 Divide 7 Return*  
*Point Line 3.150 3 0 To 3.150 3.17 0 Divide 7 Return*  
*Point Line 3.225 3 0 To 3.225 3.17 0 Divide 7 Return*  
*Point Line 3.300 3 0 To 3.300 3.17 0 Divide 7 Return*  
*Point Line 3.375 3 0 To 3.375 3.17 0 Divide 7 Return*  
*Point Line 3.450 3 0 To 3.450 3.17 0 Divide 7 Return*  
*Point Line 3.525 3 0 To 3.525 3.17 0 Divide 7 Return*  
*Point Line 3.600 3 0 To 3.600 3.17 0 Divide 7 Return*  
*Point Line 3.675 3 0 To 3.675 3.17 0 Divide 7 Return*  
*Point Line 3.750 3 0 To 3.750 3.17 0 Divide 7 Return*  
*Point Line 3.825 3 0 To 3.825 3.17 0 Divide 7 Return*  
*Point Line 3.900 3 0 To 3.900 3.17 0 Divide 7 Return*  
*Point Line 4 3 0 To 4 3.17 0 Divide 7 Return*

The smallest element size was determined by the frequency under investigation such that there would be 6 elements per wavelength. This was the recommended (default) element size given by the SYSNOISE and also is in line with the findings of previous researchers discussed earlier. However it was found that 12 elements per wavelength were more likely to give reasonable results for some of the geometries under investigation. The maximum element size was 0.025 m for the earth mounds with multiple edges and 0.01 m for the multiple edges on the ground or on rectangular barriers.

The model elements consist of straight-line segments with no thickness. This also applies to the multiple edges. All elements, by default, are assumed to be acoustically



reflective, unless otherwise explicitly allocated impedance properties within SYSNOISE.

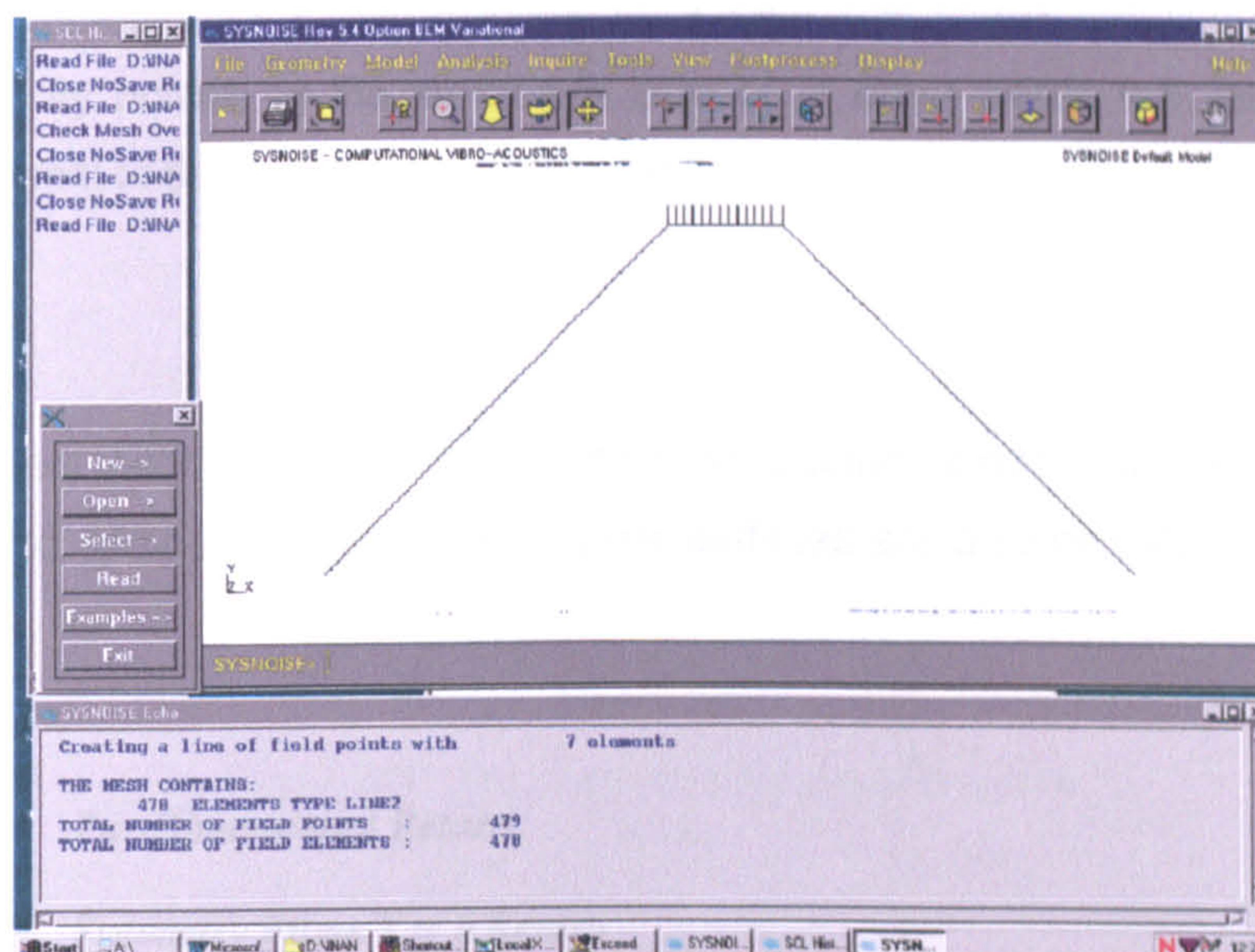


Figure 10.3 : The geometry pre-processed as field points in SYSNOISE

The start and end coordinates of each segment comprising the model geometry (x and y coordinates), and the number of elements within each straight segment were defined. In this example, the lower left hand side of model is taken as the origin, having the coordinates of zero. As it stands, these points are defined to be 'receiver points' within the SYSNOISE. These coordinates were saved as a text file and the model was cleared. Before these were loaded back into the software as the geometry mesh, the numerical modelling option had to be defined as described earlier. These steps are shown below.

*Export Point Format Free File example\_01 Return*

*Close Return*

*New Name 'example\_01' Model 1 File Example\_01.sdb Return*

*Option BEM Indirect Variational Uncoupled Unbaffled Frequency Return*

*Import Mesh Format Free File example\_01 Return*

All models investigated in this research programme are modelled as 2-dimensional models. Therefore the z coordinate which would determine the length of the barrier are



set to zero, implying that all models are infinitely long when translated to a 3-dimensional model.

The ground surface was modelled by defining a symmetry plane where it would be situated. Symmetry plane corresponds to a rigid half-space condition, where the particle velocity normal to the surface is zero or in other words the variation of the pressure normal to the surface is equal to zero.

$$\frac{\partial p}{\partial n} = 0 \quad \text{Equation 10.7}$$

This plane not only simulates an infinite rigid ground surface, but also saves the modelling and computation time. The barrier surfaces are also defined as having zero admittance.

*TwoDimensional Return*

*Symmetry Plane Y = 0 Return*

*Check Mesh Merge Return*

*Material Fluid*

*Name 'air'*

*Sound 3.4000e+002 Rho 1.2250e+000*

*Return*

The medium is a homogenous air with a standard impedance value of  $\rho c$ , with air density  $\rho = 1.225 \text{ kg} / \text{m}^3$  and air velocity  $c = 340 \text{ m} / \text{s}$ .



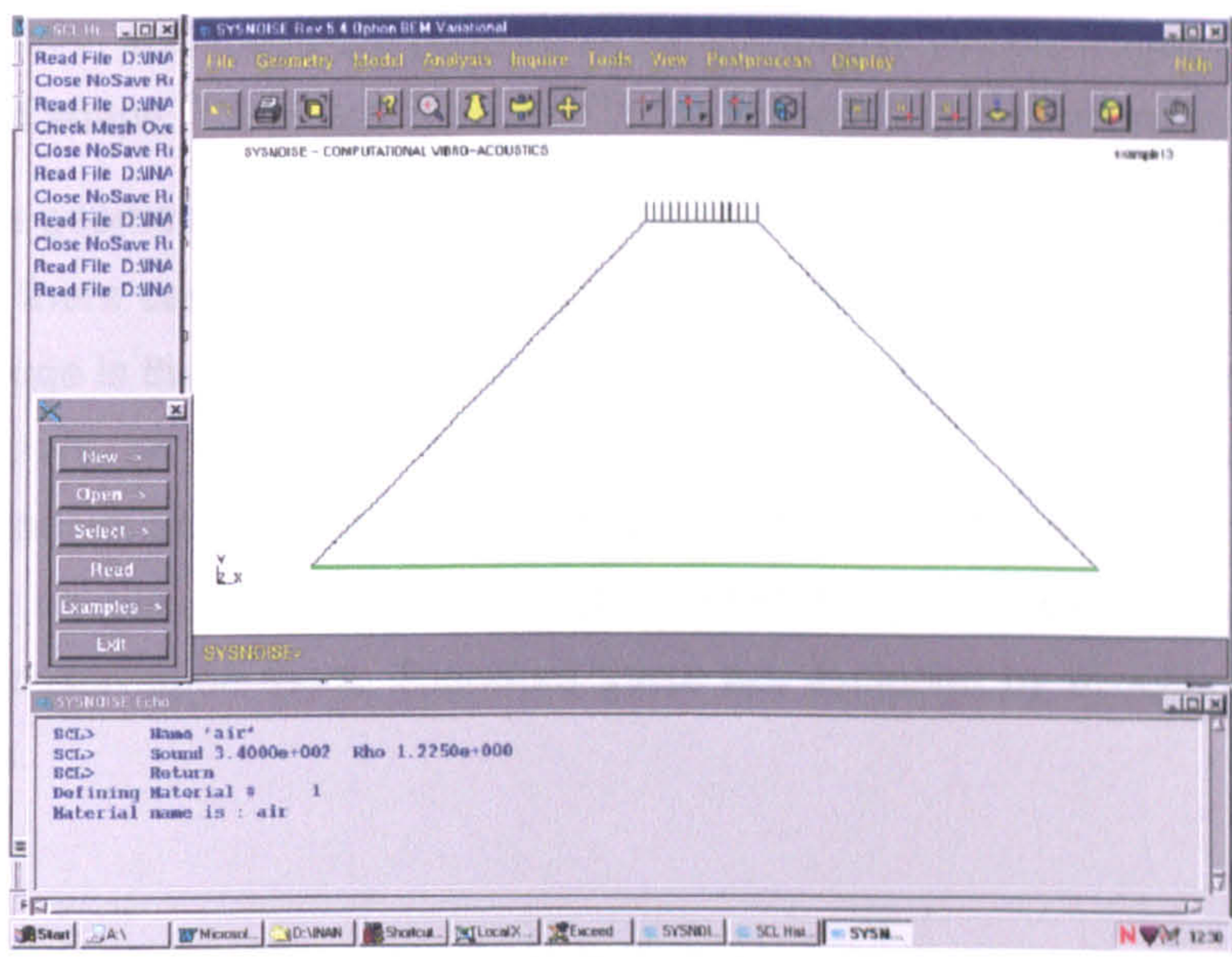


Figure 10.4 : The model with the symmetry plane

The imported mesh is checked for element normal vector directions and these are corrected if they do not conform to the rule that all should be facing outwards, away from the closed volume. This is particularly important with the rib structures where it is not immediately obvious which direction these should be facing.

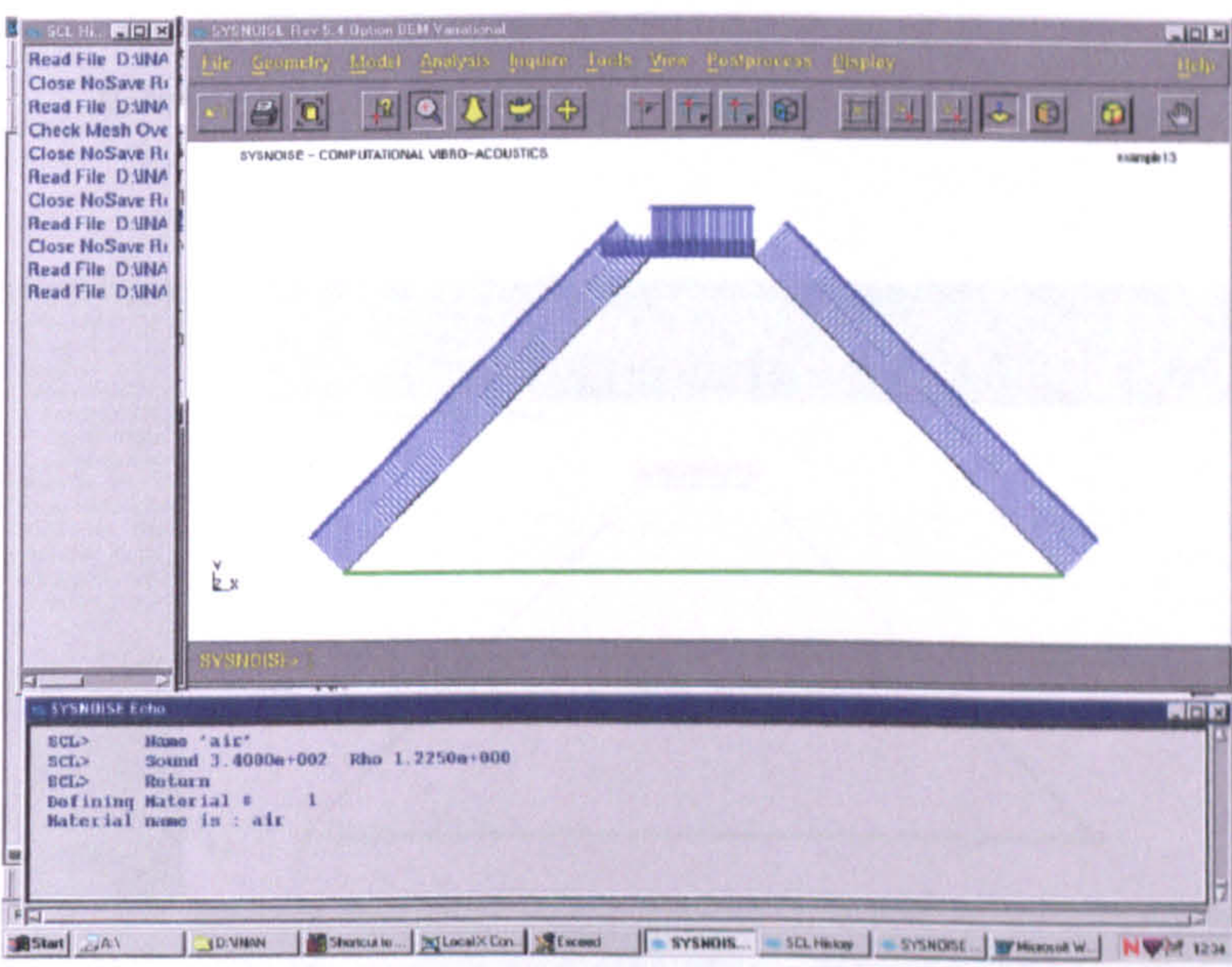


Figure 10.5 : Element normal vectors

These are handled in a consistent manner and it can be seen above that the element vectors are facing away from the closed volume where elements form part of the



closed geometry, and these are pointing to the left for the vertical edges which do not form a closed shape. These are discussed in the forthcoming section in further detail.

Following the geometry mesh corrections, boundary conditions are defined. Where free edges exist, there can be no changes in pressure across the edges. The fluid on one side of the edge is the same as the fluid on the other. In physical terms this means that the rib structure on top of the earth mound is surrounded by air, which forms a continuous medium and has uniform properties. However, the two element nodes which are situated on the symmetry plane, represented by  $y = 0$  should not have this condition imposed upon them. Therefore these are excluded by allocating these into different sets.

```
Set Name "Envelope" Envelope Return
```

```
Set Name "Symmetry"
```

```
Faces y=0
```

```
Return
```

```
Set Name "Free Edges" Difference 1 2 Return
```

```
Boundary Jump Pressure Real 0 Imag 0
```

```
Nodes set 3
```

```
Return
```

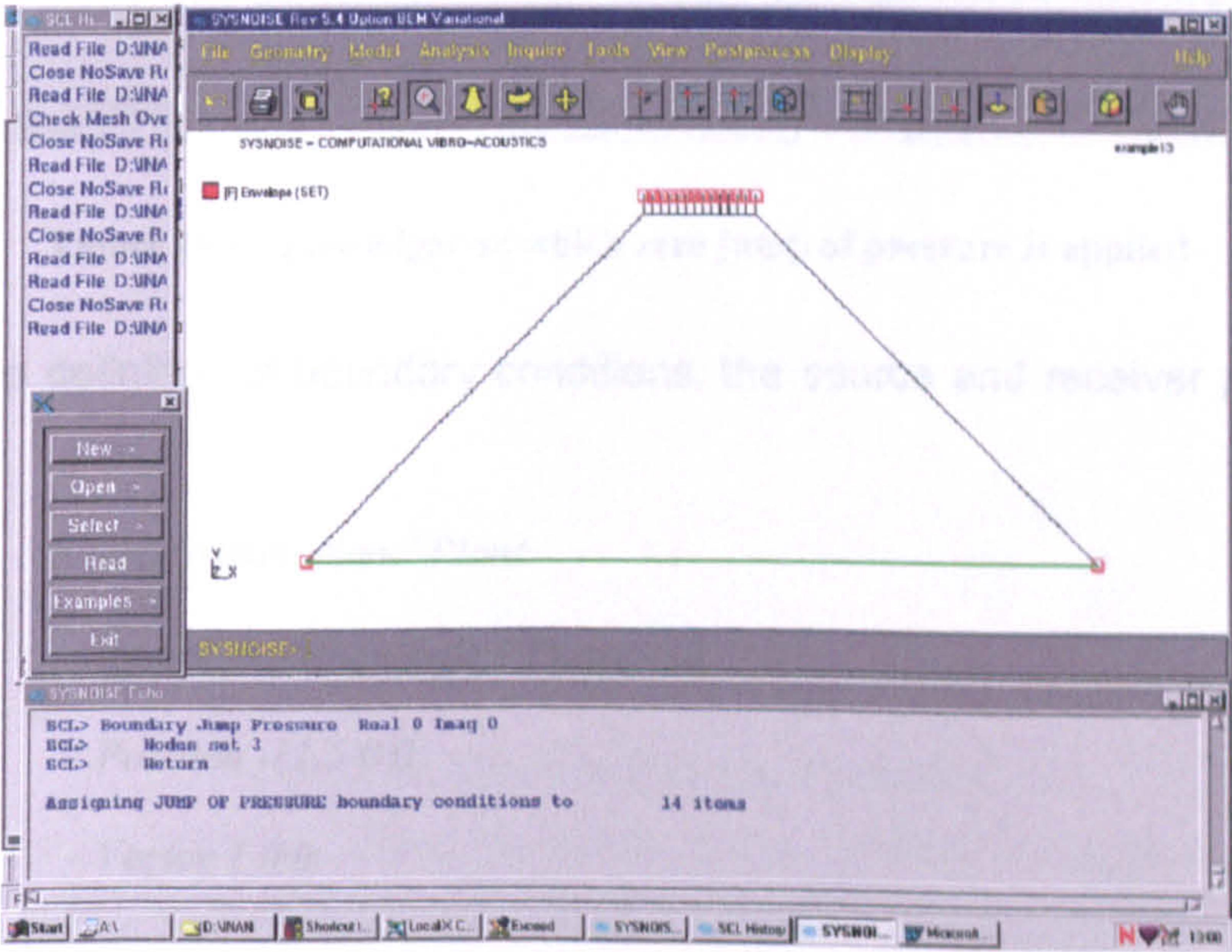


Figure 10.6 : All free edges forming the model



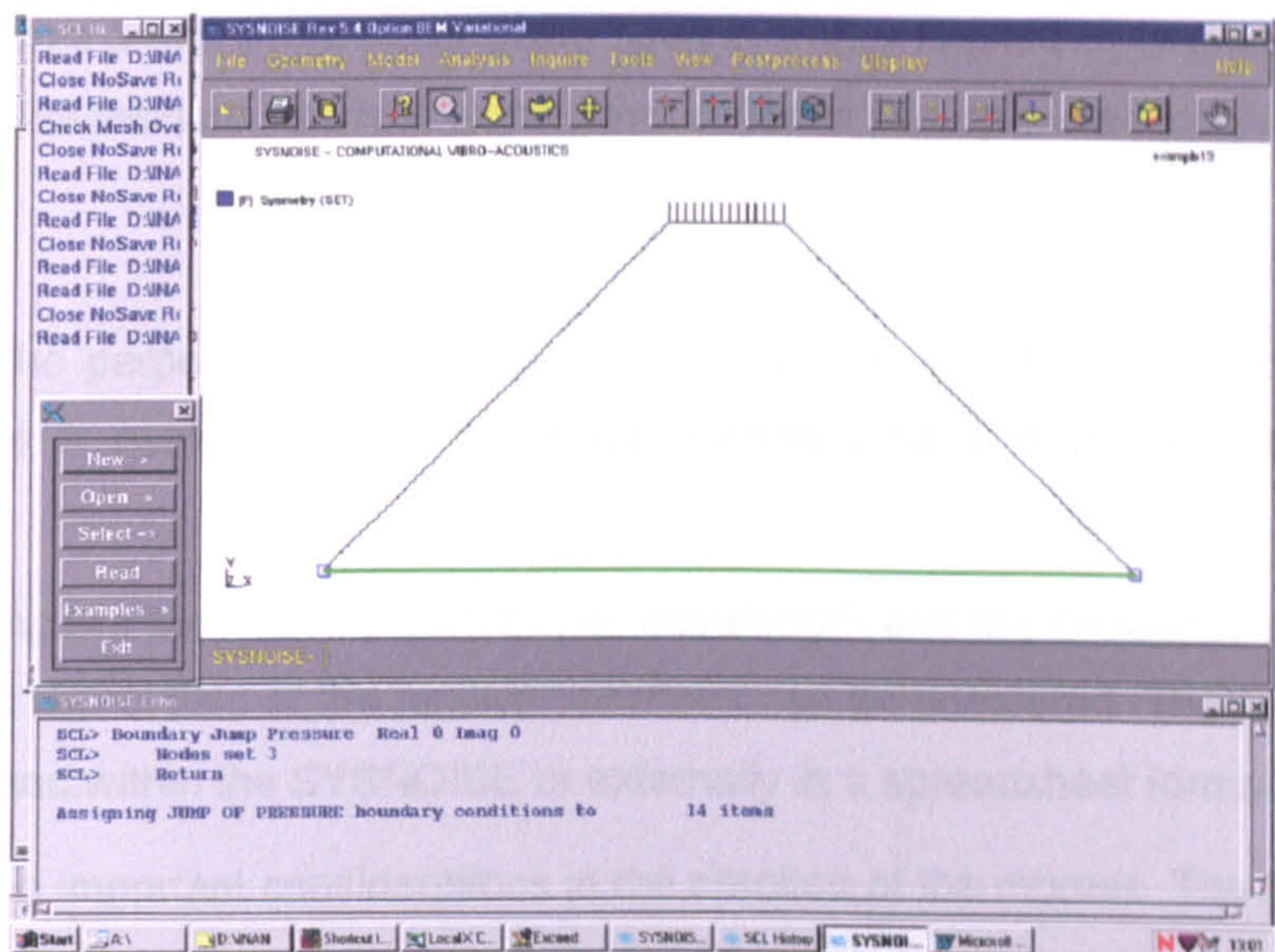


Figure 10.7 : Free edges on symmetry plane

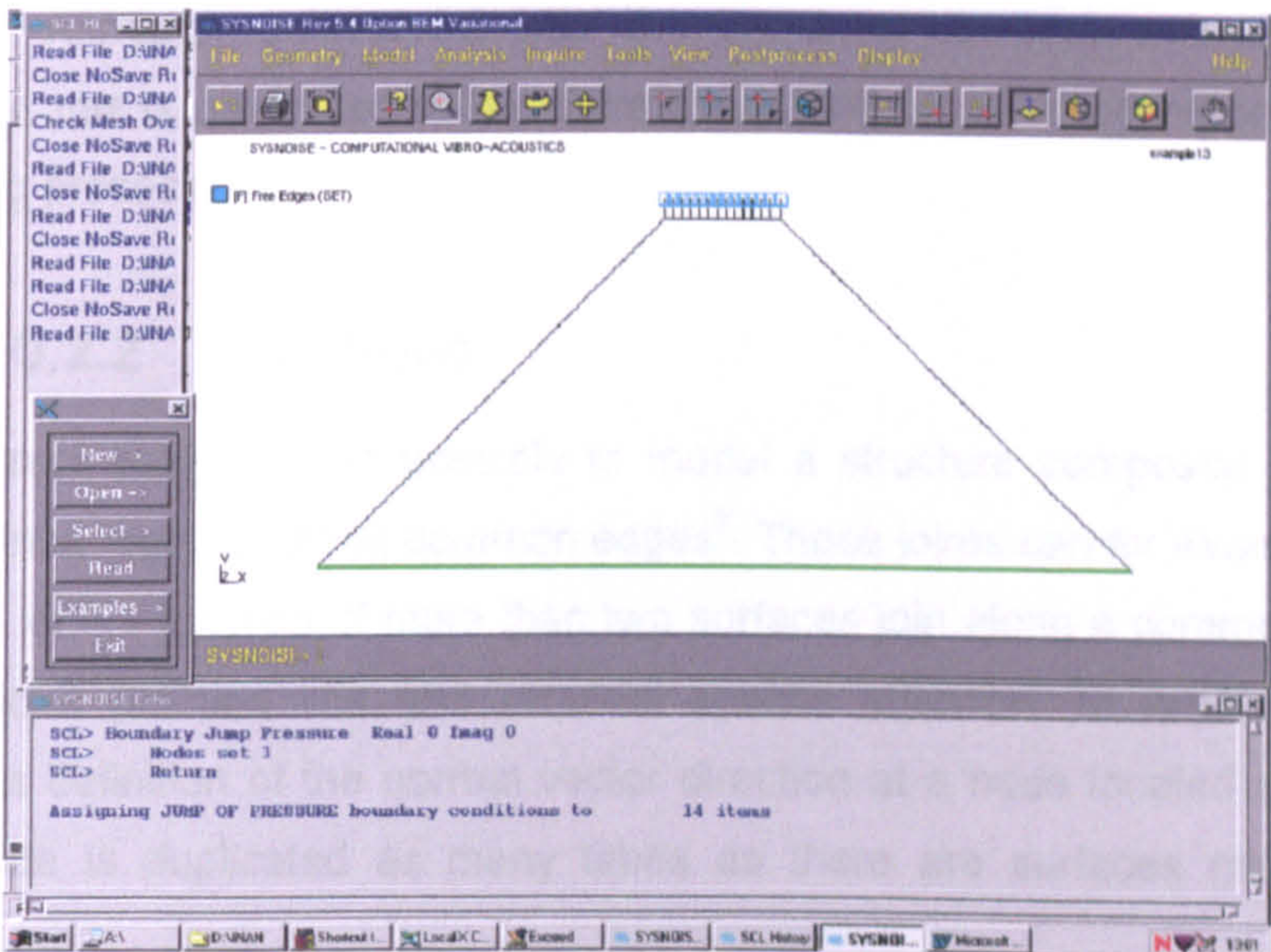


Figure 10.8 : Free edges on which zero jump of pressure is applied

Following the definition of boundary conditions, the source and receiver positions are described.

Source Name 'plane' Plane

Amplitude Magnitude 1 Phase -30

Position -11.5 0 0

Vector 1 0 0

Return

Point Plane 7,0.5,0 To 7,5,0 Divide 9 To 20,0.5,0 Divide 28 Return



The source was a two-dimensional plane source. It was defined by a given magnitude and phase. The incident field of a plane wave varies in free space as follows.

$$p = A e^{-ikd} \quad \text{Equation 10.8}$$

where  $d$  is the perpendicular distance from the source plane to the point where the incident field is evaluated,  $k$  is the wave number and  $A$  is the incident pressure amplitude.

After choosing the number of elements per wavelength and the frequency range for the analysis, the sound field at the receiver locations can be computed. The results can be post-processed within the SYSNOISE or externally in a spreadsheet format.

There are two important considerations in the creation of the models. The first one is at the pre-processing stage and the second is at the post-processing stage. These are on the treatment of model 'junctions' and the consideration of 'irregular frequencies' respectively. Although SYSNOISE has the capability to deal with the junctions automatically, this is discussed below since it was one of the most important steps in the modelling process.

## 10.2.2 Junctions

In BEM Indirect analysis, it is possible to model a structure composed of sub-parts which are joined together along common edges<sup>8</sup>. These joints can for example take the form of a T - or X - junction. If more than two surfaces join along a common edge, this line is called a junction line and requires special attention. In order to have an unambiguous definition of the normal vector direction at a node located on a junction line, this node is duplicated as many times as there are surfaces meeting at the junction.



Figure 10.9 : Node duplication at junctions

As the node duplication effectively disconnects the different surfaces meeting at the junction, an additional compatibility equation is necessary for a correct treatment of the pressure discontinuities  $\mu_1 \mu_2 \mu_3$  across each of the surfaces. This compatibility equation or junction constraint expresses the requirement that the sum of the pressure



discontinuities across all surfaces meeting at the junction line, in sequence and observing the relevant orientations of the element normals, is equal to zero.

$$c_1 \cdot \mu_1 + c_2 \cdot \mu_2 + c_3 \cdot \mu_3 = 0$$

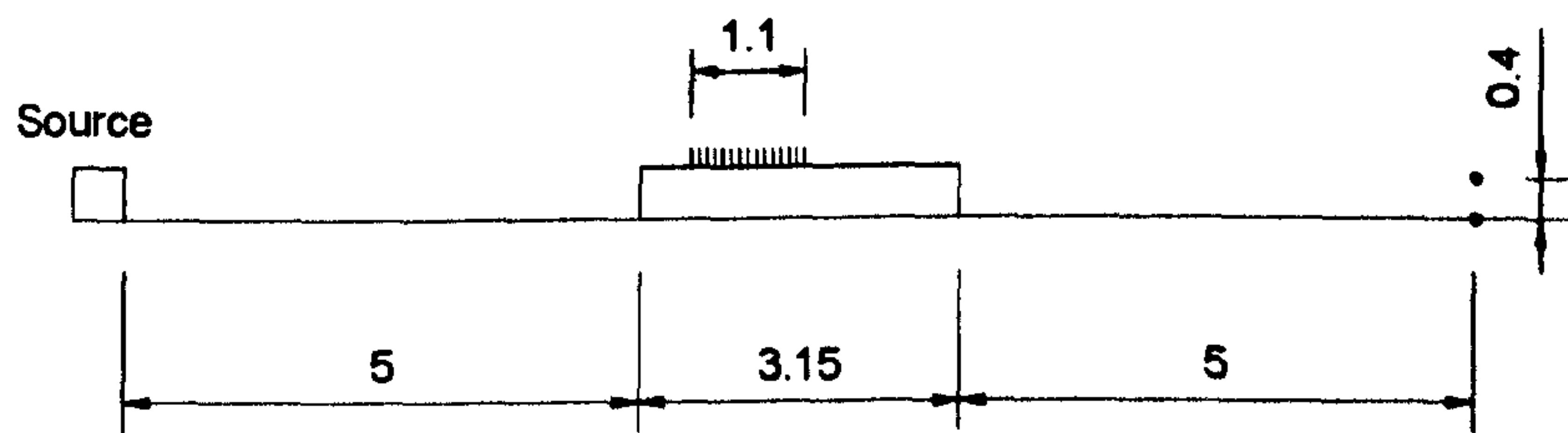
$c_1$ ,  $c_2$  and  $c_3$  have a value of +1 or -1 depending on the relative orientation of the element normals to the surface at the junction.

Whenever the model has free edges, zero jump of pressure has to be applied as explained above, since the fluid on both sides are in direct contact and there is no mechanism to support a pressure difference. This pressure continuity is defined as follows.

$$\mu = 0$$

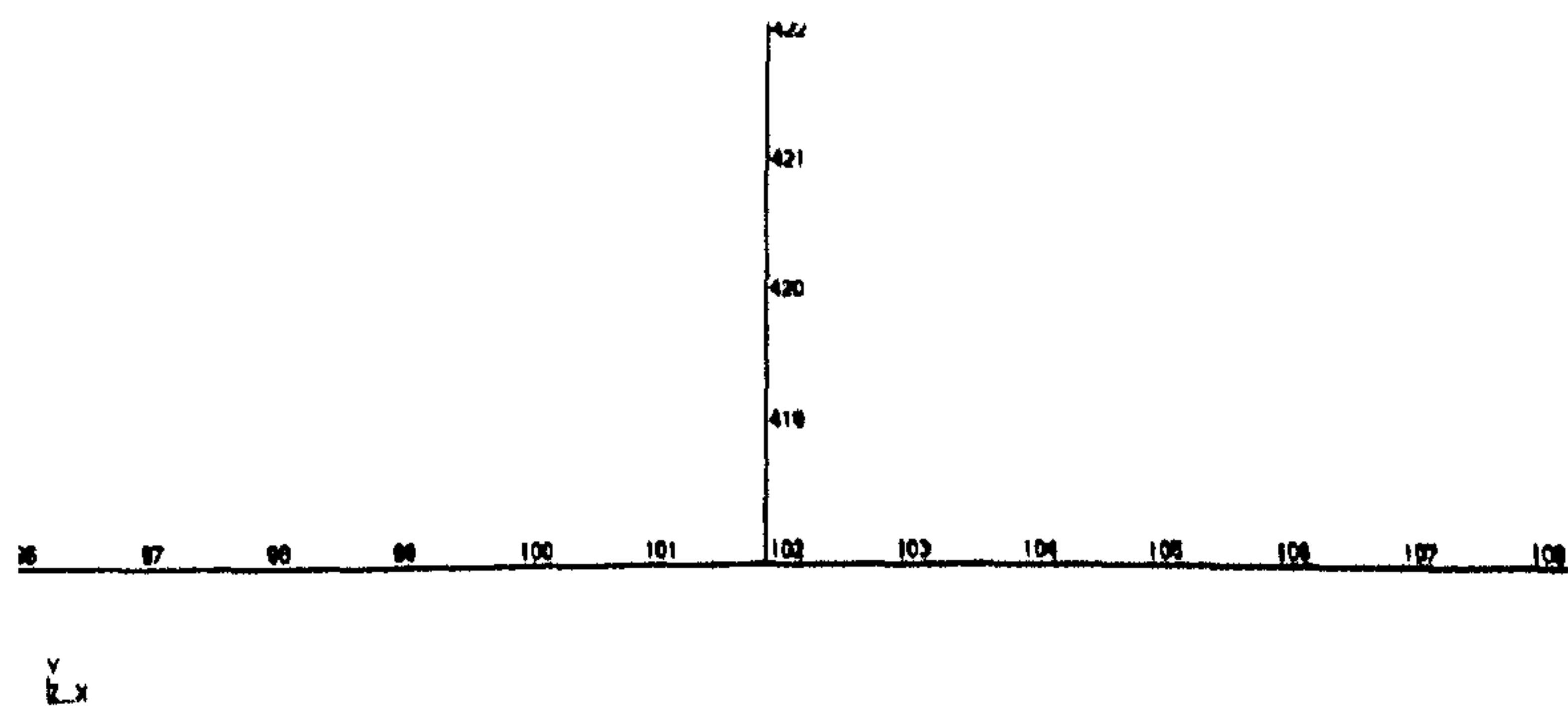
**Equation 10.9**

The effect of junctions on the sound pressure field can be explained with the aid of an example geometry as shown below.



**Figure 10.10 : The geometry for investigating the influence of junctions**

The sound pressure levels were computed at the receivers shown with and without the use of node duplication at the intersection points between the vertical free edges and the horizontal top part of the rectangle.



**Figure 10.11 : Element nodes as modelled originally**



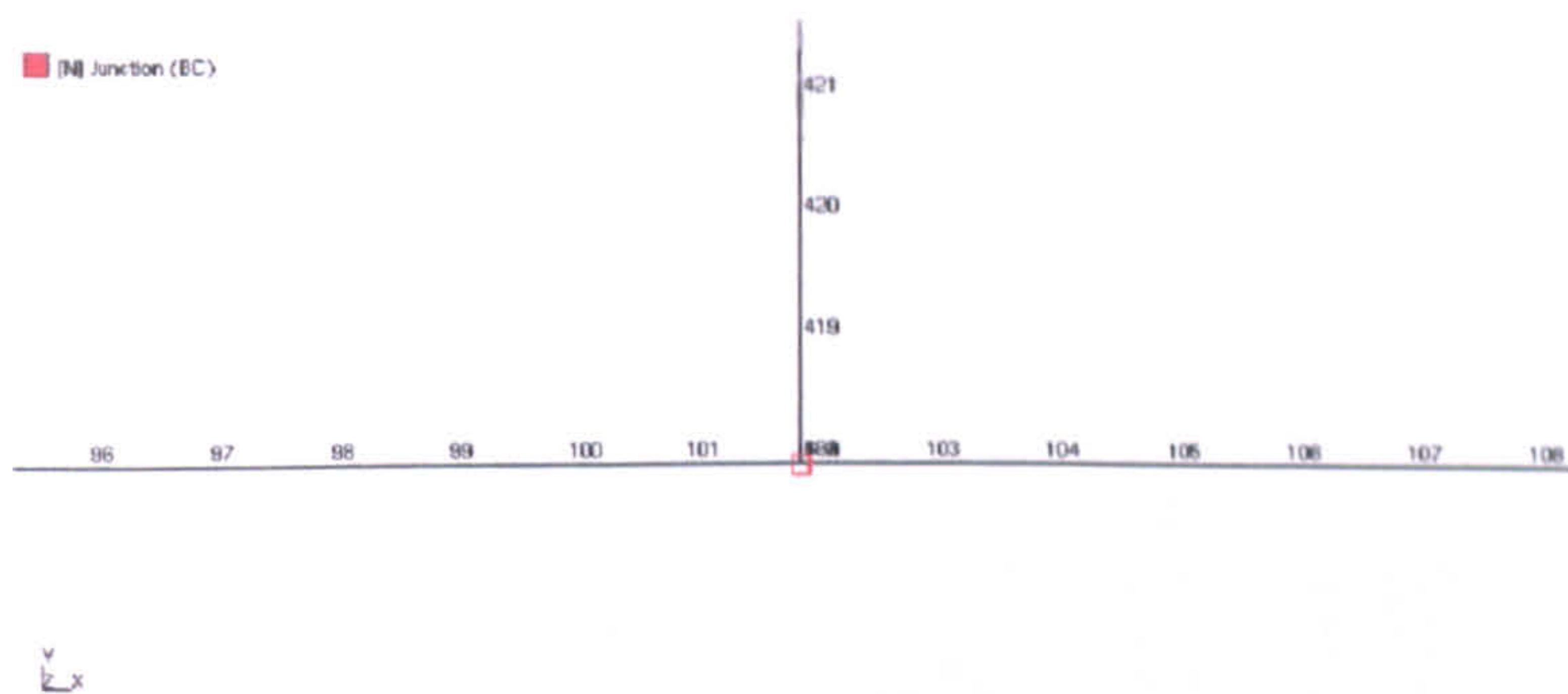


Figure 10.12 : Node duplication at junctions

Figure 10.11 and Figure 10.12 show the additional node point generated at the intersection of the first vertical edge with the horizontal elements on top of the rectangle. The differences in the calculated sound fields are compared below.

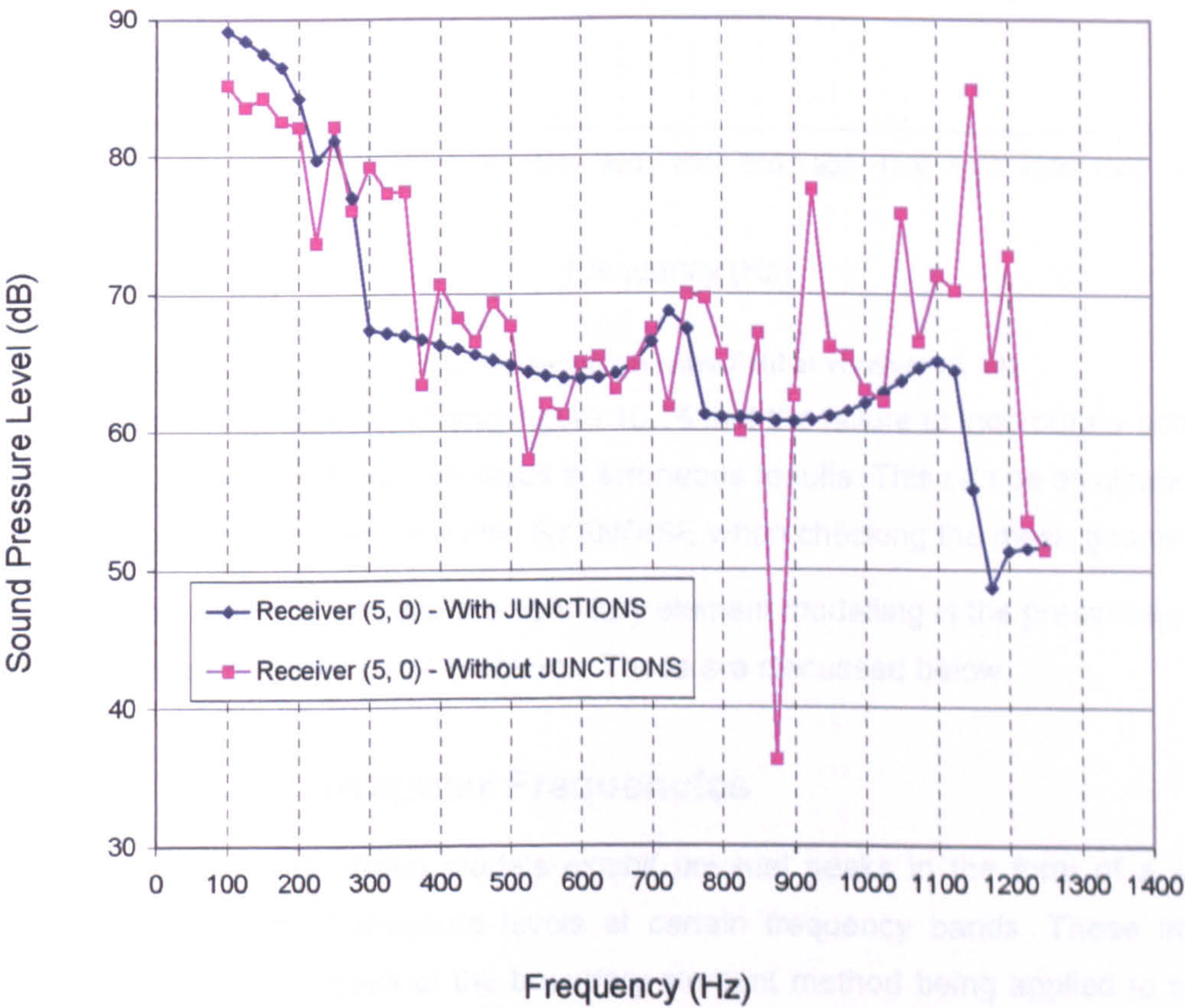
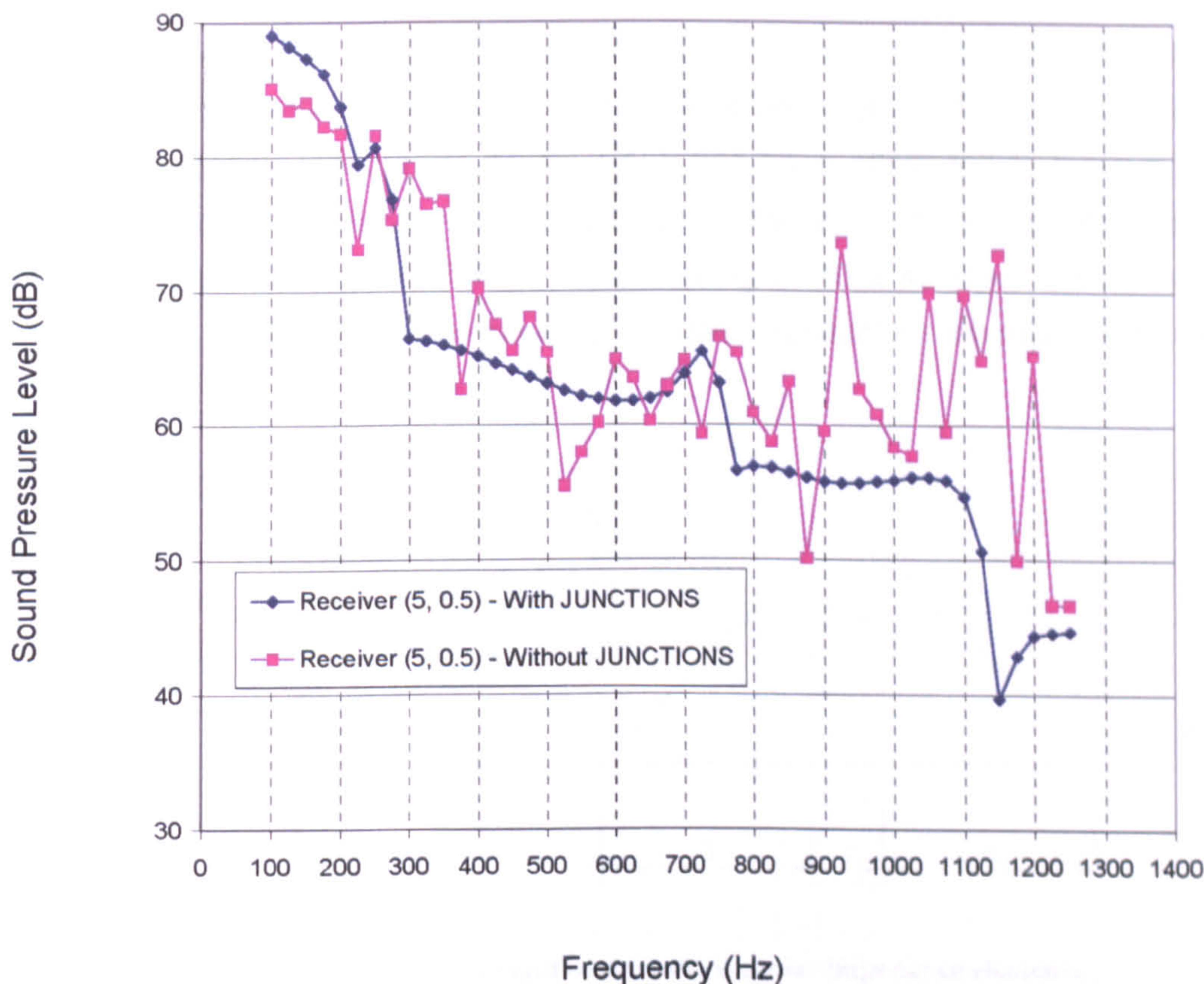


Figure 10.13 : The effects of junctions on sound pressure field at receiver (5,0)





**Figure 10.14 : The effects of junctions on sound pressure field at receiver (5, 04)**

It can be seen in Figure 10.13 and Figure 10.14 that the failure to incorporate additional node points at the junctions can result in erroneous results. This can be eliminated at the mesh generation stage or within SYSNOISE when checking the mesh geometry.

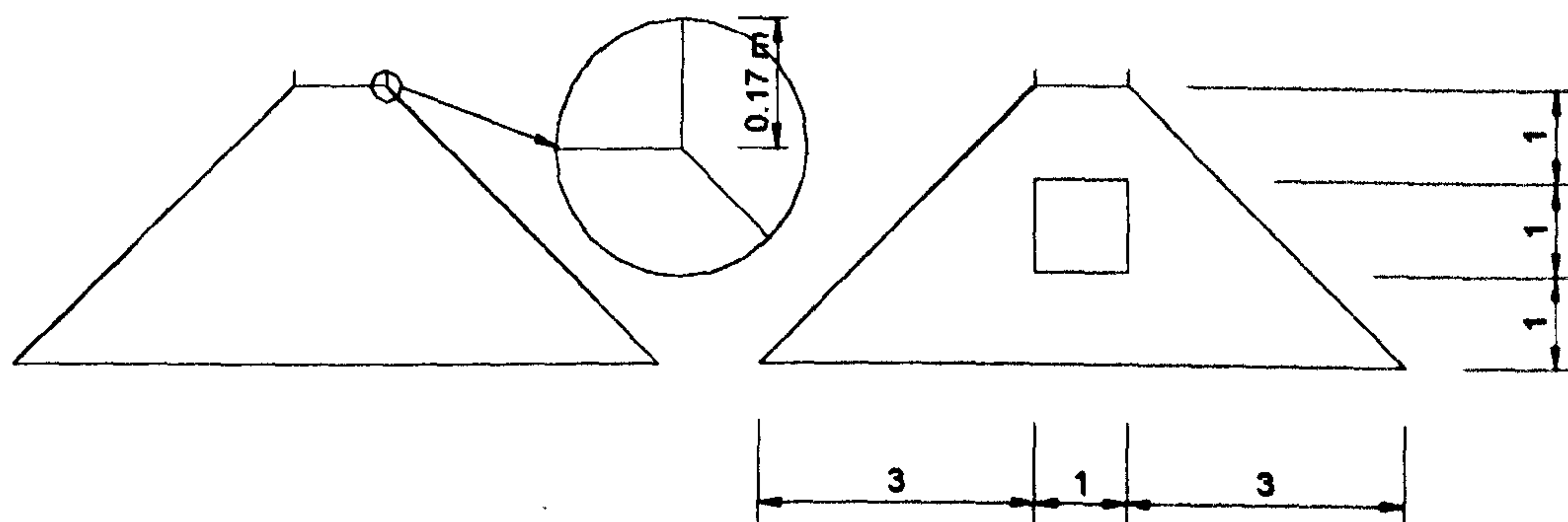
Another potential problem with the boundary element modelling is the presence of irregular frequencies for some problems. These are discussed below.

### 10.2.3 Irregular Frequencies

It was observed that certain models exhibit unusual peaks in the form of a sudden increase in the sound pressure levels at certain frequency bands. These irregular frequencies are as a result of the boundary element method being applied to exterior problems. The non - unique solution occurs whenever the vibrating surface is closed and excitation frequency corresponds to a resonance frequency of the associated interior problem<sup>9</sup>. In Indirect boundary element methods, these singularities are suppressed by addition of internal elements to the cavity enclosed by the boundary mesh. These additional elements are allocated "singular boundary" conditions where the real part of the given admittance must be positive.

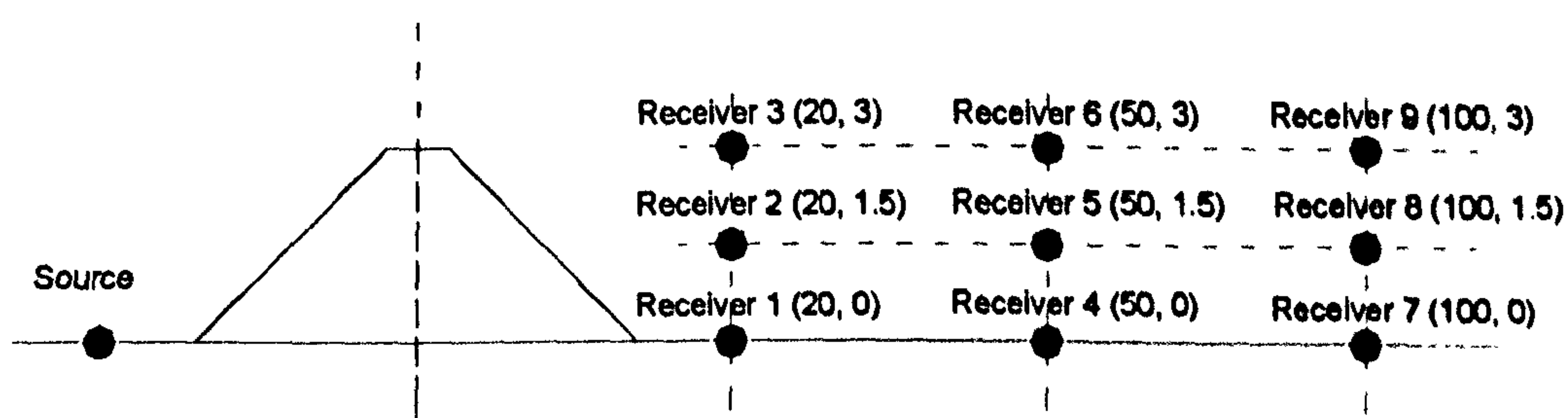


This is explained below with an example geometry where irregular frequencies appear at 1400 Hz and are restricted to that specific frequency throughout the receiver locations under investigation. This geometry will be the subject of further investigations in the forthcoming sections, as 'Model 12'. It has been attempted to remove these irregularities by the addition of a square mesh in the centre of the enclosed volume. This mesh had dimensions of 1 x 1 m, consisting of 40 x 40 linear elements. The details of the model with and without the singular impedance elements are shown in Figure 10.15.



**Figure 10.15 : Model with and without the singular impedance elements.**

Sound pressure levels have been calculated at 9 receivers with and without singular impedance elements. The receiver locations 1 to 9 are as shown in Figure 10.16. The receivers are referred to as (x, y) to represent their horizontal and vertical distances from the ground coordinates of the centreline of the earth mound. The source is 15 m from the centreline and is situated on the ground.



**Figure 10.16 : The source and receivers for investigating irregular frequencies**

The sound pressure levels for the geometries with and without the singular impedance elements are shown in Figure 10.17 for receiver 4. The differences in the sound pressure levels due to suppressed singularities at 1400 Hz for all receiver positions are shown in Figure 10.18. The differences vary between 0 - 12 dB depending on the receiver location. The neighbouring frequency of 1300 Hz is included for comparison to show that the addition of the extra elements did not affect the physical model, except removing the unwanted peaks caused by the nature of the mathematical model.



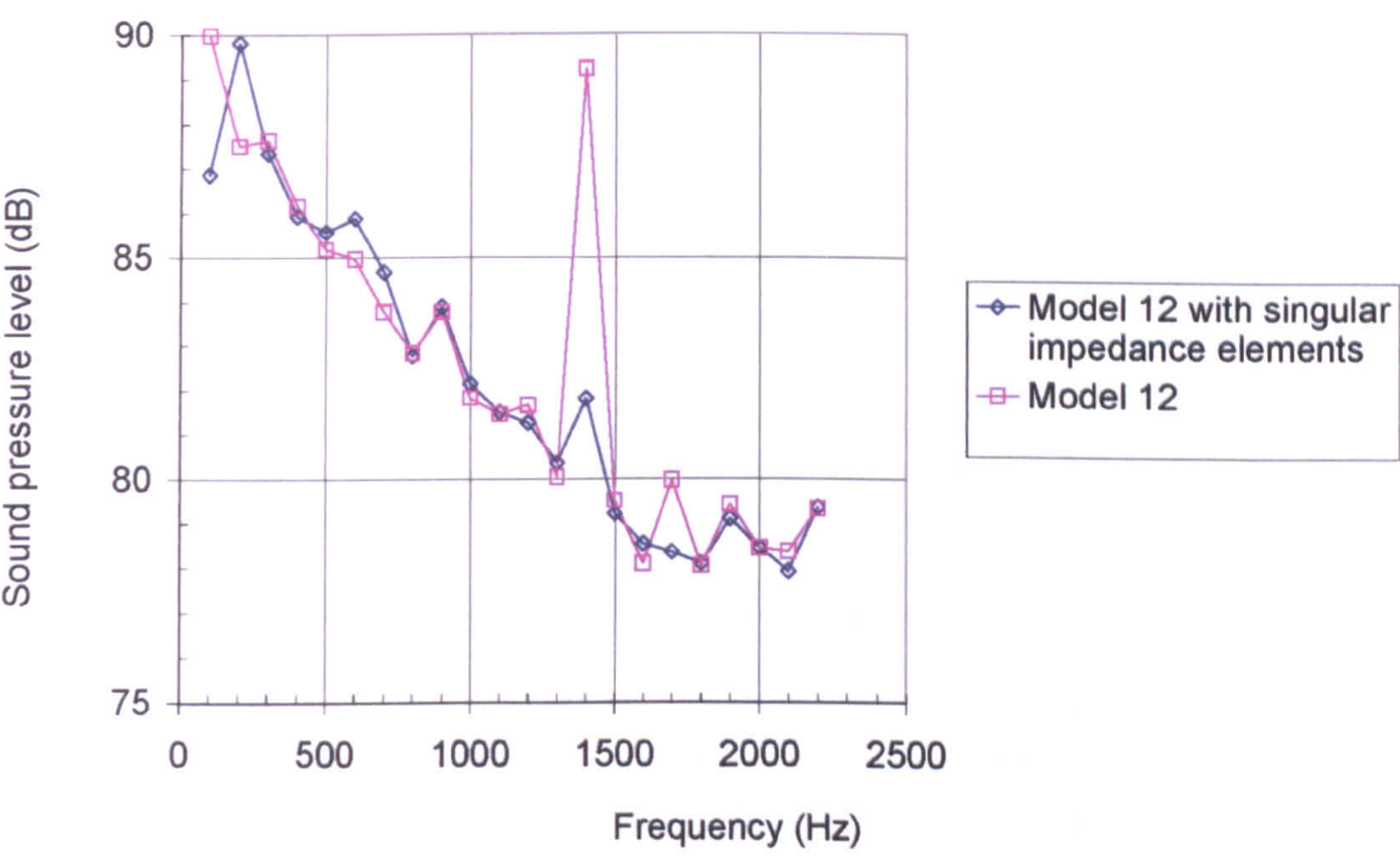


Figure 10.17 : Differences in sound pressure levels at receiver 4 due to singular impedance elements.



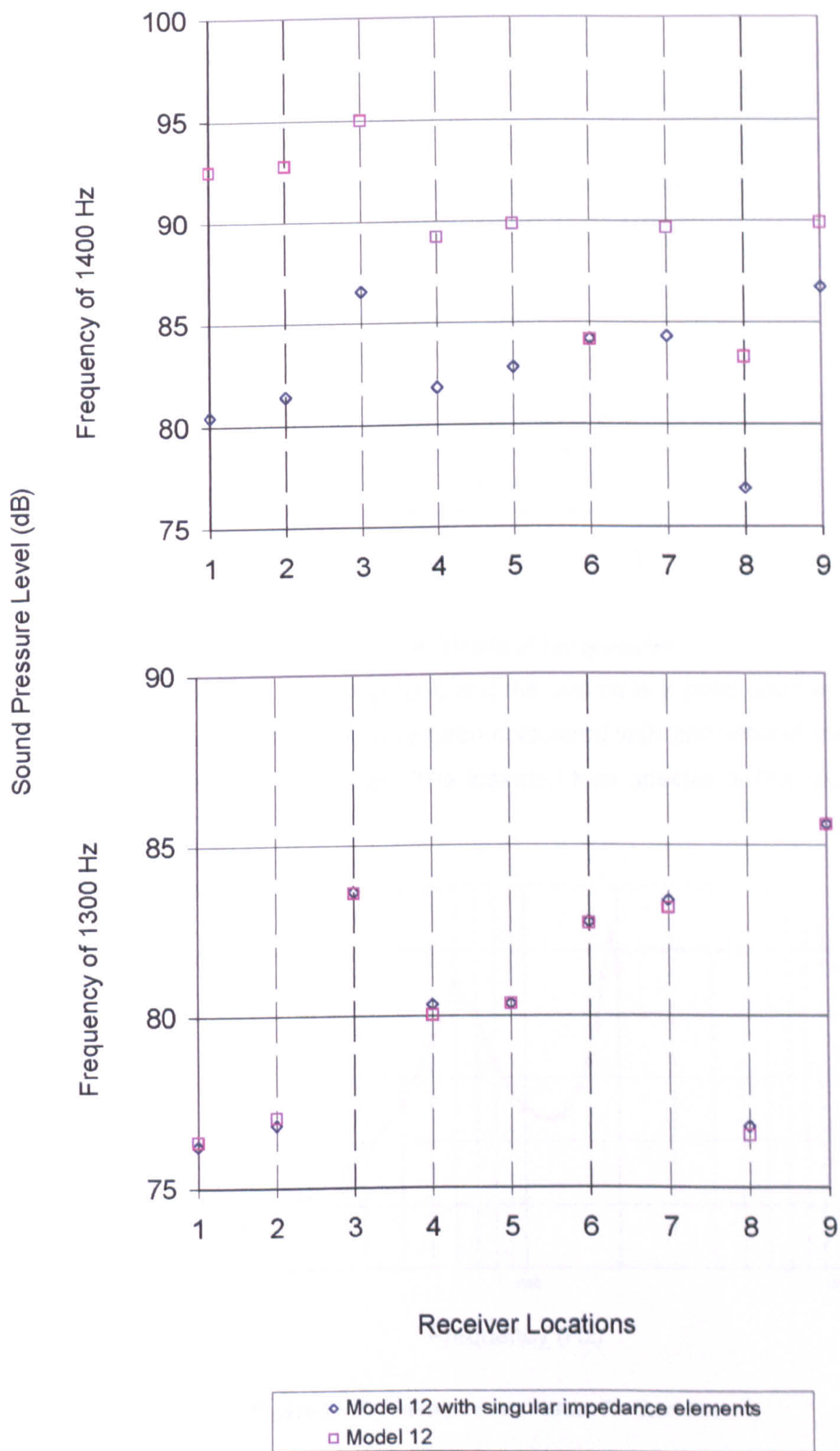


Figure 10.18 : Differences in sound pressure levels at 1400 and 1300 Hz throughout receivers 1 - 9.



### 10.3 MODELLING OF A TEST GEOMETRY FROM LITERATURE

In order to show the applicability of the numerical model, the following geometry was selected as a test case. This geometry has previously been studied by Lai<sup>10</sup> using SYSNOISE and direct comparisons of calculated insertion loss spectra can be made. The simplicity of the geometry also allows qualitative observations to be made easily on the expected and observed locations of interference peaks.

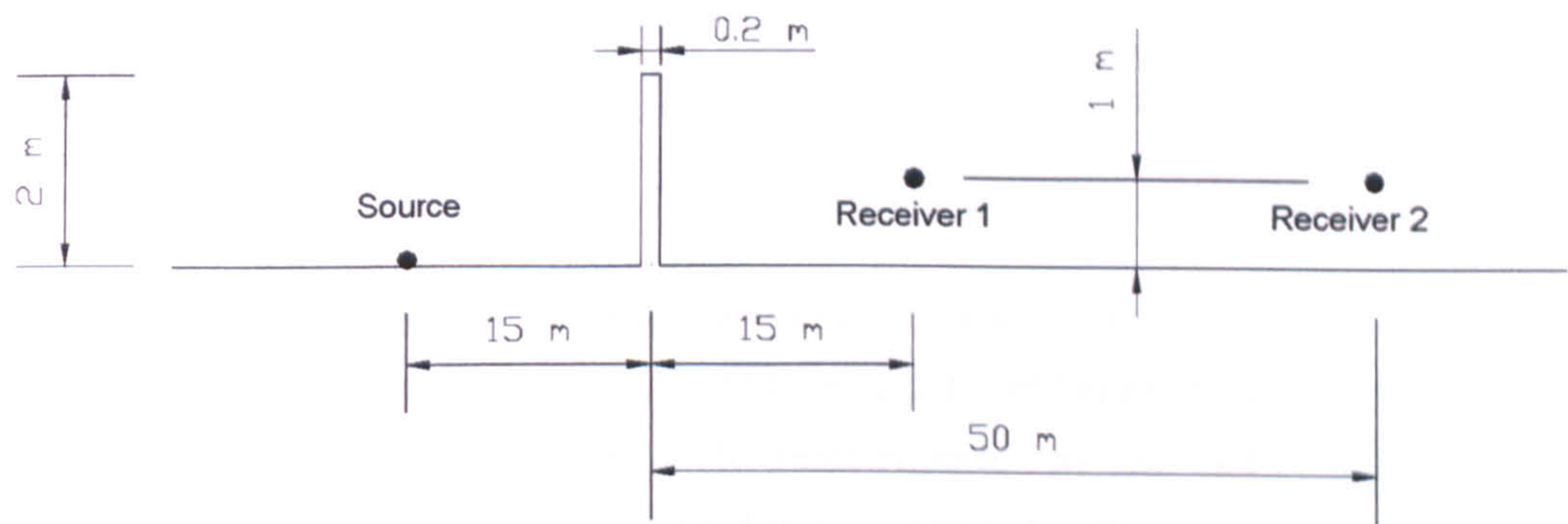


Figure 10.19 : Details of Lai geometry

The ground is modelled as hard ground and the source is a point source (cylindrical in 3D). The sound pressure levels have been calculated with and without the barrier, but with ground present in both cases. The insertion loss spectra at the receivers under consideration are shown below.

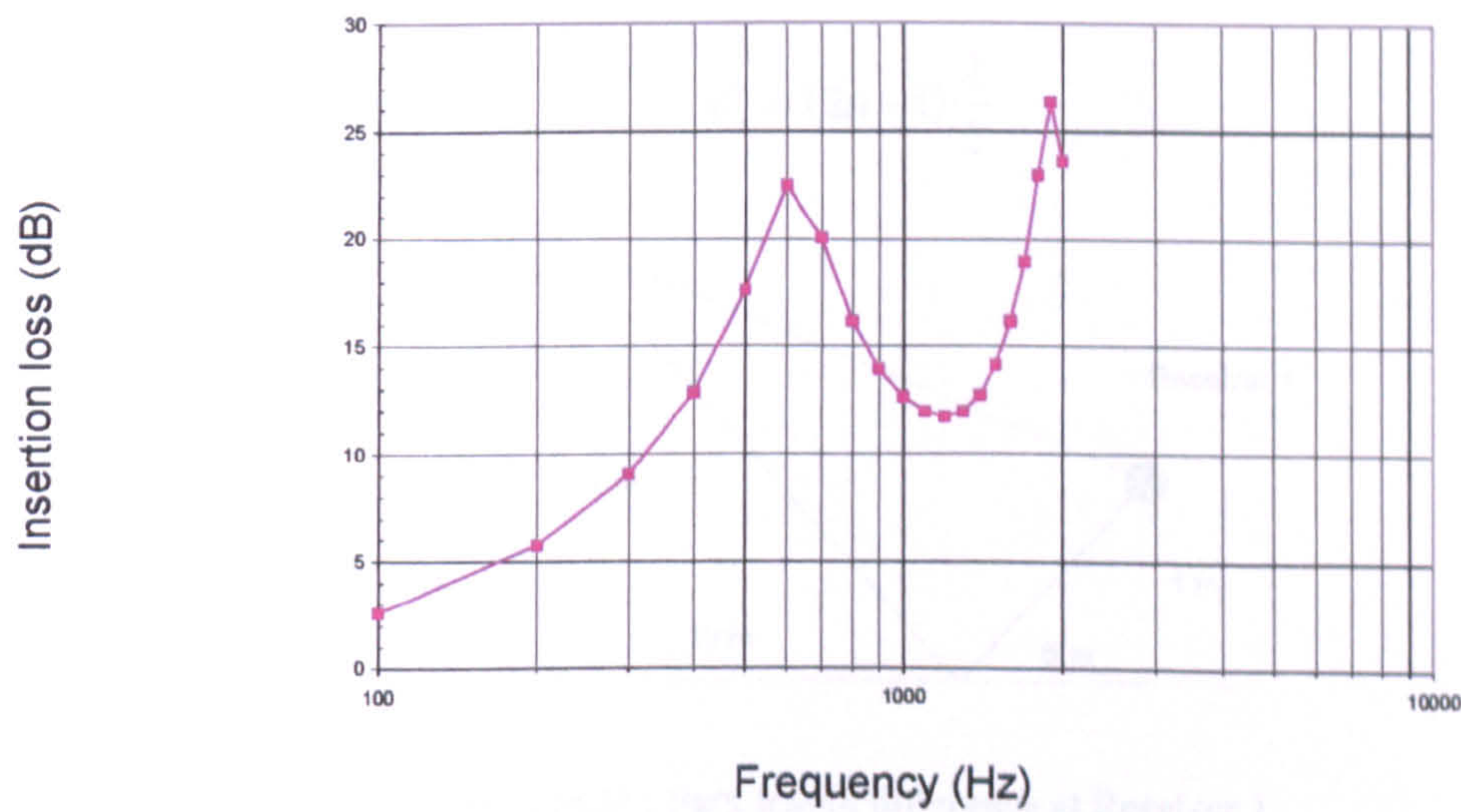


Figure 10.20 : Insertion loss values for Receiver 1



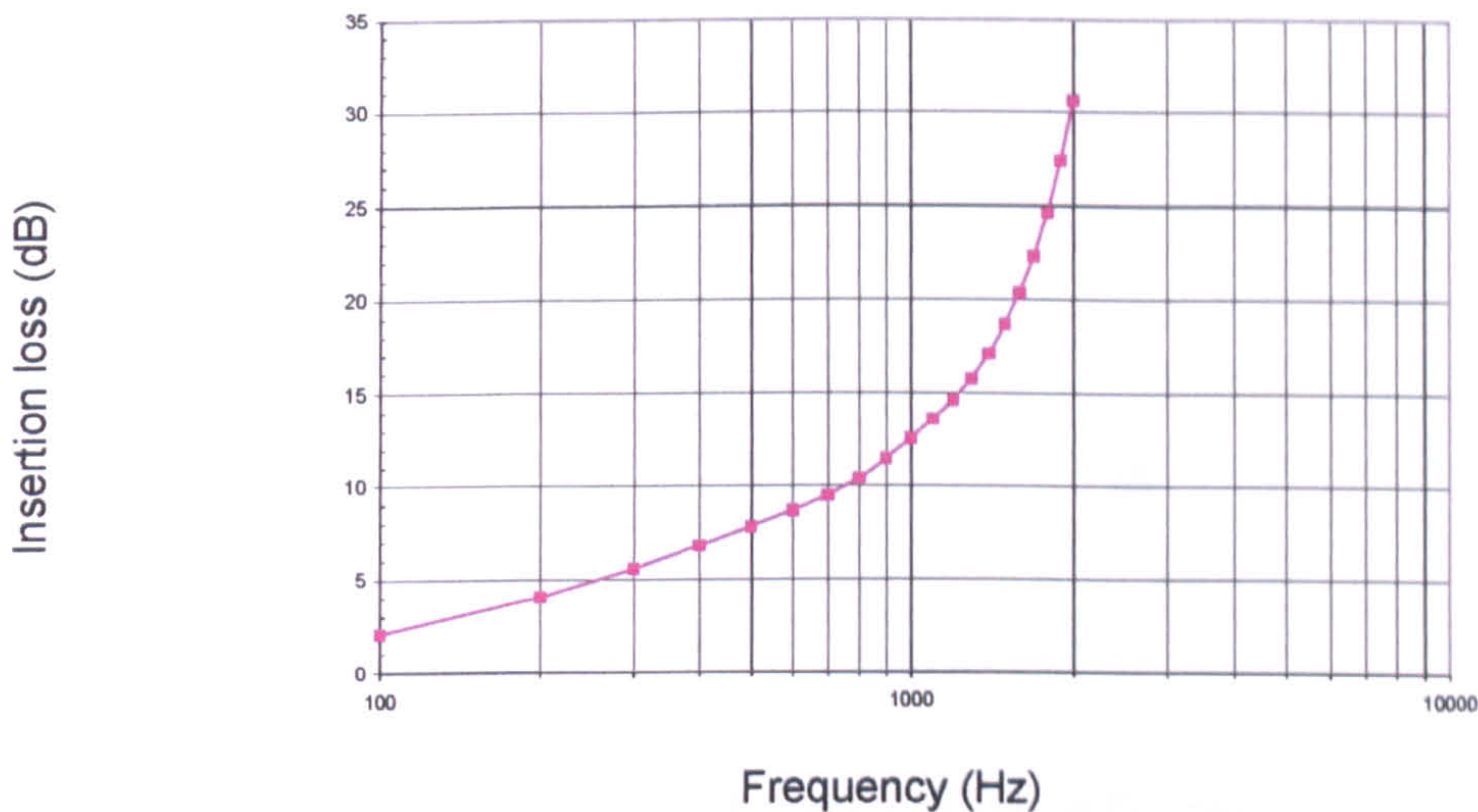


Figure 10.21 : Insertion loss values for Receiver 2

The graphs of insertion loss are shown in Figure 10.20 and Figure 10.21 for receivers 1 and 2 respectively and they are identical to those reported by Lai. The sound pressure field has been calculated with and without the barrier but with the ground present in both cases and the insertion loss was calculated.

The path length difference in presence of a barrier between direct and ground reflected rays can be represented as  $\delta_x$ . Over a hard ground, attenuation maxima (destructive interference) occur at frequencies corresponding to path length differences,  $\delta_x$ , which are odd multiples of half-wavelength. These frequencies can be represented as follows:

$$\delta_x = (2n + 1) \frac{\lambda}{2}$$

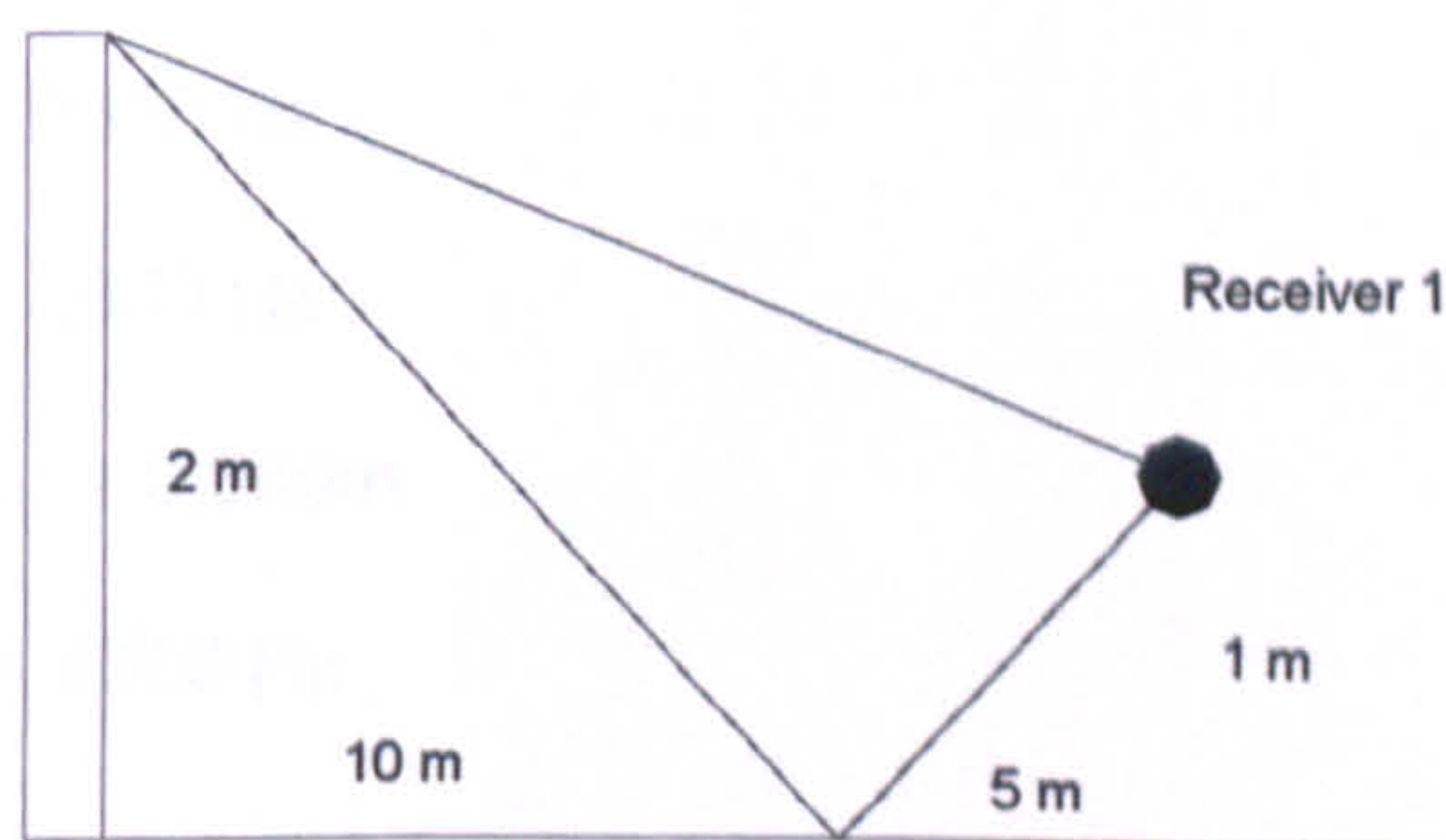


Figure 10.22 : Path length difference at Receiver 1

In the case of receiver 1  $\delta_x = 0.264\text{m}$

For  $n = 0$ ,  $f_1 = 651 \text{ Hz}$

For  $n = 1$ ,  $f_2 = 1954 \text{ Hz}$

For  $n = 2$ ,  $f_3 = 3258 \text{ Hz}$



The first two of these can clearly be identified in the insertion loss graph for receiver 1. The third frequency is beyond the frequency range under consideration.

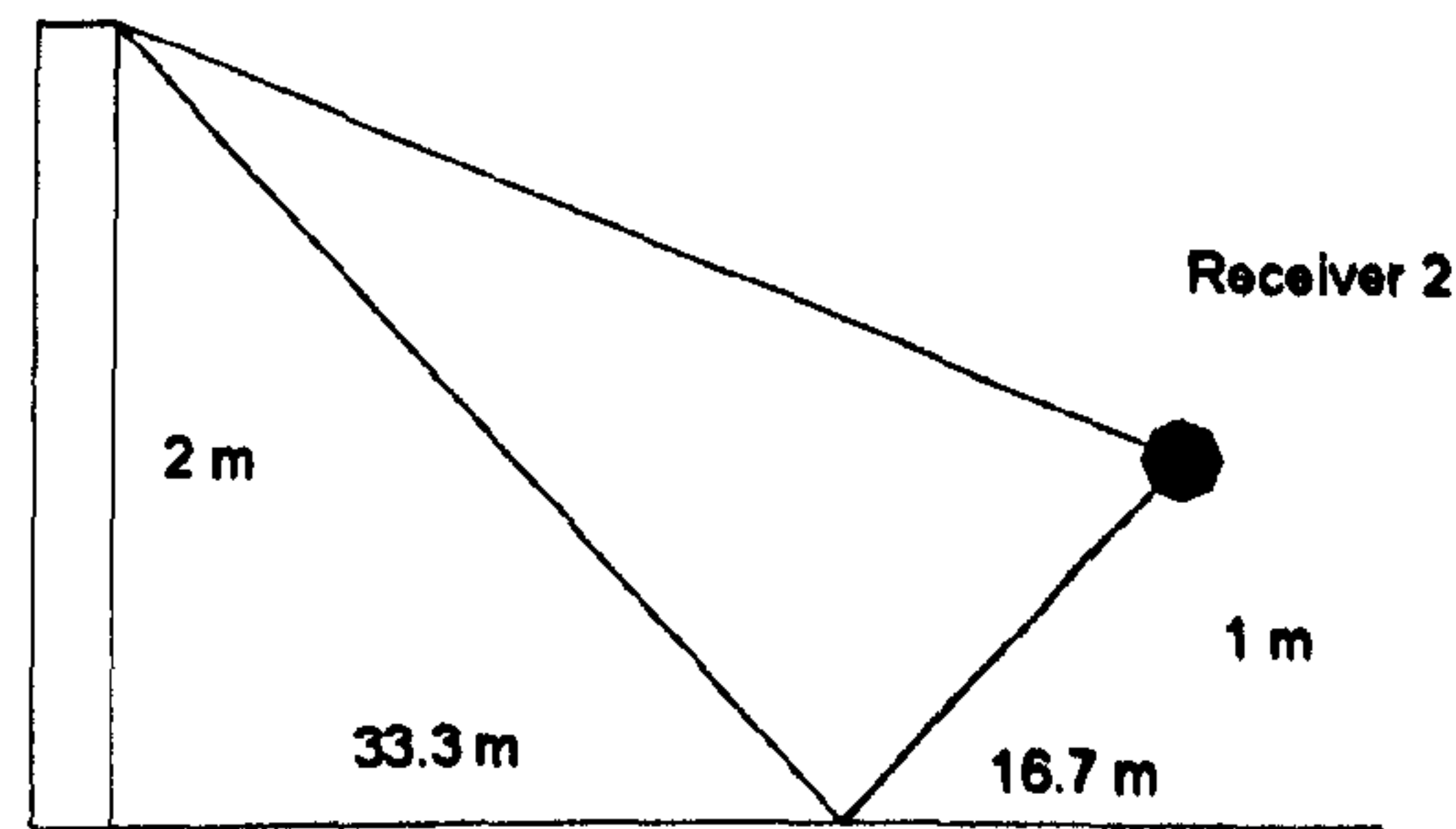


Figure 10.23 : Path length difference at Receiver 2

In the case of receiver 2  $\delta_x = 0.080\text{m}$

$$\text{For } n = 0, \quad f_1 = 2150 \text{ Hz}$$

$$\text{For } n = 1, \quad f_2 = 6450 \text{ Hz}$$

The first maxima occurs just beyond the frequency range considered and there are no other interference effects visible within this range as predicted by the above equation.

On the other hand, constructive interference are expected to occur at frequencies which are even multiples of half-wavelength. This can be represented as shown below.

$$\delta_x = (2n) \frac{\lambda}{2}$$

In the case of receiver 1  $\delta_x = 0.264\text{m}$

$$\text{For } n = 1, \quad f_1 = 1303 \text{ Hz}$$

$$\text{For } n = 2, \quad f_2 = 2600 \text{ Hz}$$

$$\text{For } n = 3, \quad f_3 = 3900 \text{ Hz}$$

In the case of receiver 2  $\delta_x = 0.080\text{m}$

$$\text{For } n = 1, \quad f_1 = 4300 \text{ Hz}$$

Only the first constructive interference frequency for receiver 1 is within the measured range and this can be seen in Figure 10.22.

The maxima and minima in insertion loss spectra are located at the frequencies as would be expected by a simple interference approach for a hard ground with no phase change on reflection. This test geometry verified the way the numerical model has been implemented.



10.4 NUMERICAL MODELLING OF SELECTED GEOMETRIES INVESTIGATED BY PHYSICAL MODELLING

Four sets of geometries investigated in previous chapters have been modelled using the numerical method described in this chapter. The first set of geometry consists of the rib structure which was used to investigate the effects of attenuations and amplifications at various diffraction angles. The second set of geometries consisting of a series of edges on the ground includes three models having 14-edge configurations with different heights. The third set of geometries involving low rectangular barriers similarly uses three models with different edge conditions. The fourth consists of a single geometry of reactive earth mound to represent the largest geometries. This model was considered to be the most likely candidate where a reactive surface could be realised due to the number of edges involved.

The source heights in the numerical models are taken as 0.25m above the ground to represent the physical centre of the sources. All ground and barrier surfaces are modelled as acoustically hard. The details of models and the comparisons obtained by physical and numerical modelling are discussed below.

10.4.1 The rib structure

This geometry compared a single edge case to the 21-edge case at 7 receiver heights. These are shown in Figure 10.24.

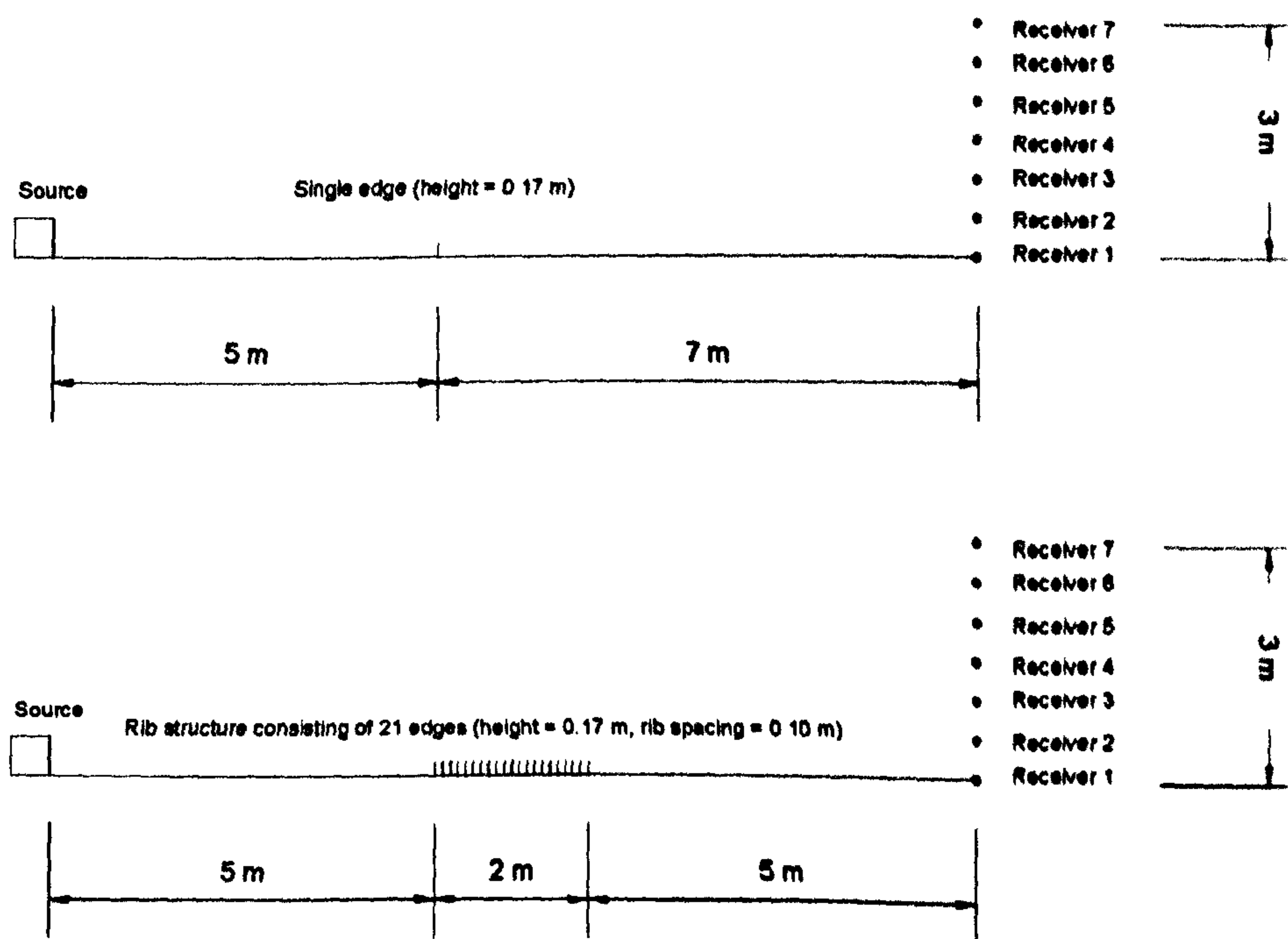


Figure 10.24 : Experimental set-up investigating various receiver heights



The relative improvements of the 21-edge case over the single edge case are shown in Figure 10.25.

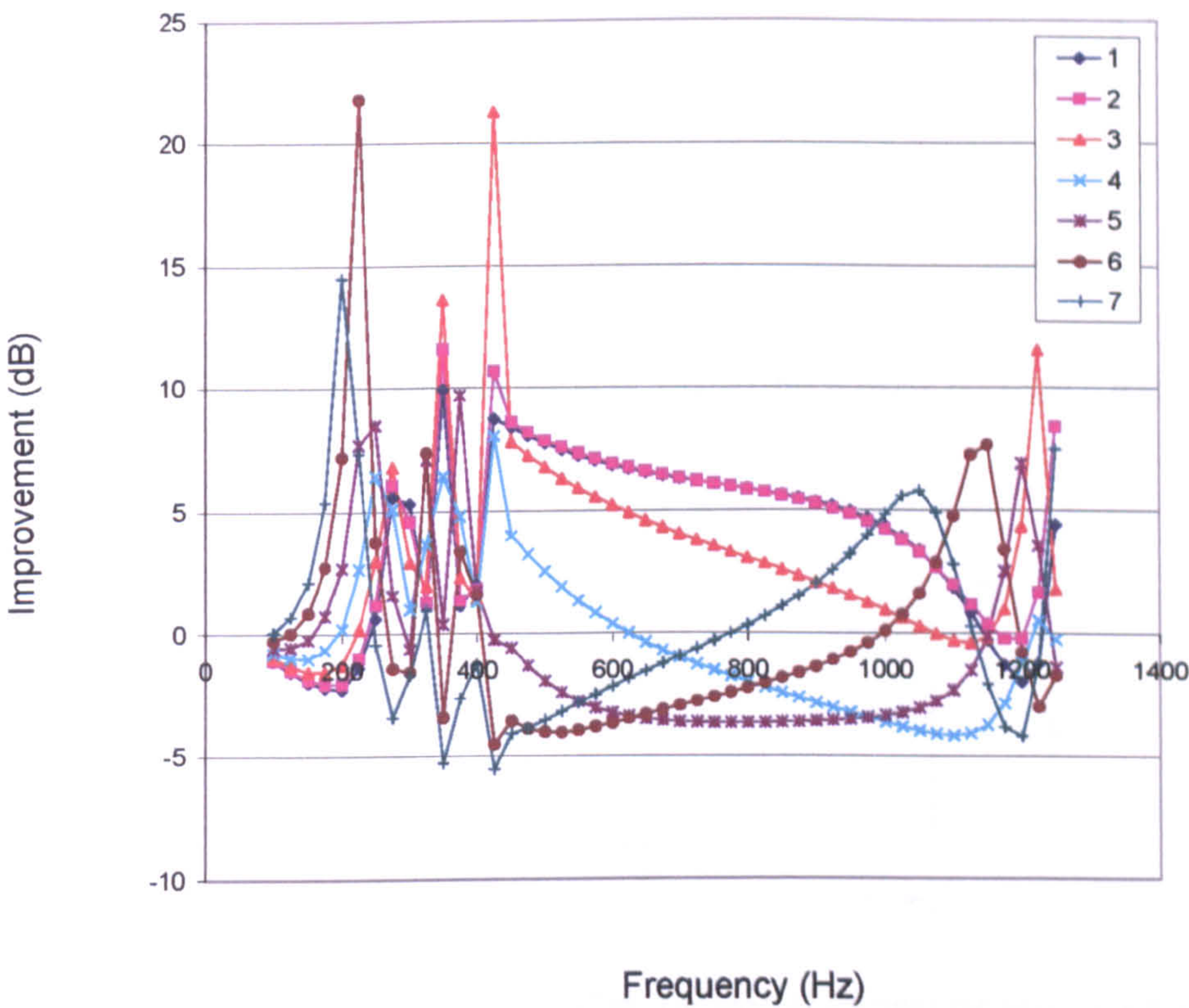


Figure 10.25 : The effect of 21 edges over a single edge

10.4.2 The edges on the ground

Three models have been used for modelling the configurations involving edges on the ground. These represent three different well depths of 14-edge cases compared with their equivalent 1-edge cases. The single edges are all situated 5m from the source. The details of the geometries are shown in Figure 10.26 to Figure 10.28. All dimensions are in metres. The improvements obtained by these geometries are shown in Figure 10.29 to Figure 10.31.



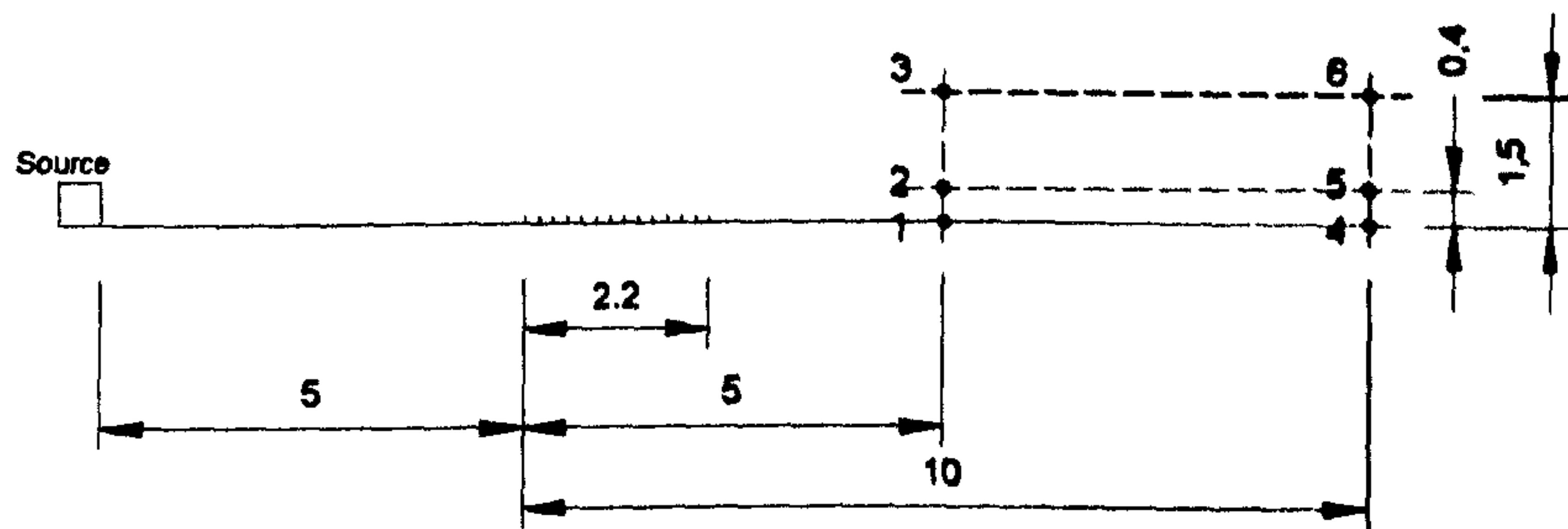


Figure 10.26 : The height of the wells is 0.08 m. The spacing between the edges is 0.17 m.

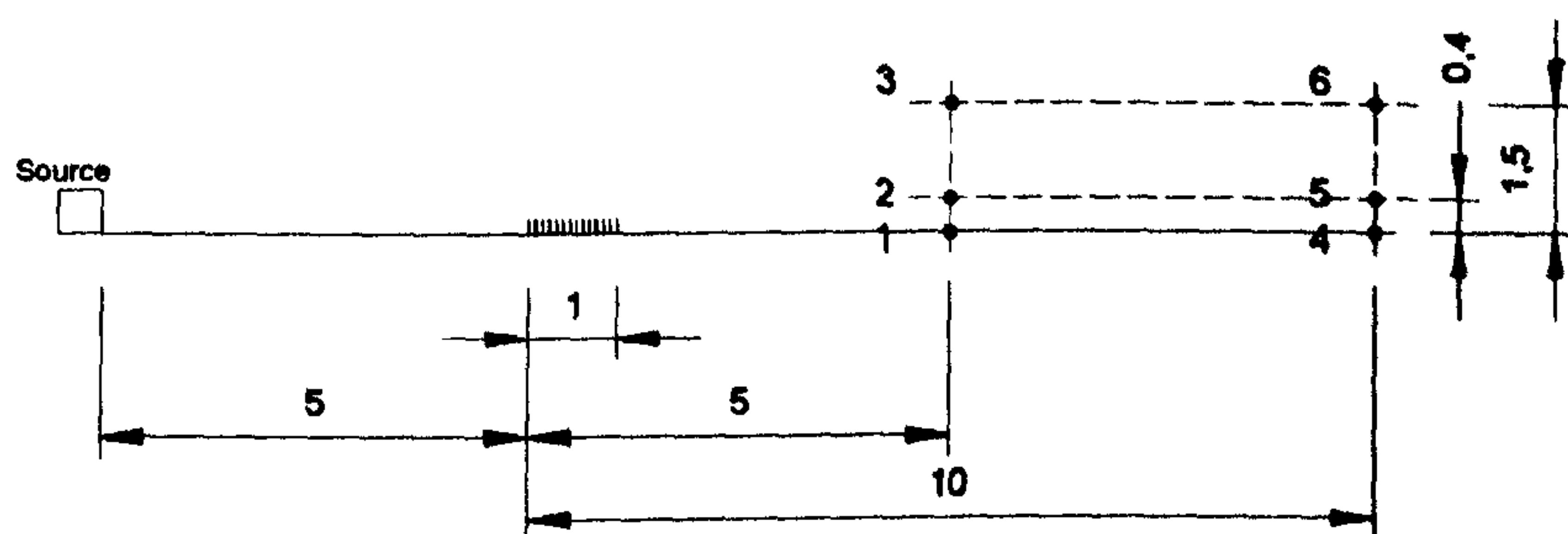


Figure 10.27 : The height of the wells is 0.17 m. The spacing between the edges is 0.08 m.

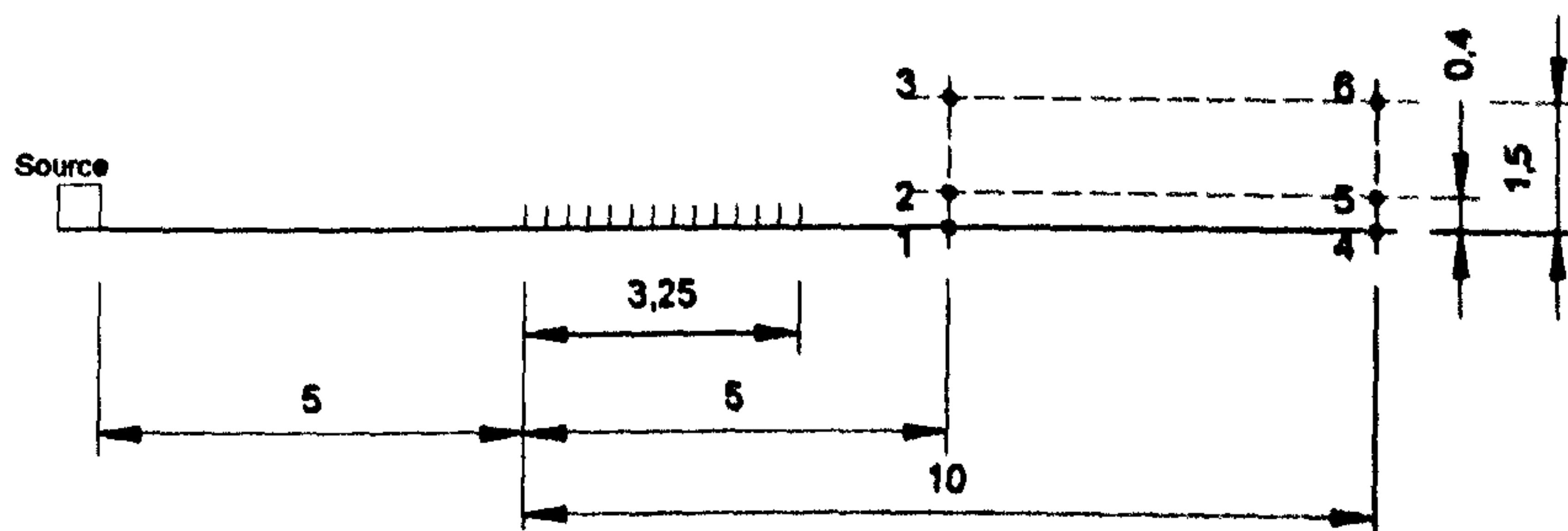


Figure 10.28 : The height of the wells is 0.25 m. The spacing between the edges is 0.25 m.



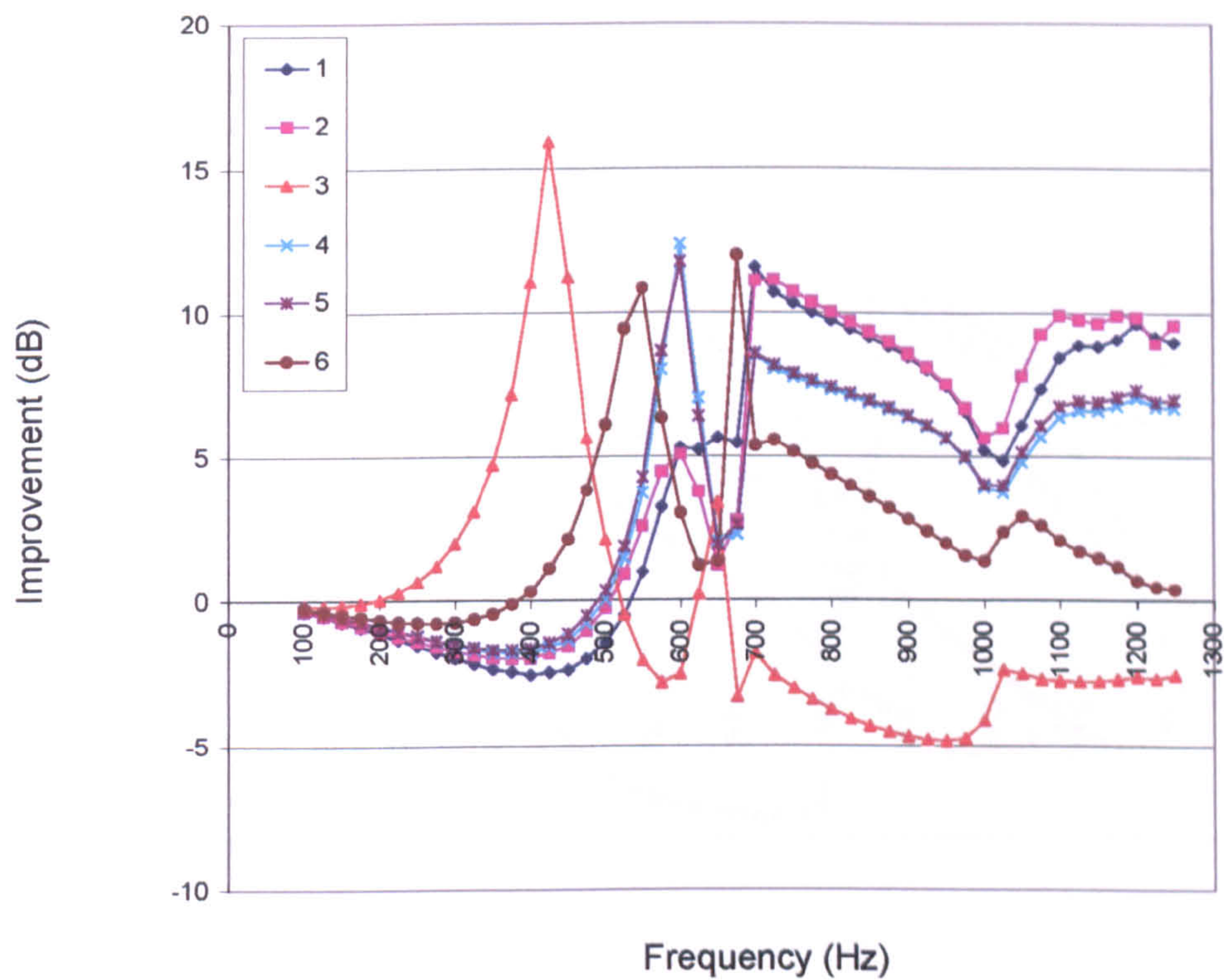


Figure 10.29 : Effect of 14 x 0.08m edges relative to a single edge (on the ground)

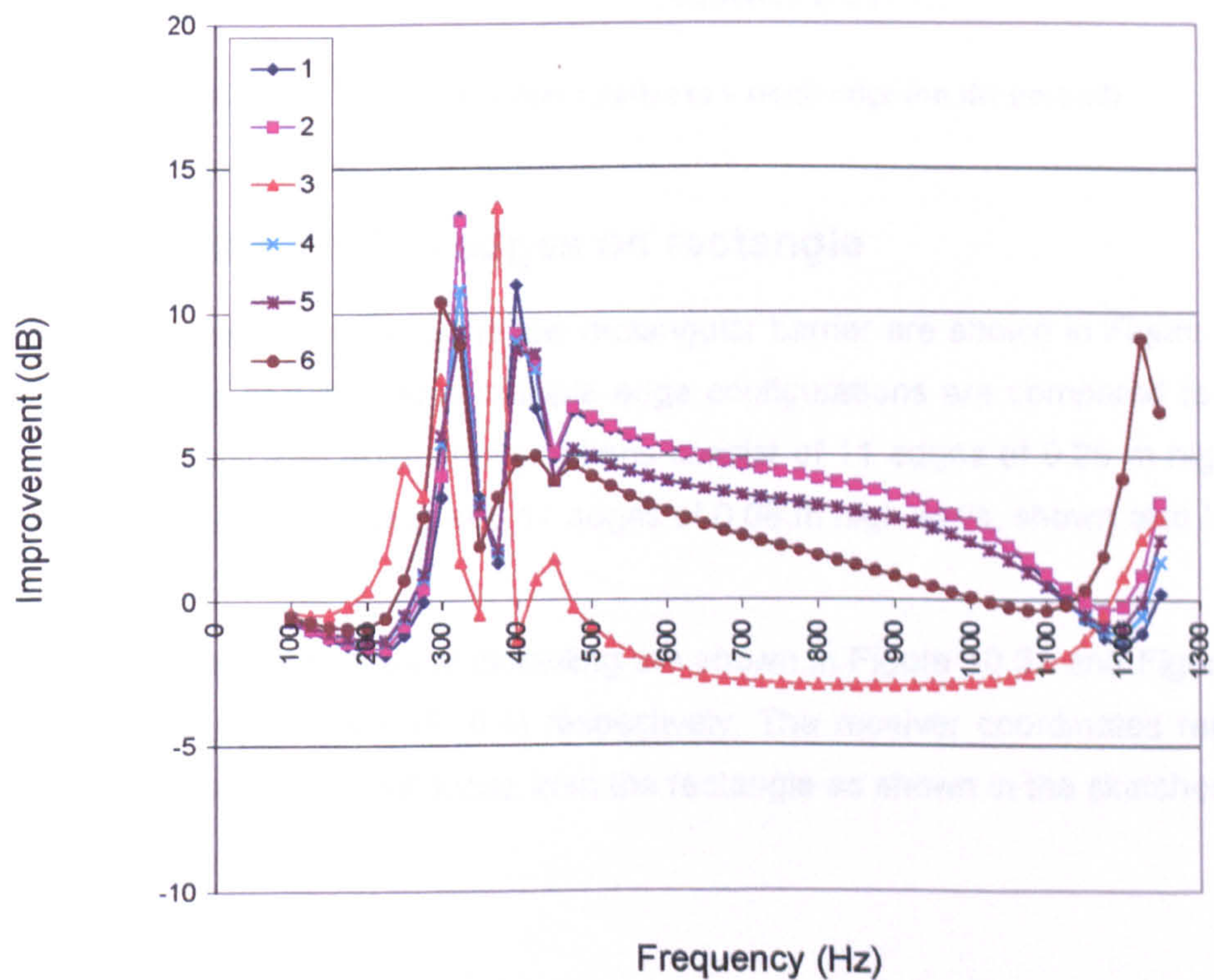


Figure 10.30 : Effect of 14 x 0.17m edges relative to a single edge (on the ground)



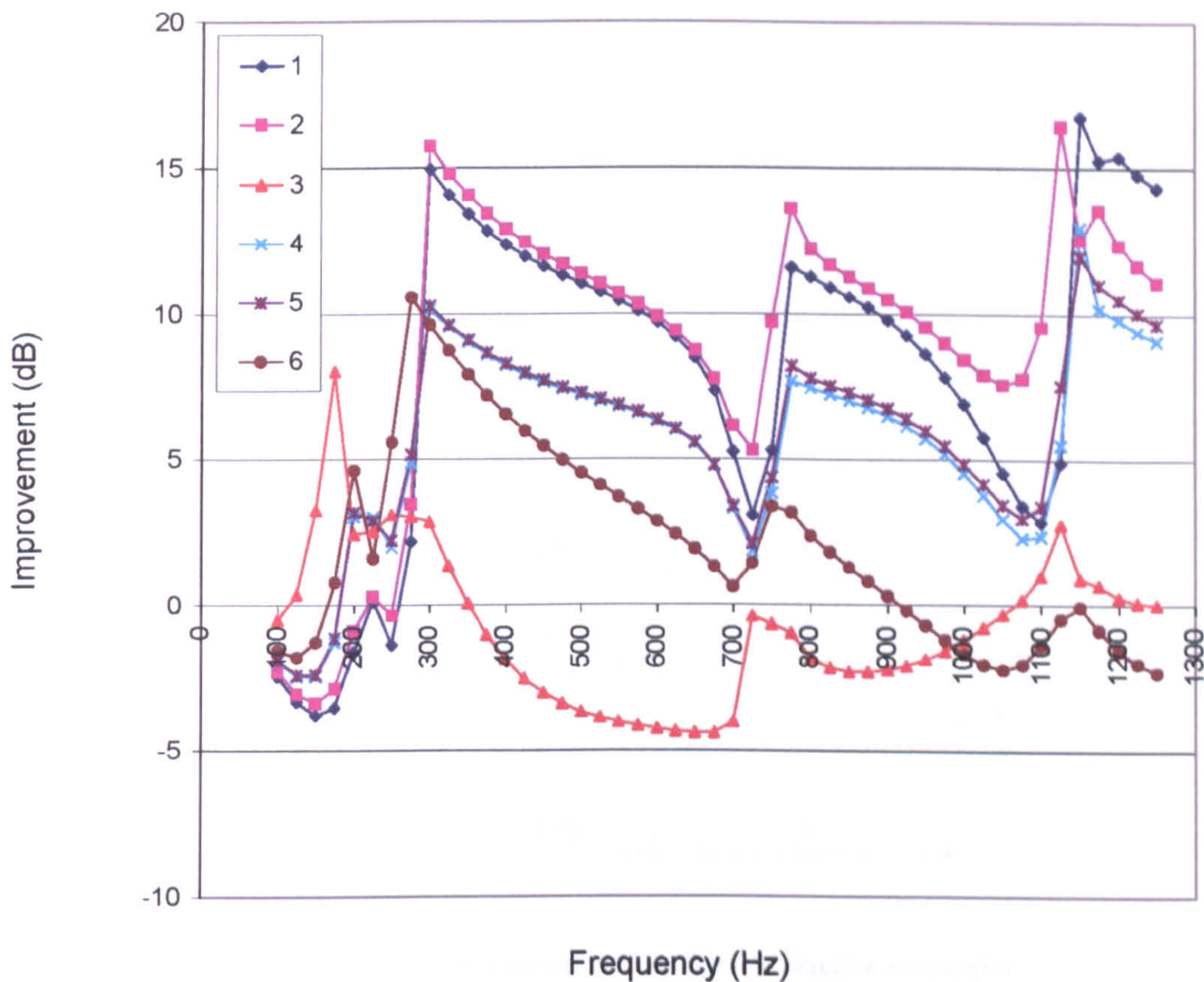


Figure 10.31 : Effect of 14 x 0.25m edges relative to a single edge (on the ground)

### 10.4.3 The edges on rectangle

The three models involving the low rectangular barrier are shown in Figure 10.32. The performances of the various multiple edge configurations are compared to that of the plain rectangle. The edge configurations consist of 11 edges of 0.25 m high wells, 15 edges of 0.17 m high wells and 14 edges of 0.08 m high wells, shown also in this order in Figure 10.32.

The results of the numerical modelling are shown in Figure 10.33 and Figure 10.34 for the receivers (5, 0) and (5, 0.4) respectively. The receiver coordinates represent the horizontal and vertical distances from the rectangle as shown in the sketches.



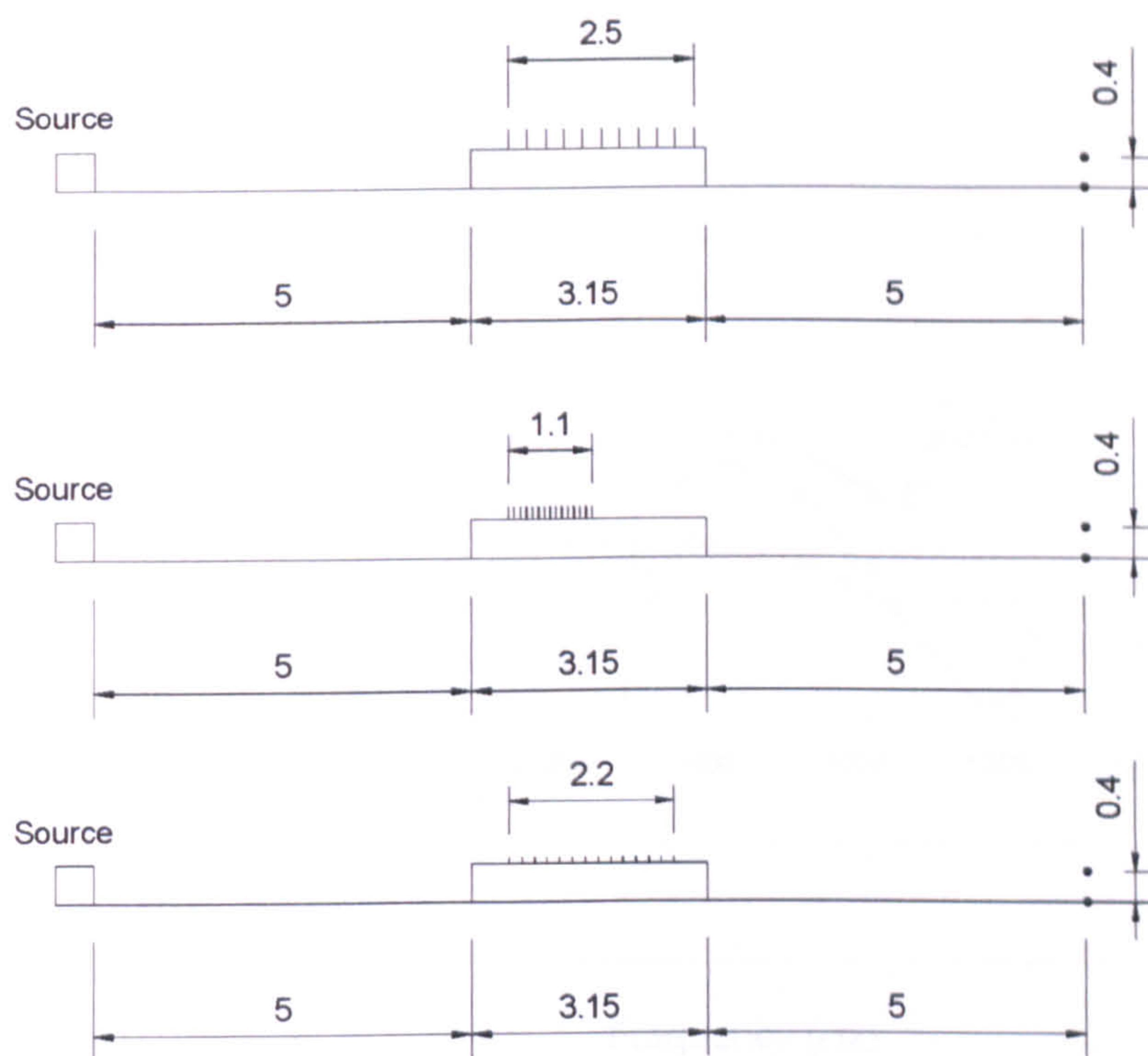


Figure 10.32 : Experimental set-up for the reactive rectangles

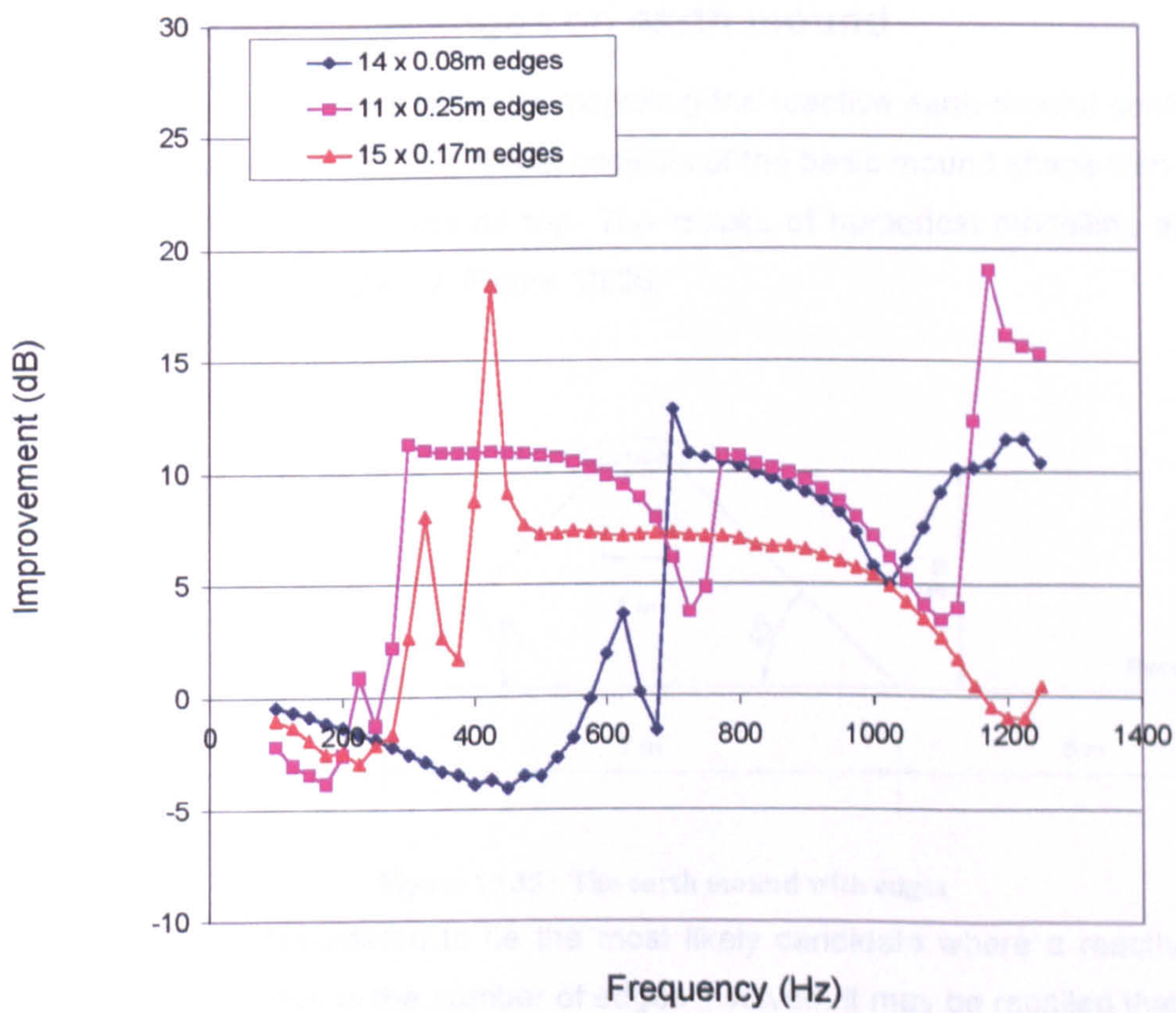


Figure 10.33 : Effect of reactive configurations over a plain rectangle (receiver 5, 0)



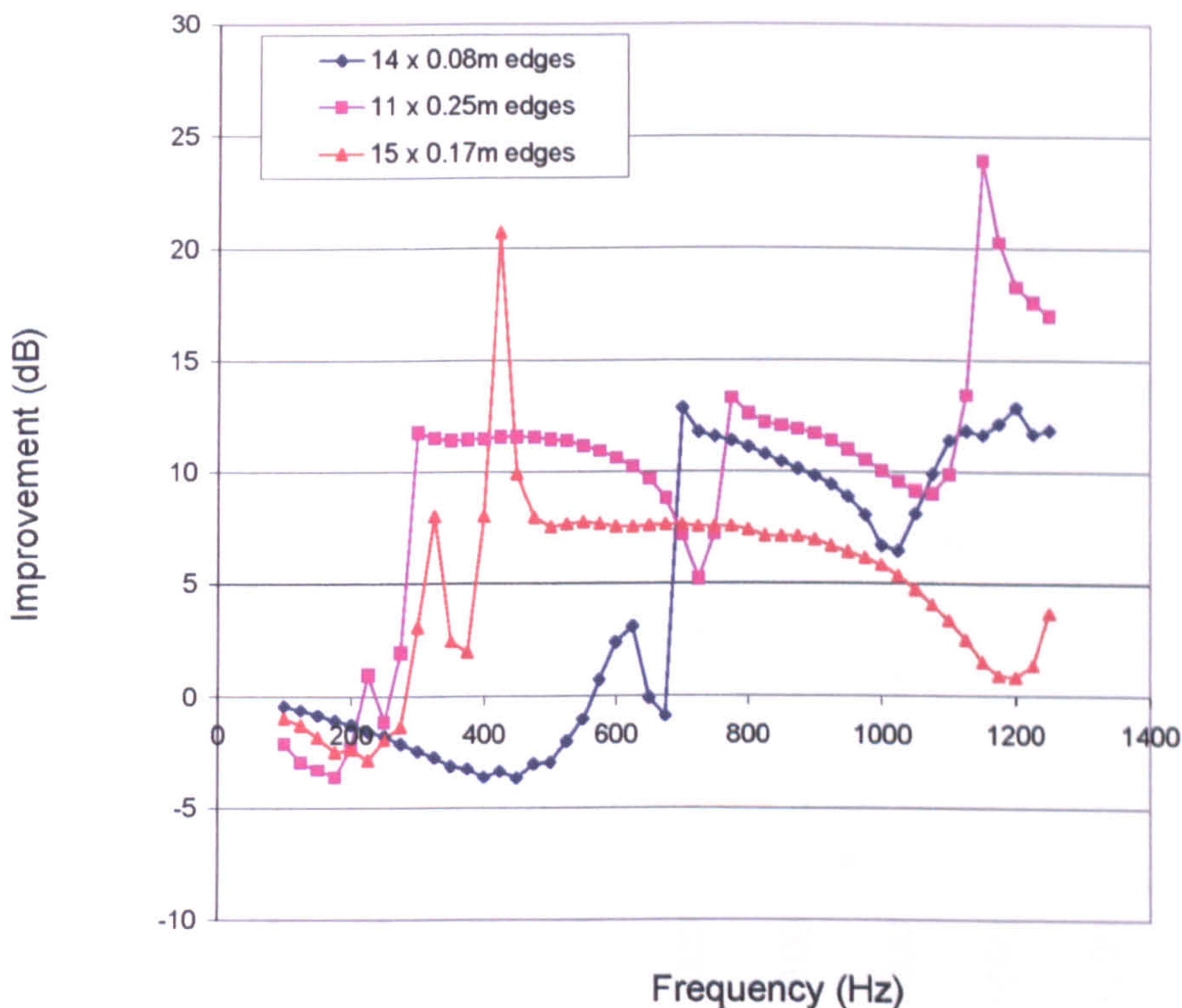


Figure 10.34 : Effect of reactive configurations over a plain rectangle (receiver 5, 0.4)

### 10.4.4 The edges on earth mound

The geometry that was selected for modelling the reactive earth mound configurations is shown in Figure 10.35. This model consists of the basic mound shape with 10 edges of 0.17m high wells attached on top. The results of numerical modelling at a single receiver position are shown in Figure 10.36.

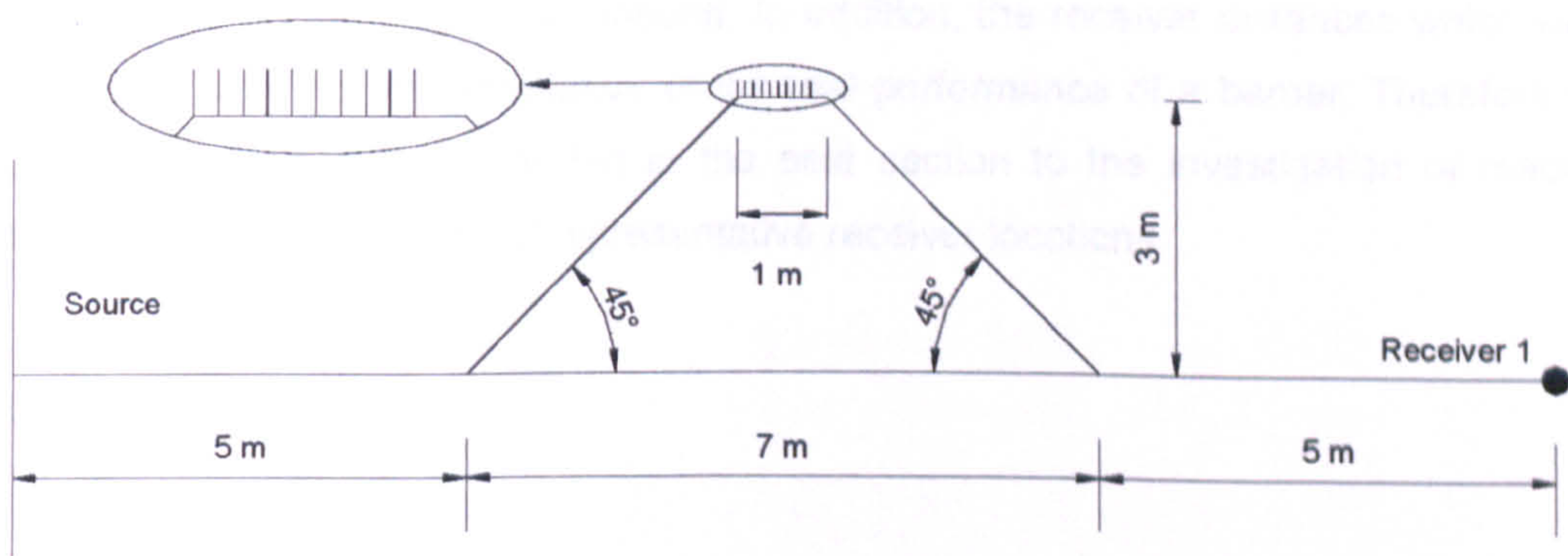
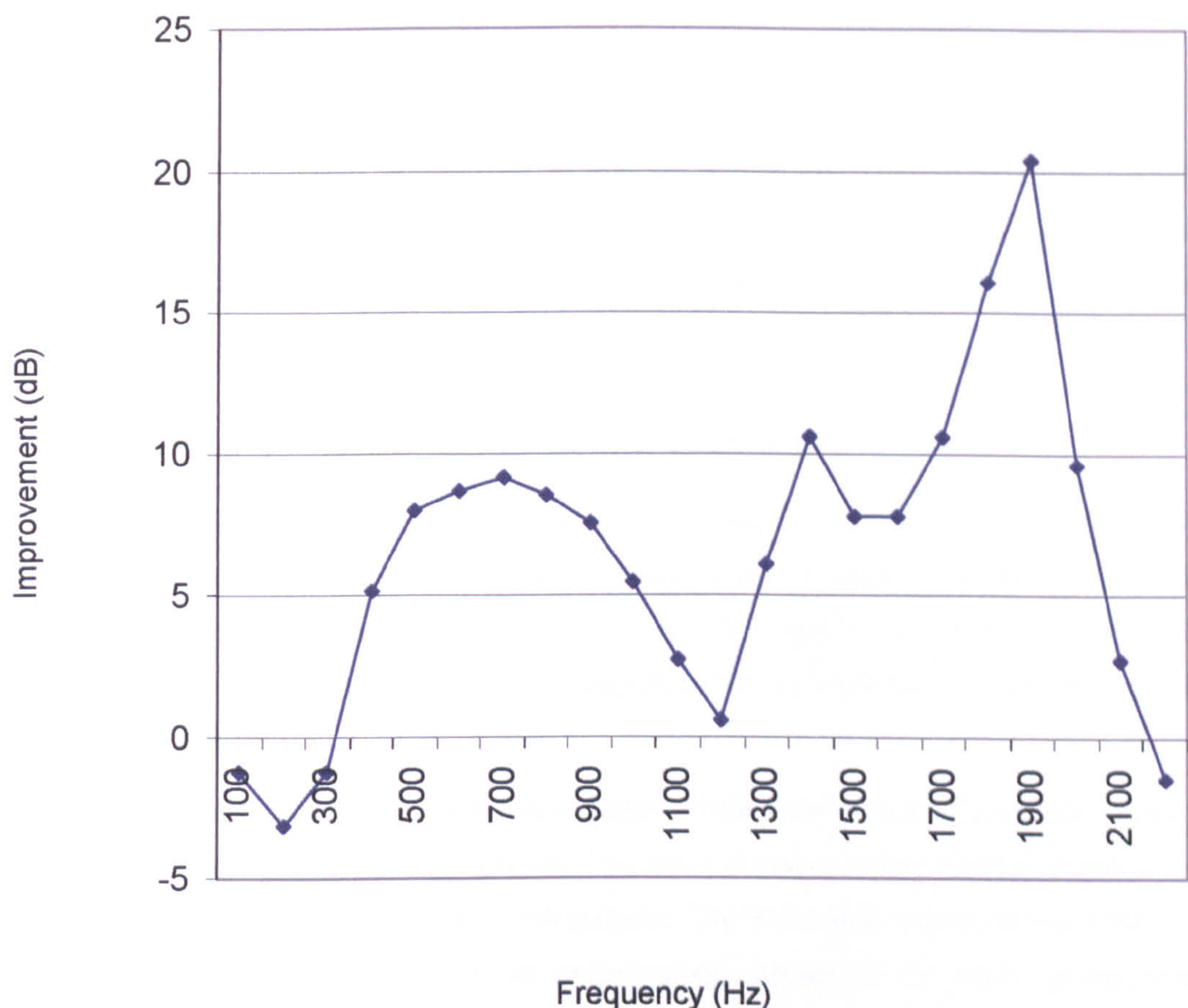


Figure 10.35 : The earth mound with edges

This model was considered to be the most likely candidate where a reactive surface could be realised due to the number of edges involved. It may be recalled that the other two edge heights were represented by 5 edges on top of a mound.





**Figure 10.36 : The effect of multiple edges on top of a plain earth mound**

The numerical modelling results presented in this section will be used in the next chapter for comparing and validating the findings of physical modelling undertaken previously. As it may be recalled, the practical limitations associated with physical modelling, in some instances, did not allow sufficient number of edges to be investigated on top of an earth mound. In addition, the receiver distances which were examined were not representative of the real performance of a barrier. Therefore the numerical modelling is extended in the next section to the investigation of reactive earth mounds at a number of representative receiver locations.



# 10.5 MODIFICATIONS TO AN EXISTING EARTH MOUND

The numerical modelling undertaken in this section is intended to result in acoustic guidance on the potential ways on how the performance of an existing earth mound could be improved. This will be used in the forthcoming chapters to supplement the advice provided in chapter 4.

## 10.5.1 Description of the Geometry

The relative performance of 16 configurations were studied and compared with a reference profile. The reference profile is a plain reflective trapezoidal barrier as shown in Figure 10.37. It has a vertical height of 3 m and top and bottom widths of 1 m and 7 m respectively. The slope angles are 45 degrees. This is identical to those investigated in previous chapters.

A single source location was selected to observe the relative sound pressure levels at 9 receiver locations behind each profile. The source was a plane source located 15 m from the centreline of the mound on the ground. The 9 receiver positions were selected in a way to provide realistic overall performance indicators for each configuration. These have been previously investigated by others<sup>3,11</sup>. The receivers were located 20 m, 50 m and 100 m from the barrier centreline, situated at three different heights, namely on the ground and 1.5 m and 3 m above the ground.

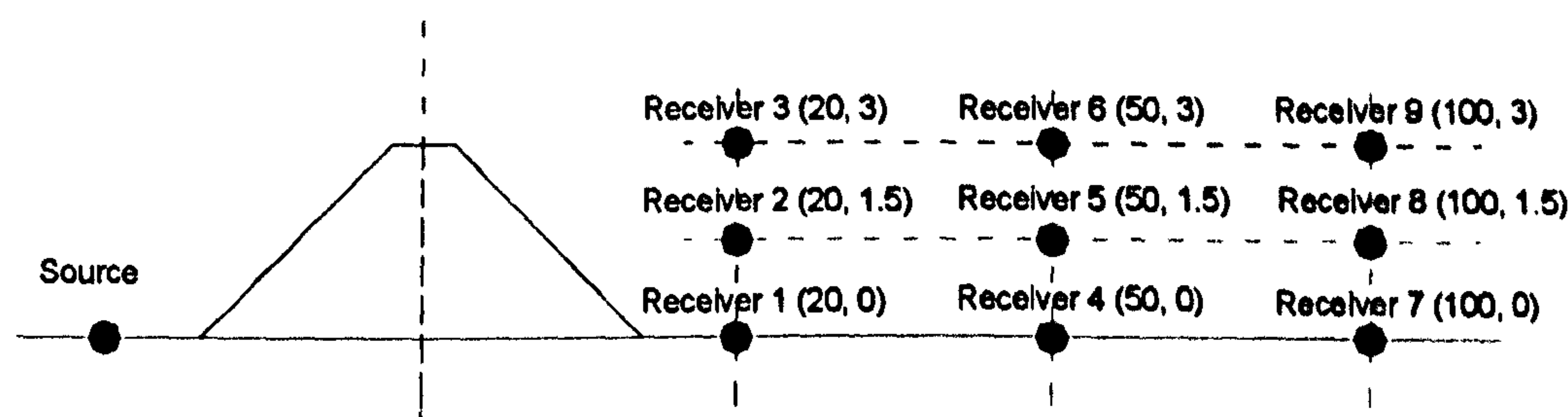


Figure 10.37 : The basic earth mound geometry and receivers locations

The reasons for considering these receivers in assessing the performance of different profiles can be summarised in Table 10-1 and Table 10-2.



Vertical height (m)	The reason of preference
0	no interference dips from ground reflected paths
1.5	'typical' height for a receiver
3	'typical' height of a ground floor of a building

**Table 10-1 : Vertical receiver heights**

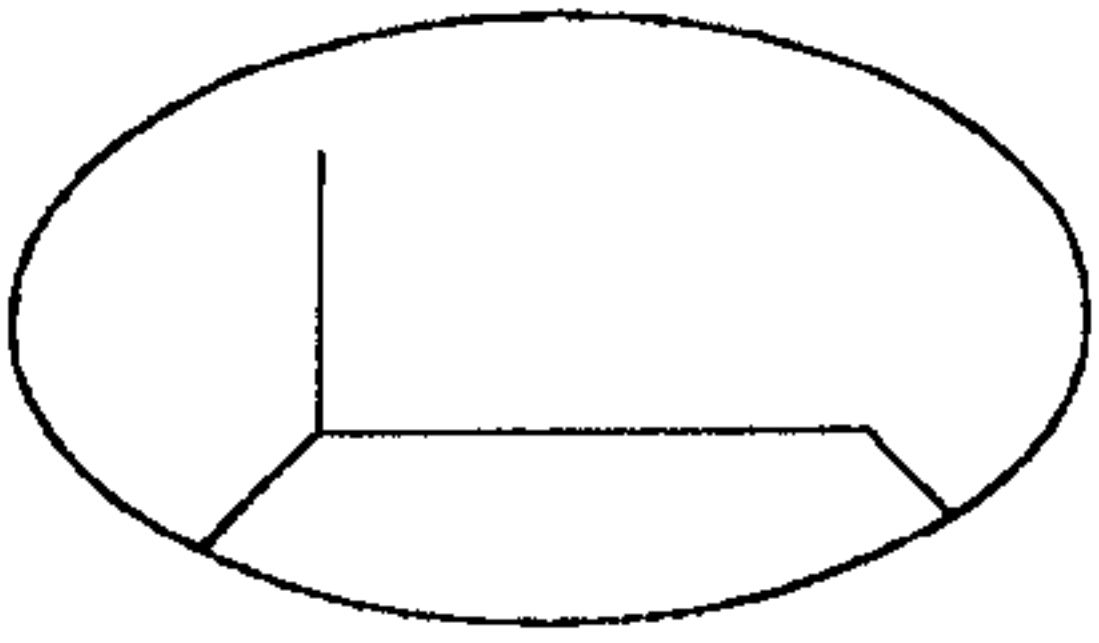
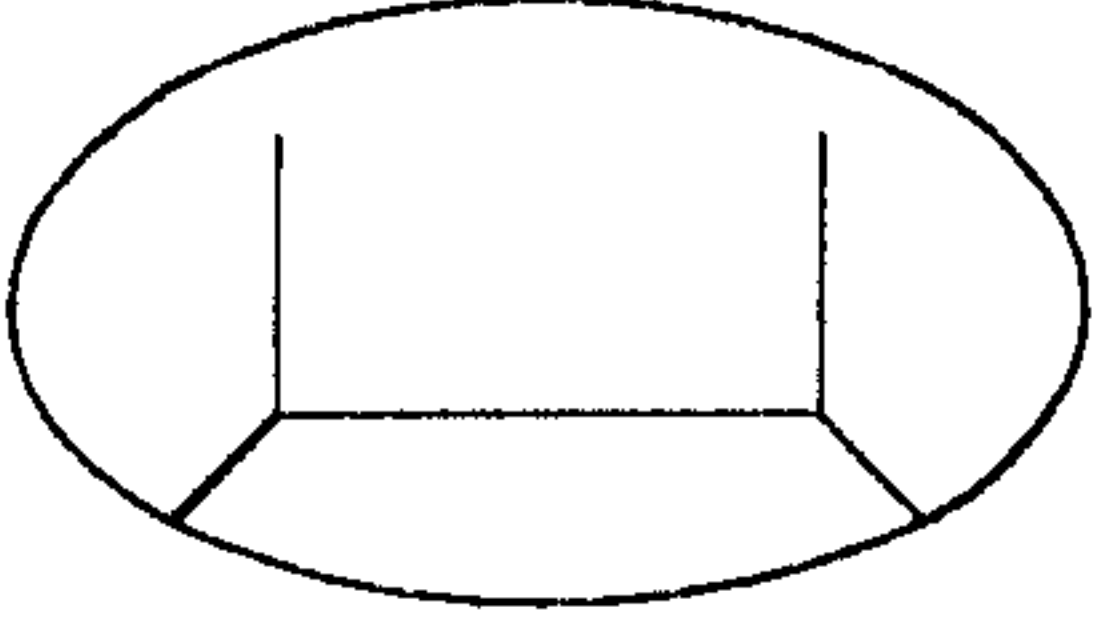
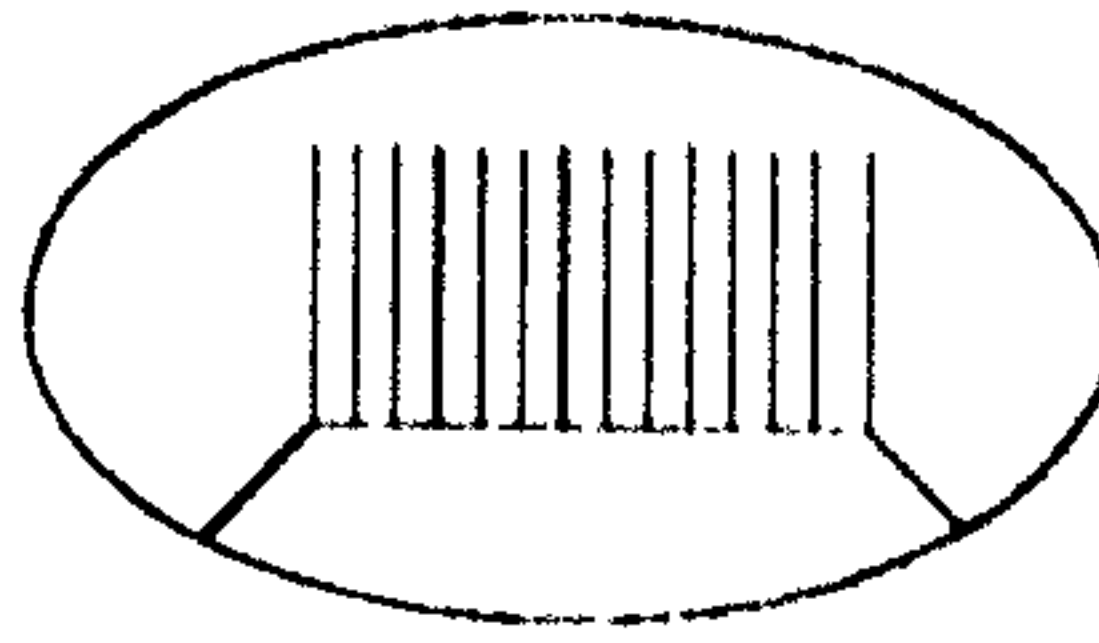
The ear position of an average person is generally assumed to be located 1.5m above the ground. The height of a single storey building is typically taken as 3m. The receivers on the ground are intended to eliminate the ground reflected paths. When the spectra obtained at these receivers with and without the multiple edges are compared, the relative differences can be appreciated more readily. It should also be noted that another receiver height generally used in noise assessments is 4.5m, which represents the height of a typical bedroom window, commonly situated on the first floor of a residential house. This receiver height is not considered as part of the following numerical modelling, and the accompanying acoustical advice.

Horizontal distance (m)	The reason of preference
20	'typical' lower limit for barriers beyond which different profiles exhibit consistent trends relative to each other
50	represents an in-between case for horizontal distance range considered
100	'typical' upper limit for considering noise barriers in practice

**Table 10-2 : Horizontal distances of receivers**

The edge conditions, which will be compared to the plain earth mound, are shown in Figure 10.38. These consisted of single, double and multiple edge configurations. The number of edges was 14 in the case of all multiple edge profiles. The heights of the edges investigated consisted of six different heights. The smallest three of these heights have been the subject of extensive investigations as part of the physical scale modelling. These are summarised below.



Edge height (m)	Modifications made to the horizontal top.		
			
2	Model 1	Model 2	<i>N / A</i>
1	Model 3	Model 4	<i>N / A</i>
0.5	Model 5	Model 6	Model 7
0.25	Model 8	Model 9	Model 10
0.17	Model 11	Model 12	Model 13
0.08	Model 14	Model 15	Model 16

**Figure 10.38 : The details of the modifications made on top of the basic shape.**

The frequencies under investigation are between 100 Hz and 2200 Hz inclusive, in linear steps of 100 Hz. In order to be able to compare various configurations against each other, a sensible rating system needs to be devised. There are alternative, more complex, barrier rating systems<sup>4</sup>, however for the purposes of this work, the following comparison is assumed to suffice.

The single figure performance indicators were determined for each one of the models above, relative to the reference profile. The differences in the sound pressure levels were calculated for each one of the 22 linear frequency steps.

$$\Delta f_x = (SPL_{reference} - SPL_{model}) \text{dB}$$

Equation 10.10

where  $x = 1$  to 22, corresponding to each linear frequency step between 100 Hz and 2200 Hz. These differences were averaged linearly throughout the spectrum to obtain values in decibels at each receiver location.



$$f(y)_{average} = \left( \frac{\Delta f_1 + \Delta f_2 + \dots \Delta f_{22}}{22} \right) \text{ dB}$$

Equation 10.11

where  $y = 1$  to  $9$ , corresponding to each receiver location under consideration. The average of these values for the  $9$  receiver locations provided a single value thought to be representative of the relative performance of each profile, over that of the basic shape.

$$Single\ Figure\ Performance\ Indicator = \left( \frac{f(1)_{average} + \dots + f(9)_{average}}{9} \right)$$

Equation 10.12

Logarithmic averaging throughout the spectrum is specifically avoided. The output broadband spectra at any given receiver are not constant throughout the spectra and the output decreases with increased frequency. Therefore, any such averaging will place emphasis to the lower frequency noise levels, and any potential gains, which are expected at the higher ends of the spectrum, will be masked. The findings of numerical modelling are given below.

### 10.5.2 Numerical Modelling Results

Before presenting the relative improvements of various configurations, the insertion loss of the basic shape was calculated in  $25\text{ Hz}$  linear steps. The single figure performance indicators are shown in Table 10-3. These are based on the linear averaging described above. Due to the magnitude of the destructive interference at the receivers which are  $1.5\text{m}$  above the ground, the insertion loss values at these receivers are the highest. Similarly, this applies to the receivers which are  $3\text{m}$  high, to a lesser extent.

Receiver	1	2	3	4	5	6	7	8	9
Mean Insertion Loss (dB)	12.5	16.8	14.3	11.5	16.1	15.3	10.9	17.1	15.8

Table 10-3 : Mean insertion loss of the basic earth mound at various receivers

The insertion loss spectra are shown in Figure 10.39 to Figure 10.41 for the receivers at  $20\text{m}$ ,  $50\text{m}$  and  $100\text{m}$  away from the barrier centreline respectively. The interference patterns for the receivers above the ground correspond to the odd multiples of half-wavelength of the path length difference between the direct and the ground reflected paths on the source side. The ground is modelled as acoustically hard and therefore there is no phase change on reflection. It can be seen that the insertion loss values for receivers on the ground do not have an interference pattern.



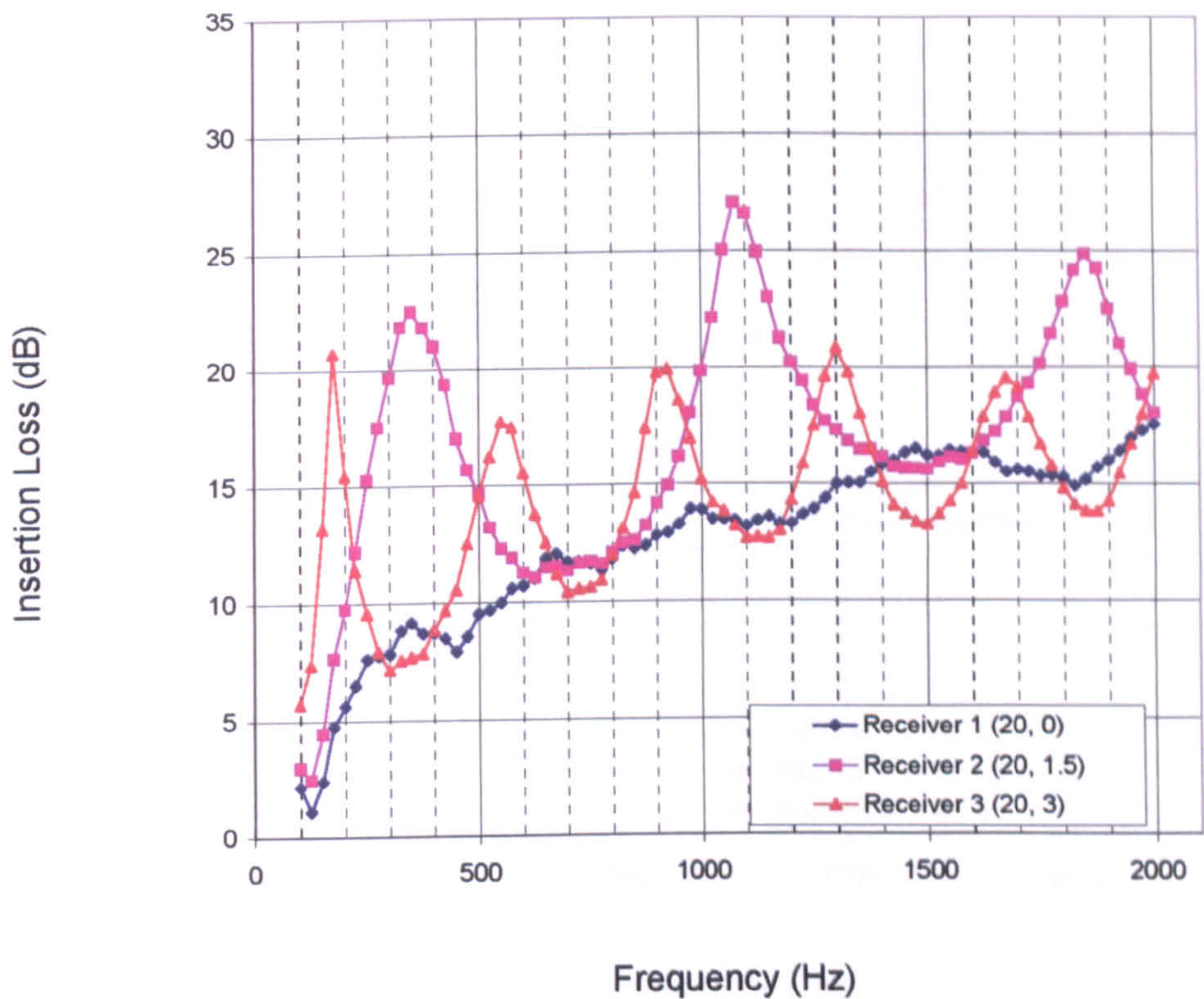


Figure 10.39 : Insertion loss spectra for receivers 20m from the centreline

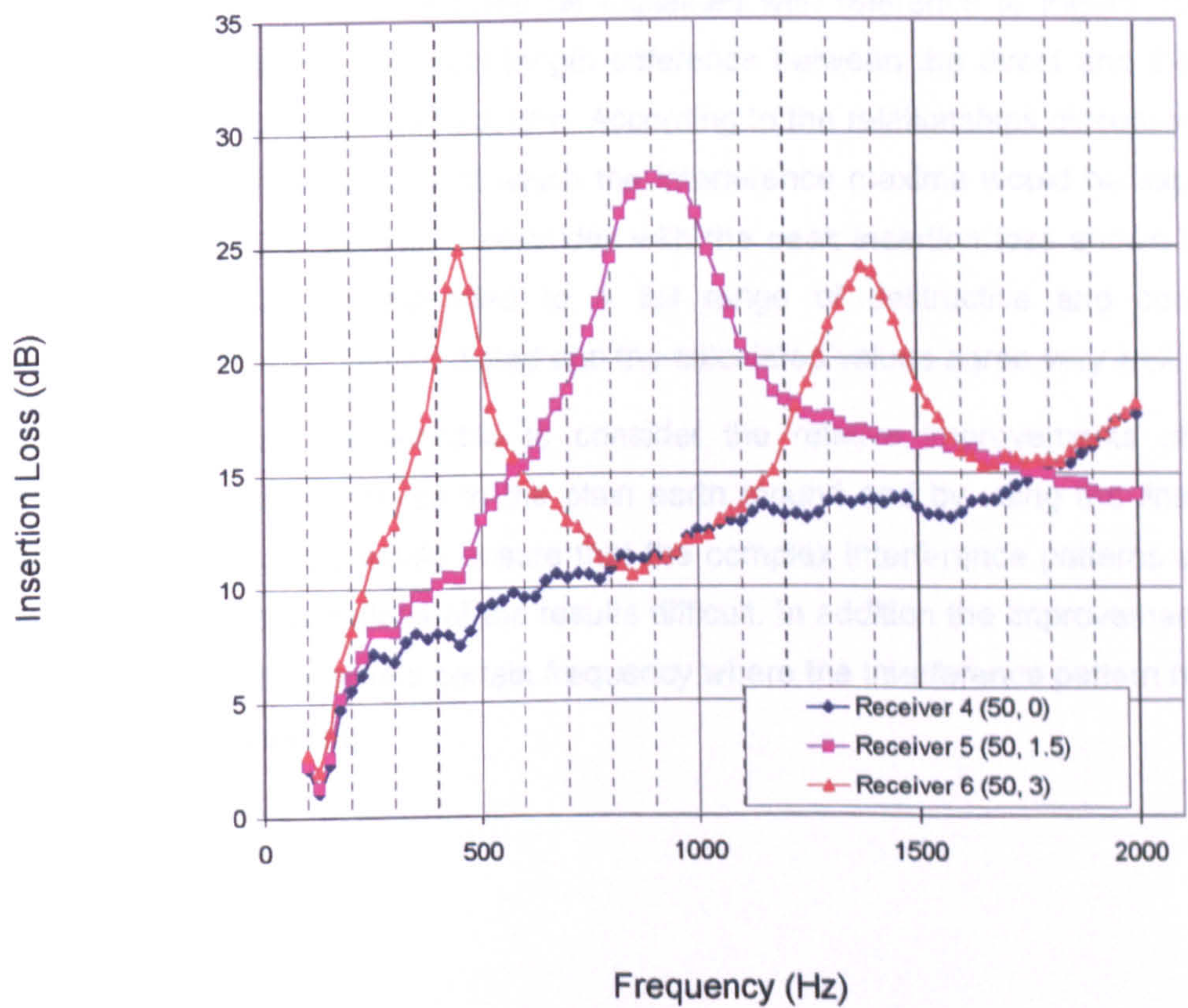
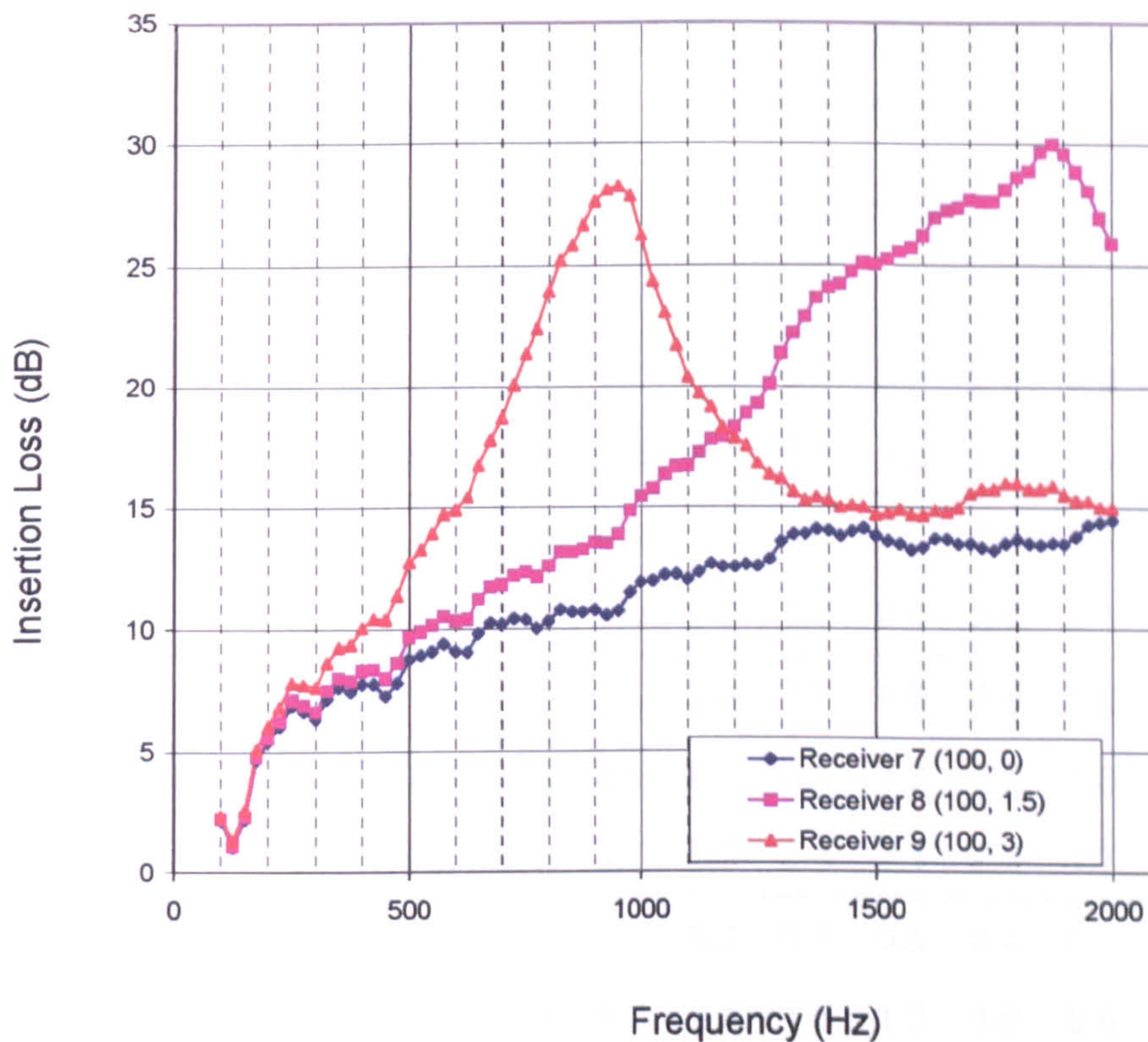


Figure 10.40 : Insertion loss values for receivers 50m from the centreline





**Figure 10.41 : Insertion loss values for receivers 100m from the centreline**

The destructive interference could be explained with reference to Figure 10.41. For instance at receiver 9, the path length difference between the direct and the ground reflected paths corresponds to 0.18m. According to the relationships discussed earlier, the corresponding frequency at which the interference maxima would be expected to occur is around 940 Hz and it coincides with the peak insertion loss shown in Figure 10.41. These can be extended to a full range of destructive and constructive interference patterns. The predicted and the calculated values agree very well.

Therefore it would be sensible to consider the relative improvements of various configurations with reference to the plain earth mound and by using the linear rating described earlier. This would ensure that the complex interference patterns above do not make the interpretations of the results difficult. In addition the improvements would not be prejudiced towards a certain frequency where the interference pattern happened to be particularly strong.

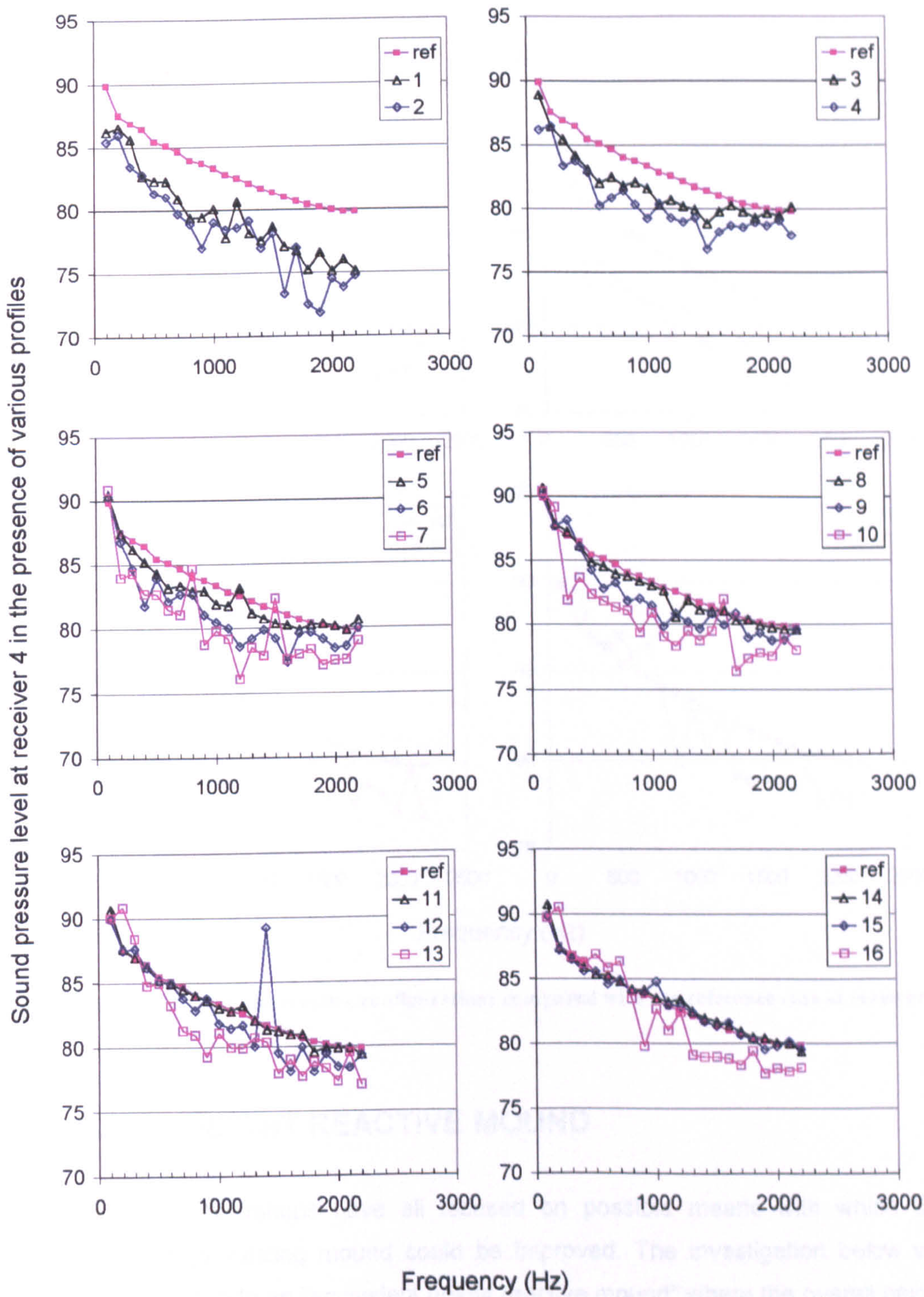


The results of the rating system described earlier are summarised in Table 10-4 which shows the relative improvement over the insertion loss of the basic shape in dB.

	Designated model number	Receiver Location									Mean AIL
		1	2	3	4	5	6	7	8	9	
		3.8	4.8	8.2	3.6	5.4	5.6	2.8	3.2	4.2	
		6.1	6.5	10.6	4.8	6.0	6.5	3.6	4.0	4.8	
		2.6	2.6	4.4	1.5	4.4	2.7	1.8	1.9	2.4	
		4.2	4.3	6.0	2.8	5.3	3.5	2.6	2.4	2.8	
		0.9	1.4	2.5	0.6	1.7	1.5	0.9	1.2	1.1	
		3.5	3.0	3.4	2.0	3.1	2.0	1.8	1.6	1.6	
		6.2	5.0	3.7	2.7	3.4	2.1	2.2	1.7	1.7	
		0.5	0.7	1.0	0.3	0.7	0.6	0.4	0.5	0.5	
	9	1.7	1.7	1.7	1.1	1.5	1.3	1.0	0.9	0.9	1.3
	10	6.0	3.3	2.6	2.5	2.4	1.5	1.7	1.2	1.2	2.5
	11	0.2	0.4	0.5	0.1	0.4	0.4	0.2	0.3	0.3	0.3
	12	1.0	0.8	0.9	0.6	0.8	0.9	0.5	0.3	0.5	0.7
	13	4.7	2.7	2.2	1.7	1.4	0.9	1.2	0.9	0.8	1.8
	14	-0.3	0.0	0.0	-0.2	0.0	0.0	0.0	0.0	0.0	0.0
	15	0.0	0.3	0.2	0.0	0.2	0.3	0.1	0.1	0.1	0.1
	16	2.0	2.0	1.2	1.0	1.0	0.6	0.7	0.5	0.5	1.1

Table 10-4 : Change in the mean insertion loss AIL of an earth mound for various configurations.





**Figure 10.42 : Spectra at receiver 4 comparing profiles with the same edge heights to the reference case.**



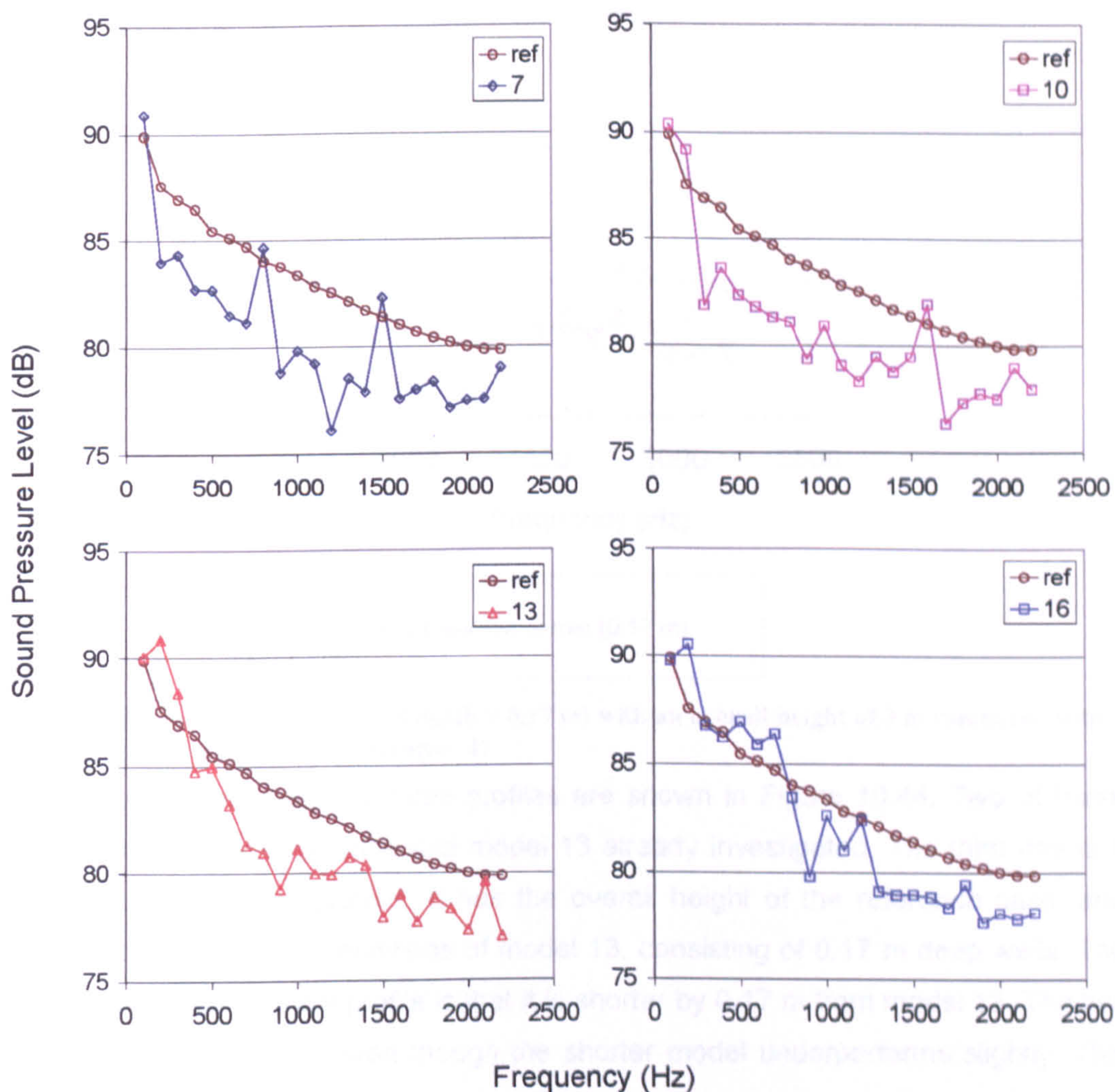


Figure 10.43 : Spectra of the reactive configurations compared with the reference case at receiver 4.

## 10.6 EQUAL HEIGHT REACTIVE MOUND

The previous configurations have all focused on possible means with which the performance of an existing mound could be improved. The investigation below will extend this approach to an "equivalent height reactive mound" where the overall height of the barrier including the reactive well height will be 3 m. The basic shape will effectively retain its slope angle and the length of the horizontal top and will be cropped from the base by an amount equal to the height of the wells added onto the top. Two configurations that will be examined are the 0.17 m and 0.25 m deep reactive wells. The spectra will be presented for receiver 4 as before.



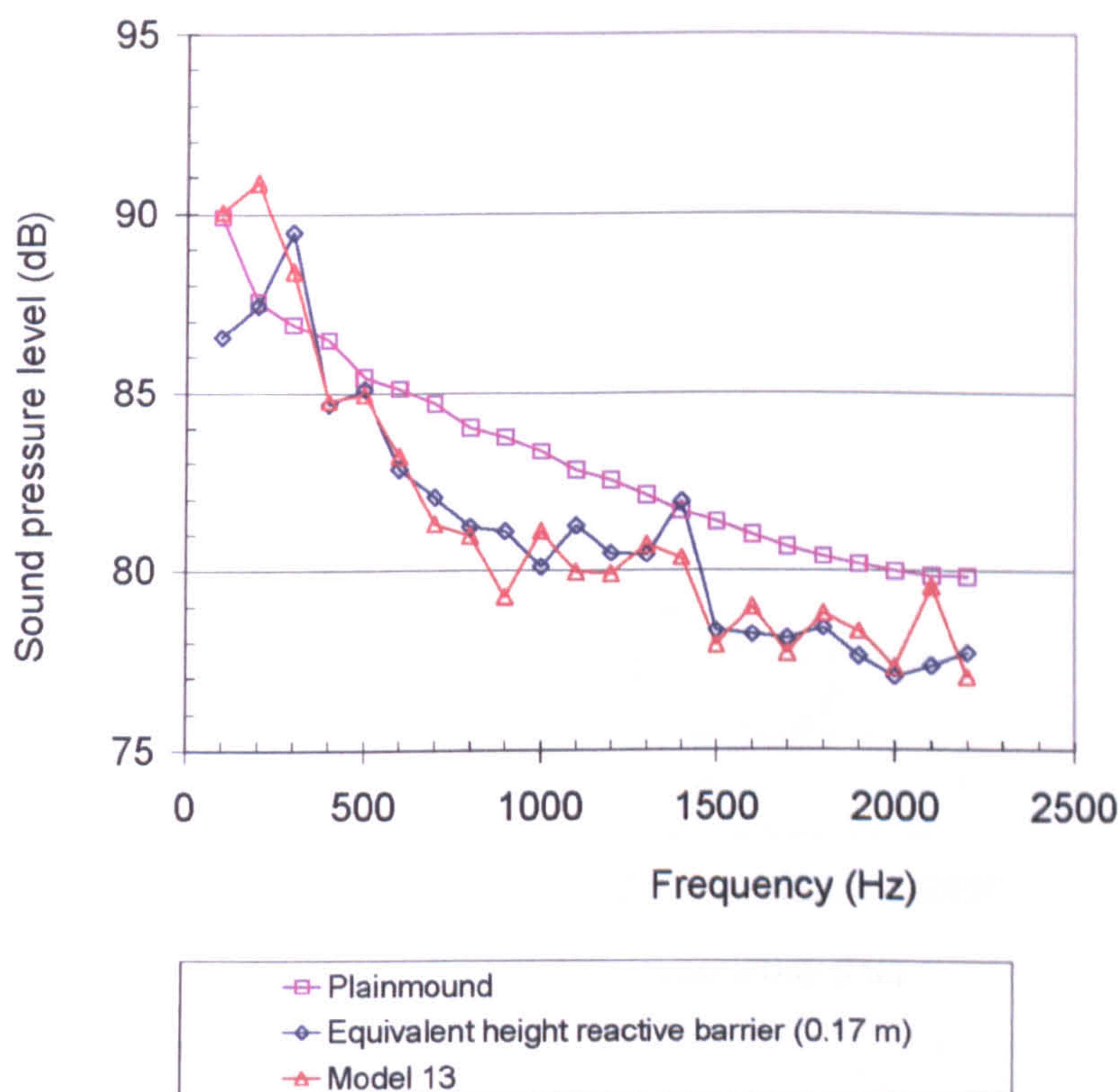


Figure 10.44 : Reactive mound (well depth = 0.17 m) with an overall height of 3 m compared with the reference case and model 13 (receiver 4).

The relative performances of three profiles are shown in Figure 10.44. Two of these profiles are the reference case and model 13 already investigated. The third one is a combination of the two profiles. It has the overall height of the reference case, and possesses the same top conditions of model 13, consisting of 0.17 m deep wells. The main difference of the new profile is that it is shorter by 0.17 m from model 13. The two profiles perform similarly, even though the shorter model underperforms slightly. This could be due to the smaller path length difference.



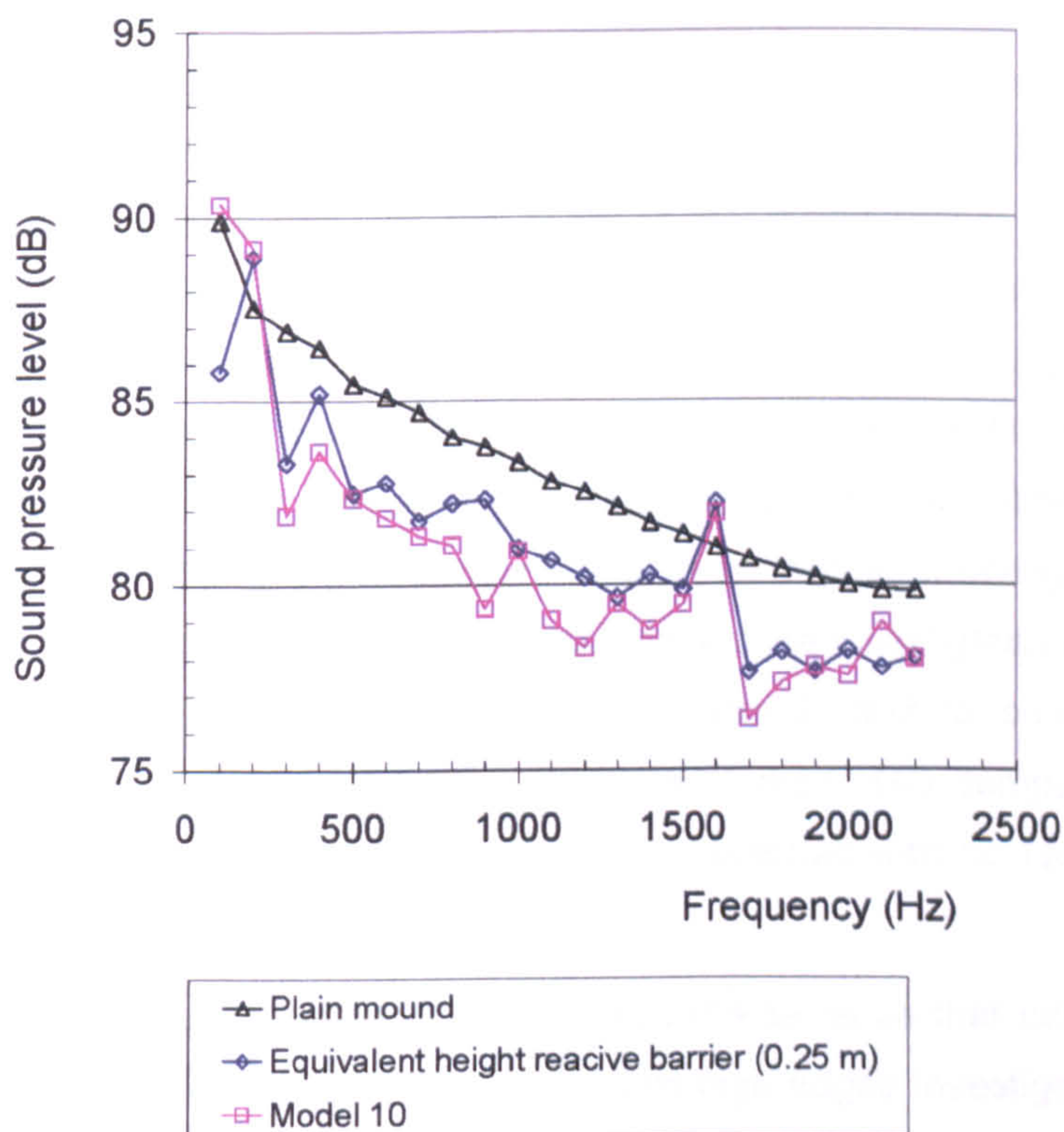


Figure 10.45 : Reactive mound (well depth = 0.25 m) with an overall height of 3 m compared with the reference case and model 10 (receiver 4).

The performance of the equal height reactive barrier in the case of 0.25 m high wells is visibly less than model 10. This difference is due to larger path length difference.

When trying to adopt these reactive designs to an "equivalent height" case, the above findings should be kept in mind. As the difference between the single and double configurations increase, as it is the case with increased edge height, the well depth of a newly designed reactive barrier will need to be larger to match the performance of the configurations investigated above which are for existing mounds. This is due the increased effect of the double edges.

In the 0.17 m case the single or double configurations made no difference and therefore an equivalent height barrier performed very similar to the reactive configuration which was added on top of an existing barrier. In 0.25 m high edges, single and double configurations do make a difference and hence the resulting equivalent height reactive configuration will perform less than the reactive case reported above. Therefore if the same performance is intended the new design either needs to be made higher or the well depth should be increased.



# 10.7 DISCUSSION

This chapter consisted of three main parts. In the first part, the details of the numerical modelling carried out by SYSNOISE are described. The indirect boundary element methods was used as the basis of the mathematical model. A geometry from the literature is used to verify the way the numerical model has been implemented. The second part is on the numerical modelling of selected geometries which were investigated in previous chapters by physical scale modelling. The findings of these will be used in the forthcoming chapters to aid the validation of the physical modelling results. The third part concentrated on earth mound configurations with single, double and multiple top edge conditions. These were investigated with a view to extending the acoustic design guidance on earth mounds and to supplement the advice in the previously proposed barrier selection method. The computer modelling also allowed more realistic receiver locations to be selected with no restrictions on their horizontal extent.

The reference geometry chosen was the same as that used in physical modelling. In addition to the 0.08, 0.17 and 0.25 m high edges investigated earlier, 0.5, 1 and 2 m high barriers were also examined. These were thought to be the more likely candidates which could have currently been implemented in practice as conventional barriers on top of earth mounds. All heights listed above have been tested as both single and double edge configurations. The edge heights smaller than and including the 0.5 m high edge have been tested as reactive configurations, in the form of multiple edges organised as a series of wells. The total number of modifications were 16 as detailed in Figure 10.38. Single value performance indicators were determined according to the sound pressure levels observed with and without the modification, with the reference geometry present in both cases. This rating system enabled the performance of each modification to be compared relative to that of the plain earth mound.

Edge height (m)	Single	Double	Multiple
2	4.6	5.9	N/A
1	2.7	3.8	N/A
0.5	1.3	2.4	3.2
0.25	0.6	1.3	2.5
0.17	0.3	0.7	1.8
0.08	0	0.1	1.1

Table 10-5 : Mean additional insertion loss values in dB for various configurations (all receivers)



The mean insertion loss values at the receivers considered for various configurations is summarised in Table 10-5. As it would be expected, double edge configurations performed better than the single edge cases possibly due to change in the path length or due to multiple diffraction effects. As the edge height decreased, the difference between the single and double cases diminished. The differences are 1.3 dB for the 2 m high barriers and 0.1 dB for the 0.08 m high edges. The reactive configurations in turn performed better than their equal height double-edge counterparts. Between the double and reactive configurations the path length remains the same and therefore any recorded gains could be attributed to multiple diffraction effects or the soft pressure release surface as discussed in previous chapters. The reactive configurations provided approximately 1 dB additional gains over the double - edge cases and 1 to 2 dB additional gains over the single edge cases. It has been shown that as the angular displacement of the receiver into the shadow is increased, the differences in attenuation values between a hard and soft - or indeed between hard and absorbent - boundary conditions are also increased<sup>12</sup>. The receiver positions closer to the barrier gave more substantial gains and these values decreased as the receivers were further away from the barrier. The receiver position with the maximum angular displacement into the shadow zone - receiver 1 - provided 2 to 4 dB additional attenuations over the double-edge cases. Compared with the performance of a plain mound, the additional attenuations were 2 to 6 dB. This is shown in Table 10-6.

Edge height (m)	Single	Double	Multiple
2	3.8	6.1	N/A
1	2.6	4.2	N/A
0.5	0.9	3.5	6.2
0.25	0.5	1.7	6.0
0.17	0.2	1.0	4.7
0.08	-0.2	0	2.0

Table 10-6 : Additional attenuations in dB for various configurations at Receiver 1

When we look at the spectra of gains in Figure 10.42, it is possible to find evidence concerning the lowest frequency for which the surface would be considered reactive. These frequencies seem to lie around 200, 300, 400 and 900 Hz respectively for the reactive configurations with 0.5, 0.25, 0.17 and the 0.08 m deep wells. They are characterised by the relative performance crossing to the positive side from negative gains and from then onwards providing positive contributions. The predicted frequencies are 170 Hz, 340 Hz, 500 Hz and 1000 Hz respectively. These spectra are for a single receiver location. If receivers which are closer to the barrier and situated more in the shadow are to be examined these gains will possibly be much larger at



those frequencies. However, as it stands, the expected gains at the predicted frequencies are very modest. When the rest of the spectrum is considered for a given reactive profile at the predicted frequencies and higher, the superior performance of these profiles are visible. It should be noted that the overall width of the reactive surface is 1 m and this limits the lower limit of the frequencies which can be realised by the reactive surface even though it is designed for a specific resonant frequency. Discussions in previous chapter have suggested that these frequencies should be smaller than the half-wavelength of the total width of the surface and this could mean the smallest noticeable resonant frequency is 680 Hz. In the cases where having an earth mound with a horizontal top which is wide enough, extending the multiple edges to the slopes could be considered. This is beyond the scope of this work.

Figure 10.43 shows the reactive configurations alone compared with the plain mound at a receiver resting on the ground. Therefore the interference effects due to ground reflected paths are eliminated. The cut-off frequencies where the relative performance of a reactive configuration improves coincide with the lowest frequency for which they can be considered reactive. As the well depth becomes shallower, the range of the spectrum for which the performance of the reactive profile diminishes, increases.

Two cases of "equal height reactive barriers" have also been investigated. Figure 10.44 and Figure 10.45 show the equal height (i.e. the overall height is 3 m) reactive mounds with well depths of 0.17 m and 0.25 m respectively. They are shown to perform better than a plain mound but slightly less than their counterparts which are higher by the same amount of the well depth under consideration. This work was intended to demonstrate that if these reactive configurations are considered at an early design stage, the earth mound can be made shorter. However, the reduction in height will somewhat be less than the reactive well depth if the performance of the above reported cases are to be matched. Otherwise, the equal height reactive cases are shown to be superior.

## 10.8 CONCLUSIONS

This chapter provided the details of the numerical modelling carried out by indirect boundary element methods using the software package called SYSNOISE. A geometry from the literature was used to verify the way the numerical model was implemented.

A number of earth mound configurations with single, double and multiple top edge conditions were investigated. These will be used in the forthcoming chapters to extend the acoustic design guidance on earth mounds and to supplement the advice provided in the previously proposed barrier selection method in chapter 4.



Some of the geometries investigated in previous chapters as part of physical scale modelling were modelled using the numerical modelling described. The next chapter is a comparison of the findings of the numerical modelling with the physical modelling results. This comparison aims to validate the results of the uniform field experiments and the tests undertaken in semi-anechoic chambers.



## 10.9 REFERENCES

- 
- <sup>1</sup> BANERJEE, P.K., The Boundary Element Methods in Engineering, 2nd edition, McGraw Hill Book Company, ISBN 0-07-707769-5, 1994
- <sup>2</sup> SEZNEC, R., Diffraction of Sound Around Barriers: Use of Boundary Elements Technique, Journal of Sound and Vibration, 73 (2), 1980, 195 - 209
- <sup>3</sup> HOTHERSALL, D.C., CHANDLER-WILDE, S.N., HAJMIRZAE, M.N., Efficiency of Single Noise Barriers, Journal of Sound and Vibration, 146 (2), 1991, 303 - 322
- <sup>4</sup> FYFE, K.R., and HARRISON, C.C., Modelling of Road Noise and Optimal Barrier Design, Canada Mortgage and Housing Corporation (CMHC), CMHC CR File 6585-F039, March 1995
- <sup>5</sup> CISKOWSKI, R.D., BREBBIA, C.A. (Editors), Boundary Element Methods in Acoustics, Co-publishers: Computational Mechanics Publications, Elsevier Applied Science, ISBN 1-85312-104-5, Computational Mechanics Publications, Southampton, Chapter 11 - Applications in Environmental Noise, by ANTES, H., 1991, 225 - 290
- <sup>6</sup> SYSNOISE User's Manual, Revision 5.4, Numerical Integration Technologies, Leuven, Belgium, 1994, Section 1.2.2, Boundary element methods
- <sup>7</sup> SYSNOISE User's Manual, Revision 5.4, Numerical Integration Technologies, Leuven, Belgium, 1994, Section 5.2.4, Formulation, page 5-11
- <sup>8</sup> SYSNOISE User's Manual, Revision 5.4, Numerical Integration Technologies, Leuven, Belgium, 1994, Section 5.10, Surface Junctions
- <sup>9</sup> SYSNOISE User's Manual, Revision 5.4, Numerical Integration Technologies, Leuven, Belgium, 1994, Section 5.18, Irregular Frequencies
- <sup>10</sup> LAI, J.C.S. (1995) *Application of the boundary element method to assessment of road traffic noise barriers*. Proc. of Sysnoise 2nd Users Meeting, Leuven, Belgium June 26-28, 1995 IV.2, 1-12
- <sup>11</sup> HOTHERSALL, D., Modelling Performance of Noise Barriers, Eurosymposium 1992, The Mitigation of Traffic Noise in Urban Areas, Nantes, France, 247-258, 12-15 May 1992
- <sup>12</sup> BUTLER, G.F., A Note on Improving The Attenuation Given By A Noise Barrier, Journal of Sound and Vibration, 32 (3), 1974, 367 - 369



# **11 COMPARISON OF MODELLING RESULTS**

The previous chapter provided the details of the numerical modelling undertaken by SYSNOISE using boundary element methods. This chapter compares the findings of physical modelling carried out in Chapters 8 and 9 with the findings of numerical modelling undertaken in Chapter 10. This comparison is aimed at determining the extent of validity and general applicability of the three modelling techniques used.

## **11.1 VALIDATION OF THE RESULTS FROM THE SCALE MODELLING**

The model dimensions and frequencies reported in this chapter have been scaled in accordance with the scale factor of 1:10 to represent the real dimensions. The numerical modelling was undertaken to represent real dimensions and frequencies and therefore these are reported as they are.

It will be recalled that the uniform field experiments were carried out at 1/24 octave band frequencies between 2kHz and 22kHz and the semi-anechoic chamber experiments were undertaken at 1/3 octave band frequencies between 1.6 kHz and 12.5 kHz. Therefore the comparisons are limited to 1/3 octave band frequencies between 1.6 kHz and 12.5 kHz. The uniform field experiments were accordingly energy averaged to represent the 1/3 octave bands. The higher frequencies than 12.5 kHz, i.e. those corresponding to 16 kHz and 20 kHz are not considered in the comparisons.

Four sets of geometries investigated in previous chapters are selected for comparison and validation purposes. The first set of geometries consisting of a series of edges on the ground includes three models having 14-edge configurations with different heights. The second set of geometries involving low rectangular barriers similarly uses three models with different edge conditions. The third consists of a single geometry of reactive earth mound to represent the largest geometries. This model was considered to be the most likely candidate where a reactive surface could be realised due to the number of edges involved. The fourth set consists of the rib structure which was used to investigate the effects of attenuations and amplifications at various diffraction angles.

The source height in the numerical models is taken as 0.25m above the ground to represent the physical centre of the sources. All ground and barrier surfaces are modelled as acoustically hard.

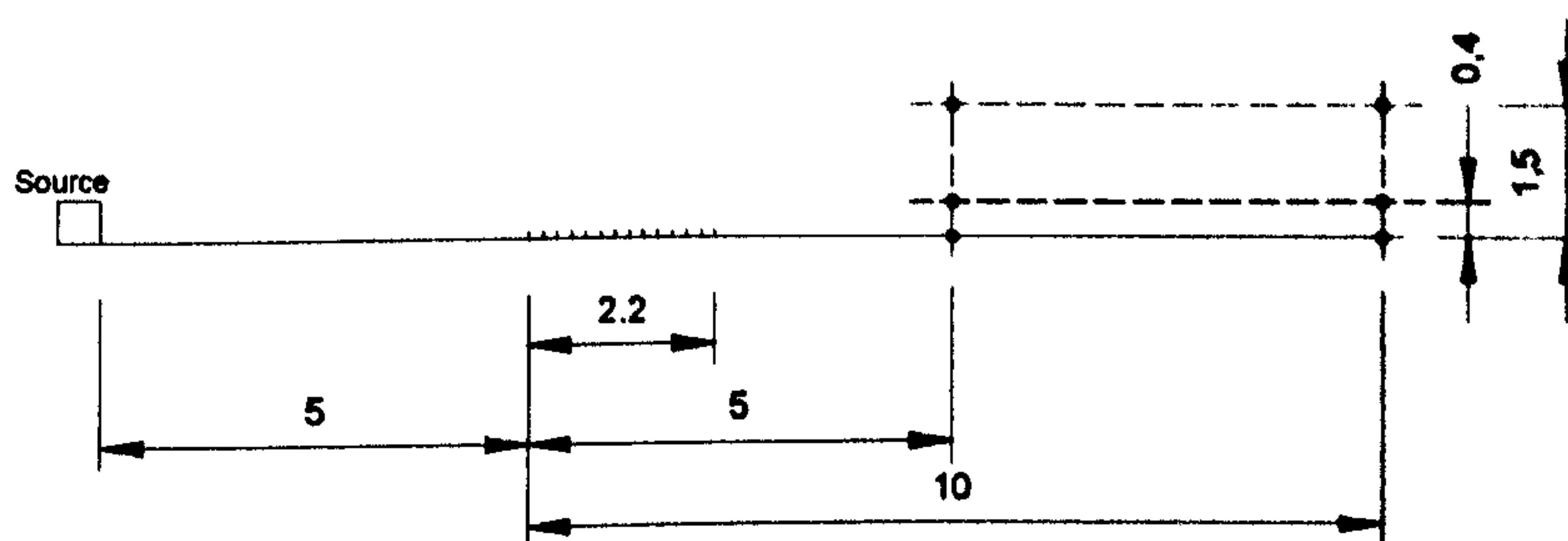


The details of models and the comparisons obtained by physical and numerical modelling are shown below.

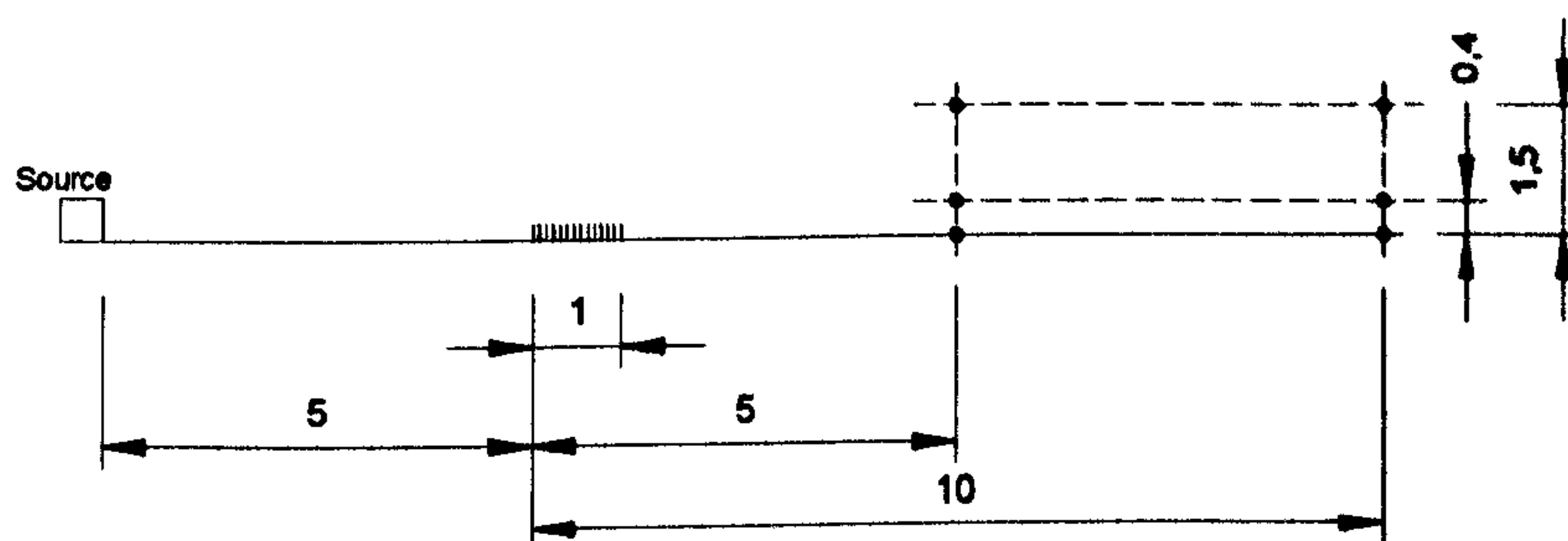
### **11.1.1 Edges on the Ground**

Three models have been used for comparing modelling results for the configurations involving edges on the ground. These represent three different well depths of 14-edge cases compared with their equivalent 1-edge cases. The single edges are all situated 5m from the source. The receivers are referred to as (x, y) to represent their horizontal and vertical distances respectively, as measured from the ground coordinates of the first edge. The details of the geometries are shown in Figure 11.1 to Figure 11.3. All dimensions are in metres. The comparisons are shown in Figure 11.4 to Figure 11.6.

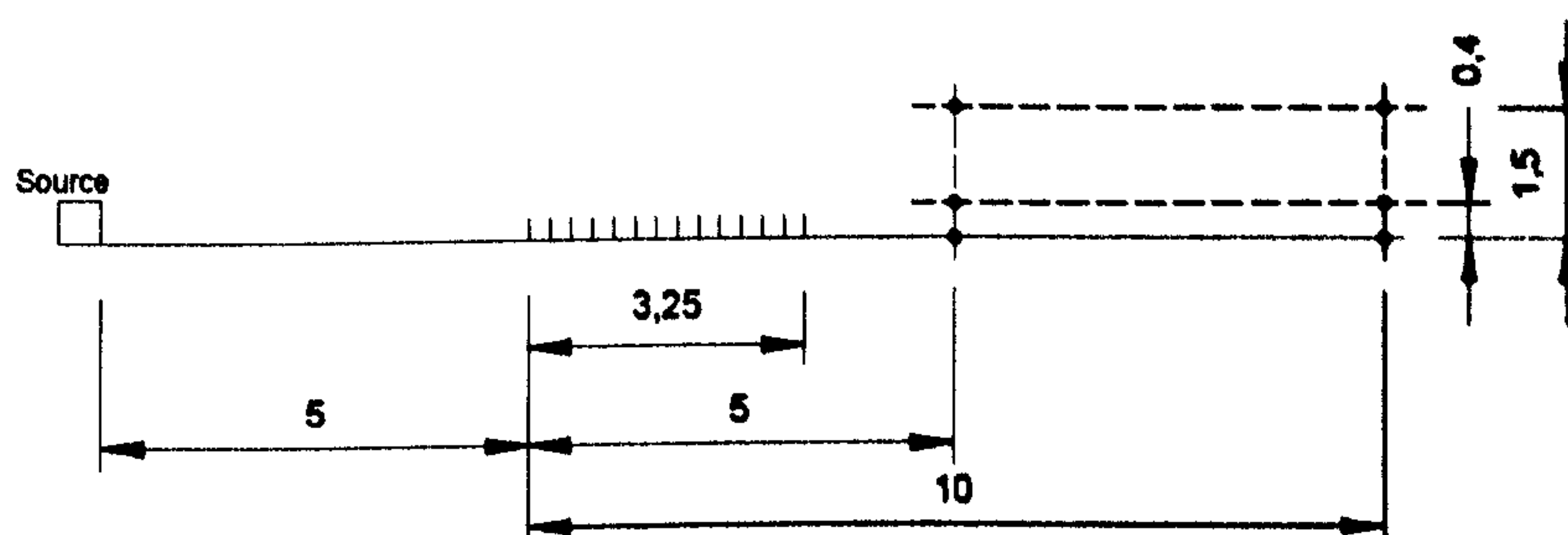




**Figure 11.1 : The height of the wells is 0.08 m. The spacing between the edges is 0.17 m.**



**Figure 11.2 : The height of the wells is 0.17 m. The spacing between the edges is 0.08 m.**



**Figure 11.3 : The height of the wells is 0.25 m. The spacing between the edges is 0.25 m.**



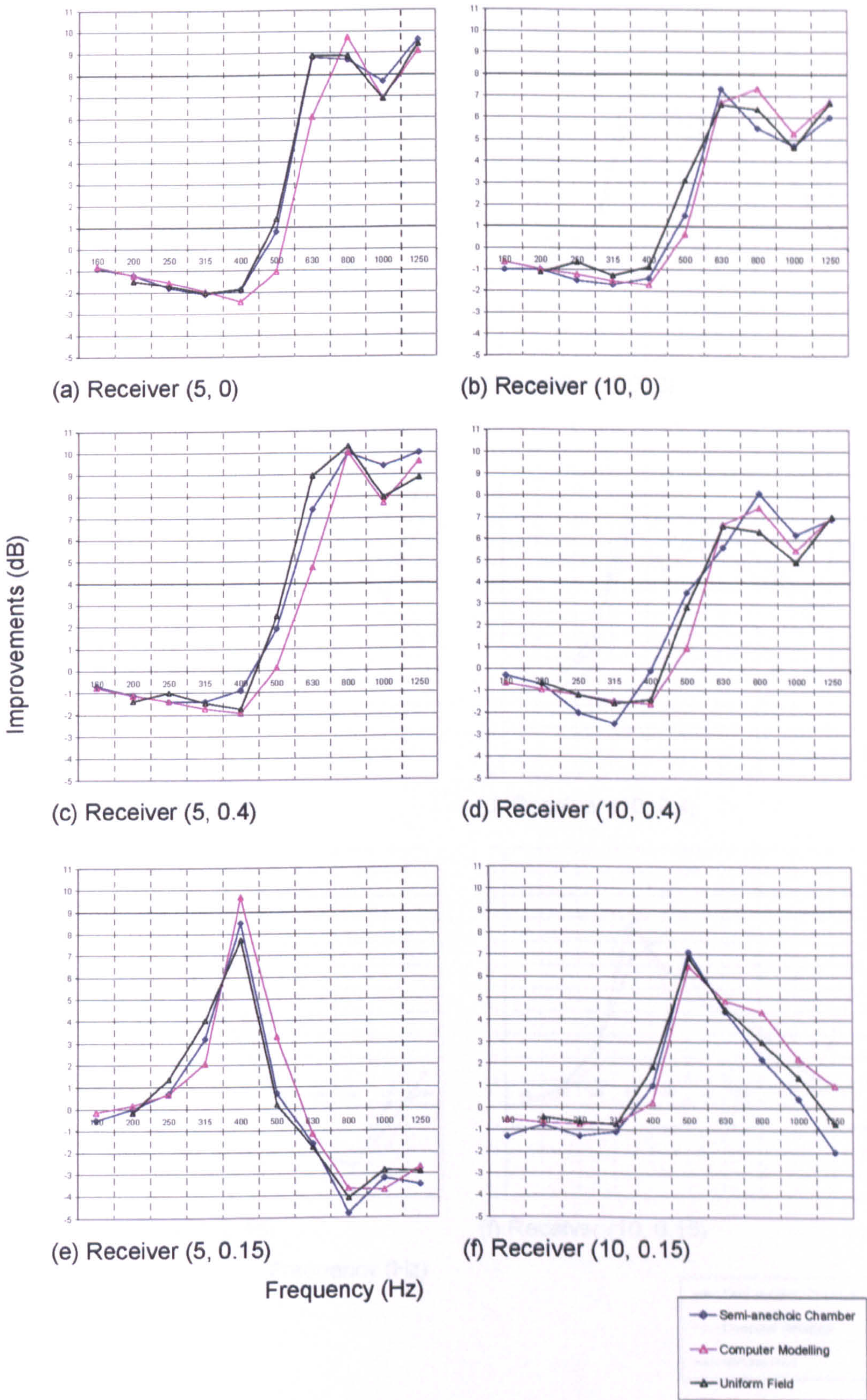


Figure 11.4 : Effects of 0.08m wells on the ground



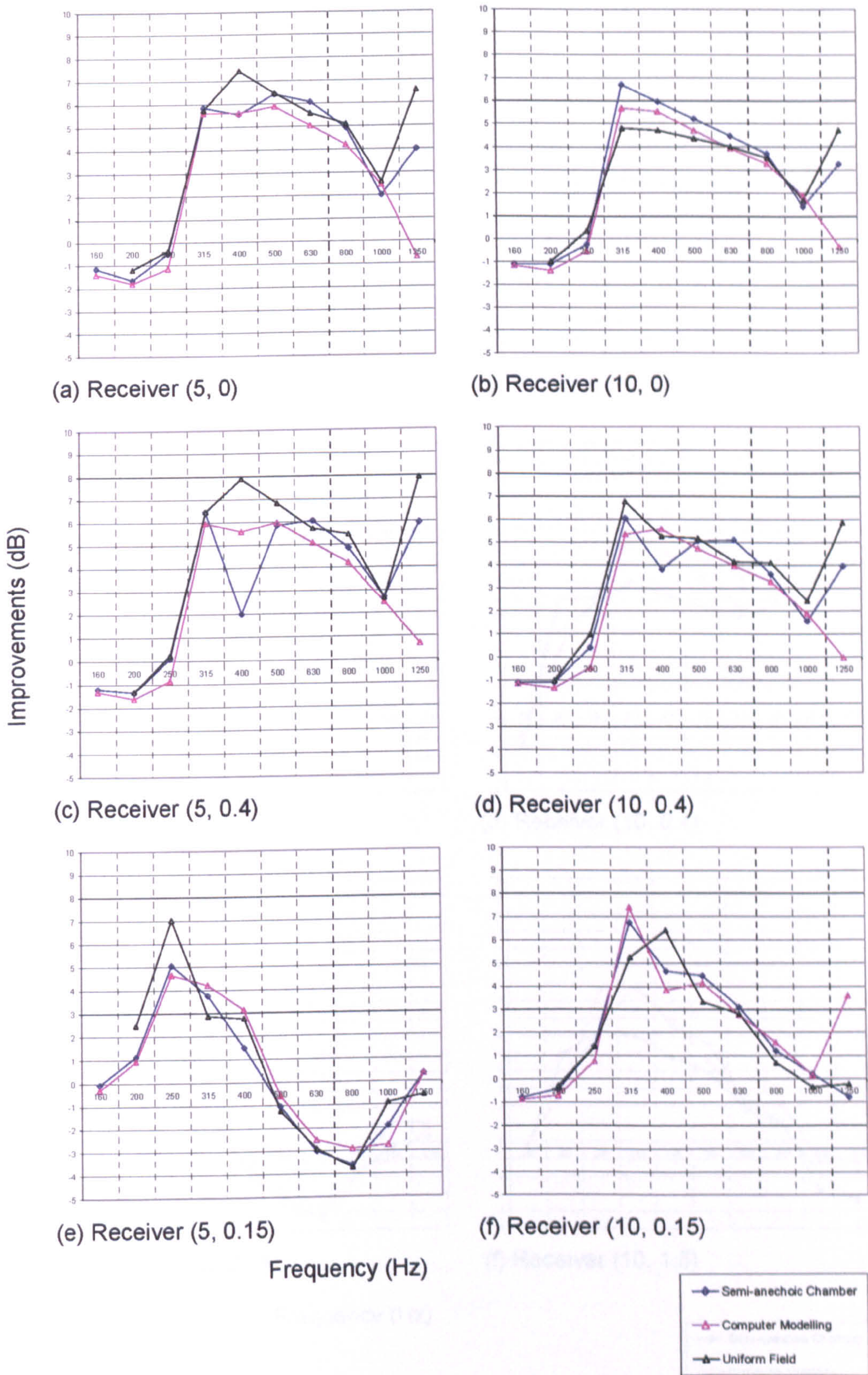
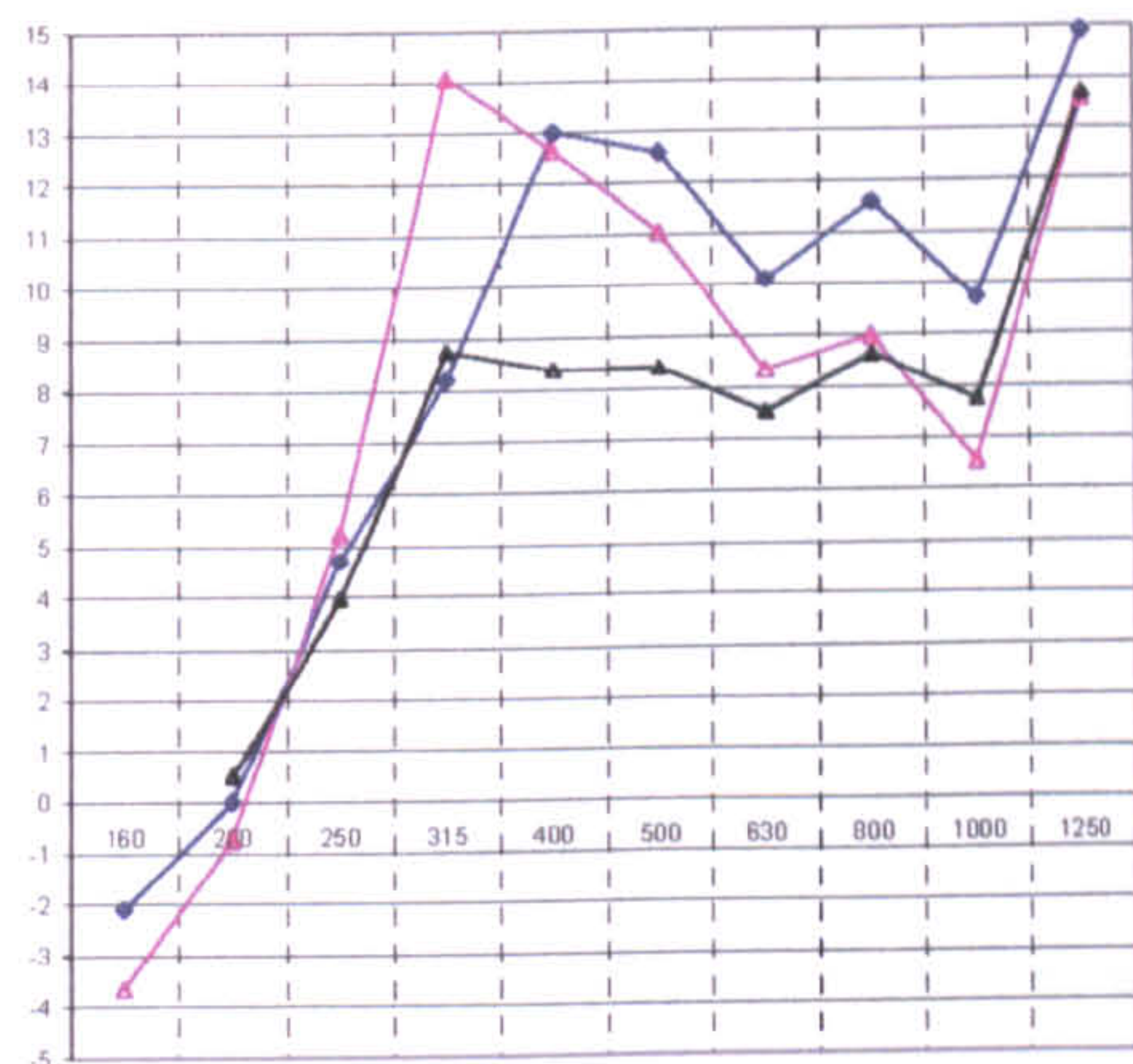
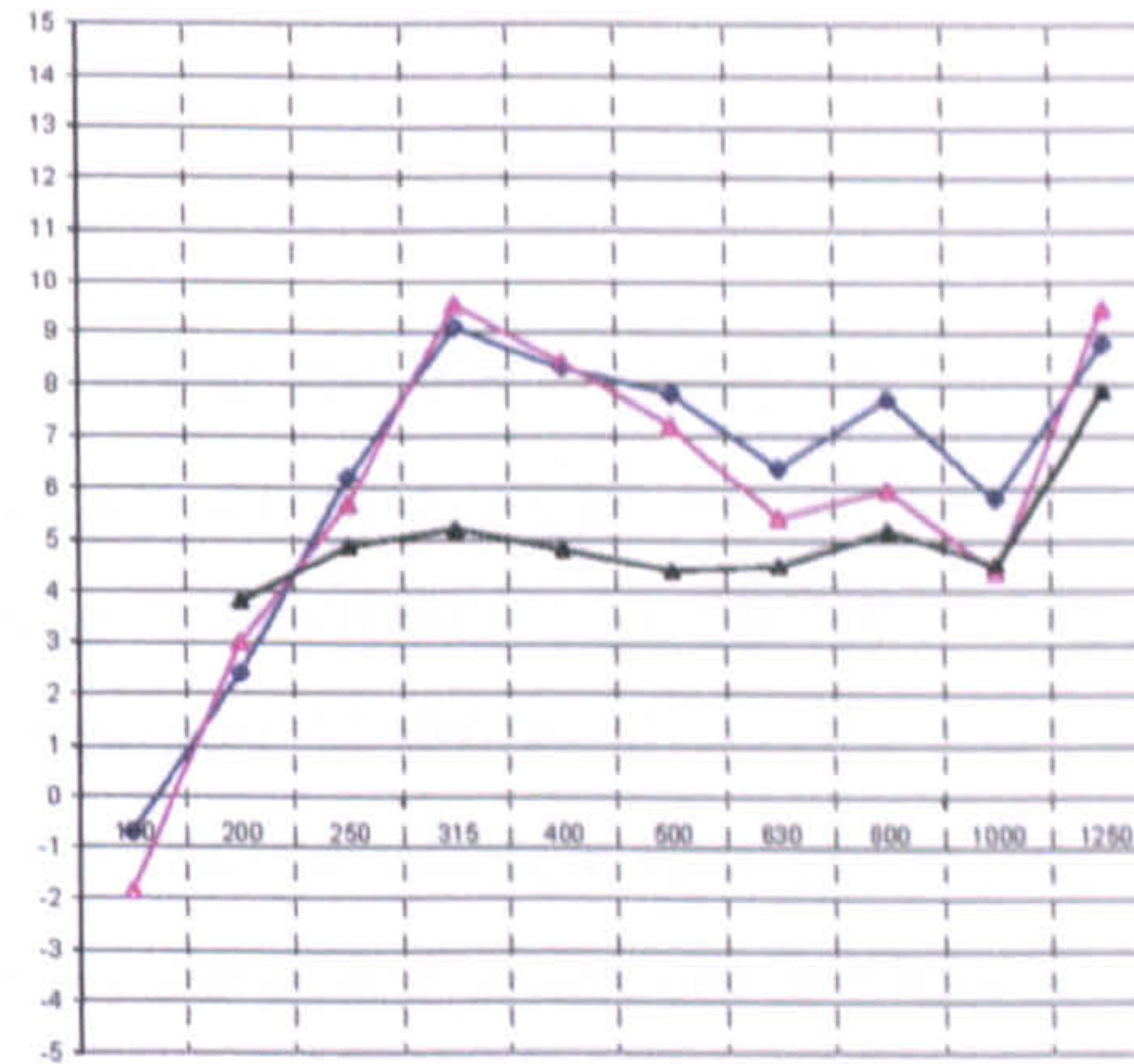


Figure 11.5 : Effects of 0.17m wells on the ground

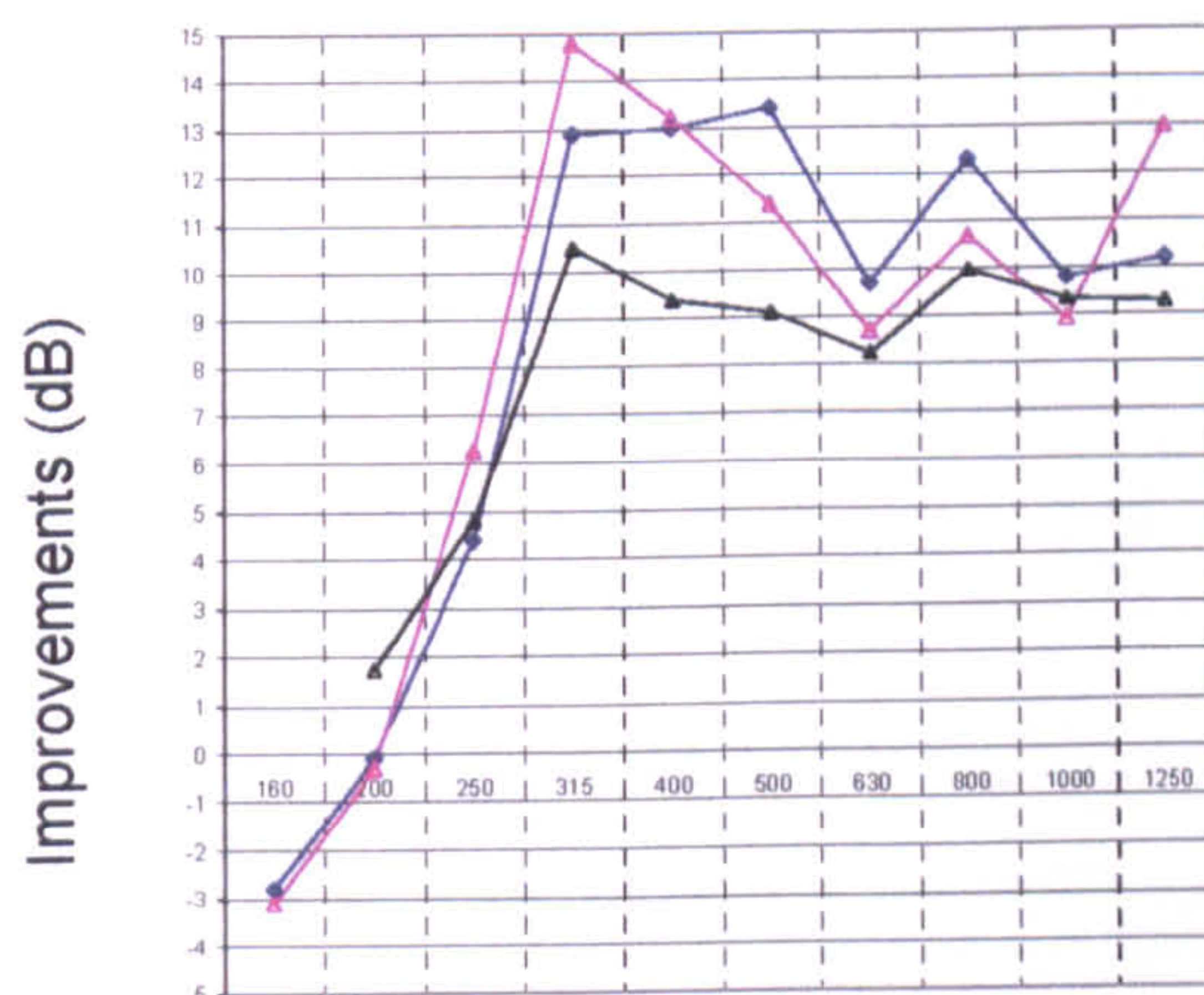




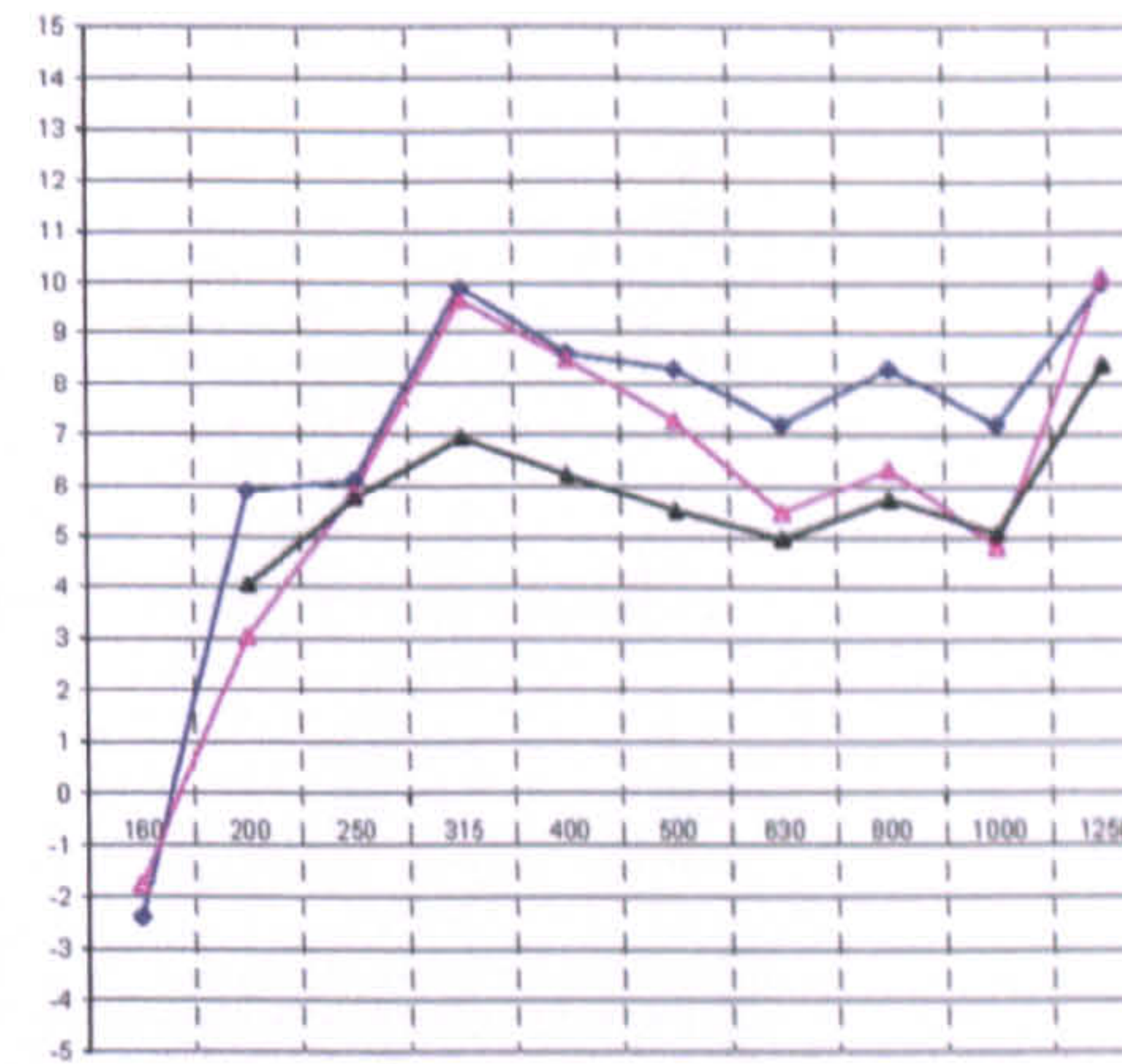
(a) Receiver (5, 0)



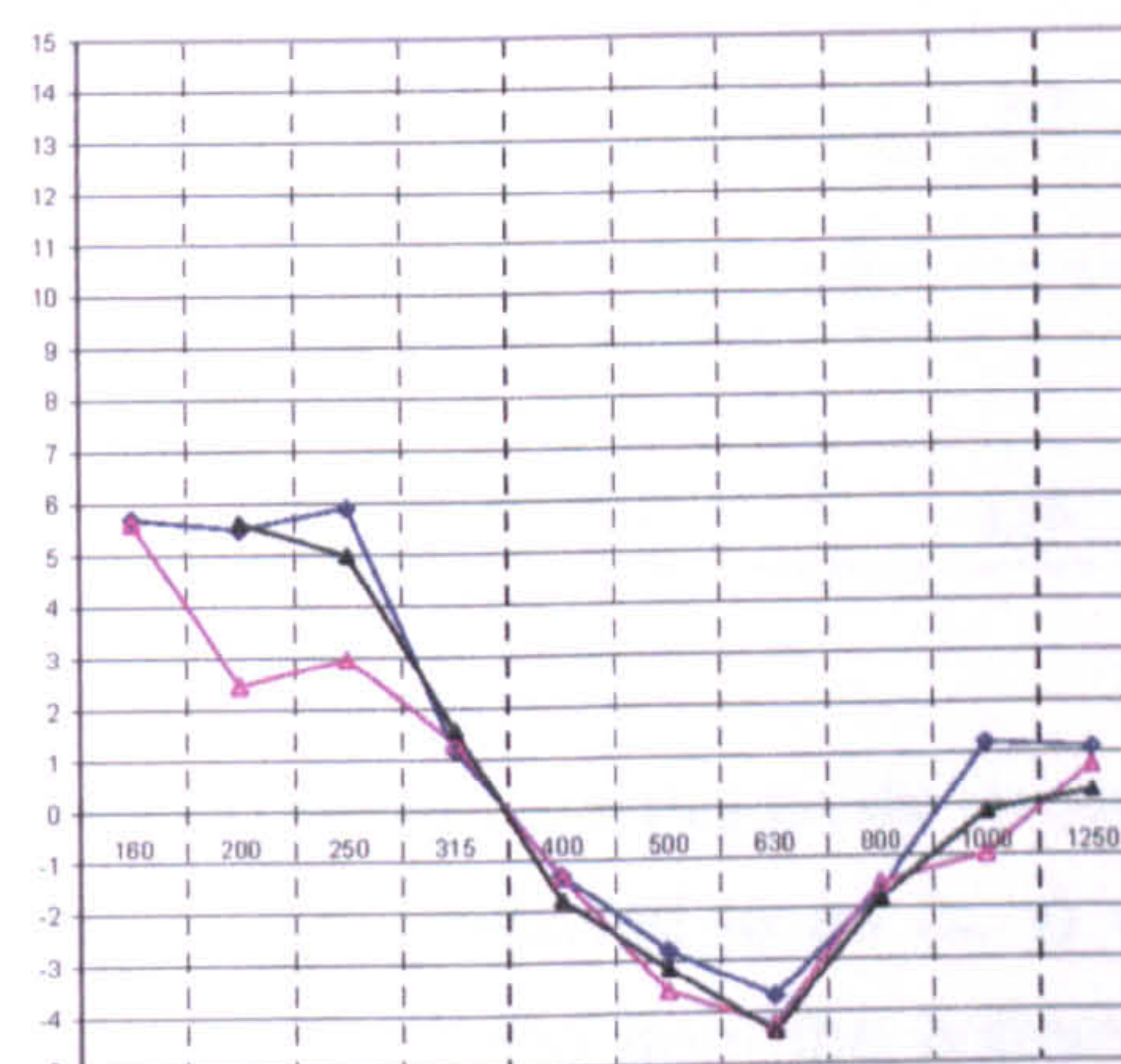
(b) Receiver (10, 0)



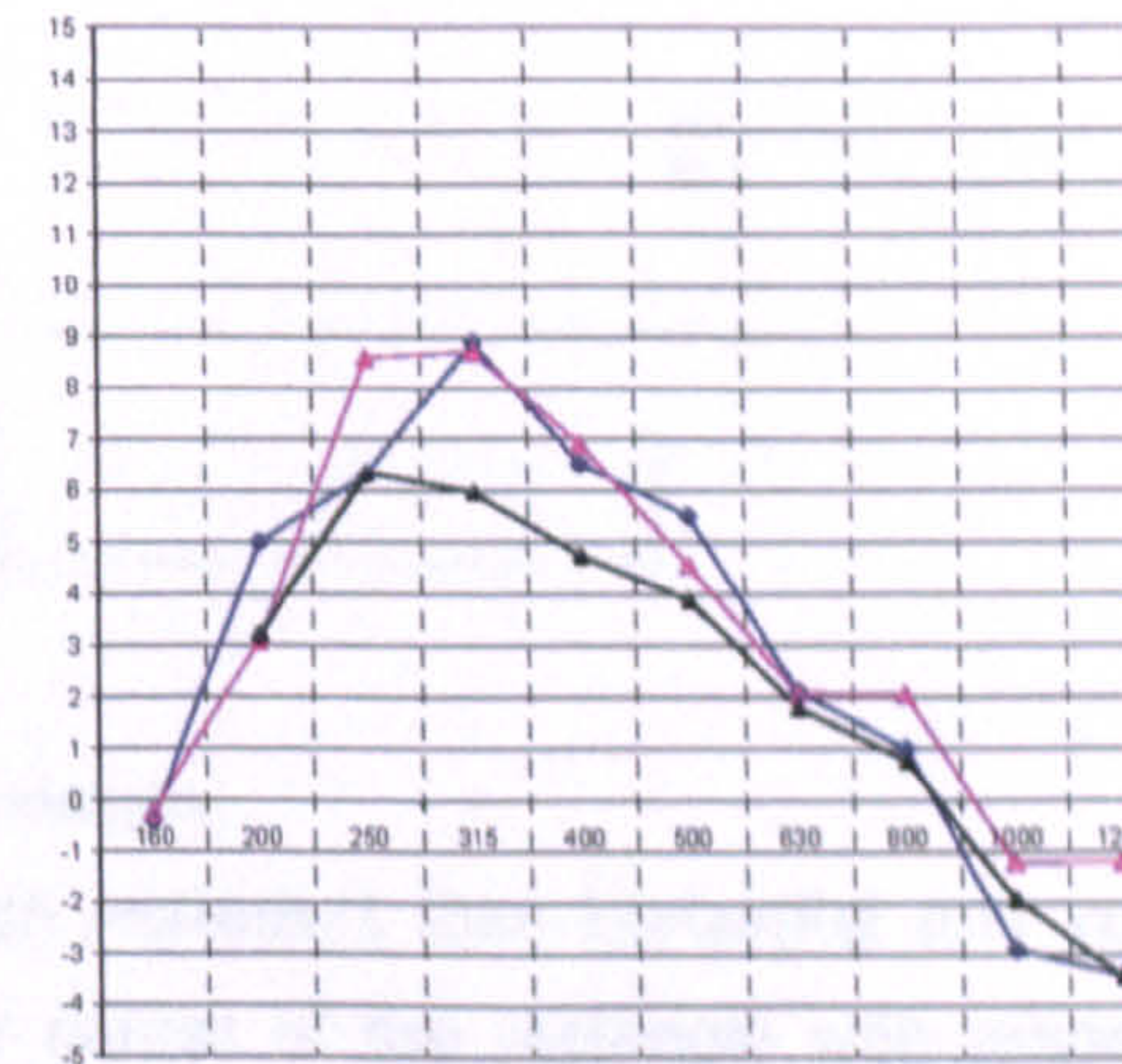
(c) Receiver (5, 0.4)



(d) Receiver (10, 0.4)



(e) Receiver (5, 0.15)



(f) Receiver (10, 1.5)

Frequency (Hz)

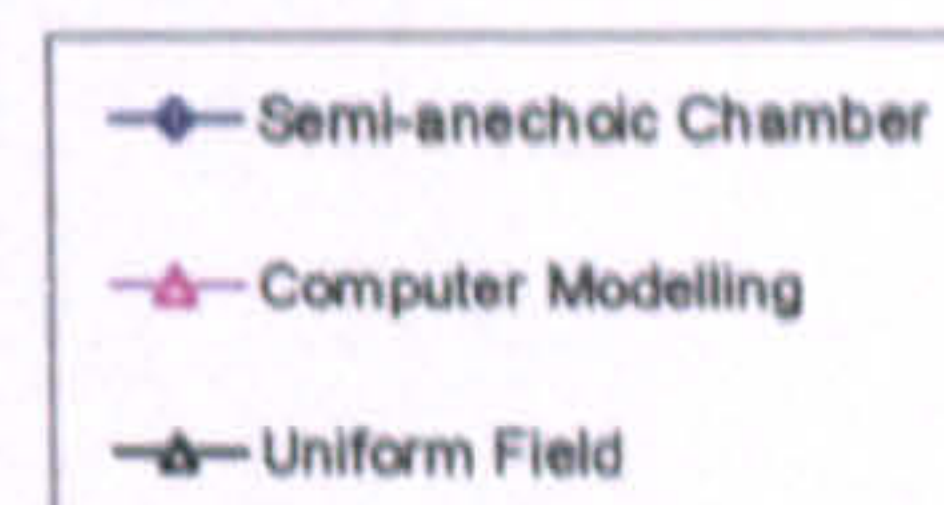


Figure 11.6 : Effects of 0.25m wells on the ground



### 11.1.2 Edges on Rectangle

The three models chosen for comparisons involving the low rectangular barrier are shown below. The performances of the various multiple edge configurations are compared to that of the plain rectangle. The edge configurations consist of 11 edges of 0.25 m high wells, 15 edges of 0.17 m high wells and 14 edges of 0.08 m high wells. These are shown in Figure 11.7 in this order. The nearest vertical side of the rectangle is situated 5m from the source. The first edge on top of the rectangle is situated 0.5m from the vertical side (i.e. 5.5m from source).

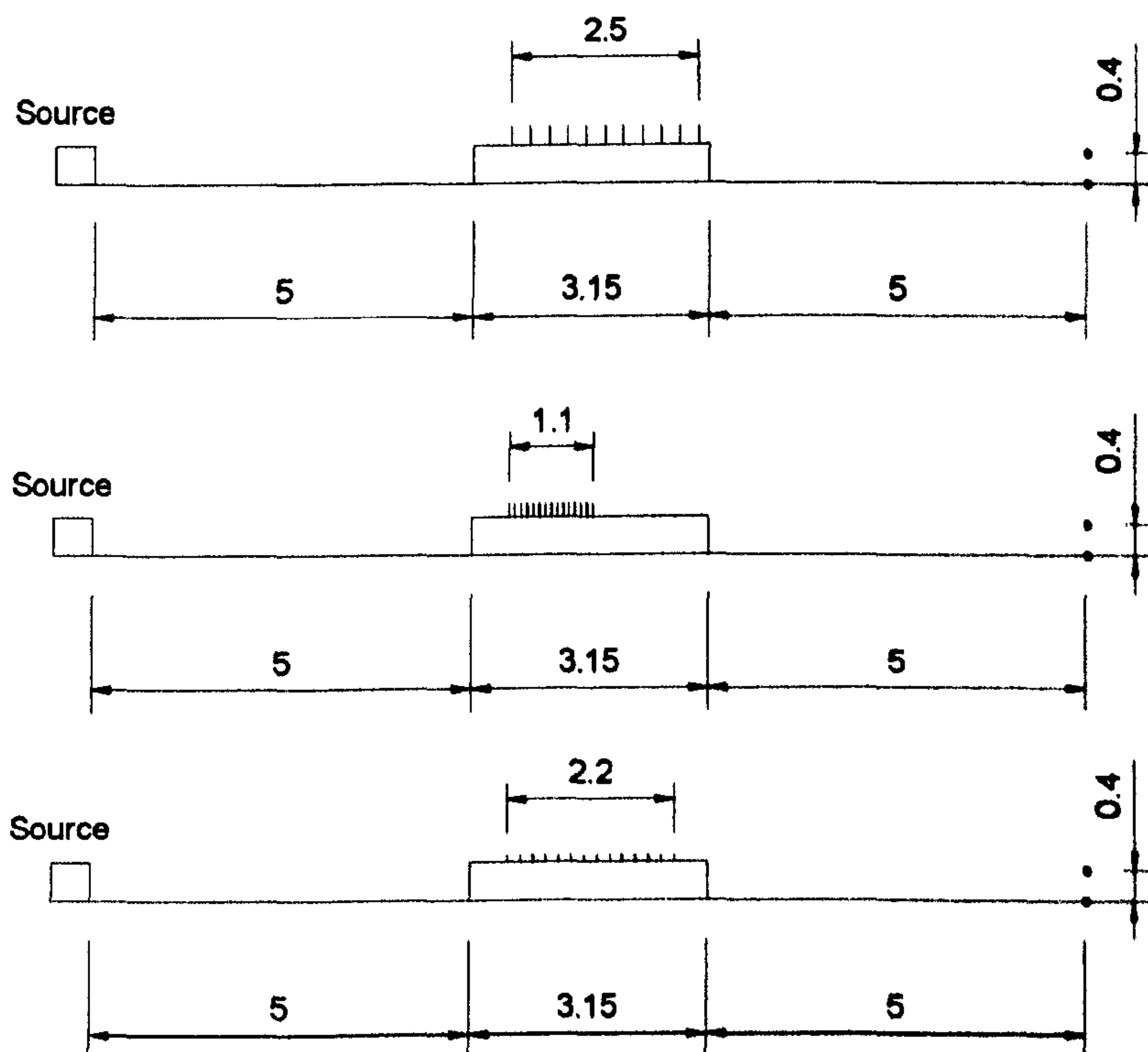


Figure 11.7 : Experimental set-up for the reactive rectangles

The receivers are referred to as (x, y) which represent their horizontal and vertical distances as measured from the bottom far corner of the rectangle with respect to source. All dimensions are in metres. The height of the rectangles is 0.5m in all cases. The results of comparisons are shown in Figure 11.8.



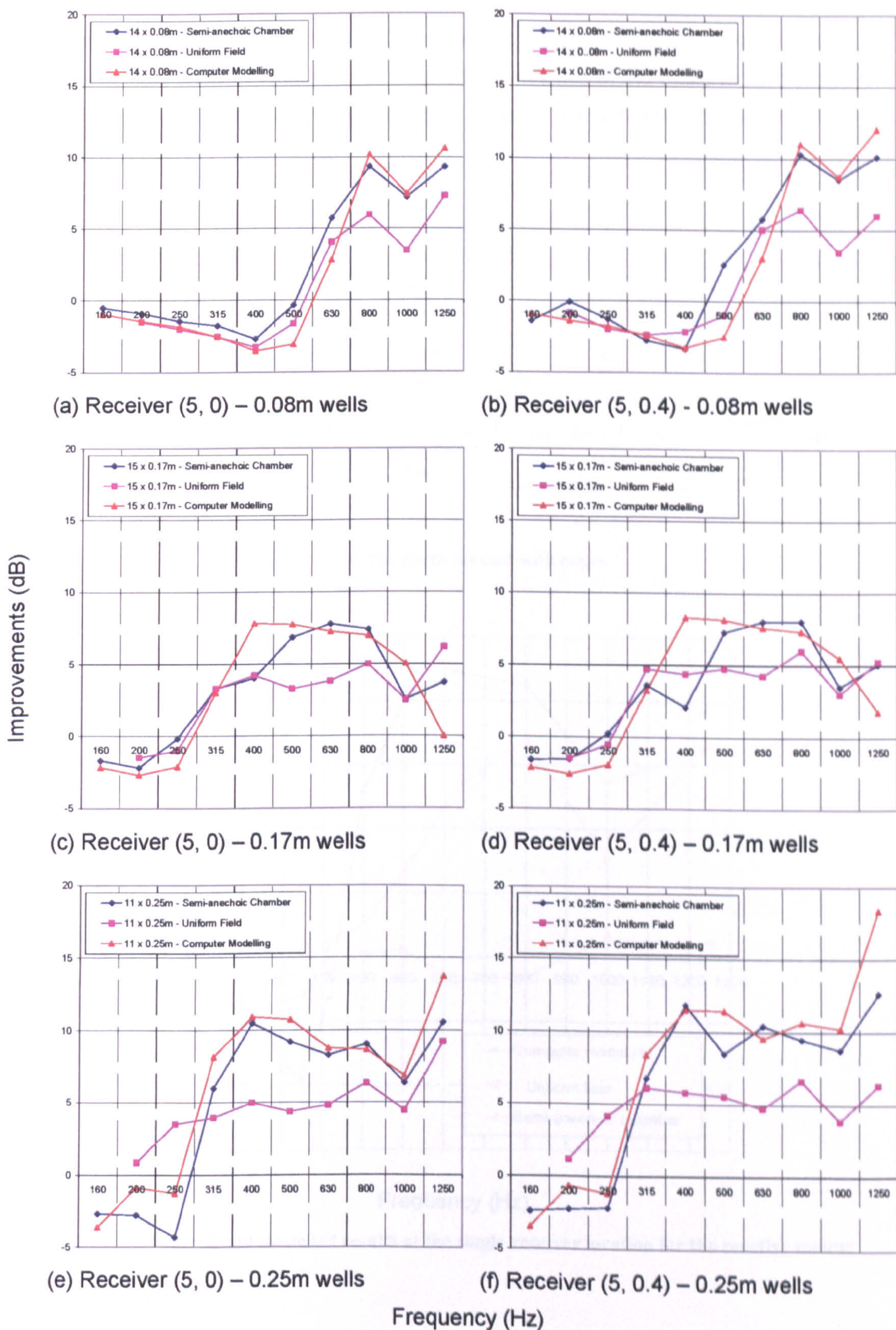


Figure 11.8 : Effect of reactive configurations over a plain rectangle



### 11.1.3 Edges on Earth Mound

The geometry selected for comparing the modelling results of reactive earth mound configurations is shown in Figure 11.9. This model consists of the basic mound shape with 10 edges of 0.17m high wells attached on top. The comparisons of modelling results are shown in Figure 11.10.

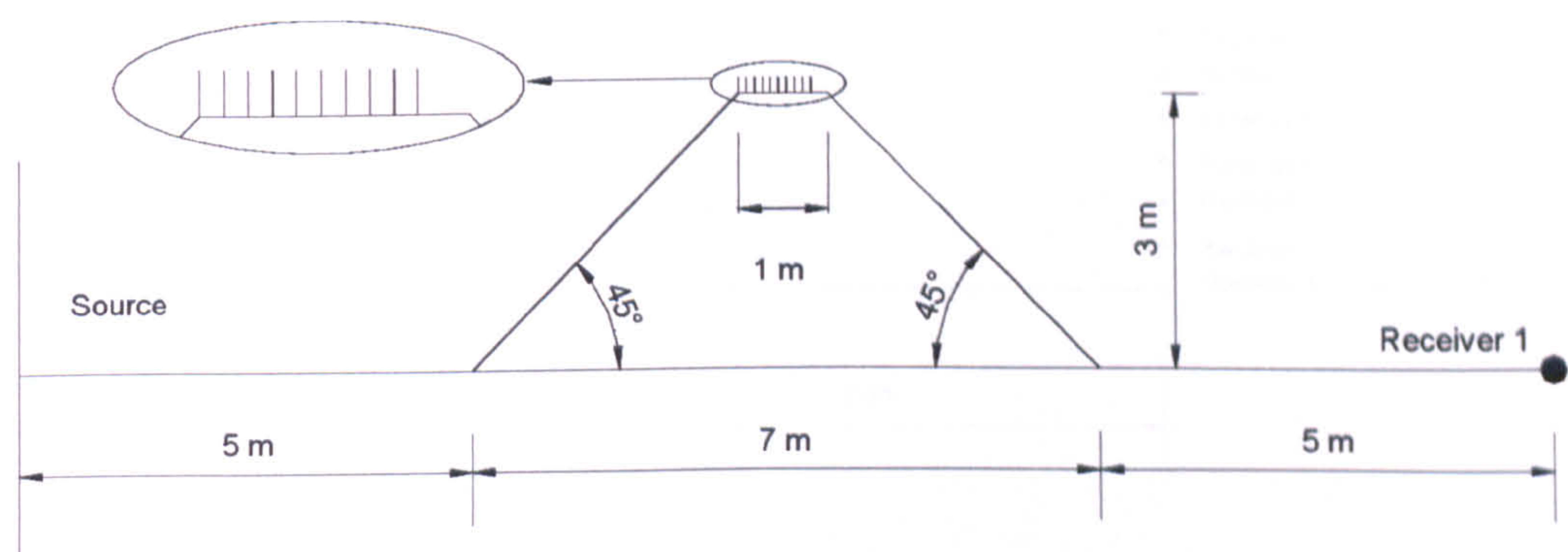


Figure 11.9 : The earth mound with edges

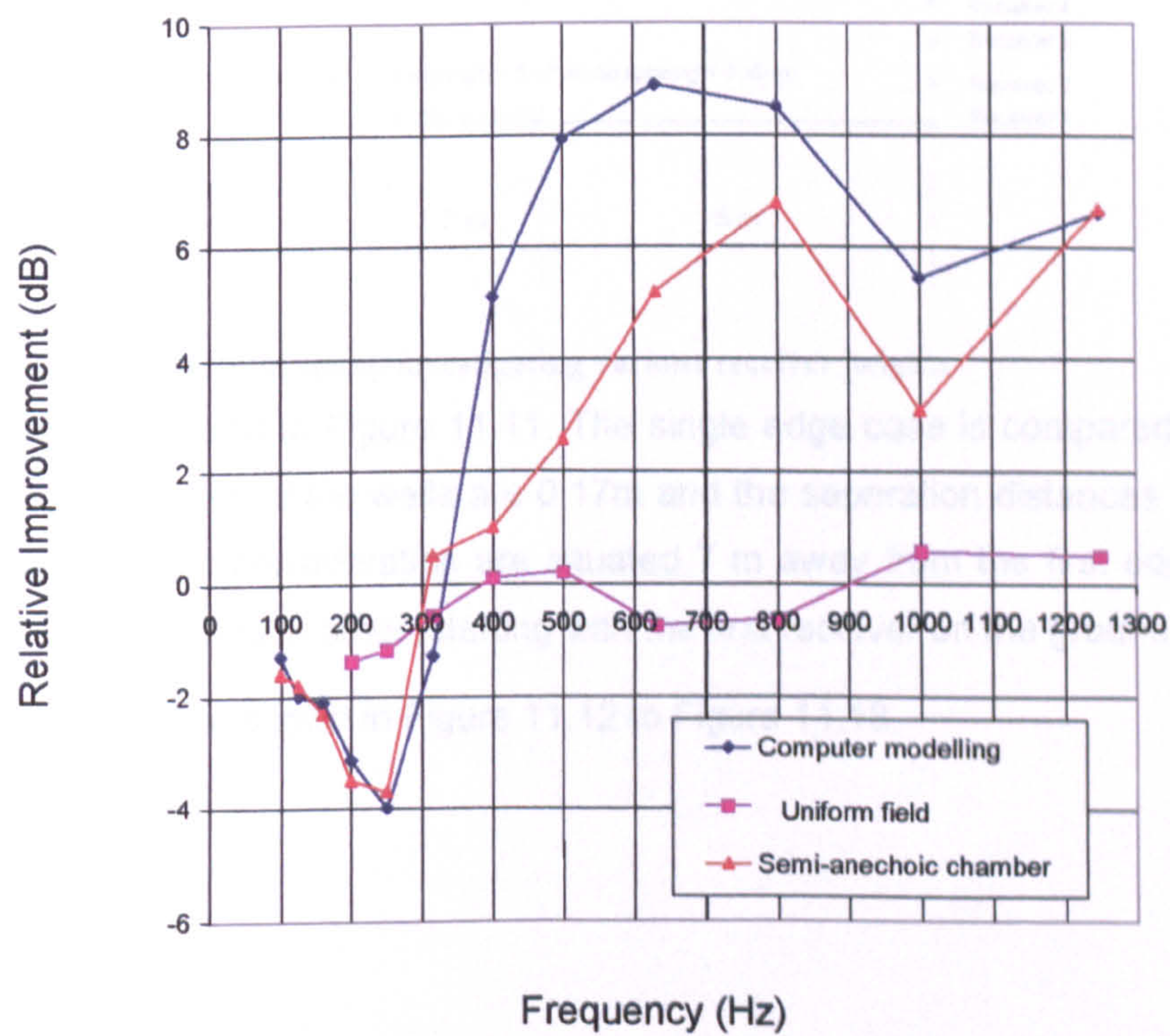


Figure 11.10 : Measured and modelled results at the single receiver location for the reactive mound geometry.



### 11.1.4 Effects of Rib-structure at Different Receiver Heights

As recalled, these tests were carried out in the semi-anechoic chamber to supplement some of the findings of the uniform field experiments. Therefore the comparisons of the results are limited to those obtained in semi-anechoic chamber and those which resulted from numerical modelling.

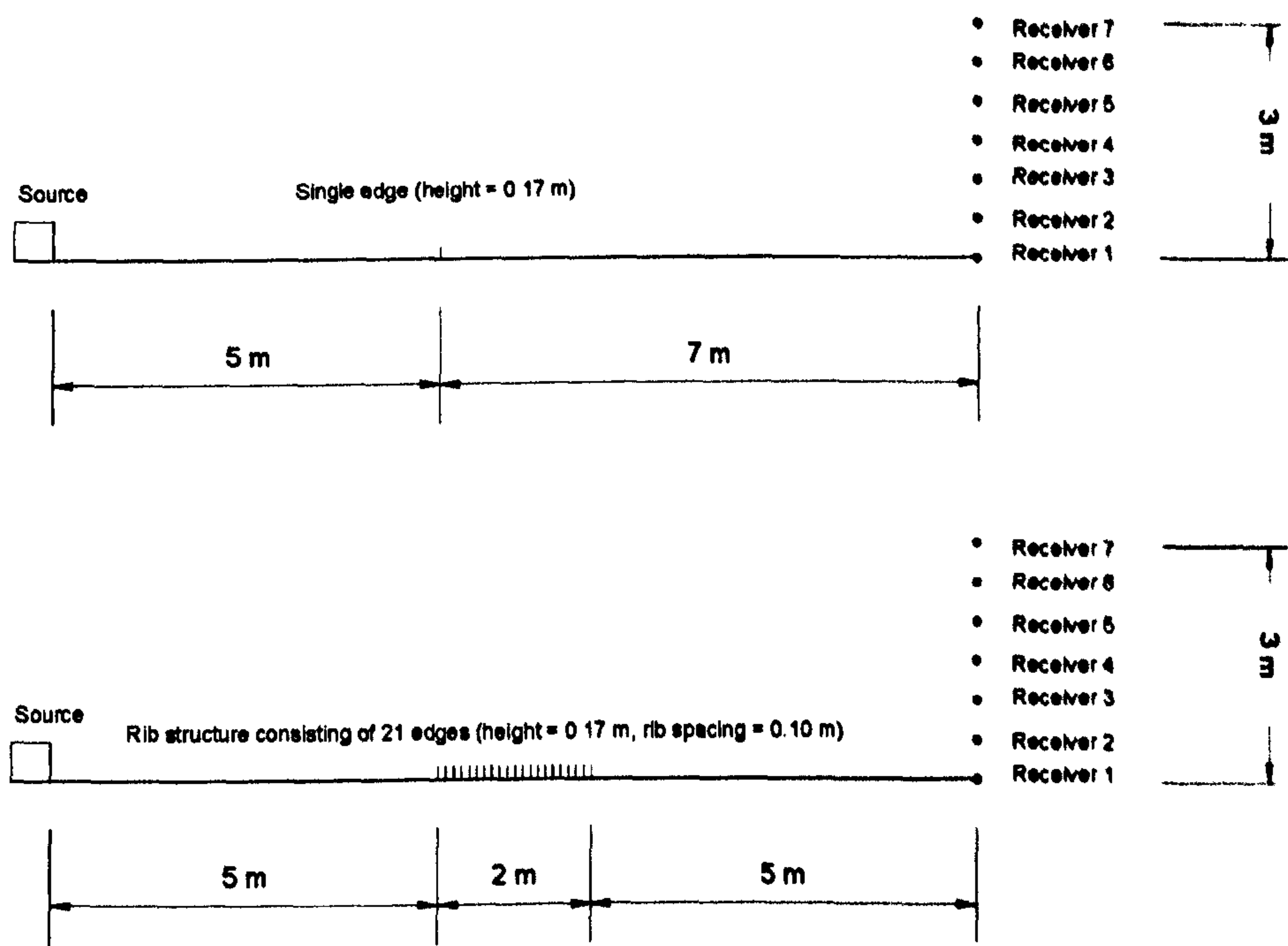


Figure 11.11 : Experimental set-up investigating various receiver heights

The models are shown in Figure 11.11. The single edge case is compared to the 21-edge case. The depth of the wells are 0.17m and the separation distances are 0.08m. The receivers under consideration are situated 7 m away from the first edge and are situated 0.5m above each other, starting with the first receiver on the ground.

The comparisons are shown in Figure 11.12 to Figure 11.18.



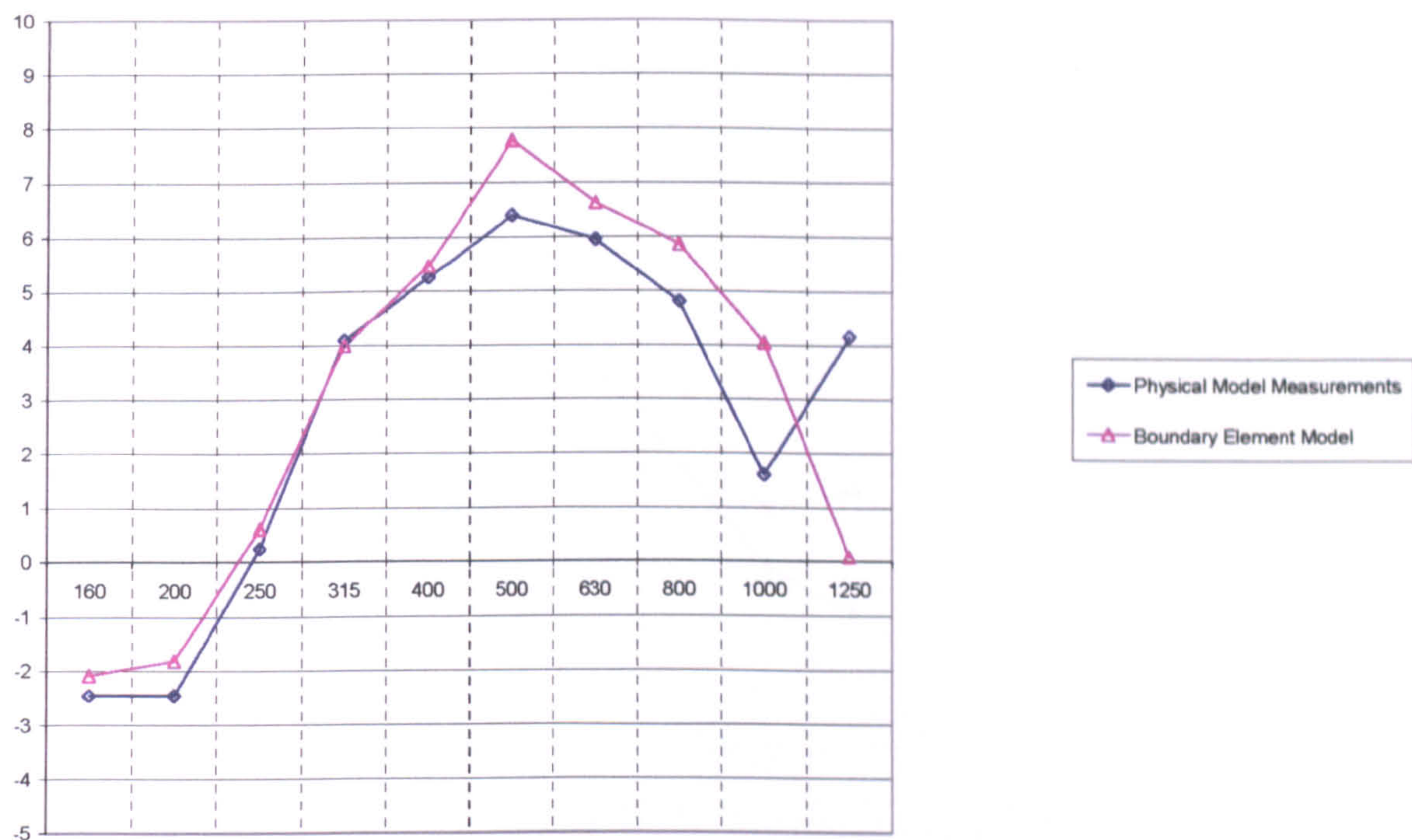


Figure 11.12 : Receiver height = 0

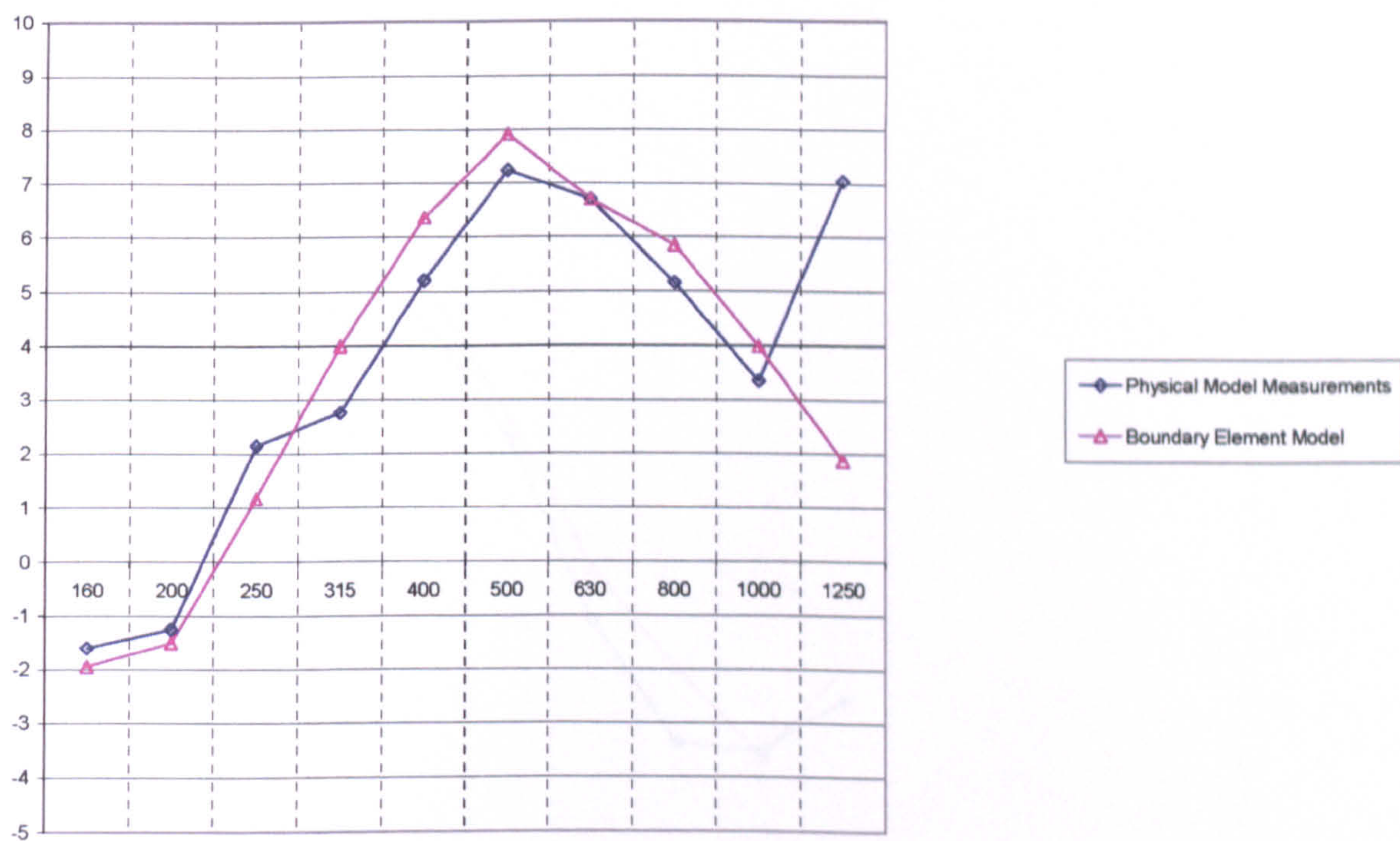


Figure 11.13 : Receiver height = 0.5m



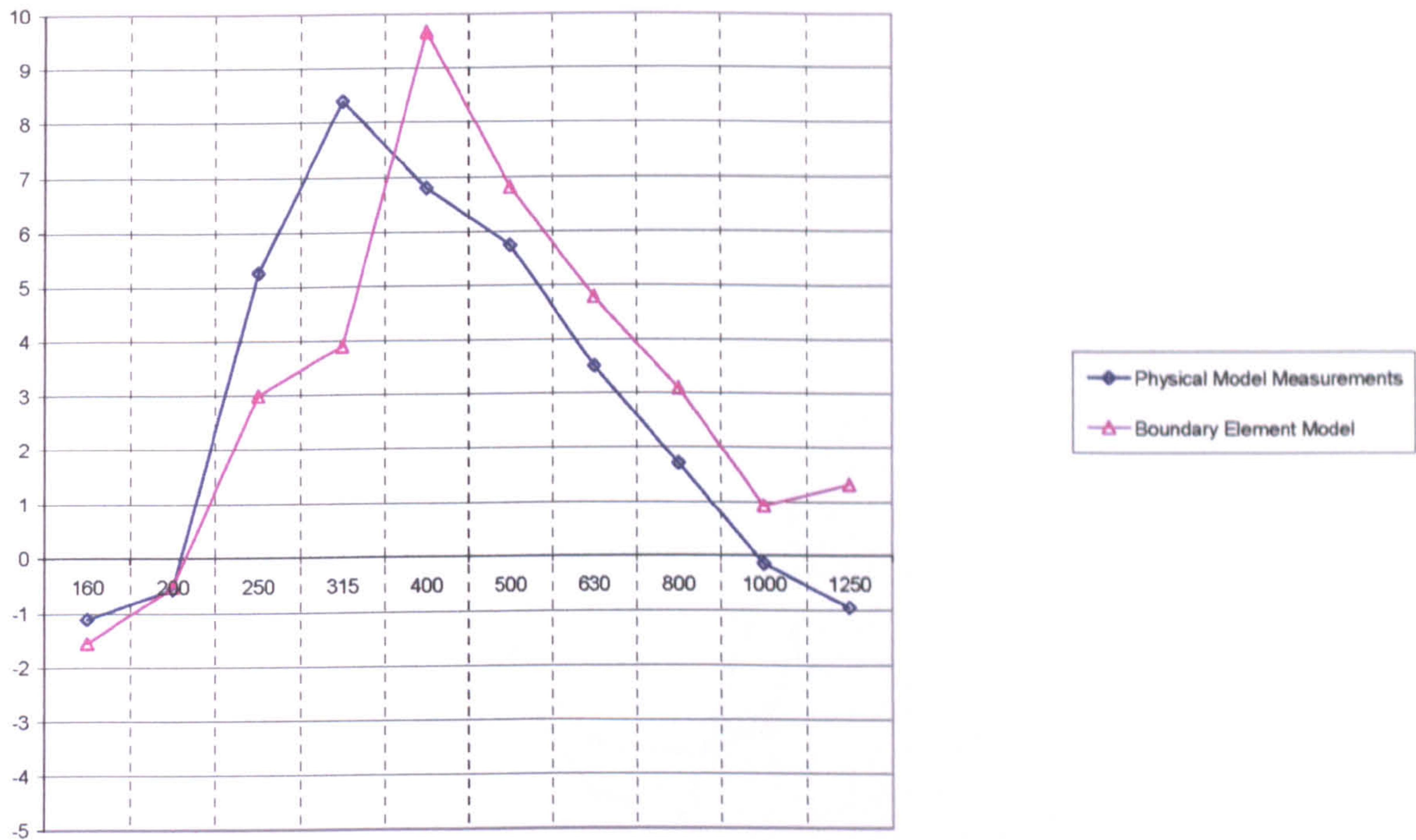


Figure 11.14 : Receiver height = 1m

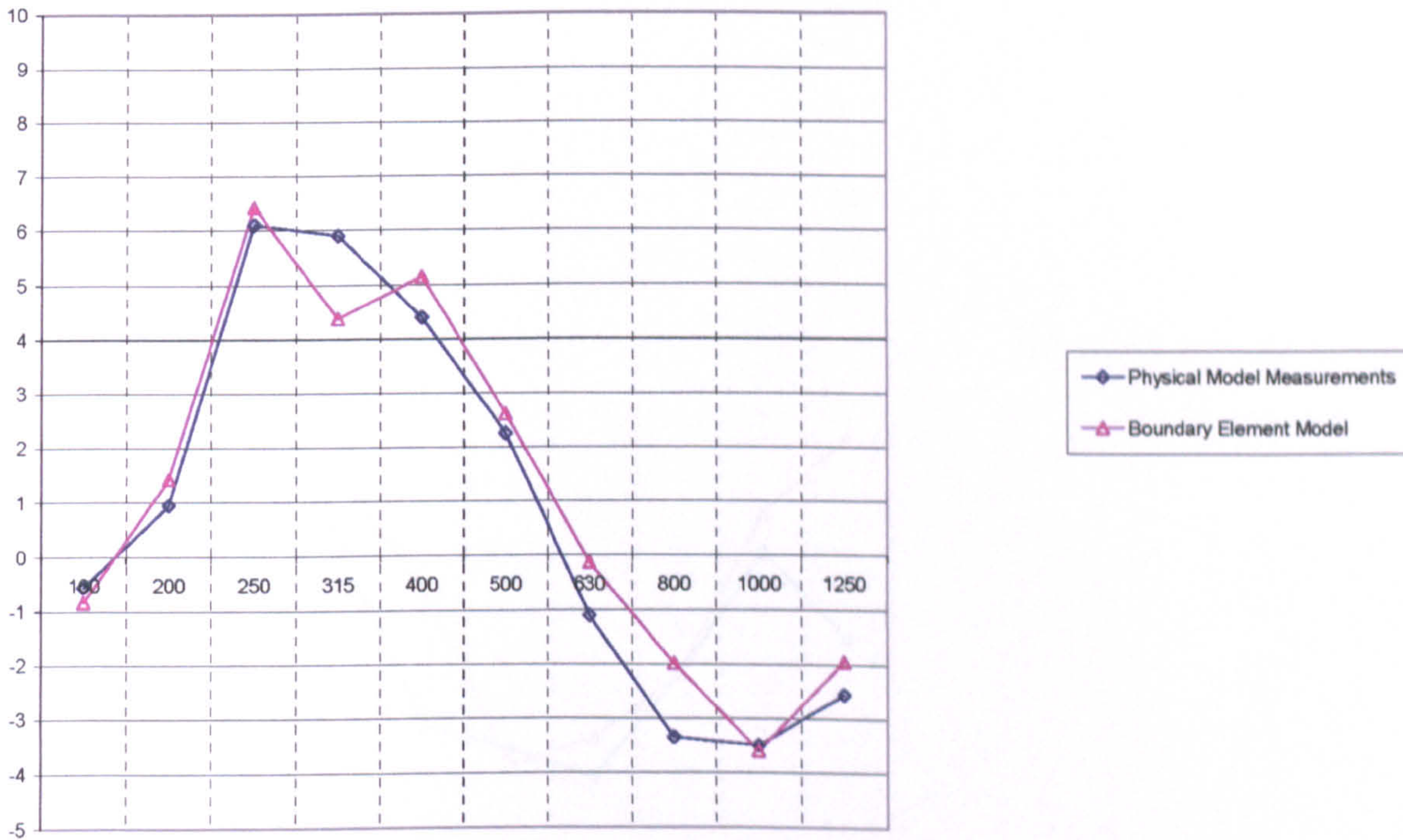


Figure 11.15 : Receiver height = 1.5m



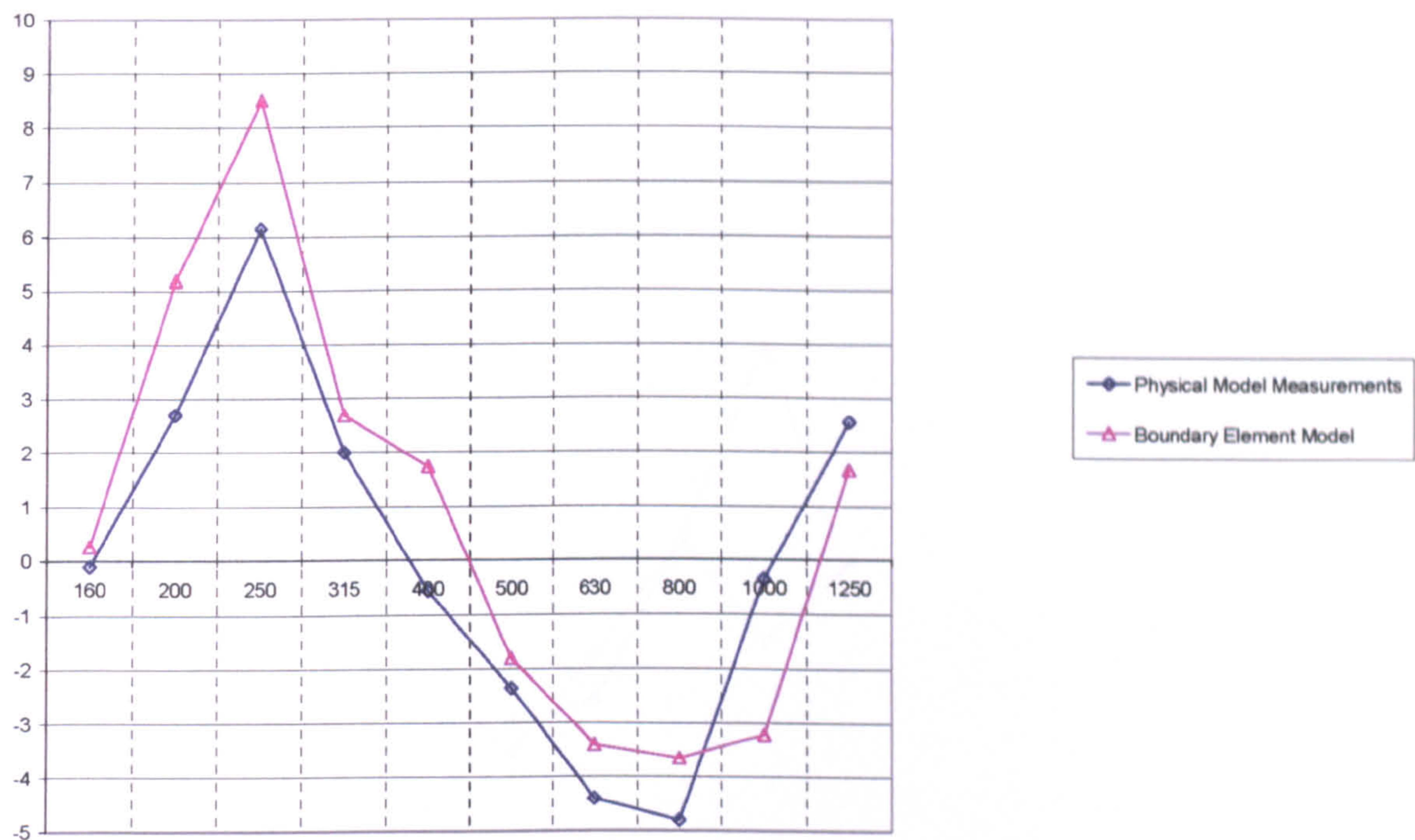


Figure 11.16 : Receiver height = 2m

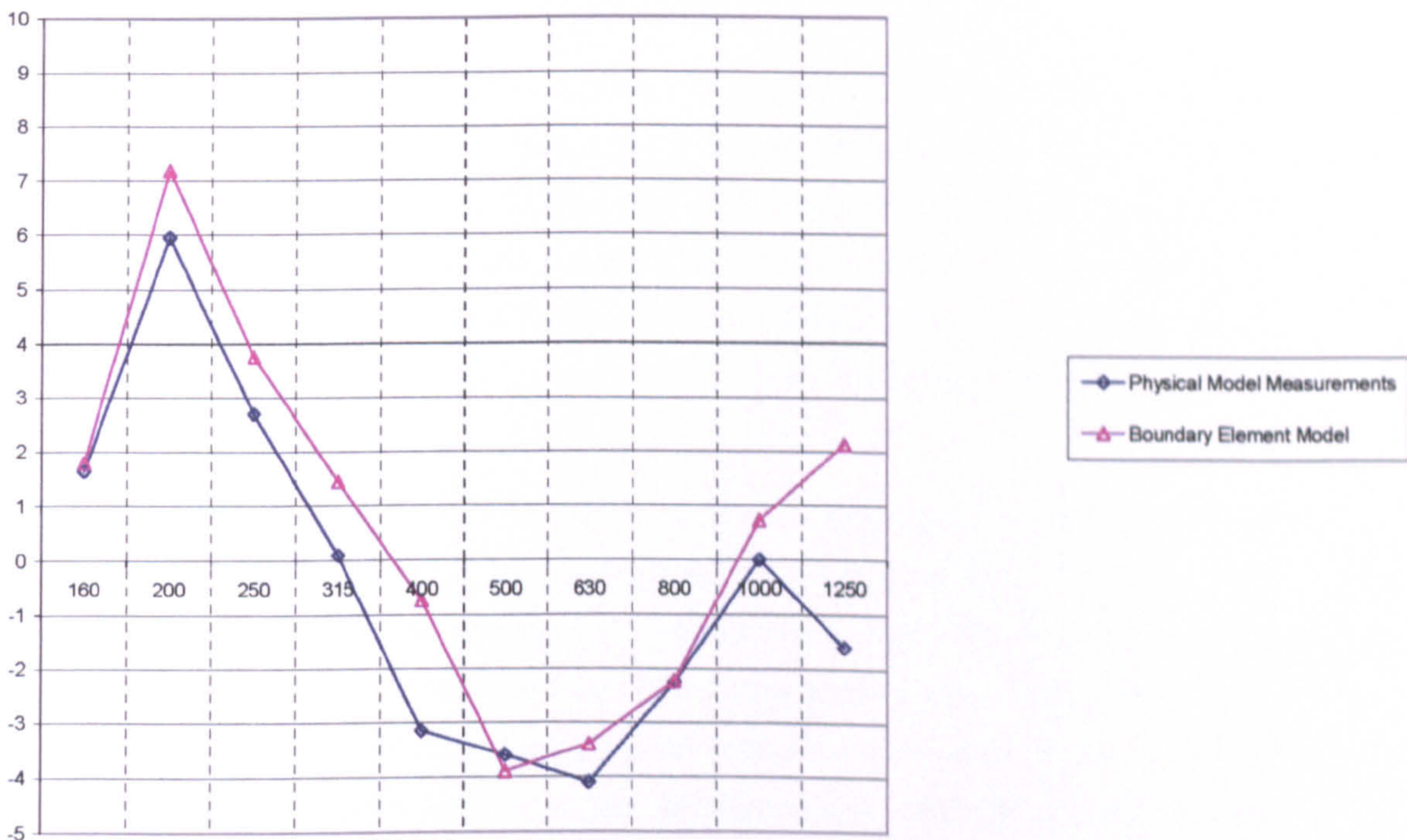


Figure 11.17 : Receiver height = 2.5m



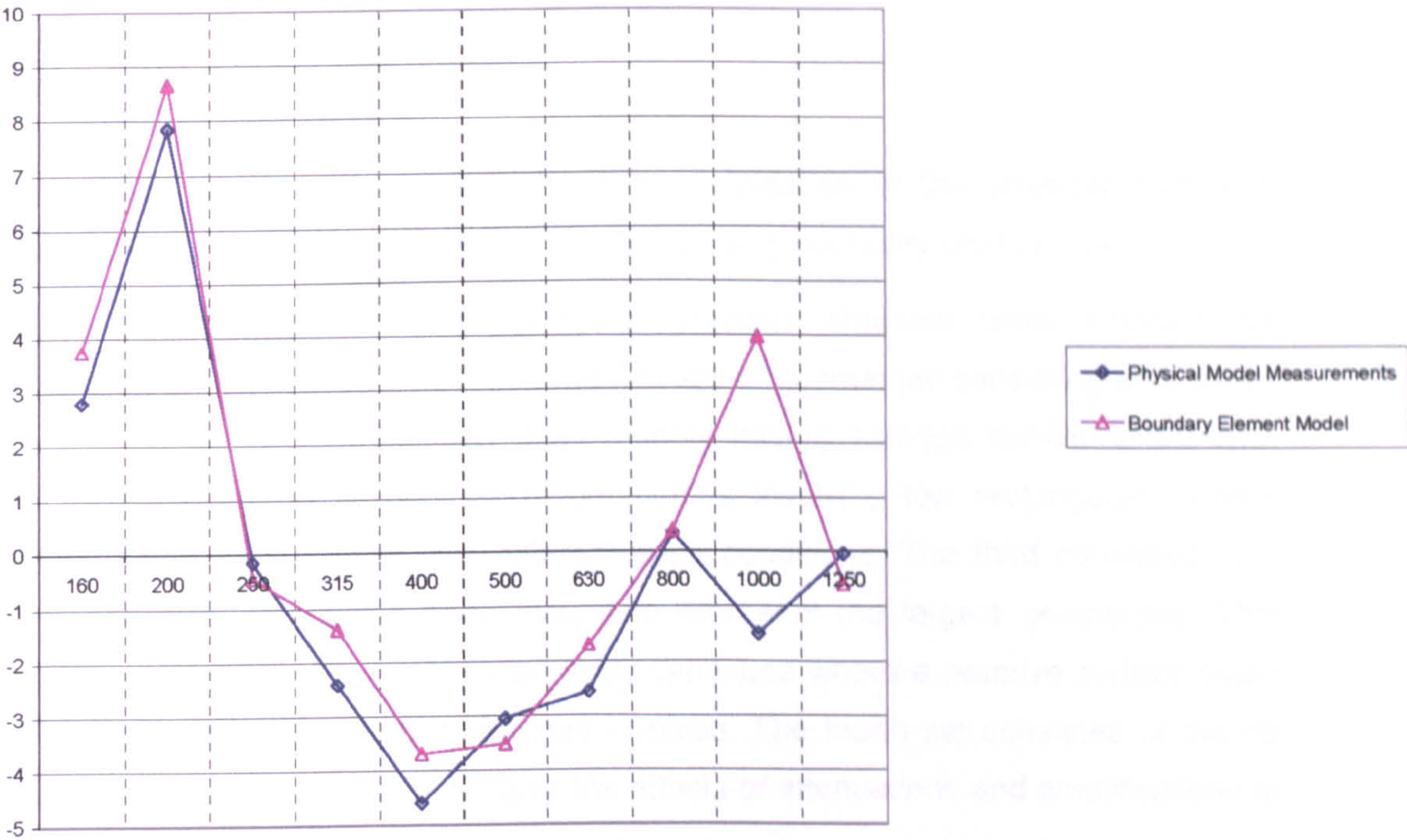


Figure 11.18 : Receiver height = 3m



## **11.2 DISCUSSIONS**

This chapter was mainly concerned with the validation of the physical modelling techniques by comparing to numerical modelling using boundary element methods.

Four sets of geometries investigated in previous chapters were selected for comparison and validation purposes. The first set of geometries consisting of a series of edges on the ground included three models having 14-edge configurations with different heights. The second set of geometries involving low rectangular barriers similarly used three models with different edge conditions. The third consisted of a single geometry of reactive earth mound to represent the largest geometries. This model was considered to be the most likely candidate where a reactive surface could be realised due to the number of edges involved. The fourth set consisted of the rib structure which was used to investigate the effects of attenuations and amplifications at various diffraction angles.

### **11.2.1 Edges on the ground**

The 0.8 m deep wells generally provided very good agreements at all receivers. The results were overall within 2 dB of each other or better. Similarly, the 0.17m wells gave generally very good agreements. The exception is the general lack of correlation at high frequencies. At 1250 Hz, although the physical modelling results were within 2 dB of each other, the numerical modelling gave some inconsistent results. At 400 Hz for the receiver (5, 0.4), it can be seen that there is poor agreement between all three methods.

At the receivers 1.5 m above ground, the 0.25 m wells gave good agreements for all three methods. At the remaining receivers, attenuations obtained by uniform field experiments were under measured by 1 to 4 dB at mid to high frequencies compared with semi-anechoic chamber experiments. Good agreements were obtained at lower frequencies for all three methods. The numerical modelling provided attenuation values which are in closer agreement with the semi-anechoic chamber results at mid frequencies and with uniform field experiments at highest frequencies.

Generally, the well depths of 0.08 m and 0.17 m provided very good agreements between the magnitudes of improvements obtained by all three methods. The well depths 0.25 m gave good to reasonable agreements for the findings of all three methods. Overall, all three well depths provided good qualitative agreements.



### **11.2.2 Edges on rectangle**

The 0.8m wells yielded very good agreements at frequencies corresponding to quarter-wavelength of the well depth or lower. The attenuations measured by uniform field tests were lower by 4 to 5 dB at higher end of the spectrum compared with semi-anechoic chamber and numerical modelling. Overall, reasonable qualitative agreements were obtained for this geometry. The agreement between numerical modelling results and semi-anechoic chamber experiments were found to be very good.

The 0.17m wells provided very good agreements at frequencies corresponding to quarter-wavelength of the well depth or lower. There was very good correlation between two physical modelling techniques at the highest frequency under consideration which is 1250 Hz. The inconsistencies in numerical modelling results have been observed at this frequency as noted above. The findings of the uniform field experiments indicated that the mid-frequency range of frequencies were under measured by 4 to 5 dB compared with semi-anechoic chamber experiments. Generally the correlations between numerical modelling and semi-anechoic chamber results are very good except at 400 Hz and the problematic frequency of 1250 Hz. Overall, reasonable qualitative agreements could be identified.

The 0.25m wells gave very good correlations between semi-anechoic chamber experiments and numerical modelling results. The inconsistency of numerical modelling predictions at 1250 Hz was noted at this geometry as well. Uniform field experiments, when compared with these, gave intolerable qualitative and quantitative agreements. The attenuations obtained by this method were consistently under-measured by 3 to 6 dB at frequencies higher than those corresponding to quarter-wavelength of well depth and these were over measured by a similar amount at lower frequencies. Overall, as the attenuations due to the edges increased, the lack of correlations in uniform field experiments was more prominent. The semi-anechoic chamber tests and the numerical modelling results using boundary element methods gave very good correlations.

### **11.2.3 Earth Mound**

The uniform field experiments gave negligible relative Improvement values as noted in Chapter 8. This was considered to be due to the increased effects of the reverberant field masking the attenuations. This is supported by the substantial attenuations observed by physical modelling carried out in the semi-anechoic chamber and the numerical modelling.

The results of numerical modelling and semi-anechoic chamber tests yielded very good correlations at frequencies less than 315 Hz. The differences between the two were



less than 1 dB. The agreements were reasonable at frequencies greater than 800 Hz. The semi-anechoic chamber results are shown to be up to 2 dB lower. The differences are more prominent especially when the attenuations are great. However at frequencies centred around 500 Hz, the semi-anechoic chamber tests yielded values which were 4 to 6 dB lower than the findings of numerical model. These large discrepancies are thought to be mainly due to the practical difficulties associated with attaching the edges on top of the mound. The irregularities in the floor surface and the model dimensions meant the edges could not be secured in a way to form an integral part of the mound. Considerable attention was devoted to fixing these onto the earth mound model in such a way that there would not be any gaps left. These would have prevented some of the sound waves from taking a direct path over the reactive surface and instead they would propagate through the gaps underneath the edges. This would have resulted in the reactive surface not being fully realised. It is noted that 500 Hz is the resonant frequency corresponding to these well depths and the attenuations which have been adversely affected are centred around this frequency band.

This geometry showed that uniform field experiments would not be suitable for the largest geometries where the attenuations are expected to be greatest. It was found that there were some discrepancies at around the resonant frequencies between the findings of semi-anechoic chamber experiments and numerical modelling results. This was attributed to the reactive surface not being fully realised due to irregularities in the physical model.

#### **11.2.4 Rib-structure**

This geometry compared semi-anechoic experiments with numerical modelling. Generally it was found that the numerical modelling results and the semi-anechoic chamber experiments are within 2 dB of each other or better. The numerical modelling generally tends to yield the higher improvements of the two methods.

The inconsistencies observed previously at 1250 Hz with the results of numerical modelling are also seen in these experiments. These are prominent especially at receiver heights of 0m, 0.5m and 2.5m. A similar comment can be made for 1000 Hz at receiver which is 3m high. Overall, the numerical modelling attenuations agreed reasonably well with those obtained by semi-anechoic chamber experiments.



## **11.3 CONCLUSIONS**

This chapter was mainly concerned with the validation of the physical modelling techniques by comparing to numerical modelling using boundary element methods.

This comparison showed that uniform field experiments can be used to investigate various small sized geometries. An increase in the size of model geometries resulted in reduced correlations in uniform field modelling results. This is likely to be due to increased effects of the reverberant field. However it was found that reasonable qualitative agreements were possible and this technique could be useful for investigation of the relative performance of small sized barriers.

At the largest geometries where attenuations are expected to be very high, it was concluded that uniform field experiments could not be used for the investigation of small additional attenuations. The reverberant field would mask any potential reductions and no sensible comparisons could be made.

The comparison of the modelling work undertaken by different methods indicated that generally there is a very good correlation between the semi-anechoic chamber experiments and numerical modelling results. At high frequencies, the numerical modelling can give inconsistent results due to the shortcoming of boundary element methods at high frequencies. For the reactive earth mound configuration used for comparisons, it was found that around the corresponding resonant frequency, the semi-anechoic chamber results were in poor agreement with the numerical modelling results. This was attributed to the irregularities in physical model.



## **12 GENERAL DISCUSSION**

### **12.1 BACKGROUND**

Environmental noise, caused by traffic, industrial and recreational activities is one of the main local environmental problems and the source of an increasing number of complaints from the public. Generally however action to reduce environmental noise has had a lower priority than that taken to address other environmental problems such as air and water pollution.

Regarding research on environmental noise, Europe has been lagging behind North America and Japan. The European Commission Green Paper on "Future Noise Policy", which recently became a new directive, stresses the fact that in Europe the data available on noise exposure is generally poor in comparison to that collected to measure other environmental problems and often difficult to compare due to the different measurement and assessment methods. According to the statistics in the Green Paper, it has been estimated that around 20 % of the European Union's population or close to 80 million people suffer from noise levels that scientists and health experts consider to be unacceptable which is a level more than 65 dB(A), where most people become annoyed, where sleep is disturbed and where adverse health effects are to be feared. An additional 170 million citizens are living in so-called 'grey areas', which are areas subject to levels between 55 and 65 dB(A), where the noise levels are such to cause serious annoyance during the daytime. The estimates of the economical costs of transport noise to the society range from 0.2 % to 2 % of GDP. Using the lower estimate of 0.2% of GDP represents an annual cost to society of over 12 billion ECU.

With regard to nuisance due to excessive noise levels, road traffic noise is the main culprit as it accounts for the 90 % of the cases experienced by the 80 million people exposed to levels more than 65 dB(A). Thanks to the legislations and technological progress significant reductions of noise from individual sources have been achieved since 1970. However data covering the past 15 years do not show significant improvements in exposure to environmental noise especially road traffic noise. The growth and spread of traffic in space and time and the development of leisure activities and tourism have partly offset the technological improvements. In the case of motor vehicles other factors such as the dominance of tyre noise above quite low speeds (50



km/h) and the absence of regular noise inspection and maintenance procedures are also important.

Road traffic noise attracted a number of solutions depending on the nature of the problem and the political / legislative arrangements in the specific countries. In the U.K., the Land Compensation Act 1973 encouraged sound insulation of properties and paying for the land subjected to noise levels set by the legislation. By offering double-glazing noise was kept out of the homes. This only avoided the problem rather than solving it and it did not take into consideration the need for the people to open their windows or use their gardens, in which case this particular noise control would be rendered useless.

Traffic management is another means of traffic noise control. Two main parameters affecting traffic noise are traffic speed and composition. Traffic management attempts to control these two parameters by various measures. These include traffic control devices, prohibition of certain vehicle types during certain times from sensitive areas, modification of speed limits or horizontal/ vertical realignment of the traffic relative to the noise sensitive areas. These measures do have their practical limitations and some may also require a strict enforcing (control / policing) mechanism until they take effect.

Two of the more commonly preferred and implemented noise mitigation measures are the use of barriers and alternative road surfaces. In U.K. porous road surfaces were developed to allow water to drain rapidly through the surface material and consequently help to prevent water forming on the surface during heavy rainfall. These surfaces reduce spay from passing vehicles and give better skid resistance. However, it's been realised that in addition to the reduction in the so called "splash noise", the tyre/road generated noise was also absorbed to some extent due to the porous nature of the road surface under dry conditions. This technique of noise control "at the source" has been developed over the years and implemented into practice. Durability, maintenance, reduction of acoustic effectiveness in time and cost (both application and maintenance) are still a concern. However promising progress has been made and reductions in traffic noise in real life situations are encouraging. The use of this method is also emphasised in the EU Green Paper.

Most commonly preferred traffic noise control method has been the use of noise barriers. Although it is a method of noise control by intercepting the transmission path, due to the ease of implementation and its effectiveness, it attracted wide interest among the scientific community. This method has the advantage over noise insulation that it protects people more effectively, whether they are inside or outside their homes. Barriers take immediate effect and do not require a transition period required by certain traffic management measures. Although noise control at source is always more



effective, low noise surfaces are still in the process of being developed and require technical expertise -not possessed by developing countries -to be implemented. Problems inhibiting their implementation may be overcome over the years but low noise surfaces may still be required to be used in conjunction with noise barriers for a more effective traffic noise control.

It is environmentally more acceptable to address the problem at the source rather than at the receiver. The sound insulation of the properties is simply to avoid the problem. Low noise surfaces, if they could be effective on their own, would be the best way to control noise at its source. However, low noise surfaces are unable to offer a full solution to the problem currently and are likely to be used in conjunction with environmental noise barriers. When built as close to the traffic source as possible, the screening becomes a method of control at the source containing the noise within the corridor around the road. In addition, there are continuing reservations about the cost, durability, maintenance requirements and the long-term acoustic performance of alternative road surfaces. The indecisiveness of the Highway Agency as to which surface to adopt indicates these surfaces are passing through a dynamic research and development stage. The maximum allowable noise levels in the U.K., highest of all European countries, is also making the noise problem appear smaller than it actually is. Possible lowering of these levels is bound to demand more effective solutions possibly incorporating barriers and low noise surfaces. The growth and spread of traffic in space and time, when added on top of all these, is expected to make the semi-urban and rural areas more susceptible to noise impacts.

Currently screening provides the well-proven, widely used option for securing considerable reductions in roadside noise levels with no long-term decrease in performance. Barriers can also have the added advantage over alternative road surfaces of reducing dust, dirt, litter, fumes and highlight glare from the highways and improving the visual quality of the surroundings if well-conceived. The expertise needed in the design, construction and maintenance of special road surfaces is not essential in the case of noise barriers, provided basic guidelines are made available for the designers by experts. When the developing countries reach the awareness of the developed nations in accepting the adverse impacts of noise on the built environment, barriers are the likely candidates to offer off-the-shelf solutions for their needs which will also be economically, aesthetically, acoustically and environmentally effective. The role of environmental noise barriers in road traffic noise control is not thought to diminish in any case at a foreseeable future. There is presently a need for research into environmentally sensitive noise barriers with enhanced acoustic performance.



## **12.2 IDENTIFYING RESEARCH NEEDS**

Before undertaking detailed research into noise barriers, factors affecting sound propagation in outdoor environments were reviewed. This demonstrated that atmospheric and ground effects were very important in influencing the actual performance of barriers. It was argued that when assessing the relative performance of different barrier shapes it would be reasonable to minimise atmospheric and ground effects such that the acoustic benefits of various shapes could be determined free from external factors.

As part of this research programme, an extensive review of the up-to-date work carried out on environmental barriers was undertaken which covered both theory and practice. Different types of noise barriers were also reviewed. This has shown that a great deal of theoretical work has been done on the modelling and performance prediction of barriers, especially on those designed for the urban context. However, it was found that the on-site performance of barriers was not well documented. This work resulted in recommendations on further research needs in the general field of environmental noise control by means of barriers.

A number of official documents provide guidance on the general aspects of barriers. Most of the advice on the acoustical aspects is applicable for the wall type barriers which are commonly used in urban surroundings. Spread and growth of traffic in space and time will continue to shift the noise problem to semi-urban and rural areas. These surroundings demand differing solutions. Factors affecting the decisions for implementing a solution are not solely acoustics. Traditionally, noise solutions for such surroundings have been earth mounds. Apart from combining them with conventional barriers, there have not been any serious attempts to enhance their performance further without increasing their overall height or diminishing their aesthetic appeal. Also such solutions would have implications for a shorter earth barrier requirement for similar performance. Considering that the amount of material required for their construction and the horizontal land-take are the two factors which restrict their use, this could make the earth barriers clear favourites in noise control solutions in sensitive environments. The previous work by others showed that barriers with multiple diffracting edges are the most efficient designs. More recent work revealed that barriers with reactive surfaces are equally promising if not superior. However, attention in the case of both was given to the applications involving wall type barriers.

With numerical modelling techniques being improved and the inventory of noise barriers being extended continuously, the designers are drawn away from the real problem. The real problem is an environmental one. The solution should address it



accordingly in a practical and efficient manner. One has to remember that noise control has its limits in reality and physical parameters that could possibly be modified to obtain enhanced barrier performance are only a few. The people who are involved in implementation of noise barriers into real life, need substantial information on all these issues. The plethora of noise barrier types and availability of many mathematical models should not mislead the designer into the belief that acoustic solutions are endless. This only complicates the decision making in design. The designer should be distanced from the technicalities.

Therefore as part of this work, the initial attention was directed towards the need for a simplified approach to selecting barriers used in controlling road traffic noise. This approach would be of benefit particularly to those non-acousticians who are part of the decision making process. It was also identified that there is a need for noise barrier solutions which address the environmental dimension of the problem.

### **12.3 A SIMPLIFIED METHOD FOR BARRIER SELECTION**

The main source of advice in the UK for the design of environmental barriers is the Manual for the Design of Roads and Bridges (Volume 10, Section 5, Parts 1 and 2). The information contained in this document is often difficult to interpret particularly when the designer is inexperienced.

The abundance of different barrier shapes have been pointed out in Chapter 3. Only the most promising profiles have been incorporated into this design method where on-site performance investigations by others indicated positive gains. The design process for new barriers can be undertaken in two stages. Initially, the most favourable type of barrier is selected on the basis of availability of space for erection and the cost implications. The second stage is where the type of acoustic treatment to be applied to the barrier is selected on the basis of some simple logical tests, where no specialist knowledge of acoustics is required. Considering the average insertion loss of barriers in practice was observed to lie between 5 and 12 dB(A), the targeted insertion loss values should be at least 10 dB(A). This reduction will be subjectively perceived as halving the noise levels.

Similarly a design procedure, for improving the performance of existing wall type barriers, based on simple yes/no tests and little knowledge of acoustics was proposed. The main advantage of both methods is the shortening of the design process and the reduction in the costs of afterthought mitigation measures. The reported benefits of the discussed modifications vary. However, almost all are said to have made only modest contributions to an existing barrier, up to about 3 dB(A) in real life applications. An



existing barrier may already possess a high degree of screening performance and it may prove difficult to enhance this performance greatly. Realistically, 3 dB(A) should be the targeted additional increase in the acoustic performance, which is subjectively the smallest noticeable change in noise levels.

It was emphasised that design philosophy of barriers is a complex process and acoustics is only one of the many pieces of the jigsaw puzzle. Therefore non-acoustical aspects of these modifications should also be carefully addressed.

Earth mounds and wall type barriers were generally given equal emphasis as part of this method as being the two main barrier types. In certain environmentally sensitive situations, the earth mounds were given priority of choice over wall type barriers, whenever practicalities permit their applications. However this could not be supported by additional advice on acoustic aspects of new and existing earth mounds.

These guidelines condensed some of the large amount of research carried out on noise barriers into a simple and practical format. It also served the purpose of identifying further research needs.

## **12.4 EXPLORATORY WORK**

The limited information available on acoustical characteristics of earth mounds has indicated that there is a need for further research into these. The design criteria related to barriers can be listed as acoustics, aesthetics, cost, acceptability, environmental friendliness, and engineering aspects such as stability, durability, serviceability and deformation resistance, maintenance and repair conditions and aspects of traffic safety. The earth mounds readily satisfy many of these aspects and possess some additional characteristics which make them a better choice in certain localities compared with wall type barriers. In order to improve their acoustic performance and to off-set their non-acoustic limitations, additional research was required.

The three available techniques for the investigation of the performance of traffic noise barriers were identified in Chapter 3. These are on-site measurements as well as analytical and physical modelling. Therefore exploratory work was directed towards identifying which techniques would be better suited for the purposes of this investigation.

Preliminary on-site measurements were undertaken to assess the noise reduction potential of an earth mound. This noise assessment was useful in identifying the insertion loss value for a typical earth mound. Practical difficulties involved with on-site measurements, such as the identification of a suitable site, planning, mobilisation of



equipment, time and manpower required for a representative survey and atmospheric conditions, were also realised. Since the aim of this research is to develop an alternative barrier profile, it was decided that further on-site measurements would be undertaken if modelling techniques indicated that such a barrier is likely to exhibit superior acoustic performance on-site.

Compared with conventional barriers, earth mounds are slightly compromised in terms of acoustic performance and their implementation can require extensive areas of land and considerable utility relocations. The acoustics can be enhanced by the use of a wall on top of a mound, but that may diminish the aesthetics. Instead of a single conventional height barrier on top of a mound, multiple small height edges could be incorporated, maximising the acoustics and minimising the visual impact on the surroundings.

Physical modelling work was carried out which examined the potential benefits of modifications on top of earth mounds. This investigation did not provide any conclusive evidence in support or against the use of small height barriers on a plain earth mound. However there was limited evidence that a series of multiple edges on top of an earth mound type barrier could be beneficial at selected frequencies. It was decided to explore these concepts in further detail under better-controlled conditions.

The exploratory experimental work using physical modelling under uniform field conditions and on-site measurements determined the methodology for investigation for the rest of this research programme. Accordingly, physical and numerical modelling would be undertaken to investigate the use of multiple edges on top of earth-mounds.

Before undertaking the experimental work, a theoretical appraisal was undertaken into rib structures. The approaches employed in the study of resonators and gratings were used to explain the likely physical mechanisms and the parameters responsible for the noise attenuations achieved by rib structures. These were found to depend on a number of factors including the wavelength of the incident wave, depth and width of wells, total number of diffracting elements, source and receiver location, the nature of the individual diffracting elements, total distance covered by diffracting elements, and the proportion of source-to-receiver distance covered by the diffracting elements.

It was found that the low frequency limit of attenuations was mainly determined by well depth and the high frequency limit was influenced by well width. Scattering effects were identified to be the main noise attenuation mechanism at lower frequencies and diffraction effects were likely to be the main mechanism at higher frequencies. Therefore a combined grating/ resonator approach could be more appropriate for explaining the noise attenuations by rib structures. These findings were investigated by physical modelling.



## **12.5 MAIN MODELLING WORK**

Before undertaking modelling work, the uniform testing space, the sound source and the modelling materials to be used for physical scale modelling purposes were characterised. Reverberation time measurements were carried out to find out the suitability of the testing space for modelling work and to quantify the effects of the reverberant field. Directivity tests helped determine the source characteristics. Impedance tube measurements revealed the absorptive behaviour of the modelling materials used. The findings of previous research by others, using airflow resistivity experiments, were presented in support of some of the findings of impedance tube measurements.

The investigation into the experimental set-up indicated that even though the testing space is not a purpose built anechoic chamber, it could still be possible to undertake relative performance investigations of different barrier profiles. The magnitude of the effects of the reflections was identified as being dependent on the choice of source - to - receiver distance and the geometry. Having determined the source and room characteristics, the effects of the reverberant field on the direct component of sound could be identified.

Therefore two geometries from the literature were used as reference cases to quantify the probable effects of the reverberant field. It was found that in the cases where the direct sound is not already attenuated too much, reasonable insertion values could be obtained. In the cases where the direct sound was reduced to levels comparable to reverberant levels, it would not be possible to obtain the true performance of a configuration. In this case, a relative performance investigation could be possible. In the extreme case where the direct field was reduced to levels 10 dB smaller than the reverberant field, no gains of any magnitude would be recorded.

Therefore for the small geometries where the path length difference is small and where the overall source - to - receiver distance remains within the direct field range as much as possible, a reasonable representation of the actual insertion loss values would be possible. For larger geometries where the path length difference becomes larger and when larger insertion loss values are to be expected, the attenuations that can be achieved would likely to be limited. A good qualitative agreement may be obtained for potentially high insertion losses.

Following the investigation into experimental set-up, uniform field experiments looked at a number of models consisting of a series of wells on the ground and on top of other earth mound type barriers.



Initially, the progressive increase in the number of edges was investigated. The sound pressure levels were monitored at a single receiver location which was chosen such that the line-of-sight from the physical centre of the source to the receiver was grazing the top of the edge. This would ensure the subsequent addition of edges in the direction of the receiver would not affect the path length of the sound. The sound pressure levels were reduced with the increased number of edges indicating the clear benefits of increased edge numbers. The insertion loss provided by the 8 - edge case was higher than a single edge by 5 to 10 dB throughout the spectrum. The insertion loss value of the single edge was 4.5 dB as would be expected due to the line-of-sight grazing the top part of the edge. The improvement in the insertion loss provided by the 8 - edges was 6.9 dB bringing the total insertion loss to 11.4 dB without any additional increase in the height of the barrier.

Having established the potential benefits of progressive increase in the number of edges, it was decided to examine the effects of doubling the number of wells, and hence the width of the reactive surface. An array of six receiver locations was chosen which would provide evidence as to how the spectrum behind the reactive surface is affected at various distances and heights. Two of these were in the shadow zone, two were along the line-of-sight from the source grazing the top of the edges, and the remaining two were clearly visible from the source location. Provided the line-of-sight from the source to the receiver was intercepted, the increased number of edges enhanced the improvement in performance. The spectrums of the improvements relative to the single edge case for the receivers in the shadow zone showed a distinctive "stepped" shape, where the distinctive peaks were followed by linear reductions in the gains.

In the experiments under consideration the channel depth was 0.025 m and the frequency corresponding to quarter-wavelength of the well depth was approximately 3.4 kHz. The subsequent peaks in improvements appeared to be 1.5 times the previous peak frequency. This relationship did not hold for receivers which were not obstructed from a straight line drawn from the source. These experiments supported the observation of others concerning the minimum frequency for which the maximum attenuations would be realised. A diffraction grating approach did not reveal any conclusive relationships. For the geometry under investigation only the zero diffraction orders would be valid at grazing incidence and this would apply to all frequencies. At diffraction angles other than at grazing incidence (i.e. the receiver 1.5m high), the grating separation was too small to give any physically realisable diffraction orders within the range of frequencies considered.



These observations were extended to different well depths. The attenuations recorded in the case of well depths of 0.008 m and 0.017 m were still substantial even though any potential peak frequencies were less readily identifiable. The lowest frequencies at which maximum attenuations for these two well depths occurred were around 10.625 kHz and 5 kHz respectively. However the experimental results indicated that these were around 5.7 kHz and 3.2 kHz respectively. It should be noted that the total widths of the two reactive surfaces were not equal. It was considered that different aspect ratios of well depth to separation distance in conjunction with different reactive surface widths could reveal a more conclusive relationship. This would require further parametric studies.

Comparing the single value indicators it was found the relative performance of a reactive surface at any given receiver location diminished with reduced well depth. Excluding the receiver locations which were visible from the source, the gains over the single - edge cases on average were 3.7 dB, 4.3 dB and 6.9 dB for well depths of 0.008 m, 0.017 m and 0.025 m respectively.

This thought was extended one step further, and the reactive surface was incorporated on top of a low rectangular barrier. The results showed that the reactive configurations including the edges and the reflective rectangle provided gains in excess of that offered by the rectangle alone or a rectangle with a single edge on top. When the edge heights were translated into real dimensions using 1:10 scale, these gains were more readily appreciated. The reactive configuration consisting of 0.17 m wells matched the performance of a single barrier of 0.5 m height, even though it is shorter by a threefold.

The insertion loss of the rectangle and the reactive rectangle with three well depths were compared for two receiver locations. All three reactive rectangle systems performed better than the plain rectangle at both receiver locations except at low frequencies. As the well depth was increased, the low frequency performance was clearly enhanced while the rest of the spectrum remained similar for all systems. Therefore there would be an optimum depth where the low frequency performance would be positive. In this case, this depth appeared to be 0.25 m for the specific geometry investigated at a scale factor of 1:10.

The high frequency performance for all three well depths at both receivers and the contributions to the performance approached zero at around 20 kHz. Positive contributions at mid-frequencies for all three systems at both receivers (except at 10 kHz) are prominent. The frequency range of 5 – 15 kHz where favourable contributions were noted would represent the peak of the A-weighted traffic noise spectrum corresponding to a range of 500 Hz to 1500 Hz at the scale factor of 1:10.



Having realised these favourable gains on small height barriers, the wells were placed on top of an earth mound. The findings were inconsistent and the contributions to the performance were small. This was considered to be due to the limitations of the testing room. Increased path length meant the contributions from the reverberant sound were masking any potential gains that might have been present. The predicted lowest frequencies for the reactive surface to be realised were not clearly visible as before.

The physical scale modelling under uniform field conditions did confirm the benefits of a series of wells for small geometries but failed to provide any concrete evidence in the case of large geometries, even though very small gains were still reported. Considering the limitations of the testing method it was decided to repeat these experiments in a semi-anechoic chamber to test their validity.

The experiments were repeated in two different semi-anechoic chambers with an aim to identify the limitations of the uniform field experiments. Additional experiments were also undertaken to supplement the findings of uniform field experiments and to understand the likely mechanisms of noise attenuation involved in the case of rib structures consisting of a series of edges or wells.

It was found that mainly the depth of the wells determined the lower frequency limit of attenuations. At frequencies lower than the limiting frequency, the insertion loss of the rib structures were found to be negative. The effectiveness of the pressure release surface appeared to be restricted to the vicinity of the wells and the attenuations were greatest for receivers which were situated at propagation angles and horizontal distances close to the reactive surface. The high frequency performance appeared to be dependent on diffraction effects characterised by the overall surface area of the wells and the total number of edges. This was not necessarily the case for receivers which were in direct line of sight of the source. It was found that there was an optimum number of edges for the most favourable attenuations. However this depended on the diffraction angles and the frequencies.

As the diffraction angles measured from the grating normal were reduced, the attenuations were observed to shift to lower frequencies. The high frequency gains at these receivers were negative. For the maximum attenuations at resonant frequencies to be realised, the wavelength of the sound wave has to be smaller than the half-wavelength of the overall width of the reactive surface.

The geometries considered did not enable a clear relationship to be established for attenuations at various diffraction angles. The separation distance between the edges and the nature of the scattering objects have not been investigated as part of this work.



The semi-anechoic chamber experiments verified the usefulness of uniform field experiments under certain conditions. At smaller geometries (edges on the ground), good qualitative and quantitative agreements were obtained. At medium sized geometries (rectangular barriers) good qualitative agreements were obtained although the magnitude of some of the improvements at certain frequencies were somewhat limited by the presence of the reverberant field. At large geometries (earth mounds) single performance indicators were similar partly because the earth mound configurations did not provide substantial additional attenuations at the receivers under consideration. The frequency spectra obtained by semi-anechoic chamber measurements for large geometries showed that at higher frequencies, uniform field experiments failed to realise the substantial attenuations.

Following the physical modelling work, numerical modelling was undertaken in three parts. In the first part, the details of the numerical modelling carried out by SYSNOISE were described. The indirect boundary element methods was used as the basis of the mathematical model. A geometry from the literature was used to verify the way the numerical model has been implemented. The second part was on the numerical modelling of selected geometries which were investigated by physical scale modelling. The findings of these were used to aid the validation of the physical modelling results. The third part concentrated on earth mound configurations with single, double and multiple top edge conditions. These were investigated with a view to extending the acoustic design guidance on earth mounds and to supplement the advice in the previously proposed barrier selection method. The computer modelling also allowed more realistic receiver locations to be selected with no restrictions on their horizontal extent.

The earth mound configurations consisted of the variations of a basic earth mound geometry studied comprising single, double and multiple edges on its top. The basic geometry chosen was the same as that used in physical modelling. In addition to the 0.08, 0.17 and 0.25 m high edges investigated earlier, 0.5, 1 and 2 m high barriers were also examined. These were considered to be the most likely candidates which could have currently been implemented in practice as conventional barriers on top of earth mounds. All heights listed above have been tested as both single and double edge configurations. The edge heights smaller than and including the 0.5 m high edge have been tested as reactive configurations, in the form of multiple edges organised as a series of wells. The total number of modifications were 16. Single figure performance indicators were determined according to the sound pressure levels observed with and without the modification, with the reference geometry present in both cases. This rating system enabled the performance of each modification to be compared relative to that of the plain earth mound.



As it would be expected, double edge configurations performed better than the single edge cases possibly due to change in the path length or due to multiple diffraction. As the edge height decreased, the difference between the single and double cases diminished. The differences are 1.3 dB for the 2 m high barriers and 0.1 dB for the 0.08 m high edges. The reactive configurations in turn performed better than their equal height double-edge counterparts. Between the double and reactive configurations, one can not talk about a change in the path length and therefore any recorded gains should be due to multiple diffraction or the soft pressure release as envisaged in the previous chapters. The reactive configurations provided around 1 dB additional gains over the double - edge cases and 1.6 dB additional gains over the single edge cases. It has been shown that as the angular displacement of the receiver into the shadow is increased, the differences in attenuation values between a hard and soft - or indeed between hard and absorbent - boundary conditions are also increased. The receiver positions closer to the barrier gave more substantial gains and these values decreased as the receivers were further away from the barrier. The receiver position with the maximum angular displacement into the shadow zone - receiver 1 - on average provided 3 dB additional attenuation over the double-edge cases. This value was raised to 4.7 dB when the relative performance over the plain mound was considered.

The spectra of gains for a receiver situated on the ground provided evidence concerning the lowest frequency for which the surface would be considered reactive. These frequencies seem to lie around the predicted frequencies and they are characterised by the transition in the relative performance from positive to negative gains and from then onwards providing positive contributions. However the expected gains at the predicted frequencies are very modest. When the rest of the spectrum is considered for a given reactive profile at the predicted frequencies and there onwards, the superior performance of these profiles are visible. The "cut-off" frequencies where the relative performance of a reactive configuration improves coincide with the lowest frequency for which they can be considered reactive. As the well depth becomes shallower the range of the spectrum, for which the performance of the reactive profile diminishes, increases.

The boundary element modelling was mainly concerned with the modifications made to an existing earth mound. Two cases of "equal height reactive barriers" have also been investigated. This work was intended to demonstrate that if these reactive configurations are considered at an early design stage, the earth mound can be made shorter. However, the reduction in height will somewhat be less than the reactive well depth if the performance of the above reported cases are to be matched. Otherwise, the equal height reactive cases are shown to be superior.



The physical modelling techniques were validated by comparing the results to findings of numerical modelling using boundary element methods. Four sets of geometries investigated by physical modelling were selected for comparison and validation purposes.

The first set of geometries consisting of a series of edges on the ground included three models having 14-edge configurations with different heights.

The 0.8 m deep wells generally provided very good agreements at all receivers. The results were overall within 2 dB of each other or better. Similarly, the 0.17m wells gave generally very good agreements. The exception is the general lack of correlation at high frequencies. At 1250 Hz, although the physical modelling results were within 2 dB of each other, the numerical modelling gave some inconsistent results. At 400 Hz for the receiver (5, 0.4), it can be seen that there is poor agreement between all three methods. At the receivers 1.5 m above ground, the 0.25 m wells gave good agreements for all three methods. At the remaining receivers, attenuations obtained by uniform field experiments were under measured by 1 to 4 dB at mid to high frequencies compared with semi-anechoic chamber experiments. Good agreements were obtained at lower frequencies for all three methods. The numerical modelling provided attenuation values which are in closer agreement with the semi-anechoic chamber results at mid frequencies and with uniform field experiments at highest frequencies.

Generally, the well depths of 0.08 m and 0.17 m provided very good agreements between the magnitudes of improvements obtained by all three methods. The well depths 0.25 m gave good to reasonable agreements for the findings of all three methods. Overall, all three well depths provided good qualitative agreements.

The second set of geometries involving low rectangular barriers similarly used three models with different edge conditions.

The 0.8m wells yielded very good agreements at frequencies corresponding to quarter-wavelength of the well depth or lower. The attenuations measured by uniform field tests were lower by 4 to 5 dB at higher end of the spectrum compared with semi-anechoic chamber and numerical modelling. Overall, reasonable qualitative agreements were obtained for this geometry. The agreement between numerical modelling results and semi-anechoic chamber experiments were found to be very good.

The 0.17m wells provided very good agreements at frequencies corresponding to quarter-wavelength of the well depth or lower. There was very good correlation between two physical modelling techniques at the highest frequency under consideration which is 1250 Hz. The inconsistencies in numerical modelling results have been observed at this frequency as noted above. The findings of the uniform field



experiments indicated that the mid-frequency range of frequencies were under measured by 4 to 5 dB compared with semi-anechoic chamber experiments. Generally the correlations between numerical modelling and semi-anechoic chamber results are very good except at 400 Hz and the problematic frequency of 1250 Hz. Overall, reasonable qualitative agreements could be identified.

The 0.25m wells gave very good correlations between semi-anechoic chamber experiments and numerical modelling results. The inconsistency of numerical modelling predictions at 1250 Hz was noted at this geometry as well. Uniform field experiments, when compared with these, gave intolerable qualitative and quantitative agreements. The attenuations obtained by this method were consistently under-measured by 3 to 6 dB at frequencies higher than those corresponding to quarter-wavelength of well depth and these were over measured by a similar amount at lower frequencies. Overall, as the attenuations due to the edges increased, the lack of correlations in uniform field experiments was more prominent. The semi-anechoic chamber tests and the numerical modelling results using boundary element methods gave very good correlations.

The third consisted of a single geometry of reactive earth mound to represent the largest geometries. This model was considered to be the most likely candidate where a reactive surface could be realised due to the number of edges involved.

The uniform field experiments gave negligible relative improvement values as noted in Chapter 8. This was considered to be due to the increased effects of the reverberant field masking the attenuations. This is supported by the substantial attenuations observed by physical modelling carried out in the semi-anechoic chamber and the numerical modelling.

The results of numerical modelling and semi-anechoic chamber tests yielded very good correlations at frequencies less than 315 Hz. The differences between the two were less than 1 dB. The agreements were reasonable at frequencies greater than 800 Hz. The semi-anechoic chamber results are shown to be up to 2 dB lower. The differences are more prominent especially when the attenuations are great. However at frequencies centred around 500 Hz, the semi-anechoic chamber tests yielded values which were 4 to 6 dB lower than the findings of numerical model. These large discrepancies are thought to be mainly due to the practical difficulties associated with attaching the edges on top of the mound. The irregularities in the floor surface and the model dimensions meant the edges could not be secured in a way to form an integral part of the mound. Considerable attention was devoted to fixing these onto the earth mound model in such a way that there would not be any gaps left. These would have prevented some of the sound waves from taking a direct path over the reactive surface and instead they would propagate through the gaps underneath the edges. This would



have resulted in the reactive surface not being fully realised. It is noted that 500 Hz is the resonant frequency corresponding to these well depths and the attenuations which have been adversely affected are centred around this frequency band.

This geometry showed that uniform field experiments would not be suitable for the largest geometries where the attenuations are expected to be greatest. It was found that there were some discrepancies at around the resonant frequencies between the findings of semi-anechoic chamber experiments and numerical modelling results. This was attributed to the reactive surface not being fully realised due to irregularities in the physical model.

The fourth set consisted of the rib structure which was used to investigate the effects of attenuations and amplifications at various diffraction angles.

This geometry compared semi-anechoic experiments with numerical modelling. Generally it was found that the numerical modelling results and the semi-anechoic chamber experiments are within 2 dB of each other or better. The numerical modelling generally tends to yield the higher improvements of the two methods.

The inconsistencies observed previously at 1250 Hz with the results of numerical modelling are also seen in these experiments. These are prominent especially at receiver heights of 0m, 0.5m and 2.5m. A similar comment can be made for 1000 Hz at receiver which is 3m high. Overall, the numerical modelling attenuations agreed reasonably well with those obtained by semi-anechoic chamber experiments.

## **12.6 EXTENDING GUIDANCE ON EXISTING EARTH MOUNDS**

Acoustic guidance on existing earth mounds can be provided in the form of flow-chart diagrams as proposed for the wall type barriers earlier. As recalled, the guidance on wall type barriers was based on extensive work done by others. Modelling work, either physical or analytical, combined with on-site performance checks confirmed the performance of the barrier profiles included in the earlier flow-charts.

The guidance proposed below is based on the modelling work undertaken herein. Therefore the validity of the guidance is subject to the limitations of this work and the underlying assumptions. Some of these assumptions can be listed as follows:

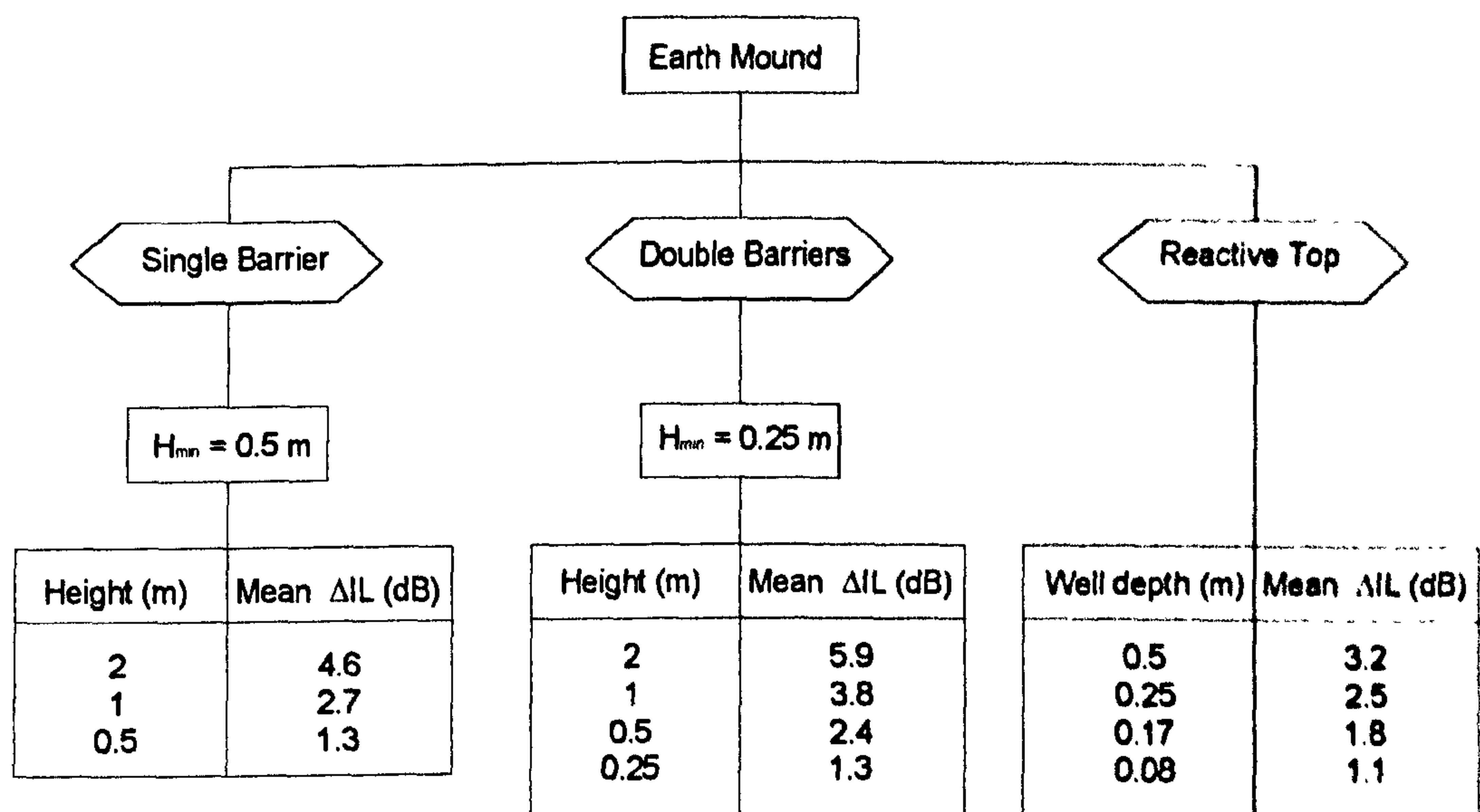
- The single figure performance indicators provided are strictly limited to the source / receiver configurations investigated and the rating system applied.



- The guidance is based upon the basic shape with a fixed height, base and top width and slope angles.
- Any multiple reflections that might exist do not affect the performance adversely.
- An increase in the height of an existing earth mound is possible / acceptable.
- The insertion loss of the basic shape is very similar to those obtained by others and values tabulated below can be added on these cumulatively.
- Extra barriers to be added on top are "thin" compared with the wavelengths under consideration, with sufficient transmission loss through the chosen barrier material, and no gaps exist between the added barrier and the existing earth mound to allow leakage of sound in an unfavourable way.
- All the materials used including the ground, extra barriers / edges and the existing earth mound are hard (reflective).
- The source is an infinite two-dimensional plane source perpendicular to the ground surface and the source / receiver plane.
- The roadway and the barrier are parallel and of infinite length with no vertical or horizontal variations in the physical dimensions along the longitudinal direction.
- The reactive surface to be applied on top of an existing mound is based on the fixed width and number of wells investigated.
- The atmosphere is homogeneous with no variations in the sound speed or the air density.

It is obvious that the performance of these applications need to be validated on-site with realistic ground characteristics, atmospheric conditions and traffic compositions before any guidance can have practical importance. Figure 12.1 shows the possible improvements which can be made to an existing earth mound and their effects on the mean insertion loss are tabulated. These can be in the form of single, double or reactive modifications. It is emphasised that the smallest single barrier to improve the mean insertion loss by more than at least a decibel is 0.5 m. In the case of double barriers, 0.25 m matches this performance.





**Figure 12.1 : Improvements to existing earth mound type barriers.**

It is hoped this guidance can augment the advice provided in the official barrier design guidelines of the U.K.. The contradictory nature of these were discussed in Chapter 4.

Alternatively, the information can be presented in the form of a graph, as seen in Figure 12.2. In addition to the change in the mean insertion loss values provided above, data is provided for receiver 2 which corresponds to a receiver height of 1.5 m situated in the deep shadow zone, 20 m from the barrier centreline. These set of curves show that improvements depend on the receiver location. These modifications therefore represent a better potential if receivers up to, for instance, 20 m are to be considered.



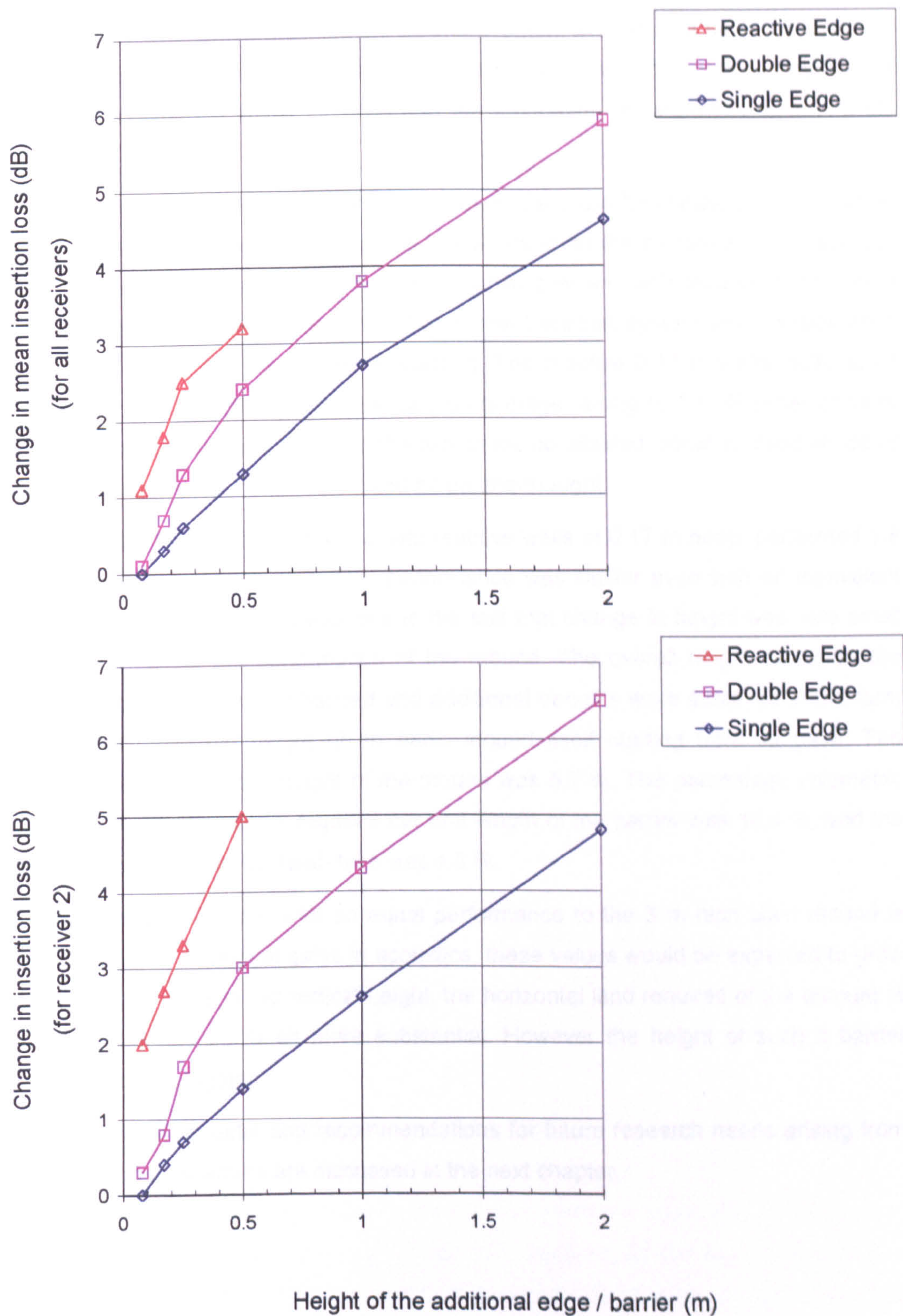


Figure 12.2 : Change in insertion loss of an existing earth mound due to various modifications.

The reactive configuration with 0.25 m deep wells on average performed almost as well as the single 1 m tall barrier. When considering how to improve the performance of an



existing earth mound, the governing factor for choosing between these two would not be acoustics. The former provided 2.5 dB improvement whereas the latter matched this with 2.7 dB. The fabrication costs of a series of wells would therefore need to be balanced against the visual intrusion and the foundation requirements of a 1 m tall barrier.

Similarly, reactive configuration with 0.17 m deep wells can be compared with a single small barrier with a height of 0.5 m. The former improves the performance on average by 1.8 dB and the latter by 1.3 dB when installed over an earth mound. A 0.5m high barrier could still require some form of permanent support system with consideration given to the wind loading on the foundations. The reactive 0.17 m wells, quite apart from performing 0.5 dB better acoustically on average raising to 1.4 dB better or more when the receiver locations close to the barrier are considered, could be fixed on top of an earth mound easier when conceived as an afterthought.

It was shown that a reactive mound with reactive wells of 0.17 m deep, performed 1.8 dB better than a plain mound. This performance was similar even with an equivalent height reactive mound. This was due to the fact that change in height was very small and it didn't affect the performance of the mound. The overall height remained the same, the acoustics was enhanced and additional benefits were achieved in the form of a reduction in the height of an earth mound itself starting from its base. The reduction achieved in the height of the mound was 5.7 %. The percentage volumetric reduction in the fill material required per unit length of the barrier was 10.4 %, and the reduction in the horizontal land- take was 4.8 %.

If a reactive earth barrier with an equal performance to the 3 m high plain mound is desired, with no additional gains in acoustics, these values would be expected to grow larger and the gains in the vertical height, the horizontal land required or the amount of fill material would be much more substantial. However the height of such a barrier needs to be investigated.

The concluding remarks and recommendations for future research needs arising from this research programme are discussed in the next chapter.



## **13 CONCLUSIONS AND FUTURE WORK**

This research programme was concerned with the design of road traffic noise barriers, in particular, the use of low-height multiple-walls on the ground and on top of earth mound type barriers. These noise reducing devices have been referred to as 'rib structures' throughout most of this work (see Chapter 6).

A comprehensive review of literature<sup>1</sup> (Chapter 3), the proposal of a new barrier selection method (Chapter 4) and the preliminary experimental work (Chapter 5) have all contributed to the development of this barrier type. The main findings of the investigation into the acoustic properties of rib structures are summarised below.

### **13.1 MODELLING**

A detailed investigation was undertaken into the acoustic performance of multiple-walls using physical and numerical modelling techniques. Physical scale modelling experiments were carried out both under uniform field conditions and in two different semi-anechoic chambers in the presence of a continuous noise source, using a model scale of 1:10. Numerical modelling was applied using indirect boundary element method formulation. The commercial software named SYSNOISE was employed for the computations. It was found that numerical modelling results and the semi-anechoic chamber experiments generally agreed very well. The level of accuracy of the uniform field experiments depended on the choice of source and receiver locations as well as the size of the model geometry. These are discussed in Chapters 7 to 11.

### **13.2 AN ALTERNATIVE BARRIER TYPE**

Although previous researchers investigated similar applications situated on the ground<sup>2</sup> and on top of conventional barriers<sup>3,4</sup> these investigations did not explore in detail the influence of various parameters on sound attenuation or the associated attenuation mechanisms.



### **13.2.1 Physical Parameters**

The work undertaken as part of this research project has shown that a number of physical parameters are likely to influence noise propagation over rib structures. These were identified as follows.

- Wavelength of the incident wave,  $\lambda$
- Well depth,  $d$
- Total number of diffracting elements,  $N$
- Well width, or horizontal spacing between adjacent elements,  $w$
- Source location determining angle of the incident wave,  $\alpha$
- Receiver location, with respect to the order of diffracted wave,  $\beta$
- Nature of the individual diffracting element,  $F$
- Total distance covered by diffracting elements,  $L$
- Proportion of source-to-receiver distance ( $X$ ) to that covered by diffracting elements,  $X / L$

### **13.2.2 Attenuation Mechanisms**

This work also discussed the likely noise attenuation mechanisms by rib structures. In addition to the long wave scattering effects and diffraction effects, it was shown that surface wave generation mechanisms and interference effects played a significant part.

Long wave scattering effects were identified to be the main noise attenuation mechanism at lower frequencies. Surface wave generation mechanisms were shown to reduce the performance of rib structures at frequencies lower than those corresponding to quarter wavelength of the depth of the wells. Diffraction effects were likely to be the main mechanism at higher frequencies. Interference between direct paths and multiply reflected paths (within the grooves) caused constructive and destructive interference peaks at certain frequencies for some of the geometries considered.

## **13.3 SPECIFIC FINDINGS**

This investigation resulted in acoustic advice on the use of multiple walls both on their own and on top of earth mounds. Under favourable conditions, the multiple-wall configurations were shown to give substantial attenuations. The full implications of these results can be better appreciated when evaluated against the traditional noise



barrier design principles. These maintain that (1) a barrier should at least intercept the line-of-sight from source to receiver (2) to improve performance of a barrier 'path length difference' would need to be increased (3) at low frequencies, barriers are not very effective due to their size. The following are some specific outcomes which contradict these principles.

At 1250 Hz, noise attenuations of up to 26 dB have been measured for a receiver in the shadow zone (Figure 9.11). This frequency is where A-weighted road traffic noise spectrum typically peaks. The configuration consisted of 17 edges (0.25m high) situated on the ground and the 'path length difference' was very small. According to the 'path length difference' approach, in order to match this performance, a conventional noise barrier would need to be 4.4m high. This height is around 17 times higher than that considered above. The improvements were substantial throughout the spectrum as indicated by noise reductions of around 18 dB at 400 Hz.

For a receiver in illuminated zone situated 1.5m above ground, the edge configuration described above gave attenuations up to 11 dB at 315 Hz (Figure 9.16). A different configuration which consisted of 21 edges (0.17m high) on the ground gave around 8 dB improvements at 200 Hz for a receiver in illuminated zone situated 3m above ground (Figure 9.24). Considering the size of the barrier and the location of the receivers, these are significant attenuations at low frequencies.

Multiple-edge configurations on the ground would be most effective when used as a noise control measure at source. A conventional noise barrier situated at the edge of the road is generally designed for mitigating near-side traffic. However it loses its effectiveness against far-side traffic due to increased source distances. Therefore the use of a series of edges in central reservations of dual carriageways would act as a noise mitigation measure for far-side traffic on both sides of the carriageway.

The examples above demonstrate that substantial attenuations are possible throughout frequency spectrum for receivers at grazing incidence and in shadow zone without the need for large 'path length differences'. Although significant noise reductions are also achievable for receivers in illuminated zone, these show strong frequency dependence.

Where the height of a series of edges on their own is not sufficient to intercept the line of sight, consideration should be given to elevating them using other structures. For example a configuration consisting of 11 edges (0.25m high) placed on top of a 0.5m high barrier gave an insertion loss of 23 dB at 400 Hz and 31 dB at 1250 Hz for a receiver in shadow zone (Figure 9.40). This configuration would be applicable to roadside situations placed on a low earth mound.



When used on top of a 3m high earth mound with a 1m wide horizontal top, multiple-edge configurations gave up to 8 dB attenuations at high frequencies (Figure 9.44). These were offset to some extent by amplifications at low frequencies. However the assessment of traffic noise using A-weighting and the logarithmic nature of addition of sound would ensure the overall benefits are substantial. If used on top of wider mounds or on the slopes of mounds, these would be expected to provide even greater attenuations.

For instance, design graphs in Figure 12.2 show that 0.3m high wells on top of a 3m high earth mound can give around 3.5 dB improvement over an existing mound in single figures. The graphs also show that the same improvement could be provided by a single barrier of about 1.5m high. It should be noted that a 3m high mound has an insertion loss of 17 dB (Table 10-3) and an additional 3.5 dB would be considered substantial in environmental noise situations. This is also a considerable reduction in the height of the additional barrier amounting to 80% reductions in height.

All of these multiple-edge configurations have shown that significant acoustic benefits can be obtained without the need to compromise aesthetic or visual qualities of barriers. In addition, the reduced overall height of these barriers would have important implications on their structural design.

## **13.4 RESEARCH FINDINGS**

The summary of the main findings of this work is shown below.

1. A comprehensive state-of-the-art review was undertaken on the research carried out on noise barriers. This was presented in Chapter 3 (also see Appendix A).
2. A simplified approach was put forward for selecting the type of noise barrier in controlling road traffic noise. This approach would be of benefit particularly to those non-acousticians who are part of the decision making process. This is shown in Chapter 4.
3. The physical parameters and noise attenuation mechanisms involved in the design of rib structures were identified. It was discussed that a combined approach used in the study of resonators and diffraction gratings as well as surface wave generation mechanisms and interference effects would be more appropriate for their study. These were discussed in Chapter 6.
4. It was shown that physical modelling under uniform field conditions using a continuous noise source could be undertaken. It was demonstrated that their



applicability depended on the source-receiver locations and the size of the geometry under consideration.

5. The barrier selection method was extended to include the acoustic aspects of existing earth mounds with single or multiple edges on their top. The details can be found in Chapter 12.
6. The rib structures used on the ground and on other earth mound type barriers were shown to provide substantial noise attenuations. This was especially the case when the propagation path was grazing the top of the reactive surfaces. Noise attenuations of up to 26 dB have been measured under favourable conditions, without an increase in barrier height. Noise reductions were also noted at receivers in the illuminated zone. These were frequency dependent and varied with diffraction angles. It is considered this noise mitigation method could be very beneficial especially in central reservations of roads, where a conventional noise barrier would not be appropriate. These can also be used on either side of the road, or on top of garages or other buildings.

In order to fully develop a design method certain aspects of this work needs to be investigated further. These are outlined below.

## **13.5 FUTURE WORK**

- A more detailed parametric study into the relationship between the well depth, well width, the number of edges and the overall width of the reactive surface and other parameters identified as part of this research. These include the nature of the scattering surfaces and the effects of non-periodic spacing on different receiver locations.
- Further research on the four mechanisms identified as part of this work to propose a combined analytical model. This work would need to establish the exact nature of the relationships between these mechanisms and also identify additional mechanisms that may be influencing the acoustic performance of rib structures.
- On - site measurements of the acoustic performance of rib structures under real atmospheric conditions. There is a need to verify their performance when used in central reservations, on the sides of the roads, on top of garages and other buildings and on top of earth mounds.



- A detailed study is required into the non - acoustical aspects of a rib structure. Such aspects include materials, cost, drainage, engineering, maintenance and support systems.
- The uses of rib structures on the rest of the slopes of an earth mound need to be investigated. Crib walls could be the potential naturally occurring barriers for investigating this aspect.
- The simplified design method discussed in Chapters 4 and 12 would need to be extended further to develop of a "knowledge based system" for the design of road traffic noise barriers. This would be useful to all decision makers who may not have a background in acoustics.



## **13.6 REFERENCES**

- 
- <sup>1</sup> EKICI, I. and BOUGDAH, H.N., A Review of Research on Environmental Noise Barriers, Building Acoustics, Volume 10, Number 4, 289 - 323, 2003
- <sup>2</sup> Van Der HEIJDEN, L.A.M. A and Martens, M.J.M., Traffic Noise Reduction by Means of Surface Wave Exclusion Above Parallel Grooves In The Roadside, Applied Acoustics, 15, 329-339, 1982
- <sup>3</sup> FUJIWARA, K., HOTHERSALL, D.C. and KIM, C., Noise Barriers with Reactive Surfaces, Applied Acoustics, Vol. 53, No 4, 255-272, 1998
- <sup>4</sup> OKUBO, T. and FUJIWARA, K., Efficiency of A Noise Barrier on the Ground With An Acoustically Soft Cylindrical Edge, Journal of Sound and Vibration, 216(5), 771-790, Article No. sv981720, 1998